UNCLASSIFIED

AD NUMBER

AD844671

NEW LIMITATION CHANGE

TO

Approved for public release, distribution unlimited

FROM

Distribution authorized to U.S. Gov't. agencies and their contractors; Administrative/Opertional Use; Sep 1968. Other requests shall be referred to Air Force Aero Propulsion Lab., Wright-Patterson AFB, OH 45433.

AUTHORITY

AFAPL ltr, 12 Apr 1972

THIS PAGE IS UNCLASSIFIED

AFAPL-TR-67-114
Part II

AD844671

VAPORIZING AND ENDOTHERMIC FUELS FOR ADVANCED ENGINE APPLICATION

Part II. Studies of Thermal and Catalytic Reactions, Thermal Stabilities, and Combustion Properties of Hydrocarbon Fuels

A.C. Nixon, G.H. Ackerman, L.E. Faith, H.T. Henderson,
A.W. Ritchie, L.B. Ryland

Shell Development Company,
A Division of Shell Oil Company

TECHNICAL REPORT AFAPL-TR-67-114, Part II
September 1968

This document is subject to special export controls and each transmittal to foreign governments or foreign nationals may be made only with prior approval of the Air Force Aero Propulsion Laboratory. / AFPL

Air Force Aero Propulsion Laboratory
Air Force Systems Command
Wright-Patterson Air Force Base, Ohio

362

FOREWORD

This report was prepared by Shell Development Company, Emeryville, California, under U.S. Air Force Contract No. AF 33(615)-3789. The contract was initiated under Project No. 3048, Task No. 304801. The work was administered under the direction of the Aero Propulsion Laboratory, Mr. H. L. Lander, Project Engineer, AFPL.

This report covers work for June 1967 to June 1968.

A. C. Nixon was principal investigator and project supervisor for Shell Development Company. The professional staff participating in the investigation was comprised of: G. H. Ackerman, L. E. Faith, H. T. Henderson, A. W. Ritchie, and L. B. Ryland.

This report was submitted by the authors

This technical report has been reviewed and is approved.

Arthur V. Churchill
ARTHUR V. CHURCHILL, Chief
Fuels, Lubrication and Hazards Branch
Support Technology Division

ABSTRACT

Investigation of the feasibility of using endothermic reactions of hydrocarbons to augment the latent and sensible heat of fuels for cooling engines operating under a high mach number regime is continuing. The literature continues to maintain the desirability and feasibility of producing vehicles with hypersonic flight speeds; some areas of advantage for hydrocarbons are suggested.

The dehydrogenation of Decalin over a platinum/Al_2O_3 catalyst has been studied extensively on a laboratory scale covering the temperature region up to 1200°F and pressures to 10 atms, in both once through and differential systems, in order to provide kinetic data for the construction of a mathematical model. Studies on the thermal reaction of SHELLDYNE and its hydrogen treated derivative indicate that the hydrogen treating increased the stability by a factor of 1500 (the reactivity of SHELLDYNE-H is about the same as that of Decalin).

Production of catalysts ~~under our catalyst development program~~ have turned up a number of the 536 catalysts examined that are more active than our standard Pt/Al_2O_3 catalyst, but no breakthrough in either activity or cost has been achieved. Further testing has shown that catalysts which demonstrate improved activity with MCH do the same with Decalin and has confirmed the observation that improved catalyst stability is associated with small pore size. Our efforts to reduce the heat transfer and pressure drop problems inherent in a bed catalyst by applying the catalyst to the wall of the heat exchange tube have met with some success. Studies on molecular and dispersed catalysts are underway. A pulse reactor to be used in this study has been successfully operated with MCH.

Heat transfer studies in a simulated single tube fuel system have confirmed the mathematical model for the catalytic dehydrogenation of MCH up to a heat flux of 600,000 Btu/hr/sq ft. They also indicate the necessity for catalysts of higher activity and stability such as are available from our catalyst development program. Heat transfer studies with nonreactive cooling to be applied with a regenerative ramjet indicate maximum temperature limits of 1350°F for tube wall and 1150°F for the fluid. A maximum heat flux of $8^5 \times 10^6$ Btu/hr/sq ft has been achieved to date. Satisfactory correlations of the Dittus/Boelter type have been developed for the super critical region but are less satisfactory in the critical and subcritical regions.

In studying the effect of environment on the thermal stability of Decalin at 600°F, it was found that exposure to high surface areas of iron, copper and chromium had a deleterious affect which could be largely controlled with MDA.

SHELLDYNE-H was found to have a satisfactorily short ignition delay in shock tube studies compared to other hydrocarbon systems. An interesting "double delay" behavior was observed with SHELLDYNE itself. The thermodynamic and transport properties of trans-Decalin, SHELLDYNE and JP-7 and a bibliography of recent literature of interest are included.

TABLE OF CONTENTS

PAGE

Introduction 1

Summary 4

Considerations Affecting Applications 6

Laboratory Reaction Studies 13

  Thermal Reaction of SHELLDYNE® H and SHELLDYNE 13

    SHELLDYNE H 17

    SHELLDYNE 17

    Comparison With Decalin 17

    Discussion 24

  Dehydrogenation of Methylcyclohexane in a Pulse Reactor 24

  Dehydrogenation of Decalin Over Various Catalysts 32

    Results 34

    Effect of Pore Volume on Catalyst Stability 44

  Dehydrogenation of Decalin: Diluted-Bed Reactor 44

    Results 50

    Summary 63

  Bench-Scale Catalyst Evaluation Tests With Methylcyclohexane 66

Conventional Catalysts and Catalytic Coatings 69

  Conventional Catalysts 69

    Preparation 69

    MICTR Evaluation With MCH and n-Heptane 70

  Catalytic Coatings 78

    Preparation and Granular Evaluation With MCH 78

    Coating Evaluation With MCH 83

Nonconventional Catalyst Systems 86

TABLE OF CONTENTS (Contd)

PAGE

Homogeneous and Dispersed Catalysis 86

Feasibility Calculations on Dispersed Phase Catalysis 89

Thermal Stability 92

Tube Deposit Rating Methods 92

Direct Heat Transfer Coefficient Measurements 93

Complete Combustion of Tube Deposits 94

Radiative Methods 97

Infrared 98

Solvent Deposit Removal 98

Electron Micrography 101

Summary of Deposit Rating Methods 104

Modification of the SD Coker: SD/M-7 105

Effect of Metal Environment on Decalin Thermal Stability 106

SD/M-7 Coker Cleanup Procedure 110

Influence of Solvent Contamination on SD/M-7 Coker Ratings . . . 110

Thermal Stability of SHELLDYNE and SHELLDYNE H 112

Thermal Stability of P and W 535 Jet Fuel 112

Fuel System Simulation Test Rig 114

Catalytic Dehydrogenation of MCH Over UOP-R8 114

0.277" ID x 2-ft Long Reactor 114

Cooling Program, Experimental Study 126

0.277" ID x 2-ft Long Heat Transfer Section 130

0.0265" ID x 6" and 4" Heat Transfer Sections 134

Model of a Packed Bed Reactor 152

Influence of Physical Properties 152

TABLE OF CONTENTS (Contd)

PAGE

Reaction Kinetics for MCH Dehydrogenation 152
  Kinetic Parameters From FSSTR Data 152
  Kinetic Parameters From Bench-Scale Data 158
  Comparison of Results 160
Reaction Kinetics for Decalin Dehydrogenation 167
  Decalin-Tetralin-Naphthalene Equilibria 167
  Kinetic Parameters From Bench-Scale Data 169
Model of a Regenerative Heat Exchanger for Missile Application 169
  Model Development 169
  Comparison With Experiments 174
Shock Tube Studies of Ignition Delays of Hydrocarbons 175
  Experimental Work 175
  Data Analysis 181
  Results 181
Estimation of Physical Properties of Hydrocarbons 186
  Description of Estimation Methods 196
Present Status and Future Projections 198
References 203
Appendix 207
Bibliography 291
Subject Index for Bibliography 346

ILLUSTRATIONS

FIGURE PAGE

1. Factors Affecting Ablative Effectiveness 9
2. Variation of Overall Thermal Efficiency With Mach Number 11
3. GLC Chromatogram of SHELLDYNE 14
4. GLC Chromatogram of SHELLDYNE H 15
5. Secondary Furnace Liner for 1/4" OD Reactor Tube 18
6. Reactor Temperature Profile 19
7. Dehydrogenation of Methylcyclohexane Pulse Reactor. Effect of LHSV on Conversion 28
8. Dehydrogenation of Decalin Over Various Catalysts. Effect of Temperature on Conversion 36
9. Dehydrogenation of Decalin Over Various Catalysts. Temperature Coefficient 37
10. Dehydrogenation of Decalin Over Various Catalysts. Effect of Temperature on Selectivity for Naphthalene 38
11. Dehydrogenation of Decalin Over Various Catalysts. Effect of Temperature on Stability: 842 to 1022°F 40
12. Dehydrogenation of Decalin Over Various Catalysts. Effect of Temperature on Stability: 842 to 1202°F 41
13. Dehydrogenation of Decalin Over Various Catalysts. Effect of Pore Size on Catalyst Stability 47
14. Diluted Bed Reactor 49
15. Equilibrium Constants for Decalin System 51
16. Equilibrium Composition for Decalin System 52
17. Dehydrogenation of Decalin: Diluted Bed Reactor. Temperature Coefficient 58
18. Dehydrogenation of Decalin: Diluted Bed Reactor. Effect of Pressure 60
19. Isomerization of Decalin: cis-trans Equilibrium 64
20. Calculated Dehydrogenation of MCH by Vapor Phase Catalysis . . . 91

ILLUSTRATIONS (Contd)

FIGURE PAGE

21. Combustion Tube Rater Design 96

22. Electron Micrographs of a Clean Stainless Steel Coker Filter Element at 60x, 100x, and 300x Magnifications 102

23. Electron Micrographs of a Stainless Steel Coker Filter Element at 100x Magnification, Following Run With SHELLDYNE at 6 lb/hr and 675°F in the SD/M-7 Coker 103

24. Revised Fuel System for the SD/M-7 Coker 111

25. FSSTR-Flow Sketch of Fuel System Simulation Test Rig 115

26. FSSTR-0.277" ID x 2-ft Long Reactor Section 116

27. FSSTR-Comparison of Sheathed and Bare Wire Thermocouples on 2-ft Reactor Section 118

28. FSSTR-Heat Loss From 2-ft Reactor Section 119

29. FSSTR-MCH Over UOP-R8 in 2-ft Reactor: Catalyst Bed Exit Fluid Temperature 124

30. FSSTR-MCH Over UOP-R8 in 2-ft Reactor: Decline in Catalyst Activity during Series 10018-55 125

31. FSSTR-MCH Over UOP-R8 in 2-ft Reactor: Effect of Coke Deposition on Tube Wall Temperature, Series 10018-55 127

32. FSSTR-MCH Over UOP-R8 in 2-ft Reactor: Effect of Coke Deposition on Tube Wall Temperature, Series 10018-64 128

33. FSSTR-MCH Over UOP-R8 in 2-ft Reactor: Coke Formation From Series 10018-55 129

34. FSSTR-0.277" ID x 2-ft Long Heat Transfer Section 132

35. FSSTR-Heat Transfer to MCH in Empty 0.277" ID x 2-ft Long Heat Transfer Section: Variation of Tube Wall Temperature With Thermocouple Location 133

36. FSSTR-Example of Heat Loss Measurement from 2-ft Long Heat Transfer Section 135

37. FSSTR-Miniature Heat Transfer Section Test Stand 136

38. FSSTR-Miniature Heat Transfer Section: Reactor No. 10018-82 . . . 137

39. FSSTR-Miniature Heat Transfer Section: Reactor No. 10018-97 . . . 138

ILLUSTRATIONS (Contd)

FIGURE PAGE

40. FSSTR-Miniature Heat Transfer Section: Reactor No. 10018-103 + 110 139

41. FSSTR-Miniature Heat Transfer Section: Reactor No. 10018-122 . 140

42. FSSTR-Example of Tube Wall Temperature Data From Miniature Heat Transfer Section, Run 10018-101-13:01 142

43. FSSTR-Effect of Inverting Miniature Heat Transfer Section on Tube Wall Temperatures 143

44. FSSTR-Tube Heat Loss From Miniature Heat Transfer Sections . . 145

45. FSSTR-End Fitting Heat Loss From Miniature Heat Transfer Sections 146

46. FSSTR-Thermal Conductivity and Electrical Resistivity Used for Type 316 SS Miniature Heat Transfer Sections 150

47. Calculated Profiles for MCH Dehydrogenation in the FSSTR From FSSTR Kinetic Data - Run 50-1610 156

48. Calculated Profiles for MCH Dehydrogenation in the FSSTR From FSSTR Kinetic Data - Run 62-1419 157

49. Calculated Profiles for MCH Dehydrogenation in the FSSTR From Bench-Scale Kinetic Data - Run 50-1610 165

50. Calculated Profiles for MCH Dehydrogenation in the FSSTR From Bench-Scale Kinetic Data - Run 62-1419 166

51. Equilibrium Conversions of the Decalin-Tetralin-Naphthalene System 170

52. Calculated and Experimental Temperature Profiles for Regenerative Heat Transfer Studies - Run 78-1110 176

53. Calculated and Experimental Temperature Profiles for Regenerative Heat Transfer Studies - Run 78-1225 177

54. Calculated and Experimental Temperature Profiles for Regenerative Heat Transfer Studies - Run 78-1535 178

55. Calculated and Experimental Temperature Profiles for Regenerative Heat Transfer Studies - Run 130-1411 179

56. Calculated and Experimental Temperature Profiles for Regenerative Heat Transfer Studies - Run 133-1430 180

ILLUSTRATIONS (Contd)

FIGURE		PAGE
57.	Oscilloscope Traces of Pressure and CO_2 Infrared Emission in Shock Tube Runs	182
58.	Correlation of Ignition Delays for n-Octane-Oxygen-Argon . . .	187
59.	Correlation of Ignition Delays for Decalin-Oxygen-Argon	188
60.	Correlation of Ignition Delays for SHELLDYNE-Oxygen-Argon . . .	189
61.	Ignition Delay Times for SHELLDYNE-Oxygen-Argon	190
62.	Correlation of Ignition Delays for SHELLDYNE H-Oxygen-Argon . .	191
63.	Correlation of Ignition Delays for DMD-Oxygen-Argon	192
64.	Comparison of Ignition Delay Correlations for DMD, SHELLDYNE, SHELLDYNE H, Decalin and n-Octane	193
65.	Correlation of Ignition Delays for SHELLDYNE-Decalin-Oxygen-Argon	194
66.	Correlation of Ignition Delays for SHELLDYNE-Binor-S-Oxygen-Argon	195
67.	Secondary Furnace Liner for Pulse Reactor	211
68.	Pulse Reactor: Schematic	212
69.	Pulse Reactor System	213
70.	GLC Analysis System	214
71.	GLC Chromatogram of Diethylcyclohexane Isomers: Capillary Column	222
72.	GLC Chromatogram of Diethylcyclohexane Isomers: Packed Column.	223
73.	GLC Analysis of Adsorbate From Decalin Purification	253

TABLES

TABLE PAGE

1. Some Physical Properties of SHELLDYNE and SHELLDYNE H 16
2. Thermal Reaction of SHELLDYNE H 20
3. Thermal Reaction of SHELLDYNE H. Product Distribution 21
4. Thermal Reaction of SHELLDYNE 22
5. Thermal Reaction of SHELLDYNE. Product Analyses 23
6. Thermal Reaction of Decalin 25
7. Comparison of Reactivities of SHELLDYNE H and SHELLDYNE 25
8. Dehydrogenation of Methylcyclohexane: Pulse Reactor. Effect of Space Velocity on Conversion at 662°F 27
9. Dehydrogenation of Methylcyclohexane: Pulse Reactor. Catalyst Stability 29
10. Dehydrogenation of Methylcyclohexane: Pulse Reactor. Effect of Space Velocity on Conversion at 752°F 30
11. Dehydrogenation of Methylcyclohexane: Pulse Reactor. Effect of Catalyst Pretreatment on Stability 31
12. Dehydrogenation of Decalin Over Various Catalysts. Relative Activities and Stabilities 35
13. Dehydrogenation of Decalin Over Sinclair-Baker RD-150 Catalyst . . 42
14. Dehydrogenation of Decalin Over Shell 107B Laboratory Catalyst . . 43
15. Dehydrogenation of Decalin Over Various Catalysts. Summary Table . 45
16. Physical Properties of Various Catalysts 46
17. Dehydrogenation of Decalin and Tetralin. Feed Compositions 48
18. Dehydrogenation of Decalin: Diluted Bed Reactor. Effect of Temperature and Space Velocity on Conversion 53
19. Dehydrogenation of Decalin: Diluted Bed Reactor. Effect of Pressure 54
20. Dehydrogenation of Decalin: Diluted Bed Reactor. Effect of Temperature 56
21. Dehydrogenation of Decalin: Diluted-Bed Reactor. Apparent Activation Energies 57

TABLES (Contd)

TABLE		PAGE
22.	Dehydrogenation of Decalin: Diluted Bed Reactor. Effect of Pressure at 752°F	59
23.	Dehydrogenation of Decalin Mixtures	62
24.	Dehydrogenation of Decalin-Tetralin Mixtures	65
25.	Dehydrogenation of Methylcyclohexane. Evaluation of Various Catalysts	67
26.	Relative Rates of MCH Dehydrogenation by the More Active Catalysts.	71
27.	Effect of Neutralization of Platinum Impregnate by Various Acids on MCH Dehydrogenation Activity	72
28.	Relative MCH Dehydrogenation Rates of Several Older Supported Pt Catalysts	73
29.	Relative MCH Dehydrogenation Rates With Various Single Metals on Several Supports	74
30.	Relative MCH Dehydrogenation Rates With Supported Variable Composition Bimetallics	75
31.	Relative MCH Dehydrogenation Rates With Variable Composition Bimetallics on a Type 1 Support	76
32.	Relative MCH Dehydrogenation Rates With Variable Composition Trimetallics on a Type 1 Support	76
33.	Relative MCH Dehydrogenation Rates With Various Amounts of Supported Bimetallics and Trimetallics	77
34.	Relative MCH Dehydrogenation Rates With Various Candidate Catalytic Coatings (Granular)	79
35.	Relative MCH Dehydrogenation Rates With Various Candidate Catalytic Coatings (Granular)	82
36.	Evaluation of MCH Dehydrogenation With Various Catalytically Coated Tubes With Different Physical Arrangements	85
37.	Dispersed Phase Dehydrogenation of MCH	87
38.	Candidate Solubilizing Agents for Dispersed Phase Catalysts	88
39.	MCH Dehydrogenation: Vapor Phase Catalysis	92
40.	Combustor Tube Rater Results on Polystyrene "Deposits"	95

TABLES (Contd)

TABLE PAGE

41. Solvent Deposit Removal Tests 100

42. Estimated Minimum Detection Levels for Five Different Coker Tube Rating Techniques 104

43. Effect of Total Pressure on Dissolved Oxygen Concentration in a 0.78 Specific Gravity Hydrocarbon With an Equilibrating Gas Containing 1 ppm 106

44. Effects of Metal Environments on Thermal Stability of Decalin (F-139) With and Without Metal Deactivator (MDA) 108

45. Chemical Analysis of 316 Stainless Steel 109

46. Effect of Metal Deactivator (240 ppm) on Thermal Stability of Decalin 110

47. Comparison of Thermal Stability of SHELLDYNE, SHELLDYNE-H and Decalin 113

48. FSSTR-MCH Over UOP-R8 in 2-Ft Reactor: Data Summary 120

49. FSSTR-Heat Transfer to MCH in 0.277" ID x 2-Ft Long Heat Transfer Section: Data Summary 131

50. FSSTR-Summary of Operating Conditions for Miniature Heat Transfer Sections 147

51. Effect of Changes in Physical Properties on MCH Dehydrogenation . . 153

52. Calculated and Experimental Results for MCH Dehydrogenation in the Packed Bed Reactor 155

53. Dehydrogenation Rates for Pure MCH 160

54. Data for the Packed Bed Program Predictions of MCH Dehydrogenation Runs 161

55. Experimental and Predicted Results for MCH Dehydrogenation in the FSSTR (0.277-in. D x 9.81-ft L) 162

56. Experimental and Predicted Results for MCH Dehydrogenation in the FSSTR (0.652-in. D x 9.55-ft L) 163

57. Experimental and Predicted Results for MCH Dehydrogenation in the FSSTR (0.277-in. D x 2.04-ft L) 164

58. Ignition Delay Parameters in Equation (57) 164

TABLES (Contd)

TABLE PAGE

59. Ignition Delay Parameters in Equation (38) 185

60. Dehydrogenation of Decalin Over Various Catalysts 215

61. Dehydrogenation of Decalin Over Shell 46 Laboratory Catalyst . . . 216

62. Dehydrogenation of Decalin Over Shell 108 Laboratory Catalyst . . 217

63. Dehydrogenation of Decalin Over Shell 107A Laboratory Catalyst . . 218

64. Dehydrogenation of Decalin Over Shell 91A Laboratory Catalyst . . 219

65. Dehydrogenation of Decalin Over Shell 105B Laboratory Catalyst . . 220

66. MCH Dehydrogenation With Various Catalysts in MICTR: Runs 263-450. 224

67. MCH Dehydrogenation With Various Catalysts in MICTR: Runs 484-572. 233

68. MCH Dehydrogenation With Various Catalysts in MICTR: Runs 573-676. 235

69. MCH Dehydrogenation With Various Catalysts in MICTR: Various Supports 243

70. n-Heptane Dehydrocyclization With Various Catalysts in MICTR . . . 244

71. GLC Analyses of RAF-161-60 Decalin 247

72. Dehydrogenation of RAF-161-60 Decalin 249

73. Comparative Effectiveness of Davison Grades 950 and 28 Silica gel in the Purification of RAF-161-60 Decalin 250

74. FSSTR-Heat Transfer to MCH in Empty 3/8" OD x 10 Ft Long Sections: Data Summary 254

75. FSSTR: Data Summary Series 10018-90. Heat Transfer to MCH in Miniature Heat Transfer Section 256

76. FSSTR: Data Summary Series 10018-94. Heat Transfer to MCH in Miniature Heat Transfer Section 257

77. FSSTR: Data Summary Series 10018-98. Heat Transfer to Nitrogen in Miniature Heat Transfer Section 258

78. FSSTR: Data Summary Series 10018-101. Heat Transfer to Water in Miniature Heat Transfer Section 259

79. FSSTR: Data Summary Series 10018-108. Heat Transfer to Water in Miniature Heat Transfer Section 260

TABLES (Contd)

TABLE Page

80. FSSTR: Data Summary Series 10018-116: Heat Transfer to Water in Miniature Heat Transfer Section 261

81. FSSTR: Data Summary Series 10018-119. Heat Transfer to Water in Miniature Heat Transfer Section 262

82. FSSTR: Data Summary Series 10018-126. Heat Transfer to Water in Miniature Heat Transfer Section 263

83. FSSTR: Data Summary Series 10018-127. Heat Transfer to MCH in Miniature Heat Transfer Section 264

84. FSSTR: Data Summary Series 10018-129. Heat Transfer to MCH in Miniature Heat Transfer Section 265

85. FSSTR: Data Summary Series 10018-130. Heat Transfer to MCH in Miniature Heat Transfer Section 266

86. FSSTR-Data Summary Series 10018-131: Heat Transfer to MCH in Miniature Heat Transfer Section 267

87. FSSTR: Data Summary Series 10018-132. Heat Transfer to MCH in Miniature Heat Transfer Section 268

88. FSSTR: Data Summary Series 10018-133. Heat Transfer to MCH in Miniature Heat Transfer Section 269

89. Ignition Delays for n-Octane-Oxygen-Argon 270

90. Ignition Delays for Decalin-Oxygen-Argon 273

91. Ignition Delays for SHELLDYNE-Oxygen-Argon 275

92. Ignition Delays for SHELLDYNE H-Oxygen-Argon-Mixtures 277

93. Ignition Delays for DMD-Oxygen-Argon 279

94. Ignition Delays for SHELLDYNE-Decalin-Oxygen-Argon 280

95. Ignition Delays for SHELLDYNE-Binor S-Oxygen-Argon 281

96. Characteristic Properties of F-71. 282

97. Liquid Properties of F-71 at Saturation Pressure 282

98. Gas Properties of F-71 283

99. Characteristic Properties of trans-Decalin 284

TABLES (Contd)

TABLE PAGE

100. Liquid Properties of trans-Decalin at Saturation Pressure 284

101. Gas Properties of trans-Decalin 285

102. Characteristic Properties of SHELLDYNE II 286

103. Liquid Properties of SHELLDYNE at Saturation Pressure 287

104. Gas Properties of SHELLDYNE 288

VAPORIZING AND ENDOTHERMIC FUELS FOR ADVANCED ENGINE APPLICATION

Introduction

The objective of this study is to provide the information necessary for specifying fuels which will be capable of providing cooling and propulsion for engines powering aircraft in the speed range above Mach 3. The fuel will provide cooling by giving up its latent and sensible heat and by undergoing endothermic reactions before it is fed into the engine as vaporized fuel. Practically, this could be in the temperature range up to about 1400°F. In order for the fuel to function in this manner, it must have excellent thermal stability up to the temperature at which reaction occurs and also in the post-reaction portion of the heat exchanger, to avoid fouling problems. Work under early Air Force contracts served to establish many of the parameters which obtain in delineating the boundaries of the problem. Work was done under our previous contract[1-3] to define more closely the advantages and limitations for the application of hydrocarbon fuels. In that contract it was intended to develop specifications for a fuel or fuels which could be utilized for advanced engine application and to design methods and equipment for testing the properties of such a fuel.

In order to allow precise definition of the fuel, we studied various problems that could arise in several parts of the fuel-combustion system. These included thermal stability problems which could originate in the fuel tanks or in the various metering devices and fuel lines; deposition or coking problems which could affect the efficiency of heat exchanger-reactor devices and catalysts, or plug fuel nozzles; and combustion parameters which could affect the design or operation of the combustion chambers. In order to provide a sound basis for the selection or rejection of fuels, we endeavored to relate the various phenomena observed to the physical and chemical properties of the fuels studied.

The problem areas and approaches used were broken down in the following manner: we improved a previously designed coker apparatus to permit it to be used to study the thermal stability of possible fuels and components at temperatures up to 900°F. We studied possible thermal and catalytic reactions in laboratory scale equipment in order to test the reactivity of fuels and the suitability of selected catalysts. The heat sinks available in the hydrocarbons tested were calculated from thermodynamic properties of the reactants and products. A fuel system simulation test rig (FSSTR) was constructed and used to provide data on hydrocarbon systems. A computer program for simulating the behavior of a packed bed reactor was modified to accept and correlate the results obtained in the fuels system simulator. The subsonic combustion properties of selected fuels and reaction products were observed in a small scale combustor while the ignition-delay behavior of the same fuels and products was studied in a single-diaphragm shock tube to give an indication of supersonic combustion properties.

---

[1] See References.

Studies done under the previous contract indicated the general feasibility of the endothermic reaction approach, particularly the utilization of catalytic dehydrogenation reactions. Our best results have been achieved with the platinum/alumina-methylcyclohexane combination. With this combination, the possibility of achieving the original conceptual goal of 2000 Btu per pound of fuel total heat sink seems possible. The importance of restricting the oxygen content to very low levels to reduce heat exchanger problems was also indicated. Operations with the fuel system simulation test unit (FSSTR) have provided valuable data for heat exchanger design calculations and demonstrated the possibility of high space velocity and long catalyst life with the MCH system. Limitation of thermal cracking of hydrocarbons to a relatively low heat sink of about 300 Btu per pound due to hydrogen transfer reaction was demonstrated. The mathematical model for the cylindrical axial flow reactor was found to be adequate to the extent of its present development. The combustion studies suggest that the possibilities of burning the proposed feed materials and the products of their dehydrogenation under both subsonic and supersonic combustion conditions are promising.

Under the present contract we are continuing and extending the work done under the previous contract with some changes in emphasis. We are continuing to survey the pertinent literature and will issue bibliographies from time to time. We will continue to consider various feed materials which might be useful in this application and assess the probability of their being successful candidate materials. Such candidates are screened in our small scale equipment for reactivity and effect on catalyst life and their thermal stability under heat exchange conditions. Successful candidate materials are tested with improved catalysts and also under larger scale conditions as represented by our fuel system simulation test rig.

In the previous contract only a limited number of catalysts, selected for their probable activity, were tested with a variety of feed materials. The reactions of interest in that program included dehydrogenation, dehydrocyclization and depolymerization. In the present program we are conducting an extensive catalyst development program for new catalysts for these types of reactions. This involves the small scale preparation of a wide variety of catalysts in which catalytic elements (e.g., transition metals) are deposited on substrates and modified by a variety of noncatalytic elements such as, for example, the alkalies, alkaline earths, and halogens. Other catalysts are prepared containing metallic oxides and acidic sites. Such catalysts are tested initially in a small scale apparatus ("micro scale catalyst test reactor", MICTR) which allows rapid screening with standard feed materials such as MCH, n-heptane and tetraisobutylene. In addition to the attempt to prepare superior conventional type catalysts in which catalytic materials are mounted on substrate granules, attempts are being made to prepare nonconventional catalysts in which the catalytic material is mounted in a special way designed to minimize pressure drop, or is previously dispersed in the feed material, or is formed by decomposition in the heated zone. Such nonconventional catalysts are tested with MCH in a variety of equipment prior to being used with other feed materials developed as a result of the program mentioned above.

The computerized mathematical model mentioned above has been carried to the point where good representation of the FSSTR experimental results was possible with different size tubes and catalyst dispositions and variable heat flux and temperatures along the tube length. Difficulty was encountered in representing different tube lengths, LHSV's and heat fluxes but this appears to have been resolved. The program will eventually include latent and sensible heat sinks both before and after the reaction zone, and the mating of a reactor-exchanger with a heat source such as a combustor or a leading edge. This latter step, of course, will require collaboration with engine manufacturers who are working on the combustor design part of the overall program.

Extension of the program towards an aircraft system requires that considerably more work be done on the supersonic combustion aspects of the problem. We are continuing our studies in the shock tube with high molecular weight fuels and their dehydrogenation products. Fuels utilized by engine companies may also be examined in the shock tube to obtain correlation with the results observed by them in their laboratory studies. We also contemplate completing our work on the examination of subsonic combustion in the small burner developed under the previous contract with the additional feature of obtaining quantitative data on the radiation emitted, as a function of fuel composition and burner conditions.

An important consideration in any system which attempts to use the fuel for cooling is the thermal stability of the fuel in the exchanger portion portions of the fuel system. In our previous contract we used the SD Coker for evaluating the thermal stability both of feed material and of products produced by both thermal and catalytic reactions. Examination of the products suffers from the serious deficiency that inevitably a time lapse and some handling has to occur, before the products of reaction are tested. We have therefore constructed a new piece of equipment under the present contract for establishing a standard test for both catalysts and fuels. This unit, called the Catalyst and Fuel Stability Test Rig (CAFSTR), permits simulation of the thermal environment and representative contact times all the way from the fuel tank to the engine inlet. Fuels will be tested using a standard catalyst, while catalysts will be tested using a standard fuel.

Specific support is also being furnished to contractors in the cooling program. This support consists of consultation with respect to problems encountered in the study programs, the furnishing of technical data required for the solution of design problems or for the carrying out of experimental investigations.

Summary

Work to bring our knowledge of the Decalin system up to that we have of MCH has continued. Because of the existence of two isomers in the feed and the two-step nature of the dehydrogenation, the Decalin system is considerably more complicated than MCH. Kinetic data has been obtained in diluted beds and under recycle conditions allowing for completion of a mathematical model for the system.

The thermal reactivity of the high density fuel, SHELLDYNE,® and the effect of hydrogen treatment on this reactivity has been studied in our bench scale reactors. SHELLDYNE was studied over the temperature range 770 to 940°F at pressures up to 10 atms. The thermal reactivity increased with both temperature and contact time. In the all metal system used, SHELLDYNE was found to be quite reactive leading to coking at the higher contact times and temperatures; pressure had little effect. Hydrogen treating gave a much more thermally stable product as was evidenced in studies covering the temperature range 1022 to 1202°F and pressures to 10 atms. It is estimated that SHELLDYNE is 1500 times as reactive as the hydrogen-treated material. In both cases, the different isomers had different rates of reaction. SHELLDYNE H was found to be only slightly more reactive than Decalin. Testing of catalysts prepared under our catalyst development program has continued. The general procedure is to screen the catalysts rapidly with MCH as the test fluid, examining promising catalysts more extensively under bench scale conditions with MCH and if they are still favorable, utilize Decalin as a further test fluid. A group of six catalysts that appeared promising under bench scale conditions with MCH have now been tested further with Decalin. Out of this study has come a number of catalysts of improved activity and stability with both MCH and Decalin. Further evidence that the stability of the catalyst is related inversely to the pore size of the support have been obtained. An additional five catalysts which had appeared promising under micro scale test conditions have been evaluated in bench scale reactor testing. On the basis of preliminary work two of the catalysts appear 12 and 16% more active than the standard catalyst. Additional catalysts have also been prepared and submitted to micro scale testing. The total number of catalysts prepared under our program or obtained from proprietory or commercial sources now stands at 536. During this period, the effect of neutralizing the platinizing solutions with different acids has been investigated with some favorable effects noted. Although most of the catalysts prepared have less activity than the standard material, twelve new materials have been found this quarter which are more active. One interesting case of a bimetallic system has been found in which the synergistic effect of an inactive metal on a slightly active metal has been observed. Attempts have also been made to find catalysts which will be active for the dehydrocyclolization of n-heptane to toluene to take advantage of the additional heat sink available in this way. Some moderately active catalysts were discovered but none of sufficient activity to serve the purpose. Cracking was a common side reaction.

More success has been had with attempts to develop a nonconventional configuration in which the catalyst is attached to the heat exchanger tube wall. Considerable experimental work has been done to develop ways of getting good bonding to the metal surface without destroying the good catalytic activity of the basic catalyst formulation and developing a technique for

applying the coatings to the inside surface of tubes. This seems to have been satisfactorily solved and a number of tubes were prepared with coating thicknesses ranging from 3.5 to 13 mils. In the area of developing particulate or molecularly dispersed catalysts, a number of possible compounds have been prepared or purchased. These will be tested out in two different types of apparatus, an injection autoclave and a pulse reactor. Preliminary work in the latter has turned up three model compounds that show some activity with MCH in this mode of application.

Work on the development of mathematical models to represent both reactive and nonreactive heat sink situations has continued. Difficulties in the development of a satisfactory model to represent the Decalin system in which dehydrogenation to tetralin and naphthalene occurs necessitated the acquisition of additional kinetic data under low conversion conditions. Also, the regenerative heat exchanger model for nonreactive cooling has required continual modification to represent experimental results. It now appears satisfactory in the super-critical region but not below.

Physical and transport properties for SHELLDYNE, a typical JP-7 and trans-Decalin have been calculated using the presently best regarded computation systems. These data are included in this report and have been transmitted to interested investigators. A 1500 gallon batch of Decalin has been purified by silica gel treatment.

The experimental study for very high heat flux conditions in support of the nonreactive cooling program has been continued using heat exchange systems made up of four- and six-inch lengths of 26.5 mil ID tubing in the modified FSSTR (the "mini-FSSTR"). Six sections have been constructed to date, all basically of the same design. These have been utilized in a series of tests with nitrogen, MCH, and water as the test fluids. Operating at flow rates up to 14 x 10^6 lbs/sq ft/hr, a heat flux of up to 8 million Btu/hr/sq ft was achieved with a maximum outlet temperature of about 900°F and a maximum inlet pressure of 1000 psi. Plugging and burn-out conditions were reached during some of these experiments, however, in only one case due to coking.

Efforts to develop a simple and reproducible method of rating deposits on CAFSTR tubes has been continued. Methods favored include solvent removal of deposits, combustion and electron reflection. A large group of selected solvents were tested for their effects on deposits formed from Decalin and jet fuel in the ASTM coker, heating the solvent at 100°C for one hour. The only promising solvent found was dimethylformamide which appeared to be capable of removing substantially all the deposit although two treatments are required. Some results on other methods of rating have been obtained.

The SD-coker has been modified to maintain the feed side of the system at system pressure so that the Zenith pump utilized serves merely as a metering device, thus avoiding the occurrence of pump wear. This system seems to be performing quite satisfactorily. Hydrogen treating SHELLDYNE improved its stability substantially. Examination of the effect of powdered metals in Decalin revealed the combination Fe/MDA may be very deleterious.

Indications of the supersonic combustion behavior of three possible high density fuel components have been obtained by measuring ignition delays in the single diaphragm shock tube at temperatures to 2500°F and 25 psia pressure. The order of decreasing ignition delay found was dimethano-Decalin = SHELLDYNE, octane, SHELLDYNE H. All fuels had about the same energy of activation of combustion (40 kcal). SHELLDYNE showed a peculiar "double-delay" behavior wich so far remains inexplicable.

Considerations Affecting Applications

An interesting paper has recently been published by Ferri[4] (Review of Scramjet Propulsion Technology) which, although directed towards the use of LH_2 fuel, and the combustion process rather than cooling, has some pertinent points. He points out the importance of good cooling since the maximum pressure rise across the combustor in the absence of separation depends strongly on the wall temperature in the region of separation. He notes that the most severe cooling and heat requirements occur in the burner. Good burner design requires that the values of both the heat that must be removed and the maximum heat transfer coefficient should be minimized but at the same time the engine wall thickness must be kept within practical limits. His remarks emphasize the necessity to extend our knowledge of cooling techniques to the utmost in order to develop cooling systems of great flexibility that will not unduly constrain the engine designer.

An interesting application of the endothermic reaction principle can be made in the case of ablative thermal protective systems. This would involve incorporating into the material, a mixture of a high boiling naphthene and a finely divided supported, or molecularly dispersed, dehydrogenation catalyst. As the material heated up as the vehicle entered the atmosphere, one of the early reactions that would take place would be the dehydrogenation of the naphthene to an aromatic and hydrogen with the resulting ejection of the latter from the solid or liquid layer. As explained by E. W. Ungar[5] the heat transfer rate at the gas interface is substantially reduced from the usual value by gas injection. He noted:

> "Injection of gas into the boundary layer cools the gas adjacent to the surface and thickens the layer, thus reducing heat transfer rates. The effectiveness of the injected gas in reducing heat transfer increases as the molecular weight of the injected gas is decreased. Figure 5 (1A) shows the reduction in heat transfer rate, as measured by the Stanton number, as the injection rate, as measured by the blowing parameter, is increased. The Stanton number (St) is defined by
>
> $$St \equiv \dot{q}[\rho_e u_e(\Delta h)]$$
>
> where $\dot{q}$ is the heat flux; ρ_e is the density at the edge of the gas boundary layer; u_e is the velocity at the edge of the gas boundary layer; and Δh is the difference between the gas recovery enthalpy and gas enthalpy at the temperature of the wall. The injection rate as measured by the blowing parameter is the ratio of the mass injection rate to the product of the streamwise mass flux and the Stanton number without gas injection. Curves are shown for the injection of air into air and hydrogen into air for both a

> laminar stagnation point (3) and flat plate without gas-phase reactions (4). In addition, an experimental curve is shown for air-air with turbulent flow on a flat plate (5). Thus (i) the heat transfer rate reduction is large in all cases, (ii) hydrogen reduces the heat transfer rate more than air, and (iii) turbulent boundary layer flow reduces the effectiveness of gas injection.
>
> "The efficiency of an ablative material is frequently measured by the effective heat of ablation defined by
>
> $$H_{eff} = \dot{q}_0 | \dot{m}$$
>
> where H_{eff} is the effective heat of ablation, and $\dot{q}_0$ is the heat transfer to a nonablating surface at temperature T_w. The effective heat of ablation includes gas-injection effects. The effective heat of ablation is strongly dependent on the exposure conditions as a result of the factors discussed above. For illustration, Fig. 6 (1B) shows the effective heat of ablation of ice as a function of the external temperature. The curves were computed at three pressures by Roberts (6) to show the effect of boiling point. The various components of effective heat of ablation are shown on the figure. It is clear that vaporization is the dominant factor and that the effectiveness of ice improves dramatically with increasing external temperature. At the leading edge of the vehicle, the external temperatures shown in Fig. 6 (1B) are equivalent to the stagnation temperatures shown in Fig. 1. The increase in effective heat of ablation with severity of environment is a desirable characteristic which is generally common to gas-producing ablators. To carry the illustration further, the previously mentioned flight condition of 6 km/sec at an altitude of 30 km would lead to an effective heat of ablation in excess of 1200 calories per gram if the vehicle utilized ice as a heat shield."

Another method of application of this same principle could be achieved by selection of the proper plastic for the fabrication of the thermal protection system. In this case, a plastic is selected containing naphthene rings as an integral part of the molecular structure. For instance, such a plastic might be polymerized cyclohexylethylene, (i.e., hydrogenated polystyrene). Into this would be incorporated a finely divided or molecularly dispersed dehydrogenation catalyst. When this layer heated up the initial reaction would be to dehydrogenate the cyclohexyl rings giving a very effective ablative system, since as Ungar explains in the section quoted above, hydrogen is a very effective gas in reducing the heat transfer at the ablating surface.

An interesting comparison between the performance of various fuels has been made by Amin and Molder[6] in a paper entitled "Performance Comparison of Gun-Launched Scramjets for Various Fuels". The fuels compared are kerosene, triethyl aluminum (TEA), liquid hydrogen, and SHELLDYNE. The author used the following parameters for the scramjet engine powered gun-launched vehicle:

SCRAMJET ENGINE PARAMETERS USED TO CALCULATE PERFORMANCE

Parameter	Value
Intake area ratio, A_1/A_3	12.5
Intake efficiency, K_d[a)]	0.94
Fuel total pressure, psf	200,000
Fuel total temperature, °R	550
Downstream fuel injection angle, deg	45
Combustor area ratio, A_5/A_3	3.5
Average pressure factor, n[b)]	1
Exit/inlet area ratio, A_7/A_1	1

a) K_d = "process efficiency" = $(h_3 - h')/(h_3 - h_1)$ where the superscript prime denotes conditions obtained when the air at station 3 is expanded isentropically until $p_3 = p_1$ and h is static enthalpy.

b) Defined by $\bar{p} = p_3 + n(p_5 - p_3)$ where $\bar{p}$ is static pressure and p is the average pressure required to calculate the thrust on the combustor internal walls.

Although they evaluated both volume limited and weight limited vehicles, they consider the volume limited case to be more practical. The authors concluded that "SHELLDYNE was the best of the four fuels considered for volume limited scramjet vehicles. There is no significant theoretical performance difference between the TEA and kerosene but the former might give better performance in practice because of it's greater reactivity. Nonoptimized single stage 90° gun-launched scramjet vehicles using these fuels are theoretically capable of accelerating a 200-lb payload from Mach 5 to Mach 9 during ascent and reaching an altitude of approximately 200 miles". For 90° launching, the actual values of the apogee calculated out to be 275, 215, 205 and 78 miles for SHELLDYNE, kerosene, TEA and LH_2, respectively. At 45° launch, the range in miles (in the same order) would be 405, 316, 301, and 115.

In consideration of the state of knowledge with respect to the kinetics of hydrocarbon air supersonic combustion, it is apparent that there is a need for much further work in this field. This is evident from a study of the analysis of nonequilibrium hydrocarbon air combustion presented in the paper by W. Chinitz and P. Baurer[7)] which is a good summation of the complexity of the kinetic situation in this sort of system and the difficulty of agreeing on the nature and importance of such a fundamental parameter as the ignition delay time. In view of the problems which have been encountered in achieving successful piloting of a hydrocarbon scramjet especially if air rather than pure oxygen is used as the pilot flame oxidant, it is suggested that further investigation of the effect of various types of additives on the ignition delay and also on the oxidation rate following the onset of ignition is urgently needed. The first approach to obtaining this sort of data can probably best be made in a shock tube.

An interesting analysis of aircraft engines development was made recently by A. A. Lombard.[8)] He points out that the best way to increase the

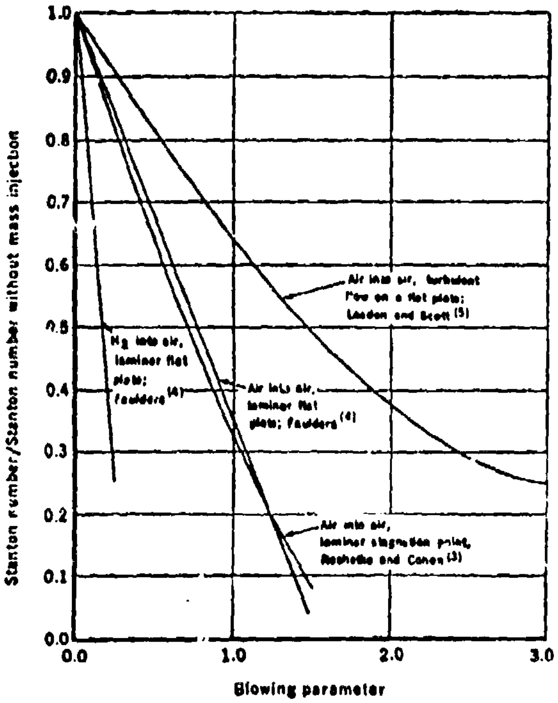

A. Heat Transfer Reduction Due to Gas Injection

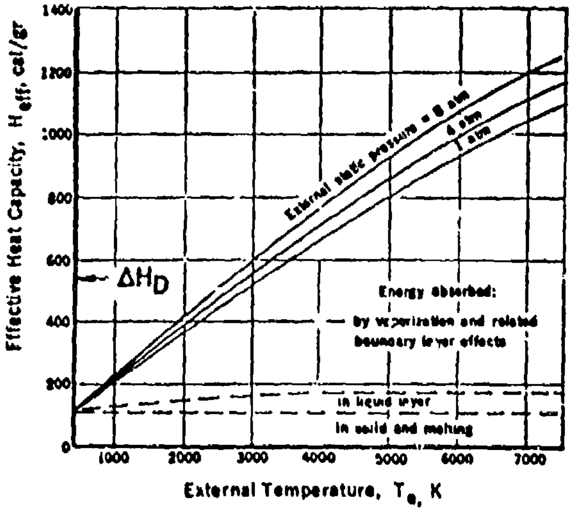

B. Variation of Effective Heat Capacity H_{eff} of Ice With External Temperature T_e for Axisymmetric Flow

ΔH_D = Heat of Dehydration of Cyclohexane

Figure 1. FACTORS AFFECTING ABLATIVE EFFECTIVENESS
Ungar, Science, Vol. 158, 1967

overall thermal efficiency of a power plant is to fly faster. A lot of difficult engineering in an engine is only necessary because of the low design speed - since the jet velocity must be low. Figure 2 is an illustration taken from Figure 52 in his paper which shows how the overall thermal efficiency of a range of engines varies with design Mach number. He states "this is an envelope curve in that from 0.8 to above 2 Mach number the curve represents the efficiencies of a range of turbo fan engines, from 2 to just below Mach 3 a range of pure jet engines and from Mach 3 onwards ramjets. It is very clear that at higher Mach numbers utilization of energy is very good indeed." And again, "as we go still higher in design Mach number the design of an air-breathing power plant becomes even more difficult. At a Mach number of 7 in the stratosphere the total temperature of the air entering the engine is over 2000°C and the combustion temperature must be of the order of 3000°C in order to achieve a worthwhile thrust. Quite apart from the metallurgical problems, there are big problems connected with the dissociation of the products of combustion of normal fuels which makes the attainment of these temperatures difficult."

It is evident that considerable incentive exists for the development of a multiple purpose additive. One which will act as a dehydrogenation catalyst in the heat exchanger of the engine, will act as a combustion catalyst in the combustion chamber and will act as a recombination catalyst in the nozzle section of the engine. While it may be visionary to hope that this can be achieved, there are compounds of metals and oxides that have properties which encourage us to continue dreaming.

Some interesting papers having to do with heat transfer and boundary layer flow have appeared recently which are pertinent to the present investigation. Lewis, Kubota and Lees published an article[9] in the A.I.A.A. Journal for January 1968, p. 7 on an "Experimental Investigation of Supersonic Laminar Two Dimensional Boundary Layer Separation in a Compression Corner With and Without Cooling". They compared the surface pressure distribution for cold wall with the adiabatic configuration for a laminar interaction and observed the dependence on Reynolds number for both laminar and transitional interaction. The free interaction similarity suggested by Chapman was empirically tested and found to be a good approximation for the adiabatic configuration but it failed to correlate the cooled case with the adiabatic case. The scaling suggested by Curle was tested and found to eliminate this deficiency.

Also in the same journal, p. 15, the paper by Barry E. Edney[10] related the "Effects of Shock Impingement on the Heat Transfer Around Blunt Bodies". He reported that an extraneous shock impingeing on a blunt body in hypersonic flow altered the flow around the body and increased the local heat transfer rate near the impingement point. A physical model was set up which predicted variations in shock interference patterns and surface pressure distributions and of the intensity in the extent of the peak heating, in accordance with the experimental findings.

The February issue of the same journal (p. 193), Laganelli, Aimes, and Hartnett[11] wrote on the "Transpiration Cooling in a Laminar Boundary Layer Solid Wall Upstream Effects" in which they developed an analytical model for this type of cooling. It was found that the solid leading edge had a significant effect on the magnitude of the skin friction coefficient over the transpiration surface. They concluded that further investigations would be

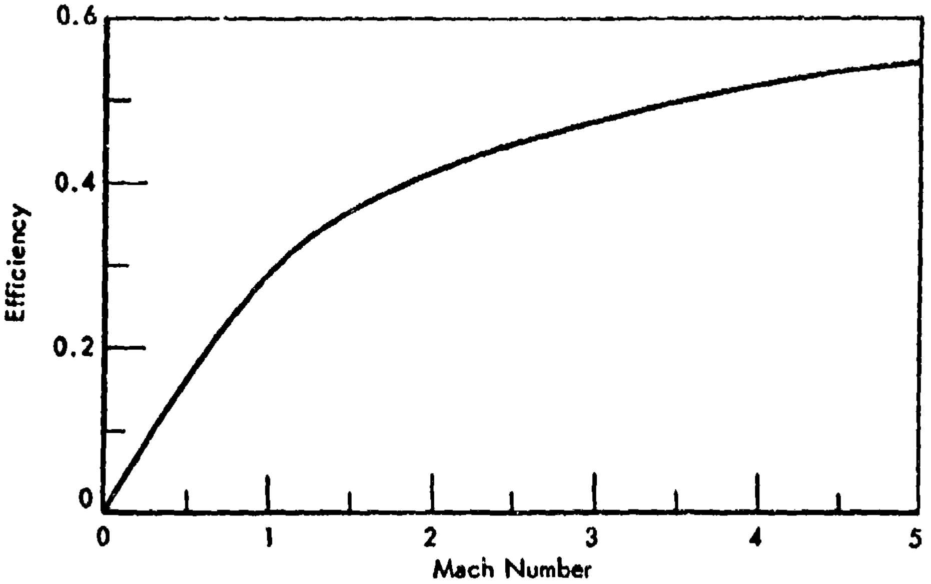

Figure 2. VARIATION OF OVERALL THERMAL EFFICIENCY WITH MACH NUMBER

required for transpiration systems particularly systems which include a non-porous leading edge, since this increases local skin friction.

Also, F. W. Spaid and E. E. Zudukoski[12] describe a "Study of the Interaction of Gaseous Jets From Transfer Slots With Supersonic External Flows". This was an analytic and experimental investigation at Mach numbers up to 4.5. A correlation of data obtained from experiments with finite span slots demonstrates that the effect of jet penetration height and the slot span are the important characteristic dimensions of such flow fields.

In the March issue of the A.I.A.A. Journal, E. J. Felderman[13] on p. 408 writes on the "Heat Transfer and Shear Stress of the Shock Induced Unsteady Boundary Layer on a Flat Plate" in which he examined the development of the boundary layer following the passage of the initial shock wave over a semi-infinite flat plate mounted in the shock tube. Both experimental and analytical solutions of the problem were sought. Data obtained over a range of shock Mach numbers, initial channel pressures and position on the plate agreed well with the theoretical calculations.

An interesting paper on the "Diffusion of Gases and Porous Solids Over a Thousand-Fold Pressure Range" was offered in Chemical Engineering Science 1967 Vol. 22, p. 11 by Henry Cunningham and Jim Geankoplis[14] in which they showed that the experimental diffusivities of gases in alumina and in porous Vicor compared closely with those predicted by the raw field effectiveness factor model and the Wakao and Smith random pore model, as did the data on Vicor.

A paper by M. F. L. Johnson and J. Moil[15] in the Division of Petroleum Chemistry Preprints, ACS Chicago Meeting, September 1967 on the origin and types of pores in some alumina catalysts indicated that the authors were able to distinguish as many as three different pore systems in alumina and alumina catalysts. This data is mainly useful in calculating effective diffusion coefficients.

A paper by S. Landa, J. Vais, and J. Berkhard[16] published in the Collection Czech. Chem. Commun. 32 No. 2, p. 570, February 1967 dealt with adamatene and its derivatives. This is interesting because of the possibility of using an adamantane derivative as a high density thermally stable fuel.

A paper by Kunugi, Tominaga, and Abiko[17] on a kinetic study of the pyrolysis of propane in the presence of hydrogen appeared in the Sekiyu Gakkai Shi, No. 11, 1966 (Japan).

An article appearing in Kinetic Catalysis Chemical Engineering Symposium Series No. 73 Vol. 63, 1967 by R. L. Smith and C. D. Prater[18] on "Some Capabilities and Limitations of Kinetic Studies in Heterogeneous Catalysis as Illustrated by Cyclohexane-Cyclohexene-Benzene Inter-Conversion Over A Supported Platinum Catalyst" shed some light on the mechanism of this important reaction. They gave some kinetic information on the various steps involved with the general conclusion that cyclohexene is not a necessary intermediate in the dehydrogenation of cyclohexane.

Laboratory Reaction Studies

Laboratory studies of candidate endothermic fuels and catalyst systems were continued in our bench-scale reactors.

The relative reactivities of SHELLDYNE, hydrogen treated SHELLDYNE (SHELLDYNE H) and Decalin for thermal reaction were determined.

A pulse reactor was constructed for use in studying catalytic reactions under fixed bed and dispersed phase conditions. A brief study of the dehydrogenation of methylcyclohexane over our standard 1% Pt on Al_2O_3 catalyst was done in this system at liquid hourly space velocities (LHSV) up to 4265.

Several commercial and laboratory-developed catalysts that were promising for the dehydrogenation of methylcyclohexane were evaluated for the dehydrogenation of Decalin in our conventional flow reactor.

Studies on the dehydrogenation of Decalin, tetralin and mixtures of the same were carried out in a highly diluted catalyst bed, in order to obtain kinetic data for formulating a mathematical model for this reaction.

A few catalysts that appeared promising for the dehydrogenation of methylcyclohexane under micro-scale testing (MICTR) were further evaluated in our bench-scale reactor.

Thermal Reaction of SHELLDYNE H and SHELLDYNE

SHELLDYNE is the trade name of a high density, high energy fuel developed by Shell[a] for use in air breathing and rocket engines. This fuel is not prepared from crude oil by conventional processes, but is manufactured from specific chemical intermediates. It has moderately good storage and thermal stability which is improved by hydrogen treatment. As SHELLDYNE is being considered for use as an advanced fuel both SHELLDYNE and hydrogen treated SHELLDYNE (SHELLDYNE H) were evaluated for thermal reactivity in our bench-scale reactor.

Some physical properties of SHELLDYNE and SHELLDYNE H are tabulated below. It is evident that hydrogen treatment increased the viscosity slightly and somewhat lowered the density, RI, freezing point and heat of combustion (Table 1).

SHELLDYNE consists of numerous isomeric compound of which three isomers made up 85% of the material. These were present in the ratios: I:II:III = 16:21:48. Figures 3 and 4 show GLC analyses of SHELLDYNE and SHELLDYNE H respectively. The chromatographs have the same general pattern, but the emergence times of the SHELLDYNE H components are longer however.

Both SHELLDYNE and SHELLDYNE H were tested under conditions of vapor phase thermal reaction at furnace block temperatures of 752-1202°F and 1-10 atm pressure. Both feeds were tested in a 1/4" OD stainless steel tube

---

[a] Information and experimental quantities may be obtained from Shell Oil Company, Products Application Department, New York.

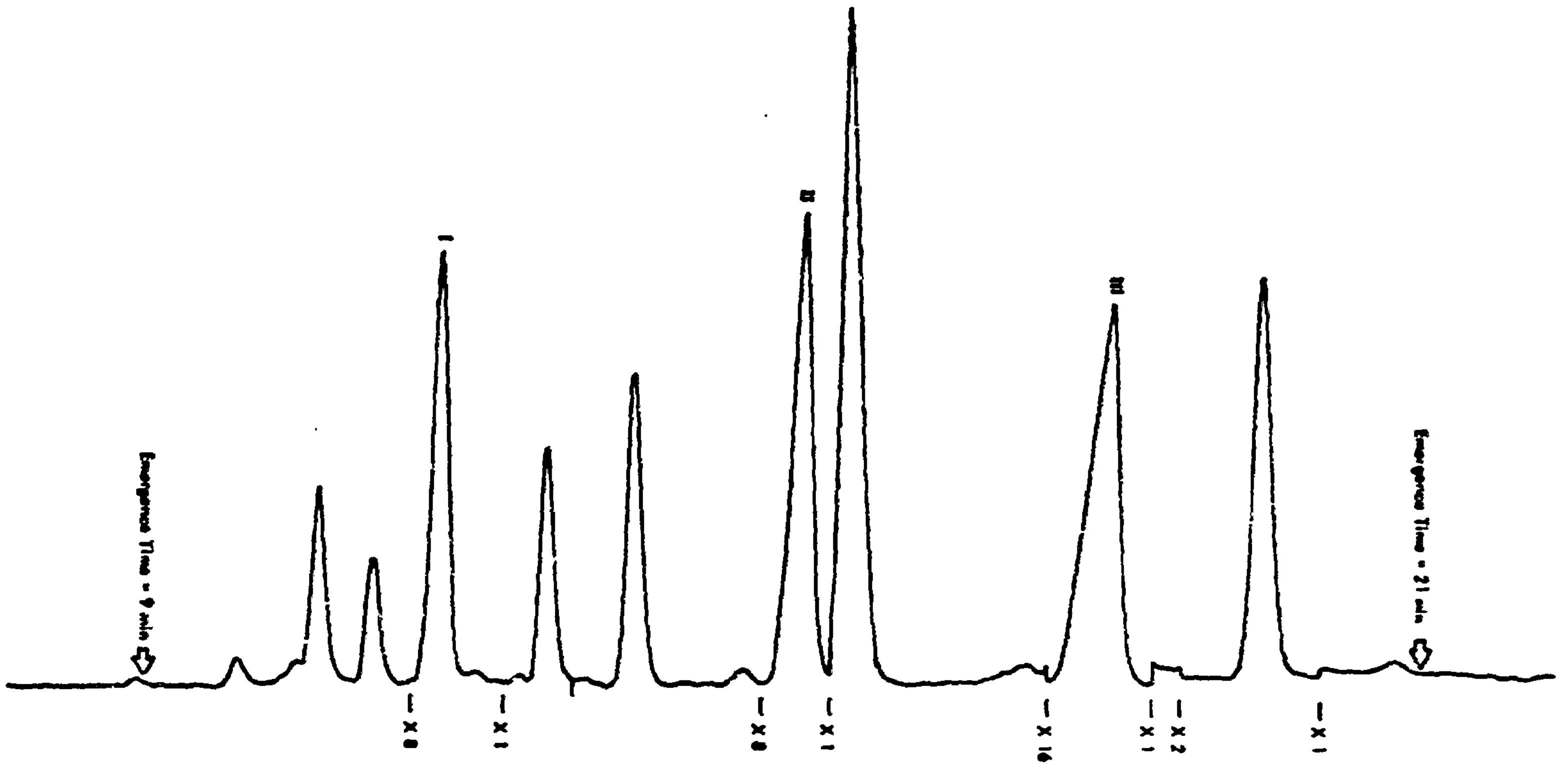

Figure 3. GLC CHROMATOGRAM OF SHELLDYNE

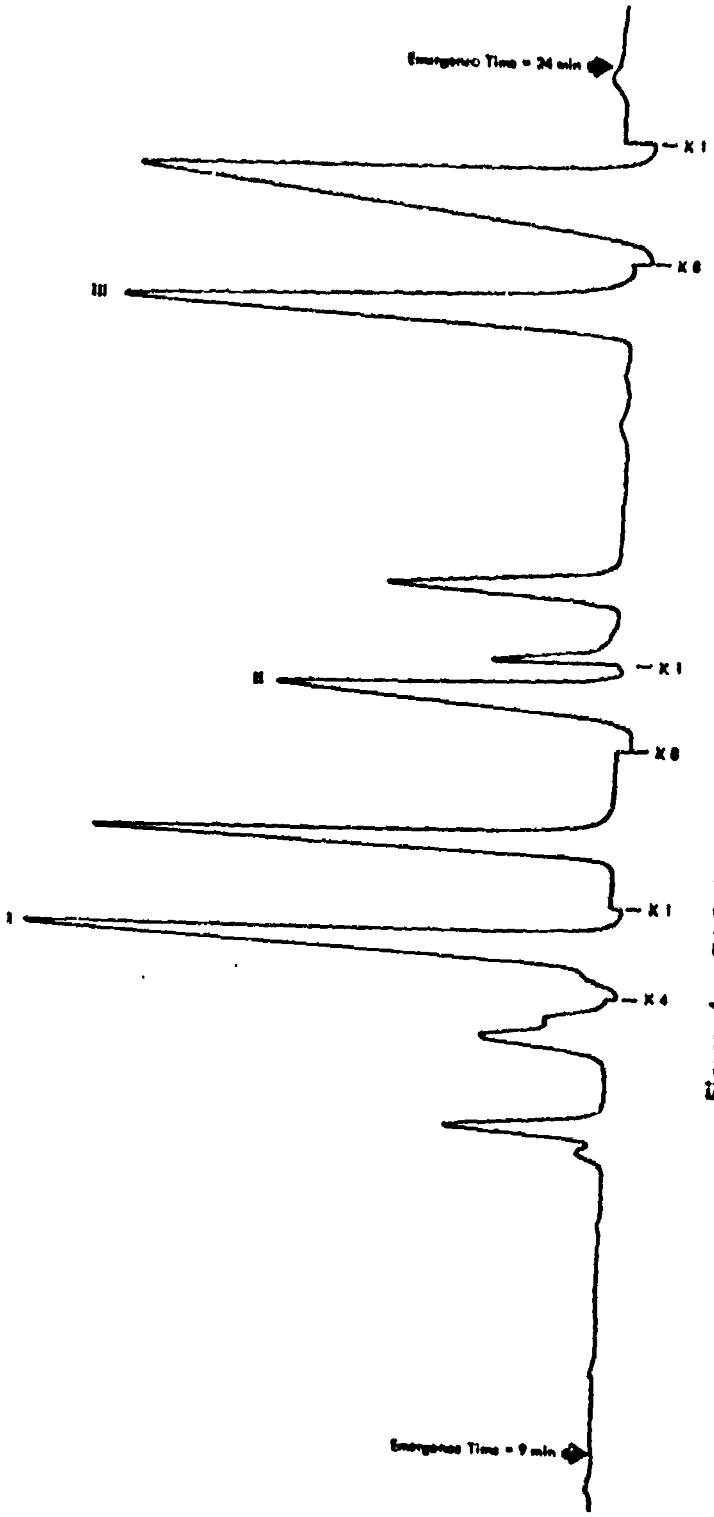

Figure 4. GLC CHROMATOGRAM OF SHELLDYNE H

Table 1. SOME PHYSICAL PROPERTIES OF "SHELLDYNE" AND "SHELLDYNE" H

	SHELLDYNE	SHELLDYNE H
Boiling Point	482-89	500
Freezing Point, °F	-24	(-85)[a]
Specific Gravity, 60°F/60°F	1.100	1.081
Viscosity, cs		
212°F	2.89	3.19
68°F	20.2	26.2
Refractive Index (68°F)	1.5479	1.5401
Pounds/gal (US)	9.16	9.02
Heat of Combustion, Btu/gal	163,830	160,390

a) This material did not show a sharp freezing point but became more viscous with decreasing temperature. At -85°F the liquid could no longer be stirred.

with no packing in the tube.[a] In addition SHELLDYNE was tested in our 5/8" ID standard reactor tube packed with 10-20 mesh quartz chips.

In the 1/4" OD tube the wall temperature was measured at seven points along the tube. The points were 1-1/2 inches apart and the top point was one inch below the top of the secondary liner (Figure 5). The portion of the tube above the secondary furnace liner served as a pre-heat section and was kept at 770°F. The temperature of the reactor wall varied down the tube and Figure 6 shows the temperature variation for a furnace block temperature of 1202°F.

The maximum reaction rate will occur in the region of maximum temperature. Presumably the rate in that portion of the tube whose temperature was 18°F (10°C) or more below the maximum temperature, did not contribute appreciably to the overall rate. Thus the "effective" volume of the tube was that portion of the tube whose temperature was within 18°F of the maximum wall temperature, and whose volume was determined from a plot such as Figure 6. The "effective" reactor temperature was taken as 9°F below the maximum temperature and space velocities and Apparent Contact Times (ACT) were calculated based on the effective volume and effective reactor temperature.

In the 5/8" ID reactor tube the space velocities and contact times were based on the volume of quartz chips (20 ml) and the reactor wall temperature as measured by a thermocouple pressed between the reactor well and the furnace block.

---

a) This reactor system was described in a previous report in detail, on p. 248, 254.[1]

Liquid product material was analyzed by GLC using a 165' capillary column (0.018" diam) coated with 20% polyphenyl ethers in DC 710 silicone. Gas products were analyzed by mass spectrometry. Conversions were calculated from product analyses and neglect coke or polymer formed during reaction.

SHELLDYNE H

At short contact times (0.3 to 0.8 seconds) SHELLDYNE H was reasonably stable. Thus conversions were less than 3% at 1022°F and only 5 to 10% at 1202°F (Table 2). At these contact times conversions were generally lower at higher pressures probably because the increased mass flow at the higher pressures reduced the reactor temperature. At longer contact times (3-4 seconds) increased conversion was observed. Highest conversion obtained was 51% (1202°F, 10 atm) of which about 8% was to light gas products. The liquid product was black, but no tube plugging occurred. Product material was principally cracked liquids (i.e., lighter than starting material) with some light gas at the higher conversions (Table 3). The three isomers were not equally reactive and in general at 1202°F, I was the most reactive at lower pressures and III at higher pressure (Table 3).

First order rate constants were calculated from the rate of disappearance of starting material. Using these values activation energies of 41.8 and 40.3 kcal/mole were obtained over the temperature range of 1022 to 1202°F (Runs 110, 112-1 and 111, 112-3; Table 2).

SHELLDYNE

SHELLDYNE was more reactive and less stable than the hydrogen treated material (Table 4). Thus in the 1/4" OD tube conversion at 797°F (Run 114) was about that obtained with SHELLDYNE H at 1202°F! (Run 112-3; Table 2.) Quantitatively, based on the first order rate constants and an activation energy of 41 kcal/mole, SHELLDYNE was 1500 times more reactive than SHELLDYNE H. Further, at 797°F considerable coking occurred with SHELLDYNE and the reactor began to plug after 15 minutes (Run 115, Table 4). As with SHELLDYNE H the various isomers were not equally reactive and generally the reactivity of I ≈ III > II (Table 5). At constant contact time, pressure did not appear to affect reactivity (cf Runs 114 and 115 Table 4).

In the 5/8" ID reactor tube at higher temperatures and longer contact times coking was even more severe. For example at 932°F (3.6 seconds ACT) the reactor plugged after 15 minutes while at 1022°F (4.5 seconds ACT) plugging occurred after only about five minutes reaction time! Further, before the tube plugged a hot spot appeared and moved down the quartz bed and the temperature in the bed rose to over 1292°F even though the block temperature was only 1022°F!

In both sets of experiments the reaction products were principally liquid cracked material and light gas.

Comparison With Decalin

In order to relate the stability and reactivity of SHELLDYNE H and SHELLDYNE to the naphthenes examined earlier,1)3) a few experiments were done with F-113 Decalin in the 1/4" OD reactor tube. The composition of

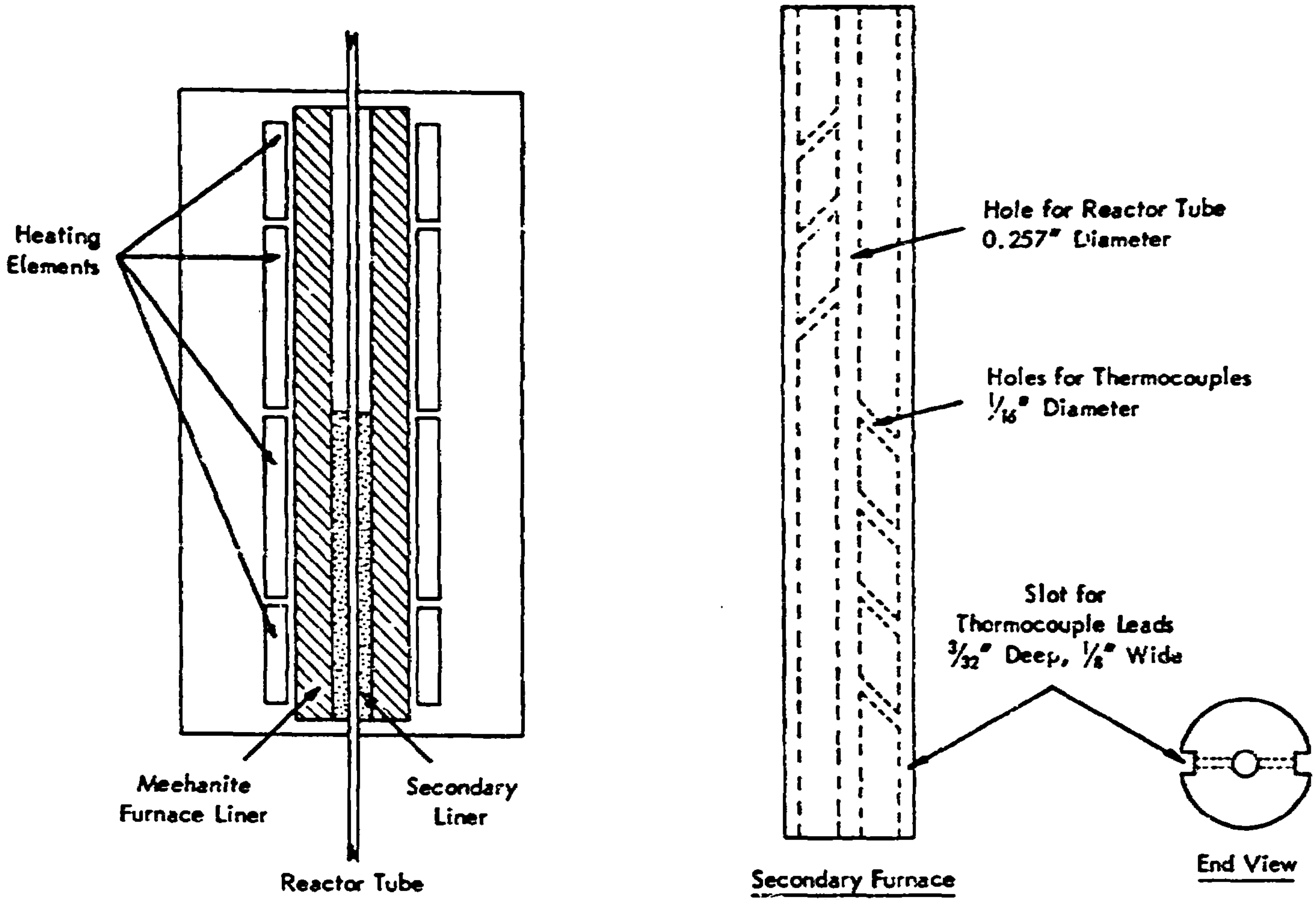
Heating Elements
Meehanite Furnace Liner
Secondary Liner
Reactor Tube
Hole for Reactor Tube 0.257" Diameter
Holes for Thermocouples 1/16" Diameter
Slot for Thermocouple Leads 3/32" Deep, 1/8" Wide
End View

Reactor Furnace with Secondary Furnace Liner in Position

Secondary Furnace Liner

Figure 5. SECONDARY FURNACE LINER FOR 1/4" O.D. REACTOR TUBE

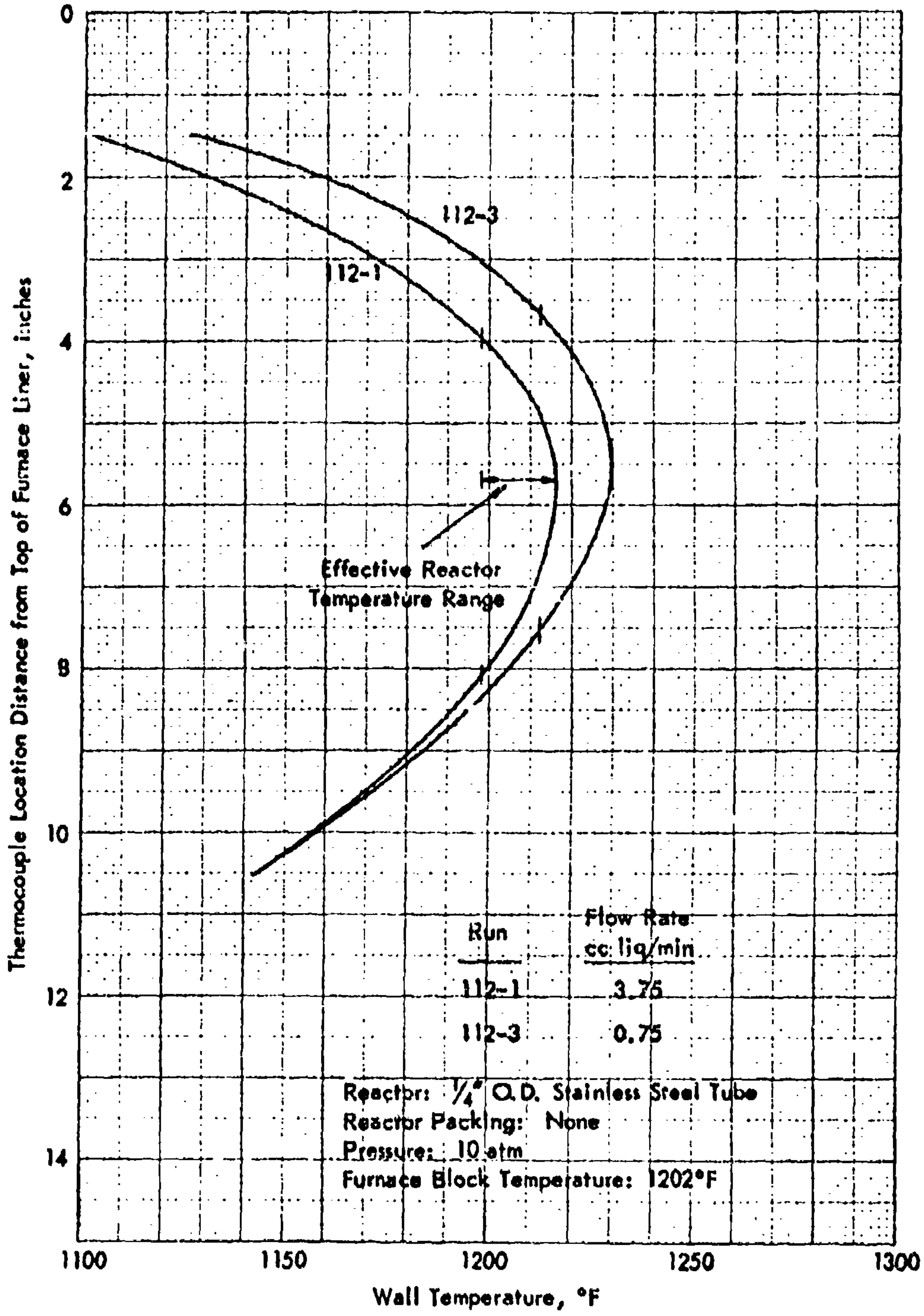

Figure 6. REACTOR TEMPERATURE PROFILE

Table 2. THERMAL REACTION OF "SHELLDYNE" H

Reactor: 1/4" OD Stainless Steel Tube
Reactor Packing: None

Run 10548-	98	99	100	101	102-1	102-2	103	104	105	106	107	108-1	108-2	109	110	111	112-1	112-3
Pressure, atm	1	5	1	5	10	1	5	10	1	5	10	1	5	10	10			
Feed Flow Rate, ml/min	0.75	3.75	0.75	3.75	7.50	0.75	3.75	7.50	0.75	3.75	7.50	0.75	3.75	7.50	3.75	0.75	3.75	0.75
Temperature, °F																		
Block	797					842			1022			1202			1022		1202	
Wall	797	781	797	788	781	855	819	812	995	975	927	1155	1136	1090	961	933	1103	1130
	802	794	802	797	788	848	838	824	1024	1006	927	1202	1177	1150	1000	1022	1172	1197
	806	801	806	802	795	855	848	833	1040	1028	1013	1226	1208	1191	1026	1040	1195	1209
	806	801	806	802	797	855	849	837	1040	1031	1022	1227	1216	1202	1031	1040	121[illegible]	1229
	802	801	801	801	797	848	848	833	1028	1022	1017	1213	1206	1194	1024	1028	1206	1213
	792	792	790	792	793	837	838	828	1004	1002	1004	1184	1182	1175	1006	1010	1180	1182
	774	774	770	774	779	815	821	815	974	975	974	1144	1144	1141	977	977	1143	1143
Effective Reactor Temperature, °F	797	793	788	793	788	846	840	828	1031	1022	1013	1220	1211	1193	1022	1031	1208	1220
Effective Reactor Volume, ml	3.36	3.04	3.37	3.04	3.51	3.49	2.60	2.74	1.95	1.92	1.50	1.64	1.54	1.50	1.93	2.13	1.[illegible]	1.71
Effective LHSV	13	74	13	74	128	13	87	154	23	117	300	27	146	300	117	[illegible]	162	26
Effective ACT, sec	0.80	0.70	0.80	0.70	0.82	0.77	0.58	0.62	0.38	0.38	0.30	0.29	0.27	0.26	0.75	4.2	0.49	3.0
SHELLDYNE Conversion, %w	0.1	0.6	0.3	0.3	1.8	0.3	1.6	0.6	2.6	0.8	2.4	10.2	7.9	5.3	2.8	5.6	25.1	51.0
First Order Rate Constant, sec^{-1}	-	-	-	-	-	-	-	-	-	-	-	0.372	0.346	0.208	0.039	0.014	0.594	0.236

Table 3. THERMAL REACTION OF "SHELLDYNE" H

Product Analyses

Reactor: 1/4" OD Stainless Steel Tube
Reactor Packing: None
U_1 = emerged before I, includes cracked liquid
U_2 = emerged after I and before II
U_3 = emerged after II and before II
U_4 = emerged after II

Run 10548-	Feed	98	99	100	101	102-1	102-3	103	104	105	106	107	108-1	108-3	109	110	111	112-1	112-3
Pressure, atm		1	5	1	5	10	1	5	10	1	5	10	1	5	10	10			
Temperature, °F																			
Block		797					842			1022			1202			1022		1202	
Effective Wall				797	793	788	846	840	828	1031	1022	1013	1220	1211	1193	1022	1031	1208	1220
Product Analysis, %w																			
U_1	2.7	2.8	2.8	2.8	2.8	2.8	2.9	2.8	2.9	3.0	3.0	3.1	10.1	8.3	5.6	3.4	7.0	19.2	36.1
I	15.5	15.2	14.7	14.9	14.6	14.5	14.9	14.7	14.9	13.5	14.8	14.4	13.0	12.9	14.8	14.6	14.7	13.0	9.1
U_2	2.8	2.8	2.8	2.7	2.8	3.1	2.9	2.9	2.8	3.3	2.9	2.7	3.6	3.3	3.4	2.9	3.0	3.3	4.5
II	22.8	23.2	22.5	22.7	22.7	22.0	23.1	22.1	22.7	21.6	22.9	22.2	20.2	21.9	21.3	20.3	20.8	17.7	12.3
U_3	3.5	3.6	3.8	3.7	3.7	4.8	3.8	4.7	3.7	5.0	3.8	4.7	4.2	4.3	4.6	6.4	5.6	5.5	3.8
III	52.6	51.5	52.2	52.0	52.4	51.8	51.5	51.9	51.9	52.6	51.9	51.3	47.7	58.3	48.1	50.8	47.3	34.3	.8.0
U_4	1.0	0.9	1.2	1.2	1.0	1.0	0.9	0.9	1.1	1.0	0.7	1.6	1.2	0.8	0.8	1.6	1.6	2.7	4.8
Light Gas	-	-	-	-	-	-	-	-	-	-	-	-	-	-	-	-	-	4.3	10.8
Conversion, %w																			
I	-	2.0	5.2	4.0	5.9	6.5	4.0	5.2	4.0	13.0	4.6	7.2	16.2	17.8	4.6	5.9	5.2	16.2	41.4
II	-	-1.8	1.4	0.5	0.5	3.6	-1.2	3.2	0.5	5.4	0.4	2.7	11.5	4.0	6.8	11.0	8.8	22.4	46.1
III	-	2.2	0.8	1.2	0.4	1.6	2.2	1.4	1.4	0.0	1.4	2.6	9.4	8.2	8.6	3.4	10.1	34.8	63.9
Total	-	0.1	0.6	0.3	0.5	1.8	0.3	1.6	0.6	2.6	0.8	2.4	10.2	7.9	5.3	2.8	5.6	25.1	51.0

Table 4. THERMAL REACTION OF "SHELLDYNE"

Run 10548-	94	95	98	114	115	64	65	67	68	69	70-1	70-3
Reactor	← 1/4" OD stainless steel tube →					← 5/8" ID stainless steel tube →						
Reactor Packing	← none →					← Quartz chips; 10-20 mesh →						
Reactor Volume						← 20 ml →						
Pressure, atm	1	5	10	1	5	10	1	1	1	1	4.3	7.7
Feed Flow Rate, ml/min	0.75	0.75	0.75	0.75	3.75	← 11.7 →						
Temperature, °F												
Block	← 797 →					1022	752	752	842	932	932	932
Wall	778	790	788	795	779	995	716	734	820	900	8[illegible]2	939
	799	799	801	801	790	-	-	-	-	-	-	-
	806	806	808	804	797	-	-	-	-	-	-	-
	806	806	810	808	799	-	-	-	-	-	-	-
	802	802	806	802	799	-	-	-	-	-	-	-
	792	792	796	792	792	-	-	-	-	-	-	-
	772	774	777	772	774	-	-	-	-	-	-	-
Effective Reactor Temperature, °F	797	797	801	797	790	-	-	-	-	-	-	-
Effective Reactor Volume, ml	3.1	3.1	3.1	3.0	3.4	-	-	-	-	-	-	-
Effective LHSV	14.5	14.5	14.5	15	66	← 20 →						
Effective ACT, seconds	0.71	3.6	7.1	0.69	0.79	4.48	0.55	0.54	0.51	0.48	2.1	3.6
% SHELLDYNE Converted to Light Gas	9.7	33.1	40.4	5.7	13.0	-	1.5	9.[illegible][b]	6.8	6.4	3.4	35.4
SHELLDYNE Conversion, %m	[illegible].8	62.9	79.0	24.0	25.6[d]	88.8[a][c]	3.0	3.6[a]	19.8	47.7	63.8	90.0[d]
First Order Rate Constants, sec^{-1}	0.490	0.274	0.216	0.391	0.382	-	-	-	-	-	-	-

a) Neglects conversion to light gas.
b) Flow rate not steady during the run. Conversion neglects light gas fraction.
c) Reactor plugged after ~5 minutes.
d) Reactor plugged after ~15 minutes.

Table 5. THERMAL REACTION OF "SHELLDYNE"

Product Analyses

U_1 = emerged before I, includes cracked liquid
U_2 = emerged after I and before II
U_3 = emerged after II and before III
U_4 = emerged after III

Run 10548-	Feed	94	93	96	114	115	64	65	67	68	69	70-1	70-3
Reactor	1/4" OD stainless steel tube						5/8" ID stainless steel tube						
Reactor Packing	none						Quartz chips						
Reactor Volume							20 ml						
Pressure, atm	-	1	5	10	1	5							
Temperature, °F	-												
Block	-	797					1022	752	752	842	932		
Effective Wall	-	797	797	801	797	790	995	716	734	820	900	892	93[illegible]
Product Anal., %w													
U_1	2.1	19.8	28.2	34.0	18.6	17.9	5.2	2.8	4.0	13.1	41.2	55.8	48.6
I	14.0	10.6	5.0	1.9	11.1	9.8	0.0	15.2	13.4	10.4	6.8	3.8	0.0
U_2	2.9	0.4	0.4	0.9	0.5	0.7	1.4	1.4	1.2	0.6	0.3	0.4	0.6
II	21.1	18.2	11.4	7.2	19.5	16.9	5.5	20.5	18.7	19.8	17.2	15.4	4.9
U_3	3.6	3.2	2.6	4.7	3.4	3.1	2.1	3.5	3.2	3.4	3.0	3.1	6.5
III	52.2	33.7	13.5	5.4	35.2	33.2	0.6	49.8	45.3	40.5	19.8	8.5	2.7
U_4	7.1	4.8	5.7	5.5	6.0	5.4	5.0	5.3	5.0	5.9	4.9	6.6	1.3
Light Gas	0.0	9.7	33.1	40.4	5.7	13.0	(a)(c)	1.5	9.2$^{b)}$	6.4	6.4	6.4	35.4
Conversion, %w													
I	-	27.4	45.8	87.0	24.0	32.9	100	-4	8.3$^{a)}$	28.8	53.4	74.0	100$^{d)}$
II	-	13.7	46.0	65.9	7.6	19.9	73.9$^{a)}$ c)	2.8	11.4$^{a)}$	6.2	18.4	27.0	36.8$^{d)}$
III	-	35.4	73.9	89.7	32.6	36.4	98.5$^{a)}$ c)	4.6	13.3$^{a)}$	22.4	62.1	83.8	94.8$^{d)}$
Total	-	29.8	62.9	79.0	24.0	25.6	88.6$^{a)}$ c)	3.0	3.6$^{a)}$	19.8	47.7	63.8	90.0$^{d)}$

a) Neglects light gas.
b) Values suspect due to flow rate not steady during run.
c) Reactor plugged after about 5 minutes.
d) Reactor plugged after 15 minutes.

this Decalin (DHN) was 25.1% trans-DHN, 74.5% cis-DHN and 0.4% tetralin. The data for a series of runs at 1202°F, 10 atm pressure, and various contact times are presented in Table 6. With this naphthene no coking was observed, although the product at the highest contact times was dark (Run 120). Comparing conversions and rate constants for Runs 119-3 and 120 (Decalin) with Runs 112-1 and 112-3 (SHELLDYNE H; Table 4, values in parentheses Table 6) it appears that SHELLDYNE H is slightly more reactive than Decalin.

Discussion

From the work completed thus far it is evident that SHELLDYNE is highly reactive when in contact with metal at 797°F and higher. Hydrogen treatment improves stability and reduces reactivity by a factor of about 1500. Based on conversions comparable reactivities for SHELLDYNE H were observed at temperatures 350-400°F higher than for SHELLDYNE. Pertinent data are summarized in Table 7.

Pressure did not affect the reactivity of either species. Hydrogen treating increased the viscosity by about 10-30% and decreased the density by about 2%.

Presumably the metal reactor catalyzes the decompositions of SHELLDYNE to coke as other researchers have pyrolysed SHELLDYNE components in a Pyrex tube cleanly and without coking at temperatures up to 842°F and at contact times up to 6 minutes. Some studies on the effect of metal surface on SHELLDYNE reactivity will be done.

From the work carried out thus far it is evident that at elevated temperatures SHELLDYNE H has much greater stability than SHELLDYNE, and hence is a more attracive high density fuel under high temperature conditions. In a later section of this report (page) it is shown that in Coker-type thermal stability tests SHELLDYNE H was also more stable. Thus it appears that SHELLDYNE H was superior to SHELLDYNE on all counts except for a 2% loss in gravity and heat of combustion and a small increase in viscosity (Table 1).

Dehydrogenation of Methylcyclohexane in a Pulse Reactor

A small pulse reactor has been constructed for studying catalytic reactions under both fixed bed and dispersed phase conditions. Some of the advantages of such a system over the conventional flow reactors are:

a) Heat transfer effects within the reactor can be virtually eliminated.

b) It is a rapid method for studying reactions under varying conditions.

c) High space velocities can be achieved with only a small amount of feed.

To date the pulse reactor technique has been confined primarily to exploratory and reaction mechanism studies. Recently, however, R. P. Merrill20) has suggested a method for obtaining reaction rate data from pulse reactor studies.

Table 6. THERMAL REACTION OF DECALIN

Reactor:	1/4" OD Tube
Reactor Packing:	None
Block Temperature:	1202°F
Feed:	F-113 Decalin

Run	117	118	119-1	119-3	120
Pressure, atm	1	5	10	10	10
Feed Flow Rate	0.75	3.75	7.50	3.75	0.75
Wall Temperature, °F	1157 1202 1227 1227 1211 1184 1143	1132 1185 1213 1211 1202 1119 1144	1094 1166 1197 1195 1193 1172 1139	1128 1179 1211 1211 1202 1179 1143	1150 1197 1222 1222 1208 1182 1143
Effective Reactor Temperature, °F	1218	1204	1188	1202	1213
Effective Reactor Volume, ml	1.46	1.42	1.75	1.42	1.36
Effective LHSV	31	158	257	158	33
Effective Contact Time, sec	0.25	0.25	0.31	0.50	2.36
DHN Conversion, %w	3.0 (10.2)	4.8 (7.9)	2.1 (5.3)	13.9 (25.1)	59.6 (51.0)
First Order Rate Constant, sec	0.136 (0.372)	0.218 (0.346)	0.079 (0.208)	0.317 (0.594)	0.405 (0.236)

Table 7. COMPARISON OF REACTIVITIES OF "SHELLDYNE" H AND "SHELLDYNE"

SHELLDYNE H			SHELLDYNE		
Block Temperature, °F	Contact Time, sec	Conversion, %w	Block Temperature, °F	Contact Time, sec	Conversion, %w
1022	0.8	2.8	752	0.5	3.0
1022	4.2	5.6	797	0.7	24.0
1202	3.0	51.0	797	3.6	51.0

A brief study was made of the dehydrogenation of methylcyclohexane reaction using the pulse reactor technique. In this system a stream of carrier gas flowed through the reactor continously. At the desired time a small amount of feed (ca 1 microliter) was injected into the carrier gas stream and subsequently passed over the catalyst as a "pulse". Reaction products or a slip-stream sample thereof, were led directly into a GLC for analysis. In the pulse reactor system there was virtually no heat transfer effect within the reactor. The apparatus and procedure for carrying out the experiments are described in detail in the Appendix.

Experiments were carried out at 10 atm pressure, 572° to 752°F and at carrier gas flow rates that correspond to MCH liquid hourly space velocities (LHSV) up to 4265. Both helium and hydrogen were used as carrier gas; one microliter of liquid MCH was injected as a pulse. The catalyst was 0.25 g of our standard 1% Pt on Al_2O_3 laboratory catalyst and was diluted with 1.25 ml quartz chips to give a total bed length of 3 inches.

In this reactor system high MCH conversions were obtained at much higher space velocities and much lower reactor temperatures than were obtained in the bench-scale test reactor. For example, 95% MCH conversion was obtained in the bench-scale reactor at 1200°F and LHSV of 100, and in the pulse reactor at 662°F and LHSV of 1000. Further, at 752°F in the pulse reactor 85% MCH conversion was obtained at an LHSV of 4265.

Conversion declined with increased space velocity, as shown in a series of bracketted runs at 662°F with helium carrier gas (Table 8). Figure 7 shows conversion as a function of LHSV. At the highest LHSV tested (4265), an MCH conversion of 68% was observed. Selectivities for toluene were 99+%. Catalyst activity did not change during these tests as the conversions were about the same in the initial and final runs.

At higher temperature there was catalyst deactivation in a series of tests at high space velocity. Thus at 752°F at LHSV of 4265 with helium carrier gas, conversion declined for 71% to 60% with successive MCH pulses (Table 9; Runs 5, 6-1, 6-2).

Injecting larger MCH pulses (10 ml) seemed to enhance the deactivation (Table 9, Runs 6-3, 7-1, 7-2). Changing to H_2 carrier gas appeared to restore activity somewhat (Table 9; Runs 8-1, 8-2).

Table 8. DEHYDROGENATION OF METHYLCYCLOHEXANE: PULSE REACTOR

Effect of Space Velocity on Conversion at 662°F

Catalyst:	1% Pt on Al_2O_3	Pressure:	10 atm
Catalyst Volume:	0.25 ml	Carrier Gas:	He
Feed:	Pure MCH	Temperature:	662°F
Pulse Volume:	1 µl, liquid		

Catalyst Diluted With 1.25 ml Quartz Chips

Run No. 10548-	194-	195-1	195-2	195-3	195-4	196-1	196-2	196-3	196-4
LHSV	534	1068	534	2150	534	3200	534	4265	534
Temperature, °F									
Wall	651-58	649-56	651-58	648-58	649-56	649-58	651-56	651-56	651-58
Preheater	705	743	748	795	689	905	671	959	743
Product Analysis, %w									
Cracked, liq	1.8	0.6	0.6	0.6	0.5	0.3	0.5	0.3	0.4
MCH	3.6	5.0	2.7	10.8	2.7	18.7	2.8	31.9	3.2
Toluene	94.6	94.4	96.7	88.6	96.8	81.0	96.7	67.8	96.4
MCH Conversion, %w	96.4	95.0	97.3	89.2	97.3	81.3	97.2	68.1	96.8
Selectivity for Toluene, %w	98.2	99.4	99.5	99.4	99.5	99.7	99.6	99.6	99.6

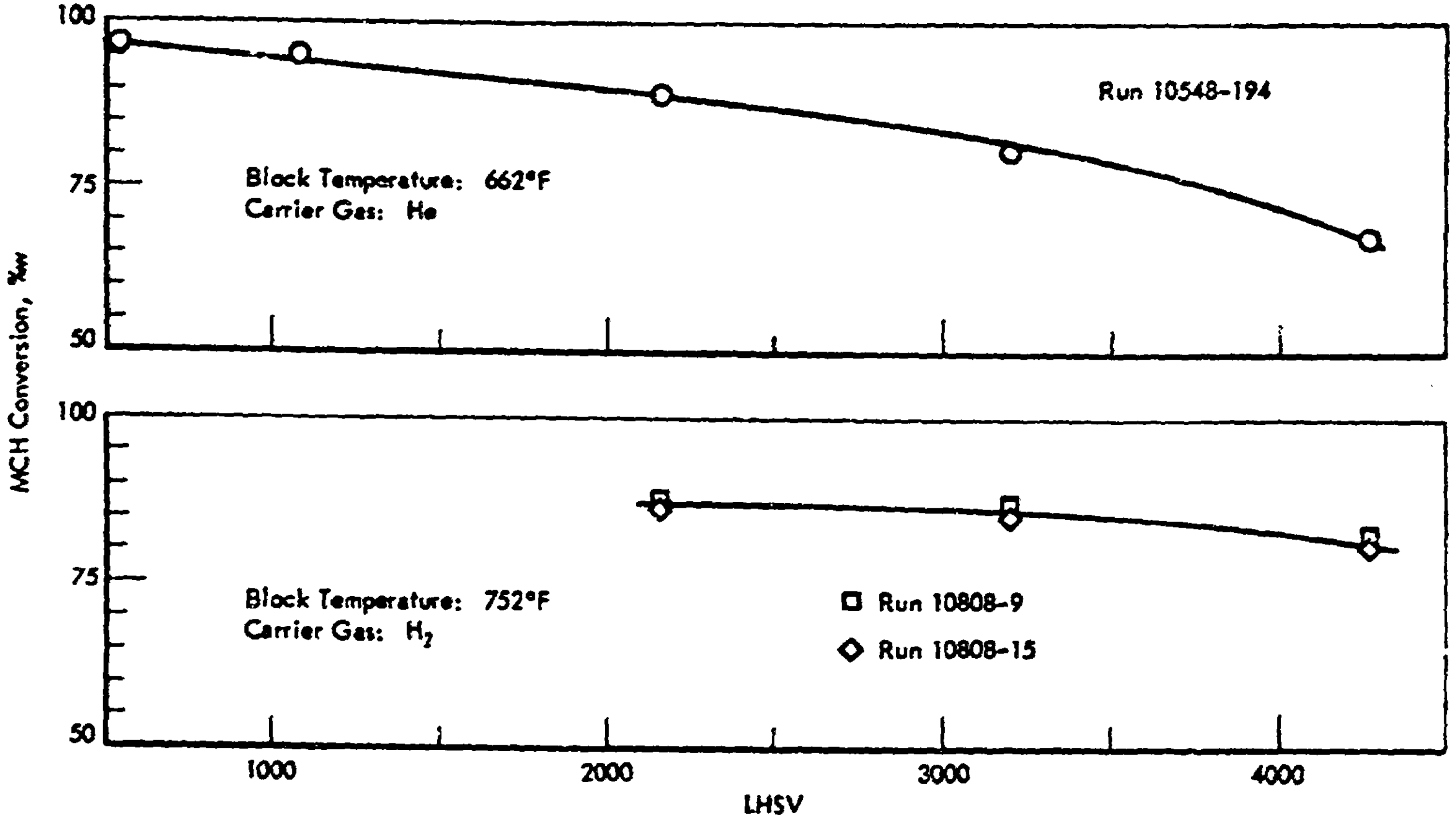

Figure 7. DEHYDROGENATION OF METHYLCYCLOHEXANE: PULSE REACTOR – EFFECT OF LHSV ON CONVERSIÓN

Pressure: 10 atm
Catalyst Volume: 0.25 ml
Catalyst: 1% Pt on Al_2O_3
Catalyst Diluted with 1.25 ml Quartz Chips

Table 9. DEHYDROGENATION OF METHYLCYCLOHEXANE: PULSE REACTOR

Catalyst Stability

Catalyst:	1% Pt on Al_2O_3	Pulse Volume:	1 µl, Liquid
Catalyst Volume:	0.25 ml	Pressure:	10 atm
Feed:	Pure MCH	Temperature:	752°F

Catalyst Diluted With 1.25 ml Quartz Chips

Run No. 10808-	5	6-1	6-2	6-3[a)]	7-1[a)]	7-2[a)]	8-1	8-2
Carrier Gas	← He					→	← H_2	→
LHSV	4265	3200	4265	4265[a)]	4265[a)]	4265[a)]	4265	4265
Temperature, °F								
Wall	743-48	743-48	743-48	743-48	743-48	743-48	743-48	743-48
Preheater	842	892	869	842	840	842	842	842
Product Analysis, %w								
Cracked, liq	3.4	2.1	0.9	0.5	0.5	0.2	0.3	0.2
MCH	28.9	29.9	39.8	51.6	54.4	59.0	35.8	32.1
Toluene	67.7	68.0	59.3	47.9	45.1	40.8	[illegible]	67.7
MCH Conversion, %w	71.1	70.1	60.2	48.3[a)]	45.6[a)]	41.1[a)]	64.2	67.9
Selectivity for Toluene, %w	95.2	97.0	98.3	99.1	99.0	99.3	99.5	99.7

a) 10 µl MCH injected before this pulse.

Higher conversions and no catalyst deactivation were observed at 752°F using hydrogen carrier gas. Thus at LHSV of 4265, 83-85% MCH conversion was obtained, and in a series of bracketted runs the initial and final conversions were about the same (Table 10). Selectivities for toluene were 92+% and more cracked products were made at the higher temperature. Conversion as a function of space velocity is shown in Figure 7.

Table 10. DEHYDROGENATION OF METHYLCYCLOHEXANE: PULSE REACTOR

Effect of Space Velocity on Conversion at 752°F

Catalyst:	1% Pt on Al_2O_3	Pressure:	10 atm
Catalyst Volume:	0.25 ml	Carrier Gas:	H_2
Feed:	Pure MCH	Temperature:	752°F
Pulse Volume:	1 µl, Liquid	Run 10808-9	

Catalyst Diluted With 1.25 ml Quartz Chips

Run No. 10808-	9-1	10-1	10-2	10-3	10-4	11-1
LHSV	4265	4265	3200	4265	2150	4265
Temperature, °F						
Wall	743-47	743-47	743-47	743-47	743-47	741-47
Preheater	882	882	959	871	874	831
Product Analysis, %w						
Cracked, liq	2.6	6.6	5.9	5.0	6.5	3.9
MCH	17.6	15.5	13.2	16.0	11.9	17.2
Toluene	79.8	77.9	80.9	79.0	81.5	78.9
MCH Conversion, %w	82.4	84.5	86.8	84.0	88.1	82.8
Selectivity for Toluene, %w	96.9	92.2	93.2	94.0	92.6	95.2

The activity of freshly reduced catalyst was considerably greater in the pulse reactor than in the bench-scale reactor. This could have been because in the latter system the catalyst was pretreated with pure MCH for 10 minutes prior to starting the runs and hence partially deactivated. Accordingly a series of experiments was done in the pulse reactor after pretreating the fresh catalyst with MCH. The pretreatment consisted of flowing pure MCH over the fresh catalyst for 15 minutes at 10 atm pressure and 662°F (no H_2 or He present). The reactor was then flushed with helium and successive pulses of MCH were injected over the catalyst. For tests at 752°F, H_2 was the carrier gas; at lower temperatures He was the carrier gas. The data are tabulated in Table 11 in the order in which the experiments were done. The conversion values obtained with no catalyst pretreatment are shown in parentheses for comparison.

Table 11. DEHYDROGENATION OF METHYLCYCLOHEXANE: PULSE REACTOR

Effect of Catalyst Pretreatment on Stability

Catalyst:	1% Pt on Al_2O_3	Catalyst pretreated with pure MCH at LHSV of 100, 10 atm press., and 662°F for 15 min prior to these runs.
Catalyst Volume:	0.25 ml	
Feed:	Pure MCH	
Pulse Volume:	1 µl, Liquid	
Pressure:	10 atm	

Catalyst Diluted With 1.25 ml Quartz Chips

Run No. 10808-	14-1	14-2	14-3	15-1	15-2	15-3	15-4	16-1	16-2	16-3	17-1	17-2	17-3	17-4
Carrier Gas	He				H_2				He					
LHSV	534	1068	1068	2150	4265	3200	2150	4265	1068	2150	2150	3200	4265	2150
Temperature, °F														
Furnace	662	662	707	707	752				662	662	707			
Wall	653-57	653-57	696-702	696-702	743-47	743-47	743-45	745-47	655-58	653-57	696-702	700-04	702-04	702-04
Preheater	815	806	902	851	914	903	963	932	871	838	842	974	920	956
Product Analysis, %w														
Cracked, liq	0.4	0.2	0.8	0.8	3.7	5.0	6.3	4.2	1.8	1.4	1.6	1.0	0.9	0.8
MCH	1.6	4.4	4.1	10.2	19.5	14.6	12.6	18.2	8.3	16.2	13.7	18.5	25.0	14.3
Toluene	98.0	95.4	95.1	88.0	76.8	80.4	81.1	77.6	89.9	82.4	84.7	80.5	74.1	84.9
MCH Conversion, %w	98.4 (96.4)	95.6 (95.0)	95.9	89.8	80.5 (82.4)	85.4 (86.8)	87.4 (88.1)	81.8 (82.8)	91.7	83.8	86.3	81.5	75.0	85.7
Selectivity for Toluene, %w	99.6	99.8	99.2	98.0	95.4	94.2	92.8	94.9	98.0	98.4	98.1	98.9	98.8	99.1

At 662°F conversions with the MCH pretreated catalyst were slightly greater than were observed with fresh catalyst, while at 752°F the reverse was true. This suggests that there was very little difference between the activities of the fresh and MCH pretreated catalysts and that the differences in activity in the pulse and bench-scale reactors were primarily due to heat transfer effects.

From the experiments carved out thus far it is evident that the reactivity of the MCH-platinum system was considerably greater in the pulse reactor than in the bench-scale reactor. This is shown quantitatively by comparing first order rate constants from data obtained in the two systems. In the pulse reactor the rate constant at 662°F (He) was 53.3 sec^{-1} (68% MCH conversion; data of Run 196-3, Table 8), compared to 0.60 sec^{-1} at 842°F in the bench-scale reactor.3) Converting the pulse reactor data to 842°F, using an activation energy of 11.7 k cal/mole,3) gave a rate constant of 176 sec^{-1} or about 293 times greater than was obtained in the bench-scale reactor. Thus the MCH-platinum system appears to have a potential reactivity about 300 times greater than was demonstrated in the bench-scale tests.

Presumably the higher reaction rates observed in the pulse reactor were due to heat transfer and diffusion effects that were much less adverse in the pulse reactor system. For example, in the pulse reactor the gas volume of the MCH pulse was about that of the catalyst pore volume (0.2 ml), so diffusion effects would be minimized in this system. Further, the heat of reaction for complete conversion of one microliter of MCH is about 0.55 cal. The heat capacity of the catalyst plus quartz in the pulse reactor is 0.3 cal. Thus the maximum total temperature drop in the catalyst bed per pulse was about 0.55/0.3 = 1.8°C or 3°F. A temperature difference between furnace and catalyst bed of 200°F was observed in the bench-scale reactor at high MCH conversion.3) This suggests that reactivities possibly 300 times greater could be obtained in continuous reactors if high heat transfer rates and elimination of diffusion effects in catalyst pores could be achieved.

Good catalyst stability was observed at 752°F with hydrogen carrier gas but not with helium. Presumably good stability is obtained because the coke precursors formed during dehydrogenation are reacted from the catalyst surface by hydrogen. This suggests that with helium carrier gas the hydrogen concentration in the catalyst pores due to hydrogen generated by the dehydrogenation reaction, was not great enough to remove the coke precursors, and hence the catalyst was partially poisoned. With hydrogen carrier however, a high hydrogen concentration was present in the pores, and the coke precursors were reacted rapidly from the surface.

Dehydrogenation of Decalin Over Various Catalysts

In earlier work3)18) it was shown that catalysts stable for the dehydrogenation of monocyclic naphthenes, were not necessarily stable for the dehydrogenation of dicyclic naphthenes. Thus UOP-R8 platforming catalyst was quite stable for the dehydrogenation of methylcyclohexane3) (MCH), but showed great instability for the dehydrogenation of dicyclohexyl1) (DCH) and Decalin1) (DHN). A number of commercial and laboratory-developed catalysts tested in the bench-scale apparatus had good stability for MCH dehydrogenation. It was of interest now, to evaluate a few of these catalysts for the dehydrogenation of Decalin.

The apparatus was a tubular flow reactor equipped with conventional devices for measuring feed flow rates and for collecting liquid and gas products. The reactor was a stainless steel tube (No. 347, 1/2-in. IPS) 32 in. long, 5/8 in. ID, and was heated by an electric furnace. The catalyst was contained in the annular space between the thermowell and the reactor wall. The dimensions were such that the catalyst bed had an annular thickness of 1/16 (one pellet diameter) and a length of 4-1/2 in. (7 ml volume). The complete apparatus was described in detail in a previous report.1)

Product analyses were carried out by mass spectrometry and by GLCa) from which conversions and selectivities were calculated.

Both zero and first order rate constants were calculated from the rate of disappearance of decalin using the following equations:

zero order:

$$k,\ \text{atm sec}^{-1} = \frac{LHSV}{3600} \times \frac{\rho \times 22,412}{MW} \times \frac{T}{273} \times f \qquad (1)$$

first order:

$$k,\ \text{sec}^{-1} = \frac{LHSV}{3600} \times \frac{\rho \times 22,412}{MW \times P} \times \frac{T}{273} \times 2.3 \log \frac{1}{1-f} \qquad (2)$$

where

LHSV = liquid hourly space velocity (i.e., volumes of feed/volume of catalyst bed per hour)
MW = molecular weight
P = reactor pressure in atmospheres
T = reaction temperature in °K (reactor wall temperature)
ρ = liquid density
f = fraction reacted

Relative reactivities and apparent activation energies were computed from the first-order rate constants.

The reactor wall temperature was measured by a thermocouple pressed against the outside reactor wall by the furnace block and located about 1" below the top of the catalyst bed. The catalyst bed temperatures were measured by thermocouples contained in the thermowell. The thermocouples were 1" apart and the top thermocouple was about 1/2" below the top of the catalyst bed. The "effective" catalyst temperature was somewhere between the reactor wall temperature and the catalyst bed temperature. For computing rate constants and apparent activation energies the reactor wall temperature was used, as this closer to the "effective" catalyst temperature than the thermowell temperature.

Three commerical catalysts and seven laboratory catalysts were evaluated for vapor phase dehydrogenation in the bench-scale reactor at 10 atm pressure and 842-1202°F. These were:

---

a) 5% Carbowax 1000 on Chromosorb W Column.

Catalyst	Designation
Sinclair-Baker Rd-150 0.67% Pt	RD-150
American Cyanamide Aeroform PHF-4; 0.8% Pt	PHF-4
Universal Oil Products UOP-R8; 0.75% Pt	UOP-R8
Shell Laboratory Catalysts	
10280-46	Shell 46
10280-108	Shell 108
10280-107A	Shell 107A
10280-107B	Shell 107B
10280-105B	Shell 105B
10280-45	Shell 45
10280-91A	Shell 91A

Seven milliliters of catalyst (10-20 mesh) were used in each test; F-113 DHN was the test feedstock. This Decalin contained 74.6% cis-DHN, 25.0% trans-DHN and 0.4% tetralin (THN).

Some deactivation during the runs was observed with all of the catalysts tested. Thus the catalysts were characterized as to activity by the total Decalin conversion or by the first order rate constant at 842°F, where catalyst deactivation was slight. Relative reactivity of a particular catalyst then was taken as the ratio of the first order rate constant obtained with that catalyst to the rate constant obtained with the standard catalyst at 842°F (10 atm pressure). The complete data are presented in Tables 60 through 65 in the Appendix.

Results

All of the catalysts were more active than the standard catalyst except RD-150, which was slightly less active (Table 12). Relative activities at 842°F are tabulated in Table 12, and at higher temperatures can be deduced from Figure 8, which is a plot of DHN conversion as a function of block temperature. Overall, the most active catalyst was the Shell 46, which was also the most stable. Catalyst deactivation with increasing temperature is reflected in the convex shape of some of the curves.

Apparent activation energies were calculated for both zero order and first order rate constants. Because of the extensive deactivation at the higher temperatures with some of the catalysts, only the rate constants at 842 and 932°F were used in this computation. Over this temperature region the apparent activation energies ranged from 6.5 to 11.4 kcal/mole for first order kinetics (Table 12). Lower activation energies were obtained for zero order kinetics because for a given increase in conversion, the first order rate constant increased more than the zero order constant.a) Figure 9 is an Arrhenius plot of the data in which the lines through the points at 842 and

---

a) The first order rate constant is given by $k_1 = K/t \log 1/1 - f$ and the zero order constant by $k_0 = (K'/t)f$ where f = fraction reacted.

Table 12. DEHYDROGENATION OF DECALIN OVER VARIOUS CATALYSTS

Relative Activities and Stabilities

Feed:	F-113 DHN
Catalyst Vol:	7 ml
Pressure:	10 atm
LHSV:	100

Catalyst	1% Pt on Harshaw 0104 Al_2O_3; Standard Catalyst	UOP-R8	10280-46	10280-108	10280-107A	10280-107B	10280-105B	RD-150		PHF-4	10280-45
DHN Conversion, %w, 842°F	32.8	36.2	40.2	37.5	38.9	39.1	39.3	32.5	30.4	36.2	44.8
First Order Rate Constant, sec^{-1}	0.39	0.45	0.50	0.44	0.47	0.48	0.47	0.37	0.36	0.43	0.56
Relative Activity Standard Catalyst = 1.00, 842°F	1.00	1.15	1.28	1.13	1.21	1.23	1.21	0.95	0.92	1.10	1.44
ΔT_{max}, °F at											
842	9	14	13	11	16	11	7	13	7	6	5
1022	61	160	16	16	75	34	20	54	31	126	11
1202	-	-	65	124	314[a]	160	237	-			
E_{act}, kcal/mole											
Zero Order, atm sec^{-1}	8.1	7.4	6.1	6.1	5.8	5.6	7.1	5.6	-	-	-
First Order, sec^{-1}	9.1	8.7	8.1	7.8	6.5	6.8	8.6	6.7	11.4	9.1	8.5

a) At 1112°F

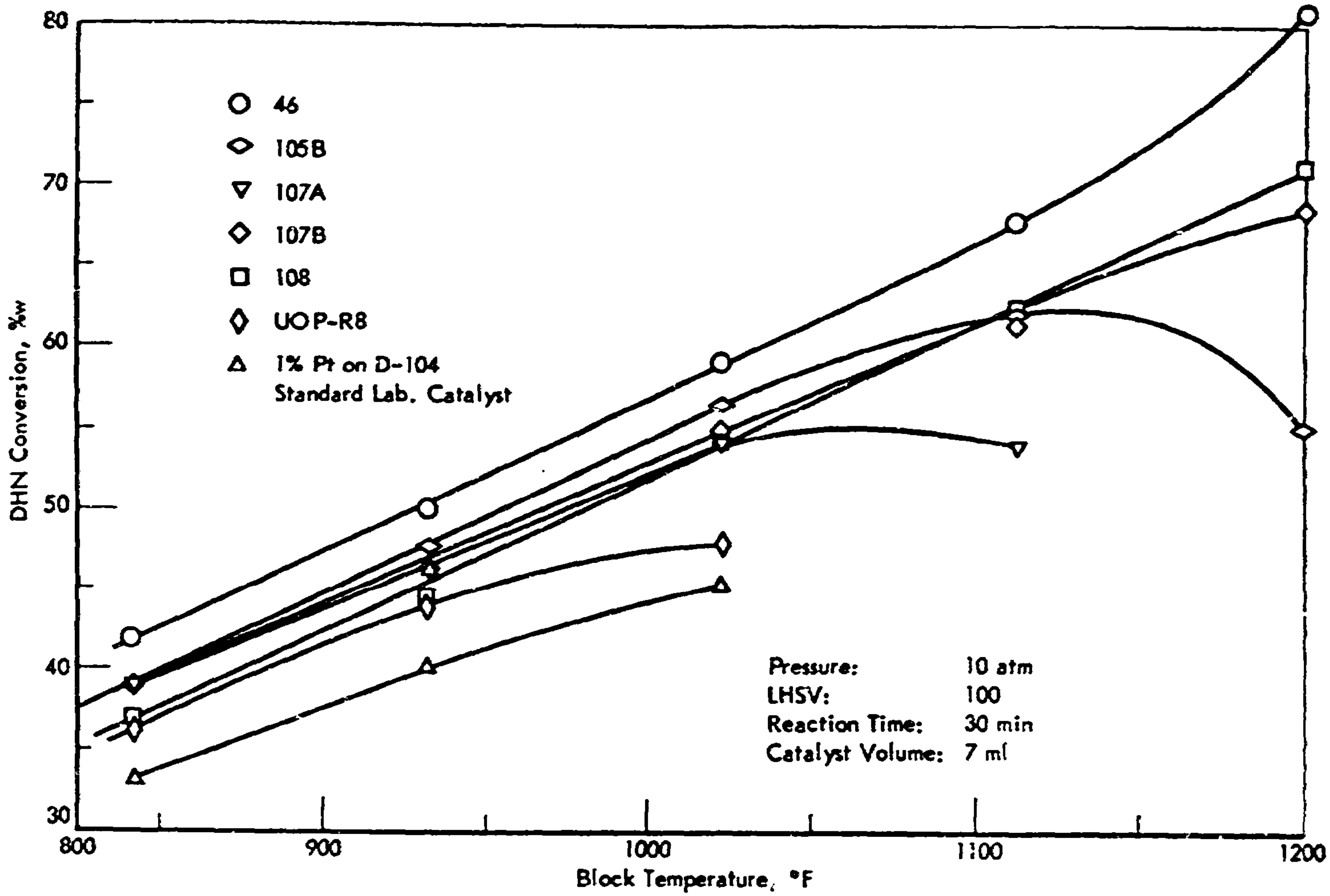

Figure 8. DEHYDROGENATION OF DECALIN OVER VARIOUS CATALYSTS: EFFECT OF TEMPERATURE ON CONVERSION

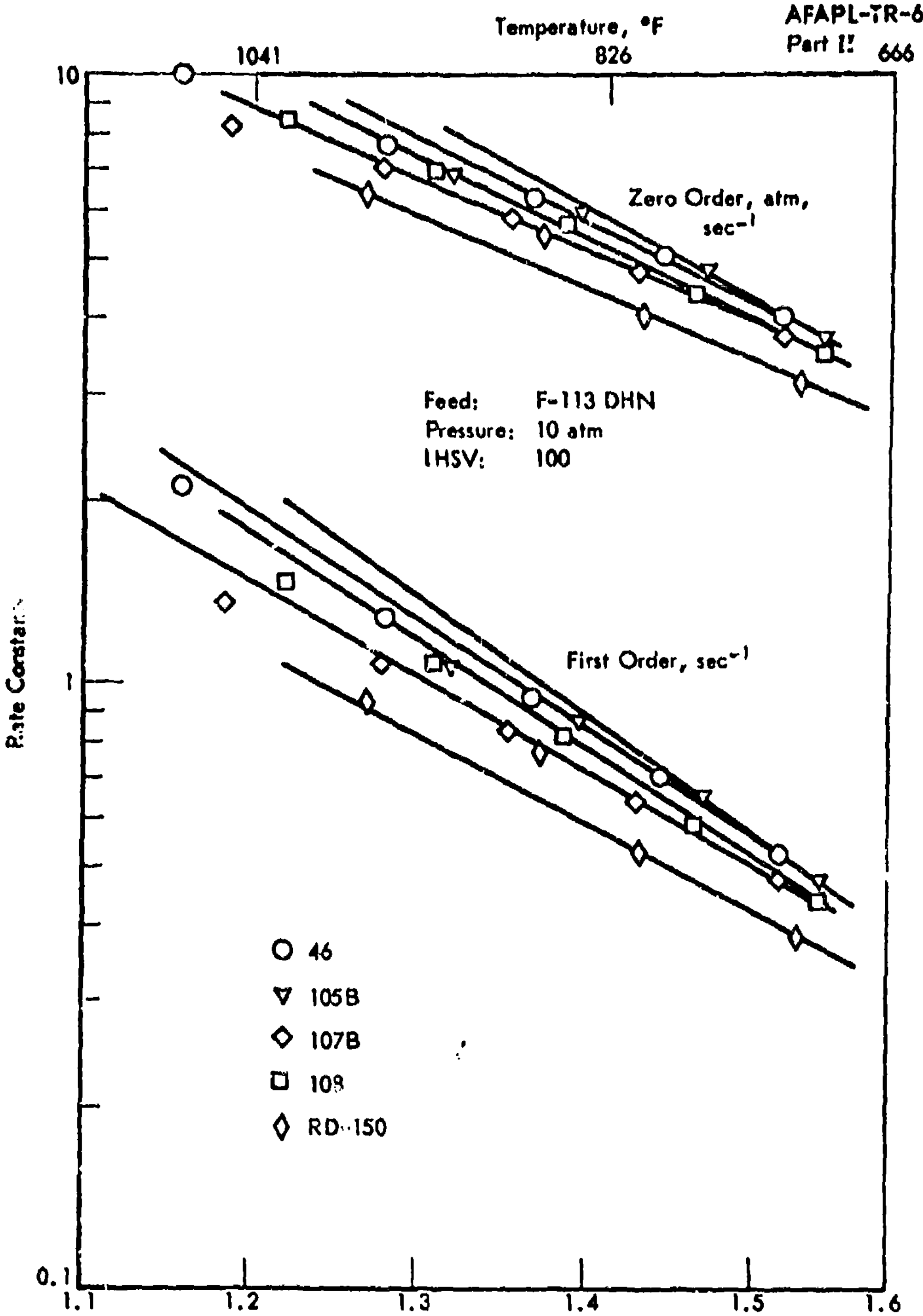

Figure 9. DEHYDROGENATION OF DECALIN OVER VARIOUS CATALYSTS: TEMPERATURE COEFFICIENT

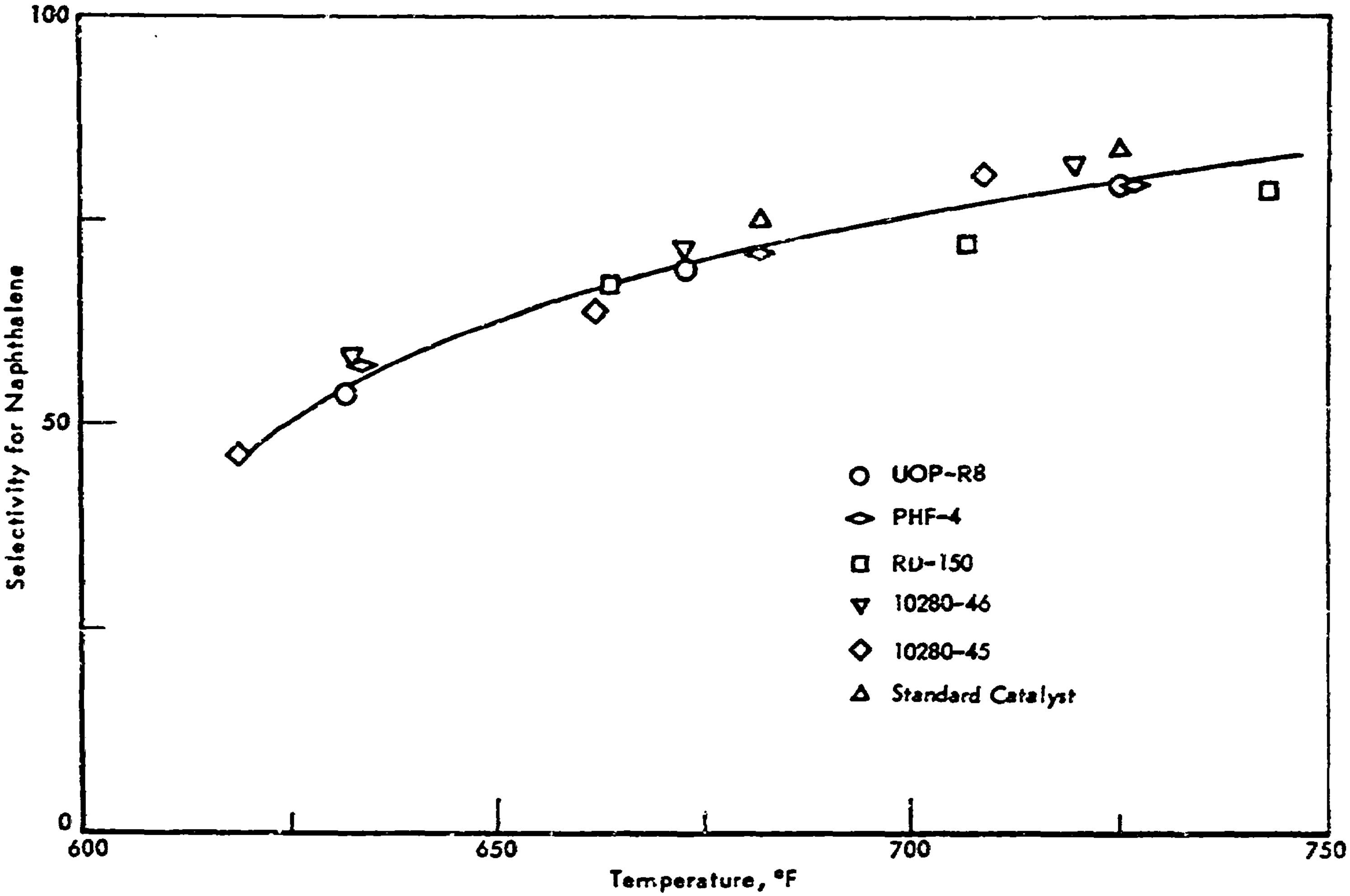

Figure 10. DEHYDROGENATION OF DECALIN OVER VARIOUS CATALYSTS: EFFECT OF TEMPERATURE ON SELECTIVITY FOR NAPHTHALENE

932°F are extrapolated over the complete temperature region. Deactivation at higher temperatures is evident as the data points fall below the extrapolated curves. The reactor wall temperatures were used for calculating the activation energies.

Selectivity for naphthalene at a given DHN conversion was different with each catalyst. This appeared to be a temperature rather than a catalytic effect, however, as in a plot of selectivity for naphthanlene as a function of "gas exit" temperature (Figure 10), the points fell reasonably close to a single line. The temperature at the bottom of the catalyst bed was taken as the gas exit temperature.

Some deactivation was observed with all of the catalysts tested (Table 12). This is shown graphically in Figures 11 and 12. These curves show the increase in catalyst bed temperature (ΔT_{max}, °F) as a function of furnace block temperature for a series of runs at 842 to 1022°F and at 842 to 1202°F respectively (at 10 atm pressure). The magnitude of the bed temperature increase was taken as a measure of catalyst deactivation. Based on this criteria the catalysts in order of their decreasing stabilities were: 46 > 108 > 107B > 91A > 105B > RD-150 > standard catalyst > 107A > UOP-R8. This evaluation depends somewhat upon the test temperature as 1022°F Shell 105B was more stable than either 107B or 91A, but was less stable than the latter two at 1202°F. It is worth pointing out that the only catalyst that had even moderate stability at 1202°F was Shell 46.

These results are for 10 atm pressure and 30-60% conversion. In previous work it was shown that at higher conversions (80-90%) both the UOP-R8 and the standard laboratory catalysts had good stability at 1022°F.1)
Presumably the other commercial catalysts would also be more stable at high conversion.

In previous work with Decalin it was observed that catalyst stability was enhanced when the operating pressure was increased from 10 to 30 atm pressure.1) Thus it was of interest to see if stability could be enhanced at higher temperatures by increasing the pressure to 30 atm.

One commercial catalyst, RD-150 and one laboratory preparation, Shell 107B, were tested over the temperature range of 842-1202°F at 30 atm pressure. With both catalysts, stability was enhanced at the higher pressure. For example with the RD-150 at 1112°F an increase in catalyst bed temperature of only 23°F was observed at 30 atm compared to 117°F at 10 atm pressure. Selectivity for THN + N was about 8-10% lower than was observed at 1022°F (Table 13). At higher temperature the catalyst was moderately stable but there was a considerable decline in both conversion and selectivity for THN + N, and a corresponding increase in yield of cracked products at both 10 and 30 atm. Presumably a hydrocracking-type reaction becomes predominant at 1202°F at both pressures (Table 13).

With Shell 107B at 1112°F only a 9°F rise in catalyst bed temperature at 30 atm (down from 36°F at 10 atm) and at 1202 a 108°F rise (down from 160°F at 10 atm) was observed (Table 14). Selectivity for THN + N at 1202°F was high at 10 atm (92.5%) but only moderate at 30 atm (77.9), and considerably more cracked products were observed at the higher pressure.

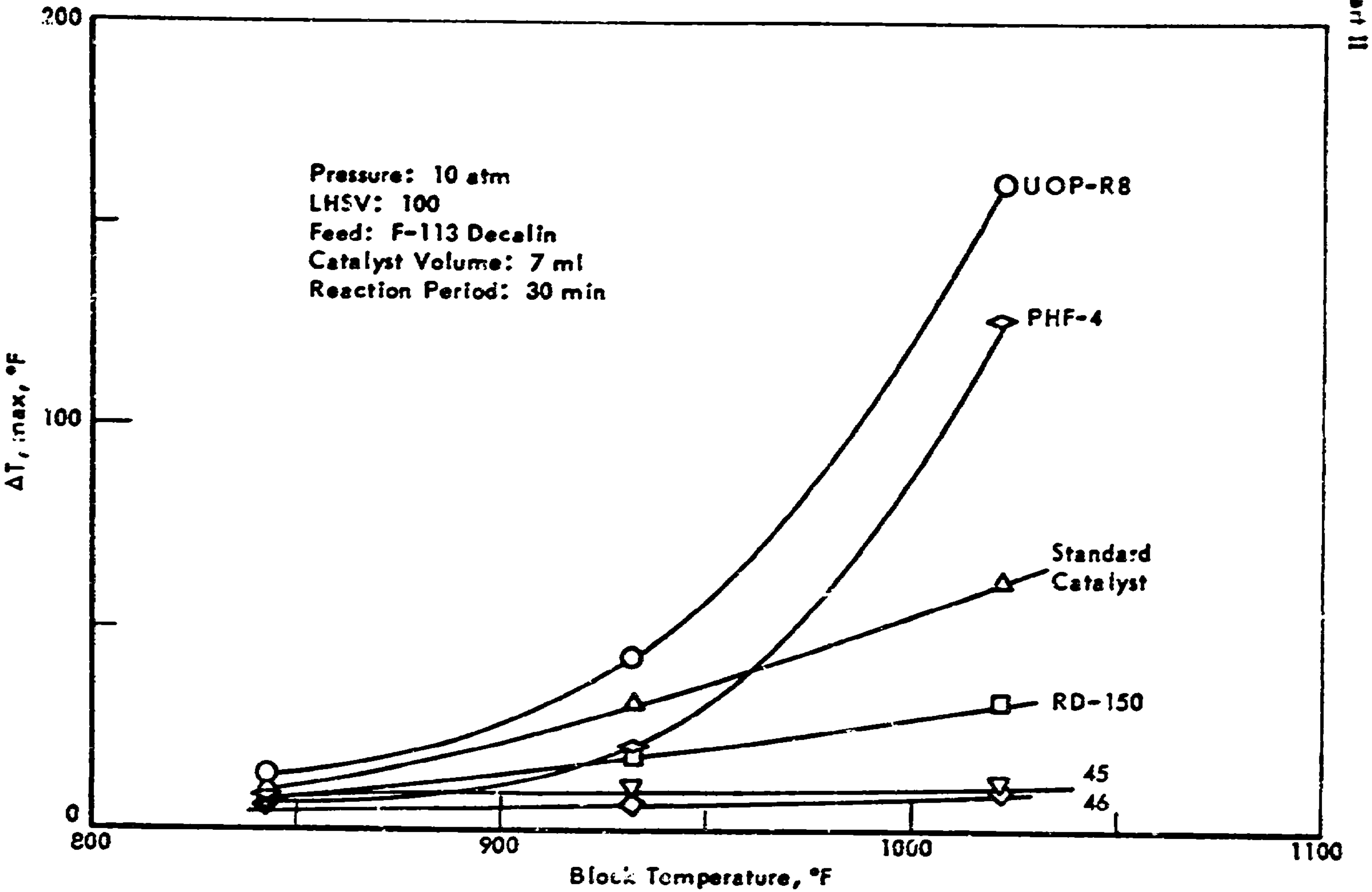

Figure 11. DEHYDROGENATION OF DECALIN OVER VARIOUS CATALYSTS: EFFECT OF TEMPERATURE ON STABILITY
842-1022°F

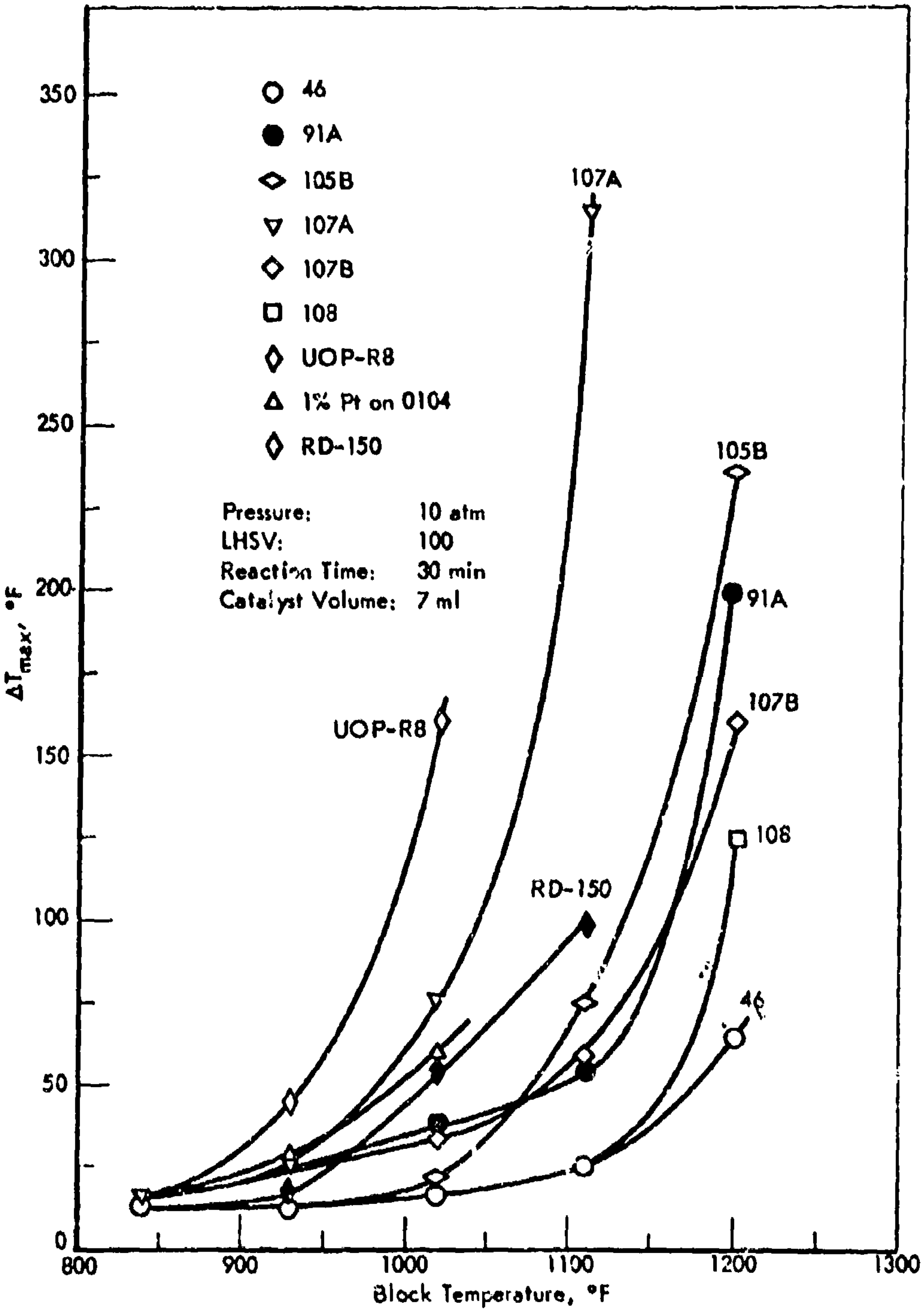

Figure 12. DEHYDROGENATION OF DECALIN OVER VARIOUS CATALYSTS EFFECT OF TEMPERATURE ON STABILITY: 842-1202°F

Table 13. DEHYDROGENATION OF DECALIN OVER SINCLAIR-BAKER RD-150 CATALYST

Catalyst Volume: 7 ml
LHSV: 100
Reaction Time: 30 min

Feed: F-113 Decalin
74.6% cis DHN
25.0% trans DHN
0.4% THN

Run No.	10548-13					10548-42					1054[illegible]				
Pressure, atm	10					10					50				
Temperature, °F															
Block	842	932	1022	1112	1202	842	932	1022	1112	1202	842	932	1022	1112	1202
Wall	718-25	732-97	846-55	928-75	1130-62	720-25	762-92	844-51	898-946	1126-57	720-27	801	851-55	921-25	1125-61
Catalyst Bed Profile	663-80	718-45	772-844	914-1031	1112-39	662-75	704-20	750-804	876-972	1117-39	667-71	709-14	745-54	734-17	[illegible]
	630-40	675-82	700-16	756-869	1062-1125	635-44	671-80	705-20	759-858	1067-1130	657-58	694-96	725-29	753-72	1071-[illegible]
	632-40	675-82	702-09	754-795	1040-1121	635-44	671-78	707-16	756-99	1053-1125	652-62	704-05	736-40	761-85	[illegible]
	642-48	687-91	718-23	725-737	1035-112[illegible]	644-51	682-87	722-27	777-94	1042-1125	671-73	716-18	732-54	[illegible]	[illegible]
ΔT max, °F[a]	17	27	72	117	-[c]	13	15	54	59	86	4	5	6	25	57[c]
Product Analysis, %w															
trans DHN	28.0	24.6	20.3	16.0	22.6	27.0	24.0	19.5	15.2	22.7	37.6	32.5	26.1	19.9	21.1
cis DHN	38.6	34.7	27.8	27.9	46.4	40.2	34.0	27.9	27.6	46.5	29.7	24.5	19.5	16.9	29.2
U[b]	0.0	0.3	1.1	5.0	11.3	0.0	0.2	1.4	5.3	12.0	0.0	0.2	0.7	2.9	15.4
THN	12.2	10.2	10.3	8.2	2.6	10.9	10.9	9.3	7.3	2.2	23.3	24.4	23.2	16.5	2.7
U[b]	0.0	0.0	0.0	0.4	3.4	0.1	0.1	0.1	0.3	3.0	0.1	0.3	0.2	0.4	2.9
N	21.1	30.0	40.3	41.1	3.7	21.7	30.6	41.2	42.9	3.6	9.2	18.0	29.5	41.1	7.4
U[b]	0.1	0.2	0.2	0.4	0.1	0.1	0.2	0.5	0.3	0.2	0.1	0.1	0.2	0.2	[illegible]
Cracked, liq.	0.0	0.0	0.0	1.0	9.8	0.0	0.0	0.1	1.1	9.8	0.0	0.0	0.1	2.1	21.1
Yield THN, %w	11.8	9.8	9.9	7.8	2.2	10.5	10.5	8.9	6.9	1.8	22.9	24.0	22.5	16.2	2.3
DHN Conversion, %w	35.1	40.5	51.8	56.0	50.7	32.5	41.8	52.0	57.0	30.5	32.4	42.3	53.8	65.0	49.8
Selectivity for THN + N, %w	99.7	98.3	96.[illegible]	87.4	19.2	99.7	98.7	96.7	87.8	17.9	99.1	99.1	97.2	90.8	19.5
Rate Constants															
Zero Order; atm sec^{-1}	3.16	4.11	5.49	6.41	5.99	3.11	4.23	5.50	6.49	5.99	3.10	4.37	5.74	7.05	6.46
First Order; sec^{-1}	0.30	0.53	0.77	0.94	0.48	0.37	0.55	0.78	0.96	0.47	0.13	0.19	0.27	0.37	0.50
E_{act}, kcal/mole	← 6.8 →		-	-	-	← 6.7 →		-	-	-	← 9.0 →		-	-	-

a) Maximum increase in catalyst bed temperature during the 30 minute run.
b) Unidentified.
c) Not significant as cold spot was moving down the catalyst head.

Table 14. DEHYDROGENATION OF DECALIN OVER SHELL 107B LABORATORY CATALYST

Catalyst Volume: 7 ml
LHSV: 100
Reaction Time: 30 min

Feed: F-113 Decalin
74.6% cis DHN
25.0% trans DHN
0.4% THN

Run No.	10342-92					10548-21				
Pressure, ata	10					30				
Temperature, °F										
Block	842	932	1022	1112	1202	842	932	1022	1112	1202
Wall	725-30	797-99	871-69	948-50	1054-87	730-32	788-86	851	916	1013-39
Catalyst Bed Profile	624-35	662-87	714-48	777-833	954-1114	644	673	709-12	750-59	941-1049
	606-14	639-51	682-94	730-47	842-957	646	671	698	732-34	842-87
	609-15	644-51	689-92	736-43	831-67	653	680	709	745	831-44
	619-22	651-60	704-04	756-54	842-44	664	693	725	766-63	856-54
ΔT max, °F[a]	11	25	34	56	160	0	0	3	9	108
Product Analysis, %w										
trans DHN	31.1	26.4	21.6	17.0	12.2	53.7	39.7	28.8	20.2	12.5
cis DHN	23.6	26.8	24.4	21.4	21.3	12.7	12.3	11.4	20.2	12.5
U[b]	0.0	0.0	0.0	0.0	0.8	0.0	0.0	0.0	0.2	4.6
THN	18.5	14.3	9.2	5.9	5.2	24.6	30.1	23.5	21.7	6.5
U[b]	0.0	0.0	0.0	0.0	0.1	0.1	0.1	0.3	0.4	0.3
N	20.6	32.3	44.8	54.9	56.3	8.8	17.6	30.0	45.1	53.5
U[b]	0.2	0.2	0.2	0.5	0.4	0.1	0.2	0.2	0.5	0.4
Cracked, liq.	0.0	0.0	0.0	0.3	3.7	0.0	0.0	0.0	1.2	11.3
Yield THN, %w	18.1	13.9	8.8	5.5	4.8	24.2	29.7	29.1	21.3	6.1
DHN Conversion, %w	39.1	46.7	54.2	61.5	66.5	32.3	47.8	59.8	69.0	76.5
Selectivity for THN + N, %w	99.5	99.6	99.6	98.7	92.5	99.4	99.0	99.8	96.3	77.9
Rate Constants										
Zero Order; atm sec^{-1}	3.77	4.75	5.82	7.01	8.23	3.20	4.83	6.34	7.68	9.09
First Order; sec^{-1}	0.48	0.64	0.84	1.09	1.36	0.13	0.22	0.32	0.43	0.58
E_{act}, kcal/mole	←16.1→									

a) Maximum increase in catalyst bed temperature during the 30 minute run.
b) Unidentified.

Thus it appears that at 1202°F increasing the reactor pressure will enhance the stability of the catalyst, but that selectivity for THN + N and in some cases DHN conversion will be reduced appreciably. Further, it appears that at these elevated pressures and temperatures a hydrocracking-type reaction becomes more important resulting in increased yields of cracked products.

The two most stable catalysts tested thus far for the dehydrogenation of decalin were the laboratory catalysts Shell 46 and Shell 108. Both catalysts had comparable stabilities at 1112°F but at 1202°F the Shell 46 was more stable. With these catalysts selectivity for THN + N was high at 1112°F and lower temperatures (98+%), but decreased by about 5-10% at 1202°F. For a given weight of platinum stability varied inversely as the pore size of the support. Increasing the operating pressure from 10 to 30 atm increased catalyst stability but at 1202°F decreased selectivity for THN+N and in one case decreased the Decalin conversion.

The Shell 46 was also the most active catalyst tested thus far and was 1.28 times more active than the standard laboratory catalyst.

Effect of Pore Volume on Catalyst Stability

In a previous report it was suggested that catalyst instability was due at least in part to the pore structure of the catalyst and that greater stability would be obtained with catalysts containing smaller pores.19) The average pore diameters of five catalysts were calculated from the surface and pore volumes and are tabulated in Table 15. These catalysts continued 0.7% to 1.0% platinum on various alumina supports; their physical properties are tabulated in Table 16. Figure 13 is a plot of catalyst bed temperature increase (ΔT_{max}, °F) as a function of average pore diameter and shows indeed that better catalyst stability was obtained with catalysts having smaller pores. (The Shell 45 was not included as the chemical composition of this catalyst was quite different from that of the other five catalysts.) While the least stable catalyst had the largest pore diameter and the most stable catalysts had the smallest pore diameter, there is an anomoly in the region of 100 A pore diameter. Thus the PHF-4 and the standard laboratory catalyst have about the same pore diameter but the catalyst bed temperature increase with the former was about twice that observed with the latter catalyst. As pore distribution for these two catalysts are about the same (Table 16), it appears that pore size is not the only factor controlling catalyst stability. This is being investigated further.

As mentioned in the previous reports it is believed that catalyst stability during the run is due to hydrogen, generated by reaction, reacting with coke precursors on the catalyst surface. Presumably in smaller pores the hydrogen partial pressure will be greater due to a higher surface to volume ratio, and hence a greater fraction of naphthene converted per unit time. This higher hydrogen pressure causes more rapid reaction with coke precursors and hence the catalyst appears to be more stable.

Dehydrogenation of Decalin: Diluted-Bed Reactor

A study of the kinetics of the dehydrogenation of Decalin has been initiated to obtain data for use in developing a computer program for this

Table 15. DEHYDROGENATION OF DECALIN OVER VARIOUS CATALYSTS

Summary Table

Feed:	F-113 DHN
Catalyst Volume:	7 ml
Pressure:	10 atm
LHSV:	100

Catalyst	842°F Block Temperature			Total Pore Volume, cc/g	ΔT_{max}, °F, Catalyst Bed at 1022°F Block Temp	Average Pore Diameter, Å
	Conv., %	Rate Constant, sec^{-1}	Relative Reactivity[b]			
1% Pt on Harshaw 0104 Al_2O_3[a]	32.8	0.39	1.00	0.266	81	106
Sinclair-Baker RD-150; 0.65% Pt	30.4	0.36	0.92	0.402	31	35
1% Pt on Al_2O_3A	40.2	0.50	1.28	0.251	9	42
Shell 45	44.8	0.56	1.44	0.377	11	104
American Cyanamide Aeroform PHF-4; 0.8% Pt	36.2	0.43	1.10	0.607	126	111
UOP-R8; 0.76% Pt	36.2	0.45	1.15	0.719	150	175

a) Standard laboratory catalyst.
b) Standard laboratory catalyst = 1.00.

Table 16. PHYSICAL PROPERTIES OF VARIOUS CATALYSTS

Catalyst		1% Pt on 0:04 Al_2O_3 (Standard Catalyst)	American Cyanamide Aerofura PHF-4; 0.6% Pt	Sinclair-Baker RD-150; 0.35% Pt		1% Pt on Al_2O_3 A Shell 46	10280-45		UOP-R8; a) 1% Pt on Al_2O_3 B
Surface Area, m^2/g		100	220	450		237	145		164
Bulk Density, g/cc (10-20 mesh size)		0.96	0.69	0.93		0.98	0.68		0.63
Total Pore Volume, cc/g		0.266	0.607	0.402		0.251	0.377		0.719
Pore Size Distribution	Pore Diameter, Å	Cumulative Volume, cc/g			Pore Diameter, Å	Cumulative Volume, cc/g		Pore Diameter, Å	Cumulative Vol, cc/g
	16	0.000	0.000	0.042	18	0.015	-	24	0.033
	17	0.000	0.000	0.061	24	0.027	0.016	35	0.024
	19	0.000	0.000	0.078	50	0.177	0.013	52	0.050
	24	0.001	0.016	0.141	97	0.206	0.075	82	0.031
	50	0.013	0.042	0.173	185	0.219	0.312	147	0.166
	102	0.085	0.193	0.255	354	0.233	0.337	235	0.328
	204	0.192	0.526	0.315	723	-	0.370	419	0.533
	454	-	-	0.371	850	0.251	0.327	850	0.850
	850	0.266	0.607	0.402					

a) Pore distribution determined on R-8 alumina base.

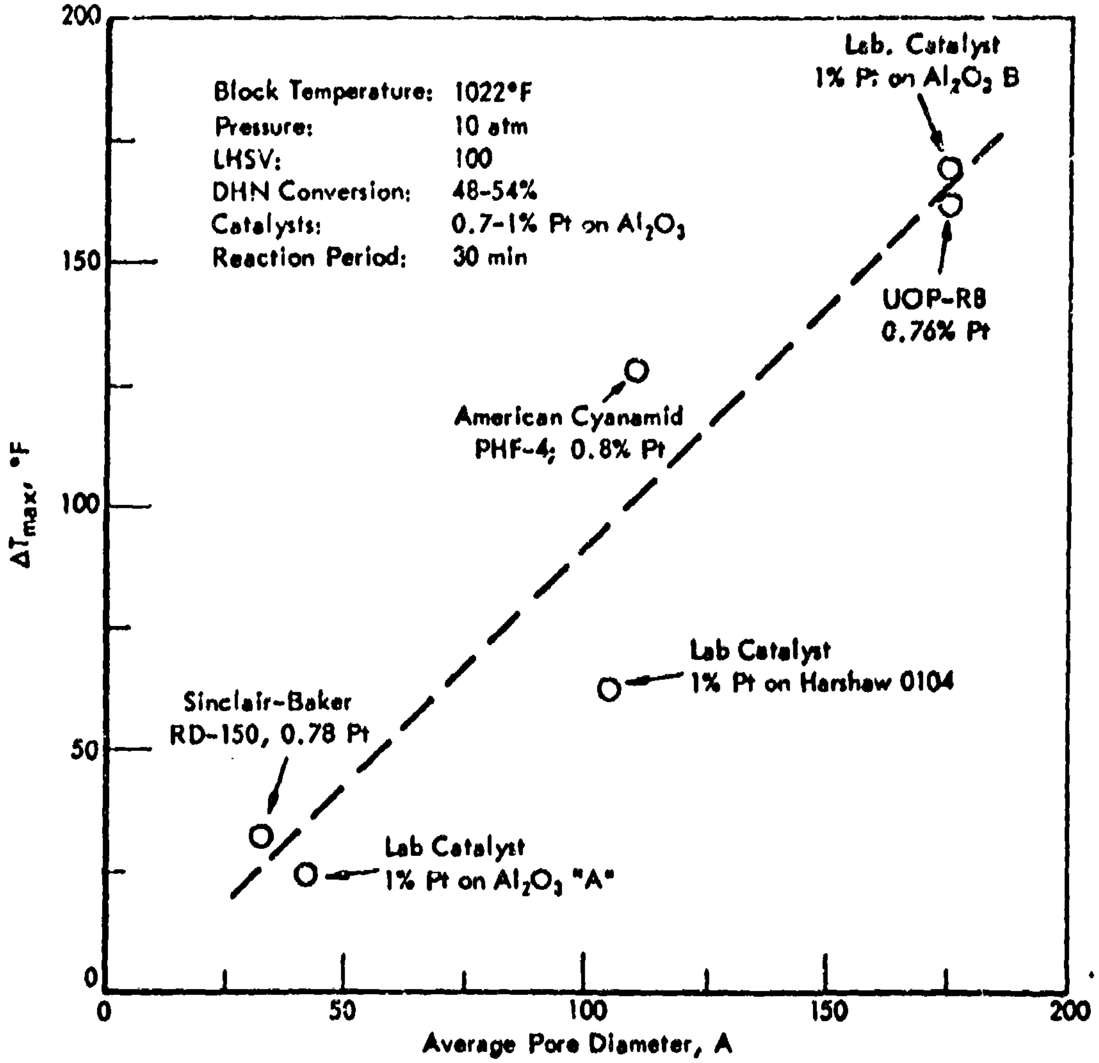

Figure 13. DEHYDROGENATION OF DECALIN OVER VARIOUS CATALYSTS: EFFECT OF PORE SIZE ON CATALYST STABILITY

reaction. For this work the catalyst was highly diluted with inert material, the reactor was operated at low conversions, and the apparatus was modified so as to try and maintain isothermal conditions within the catalyst bed as much as possible. This modification consisted of removing the 1/2-in. OD thermowell from our 5/8-in. ID reactor tube and substituting two 1/8-in. OD thermowells, one at the top and one at the bottom of the reactor tube. The top thermowell extended down 1-1/2 in. into the catalyst bed; the lower thermowell just touched the bottom of the catalyst bed. Figure 14 is a drawing of the modified reactor tube.

Results were obtained at 707 to 797°F; 10-30 atm pressure; LHSV's of 350-1400 with our standard 1% Pt on Al_2O_3 catalyst. 0.5 ml (0.48 g) catalyst was used and the catalyst was diluted with Cu granules and/or quartz chips to give a total bed volume of about 29.5 ml and a bed length of about 5-1/2 inches.

The procedure for carrying out the runs analyzing the products and calculating the rate constants were described in the previous section of this report.

The kinetics of the dehydrogenation of Decalin involve rates of: a) isomerization of cis and trans Decalin; b) dehydrogenation of cis and trans Decalin and of tetralin; c) dehydrogenation of tetralin. Thus for our study six different feeds were used that contained various amounts of cis and trans Decalin and tetralin. Hydrogen was added to those feeds containing tetralin in about stoichiometric amounts to simulate product material from Decalin dehydrogenation.

The feed compositions were:

Table 17. DEHYDROGENATION OF DECALIN AND TETRALIN

Feed Compositions

Feed Number	1	2[a)]	3	4[b)]	5[c)]	6
Liquid Composition, %w						
trans-DHN	91.0	57.0	25.0	43.6	11.8	0.1
cis-DHN	8.8	42.5	74.6	4.9	35.6	0.5
THN	0.0	0.2	0.4	50.3	51.8	97.8
N	0.0	0.0	0.0	0.6	0.4	0.8
Others	0.2	0.4	0.0	0.6	0.5	0.6
H_2 Added, moles H_2/mole THN	0.0	0.0	0.0	2.6	2.6	3.0

a) Feed 2 was 50% Feed 1 and 50% Feed 3.
b) Feed 4 is 50% THN and 50% Feed 1.
c) Feed 5 is 50% THN and 50% Feed 3.

Feeds 4 and 5 represent an approximate product mixture after dehydrogenation Decalin to 50% conversion; Feed 6 represents a product mixture of 100% conversion of Decalin to tetralin.

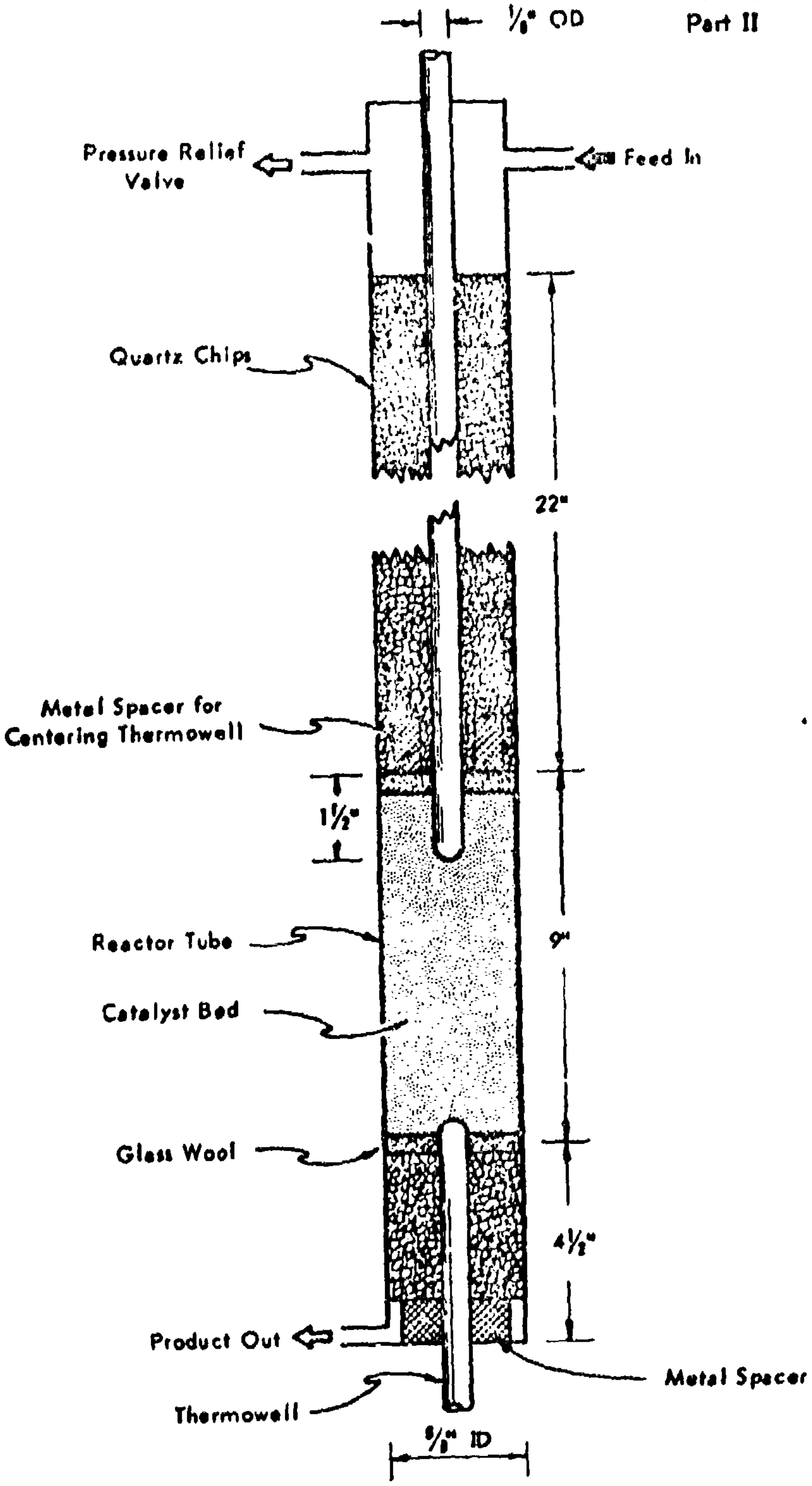
1/8" OD
Pressure Relief Valve
Feed In
Quartz Chips
22"
Metal Spacer for Centering Thermowell
1½"
Reactor Tube
9"
Catalyst Bed
Glass Wool
4½"
Product Out
Metal Spacer
Thermowell
5/8" ID

Figure 14. DILUTED BED REACTOR

The effect of process variables on reaction rates and product distribution are discussed in this section. The utilization of the experimental results for developing a computer program are discussed in another section (see page).

Results

Under our test conditions the dehydrogenation of DHN to naphthalene (N) was a two-step process with tetralin (tetrahydronaphthalene; THN) as an intermediate product. Schematically the reaction can be represented:

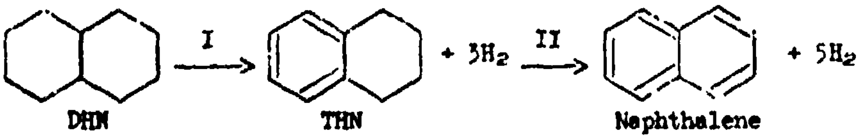

Both reactions were equilibrium limited at high conversions and in the lower temperature region at both 10 and 30 atm pressure. Reaction II was faster than I. Figure 15 shows the thermodynamic equilibrium constants for Reactions I (Kp_1) and II (Kp_2) as functions of temperature. Kp_2 was obtained by extrapolating the equilibrium data of Allam and Vlugter.[21)] Kp_1 was obtained using the data of Miyazawa and Pitzer[22)] and the calculated Kp_2. Figure 16 shows equilibrium concentrations of DHN, THN, and N at 10 and 30 atm pressure as a function of temperature using the calculated Kp_1 and Kp_2.

A preliminary series of experiments was done with F-113 Decalin (Feed 3; 74.6% cis DHN) at 707 to 797°F; 10-30 atm pressure. In this series the runs on different charges of catalyst did not give reproducible results. For example at 752°F (block temperature) LHSV of 1400 and 10 atm pressure, DHN conversion of 6.8 and 10.5% were observed for two different runs (Table 18, Runs 61 and 50-2). Presumably this nonreproducibility arose from catalyst surface contamination during catalyst pretreatment. However within any one run the catalyst was fairly stable. Thus under the same reaction conditions at 792°F only a few percent change in conversion was observed over a one hour period (Table 18, Runs 74-2 to 75-1). Increasing the space velocity at constant block temperatures gave a slight increase in reaction rate, which suggests that even at LHSV of 700 there was still a heat transfer effect within the catalyst bed. The effect of pressure was similar to that observed previously[19)] namely that with increased pressure (10 to 30 atm) conversion was not affected significantly but the rate constant declined markedly with increased pressure (Table 19).

In runs of different charges of catalyst (i.e., A, B, or C, Table 18) the absolute values of the rate constants at a given temperature were different, which suggests that the catalyst was poisoned prior to the start of the runs. With only 0.5 g catalysts small amounts of contaminents can poison an appreciable amount of catalyst surface. Thus the following changes were made in the experimental procedure to reduce the possibility of catalyst contamination.

1. The fresh catalyst was reduced in situ with hydrogen with heating at 1022°F for one hour.

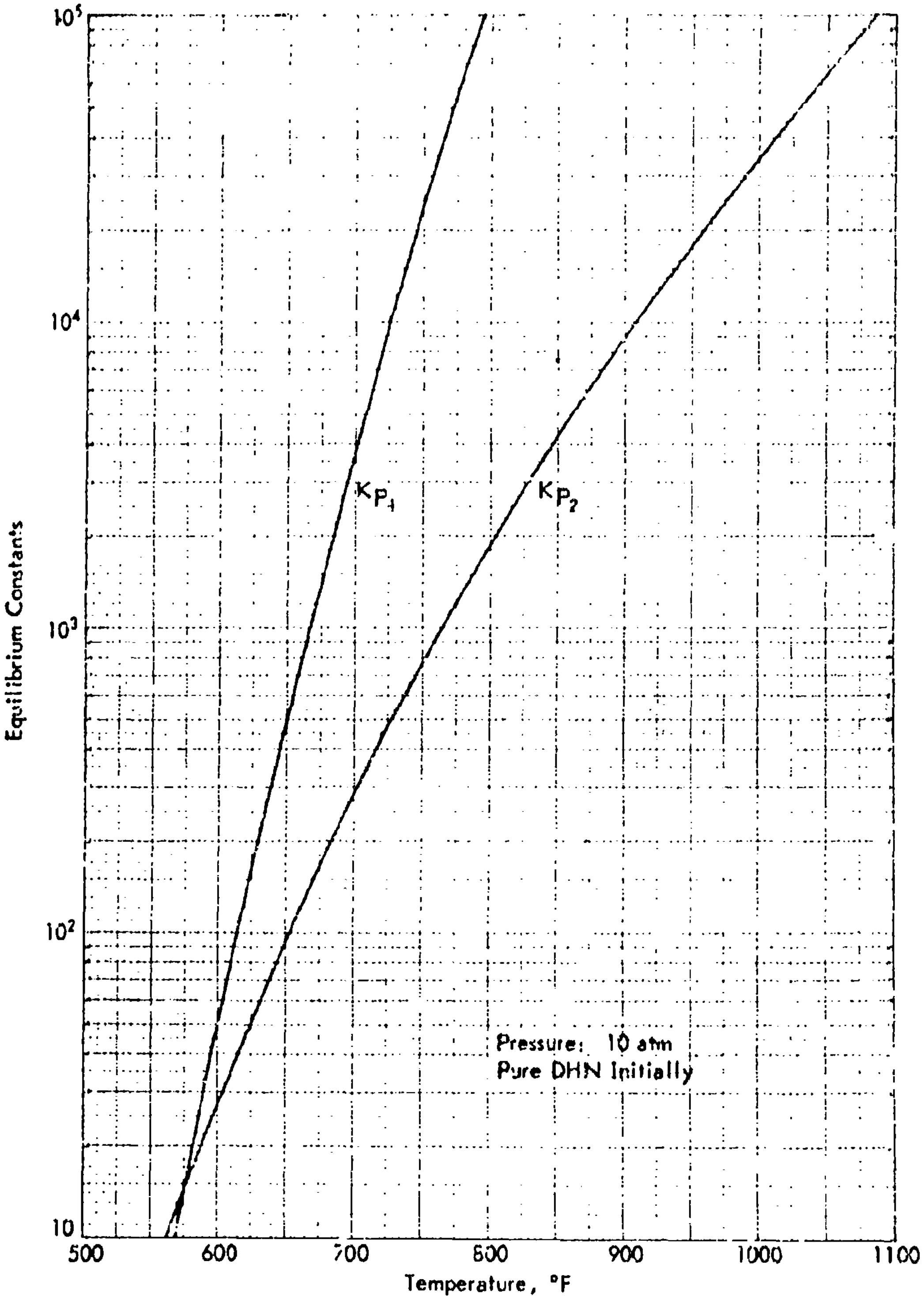

Figure 15. EQUILIBRIUM CONSTANTS FOR DECALIN SYSTEM

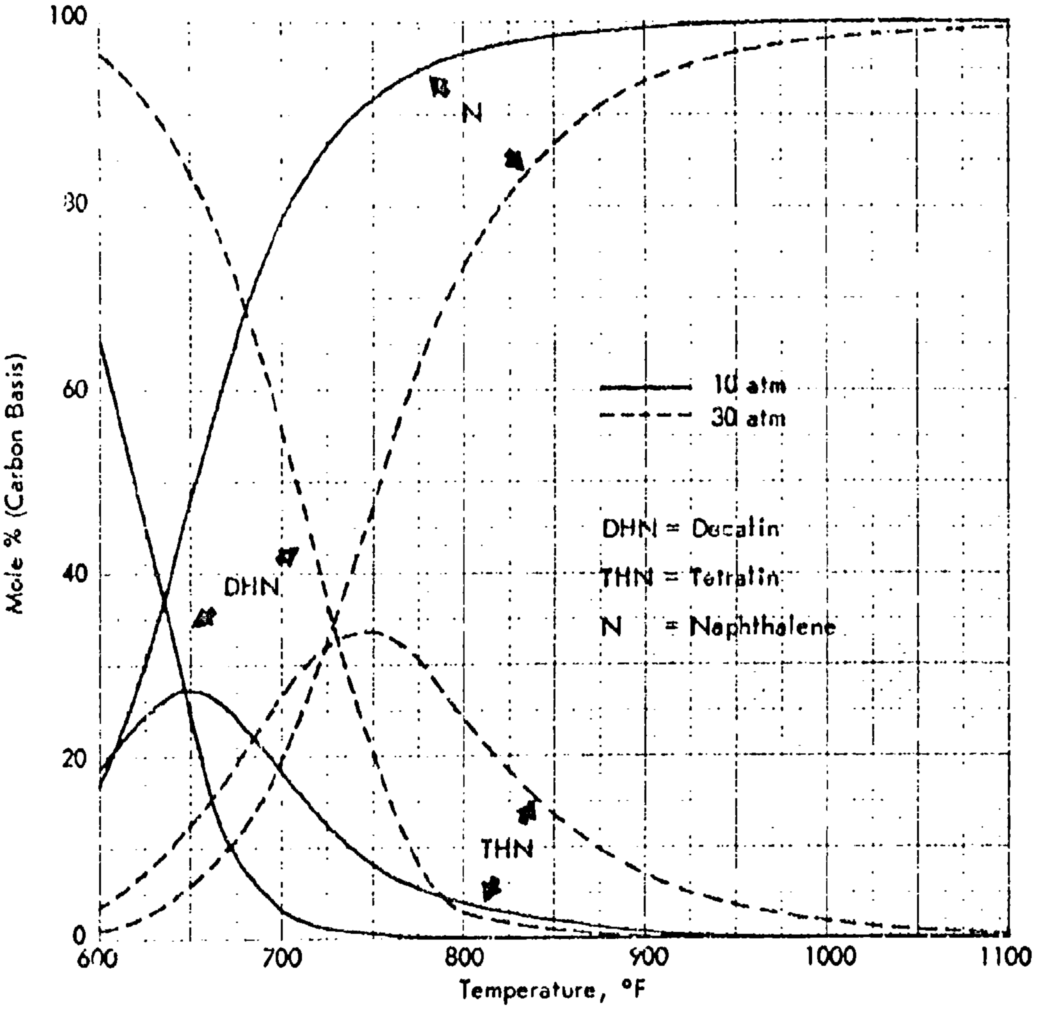

Figure 16. EQUILIBRIUM COMPOSITION OF DECALIN SYSTEM

Table 18. DEHYDROGENATION OF DECALIN: DILUTED BED REACTOR

Effect of Temperature and Space Velocity on Conversion

Catalyst:	1% Pt on Al_2O_3	Feed:	F-113 Decalin
Catalyst Volume:	0.5 ml		74.6% cis-DHN
Pressure:	10 atm		25.0% trans-DHN
			0.4% THN

Run No. 10342-	70-1	70-2	71-1	72-1	73-1	74-1	74-2	74-3	74-4	75-1	59-1	59-2	60	61	62-1	62-2	63	50-1	50-2
LHSV	700	1400	700	1400	700	1400	1400	1400	1400	1400	700	1400	700	1400	350	700	1400	1400	1400
Catalyst Change	←——— A[a] ———→										←——— B[b] ———→							← C[b] →	
Temperature, °F																			
Block	←707→		←752→			←797→					←707→		←752→		←797→			707	752
Wall	691	691	727	730	776	779	779	779	783	781	691	689	727	734	770	772	777	676	711
Catalyst Bed																			
Top	-	-	-	-	-	-	-	-	-	-	698	691	740	740	779	784	782	684	727
1-1/2 In. Below Top	673	680	705	714	741	752	757	759	761	761	-	-	-	-	-	-	-	-	-
Bottom	680	675	720	712	759	752	755	758	758	758	678	673	712	716	761	754	747	655	689
Product Analysis, %w																			
trans-DHN	26.7	25.5	25.8	24.9	24.9	24.3	24.4	24.6	24.2	24.4	26.5	25.6	25.9	25.7	22.9	24.7	24.4	26.3	25.6
cis-DHN	62.6	69.0	61.1	67.6	58.9	66.2	67.0	67.3	67.4	68.1	63.4	69.2	61.4	67.6	49.7	61.4	67.4	65.2	62.5
THN	3.6	1.9	3.9	2.9	4.3	3.1	2.8	2.9	2.6	2.8	3.6	2.0	3.6	2.5	5.6	3.7	2.6	3.4	4.1
N	7.1	3.6	9.1	4.6	11.8	6.4	5.8	5.3	5.9	4.7	[illegible]	3.2	8.6	4.7	21.5	10.1	5.6	5.1	7.9
Heavier than N	0.0	0.0	0.1	0.0	0.1	0.0	0.0	0.0	0.0	0.0	0.0	0.0	0.1	0.0	0.3	0.1	0.0	0.0	0.0
Yield THN, %w	3.1	1.5	3.5	2.5	3.9	2.7	2.4	2.4	2.2	2.4	3.2	1.6	3.4	2.1	5.2	3.3	2.2	3.0	2.7
DHN Conversion, %w	10.7	5.5	13.0	7.5	16.1	9.5	8.6	8.1	8.5	8.5	9.7	4.8	12.2	6.8	26.8	13.5	7.8	8.1	10.5
First Order Rate Constant, sec^{-1}	0.73	0.74	0.94	1.04	1.21	1.36	1.23	1.18	1.24	1.24	0.67	0.65	0.87	0.94	1.06	0.99	1.13	1.08	1.44

a) Catalyst diluted with 23 ml Cu and 6 ml quartz chips.
b) Catalyst diluted with 23 ml of Cu granules.

Table 10. DEHYDROGENATION OF DECALIN: DILUTED BED REACTOR

Effect of Pressure

Catalyst:	1% Pt on Al_2O_3	Feed:	F-113 Decalin
Catalyst Volume:	0.5 ml		74.6% cis-DHN
LHSV:	1400		25.0% trans-DHN
Block Temp:	792°F		0.4% THN
Reaction Time:	15 min		

Catalyst diluted with 23 ml Cu and 6 ml quartz chips

Run No. 10342-	76	77	78-1	78-2
Pressure, atm	10	20	30	10
Temperature, °F				
Wall	779	777	765	779
Catalyst Bed				
1/2 in. Below Top	777	770	756	779
1 in. Below Top	772	761	736	768
1-1/2 in. Below Top	763	758	732	761
Bottom	758	755	752	756
Product Analysis, %w				
trans-DHN	24.4	25.3	26.8	24.5
cis-DHN	68.1	66.8	64.7	67.4
THN	2.7	3.0	4.5	2.8
N	4.8	4.9	4.0	5.3
Yield THN, %w	2.3	2.6	4.0	2.4
DHN Conversion, %w	7.5	7.9	8.4	8.1
First Order Rate Constant, sec^{-1}	1.08	0.55	0.40	1.17

2. The Cu granules were carefully cleaned by repeated washing in hot isopropyl alcohol until they were dust-free.

3. The length of the heated lead was increased from 3 to 5 feet, to insure complete vaporization of the Decalin prior to entering the reactor.

Reproducible results were obtained after adopting the above changes.

An extended series of runs was made with F-113 Decalin (Feed 3; 74.6% cis DHN) at 707-797°F, LHSV of 700 and 1400 and at 10-20 atm pressure. At the lower pressure DHN conversions ranged from 11% to 21% at LHSV of 700 and from 6% to 11.5% at 1400°F (Table 20). The catalyst bed was not isothermal and temperature differences at 16°F at 6% conversion and 54°F at 21% conversion were observed between the top and a point 1-1/2 in. below the top of the bed. The data were reasonably reproducible and at any one temperature and space velocity the maximum variation in rate constants (3 runs) was ±12% and the closest agreement was ±6%. At a given temperature the average rate constant (3 runs) was slightly higher at the higher space velocity. This suggests that even at these high space velocities the reaction rate is limited by the heat transfer rates. Activation energies ranged from 9.2 to 12.2 kcal/mole and were slightly higher for first order kinetics (Table 21).[a] Figure 17 is an Arrhenius plot of the data. As was observed in previous work, there was some cis to trans-isomerization during the runs at the lower temperatures as shown by the increase in trans-DHN concentration in the product compared to that in the feed (Table 20).

With increased pressure (10-25 atm) at 752°F, conversions were reasonably constant at any one space velocity (Table 22, Figure 18). However the first order rate constants declined markedly with increased pressure, while the zero order constants increased slightly. This suggests that the reaction order with respect to Decalin is closer to zero order at these low conversions. Figure 18 shows the average values of three runs for conversions, zero and first order rate constants as functions of pressure. Again cis- to trans-isomerization was observed that increased with increasing pressure (Table 22).

The approximate reaction order may be calculated from the data of Table 22 by the following method. Assuming that the rate of dehydrogenation is proportional to some power of the pressure (i.e., concentration) then

$$r = kP^n$$

At low conversion the rate is equal to the fraction reacted f, per unit time, t, and

$$r = \frac{f}{t} = kP^n$$

In a flow system t is the residence time. For two different pressures at the same space velocity (i.e., constant residence time)

$$r_1 = f_1 = kP_1^n \qquad r_2 = f_2 = kP_2^n$$

---

[a] See footnote on page 25.

Table 20. DEHYDROGENATION OF DECALIN: DILUTED BED REACTOR

Effect of Temperature

Catalyst: 1% Pt on Al_2O_3
Catalyst Volume: 0.5 ml
Catalyst Weight: 0.48 g
Catalyst Size: 10-20 mesh
Pressure: 10 atm
Catalyst diluted with 23 ml Cu granules and 6 ml quartz chips

Feed: F-113 Decalin
25.0% trans-DHN
74.6% cis-DHN
0.4% THN

Catalyst Charge[a]	A	B	C	A	B	C	A	B	C	A	B	C	A	B	C	A	B	C
Run No. 10342-	130-1	135-1	142-1	131-1	136-1	142-2	132-1	137-1	143-1	152-1	157-1	144-1	133-1	138-1	144-2	134-1	139-1	145-1
LHSV	700			1400			700			1400			700			1400		
Temperature, °F	707			707			752			752			797			797		
Block																		
Wall	676	682	682	678	682	686	714	725	722	718	729	725	758	768	761	761	774	756
Catalyst Bed Profile																		
Distance From Top, in.																		
0	698	694	702	696	689	702	743	743	747	741	738	736	792	788	780	790	797	734
1/2	689	686	694	693	687	691	736	739	743	739	734	732	784	777	779	786	783	731
1	671	675	682	686	682	684	711	720	725	727	730	725	758	763	763	770	774	776
1-1/2	662	666	667	669	675	676	696	707	705	712	728	712	738	745	738	754	761	758
Bottom	678	676	675	669	671	669	714	710	714	701	712	705	752	756	750	743	748	743
Product Analysis, %w																		
trans-DHN	27.5	26.9	27.2	25.8	25.8	25.9	26.6	26.4	26.4	25.7	23.7	25.7	24.7	25.1	25.5	24.6	25.1	24.8
cis-DHN	58.8	61.4	60.5	66.0	68.0	67.6	56.0	57.9	58.0	64.6	66.0	65.9	[illegible]	56.6	55.3	63.4	65.0	[illegible]
THN	4.7	3.0	4.0	3.1	2.1	2.1	5.1	4.0	4.5	3.0	2.5	2.7	5.5	[illegible]	5.2	3.9	2.9	3.4
U[b]	0.0	0.0	0.0	0.0	0.0	0.0	0.0	0.0	0.0	0.0	0.0	0.0	0.5	0.0	0.0	0.1	0.0	0.0
N	9.0	8.1	8.3	5.1	4.1	4.4	12.2	11.6	11.0	6.7	5.9	5.7	15.1	14.0	13.9	8.0	7.1	7.1
U[b]	0.0	0.0	0.0	0.0	0.0	0.0	0.1	0.1	0.1	0.0	0.0	0.0	0.2	0.1	0.1	0.0	0.0	0.0
Yield THN, %w	4.3	3.2	3.6	2.7	1.7	1.7	4.7	3.6	4.1	2.6	2.1	2.3	5.1	3.8	4.8	3.5	2.5	3.0
DHN Conversion, %w	13.7	11.4	12.0	7.7	5.9	6.2	16.9	15.4	15.3	9.4	9.0	8.1	20.6	18.0	18.9	11.5	9.6	10.4
Selectivity for N, %w	67.8	71.0	69.2	65.4	69.5	70.9	71.8	75.3	71.9	72.3	73.8	70.4	73.0	78.8	73.6	69.0	74.0	68.3
Rate Constants																		
Zero Order, atm sec^{-1}	8.8	7.3	7.7	9.9	7.6	7.9	11.2	10.3	10.2	12.0	10.6	10.7	14.1	12.4	13.0	25.7	13.2	14.2
First Order, sec^{-1}	0.948	0.784	0.827	1.029	0.766	0.823	1.238	1.120	1.101	1.276	1.099	1.123	1.594	1.361	1.434	1.660	1.385	1.504

a) The runs in each Series (A, B, or C) were done on different charges of catalyst. The runs in any one series was done on the same charge of catalyst.

b) Unidentified.

Table 21. DEHYDROGENATION OF DECALIN: DILUTED-BED REACTOR

Apparent Activation Energies

Catalyst: 1% Pt on Al_2O_3
Catalyst Volume: 0.5 ml
Pressure: 10 atm
Temp Range: 707-797°F
Catalyst diluted with 23 ml Cu granules and 6 ml quartz chips

Run No. 10342-	130		135		142	
LHSV	700	1400	700	1400	700	1400
E_{act}, kcal/mole						
Zero Order	9.7	9.2	10.1	10.8	10.7	11.8
First Order	10.7	9.7	10.6	11.6	11.3	12.2

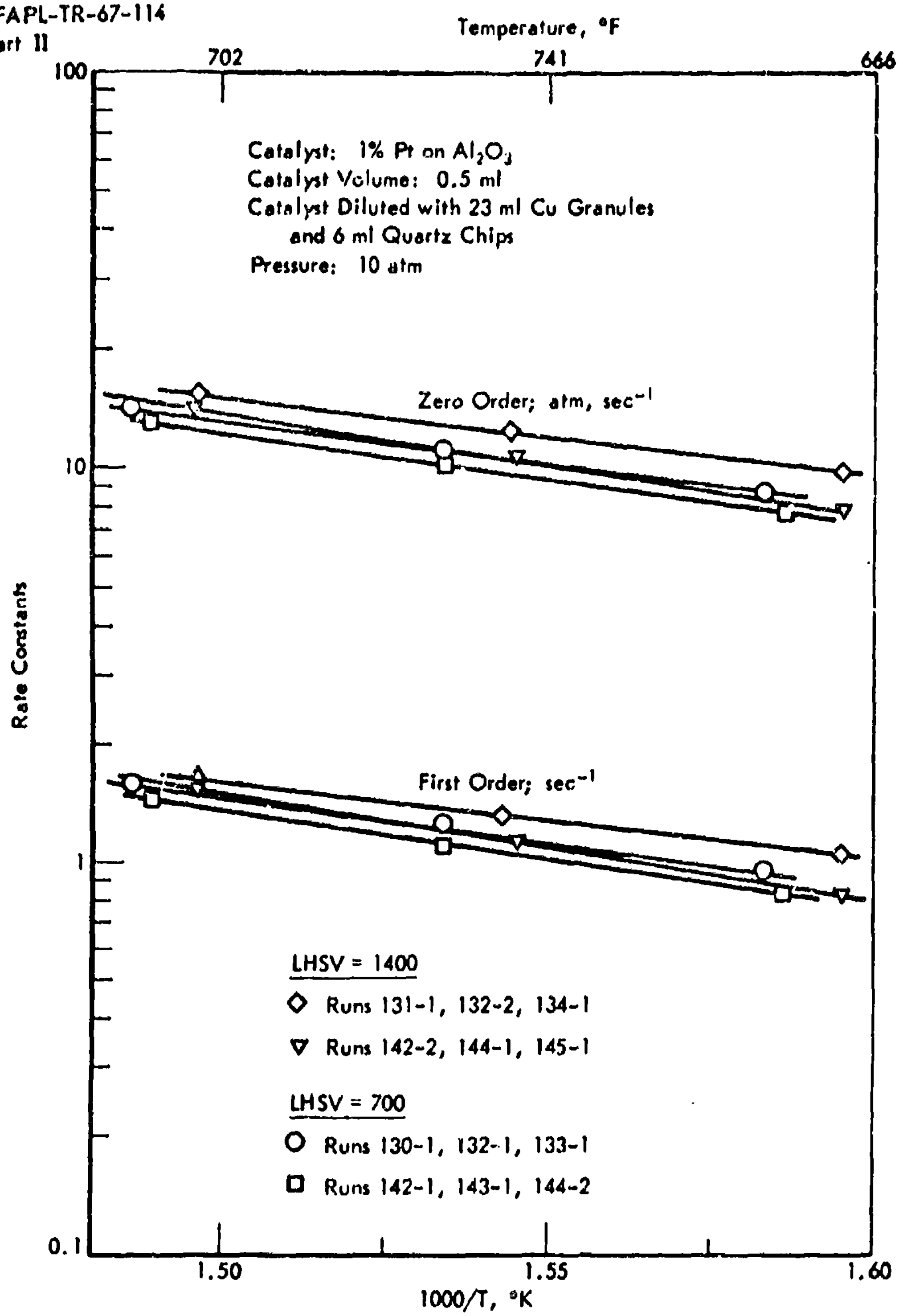

Figure 17. DEHYDROGENATION OF DECALIN: DILUTED BED REACTOR TEMPERATURE COEFFICIENT

Table 22. DEHYDROGENATION OF DECALIN: DILUTED-BED REACTOR

Effect of Pressure at 752°F

Catalyst:	1% Pt on Al_2O_3	Block Temperature:	752°F
Catalyst Volume:	0.5 ml		
Catalyst Weight:	0.48 g		
Catalyst Size:	10-20 mesh		

Catalyst diluted with 23 ml Cu granules and 6 ml quartz chips

Catalyst Charge[b]	A	B	C	A	B	C	A	B	C	A
Run No. 15342-	160-1	166-1	175-1	160-2	167-1	175-2	161-1	167-2	173-1	161-2
Pressure, atm	13						15			
LHSV	700			1400			700			1400
Temperature, °F										
Wall	730	727	729	725	730	732	727	730	729	725
Catalyst Bed Profile										
Distance From Top, in.										
-1/2	747	750	743	734	748	752	747	750	750	736
0	743	748	745	752	748	750	745	747	748	734
1/2	745	739	736	743	743	745	730	736	736	743
1	[illegible]	718	740	730	730	734	737	[illegible]	722	729
1-1/2	660	714	737	725	712	720	644	712	716	725
Bottom	720	725	728	712	718	726	723	729	726	716
Product Analysis, %										
trans-DHN	27.1	25.3	27.0	26.1	25.4	25.3	27.8	27.1	27.1	26.6
cis-DHN	54.7	57.4	55.9	63.1	65.0	65.4	55.3	58.1	57.8	62.7
THN	5.3	4.8	4.5	3.2	[illegible]	2.3	6.3	5.6	5.1	4.2
N	12.9	11.5	12.6	7.6	6.5	6.6	10.5	4.6	13.8	6.6
Un[a]	0.0	0.0	0.0	0.0	0.0	0.0	0.1	0.0	0.0	0.0
Yield THN, %	4.9	4.6	4.1	2.8	2.9	2.3	5.9	5.6	4.7	3.7
DHN Conversion, %	17.9	16.9	16.8	10.4	9.2	8.9	16.5	14.5	14.6	10.3
Selectivity for N, %	70.4	72.5	75.0	73.0	69.9	72.9	63.6	64.8	67.6	64.0
Rate Constants										
Zero Order, atm. sec^{-1}	12.8	10.7	11.2	17.8	12.5	11.9	11.2	9.6	9.9	13.7
First Order, sec^{-1}	1.52	1.17	1.25	1.65	1.29	1.26	0.790	0.722	0.729	0.998

Catalyst Charge[b]	B	C	A	B	C	A	B	C	A	B
Run No. 15342-	168-1	173-2	162-1	169-1	176-1	162-2	169-2	176-2	163-1	177-1
Pressure, atm			20						[illegible]	
LHSV			700			1400			700	
Temperature, °F										
Wall	730	734	725	732	734	723	725	729	725	723
Catalyst Bed Profile										
Distance From Top, in.										
-1/2	750	[illegible]	745	747	746	746	747	740	747	746
0	750	748	741	741	746	[illegible]	745	741	741	747
1/2	743	741	737	730	730	743	742	736	723	741
1	737	729	741	736	[illegible]	732	730	732	[illegible]	737
1-1/2	730	712	[illegible]	730	732	[illegible]	712	730	[illegible]	[illegible]
Bottom	718	712	725	720	725	714	716	712	725	729
Product Analysis, %										
trans-DHN	26.2	26.1	28.8	28.5	29.2	27.5	27.2	27.5	30.7	29.7
cis-DHN	64.1	64.5	55.7	55.5	56.6	60.8	62.5	61.9	51.8	54.8
THN	3.7	3.3	4.4	7.6	6.6	5.8	4.7	4.8	10.2	8.7
N	6.0	6.1	6.8	6.6	8.6	5.8	5.6	5.8	7.2	6.8
Un[a]	0.0	0.0	0.1	0.0	0.0	0.0	0.0	0.0	0.1	0.0
Yield THN, %	3.5	2.9	6.0	7.0	6.2	5.4	4.5	4.6	6.8	6.6
DHN Conversion, %	9.3	9.0	16.9	15.7	14.9	11.3	9.9	10.2	17.2	15.7
Selectivity for N, %	64.5	67.6	54.6	38.8	57.5	54.2	56.6	56.8	60.1	66.8
Rate Constants										
Zero Order, atm. sec^{-1}	12.4	12.0	11.9	[illegible]	17.0	15.0	15.2	15.5	11.5	10.2
First Order, sec^{-1}	0.870	0.835	0.625	0.575	0.540	0.745	0.704	0.717	0.526	0.466

Catalyst Charge[b]	C	A	B	C	A	B	C	A	B	C
Run No. 15342-	177-2	164-1	170-2	178-1	164-2	171-1	178-2	165-1	171-2	179-2
Pressure, atm					[illegible]					
LHSV		1400			700			1400		
Temperature, °F										
Wall	725	722	718	716	725	727	729	727	729	732
Catalyst Bed Profile										
Distance From Top, in.										
-1/2	746	740	747	746	740	748	742	746	740	742
0	743	[illegible]	[illegible]	743	734	747	740	734	748	750
1/2	724	742	736	[illegible]	736	736	736	740	743	740
1	734	737	[illegible]	732	737	720	722	725	730	730
1-1/2	[illegible]	734	[illegible]	[illegible]	[illegible]	712	716	727	712	722
Bottom	723	721	722	[illegible]	712	[illegible]	722	716	718	736
Product Analysis, %										
trans-DHN	30.2	29.3	29.9	29.6	26.4	21.6	26.3	27.8	27.3	25.3
cis-DHN	55.2	57.2	60.8	59.5	56.7	63.6	57.0	64.0	61.0	65.7
THN	6.5	7.0	6.1	7.0	5.1	6.7	4.5	3.3	5.3	2.7
N	7.3	6.4	6.2	6.5	11.5	13.5	11.0	6.3	6.2	6.0
Un[a]	0.0	0.0	0.0	0.0	0.1	0.0	0.0	0.0	0.0	0.0
Yield THN, %	6.9	4.5	5.8	5.9	10.9	10.1	10.6	6.5	5.8	5.6
DHN Conversion, %	16.5	12.1	9.9	10.9	16.2	14.9	14.2	9.8	9.3	8.3
Selectivity for N, %	66.8	56.5	52.6	50.6	70.2	70.6	78.6	70.6	66.6	73.5
Rate Constants										
Zero Order, atm. sec^{-1}	10.9	16.0	15.2	16.2	10.8	10.0	9.5	15.0	12.6	12.1
First Order, sec^{-1}	0.581	0.621	0.564	[illegible]	1.159	1.350	[illegible]	1.176	1.310	1.164

a) Unidentified.

b) Run A and B on same charge of catalyst; Run C on a fresh charge of catalyst. Catalyst H_2 treated for 1 hr at 932°F between runs.

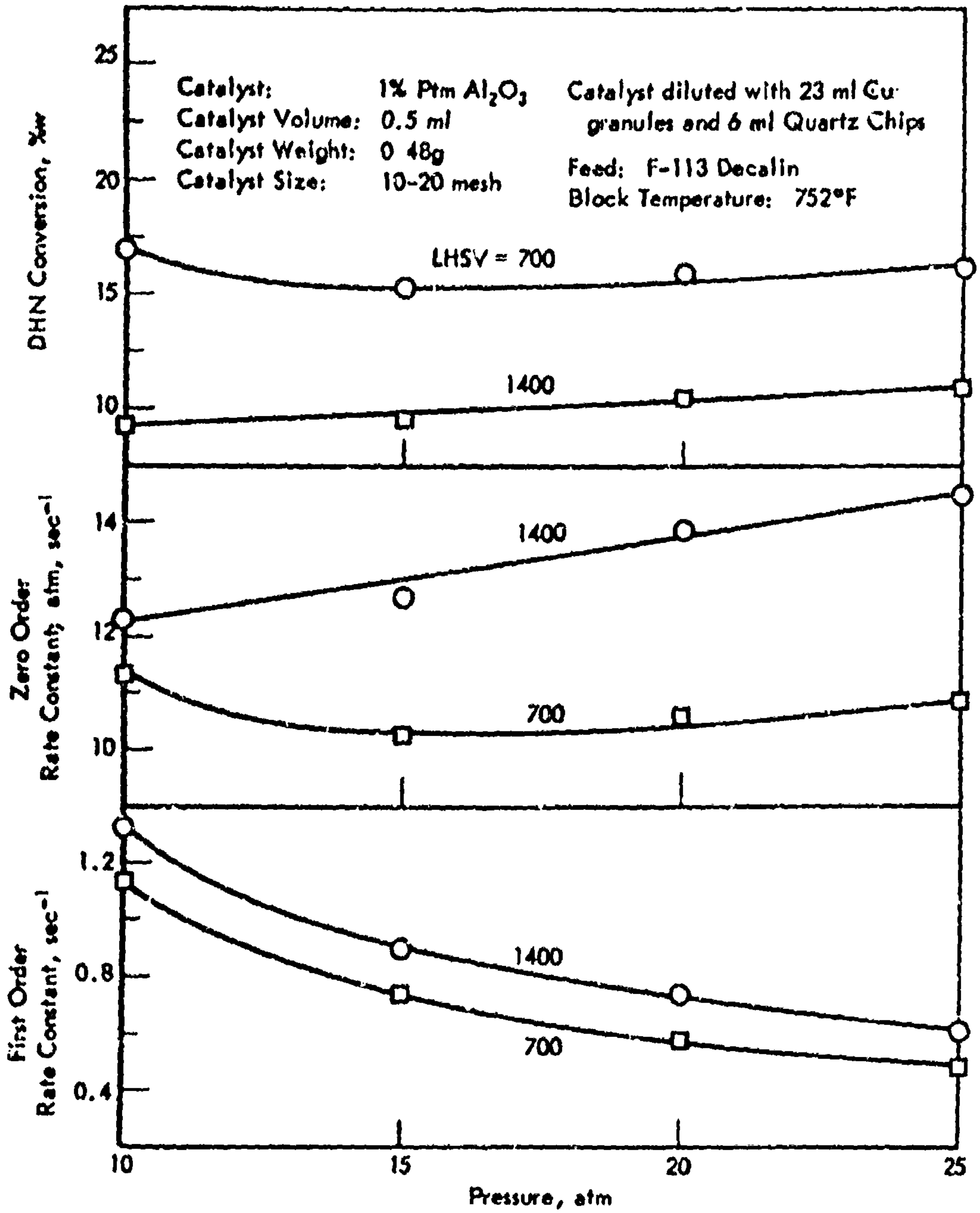

Figure 18. DEHYDROGENATION OF DECALIN: DILUTED BED REACTOR EFFECT OF PRESSURE

n then is equal to

$$n = \frac{\log \frac{f_1}{f_2}}{\log \frac{P_1}{P_2}}$$

Using the average conversion values in Table 22 10 and 20 atm, LHSV = 1400

$$n = \frac{\log \frac{10.5}{9.5}}{\log \frac{20}{10}} = \frac{0.043}{0.301} = 0.14$$

Thus the kinetic order of the dehydrogenation of Decalin reaction is about 0.14 the power of Decalin or close to zero order. This is only an approximation however as the concentration of tetralin and hydrogen may also affect the rate.

In this series of tests the reaction did not appear to be equilibrium limited as the product concentration of tetralin and naphthalene were less than the equilibrium values (Figure 16).

In another series of runs, less extensive tests were carried out with all six feedstocks. The data for those feeds containing only Decalin are presented in Table 23, and for those feeds containing tetralin are presented in Table 24.

With the feeds containing only Decalin (Nos. 1, 2, 3), reactivity appeared to be a function of isomer concentration. Thus the feed with the highest cis isomer concentration (No. 3) was the most reactive and the feed with the highest trans isomer concentration (No. 1) was the least reactive (of conversions or the rate constants). This isomer effect on Decalin reactivity was observed at higher overall conversions in previous work.1) With any one feed the reactivity of the cis isomer was greater than that of the trans when the cis concentration was over 50% (Feeds 2 and 3), but with a high trans DHN concentration (Feed 1) the reactivity of the cis isomer was greater at low space velocity (700) but at high space velocity the reverse was true. Why space velocity should effect the relative reactivities of the cis and trans DHN isomers is not clear, but it does not appear to be a temperature or conversion effect.

Overall activation energies for the first dehydrogenation step were inversely proportional to reactivity and were 12, 20, and 22 kcal/mole for Feeds 3, 2, and 1 respectively. With all three feeds pressure did not appear to effect conversion appreciably.

Some isomerization occurred concurrently with dehydrogenation. For example with Feed 3 (74.6% cis) in four of the runs there was more trans DHN in the product than in the feed, indicating cis to trans isomerization. With the high trans feed however (No. 1; 91.0% trans) the amount of cis in the product was greater than that in the feed in only one run. This suggests that the rate of cis to trans isomerization was greater than that of trans

Table 23. DEHYDROGENATION OF DECALIN MIXTURES

Catalyst	1% Pt on Al_2O_3	Catalyst Diluted With Copper Granules, ml	23
Catalyst Size, mesh	10-20	Quarts Chips, ml	6
Catalyst Volume, ml	0.5	Total Bed Length, inches	5-1/2

Feed Number	1													
Run No. 10946-	154-1	154-2	155-1	155-2	156	157-1	157-2	158	159-1	159-2	160	161-1	161-2	162-1
Feed, %w (H_2-free)														
trans-DHN	91.0													
cis-DHN	8.8													
THN	0.0													
Others	0.2													
H_2/THN mole ratio	0.0													
Pressure, atm	10	10	10	10	20	20	10	10	20	20	10	10	20	20
LHSV	786	1560	700	1400	700	1400	700	1400	700	1400	770	1400	700	1400
Temperature, °F														
Block	716						752				758			
Wall	712	700	712	704	704	704	734	736	738	736	770	772	772	773
Inches from Top of Bed														
-1/2	716	714	716	714	714	712	748	746	747	743	764	752	779	781
0	712	709	712	714	710	712	745	746	743	739	751	751	777	779
1/2	712	700	707	710	736	710	739	741	736	737	766	774	758	773
1	693	639	693	728	689	694	725	732	743	727	768	756	746	761
1-1/2	675	664	675	697	677	680	705	720	735	712	730	748	729	763
Bottom of Bed	695	687	695	695	695	684	725	718	725	716	748	745	752	763
Product Analysis, %w (H_2-free)														
trans-DHN	83.4	86.3	84.1	86.2	84.0	86.3	79.9	85.0	80.3	84.3	77.2	82.9	77.8	82.6
cis-DHN	7.7	8.6	8.1	9.0	8.0	8.6	7.7	8.4	8.1	8.4	7.4	8.6	7.5	8.3
THN	2.8	1.6	2.3	1.6	3.3	2.1	2.9	1.3	4.0	2.4	3.2	2.3	4.9	2.9
N	5.7	3.1	5.1	2.8	4.3	2.4	9.0	4.5	6.6	4.3	11.6	5.8	9.2	5.8
Others	0.4	0.4	0.4	0.4	0.4	0.4	0.5	0.4	0.4	0.4	0.6	0.4	0.5	0.5
Conversion, %w														
trans-DHN	8.3	5.6	7.6	5.2	7.7	5.0	12.2	6.4	11.1	7.2	15.2	9.1	14.5	9.2
cis-DHN	12.5	2.2	7.9	-2.0	9.1	2.3	12.5	4.6	8.0	4.6	15.9	2.3	14.6	5.6
Total DHN	8.4	5.4	7.6	4.6	7.8	4.7	12.2	6.4	10.8	6.9	15.2	8.3	14.5	8.9
Rate Constants														
First Order, sec^{-1}	0.642	0.709	0.510	0.630	0.262	0.309	0.276	0.866	0.376	0.475	1.131	1.224	0.537	0.626
Zero Order, atm, sec^{-1}	6.16	7.61	4.36	6.00	5.10	6.57	7.17	8.58	7.44	9.18	10.40	11.99	9.75	12.12
E act. kcal/mole (10 atm pressure)														
First Order Constants	19.9						22.1							
Zero Order Constants	19.6						20.6							

Feed Number	2						3					
Run No. 10946-	163-1	163-2	166	167-1	167-2	168	190-1	190-2	191-1	191-2	192-1	193-1
Feed, %w (H_2-free)												
trans-DHN	57.0						25.0					
cis-DHN	42.4						74.6					
THN	0.2						0.4					
Others	0.4						[illegible]					
H_2/THN mole ratio	0.0						[illegible]					
Pressure, atm	20	10	10	10	20	20	20	10	10	10	20	20
LHSV	750	700	1400	1400	1400	700	700	700	1400	1400	1400	700
Temperature, °F												
Block	716			758			716			754		
Wall	636	658	742	763	759	761	692	724	752	753	753	753
Inches from Top of Bed												
-1/2	710	716	715	751	772	756	712	711	711	753	[illegible]	754
0	709	724	716	773	774	751	717	717	754	751	779	751
1/2	725	727	722	776	756	772	686	732	731	[illegible]	772	[illegible]
1	676	647	709	749	[illegible]	765	675	691	[illegible]	[illegible]	[illegible]	[illegible]
1-1/2	660	682	697	757	736	732	671	697	[illegible]	736	[illegible]	749
Bottom of Bed	693	695	691	745	741	732	683	687	664	763	763	744
Product Analysis, %w (H_2-free)												
trans-DHN	57.0	55.6	56.3	53.9	54.9	53.4	28.2	25.5	24.9	24.2	25.4	26.9
cis-DHN	30.4	34.2	37.7	35.6	35.3	31.1	60.0	62.6	68.1	66.0	64.2	56.4
THN	5.8	2.6	1.8	2.5	3.2	4.3	7.3	3.7	1.9	2.6	3.9	5.9
N	6.5	7.1	3.6	7.2	5.9	10.0	6.2	8.1	4.3	7.0	6.6	10.5
Others	0.6	0.8	0.7	0.8	0.9	0.6	0.5	0.2	0.5	0.9		
Conversion, %w												
trans-DHN	0.0	2.4	1.2	5.4	3.7	4.3	-12.0	-2.0	+0.5	+3.3	-1.3	-7.5
cis-DHN	28.0	19.0	12.7	19.6	16.4	26.3	19.6	17.4	7.8	11.9	14.0	24.4
Total DHN	12.0	9.6	5.4	9.9	9.2	14.9	12.7	11.6	6.6	9.7	10.0	16.4
Rate Constants												
First Order, sec^{-1}	0.420	0.661	0.724	1.441	0.573	0.552	0.412	0.424	0.697	1.379	0.720	[illegible]
Zero Order, atm, sec^{-1}	7.627	5.471	7.033	13.480	12.538	10.220	7.26	8.52	13.21	13.41	13.61	11.26
E act. kcal/mole (10 atm pressure)												
First Order Constants			19.8						12.3			
Zero Order Constants			19.2						12.4			

to cis, although the rate of the latter reaction may have been equilibrium limited as the percent cis at equilibrium at 700°F is about 11% (Figure 19).

Pure tetralin was 3 to 4 times more reactive than Decalin (Table 24). Quantitatively base on first order rate constants, THN was 2.8-3.1 times more reactive than cis DHN (Feed 3) and 3.3-3.9 times more reactive than trans DHN (Feed 1). Tetralin conversions ranged from 15 to 32% with high selectivity for naphthalene (90-99%). Conversion of tetralin to Decalin was less than 1% except for the run at lowest temperature LHSV and highest pressure (i.e., longest contact time) where about 10% of the tetralin reacted was converted to Decalin (Run 164-1). The activation energy (first order constants) was at 15 kcal/mole, which was somewhat lower than the 24 kcal/mole calculated earlier from Decalin dehydrogenation data.[19] As was observed with Decalin, pressure did not affect conversion.

When mixed with Decalin the relative reactivity of tetralin was greater than was observed with the pure components. Thus when mixed with cis Decalin (Feed 4) based on first order rate constants the reactivity of THN was 4.5-5.5 times that of Decalin (Table 24) while with a trans DHN mixture (Feed 5) the reactivity of THN was 7.7 times that of Decalin. Activation energies for dehydrogenation of THN and DHN were lower in the mixtures than were observed for pure components.

Summary

The results obtained with Decalin and tetralin over a diluted catalyst bed at high space velocities generally were in agreement with those obtained in earlier work with an undiluted catalyst bed (7 ml catalyst; LHSV of 100);[1] namely that cis-Decalin was more reactive than trans for both dehydrogenation and isomerization. However for dehydrogenation in the diluted catalyst bed the value of the first order rate constant at 752°F, 10 atm, (1.16 $\sec^{-1}$) was about twice that obtained under standard testing (0.63 $\sec^{-1}$) and the activation energies (10 atm) were about 28% to 60% higher with the diluted bed technique. This suggests that the rate of heat transfer to the catalyst was greater in the diluted bed-high space velocity configuration which in turn lead to higher reaction rate. These results support a previous conclusion namely that during the earlier bench-scale tests the rate of heat transfer from the reactor wall to the catalyst bed was a limiting factor in the overall rate.

Pure tetralin was more reactive than Decalin for dehydrogenation and the rate of dehydrogenation of tetralin was greater than the rate of hydrogenation. The dehydrogenation of both Decalin and tetralin were about zero order in hydrocarbon. At low conversions activation energies appeared somewhat higher than those obtained in earlier work, possibly due to better heat transfer at higher conversions and temperatures. In Decalin-tetralin mixtures the relative reactivity of tetralin was greater than was observed with pure components.

Additional work will be done on the Decalin-tetralin system only if needed for the development of the computer program for this reaction.

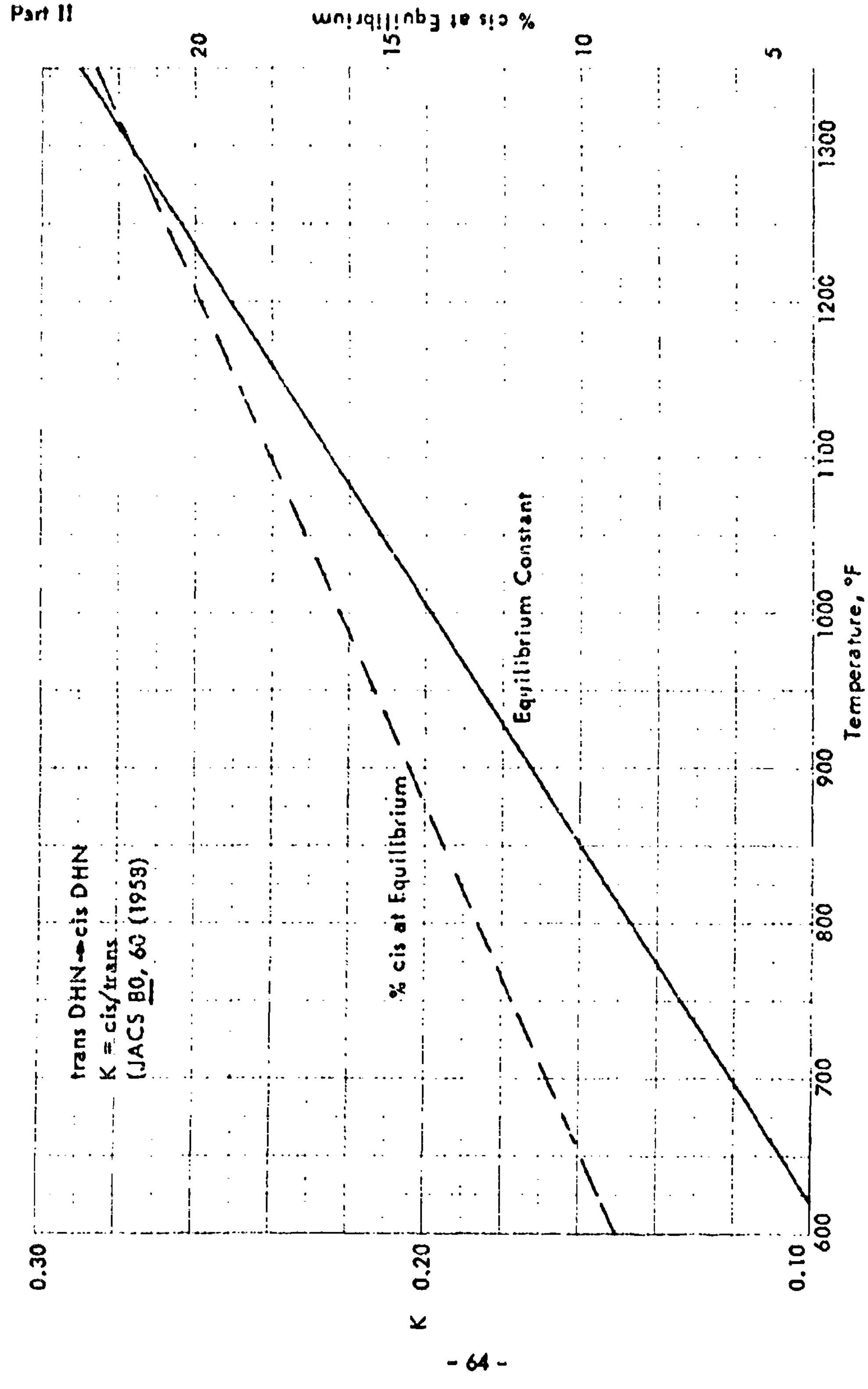

Figure 19. ISOMERIZATION OF DECALIN: cis-trans EQUILIBRIUM

Table 24. DEHYDROGENATION OF DECALIN-TETRALIN MIXTURES

Catalyst: 1% Pt on Al_2O_3
Catalyst Size: 10-20 mesh
Catalyst Volume: 0.5 ml

Catalyst Diluted With:
23 ml Copper Granules and
6 ml Quartz Chips
Total Bed Length: 5-1/2 in.

Feed No.	4						5						6					
Run No. 10548-	151-1	151-2	152	153-1	153-2	154	158-1	158-2	159	160-1	160-2	161	164-1	164-2	165	166-1	166-2	167
Feed, %w (H_2-free)																		
trans-DHN	45.6						11.8						0.1					
cis-DHN	4.9						35.6						0.5					
THN	50.5						51.8						97.9					
Others	0.6 N						0.4 N						0.9 N					
	0.6 Others						0.5 Others						0.6 Others					
H_2/THN mole ratio	2.6						2.6						3.0					
Pressure, atm	20	10	10	10	20	20	20	10	10	10	20	20	20	10	10	10	20	[illegible]
LHSV	700	700	1400	1400	1400	700	700	700	1400	1400	1400	700	700	700	1400	1400	1400	700
Temperature, °F																		
Block	716			788			716			738			716			738		
Wall	700	696	698	754	758	765	689	705	705	770	777	777	702	695	691	[illegible]	[illegible]	[illegible]
Inches from Top of Bed																		
-1/2	716	716	712	783	774	788	714	714	700	783	784	788	749	714	712	779	779	[illegible]
0	714	714	712	781	774	784	712	712	709	781	783	794	714	710	712	771	779	781
1/2	710	710	709	773	770	770	707	705	707	777	779	777	710	702	710	774	775	772
1	702	700	702	761	763	763	694	693	698	761	766	758	695	691	693	755	761	[illegible]
1-1/2	694	691	697	752	754	752	684	650	686	740	745	740	682	675	680	754	740	759
Bottom of Bed	698	695	689	743	748	759	698	691	686	738	745	756	704	695	687	743	750	761
Prod. Analysis, %w (H_2-free)																		
trans-DHN	41.3	42.0	45.8	41.4	41.9	40.3	15.0	15.2	13.2	12.7	12.8	13.1	1.6	0.3	0.2	0.2	0.4	0.5
cis-DHN	4.3	4.3	4.8	4.6	4.5	4.1	29.0	31.0	33.0	32.0	31.5	29.5	1.2	0.4	0.4	0.4	0.5	0.5
THN	37.5	34.4	37.4	35.3	36.7	31.[illegible]	39.9	36.7	40.9	37.3	39.6	35.6	74.4	73.1	82.8	73.9	76.2	66.6
N	16.4	18.8	11.4	18.1	16.4	23.3	15.5	18.[illegible]	12.5	17.8	15.5	22.2	22.2	5.5	15.9	24.7	22.0	31.6
Others	0.5	0.5	0.6	0.6	0.5	0.6	0.6	0.6	0.6	0.6	0.6	0.6	0.6	0.6	0.7	0.3	0.3	0.3
Conversion, %w																		
trans-DHN	5.2	3.6	-5.0	5.0	3.9	7.6	-27.0	-11.9	-11.9	-3.4	-7.5	-11.1						
cis-DHN	12.2	12.2	2.0	6.1	8.2	16.3	18.6	12.9	7.5	10.1	11.5	20.0						
Total DHN	6.0	4.5	-4.4	5.1	4.3	8.2	7.2	6.8	2.7	6.6	6.3	12.3						
Total THN	25.5	31.6	25.6	29.8	27.1	37.0	25.0	29.2	21.1	26.0	23.6	31.2	24.0	25.2	15.3	24.4	22.1	31.9
THN Converted To, %w																		
N													21.8	24.9	15.2	24.1	21.4	31.1
DHN													2.2	0.1	0.1	0.1	0.2	0.3
Rate Constants																		
THN																		
First Order; sec^{-1}	1.11	2.55	4.45	5.56	2.50	1.84	0.990	2.60	3.54	5.14	2.12	1.49	0.926	2.161	2.478	4.330	1.905	[illegible]
Zero Order; atm, sec^{-1}	19.27	25.77	38.39	46.75	42.74	29.44	17.38	22.00	31.54	45.68	37.11	24.75	14.22	16.24	19.74	32.62	29.31	21.49
DHN																		
First Order, sec^{-1}	0.204	0.300	-	0.721	0.299	0.294	0.249	0.466	0.388	0.956	0.486	0.452	-	-	-	-	-	-
Zero Order; atm, sec^{-1}	3.92	2.94	-	6.94	5.88	5.66	4.72	4.44	3.[illegible]0	8.95	9.27	8.46	-	-	-	-	-	-
E.Act., kcal/mole																		
THN																		
First Order	12.7 (20 atm)						10.1 (20 atm)						15.1 (10 atm)					
Zero Order	10.7 (20 atm)						9.6						13.6					
DHN																		
First Order	9.5 (20 atm)						16.0 (20 atm)											
Zero Order	9.5						15.8											

Bench-Scale Catalyst Evaluation Tests With Methylcyclohexane

A number of catalysts that appeared promising under micro-scale testing (MICTR) were evaluated in the bench-scale reactor. These catalysts consisted of active metals mounted on various supports. A test procedure has been described in a previous report[17] which gives a measure of the effect of temperature, pressure, space velocity (i.e., contact time) and catalyst stability over a three-hour test period using a single charge of catalyst. This test involves making a series of runs at 842 and 1022°F, 10 and 30 atm, and LHSV's of 50 and 100.

The tests were done in groups with a test with the standard laboratory catalyst done in each group for reference. Different Meehanite furnace liners were used for two groups of tests and these liners made better contact with the reactor tube wall. Presumably this better metal-to-metal contact enhanced the heat conductivity of the system and resulted in the higher MCH conversions for a given block temperature that was observed in the second and third series of runs.

The results of the tests, the conditions of each run, and the order in which the runs were made are shown in Table 25. Each catalyst was rated as to "Relative Performance". This rating was designed to show how the catalyst was performing at the end of the test, relative to the standard catalyst and quantitatively was taken as the ratio of the first order rate constant with the catalyst (k_c) to that with the standard catalyst (k_s) calculated from the MCH conversion of Run No. 7. Based on this criteria 12 of the catalysts were superior to our standard catalyst (11 to 32% more active); one performed about like the standard catalyst; and one was considerably less active and extremely unstable and deactivated badly during the initial run at 842°F

Activation energies ranged from 10.6 (standard catalyst) to 15.5 kcal/mole. These values were calculated from the rate constants obtained from the data of Runs 1 and 2. All of the activation energies were greater than that of the standard catalyst; this suggests that the new catalysts would be even more active than the standard catalyst at temperatures above 1022°F.

Table 25. DEHYDROGENATION OF METHYLCYCLOHEXANE

Evaluation of Various Catalysts

Feed: Pure MCH
Reaction Time: 20 minutes

Run Number	1	2	3	4	5	6	7	E, ACT kcal/mole	E_c/E_s	Relative Performance, k_c/k_s
Block Temperature, °F	842	← 1022 →								
Pressure, atm	10	10	30	10	10	10	10			
LHSV	100	100	100	100	50	100	100			
MCH Conversion, %w for Catalyst No.	First Series									
9874-7 a)	41.4	66.0	59.8	69.2	96.1	55.7	66.9	12.6	1.00	1.00
10280-121	43.2	71.5	60.7	72.4	95.4	70.7	70.4	11.6	1.03	1.11
10280-121; Muffled	41.9	72.6	61.2	72.2	97.5	71.4	71.4	15.5	1.37	1.15
10280-124A	42.5	73.7	62.2	74.4	98.1	73.0	72.8	13.4	1.17	1.21
10280-129	42.6	72.8	62.0	73.4	97.8	72.2	72.5	13.7	1.21	1.15
	Second Series									
9874-7	48.8	74.3	67.6	74.9	75.9	71.7	71.0	12.7	1.00	1.00
9874-73	48.0	76.2	69.3	77.4	69.6	74.9	74.4	12.0	0.95	1.12
10280-129	47.0	78.9	67.1	80.0	98.9	77.1	77.1	14.2	1.12	1.19

a) Standard catalyst.

(Continued)

Table 25 (Contd). DEHYDROGENATION OF METHYLCYCLOHEXANE

Evaluation of Various Catalysts

Run Number	1	2	3	4	5	6	7	E, ACT kcal/mole	E_c/E_s	Relative Performance, k_c/k_s
	Third Series									
9874-7[a]	43.3	68.2	61.7	70.4	94.0	67.5	68.7	10.6	1.00	1.00
10280-104B	45.2	75.3	63.0	75.0	97.8	74.6	73.7	13.4	1.26	1.36
10280-106C	44.9	72.9	63.2	73.6	97.3	72.3	72.8	12.4	1.17	1.12
10280-105B	42.4	68.3	61.1	69.8	93.6	67.5	67.7	12.2	1.16	0.97
	Fourth Series									
9874-7[a]	42.9	69.4	62.8	71.5	93.9	68.3	68.5	11.5	1.00	1.00
10280-75D	48.0	76.9	64.7	77.5	98.9	76.1	77.6	13.1	1.14	1.32
10280-43D	44.8	74.2	64.3	75.3	97.7	73.9	73.8	12.8	1.11	1.22
10280-33E	46.7	78.6	64.7	77.1	96.9	76.4	76.3	14.6	1.27	1.28
10280-43E; 1% Pt on Pelleted	45.6	76.9	66.4	77.6	98.8	75.6	75.7	12.5	1.09	1.24
10280-177A	26.7[b]	-	-	-	-	-	-	-	-	-

a) Standard catalyst.
b) Catalyst deactivated almost completely during Run 1.

Conventional Catalysts and Catalytic Coatings

The extensive catalyst preparation and testing program begun under this contract has continued.[19] The principal emphasis has been to develop catalysts that are more active and stable than the 1% Pt/alumina reference catalyst, for endothermic reactions such as naphthene dehydrogenation. Various attempts have been made to increase activity by promoting platinum with other metals or to better disperse platinum by various techniques. The search for active substitute metals or metal combinations for the very expensive platinum[31] and substitute supports for alumina has continued. Various disciplines of approach to catalysts have been considered in the following catalyst preparation studies (cf refs 23-30).

In addition methods of bonding thin catalytic coatings (i.e., 3-8 mils) to metal walls have been actively explored. Such active catalytic coatings are desirable since they provide a method of reducing pressure drop across a reacting heat absorbing zone. Some developments have been made earlier in this field, mainly for cracking and oxidation reactions.[32][33][illegible]

A total of 536 catalysts have been prepared, or obtained from proprietary and commercial sources, and nearly all of these have been evaluated. These include metal tubes catalytically coated in various ways. The granular catalysts have been screened for MCH dehydrogenation activity at 10 atm pressure, usually at LHSV 100, and at 662°, 752°, and 842°F in the micro-scale test rig (MICTR). Certain selected types of granular catalysts also have been screened for n-heptane dehydrocyclization to toluene, at LHSV 10, at 842 and 932°F, and 10 atm pressure.

A number of catalytic coatings on hypodermic tubing were screened initially. In these runs with MCH the hypodermic tubing was placed within the standard 1/4" OD reactor tube for testing. Adequate clearance for passage of the MCH and dehydrogenation products was allowed. Later the coatings were emplaced on the interior surfaces of the 1/4" OD reactor tubes for better heat transfer during the screening with MCH. Catalysts of the same composition as the coating formulation were often tested in 10-20 mesh granular form for mechanical convenience, for evaluation of the efficacy of the formulations.

The purpose of the screening tests is to obtain a quick comparison with the reference catalysts (9874-24 or 9874-139; 1% Pt/UOP R-8 type Al_2O_3), and to eliminate catalysts with activities too low to be of practical importance. After a favorable screening, some of the more active granular catalysts or their prototypes have been further evaluated for activity and life in the bench-scale reactor with MCH and Decalin at higher temperatures.[a] A sketch and photographs of the MICTR are shown in Figures 87, 88, and 89, in the appendix of reference 19, along with a description of operation details.

Conventional Catalysts

Preparation

The vast majority of catalysts have been prepared by impregnation of various supports with one or more metal salt or metal complex solutions;

---

a) Cf pages 40-42, of this report.

followed by oven drying, and reduction in situ in the MICTR prior to testing. Typically only small quantities of any particular catalyst have been prepared, i.e., a few grams to 50 grams. The amounts of metals employed are within the broad limits of 1 to 30% and most commonly within the limits of 1-10%. Since virtually all the individual metals in the periodic system that are known or can be expected to have dehydrogenating properties were studied earlier or various supports (ref 19, p 121), the principal present effort has been devoted to discovering supported bimetallic or trimetallic combinations equal to or better than supported platinum. This is particularly important in view of the rapidly increasing cost and decreasing availability of platinum during the past year,31) and the possibility of substituting cheaper metal combinations has been emphasized.

MICTR Evaluation With MCH and n-Heptane

Methylcyclohexane Dehydrogenation

The results of the MICTR tests with various catalysts are given in detail chronologically in Tables 66, 67, 68 and 70, in the Appendix of this report. Certain of the results with MCH are summarized in the following tables which contain first order rate constant comparisons with that of the reference catalysts at 752°F (1% Pt/UOP R-8 type Al_2O_3).

Granular catalysts consisting of substantial amounts of platinum on various supports such as alumina, silica, carbon, and magnesia are generally the most active in the MICTR tests. A number of these catalysts have been found to be very active at the higher temperatures used in the bench-scale test, and some of these have better activity-stability with both MCH and Decalin feed than the reference catalysts. The ratio of first order rate constants for some of the better catalysts vs that of the reference catalyst (9874-24) with MCH at LHSV 100 and 752°F are shown in Table 26. Included are typical granular catalysts and some of the earlier candidate catalytic coatings (in granular form). These and subsequent data are based on the conversion of MCH at constant catalyst volume, and since the catalyst densities vary, different weights are charged as shown in column 4 of Table 26. Thus, laboratory catalyst 9874-7 which is 36% denser than the reference catalyst has a 26% higher rate on a constant volume basis. A second factor is variation of surface area and intrinsic activity per unit area. Another factor is catalyst particle size range which is usually controlled within the limits of 10-20 mesh (compare runs 283 and 284, Table 26). For the same charging weight of catalyst 10230-24A which has a relative rate of 1.28 for 10-20 mesh particles, the rate is 1.06 for 10-14 mesh particles and 1.40 for 14-20 mesh particles. Thus, diffusivity is still an important factor influencing the rate in this particle size range.

Part of this study has been devoted to improving the performance of platinum on alumina catalysts. Earlier it was pointed out that higher activity than reference catalyst results on optimizing Pt content and using higher surface area supports.10) Also, as pointed out previously, higher density supports tend to give higher volumetric activity.

Moderate increases in the first order rates of dehydrogenation of MCH results from using complexed platinum solutions neutralized with certain acids on impregnating the same type 1 support with 4% Pt (10280-81C, 81E, and

Table 26. RELATIVE RATES OF MCH DEHYDROGENATION BY THE MORE ACTIVE CATALYSTS

Period: June, 1967 to June, 1968
Reference: 1% Pt/R-8 Al_2O_3 (9874-24; k_{ref} = 1.00)
Tests in MICTR at LHSV, 10 atm pressure at 752°F, no added hydrogen

	Catalyst			
Run No.[a]	No.	Description	Wt Tested	Relative Rate K_c/K_R (752°F)
266,268,270	9874-7	1% Pt/Harshaw 0104 Al_2O_3	0.76 g.	1.26
288	10280-45	5% Pt/type 6 support (repeat of 9874-161B)	0.56	1.26
292	10280-24A	4% Pt/support type 1 10-20 mesh	0.56	1.28
283	10280-24A	4% Pt/support type 1 14-20 mesh	0.56	1.40
284	10280-24A	4% Pt/support type 1 10-14 mesh	0.56	1.06
294	10280-39B	4% Pt/type 2 support	0.400	1.23
296	10280-43D[b]	2% Pt/pelleted type 1 support	0.67	1.28
298	10280-43E[b]	1% Pt/pelleted type 1 support	0.643	1.19
317	10280-33D[b]	4% Pt/type 2 support	0.411	1.33
351	10280-77B	2% Pt/80% type 1 support 20% type 6 binder	0.746	1.38
388	10280-83D	2% Pt/80% type 1 support 20% type 6 binder	0.702	1.23
392	10280-81D	2% Pt/type 1 support	0.705	1.38
415	10280-98B	2% Pt/40% type 1 support 40% type 1 support 20% type 6 binder	0.516	1.31
422	10280-104B	2% Pt/40% type 1 support 40% type 1 support 20% type 6 binder	0.609	1.37
423	10280-106C	2% Pt/80% type 1 support 20% type 6 binder	0.700	1.35
509	10280-121[b]	4% Pt/type 1 support	0.724	1.08

---

a) More detailed information on individual catalyst performance will be found by refering to the appropriate run number in the Appendix Tables, and Summary Tables in the text.

b) Evaluated in bench-scale, cf page 40, of this report.

(Continued)

Table 26(Contd). RELATIVE RATES OF MCH DEHYDROGENATION BY THE MORE ACTIVE CATALYSTS

Run No.[a)]	Catalyst No.	Catalyst Description	Catalyst Wt Tested	Relative Rate K_c/K_s (752°F)
526	10280-129[b)]	4% Pt/type 1 support (muffled at 1097°F)	0.697	1.21
527	10280-130E	4% Pt/type 1 support (muffled at 1097°F)	0.672	1.37

81F compared to control 81A, cf Table 27). Muffling[a)] of these catalysts in air at 1112°F prior to the usual reduction in hydrogen (at 797°F) gives various additional activity improvements in certain instances (i.e., 10280-81A, 81B, and 81D). The effect was adverse in one instance (81C) and without much effect in two other cases (81E and 81F). The higher initial rate of 81F is partly ascribable to a breakdown of particles to smaller dimensions. Generally with catalysts of the 10280-81A type, activity declines only above 1293°F muffling in air (i.e., 1444°F). (Cf catalysts of the 143 series, runs 575-578 and 595-598, Table 68, of the Appendix.) Muffling at 1112°F causes a substantial activity decline in catalysts 9874-139 and 90, and is without effect for ref catalyst 9874-7 (cf run 545 vs 554, 548 vs 555, and 558 vs 557).

Table 27. EFFECT OF NEUTRALIZATION OF PLATINUM IMPREGNATE BY VARIOUS ACIDS ON MCH DEHYDROGENATION ACTIVITY

Period: September-November 1967
Conditions: Same as for Table 26

Catalyst Number 10280-	Pt, %	Acid Used For Neutralization	Run No.	k_c/k_s (752°F)[a)] Dried	k_c/k_s (752°F)[a)] Calcined at 1112°F
81A	4[c)]	None	378,389	1.13	1.21
81B	4	1	379,390	1.18	1.39
81C	4	2	380,391	1.30	1.03
81D	4	3	381,392	1.21	1.38
81E	4	4	382,394	1.31	1.29
81F	4	5	383,395	1.49[b)]	1.45[b)]

a) k_c = first order rate constant of experimental catalyst; k_s = first order rate constant of 1% Pt/R-8 Al_2O_3 catalyst (ref).
b) The 10-20 mesh particles broke down to smaller sizes which would tend to increase activity somewhat.
c) Control.

---

a) Muffling = heating in a muffle furnace.

Various other attempts to disperse platinum on this same support, such as chemical reduction of the complex platinum salt in situ, or longer impregnation of the support with the platinum complex, gave no improvement in activity (cf 10280-143F and 176A, resp; runs 601 and 624 in Table 68, of the Appendix).

A number of older Pt/type 1 support catalysts have been retested for comparison with similar more recently prepared catalysts which appeared less active under present test conditions. Generally, their first order rate constants were lower relative to the reference catalyst, than originally found. This probably results in part from removal of fines[a] less than 20 mesh which is now routinely done. Previously it was shown that the activity increases substantially with decreasing particle size. The results are summarized in Table 28 and detailed in Table 68, of the Appendix.

Table 28. RELATIVE MCH DEHYDROGENATION RATES OF SEVERAL OLDER SUPPORTED Pt CATALYSTS

Conditions: LHSV 100, 10 atm pressure, no added hydrogen 0.9 ml 10-20 mesh catalysts diluted with quartz to 2.0 ml (catalysts prereduced at 797°F)

Run No.	Catalyst No. 9874-	Catalyst Description	k_c/k_s f)	Run No.	k_c/k_s (Older Data)
565	199A	4% Pt a)/type 1 support b)	1.09	205	1.09
570	199C	4% Pt/type 1 support c)	1.29	208	1.44
567	199D	4% Pt/type 1 support c) d)	1.17	207	1.32
568	200B	4% Pt/type 1 support c) e)	1.08	212	1.29
569	200D	4% a) Pt/type 1 support c) e)	1.32	214	1.65

a) Impregnate acidified.
b) Support used as received.
c) Support muffled at 932°F before impregnation.
d) Catalyst muffled at 1095°F in air before testing.
e) Different than used for 9874-199 catalyst series.
f) See footnote (e) Table 27.

A highly active catalyst results at 4% Pt loading of a new spherical type 1 support of high density (0.76) and high surface area (285 m^2/g) (cf catalysts 10280-91A and 91B; Table 66 of the Appendix). A large quantity)436 ml) of a catalyst of the 91B type has been made for evaluation in the FSSTR (10280-113).

A number of additional metals on various supports were also evaluated; and of these only metals A (previously noted) on type 1 or 2 supports, metal B on type 2 support, and metal D on type 1 support appear

---

a) This occurs in some cases by decrepitation resulting from contact with the impregnate solution.

promising (cf Table 29). These have been studied further in various bimetallic and trimetallic combinations on various supports (see later section).

Table 29. RELATIVE MCH DEHYDROGENATION RATES WITH VARIOUS SINGLE METALS ON SEVERAL SUPPORTS

	Catalyst Description			
Run No.	No. 10280-	Metal Type	Support Type	Kc/Ks (752°F)a)
325	140A	10% A	2	0.84
508	119E	1% A	1	0.77
671	185E	4% B	2	0.87
337	66A	4% B	2	0.46
425	102F	5% C	1	0.0
661	172	4% D	1	0.82
486	111B	20% E	1	0.12
485	111A	20% F	1	0.33
290	36	5% G	1	0.0
349	66B	5% G	2	0.0
299	42	5% N	1	0.0

a) See footnote a), Table 27.

Bimetallics

Various promoters of activity for platinum on type 1 or 2 supports have been evaluated in the MICTR. Many of these are listed in Table 30 with their relative rates at 752°F with MCH at LHSV 100. These promoters are either without beneficial effect or are deleterious to platinum activity.

Many supported bimetallics (not containing platinum) have been examined and a few of these have shown some promise. Data for one of these systems is shown in (Table 31). One of the supported (type 1) metals is completely inactive and the other supported metal alone has activity up to 752°F but becomes inactive at 842°F (10280-102F and 66A, resp). Over a wide range of compositions these two metals cooperate with a broad maximum of activity at 662-842°F. The highest rate, however, is only 80% of that of the reference catalyst.

Trimetallics

Many trimetallics on type 1 support have been evaluated in the MICTR with MCH; one of these metals was platinum. None of the metal combinations used in the explorative phase promoted platinum activity, and a number were deleterious (cf Table 32).

Some of the more promising metals were evaluated also in bimetallic or trimetallic combinations in different proportions on type 1 support (cf

Table 30. RELATIVE MCH DEHYDROGENATION RATES WITH SUPPORTED VARIABLE COMPOSITION BIMETALLICS

Period: March-May, 1963

Conditions: LHSV 100, 10 atm pressure, no added hydrogen. 0.9 ml 10-20 mesh catalyst diluted with quartz to 2.0 ml (catalysts reduced in situ).

Run No.	Catalyst No. 10280-	Bimetallic Pt	Bimetallic Promoter	K_c/K_B(752°F)
		Type 2 Support		
667	185A	4%	0% B(Control)	1.0
668	185B	3%	1% B	0.96
669	185C	2%	2% B	0.97
670	185D	1%	3% B	0.84
671	185E	0	4% B	0.87
		Type 1 Support		
624	176A	4%	0	1.14
636	157B	3%	1% B	0.87
635	157A	1%	3% B	0.86
337	66A	0	4% B	0.40
369	79B	1%	0 (Control)	1.00
370	79C	1%	1% C	0.35
371	79D	1%	1% L	0.49
372	79E	1%	1% M	0.93
3[illegible]6	42A	1%	1% M	0.44
373	79F	1%	1% N	0.60
375	80C	1%	1% F	0.68
376	80B	1%	1% E	0.68

Table 33). Once again none of these combinations produced a more active catalyst than platinum alone and some were deleterious to activity.

Table 31. RELATIVE MCH DEHYDROGENATION RATES WITH VARIABLE COMPOSITION BIMETALLICS ON A TYPE 1 SUPPORT

Period:	September-November, 1967
Conditions:	LHSV 100, 10 atm pressure, no added hydrogen 0.9 ml, 10-20 mesh catalyst diluted with quartz to 2.0 ml (catalyst reduced in situ).

Run No.	Catalyst No. 10280-	Bimetallic % C	Bimetallic % B	K_c/K_a
425	102F	5	0	C
426	102A	2	4	0.74
427	102B	5	5	0.78
428	102C	10	4	0.69
446	109B	10	2	0.74
429	102D	5	2	0.69
430	102E	5	6	0.67
337	66A	0	4	0.46

Table 32. RELATIVE MCH DEHYDROGENATION RATES WITH VARIABLE COMPOSITION TRIMETALLICS ON A TYPE 1 SUPPORT[a)]

Run No.	Catalyst No. 10280-	Trimetallic % (1)	Trimetallic % (2)	Trimetallic % (3)	K_c/K_a (752°F)
624	176A	4% Pt	0	0	1.14
657	163A	3% Pt	1% E	1% D	0.88
658	163B	3% Pt	1% F	1% D	0.91
659	163C	3% Pt	1% A	1% D	0.97
660	163D	3% Pt	1% G	1% D	1.04
664	163E	3% Pt	1% H	1% D	0.91
665	163F	3% Pt	1% I	1% D	0.72
639	159C	1% Pt	1% B	3% D	0.94
640	161A	1% Pt	1% E	3% D	0.75
641	161B	1% Pt	1% F	3% D	0.79
643	161D	1% Pt	1% G	3% D	0.89
646	161C	1% Pt	1% H	3% D	0.78
647	161F	1% Pt	1% I	3% D	0.69

a) Period: March-May, 1968, Conditions as in Table 31.

Dehydrogenation of n-Heptane

A cross-section of various catalyst types have been screened for dehydrocyclization of n-heptane to toluene, at LHSV 10, 10 atm pressure, and at 842 and 932°F, without added hydrogen. At complete conversion the combined sensible and reaction heats expected at 932°F would be about 955 Btu/lb for cracking and 1774 Btu/lb for dehydrocyclization. The results of these tests are given in Table 70 of the Appendix, with catalyst 9874-24 used as reference.

Table 33. RELATIVE MCH DEHYDROGENATION RATES WITH VARIOUS AMOUNTS OF SUPPORTED BIMETALLICS AND TRIMETALLICS

Conditions: LHSV 100, 10 atm pressure, no added hydrogen, 0.9 ml 10-20 mesh catalysts diluted with quartz to 2.0 ml (catalysts prereduced at 797°F), temperature = 752°F

Catalyst No. 10280-	Percent by Wt			Run No.	K_c/K_s a)b) (752°F)	Run No.	K_c/K_s a)c) (752°F)
	Pt	A	E				
119A	1	0	0	502	1.05	-	-
121	4	0	0	505	1.13	-	-
119E	0	1	0	508	0.77	-	-
119B	1	1	0	506	0.97	-	-
119C	1	2	0	503	1.06	-	-
119D	1	3	0	507	0.95	-	-
119G	2	1	0	512	0.92	541	1.03
119J	2	2	0	515	1.06	539	1.14
119H	3	1	0	513	1.14	538	1.25
119I	3	3	0	516	1.09	540	1.03
120D	0	0	1	520	0.13	-	-
120A	1	0	1	517	0.70	-	-
120B	1	0	2	518	0.63	-	-
120C	1	0	3	519	0.60	-	-
120E	2	0	1	521	0.79	-	-
120F	3	0	1	522	0.86	-	-
120H	3	0	2	524	0.86	-	-
120G	3	0	3	523	0.74	-	-
122A	1	1	1	532	0.94	-	-
122F	1	1	3	535	0.84	-	-
122D	1	3	3	533	0.93	-	-
122H	3	1	1	536	1.19	-	-
122E	3	3	1	534	1.11	-	-
122I	3	3	2	537	0.93	-	-
122B	3	3	3	529	1.00	-	-
122C	3	1	3	530	1.01	-	-

a) K_c = first order rate constant of experimental catalyst
K_s = first order rate constant of reference catalyst (6874-139) (1% Pt/Al_2O_3 R-8 type).
b) 250°F dried before reduction.
c) Muffled at 1112°C in air before reduction.

Many of the catalysts were completely inactive under these conditions and others formed substantial amounts of cracked products as well as toluene at the highest temperature; little or no hexenes were formed. In several instances almost complete conversion to cracked products occurred (i.e., 6749-33B, 10280-111A, 111B, and 117C; Table 70 of the Appendix). In view of the low allowable space velocity (10) as compared to MCH dehydrogenation (100-200), as well as the undesirable nature of the products, none of the catalysts tested under these conditions appears promising for heat sink usage. In cases where extensive cracking occurs carbon formation would be expected to limit catalyst life. However, a very active cracking catalyst might be useful as a dispersed phase catalyst (especially if some dehydrocyclization also occurred).

Catalytic Coatings

Preparation and Granular Evaluation With MCH

Preliminary experiments were made by coating stainless steel with thin layers of catalyst supports. Stainless steel strips (1" x 2") were first sand-blasted and then degreased with acetone, prior to coating most of the trials were made by starting with wet paste mixtures prepared from type 1 supports and various binding materials. The pastes were emplaced by smearing with a spatula on the strips and in some cases a scalp massage vibrator was used to smooth the thixotropic coating. After drying in air and at 284°F, strips with coatings having good adhesion were heated in a muffle furnace at 932°F or lower temperature for a further check. Coatings were about 20 mils in thickness. Coating candidates were also placed on the exterior of roughened hypodermic tubing,[a] stainless steel screen, or made as granular supports which after platinizing were tested in the MICTR. Evaluation of platinized granular formulations is convenient and useful to determine the catalytic efficacy of the coatings. The evaluation of mechanical properties of the earlier coatings is shown in Table 69 of the Appendix which gives the number of granular or tube catalysts derived therefrom. Good adhesion was obtained with an 80% mixture of finely ground fibrous type 1 support and particulate type 1 supports (1:1) and 20% type 6 binder (formulation I), or with a particulate type 1 supports and type 6 binder (4:1) (formulation II). Supports of this type (after platinizing) are very active for MCH dehydrogenation (cf Runs 415, 417 and 492, in Table 35, next section).

A large number of these catalysts have shown activity exceeding that of the reference catalyst and equaling that of the best previously prepared granular catalysts on the same volume or weight charging basis (i.e., 77A, 77B, 106C, 75E, 59B, 89B, 98C, 104B, 92A, 92B, 92C and 98D). The most satisfactory non-shrinking and adherent formulations are still those prepared from fibrous and particulate type 1 supports and type 6 binder. Adherence to sand blasted stainless steel strips is reasonably good, but further improvement in this respect is desirable. Attempts were made to raise activity per unit volume by using a high density (low surface area) type 1 particulate support in the formulation, but little is gained in activity per unit volume in raising the density beyond about 0.7. The best result has been obtained with catalyst coating formulation 10280-98C with 3% Pt loading (cf Table 34). Impregnation of coating materials with another metal, that is almost as active and selective as platinum at high MCH conversion, led to similar results obtained earlier with this metal on conventional supports which were side reactions leading to benzene and cracked products (catalysts 10280-104C and 106D).

---

a) 8" long x 0.11 dia. with 0.012" wall thickness, crimped at ends.

Table 34. RELATIVE MCH DEHYDROGENATION RATES WITH VARIOUS CANDIDATE CATALYTIC COATINGS (GRANULAR)

Period: September – November, 1967
Conditions: LHSV 100, 10 atm pressure, no added hydrogen
0.9 ml 10-20 mesh catalysts diluted with
quartz to 2.0 ml (catalyst reduced in situ)

Catalyst No. 10280-	% Pt	Support Description	Support Adhesion To Metal Strip	Run No.	Bulk Density	k_c/k_s[c] (752°F)
63A	4	80% type I support - 20% type 6 binder	Good	311	0.36	1.10
77A	2	40% type I support (1), 40% type I support (2) - 20% binder type 6	Good	492[f]	0.54	1.25
77B	2	80%[a] type I support - 20% binder type 6	Poor	351	0.85	1.38
106C[d]	2	80%[a] type I support - 20% binder type 6	-	423	0.77	1.35
71A	1	41% type I support (1), 41% type I[a] support (2) - 18% binder type 6	Good	339	0.47	1.00
71C	2	41% type I support (1), 41% type I[a] support (2) - 18% binder type 6	Good	340	0.50	1.16
75E	2	41% type I support (1), 41% type I[a] support (2) - 18% binder type 6	-	338	0.56	1.27
63B	4	41% type I support (1), 41% type I[a] support (2) - 18% binder type 6	Good	312	0.50	1.05
58A	4	80%[a] type I support - 20% binder type 6	Fair	306	0.77	1.08
58B	4	80%[a] type I support - 20% binder type I	Poor	314	0.58	1.10
83A	1	80% type I[b][e] support - 20% binder type 6	Good	381	0.82	0.54
83B	2	80% type I[b][e] support - 20% binder type 6	Good	386	0.81	1.11
98A	1	40% type I support (1), 40% type I[b][e] support - 20% binder type 6	Good	414	0.56	1.11
98B	2	40% type I support (1), 40% type I[b][e] support - 20% binder type 6	Good	415	0.56	1.31

a) Ball milled.
b) As received.
c) k_c = first order rate constant of experimental catalysts. k_s = first order rate constant of 1% Pt/R-8 Al_2O_3 catalyst (ref.).
d) Prepared for bench scale test evaluation.
e) Surface area 8.7 m^2/gm.
f) Repeat of Run 350, c.f. Table 66 of the Appendix.

Table 34 (Contd). RELATIVE MCH DEHYDROGENATION RATES WITH VARIOUS CANDIDATE CATALYTIC COATINGS (GRANULAR)

Catalyst No. 10280-	% Pt	Support Description	Support Adhesion To Metal Strip	Run No.	Bulk Density	k_c/k_s (752°F)
89A	1	40% type I support (1), 40% type I support[a][b] (2) - 20% binder type 6	Good	397	0.62	1.15
89B	2	40% type I support (1), 40% type I support[a][b] (2) - 20% binder type 6	Good	398	0.54	1.37
96B[c][d]	2	40% type I support (1), 40% type I support[a][b] (2) - 20% type 6 binder	-	411	0.44[e]	1.04
96C[c][d]	2	40% type I support (1), 40% type I support[a][b] (2) - 20% type 6 binder	-	412	0.67	1.20
98E	2	40% type I support (1), 40% type I support[a][b] (pelleted)	-	413	0.74	1.04
98C	3	40% type I support (1), 40% type I support[a][b] (2) - 20% type 6 binder	-	417	0.62	1.47
98D	4	40% type I support (1), 40% type I support[a][b] (2) - 20% type 6 binder	-	418	0.63	1.16
104B[f]	2	40% type I support (1), 40% type I support[a][b] (2) - 20% type 6 binder	-	422	0.67	1.37
92A	1	27% type I support (1), 53% type I support[b] (2) - 20% type 6 binder	-	405	0.75	1.28
92B	2	27% type I support (1), 53% type I support[b] (2) - 20% type 6 binder	Good	406	0.79	1.28
92C	1	13% type I support (1), 67% type I support[a][b] (2) - 20% type 6 binder	Good	408	0.79	1.31
92D	2	13% type I support (1), 67% type I support[a][b] (2) - 20% type 6 binder	Good	409	0.81	1.26
83C	1	80% type I support[b][g] - 20% type 6 binder	Poor	387	0.75	1.06
83D	2	80% type I support[b][g] - 20% type 6 binder	Poor	388	0.78	1.23
89C	1	85% type I support[a][b] - 15% type 6 binder	Fair	403	0.83	1.24
89D	2	85% type I support[a][b] - 15% type 6 binder	Fair	404	0.84	1.25

a) Ball milled.
b) Surface area 11.3 m^2/gm.
c) Impregnate carbonated.
d) Catalyst calcined at 1112°F.
e) Lower density because platinum impregnating solution added during mixing support ingredients.
f) Prepared for bench scale test evaluation.
g) As received.

Further experimentation has been carried out with the adherent synthetic fibrous-particulate type 1 support mixture with the type 6 binder (formulation I; 40:40:20). Satisfactory adherence and activity (when platinumized) result when particulate type supports ranging from 7 to ~278 m^2/g are used; the latter giving an overall surface area of ~250 m^2/g. The use of a highly alkaline type 17 binder leads to poor metal adherence and poor activity on platinization (cf run 544 and 546 of Table 67 of the Appendix). Various treatments of formulation I type support, or catalysts derived therefrom, have somewhat different effects than the corresponding treatments on conventional supported catalysts where these treatments resulted in improved activity. Acid neutralization of the impregnate decreases the relative dehydrogenation rate from 1.12 to 0.81 (catalysts 133A vs 133B, Table 35). A lower relative rate (0.98 vs 1.12) is obtained on drying the support at 259°F instead of muffling at 1112°F, before metal impregnation (cf catalysts 133C vs 133A, Table 35). A slightly decreased relative rate (1.06 vs 1.12) results from muffling the finished catalyst in air at 1112°F (cf catalysts 133D vs 133A, Table 35).

Substitution of 40% of type 2, 10, or 19 supports (formulations III, IV, or V) for 40% particulate support 1 (formula I) leads to satisfactory adhesion to stainless steel particularly if first coated with binder 18, as described below. Formulation III was designed to raise the surface area of various formulations I from the range of 120-250 m^2/gm to ca 500 m^2/gm (cf granular catalysts 117A and 117B, cf Appendix, Table 67). Granular supports of these types give catalysts with activity equal to or greater than the reference catalyst.

Addition of 12% of an oxidizable particulate metal dust (type 15) to formulation I gives some improvement in adhesion and a satisfactory granular catalyst support (cf catalysts 131A and 131B, of Appendix, Table 67). This metal in finely divided flake form was found to be highly reactive with water in the formulation, with resultant frothing and heating up to form a highly porous friable support which was not usable.

Substitution of a fibrous mineral (type 16) for the fibrous synthetic type 1 support in formulation I has been studied. The former is readily available while the latter is no longer manufactured. One finely ground sample led to a formulation (40% type 1, 40% type 16, 20% type 6 binder) that when platinized had satisfactory activity (cf catalyst 140A, Table 35). This formulation (VI) is less thixotropic when wet and gives poorer metal adhesion after muffling than formulation I. Two other samples of type 16 material give formulations which crack and strip from metal even on air drying. Formulations of this type can probably be improved as to adhesion.

There are various problems associated with bonding a thin catalytic coating onto metal so firmly that it adheres well at variable elevated temperatures and survives temperature cycling. First, there is a difference in two dimensional thermal expansion between the coating (an insulator) and the metal which on heating induces mechanical strain on the coating. Second, a tight bond is necessary between the catalytic coating and the metal wall so that coating should have some elasticity to prevent "stripping" and thus allow efficient heat exchange between the metal wall and the reacting fluid. Third, the coating itself must have good mechanical strength, so it remains in situ for a long period of time in use. An upper limit is set upon the strength of

Table 35. RELATIVE MCH DEHYDROGENATION RATES WITH VARIOUS CANDIDATE CATALYTIC COATINGS (GRANULAR)

Conditions: LHSV 100, 10 atm pressure, no added hydrogen, 0.9 ml 10-20 mesh catalysts diluted with quartz to 2.0 ml (catalysts prereduced at 797°F) (cf test data Table 67 of the Appendix). T = 752°F.

Catalyst No.	Pt, %	Support Description	Run No.	Bulk Density	k_c/k_s[a)]
9874-139	1	UOP R-8 type Al_2O_3 (ref)	543, 559	0.47	1.00
10280-133A	3	40% type 1 support (1) - 40% type 1 support (2) - 20% type 6 binder[b)]	552	0.53	1.12
" -133B	3[d)]	40% type 1 support (1) - 40% type 1 support (2) - 20% type 6 binder[b)]	563	0.53	0.81
" -133C	3	40% type 1 support (1) - 40% type 1 support (2) - 20% type 6 binder[c)]	564	0.55	0.38
" -133D	3	10280-133C muffled at 1112°F[b)]	561	0.52	1.06
" - 77A	2	40% type 1 support (1) - 40% type 1 support (2)[e)] - 20% type 6 binder	492	0.56	1.24
" -131A	3	39% type 1 support (1) - 39% type 1 support (2) - 12 oxidizable metal - 10% type 1 binder[c)]	553	0.55	1.10
" -131B	3	39% type 1 support (1) - 39% type 1 support (2) - 12 oxidizable metal - 10% type 1 binder[d)]	560	0.62	1.10
" -117A	2	40% type 1 support - 40% type 2 support - 20% type 6 binder	487	0.37	1.19
" -117B	4	40% type 1 support - 40% type 2 support - 20% type 6 binder	488	0.37	1.12
" -140A	3	40% type 1 support - 40% type 16 support - 20% type 6 binder	556	0.33	1.03

a) k_c = first order rate constant of experimental catalyst.
k_s = first order rate constant of reference catalyst 9874-139.
b) 1112°F muffled support used for impregnation.
c) 259°F dried support used for impregnation.
d) Acid neutralized impregnate.
e) Different type than used for catalyst 10280-133 series.

the catalytic coating since it must have a substantial pore volume and surface area to perform properly and therefore cannot be as hard or bonded as tightly as a sintered nonporous ceramic coating. Some of these problems can be resolved mechanically but certain of them are inherent.

The above described tests were carried out with sheared 1- x 2-in. strips of stainless steel and consequently had cambered shapes. This causes unequal stress in the longitudal direction on muffling in air and therefore an uneven strain on the catalytic coating. Mild steel strips have been obtained for coating studies which have been band sawed to shape to avoid this problem. This metal oxidizes more readily on muffling than stainless steel but this would not occur in a reducing atmosphere.

An improvement has been made in binding formulation I type material to steel surfaces. The cleaned surface is given three applications of 5% aqueous type 18 binder. Each coating is air dried, and finally the triple coat is air dried and muffled at 752°F for 1 hour. This apparently forms a glass like surface bond to the metal and in turn forms a good bond to the formulation. Also it reduces oxidation on muffling in air. All 1/4" OD reactor tubes coated with catalyst coatings were first coated with type 18 binder (cf next section, Table 36). Pt coated binder is inactive (cf run 592, in the Appendix, Table 67).

Various formulations were coated onto the walls of 1/4" OD tubing, the tubing wall thickness was usually 0.028". A fairly well controlled thickness was obtained by first partly filling the upper end of a tube with the thixotropic formulation and then drawing a Teflon plunger through (both ends tapered) with the desired diameter. The tubes were dried at 126°C, the excess coating drilled out with a No. 10 numbered drill to the desired coating length, and then muffled at 752°F. This was followed by filling the tube with the platinum or other impregnating solution, followed by drying and reduction in situ. Thicknesses were varied from ca 4 to 13 mils, and were usually around 7-1/2 to 8-1/2 mils. An effort was made to keep the platinum content in the 2-3% range. This could be determined accurately only by drilling out a catalyst coating and having the platinum content analyzed. The net gain in weight on platinizing is a very insensitive measure of platinum content because of the considerable tube weight (~38 gm) as compared to catalyst weight (0.1-1.0 gm) of which the Pt content is only 2-3%.

Coating Evaluation With MCH

The results obtained with various catalytically coated 1/4" tubes on HICTR testing with MCH are summarized in the following Table 36, and given in more detail in Table 68 of the Appendix.

At constant pump rate (90 ml/hr), corresponding to an MCH LHSV of 100 with conventional granular particles, 8" coated tubes 1 and 2 give higher relative rates than the reference catalyst, particularly on the same catalyst weight basis (cf last column of Table 36). As with all the other coated tubes described in Table 36 higher rates are obtained if quartz packing is used to create turbulence. An unpacked tube has an estimated Reynolds number of ca 350, at 752°F (i.e., lamellar flow range). In part, higher activity results from a thin longer catalyst zone (8 vs usual 4") which allows better heat exchange so the catalyst operates closer to the block temperatures than the shorter bed granular catalysts. Activity increase also has been shown with identical amounts of ref catalyst 9874-24 by doubling the diluted bed length from 4 to 8" which gave an apparent rate increase of 46%, and with the other ref catalyst (9874-139) an increase of 29% (cf runs 333 vs 334 and 603 vs 604, Appendix Tables 66 and 68). Also, finer particle size (synonymous with a thin layer) was shown earlier to give an increase in rate (cf Table 36).

Three tubes (3,4, and 5) coated with different weights and thicknesses of platinized formulation 1 gave about the same high rates without quartz packing and higher and equivalent rates with quartz packing. The highest rate of this series vs that of an equivalent weight of ref catalyst was with the tube with the thinnest coating (tube 5, quartz filled, run 610).

A thin coated tube (10) with 4" bed length gave a high relative weight rate (7.32) when quartz packed. Annular tubes 0.125" dia or 0.177" dia were centered in the catalyst tube to create turbulence. However, the increase in turbulence might be more than counterbalanced by the decrease in contact time. The relative rates decreased, and a recheck of the quartz filled coated tube showed the relative activity had declined during this series of tests, probably because of mechanical injury and loss occurring while making the physical arrangements. The experiment will be repeated.

The highest relative weight rate was obtained with a quartz filled tube (7) coated with formulation III support (cf run 600). High rates were also obtained with formulation IV coated tubes, and repeat runs with and without quartz gave about the same results.

Another metal (A) performed better, relative to platinum, on a coated tube than on granular support at high conversion, however, some benzene was formed in addition to toluene. Experience with the bench-scale tests indicates a gradual loss of activity. A second metal (D) performed fairly well but was not a serious competitor (run 617, Appendix, Table 68).

These overall results show considerable promise for the use of this catalyst coating for the proposed endothermic catalytic heat exchanger and this effort will be continued.

A few experiments were carried out with an 80 mesh Pt-Ir (90:10) screen which weighed 0.85 gm. This was loaded into a 1/4" OD reactor tube and MCH passed thru it at a rate of 45 ml/hr. The screen was inactive, in this form and also when coated with 0.23 gm of Pt black (cf runs 327 and 330, Table 66 of the Appendix).

Table 56. EVALUATION OF MCH DEHYDROGENATION WITH VARIOUS CATALYTICALLY COATED TUBES WITH DIFFERENT PHYSICAL ARRANGEMENTS

Pt impregnated unless otherwise noted
Conditions: same as for Table 55, constant pump rate (90 ml/hr)

Run No.	Catalyst No. 10280	Tube No.	Coating			Quartz in Tube	wt, % Conv to Toluene			K_c/K	Relative Rate, vs 0.42 g of catalyst
			Grams	Thickness, mils	Length		662	752	842°F		
582	151	1	0.239	7.5	8"	–	26	71	81	1.89	3.38
583			(Form 1)			X	37	76	97	2.19	3.92
584	152	2a)	0.406	11.5	8"		29	61	77	1.45	1.52
585			(Form 1)			X	41	75	96	2.11	2.22
586	158	3	1.00	15	8"		36	63	78	1.54	0.65
587			(Form 1)			X	30	71	92	1.98	0.83
588	158	4	0.663	8-1/2	8"		29	59	77	1.37	0.66
589			(Form 1)			X	31	72	93	1.95	1.20
590	158	5	0.291	~4	8"		27	64	85	1.59	2.38
591			(Form 1)			X	41	76	93	2.18	3.44
615	170	11	0.228	~6	8"		31	67	85	1.77	3.26
610			(Form 1)			X	32	81	98	2.02	3.79
627	170	10	0.0889	~6	4"		22	46	60	0.98	4.64
626			(Form 1)			X	28	62	87	1.55	7.32
634	170	10	0.0889	~6	4"	b)	23	47	62	0.97	4.64
651			(Form 1)			c)	17	40	60	0.77	3.69
676	170	10	0.0889	~6	4"	e)	15	25	31	0.44	2.12
679d)			(Form 1)			X	26	48	72	1.00	4.8
599	165	7 (Form III)	0.073	7.5	9"		27	65	83	1.60	9.4
600						X	29	74	93	2.04	11.9
649	178B	13 (Form IV)	0.327	8.5	7.75	X	32	76	96	2.17	2.73
650	178C	14 (Form IV)	0.167	8.5	4.25	X	31 2	77 7	96	2.23	5.70
672	178B f)	13	0.327	8.5	7.75	X	29	76	96	2.17	2.82
673	178C g)	14	0.167	8.5	4.25	X	28	69	93	1.77	4.53
620	173	8 (Form 1)	1.145 h)	7.5	7.5	X	25	57	68	1.28	3.76
618							37	79	96	2.40	7.05
617	173	9 (Form 1)	0.335 i)	7.5	7.5	X	26	50	64	1.05	1.33

a) Wall thickness 0.032", all others 0.028".
b) Zone above catalyst filled with quartz.
c) 0.125" diameter annular tube centered inside coated reactor tube.
d) Recheck of run 626 on original catalyst activity.
e) 0.177" diameter annular tube centered inside 1/4" OD coated reactor tube.
f) Repeat of run 650.
g) Repeat of run 651.
h) Impregnated with metal A.
i) Impregnated with metal D.

Nonconventional Catalyst Systems

Homogeneous and Dispersed Catalysis

As discussed in an earlier report[19] an area of catalyst modifications which could be extremely useful to heat sink applications involves providing a catalyst dispersed in either a discrete or molecular state, which could be introduced with the fuel in the heat exchange zone of an engine, and then proceed to the combustion chamber through the nozzle. Here we are investigating, in a preliminary way, possible fuel soluble or fuel dispersible catalytic materials, and testing them for their effect on the MCH dehydrogenation reaction.

Most of the preliminary work to date has involved the simple process of adding MCH and the catalyst in the desired amounts to a stirred autoclave and then observing the pressure rise during the vaporization and reaction. Analyses were by GLC. Several materials have shown catalytic activity at 1 percent metal (basis weight of MCH) at 800-1000°. Nearly all tests have been run in the virtual absence of oxygen.

Results from the autoclave tests have been tabulated in Table 37. Catalysts used have come from both commercial sources and lab preps. Some encouraging results have been obtained in a few cases, and actually most of the compounds tested have produced at least some activity compared to the neat MCH base case.

One material (Runs 126-129, 153-155) showed remarkable activity, and in Runs 126 and 127, with good specificity to toluene and benzene. H_2 pressure developed to high levels for these runs also. Unfortunately, the activity of this catalyst has proven to be elusive and nonreproducible. The other runs shown for this catalyst represent efforts to find the cause for this nonreproducibility, by varying temperature and oxygen content of the blanketing gas. Run 130 combined the catalyst of interest with the catalyst tested in run 125 to check out the possibility of synergism by contamination with the previous catalyst. The activity state of the autoclave surface has also been considered as a possible factor in this enigmatic behavior, but has not been investigated. So far, all efforts have failed to reproduce the excellent results of Runs 126 and 127.

Two compounds (Runs 124 and 125) gave about 50 percent total conversions, but these appear to act mainly as cracking catalysts, since most of the products were lower molecular weights than MCH. Another active catalyst which appears to fit in the cracking category is that of Runs 143, 146, 156, and 158.

Runs 118 and 119 are also of interest because of their relatively high total conversions to dehydrogenation products (ca 25 percent toluene, benzene, and methylcyclohexenes).

The degree of activity displayed by these compounds is encouraging, although most are less soluble than would be desired. The results may, in some instances, point the way to modifications in the organic ligands which will improve this and other properties. We have also been doing some work on the concept of using small amounts of special solvents (solubilizing agents)

Table 37. DISPERSED PHASE DEHYDROGENATION OF MCH

Catalyst additions = 1.0%w metal, basis weight of MCH

Catalyst Run LMP,27-	Catalyst Reference Number	Conversion to Products[b]					Maximum Pressure, psig	O₂ Content of Helium Atmosphere, ppm	Steady State Temperature, °F	Exposure Time, hours	
		Toluene	Benzene	Methylcyclohexene	Unidentified and/or Light Products	Total				At Steady State	Total
87	1	0.1	-	0.1	0.2	0.4	175	147	785	0.7	6.6
88	2	0.1	-	0.1	0.4	0.6	170	147	805	2.8	7.3
89	3	0.3	0.1	0.5	0.2	1.1	150	147	799	2.8	6.9
90	5	1.8	-	0.5	1.7	4.0	146	147	784	4.4	6.4
95	6	0.3	0.8	0.2	[illegible]	1.2	173	147	844	2.7	7.4
96	8	1.1	Trace	0.9	0.4	2.4	137	147	796	1.0	7.3
97	8	0.5	-	[illegible]	0.5	1.7	100	147	844	3.9	6.3
98	10	1.3	0.1	0.5	0.2	2.1	150	147	797	2.7	7.8
100	10	0.4	Trace	0.7	0.2	1.3	113	147	803	3.4	7.0
101	12	0.1	-	3.0	0.4	3.7	125	147	800	0.9	6.8
102	13	0.1	-	0.6	0.2	0.9	114	147	835	2.9	5.8
103	14	0.1	-	0.1	0.2	0.4	115	147	832	3.6	7.9
104	15	0.1	-	0.3	0.2	0.6	111	147	798	3.3	6.9
105	16	0.1	-	0.2	0.2	0.5	120	147	748	1.2	6.9
106	17	0.1	-	0.3	0.2	0.6	148	147	800	2.7	7.8
107	18	0.1	-	0.1	0.2	0.4	78	147	803	3.1	6.2
108	19	0.4	0.4	0.1	0.2	1.1	87	147	802	3.9	7.8
109	20	0.4	0.1	0.4	0.5	1.4	92	147	801	3.1	8.2
110	21	0.1	Trace	0.1	0.2	0.4	73	147	803	6.5	7.4
111	22	0.1	-	Trace	0.3	0.4	133	147	811	5.0	7.4
112	23	4.2	Trace	2.8	4.5	10.9	145	147	848	4.75	6.6
113	23	3.0	Trace	4.5	8.9	16.4	117	147	846	6.0	8.1
114	25	3.8	-	3.0	6.9	13.7	152	147	845	7.2	8.3
115	26	7.4	-	3.0	9.0	15.4	143	147	848	6.5	7.8
95	7	-	-	-	-	-	130	147	846	0.33	8.0
117	27	9.3	4.4	3.2	9.6	26.5	191	147	846	3.7	7.4
118	28	16.2	2.6	1.3	3.1	23.2	147	147	900	4.8	6.9
119	29	17.0	5.6	0.9	2.6	26.1	158	147	900	6.4	8.4
120	30	2.3	0.5	3.0	6.5	12.3	82	147	900	4.8	7.1
121	31	4.4[c]	2.9[c]	5.5[c]	31.8[c]	44.6[c]	252	147	901	4.5	6.8
122	32	0.6	0.5	2.4	8.6	11.9	100	147	900	4.5	5.4
123	33	[illegible]	1.5	5.4	[illegible]	23.1	109	147	900	5.8	7.0
124	34	4.4	4.1	6.8	34.5	49.8	135	147	900	4.1	7.2
125	35	3.2	3.1	6.5	39.6	52.4	148	147	907	7.0	9.8
126	36	33	47	1.7	3.1	84.8	500	147	910	4.0	6.0
132	36	5.1	1.0	0.8	2.3	9.2	126	964	900	4.0	6.2
133	36	13.3	2.5	1.1	3.0	19.9	134	(1.31%)	900	4.3	8.3
134	36	6.0	0.8	1.7	1.7	10.2	103	(Air)	900	4.3	6.6
127	36	21	30	1.1	2.0	54.1	532	147	997	6.8	8.0
128	36	0.8	0.4	0.5	1.2	2.9	73	147	799	6.3	6.9
129	36	4.8	3.9	1.1	13.7	23.5	121	147	948	6.0	7.2
130	36, 40	2.1	1.0	1.2	3.1	7.4	121	147	846	7.6	8.3
131	41	8.2	[illegible]	1.6	4.8	9.[illegible]	[illegible]	1.6	900	2.0	6.0
136	42	3.7	0.6	0.2	4.7	11.2	[illegible]	1.6	900	5.3	7.6
137	43	4.9	0.6	1.4	2.8	9.7	89	1.6	896	5.8	7.8
138	44	4.7	0.4	1.4	1.6	8.1	93	1.6	900	5.0	7.0
139	45	1.6	0.2	1.1	2.2	5.1	77	1.6	900	3.4	8.0
140	46	1.0	0.4	0.7	3.3	5.4	81	1.6	903	3.7	7.2
141	47	1.2	0.4	1.3	4.0	6.9	90	1.6	901	3.7	8.2
142	48	0.6	0.2	0.7	4.5	6.0	111	1.6	846	3.3	8.0
156	49	3.3	2.2	0.6	29.4	35.5	145	1.6	1011	2.0	3.1
158	49	3.8	4.4	0.5	27.6	36.7	195	1.6	1004	4.9	5.7
145	49	1.9	0.2	1.8	46.6	49.5	87.5	1.6	901	6.2	8.0
146	49	-	Trace	3.4	40.0	40.4	59	1.6	7.4	6.0	8.1
147	52	0.8	0.2	0.9	3.8	5.7	73	1.6	901	6.0	8.2
148	53	0.4	0.2	0.8	2.1	3.5	76	1.6	900	4.0	7.0
149	54	0.2	0.1	0.7	2.2	3.2	83	1.6	900	2.8	5.6
150	55	0.2	0.1	1.0	3.0	4.3	73	1.6	900	5.3	8.2
151	56	0.2	0.1	0.7	1.8	2.8	77	1.6	901	2.8	6.7
152	57	0.2	0.2	1.0	3.[illegible]	5.0	73	1.6	901	5.2	7.3
159	50	1.8	0.5	1.4	3.2	6.9	104	1.6	900	5.2	6.2
163	66								901	4.0	6.8
164	64								900	4.0	6.2
165	65								898	5.4	7.0
116 (no catalyst)	-	0.1	Trace	0.1	0.2	0.4	112	147	878	5.5	7.42
90 (R-8, Pt/Al₂O₃)	4	4.1	Trace	0.5	0.5	42	515	147	805	.75	8.62

a) MCH purity was 99.9%.
b) Analysis of liquid products by GLC.
c) Some of these values are erroneously high due to the presence of a solubilizing solvent added with the catalyst.

64458

to improve the solubility of organometallic compounds. Solvent agents which have been used for this purpose are listed in Table 38. A number of new catalysts have been prepared or purchased and are now available for testing.

Table 38. CANDIDATE SOLUBILIZING AGENTS FOR DISPERSED PHASE CATALYSTS

Isopropyl Alcohol
Methylene Chloride
Phorone
Morpholine
2-Nitropropane
Toluene
Ethyl Acetate
1/3 each: DMF, Acetone, n-Heptane

Acetone
Dimethylformamide (DMF)
Dimethylsulfoxide (DMS)
Piperidine
Butyric Acid
n-Heptane
Hexamethylphosphoramide

However, we have been involved recently in a reassessment of our experimental approach. The type of test described above, utilizing the 350 ml stainless steel autoclave, was only intended to be a way of taking a first look at catalyst activity. The present method suffers from the very slow heating rate, possibly over an hour being required to reach a 900°F steady-state test temperature. This is undesirable since the gradual heating regime of these tests may be detrimental to the reactivity of some of the catalysts, which would be true, for example, if the active form of the catalyst were in the nondecomposed state. We would prefer to heat the autoclave to its reaction temperature, and then add the reactant and catalyst.

A further complication with the original bomb test involved the accessibility of the reactant mixture and product vapors to the upper recesses of the stirring mechanism. Since the Magne-Dash required water cooling, the result has been a comparatively cold zone in the top of the bomb where condensation could occur. Deposits formed were difficult and time consuming to remove. Moreover, back-contamination from this source could have been the cause of some anomalous results encountered in the past. In order to improve this situation, we have obtained and adapted a non-stirred autoclave. It is planned to use a magnetic stirring bar, driven from the base, to stir this autoclave. The cover is equipped with 1/4-inch openings through which liquids can be charged, so that materials can be charged after the bomb is hot. Also, no dead space exists where contaminants can build up. The new equipment is ready to be pressure tested under temperature. We will also examine the possibility of using the pulse reactor (cf p. 21) for testing similar types of materials as catalysts for MCH dehydrogenation.

Feasibility Calculations on Dispersed Phase Catalysis

Our confidence in the ultimate success of the dispersed catalyst approach has been reinforced by the results of some rather simple calculations of the reaction possibilities between MCH and a molecularly dispersed catalyst in a flowing system. Conditions chosen were those of interest for a regeneratively cooled system. A computer program for a plug flow tubular reactor was adapted for a variable molar flow and used to calculate MCH conversion and temperature as a function of reactor length.[a]

For a plug flow tubular reactor with variable molar flow the reaction rate, according to collision theory, is

$$\frac{dy}{dt} = \Omega p\, e^{-E/RT}\, \frac{1 - f_C - y}{1 + 3y} \quad \text{where } \Omega = \sigma^2 \sqrt{\frac{8\pi kT}{\mu}}\, \frac{N_\Omega P}{RT}\, f_C, \tag{3}$$

collisions/molecule-sec; the heating rate is

$$\frac{dT}{dt} = \frac{4}{D} \times \frac{RT}{P} \times \frac{F_H}{c_p} - \frac{\Delta H_d}{c_p} \times \frac{dy/dt}{1 + 3y} \tag{4}$$

where heat is transferred through the tube wall at a constant heat flux, F_H, and the velocity is

$$\frac{dL}{dt} = \frac{4}{\pi D^2} \times \frac{RT}{P} \times n_{T_0}(1 + 3y) \tag{5}$$

The variables used in the calculations were taken from previous work and are consistent with those used in the packed bed reactor calculations:

1) Heat capacity,

for MCH $c_p = 79.1 + 0.0363(T - 1460°R)$, Btu/mole-°R

for H_2 $c_p = 7.099 + 0.00272(T - 1460°R)$

for toluene $c_p = 55.9 + 0.0238(T - 1460°R)$

total stream $c_p = \dfrac{26.1 + 4.44y + (0.0363 - 0.0043y)T}{1 + 3y}$

2) Heat of dehydrogenation,

$\Delta H_d = 92{,}500$ Btu/mole at 1460°R

$= 92{,}500 + 1.90(T - 1460°R) + 0.0022(T - 1460°R)^2$

3) Tube diameter,

$D = 3/8$ in. (cross-section area = 0.00110 ft^2)

---

[a] The program was developed and the calculation made by Dr. Roger Hite.

4) Initial flow rate,

n_{T_0} = 928 moles/hr-ft^2
= 1.08 x 10^{-4} moles/sec (LHSV = 103)

5) Heat flux,

F_H = 5 x 10^4 Btu/hr-ft^2

6) Initial temperature,

T = 1000°F

7) Tube length,

L = 10 ft

8) Activation energy,

E = 12.0 kcal/g-mole

9) Initial pressure,

P = 1000 psia (assumed constant)

10) Collision frequency, Ω

Assuming molecular diameters (σ) of 6.1 A for MCH and 3.8 A for the catalyst, the collision frequency is

$$\Omega = 11.26 \times 10^9 \frac{f_C P}{T} \text{, collisions/molecule-sec}$$

11) Collision efficiency, p.

12) Concentration of catalyst, f_C, mole percent

The results of several calculations are shown in Table 39 below. Since the reaction rate is proportional to the two unknown parameters p and f_C, these have been lumped together in the table so that the yield, temperature, and space velocity are presented as a function of the combined parameter pf_C. In Figure 20 the results have been plotted assuming a catalyst concentration of 1%m, which is a feasible concentration for a cheap catalyst (such as CuO). This shows that even at very modest collision efficiencies high reactivities are indicated in the temperature region of most interest to us (500-1200°F).

Additional mathematical exploration of this system will be done in a future period.

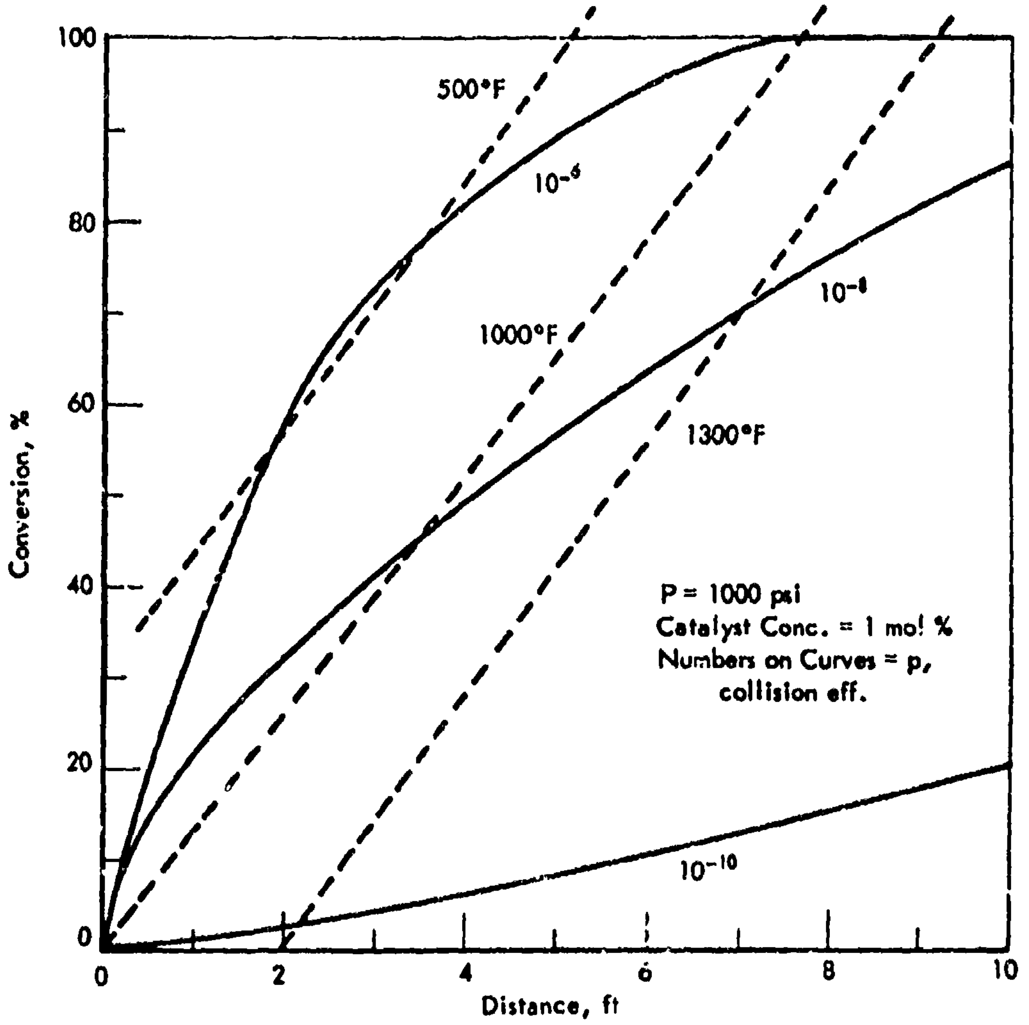

Figure 20. CALCULATED DEHYDROGENATION OF MCH BY VAPOR PHASE CATALYSIS

Table 39. MCH DEHYDROGENATION: VAPOR PHASE CATALYSIS

Distance, ft	2.5	5.0	7.5	10.0
Results for $pf_C = 10^{-6}$				
Temp, °F	491.0	635.5	946.7	1330.0
Conversion, %	67.4	89.9	99.9	100.0
Time, sec	0.70	1.19	1.54	1.79
Results for $pf_C = 10^{-8}$				
Temp, °F	947.9	1125.2	1330.9	1565.6
Conversion, %	38.0	57.5	73.7	86.2
Time, sec	0.72	1.18	1.52	1.77
Results for $pf_C = 10^{-10}$				
Temp, °F	1340.2	1625.2	1882.8	2125.3
Conversion, %	3.3	8.8	15.1	21.4
Time, sec	0.98	1.71	2.27	2.71
Results for $pf_C = 0.0$ (no catalyst)				
Temp, °F	1371.8	1695.7	1986.5	2252.7
Time, sec	1.01	1.85	2.57	3.21

Thermal Stability

Tube Deposit Rating Methods

With the objective of providing a piece of equipment which would combine a standardized test of fuel thermal stability and also of catalyst activity, the Catalyst and Fuel Stability Test Rig (CAFSTR) was designed and built last year. However, the CAFSTR heat exchangers were of similar construction to the standard ASTM-CRC coker preheater, and the assessment of fuel stability depended upon visual deposit evaluations. In conventional coker tests, these ratings are made under standard lighting conditions, by comparison with standard color code panels. While this system has served acceptably for the go, no-go type quality specifications of commercial and military jet fuels, it is basically unsatisfactory for research and development purposes because of the subjective nature of the judgment which must be rendered and the different shades of color that can be assumed by similar amounts of deposits. Moreover, in non-coker tube type heat transfer studies, Burggraf and Shayeson[44]) observed that the surface color bore no relation to loss in heat transfer coefficient.

Even within its intended scope of application, the coker's poor test repeatability has required refineries to produce fuels substantially more stable than the minimum required by the specifications; and burgeoning jet fuel demands have recently brought the need for a more quantitative fuel stability test into sharp focus.

Our own studies in the CAFSTR, where high temperatures ruled out the use of aluminum tubes, have been hampered by the development of colors of the tube metals themselves. Inconel 600, the alloy chosen for the construction of the CAFSTR heat exchanger tubes, changed color when heated, even in the presence of helium. Similar experience has been encountered with stainless steel. These colors are presumed due to surface oxidation of the metal at high temperatures, even when only trace amounts of oxygen are present.

In recognition of these critical tube deposit rating problems, we have been exploring several different methods of quantitative measurement, which include the following: 1) direct heat transfer coefficient; 2) combustion and absorption; 3) radiative; 4) infrared; 5) solvent dissolution-gravimetric; 6) electron micrography. This will be discussed separately.

Direct Heat Transfer Coefficient Measurements

The idea of using this as a quantitative method of deposit evaluation arose from the fact that fuel deposits can reduce overall heat transfer coefficients.

Calculations based on Zengel's[42)] published experimental results on the effect of deposits on heat transfer, and also on the estimated precision with which the limiting variables could be either controlled or measured, led to the conclusion that deposists as thin as 0.0001 inches (0.1 mil) should be detectable. This deposit level corresponds to a coker code rating of about 2, assuming considerable coverage of the surface.

Initially, a low temperature heat exchanger method, involving a stirred calorimeter, was developed. The test utilized an actual CAFSTR heat exchanger tube and heating element, which together with a cooling coil was immersed in the calorimeter. Heat transfer measurements were made when the calorimeter liquid temperature had reached a steady state. Actually, the wall to liquid temperature differential was monitored, using a Leeds/Northrup potentiometer, capable of reading to 1 x 10^{-4} mv (ca 0.004 °F).

Control of the voltage, cooling water, and temperature variables was recognized as of utmost importance. Voltage control to within ±1/20 volt at 110-120 volts was achieved by the use of a Superior Electric Company model IES9101 Stabiline Voltage Regulator. This instrument was used both to supply power to the CAFSTR tube and to the cooling water pump. Cooling water was supplied from a modified Colora Ultra-Thermostat constant temperature bath, and the bulk temperature was controllable to ±0.08°F at 90-95°F. The water pumping rate was about 2200 ml/min.

Although the bulk liquid temperatures could be held acceptably constant, difficulty was experienced with transient local temperatures in the stirred calorimeter, which eventually led to the abandonment of the calorimeter in favor of an annular heat exchanger arrangement.

In all experimental set-ups, comparisons were made of the ΔT (wall to liquid) for the initially clean tube and for the same tube after spray coating with (usually) 0.1 to 0.2 mil of acrylic lacquer. Our experience has been that this method, because of experimental error limits, is not sufficiently sensitive for the rating of deposits up to about the ASTM Code 4 level, but might be used for heavy deposits.

However, it is not at all certain that failure to detect the light deposits is entirely due to difficulty in maintaining adequately constant heat flows. There exist uncertainties as to the theoretical effects of low level deposits on the actual heat transfer phenomena, and these effects are dependent upon the actual mechanism of deposit buildup. For example, if the deposit is not laid down as a coherent film, but as scattered particles, the increased surface roughness could cause greater turbulence near the surface. Thus, Sherriff$^{10)}$ has shown that as surface roughness increases, the heat transfer coefficient also increases until the heights of the roughnesses reach the thickness of the laminar sublayer. The opposing effects of low deposit thermal conductivity and increased surface turbulence can have a wide range of net results in the overall heat transfer coefficient, thus destroying the usefulness of direct heat transfer measurements as a light-deposit rating technique. However, thick deposits, which form coherent layers, would reduce the heat transfer coefficient, and hence this technique would find application under such conditions; or, if test periods were protracted, heat transfer could be used as the basis for thermal stability rating. The significant philosophical question as to whether light or heavy deposits would better reflect the true performance of a fuel in a jet engine could be answered only via correlation studies which are beyond the scope of the present consideration.

Complete Combustion of Tube Deposits

A method involving complete combustion of the deposits to CO_2 and H_2O has been devised and tested. On paper, combustion offers one of the best means of rating tube deposits, having the advantage of being nearly 100 times as sensitive as the direct heat transfer coefficient method. By this method it is possible to detect deposits on a 13-inch, 5/8" diameter tube as thin as 0.001 mil uniform thickness. Since a tube code rating of 0.5 is estimated to correspond to a deposit thickness of 0.025 mil, any visible deposit should be ratable by this technique.

A schematic diagram for the combustion tube rater is shown in Figure 21. Oxygen (or air), predried and purified of any indigenous CO_2, is passed through the annular combustor with the CAFSTR preheater tube comprising the heating element. Products of the deposit combustion are trapped in suitable weighing bottles, as shown, the CO having been converted to CO_2 by passage over hot cupric oxide. CO_2 and H_2O are determined gravimetrically and back calculated to determine the total deposit weight and the coefficients in the deposit formula, C_xH_y. Sulfur, if present is picked up in the CuO furnace as $CuSO_4$, while nitrogen is trapped in the Ascarite weighing tube as KNO_3. However, the pure hydrocarbons which we are testing are probably too low in sulfur or nitrogen to cause serious error from this source. In cases of high S content fuels, the S content of the deposit could be determined by passing H_2 through the CuO tube at high temperature and converting the $CuSO_4$ to H_2S which could be trapped in caustic and titrated or otherwise determined.

On initial startup, the "clean" apparatus required several days operation at 1000°F with gas flowing to reach a steady "zero" base line, i.e., a condition where no CO_2 or water were being absorbed in the weighing tubes when deposits were known to be absent. This was undoubtedly due to oil adsorbed on the surface of the apparatus and to surface carbon. Cylinders of water pumped O_2 and N_2 are used instead of house service gas supplies to avoid introducing CO_2, CO, oil fog or other contaminants.

Following the break-in period, several runs were made on artificial deposits comprising weighed samples of polystyrene. Details of these tests are tabulated in Table 40. Also tabulated are the average deposit thicknesses of these "deposits", calculated as if they were uniformly spread over the surface of a 13-in. length, 5/8-in. OD tube. Of course, in actual CAFSTR and coker tests, the deposits are far from uniform, and the maximum local deposit thicknesses may be 2 or 3 times the average thicknesses. The code ratings listed in the table were estimated based on comparative data from coker and Minex Heat Exchanger tests by Zengel.[42] While the assumed correspondence between these two tests may be poor, the heat exchanger deposits do offer an approach to estimation of deposit thickness at various code ratings. Assuming a linear correlation, the average deposit level for a 1.0 code rating would be about 0.05 mil.

Certain drawbacks exist for the combustion method, however. First, as noted, a temperature of 1000°F or more is required to burn off the deposits. Aluminum and most of its alloys are immediately eliminated, therefore. Inconel Alloy 600, (ca 72% Ni) of which the heat exchanger tubes for the CAFSTR are constructed, is somewhat oxidized at 1000°F; strongly at 1100°F. Stainless steel also oxidizes at these temperatures. While these metals can be cleaned and polished, or perhaps even reused without polishing, the possible effect of surface metallurgical changes on test repeatability would have to be explored. After several hours at high temperature, particularly at 1100°F, the Inconel tubes develop a pronounced cellular grain structure visible to the naked eye. This cellular appearance disappears when the tube is polished, however.

Table 40. COMBUSTOR TUBE RATER RESULTS ON POLYSTYRENE "DEPOSITS"

Tube Wall Temp, °F	Gas		Deposit		Estimated[b] Max Coker Code Rating	Weight of Deposit Recovered,[a] % or Orig.
	Flow, ml/min	Composition, %, O_2	Wt, g	Average Thickness, mil		
1000	350	77	0.0348	.083	1.0	104
1000	250	28	0.0144	.034	0.5	96
1000	250	28	0.0043	.010	0	107
1000	250	46	0.0105	.025	0.5	104
1100	250	46	0.0142	.034	0.5	100
1000	200	48	0.0365	.087	1.5	69

a) Calculated from CO_2 + H_2O recovered.
b) Estimated from data of Zengel.[42]

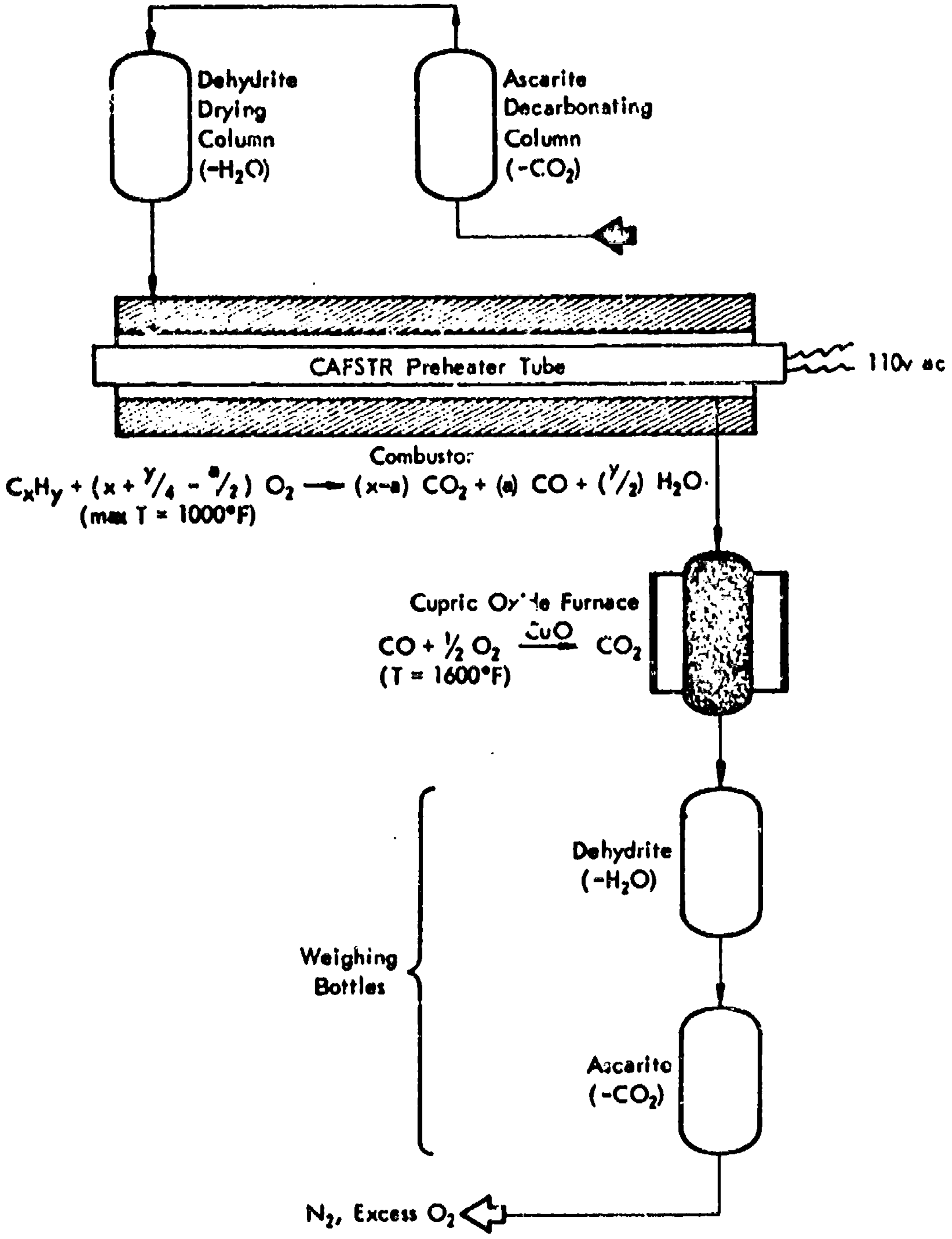
Dehydrite
Drying
Column
(-H₂O)
Ascarite
Decarbonating
Column
(-CO₂)
CAFSTR Preheater Tube
110v ac
Combustor
C_xH_y + (x + y/4 - a/2) O₂ → (x-a) CO₂ + (a) CO + (y/2) H₂O
(max T = 1000°F)
Cupric Oxide Furnace
CO + ½ O₂ →CuO→ CO₂
(T = 1600°F)
Weighing
Bottles
Dehydrite
(-H₂O)
Ascarite
(-CO₂)
N₂, Excess O₂

Figure 21. COMBUSTION TUBE RATOR DESIGN

A further difficulty was encountered when stainless steel preheater tubes of an integral heater/rating-tube construction from the Erdco Coker were used. The heater rapidly shorted-out internally causing the circuit fuse to blow. A second attempt with a new tube resulted in a similar experience. Apparently, these tubes were not designed to withstand the 1000-1100°F temperature level to which they were exposed. In our use of them in the Erdco they had probably never exceeded 800°F metal temperature.

Numerous runs have been made to establish optimum test conditions, the trade-off factors being time, temperature, oxygen concentration and total gas flow. A maximum rating time of 2 hours seemed to be a reasonable compromise. This allows about 1/2 hour heating-up time and 1-3/4 hours at oxidation temperature. Experimentation with temperature has shown 1000°F to be the practical minimum to obtain deposit burning. Then, for 1000°F and 1-3/4 hours, about 77% O_2 at 350 ml/min total flow is required to get complete combustion. Extremely heavy deposits would require still higher O_2 concentrations. At 48% O_2 and 200 ml/min total flow, for example, only 69% recovery was obtained (see Table 40), although this amount of oxygen is satisfactory for lower deposit levels.

A further operational problem involves removal of all traces of liquid test fluid from the preheater tube prior to rating. We had previously done this by rinsing with n-heptane and drying with nitrogen. However, the combustion tube rater reveals the presence of residual hydrocarbon when a clean tube has been rinsed and dried in this manner. Tests have shown that at low deposit levels these hydrocarbon residues can introduce a significant error. Present evolved practice is to rinse the tube three times with methylene chloride dry thoroughly with nitrogen, install the tube in the combustor and warm it to 100°F under 28 in. Hg vacuum for an hour, then start the gas flow and begin the combustion procedure.

A new variant on the burning method is now being investigated, in which the heat is supplied by an external furnace rather than using the internal heating element of the CAFSTR tube. It is hoped in this way to avoid overheating of the heating element, and possibly reduce oxidative attack of the surface metal. To this time, however, the background level of carbon, apparently arising from the furnace itself, has not been reduced to a satisfactory level.

The possibility of substituting GLC for the gravimetric procedure and using a laser as a heat source is also being considered.

Radiative Methods

Two methods of radiative deposit rating have been considered. First is that of direct beta radiation absorption by the deposit layer. This could be accomplished by impregnating the tube surface with a radioactive isotope such as Ni^{63}, but because of the possibility of catalytic effects on fuel deposition tendency, it would be preferable not to treat the tube surface itself. However, the direct radiation absorption technique does offer advantages in simplicity of application and should be explored.

A second approach to the radiative technique is that of β-radiation back scattering, using an external source. This method has the advantage of noncontamination of the tube surface, but the disadvantage of greater complications in implementation. Either Ni^{63} or S^{35} would seem to be good β-ray sources for this purpose.

Radiation scanning has the general advantage of being nondestructive to the deposit. Thus it would be possible to obtain comparable color code, combustion weight, and radiation counter ratings on the same tube. The radiation method also offers the advantage of being harmless to the tube metal and hence would not influence the life of the tube. It is believed that either method would be capable of detecting a 0.001 mil average film thickness, which is below the visible detection level but less sensitive than the combustion method. It is planned to scan the entire tube surface and to obtain an integrated radiation count reflecting the total deposits.

Infrared

Some thought has also been given to the development of an infrared method of tube rating, on the assumption that it would register the effects of deposits present without reflecting influences of surface film structure. The first attempts at utilizing this idea have been discouraging, however. Using the tube itself as the source of infrared, photographs were taken of the tube in a totally darkened room. Although a fast infrared type 413 Polaroid film was used, minimum conditions for the detection of even a trace of radiation were 3 minutes exposure at 600°F tube surface temperature. This was for a stationary tube. If the tube were rotated, as planned, to photograph the entire tube surface, a much longer total exposure time or higher temperature would be required.

Even 600°F may be too high a temperature to avoid detrimental deposit changes. Other problems are numerous. The temperature is far from uniform because of end effects. Optical density of the photographic image can be affected by the eccentricity of the tube axis as it is rotated in the chuck, and the chuck drive mechanism itself must be ultra smooth since the camera shutter is open constantly during the rotation. The power cord and thermocouple wires must not interfere with the free rotation of the tube, and the power input must be precisely repeatable for both the clean tube and deposit coated tube tests. Exposure times, film properties, film developing procedures, solution strengths, and camera setups must be duplicated accurately.

Having once achieved adequate control of the variables, the precision of optical density measurements must be achieved, which of course, we have not yet been in a position to do. Some means are available for improving the photographic sensitivity of the method, such as special film processing, use of higher speed film, longer exposure times or wider slit opening, reduction of the image size by changing the focal distance, and use of a faster lense; but whether these changes will accomplish the desired sensitivity is not known. The method is obviously still very much in a rudimentary stage.

Solvent Deposit Removal

Coker tube deposits cannot be recovered mechanically without the occurrence of tube damage and metal removal. It would therefore be desirable if this could be done by solvent washing. The deposits could then be recovered from the solvent and determined gravimetrically or by other means. Previously we had tried deposit removal using readily available laboratory solvents. This was done simply by wiping with a cloth dampened with the solvent at room temperature, but all such attempts were totally unsuccessful.

Since our own and the reported experience of others indicated that coker deposits of the hard, tenacious type would not be easily removed with solvents, we decided the solvent would have to be hot if it were to work at all. The deposits could then be determined by steam jet or microgum techniques.

Our experimental apparatus consists of a coker-type annular heat exchanger in which the inner coker tube is the heat source. Approximately 50 ml of test solvent is required to fill the annular space, and after filling, the device is sealed, with as little air as possible occluded. A stainless steel type pressure gage is attached, and pressure readings are taken throughout the period of the test. Arbitrarily, a temperature of 100°C was usually chosen as the maximum temperature and 300 psi as the maximum allowable pressure for the first series of runs.

Deposits were formed from either Decalin or jet fuel in an Erdco Coker and were of a hard, nonwipeable type, usually obtained at temperatures above the break point.

The experimental approach has been to select a synthetic resin structure resembling the presumed deposit structure (as deduced from the literature)45)46) as closely as possible. Then, from published solubility parameter data on resins and solvents,47)48)49)50) we have selected candidate solvents.

Results to date are tabulated in Table 41. Although the objective has not been accomplished, some interesting results were observed.

Most pronounced in its action was dimethylformamide. However, dissolution was not complete and in most cases there was still a small amount of deposit left; deposits removed were not entirely dissolved but some were merely loosened. We did find, however, that a second solvent treatment on the same tube would complete the deposit removal. A few more severe (192°C) and lengthy (2 hr) treatments removed more of the deposits but still left a few dark spots.

Under the conditions selected, none of the other solvents tested were effective in deposit removal to the extent that a recognizalbe improvement in deposit color code rating could be observed. However, several of the solvents became darkened in color, suggesting that some deposits might have been removed. Where this discoloration was observed, the temperatures were generally not high enough to have caused solvent decomposition or oxidation, unless strong catalytic effects existed.

Although M. W. Shayeson51) of General Electric Company has reported that morpholine has been found to be effective in deposit removal under some conditions, we did not find it so under the conditions of our tests.

Moreover, morpholine, in our tests, appeared to have the effect of a "developer" on the deposit appearance, i.e., to cause them to look darker,

Table 41. SOLVENT DEPOSIT REMOVAL TESTS

50-54 ml solvent surrounding a coker tube

Solvent	Temp, °C	Press., psig	Time, hr	Tube Rating		Comments
				Before	After	
Dimethyl sulfoxide	100	10	1	3.5	3.5	No effect
Phorone	100	16	1	3.5	3.5	No effect
Morpholine	100	27	2	4+	7.5	Darker
Piperidine	100	61	1	3.5	3.5	No effect
2-Nitropropane	90	200[a]	1	3.5	4.5	Darker
Diacetone alcohol	100	22	1	3.5	3.5	No effect
Amyl acetate	100	25	1	3.5	3.5	No effect
Propyl alcohol	100	102	1	3.5	3.5	No effect
sec-Butyl alcohol	100	200	1	3.5	3.5	No effect
Methylene chloride	90	198	1	3.5	3.5	No effect
Acetone	100	180	1	3.5	3.5	No effect
Methyl ethyl ketone	60	200	1	3.5	3.5	No effect
Toluene	100	190	1	3.5	3.5	No effect
Freon-II	90	200	1	3.5	3.5	No effect
Mesityl oxide	100	3	1-3/4	3.5	3.5	No effect
Tetrahydrofuran (THF)	100	170	1	3.5	3.5+	Slightly darker
Hexylene glycol diacetate	60	190	1	3.5	4.5	Darker
N,N-Dimethyl formamide (DMF)	100	32	3/4	3.5	3.5	Patches remained; most areas removed
DMF	100	26	1	3.5	0	Second consecutive treatment
DMF	100	28	1	4.0	1	Mostly removed
DMF	100	25	2	1	0	Second consecutive treatment
DMF	142	180	2	4.0	3.0	Much cleaner overall
1/3 DMF + 2/3 THF	90	190	1	3.5	3.5	No effect
1/2 DMF + 1/2 morpholine	100	90	1	4.0	7.5	Much darker
Shell solutizer[b]	100	25	1	2	3.5	Darker
Sulfolane	100	6	1	2.5	2	Possible slight improvement

a) Pressure increased during run suggesting occurrence of decomposition.
b) 6 M KOH, 3.1 M KIB.

without (we think) actually being of greater mass. The morpholine itself also turned dark. We have not tried this experiment without the deposit or metal environment to see if similar darkening of the solvent occurs. A mixture of half DMF and half morpholine appeared to have the same effect as morpholine itself.

Other solvents, such as 2-nitropropane, hexyleneglycol diacetate, tetrahydrofuran, and Shell K-2 Solutizer Solution (6.0 N KOH, 3.1 N K isobutyrate), also had this same apparent developing effect upon tube deposit color. The very fact that the deposits can thus be made to appear darker is further evidence of the inadequacy of the color code rating technique since different fuels might also vary in this property.

A further interest in solvent deposit removal is in the possible disclosure of chemical structural information about a deposit from solvent selectivity. Consequently, solvents selected for testing have covered a wide range of solubility parameters.[47][48][49][50]

This effort is still being continued with respect to solvent selection, and will also be partially repeated with respect to higher test temperatures and longer exposure times for promising solvents.

Electron Micrography

The possible use of electron microscopy for tube deposit rating is being considered, though the current intent is to merely "take a look" to see what the observations may suggest. We are thinking here in terms of deposit structure, and perhaps there is a chance for quantitative measurements as well.

We haven't yet looked at tube deposits, but Figures 22 and 23 show scanning electron micrographs[a] of stainless steel coker filters at low magnification. Figure 22 shows three shots at magnifications of 60x, 100x, and 300x of the clean filter. Figure 23 shows the same filter at 100x, three different areas, after running SHELLDYNE at 6 lb/hr and 675°F. All that can be seen by comparing these two series of photographs is how completely the filter has become plugged with debris. However, we are now preparing to repeat this comparison at about 20,000x, with the hopes of seeing the microstructure of the deposit layer on the stainless steel filter particles. We then plan to take the same sort of photographs of some sawed-up sections of a coker tube which has been previously rated on the standard Tuberator scale.

A chief disadvantage of this approach as a routine method would be its inconvenience. Also, the tube would have to be destroyed, since sections of only about 1/2 inch maximum length can be observed. The cost would be a futher deterrent. This arises not only from the cost of the electron microscope itself, but also from the laboratory preparation of the surfaces which must be made; i.e., an evaporative coating of about 75 A gold is applied at a 30° angle while the sample is being rotated. Total cost would be about 35 dollars per photograph, which must be multiplied times the number of shots necessary to describe the entire tube.

---

[a] The electron microscopy was done by R. G. Meisenheimer.

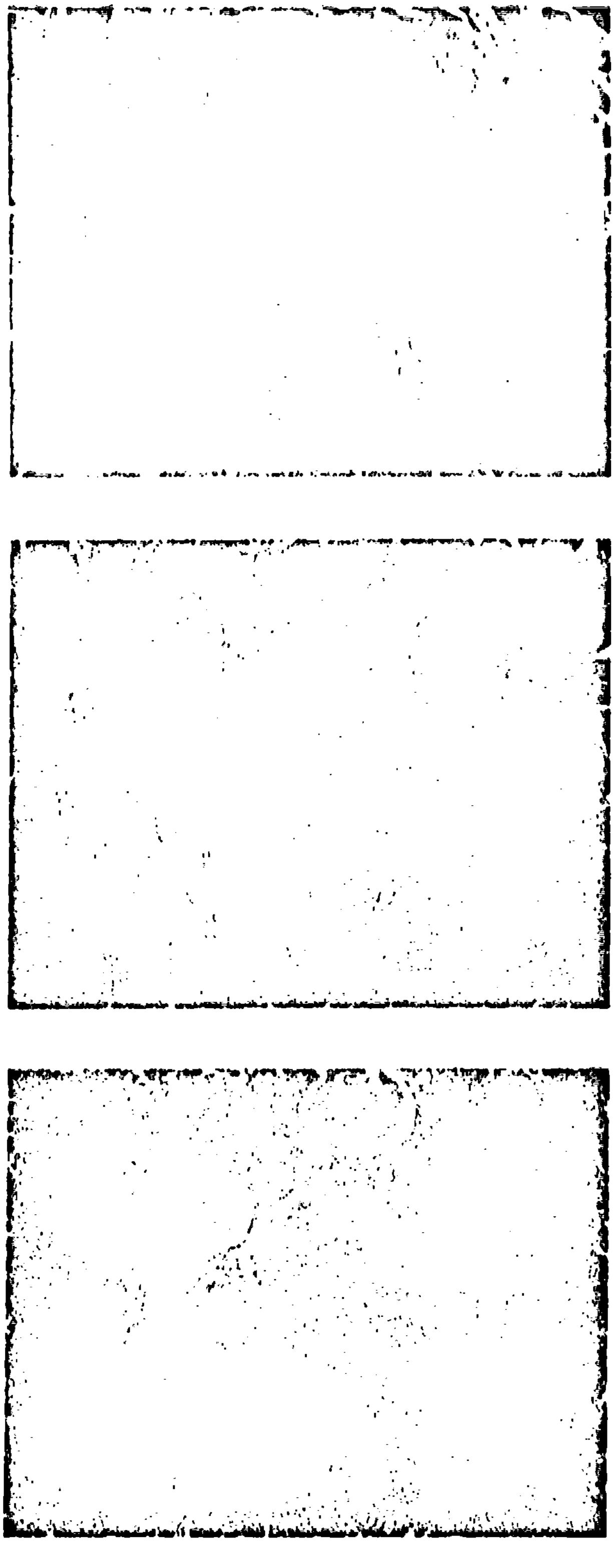

Figure 22. ELECTRON MICROGRAPHS OF A CLEAN STAINLESS STEEL COKER FILTER Element at 60X, 100X, and 300X Magnifications

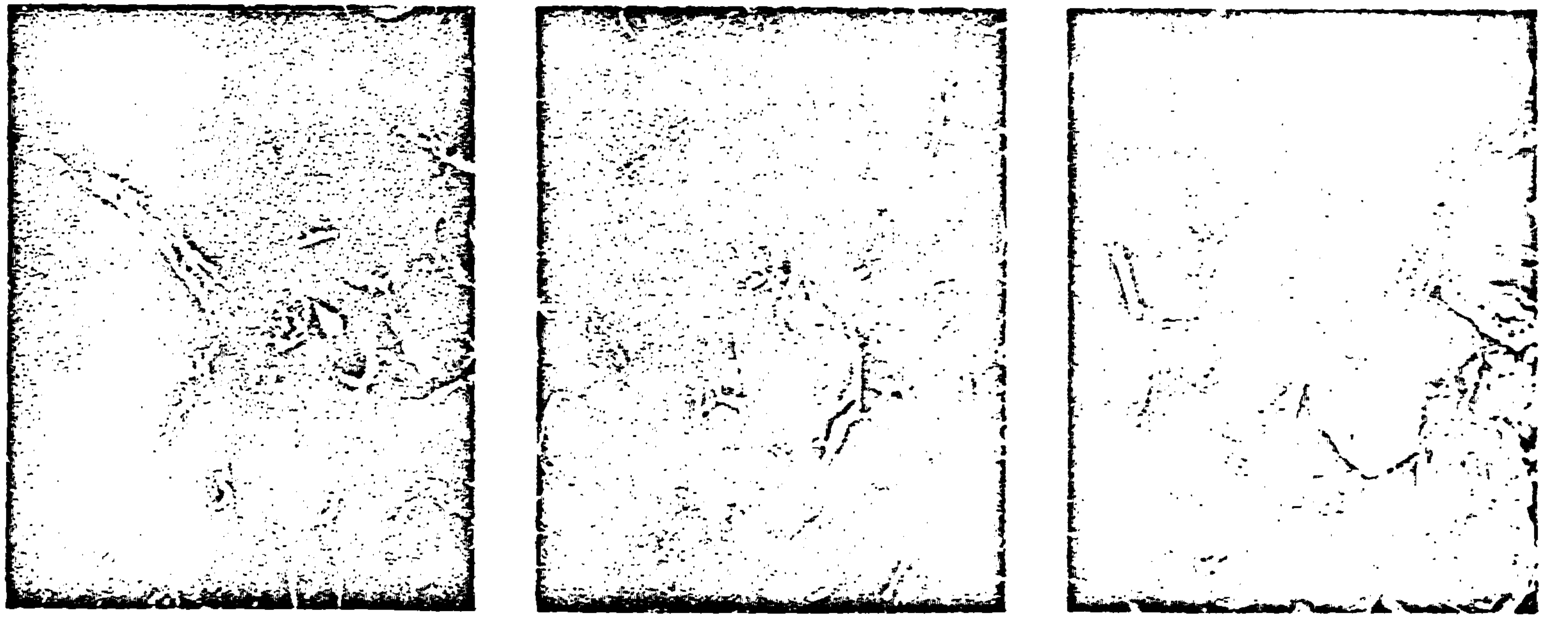

Figure 23. ELECTRON MICROGRAPHS OF A STAINLESS STEEL COKER FILTER
Element at 100X Magnification, Following Run with Shelldyne
at 6 lbs/hr and 675°F in the SD/M-7 Coker

Summary of Deposit Rating Methods

A comparison of the ASTM color code, heat transfer coefficient, combustion, radiation, and solvent deposit removal tube rating methods has been compiled in Table 42. Insufficient information is available to estimate detection levels for the infrared method.

By way of summary, it can be seen that the combustion and solvent removal techniques offer the greatest sensitivity. However, the combustion method suffers by reason of harmful tube metal effects, while the solvent method depends upon finding a suitable solvent or reactant. Beta-radiation detection ranks next in sensitivity, but the details of this approach have yet to be worked out. The measurement of heat transfer coefficients provides a sufficiently sensitive method on paper, but has not proved satisfactory experimentally. Further investigation will be necessary to select the most favorable of these methods.

Table 42. ESTIMATED MINIMUM DETECTION LEVELS FOR FIVE DIFFERENT COKER TUBE RATING TECHNIQUES

Rating Method	Average Deposit Thickness,[a)] mil	Total Deposit Weight, mg	Approx ASTM Color Code Equivalent[b)]
ASTM Color Code	0.02	10	0.5
Heat Transfer Coefficient	0.03	13	0.5
Combustion	0.0004	0.15	0
Beta-Radiation	0.001	0.5	0
Solvent Deposit Removal	0.0004	0.15	0

a) The maximum deposit thickness is probably 3-6 times the average thickness.
b) Based on average thickness of deposit.

Overall the combustion and radiative methods appear most promising, and at the present time most of our effort is directed toward the combustion method. We will also in the near future evaluate a method utilizing an H_2 ring burner or a laser as the source of combustion, with the expectation that this will be more rapid and less destructive to the tube, and particularly, to the tube heater. The possibilities of utilizing other methods of measurement, involving IR, x-ray, and dielectric properties are being studied. The success of the CAFSTR and of future coker-type testing depends upon the solution to this problem.

Modification of the SD Coker; SD/M-7

The SD Coker, as originally designed,[1][52] operated on a fuel recycle scheme and utilized a glass double reservoir to measure the fuel flow during recycle operation. This device was chosen to avoid the calibrations required with rotameters when using experimental fuels with a wide range of densities. A description of the operation of this double reservoir device has been given previously.[52]

Although the current system has been simple to operate, and satisfactorily accurate, there have been two notable defects. First, the glass reservoir and joints were subject to occasional breakage; and there was always the safety hazard that failure of the Grove pressure regulator might release full system pressure into the reservoirs and explode them.

A second problem had more to do with the inadequacy of the Zenith pump used than with the glass reservoir system itself. Particularly with lower viscosity fuels such as methylcyclohexane, pump wear has been both severe and variable. Generally, the higher the pressure developed the greater the pump wear, but this differed with individual pumps.

However, since the mating parts are machined to a tolerance of about 0.0002 in. the Zenith pump is a satisfactory metering device. Only when producing high pressures with low viscosity fluids does scuffing difficulty develop.

In our CAFSTR[a] and in the modified Erdco Coker we have gone to a gas pressure drive, which is a good system, but not readily applicable to recycle operation (which we favor because of the often limited availability of experimental fuels).

We have now modified the SD coker to eliminate the glass reservoirs. The revised system, shown in Figure 24 is designated M-7.

In this arrangement the d/p cell, besides reading pressure drop across the filter, serves as a fuel reservoir and sparge for equilibration with the pressurizing gas. The pump serves only to meter the fuel and recirculate it. Since the pump is of a volumetric displacement type, the flow rate is determined with an electronic counter which reads in tenths of rpm the rotation of the pump drive gear. Total system pressure is supplied by the sparge gas, sparging action being maintained by a slight imbalance in the settings of the sparge gas supply and system pressure regulator settings. The sight glass permits instant visual observation of the sparging rate and also doubles as a surge. The sparging rate can be observed at the Grove regulator gas discharge tube, where a simple bubble flow meter is used to quantitatively measure the sparge gas rate. A standard rate of 100 ml/min has been found satisfactory.

Since the entire fuel system is under pressure, it is necessary to replenish the oxygen reacted in the hot test zones by using a sparge gas of the proper O_2 partial pressure. Because of the effect of pressure on O_2 solubility, the required percentage of O_2 in the sparge gas is less than for atmospheric equilibration, and varies with the pressure. For example, to provide fuel which would be oxygen saturated at 1 atmosphere requires equilibration with sparge gas containing about 1.87% O_2 at 150 psig.

---

[a] Catalyst and Fuel System Test Rig.

Similarly, if a low dissolved oxygen concentration is desired, the magnitude of the total pressure imposes limitations on the minimum levels attainable. In Table 43 the equilibrium dissolved O_2 is shown versus pressure for 1 ppm oxygen concentration in the sparge gas. These values were calculated from Ostwald Coefficients for a petroleum fraction of 0.78 specific gravity at 60°F[30] and demonstrate the lower O_2 limits which may be expected. The restrictions will not be serious, however, since even 30 ppb oxygen is difficult to measure experimentally.

Table 43. EFFECT OF TOTAL PRESSURE ON DISSOLVED OXYGEN CONCENTRATION IN A 0.78 SPECIFIC GRAVITY HYDROCARBON WITH AN EQUILIBRATING GAS CONTAINING 1 PPM

Total Pressure, psi	Dissolved O_2, Parts Per Billion
150	5
250	8
400	12
600	18
1000	30

Although we intend to eventually operate the SD coker at 1000 psi pressure, operation to date has not exceeded 600 psi. Suprisingly, even at 400 psi pressure a small amount of leakage occurs between the plates of the Zenith pump, though these pumps are specified by the manufacturer for use at pressures above 1000 psi (but with viscous fluids). Apparently, the phenomenon is related to the high pressure on both inlet and outlet sides of the pump, since leakage was never a problem when the pump itself was developing the system pressure and the inlet side was near atmospheric. Thus leakage could give trouble at higher pressures. It may be possible to control this by using additional bolts or clamps.

Despite these problems, the new recycle arrangement has been found to operate quite satisfactorily. The pump operates almost without noise which indicates little wear is occurring. The fuel system requires 350 ml, and is filled to a standard mark on the Jergusen sight glass at the start of each test. This level has not been observed to change during runs. Flow rate checks are rapidly and simply made during the test using the electronic counter and have been found constant to ±0.5 percent.

Because of the avoidance of wear debris from the pump, the M-7 coker may have become a somewhat less severe test than it was previously.

Effect of Metal Environment on Decalin Thermal Stability

The presence of trace metals has long been recognized as a deterrent to good thermal stability of liquid hydrocarbon fuels. Such trace metals are always present, deriving from the construction materials of fuel system components. We have found, for example, that variations in wear rates of the SD Coker Zenith pump can cause differences in tube deposit ratings, though this could be due in part to the presence of metal in the deposit.[35]

Since trace metals are known to differ in their influence on fuel stability,[38-40] it was decided to investigate the effects on the thermal stability of Decalin of Some of the more commonly encountered metals, using the SD/M-7 Fuel Coker.

The Decalin used in these tests was prepurified by percolation through a silica gel column. Prior to the test, the Decalin was put on a laboratory shaker for a minimum of 7 hours with the chosen metal in a powdered state (ca 3 grams/liter). The powdered metal was then filtered out, using a 0.45 micron Millipore Filter, and the Decalin introduced directly into the coker. Although some tests were tried with only this pre-equilibration, the general procedure was to attempt constant re-equilibration by recirculation of the fuel through a coarser bed of the test metal throughout the test. A subsequent test was then conducted under identical conditions with about 240 ppm of the metal deactivator (MDA), N,N'-disalicylidene-1,2-propanediamine, added after filtering.

An unfortunate circumstance in the present tests is that the coker fuel system, except for the aluminum preheater tube, is 316 stainless steel throughout, thus providing a constant background of contamination with those elements present in the stainless steel. From the typical analysis of 316 stainless shown in Table 45, the large amounts of Cr, Ni, and Fe are particularly to be noted, since these are among the metals under present investigation.

The complete list of metal environments investigated includes Fe, Cu, Ni, Cr, Zn, Pb, and additional stainless steel. All runs were at 150 psig and most were at 600°F. Preliminary results are tabulated in Table 44.

Most deleterious to Decalin thermal stability ratings were copper and iron. At 600°F both caused increases of 3 code numbers in tube ratings. One difference noted between the two metals was that copper caused a significant increase in filter plugging (11.5 "Hg compared to 2.1" without copper). Iron caused no filter plugging at all. The introduction of MDA with each metal resotred the tube ratings to the "neat" Decalin stability level (Cu/MDA, 3.5/17; Fe/MDA, 3/11; metal free, 3/22). MDA also eliminated the filter plugging observed with copper (Cu, 11.5"; Cu/MDA, 1.5" Hg). At 600°F, then, MDA nullifies all of the deleterious effects of dissolved copper or iron. When iron was run by pre-equilibration alone (no re-equilibration bed in the flow stream), the ratings were essentially the same as for Decalin alone (Fe, 3/16, 0", Fe-free, 3/22, 2.6" Hg). Cu was the only metal having a significant influence on filter pressure drop.

Chromium also had a small adverse effect on Decalin ratings (Cr, 4/33, 0.8" Hg; Cr-free, 3/23, 2.1" Hg), which was not significantly improved by the addition of MDA.

The presence of nickel had no appreciable effect, although the improvement due to MDA addition which was observed without nickel was not found with nickel (Ni-free/MDA, 2/12.5; Ni/MDA, 3/14.5;). Since the coker flow system is constructed of stainless steel, as previously mentioned, we suspect the true harm contributed by Cr and Ni may be greater than that shown by these tests.

Table 44. EFFECTS OF METAL ENVIRONMENTS ON THERMAL STABILITY OF DECALIN (F-139) WITH AND WITHOUT METAL DEACTIVATOR (MDA)

Coker Runs	Temp, °F	Metal Pre-equil.	Metal Re-equil.	MDA Added, g/liter	Preheater, Watts	Tube, Max/Total	Filter, ΔP, " Hg
285, 286, 314 315, 316, 346	600	-	-	-	508	3 /22	2.1
255, 262 263a, 263B	625	-	-	-	620	3 /23	0.0
284	650	-	-	-	686	3.5/26	2.9
320	675	-	-	-	674	5 /28	0.2
287	600	-	-	0.0046	500	3 /15	0.0
295	600	-	-	0.214	505	2 /12.5	0.8
294	625	-	-	0.214	632	4.5/20.5	0.7
293	675	-	-	0.214	728	8 /20.5	0.4
288	600	Fe	-	-	499	3 /16	0.0
303	600	Fe	Fe	-	499	6 /43	0.0
304	600	Fe	Fe	0.214	499	3 /11	0.0
290	600	Cu	Cu	-	503	6 /41	11.5
291	600	Cu	Cu	0.214	505	3.5/17	1.5
327, 334	600	Ni	Ni	-	499	3 /17	0.0
317, 333	600	Ni	Ni	0.214	490	3 /14.5	0.0
308	600	Cr	Cr	-	505	4 /33	0.8
310	600	Cr	Cr	0.214	505	3.5/24.5	4.8
332	600	316SS	316SS	-	474	2 /14	0.0
331, 321	600	316SS	316SS	0.214	474	2 /10	2
319, 318, 292	600	Zn	Zn	0.214	505	1.5/10	1.5
330	600	Zn	Zn	-	464	2 /12.5	0.2
313, 325	625	Zn	Zn	-	610	3 /23	1.3
296, 301, 302, 311, 329	625	Zn	Zn	0.214	634	3 /18	0.6
297	625	Zn	-	0.214	622	4 /17.5	0.3
337	600	Pb	Pb	0.214	504	2 /17	0.0
338	600	Pb	Pb	-	498	2 /17	0.0

Table 45. CHEMICAL ANALYSIS OF 316 STAINLESS STEEL

Element	%
C	0.10
Mn	2.0
Cr	16-18
Ni	10-14
Si	1.0
Mo	3.0
Fe	62-28

In view of the results for Ni and Cr, however, the data with added 316 stainless were surprising, since the tube ratings were improved (no added stainless, 3/23; stainless added, 2/14). When MDA was added, no further effect was found.

Interestingly, at 600°F the presence of Zn and Pb gave similar improvements in tube ratings to that of 316 SS, which again were not significantly altered by the further addition of MDA. But at 625°F, no indluence of Zn occurred.

Further data will be needed to confirm the tentative conclusions stated here for Ni and Cr. However, the harmful effects of Fe and Cu, and the beneficial effects of Zn, Pb, and 316 SS represent deviations which are outside the 95 percent confidence limits for the determination of Decalin ratings, and are therefore considered reliable. The latter three metals appear to be removing something from Decalin which is harmful to its thermal stability, while Fe and Cu appear to behave as oxidation catalysts. The beneficial effect of MDA in the untreated and in the Cu and Fe treated cases is also outside the 95 percent confidence limits of the pure Decalin rating, and is therefore considered real.

When beneficial effects of MDA do occur, such as with copper and iron, the improvement is probably due to its chelating action, but this must largely occur during the first few recycles of the SD/M-7 Coker, since MDA itself is not stable above about 540°F.[a] However, the chelates of MDA would be expected to be stable at higher temperatures, and might therefore be expected to survive the 600°F coker exposure temperature. This may explain why MDA was beneficial without metal additive at 600°F, while at higher temperatures (i.e., 625-675°) the instability of the chelate itself might contribute to deposit formation. The data of Table 45 are in harmony with this hypothesis.

---

a) MDA decomposes to phenol and other lower boiling products, du Pont MDA Bulletin. Its stability would expected to be somewhat greater in dilute solution.

Table 46. EFFECT OF METAL DEACTIVATOR (240 PPM) ON THERMAL STABILITY OF DECALIN

Temp, °F	SD/M-7 Coker Tube Ratings Without MDA	 With MDA
600	3 /22	2 /12.5
625	3 /23	4.5/20.5
650	3.5/26	-
675	5 /28	8 /37

SD/M-7 Coker Cleanup Procedure

Because the M-7 Coker operates on a recycle principle, special precautions have to be taken to avoid inter-test contamination. Deposits may be laid down in the cooler and in other cold regions of the flow system, which are not readily removable by mechanical techniques such as are used in the cleanup of the preheater and test filter. Moreover, low temperature deposits laid down in one run may be partially dissolved by the test fuel of the next run, thus resulting in an experimental rating error and failure to reproduce results.

To avoid this hazard, a new procedure for cleaning the system has been developed, based upon tests of the effectiveness of various solvents in removing deposits. Solvent effectiveness has been judged from both a general knowledge of component solvency power and by the color of the solvent upon its removal from the system.

Influence of Solvent Contamination on SD/M-7 Coker Ratings

Despite the extensive care taken in trying to remove all solvent from the system following the solvent wash series, it is possible that solvent contamination might result in misleading results. The use of dimethylformamide (DMF) was of particular concern because of its nitrogenous character, although it is regarded as a very chemically stable compound.

To determine the effects of such contamination, DMF and toluene were run in the coker at 1 percent (v) concentration with Decalin. At 600°F the ratings were DMF, 2.5/10 and toluene, 2.5/14. No filter plugging occurred in either case. This compares with average ratings of 3/23 and 2.6" Hg for identical runs without DMF or toluene. In other words, neither solvent causes harm, and may even improve the thermal stability rating of Decalin (perhaps due to deposit removal from the preheater and filter due to improved solvency).

We had also been concerned whether Decalin runs following SHELLDYNE tests could have possibly suffered from contamination with SHELLDYNE. Consequently, a similar test to that with DMF was made with SHELLDYNE as the "contaminant." Results with 1 percent SHELLDYNE at 600°F were 2.5/19,

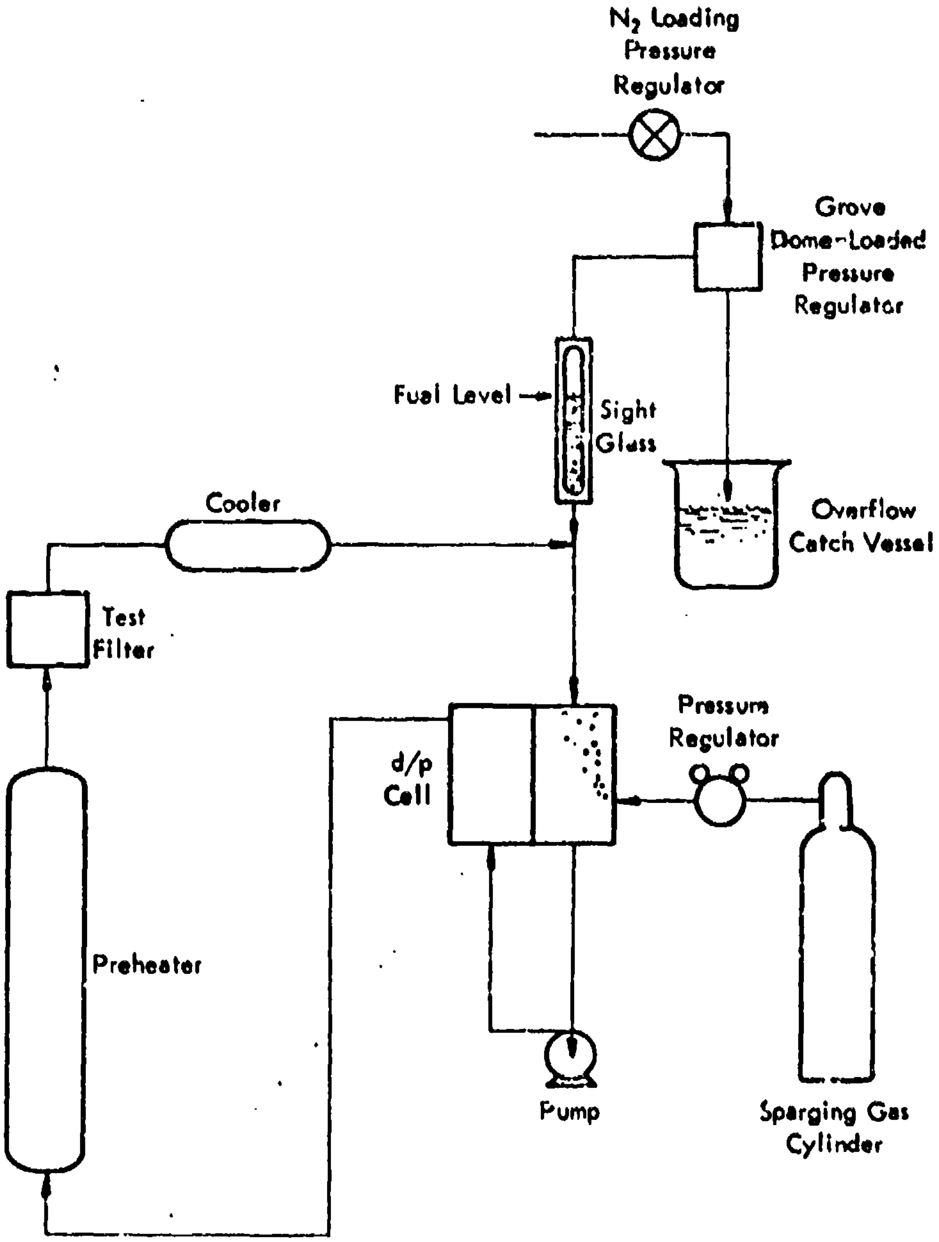
N_2 Loading Pressure Regulator
Grove Dome-Loaded Pressure Regulator
Fuel Level
Sight Glass
Overflow Catch Vessel
Cooler
Test Filter
d/p Cell
Pressure Regulator
Preheater
Pump
Sparging Gas Cylinder

Figure 24. REVISED FUEL SYSTEM FOR THE SD/M-7 COKER

and no rise in filter pressure drop--an almost identical rating to that with DMF.

Additional tests of this type will be made with other solvents which have been used, i.e., ethyl acetate and acetone.

Thermal Stability of SHELLDYNE and SHELLDYNE H

The thermal stability of SHELLDYNE, SHELLDYNE H, and Decalin was observed in the SD/M-7 Coker using the recycle mode. The results are given in Table 47. It will be noted that both SHELLDYNE and SHELLDYNE H have less tendency to form tube deposits than Decalin but much greater filter plugging tendencies. This latter attribute is probably exaggerated by the recycle mode used in the test, since on the average the charge of fuel is recycled 35 times through the heated zones. Even so SHELLDYNE H is substantially less prone to form both tube and filter deposits than the parent material.

A more recent sample of SHELLDYNE, although it had an adsorbence at 357 microns wave length 27 percent greater than the previous sample, also gave a satisfactory SD/M-7 Coker rating ($T_{2.5}$ breakpoint of 600°F). Thus, the thermal stability of the SHELLDYNE samples received have been reasonably reproducible from batch to batch, despite differences in color appearance. The latter SHELLDYNE has now been hydrogen treated for use in the mini-FSSTR studies.

Thermal Stability of P and W 535 Jet Fuel

A one-drum sample of P and W 535, a high quality JP-7 type turbine fuel, was obtained from Pratt and Whitney West Palm Beach Florida facility for use in comparative tests. This fuel is being used by P and W for most of the heat transfer testing being done at their Florida location. We have now determined the thermal stability of this fuel using the SD/M-7 Fuel Test Rig. The breakpoint temperature, $T_{2.5}$, of 600°F was found to be identical with that of Decalin. Filter plugging was almost nil (0.15" Hg). The color change in the fuel was slight, becoming a very light yellow, and low solvent coloration during the post-run cleanup indicated a low level of cold zone deposit formation.

Table 47. COMPARISON OF THERMAL STABILITY OF "SHELLDYNE," "SHELLDYNE"-H AND DECALIN

5 hr SD/M-7 Coker ratings, 6 lb/hr fuel flow rate. Recycle mode, O_2 content equivalent to equilibration with 1 atmosphere air, 150 psia.

	Fluid Temp, °F	Filter ΔP, in. Hg[f]	Tube Rating[a]
SHELLDYNE H	675	13.0	1.5/ 8
"	700	6.8	3 /22.5
"	725	-4.4	4 /23
"	(690)[b]	(10.0)[b]	(2.5/20)[b]
SHELLDYNE	575	53	0.5/ 3
"	625	ca 179	3.5/24.5
"	650	ca 305	6 /36
"	675	ca 204	1.5/10 (47 min)[c]
"	(610)[b]	(141)[b]	(2.5/18)[b]
Decalin			
F-113[d]	600	0	2.5/16.5
F-139[e]	600	0	3.0/20.5
	625	0	3 /23
	650	2.9	3.5/26
	600	0	3.0/16
	600	0	3.0/15
	(600)[b]	(0)[b]	(3.0/15)[b]

---

a) ASTM Color Code Ratings, Max/Total.
b) Interpolated tube rating breakpoint, assumed to be at code 2.5, and corresponding pressure drop.
c) Test terminated because of rapid increase in filter pressure drop.
d) Analysis: 21.5 trans, 74.5 cis, 0.4 tetralin.
e) Analysis: 33.5 trans, 65.5 cis, 0.8 tetralin.
f) Filter temperature = fluid temperature.

Fuel System Simulation Test Rig

The Fuel System Simulation Test Rig (FSSTR) has been described in detail in the three annual reports associated with the preceding contract on this subject,1)2)3) therefore no description of the unit will be included here. However, a flow scheme is repeated as Figure 25 for convenience.

During the past year the following studies have been conducted in the FSSTR:

(1) Catalytic dehydrogenation of MCH over UOP-R8 in a 0.277" ID x 2-ft long reactor section.

(2) Heat transfer to MCH in the empty 2-ft reactor section.

(3) Heat transfer to MCH, water and N_2 in 0.0265" ID x 4" and 6" long heat exchange sections.

(The last two items are part of a continuing cooling study program.)

Catalytic Dehydrogenation of MCH Over UOP-R8

A description of the reactor used in these tests as well as a report of the initial test series was included in the immediately preceding Annual Report on this project.19) For convenience, the description is repeated here and the results of the first test are incorporated with the remainder of the data.

0.277" ID x 2-ft Long Reactor

In order to permit investigation of heat flux conditions closer to those which might be encountered in combustion chamber cooling, a short reactor section was constructed and installed in the FSSTR in place of the usual 10-ft reactor section III. This reactor, a sketch of which is shown in Figure 26, was made up of a 2-ft section of 3/8 in. OD x 0.049 in. wall Hastelloy C tube welded to Ni bus bars. Compression type fittings (3/8 in.) provide inlet and outlet connections, and 1/16 in. fittings are used as glands for inlet and outlet fluid temperature thermocouples. A 1/16 in. fitting was also provided in the exit end bus bar for sample withdrawal. Tube wall (external) temperatures were measured at six locations by thermocouples spot welded to the reactor tube. The two lead wires from each junction (insulated from direct contact with the tube by ceramic cement) were wrapped 1/2 turn each in opposite directions around the tube and then passed through ceramic insulating tubes to points far from the high temperature area.

The 10-ft reactor sections normally used in the FSSTR use 1/16 in. OD, insulated junction, sheathed thermocouples welded to the tube wall for monitoring wall temperatures. The 2-ft reactor section made for this study was originally constructed in the same manner. During preliminary heating of the reactor with N_2 flow through the tube it became evident that, without a compensating heat tube surrounding the reactor, as is used around the 10-ft sections, heat leaks along the thermocouple sheaths were causing errors in temperature measurement. The use of unsheather 30-gage (0.010 in.) thermo-

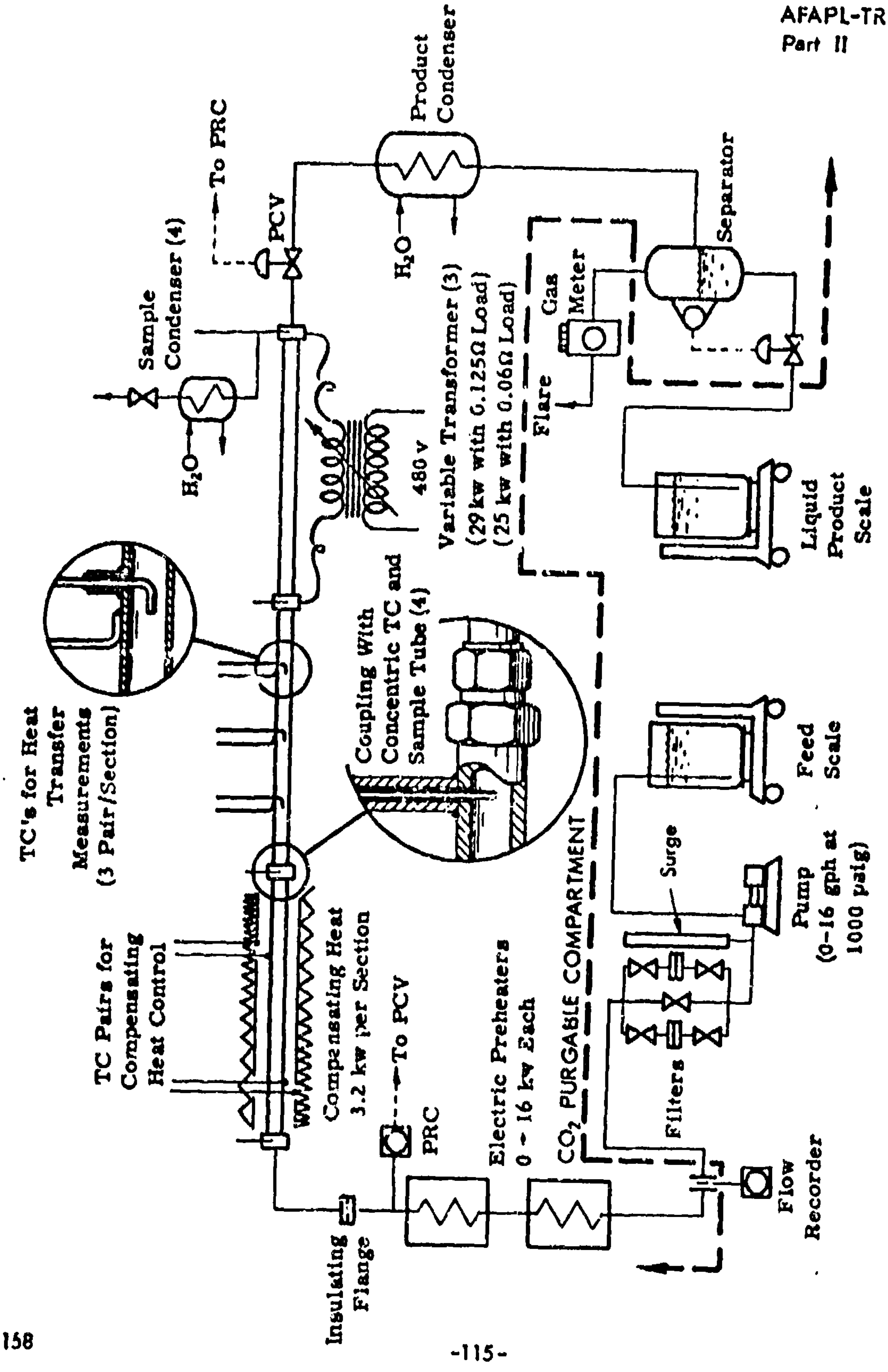
Product Condenser
To PRC
PCV
H2O
Sample Condenser (4)
H2O
480 v
Variable Transformer (3)
(29 kw with 0.125Ω Load)
(25 kw with 0.06Ω Load)
Gas Meter
Flare
Separator
Liquid Product Scale
TC's for Heat Transfer Measurements (3 Pair/Section)
Coupling With Concentric TC and Sample Tube (4)
Feed Scale
Surge
Pump (0-16 gph at 1000 psig)
Filters
CO2 PURGABLE COMPARTMENT
TC Pairs for Compensating Heat Control
Compensating Heat 3.2 kw per Section
To PCV
PRC
Electric Preheaters 0 - 16 kw Each
Insulating Flange
Flow Recorder

Figure 25. FSSTR - FLOW SKETCH OF FUEL SYSTEM SIMULATION TEST RIG

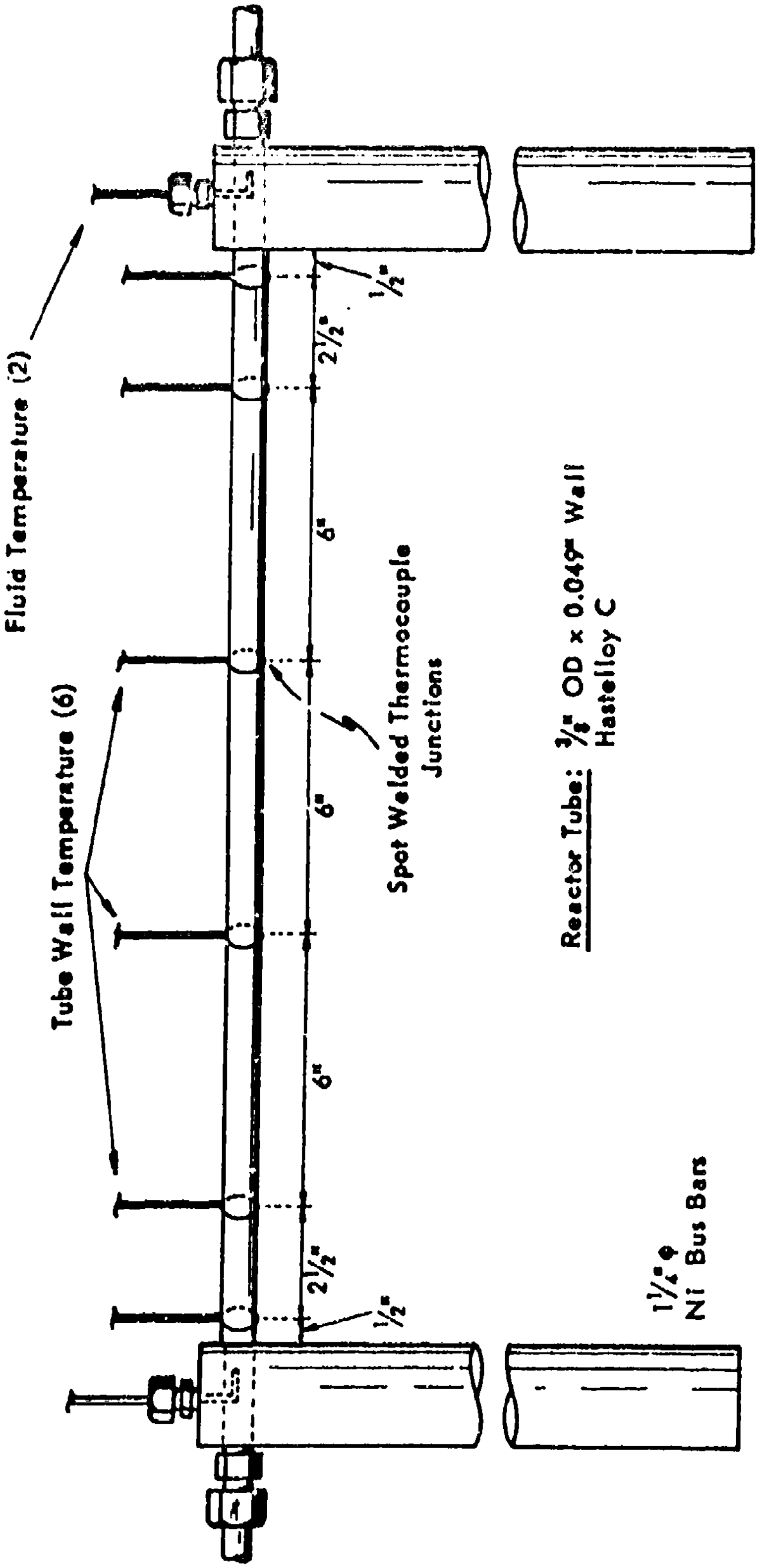
Fluid Temperature (2)
Tube Wall Temperature (6)
1/2"
2 1/2"
6"
6"
6"
2 1/2"
1/2"
Spot Welded Thermocouple Junctions
Reactor Tube: 3/8" OD x 0.049" Wall
Hastelloy C
1 1/4" φ
Ni Bus Bars

Figure 26. FSSTR - 0.277" ID x 2-FT LONG REACTOR SECTION

couples spot welded directly to the reactor was tried and proved satisfactory. A comparison of recorded temperatures obtained at the same time from the two types of couples is shown in Figure 27. The bare wire couples were used for all MCH test runs on the 2-ft reactor. Using this type of couple results in electrically hot lead wires and appropriate safety precautions had to be taken.

The electrical resistance of this reactor section is about 0.025 ohms. With the power supply presently in use, a maximum heat flux of ca 590,000 Btu/(hr · ft^2) can be reached without exceeding the 1000 ampere rating of the transformer secondary.

A measurement of heat losses from the reactor has been made by passing heated N_2 through the tube and recording the fluid temperature entering and leaving and the tube wall temperature profile. With the assumption that the tube wall temperature profile is parallel to the average N_2 temperature profile, an extrapolation of a straight line through the wall temperature points to the 0 in. and 24 in. limits (disregarding the points 1/2 in. from either end which were apparently influenced by heat leak to the bus bars) yields the N_2 temperature drop along the reactor tube proper.

Subtracting this loss from the total loss (determined from overall fluid temperature drop corrected for any power input) gives the heat loss to the two bus bars. Equal loss to each bus bar has been assumed. The heat losses so determined are shown as the solid points in Figure 28. Note that the "tube" losses agree with those determined later with the tube empty but that the "end" losses are higher than the empty tube values. This is because the outside tube wall temperature determines the heat loss from the tube and it is the outside wall temperatures which are measured, while in the case of the bus bar losses, the temperature used is that of the fluid passing through the opening in the bus bar and heat flux to the bus, depends not only on this temperature but also on the heat transfer coefficient between fluid and bus which is influenced by flow rate and also by that portion of the catalyst bed which enters the bus bar. The heat flux values given in the data summary tables have been corrected for the "tube" loss. Any overall heat balance made should incorporate both "end" and "tube" losses.

Test Runs

The initial system tested using the 2-ft reactor section was MCH over UOP-R8,Pt on Al_2O_3,catalyst. Table 48 summarizes the data obtained during the six test series making up the study. Each of the series will be described briefly in the following discussions.

The first test series (10018-50) was designed to duplicate the reactor inlet conditions and power input specified as Condition B in Table 70 of the last annual report.[19] A direct comparison of experimental data and performance predicted by the mathematical model could then be made. (This is discussed later.) A feed rate corresponding to a mass velocity of 150,000 lb/(hr·ft^2), an inlet pressure of 900 psig, and an inlet temperature of ca 900°F were established and power to the reactor was increased in steps until the specified heat flux [ca 350,000 Btu/(hr·ft)] was reached. As it became evident that the catalyst was deactivating, the test was discontinued at that point.

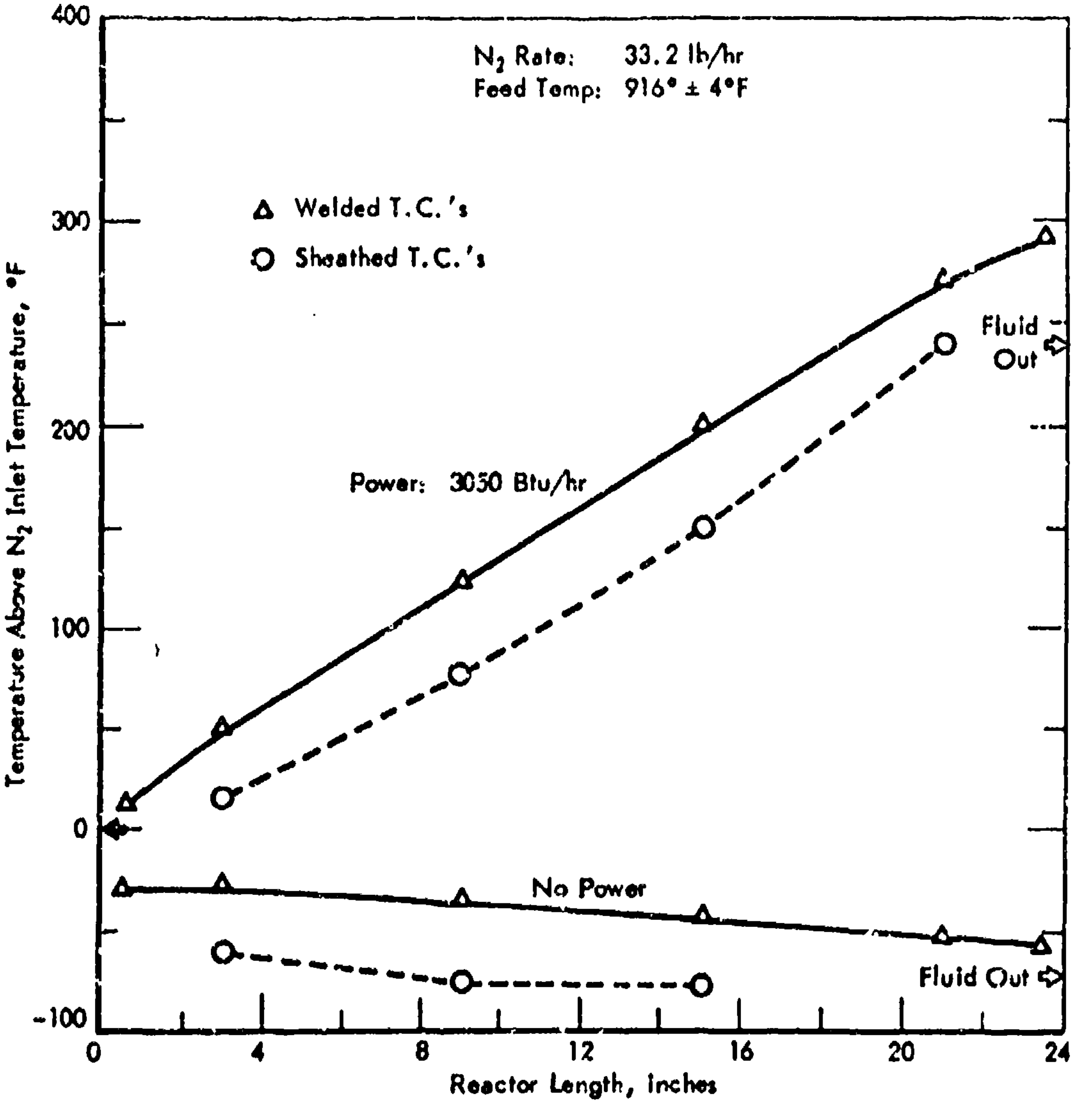

Figure 27. FSSTR - COMPARISON OF SHEATHED AND BARE WIRE THERMOCOUPLES ON 2-FT REACTOR SECTION

63586

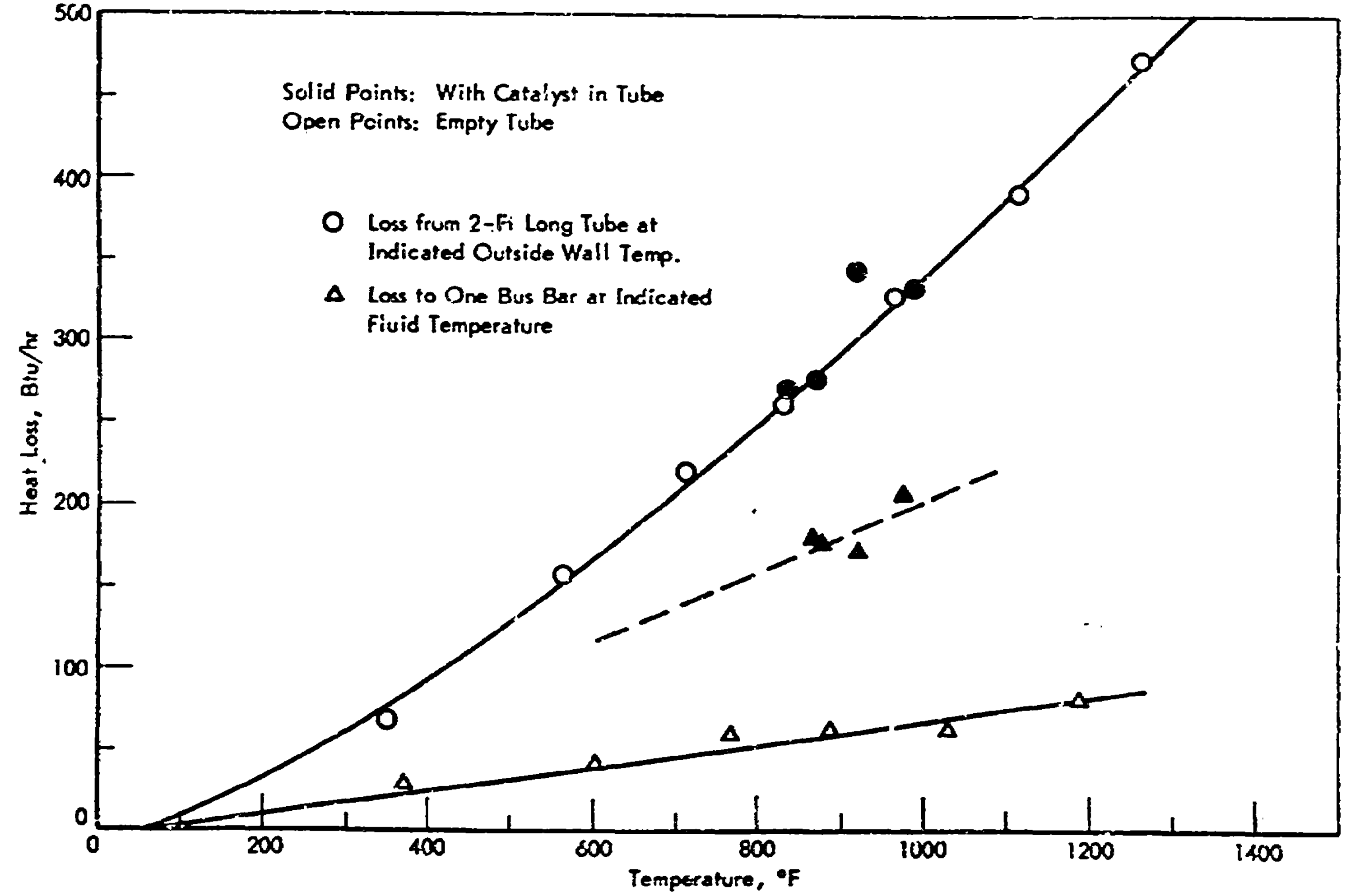

Figure 28. FSSTR - HEAT LOSS FROM 2-FT REACTOR SECTION

Table 48. FSSTR - MCH OVER UOP-R8 IN 2-FT REACTOR: DATA SUMMARY

Run 10018-	Feed Rate[a]				Heat to Fuel[d]			Temperature, °F								Press., psig		Conv.,[f] %
								Fluid		Tube Wall (Outside)[e]								
	$\frac{lb}{hr}$	gph	LHSV[b]	$\frac{lb^{c)}}{(hr)(ft^2)}$	$\frac{Btu}{hr}$	$\frac{Btu}{lb}$	$\frac{Btu}{(hr)(ft^2)}$	In	Out	1/2 in.	3 in.	9 in.	15 in.	21 in.	23-1/2 in.	In	Out	
First charge of UOP-R8 (activated 1-3/4 hr in N_2 at 1100°F)																		
50 - 12:30	64.5	16.05	1600	154,300	-225	-3.5	-1,600	898	698	863	798	736	712	700	698	865	700	15
50 - 13:10	"	"	"	"	6,000	93	41,400	901	745	897	839	787	773	771	770	837	671	21
50 - 13:50	"	"	"	"	13,200	205	91,000	895	788	925	881	841	836	841	841	886	645	29
50 - 14:30	"	"	"	"	21,500	333	148,300	895	831	962	931	901	902	913	913	885	604	39
50 - 15:10	"	"	"	"	30,600	474	211,000	896	878	1004	984	961	967	985	938	885	546	51
50 - 15:27 15:47	"	"	"	"	39,000	605	269,000	906 908	929 937	1046 1047	1032 1033	1015 1014	1024 1024	1052 1054	1062 1068	835	505	60
50 - 15:55 16:10	"	"	"	"	45,200	701	312,000	903 913	938 1011	1070 1074	1065 1069	1053 1057	1057 1071	1108 1120	1129 1149	836	466	65
50 - 16:20 16:47	"	"	"	"	52,300	811	361,000	907 900	1093 1126	1102 1094	1103 1100	1099 1099	1120 1122	1132 1212	1209 1266	885	436	65 63

(Continued)

a) Feed 99.7% MCH, 0.1% cyclohexane, 0.2% toluene.
b) LHSV based on superficial volume of 0.277-in. ID x 2-ft long reactor.
c) Mass velocity based on inside cross-section of reactor.
d) Corrected for loss along tube. Heat flux based on inside surface area.
e) Outside wall temperature at indicated distance from start of tube.
f) Moles of MCH converted per 100 moles of feed.
g) Tube wall temp rising rapidly. See separate plot of temperature-time data.

Table 48 (Contd-1). FSSTR: MCH OVER UOP-R8 IN 2-FT REACTOR

Run 10018-	Feed Rate				Power			Temperature, °F								Press., psig		Conversion, %
								Fluid		Tube Wall (Outside)								
	lb/hr	gph	LHSV	lb/(hr)(ft²)	Btu/hr	Btu/lb	Btu/(hr)(ft²)	In	Out	1/2 in.	3 in.	9 in.	15 in.	21 in.	23-1/2 in.	In	Out	
First charge of UOP-R8 (activated 1-3/4 hr in N_2 at 1100°F) (Continued)																		
52 - 11:30	64.6	10.06	1610	154,400	-230	-3.6	-1,600	900	707	876	818	750	721	710	707	885	688	14.6
52 - 12:39	"	"	"	"	26,700	413	184,000	907	906	1000	974	946	950	980	995	883	568	42
13:59								903	909	995	974	947	949	979	996			41
52 - 14:22	"	"	"	"	39,600	634	269,000	905	999	1049	1041	1025	1037	1088	1113	883	504	53
15:29								903	1011	1046	1040	1027	1039	1092	1123			51
52 - 16:00	"	"	"	"	-230	-3.6	-1,600	904	712	883	829	758	727	714	711	856	691	15.5
H_2 treat (20 minutes at 1000°F																		
55 - 11:00	64.9	10.11	1610	155,100	-230	-3.5	-1,600	904	707	808	817	750	721	709	708	883	694	13.6
55 - 11:46	"	"	"	"	38,000	586	262,000	901	1005	1039	1037	1030	1040	1093	1121	882	509	51
12:53								903	1014	1037	1036	1028	1038	1094	1125			49
14:00								900	1021	1034	1034	1029	1040	1098	1130			48
55 - 14:14	"	"	"	"	46,000	709	317,000	900	1093	1070	1080	1085	1101	1176	1220	885	465	54
14:34								905	1111	1074	1083	1089	1108	1188	1237			53
55 - 14:45	"	"	"	"	54,200	835	374,000	905	1216	1110	1129	1145	1179	1233	1357	882	418	57
14:58								901	1245	1105	1125	1144	1185	1315	(a)	885	407	54
Second charge of UOP-R8 (activated 2 hr at 1100°F)																		
60 - 13:00	64.5	10.05	1604	154,000	-225	-3.5	-1,600	900	696	860	802	739	713	700	696	854	709	14.7
60 - 13:36	"	"	"	"	41,400	642	286,000	903	926	1037	1023	1011	1027	1050	1070	892	505	63
14:03								901	933	1034	1021	1009	1024	1050	1072			61

a) Tube wall temp rising rapidly. See separate plot of temperature-time data.

(continued)

Table 48 (Contd-2). FSSTR: MCH OVER UOP-R8 IN 2-FT REACTOR

Run 10018-	Feed Rate				Power			Temperature, °F								Press., psig		Conversion, %
								Fluid		Tube Wall (Outside)								
	lb/hr	gph	LHSV	lb/(hr)(ft²)	Btu/hr	Btu/lb	Btu/(hr)(ft²)	In	Out	1/2 in.	3 in.	9 in.	15 in.	21 in.	23-1/2 in.	In	Out	
Second charge of UOP-R8 (activated 2 hr at 1100°F) (Continued)																		
62 - 11:30	25.1	3.91	625	60,000	-220	-8.8	-1,500	902	699	836	756	711	702	701	701	892	865	13.9
62 - 13:00	"	"	"	"	4,870	194	33,600	901	770	873	808	782	793	801	806	891	855	29
62 - 14:00	"	"	"	"	19,100	721	125,000	901	901	966	931	932	957	990	1019	834	836	72
62 - 14:19	"	"	"	"	24,000	954	165,000	895	1011	1002	981	990	1022	1039	1155	889	823	86
15:13								904	1042	1010	984	990	1027	1101	11159			84
16:06								900	1044	1003	980	986	1022	1101	1158			82
62 - 16:50	"	"	"	"	4,860	194	33,500	838	768	880	815	787	793	809	821	831	854	28
64 - 9:50	64.1	9.98	1593	153,200	11,300	176	77,900	71	334	183	217	294	368	439	471	902	866	
64 - 9:55	"	"	"	"	16,000	250	110,000	71	496	224	269	368	465	551	590	902	854	
64 - 10:15	"	"	"	"	22,900	357	158,000	71	610	278	335	463	579	677	713	899	863	0.0
64 - 10:25	"	"	"	"	30,200	471	208,000	72	713	339	411	566	695	797	839	896	850	0.7
64 - 10:35	"	"	"	"	38,000	593	262,000	72	804	400	485	651	793	913	959	895	836	4.5
64 - 10:50	"	"	"	"	47,900	747	330,000	72	876	473	572	758	910	1024	1059	895	810	14.1
64 - 11:05	"	"	"	"	58,200	908	401,000	72	931	545	654	855	1018	1101	1138	890	774	26
64 - 11:20	"	"	"	"	74,000	1154	510,000	73	1034	657	772	1003	1147	1219	1672	894	720	44
11:55								74	1063	660	774	1010	1150	1230	1295			42
64 - 12:05	"	"	"	"	78,000	1617	538,000	74	1103	685	799	1046	1178	1263	1337	893	705	45
12:30								74	1120	687	800	1045	1180	1269	1351			44
64 - 12:40	"	"	"	"	82,300	1280	568,000	74	1166	715	826	1081	1208	1308	(a)	893	687	47

a) Tube wall temperature rising rapidly. See separate plot of temperature-time data.

The effect of catalyst deactivation is shown in Figure 29 where the exit fluid temperature is indicated. The continuing temperature rise shown in the final runs after a step increase in power indicates that the heat sink resulting from reaction is decreasing and a corresponding amount of power is heating the product.

Even though the catalyst had evidently been slowly deactivating prior to the final power increase, the initial conversion at that level reached about 66%. Comparing this with the predicted conversion of 57% indicated that some modification of the model would be required.

Series 10018-52 was run at the same reaction inlet conditions as the preceding series as a check on the previous results. Longer lined-out periods of operation confirmed that deactivation was proceeding at temperatures at least as low as 900°F.

As tests in the bench-scale reactor (Figure 6)[10] had shown some temporary improvement in catalyst activity resulting from hydrogen treatment, this procedure was tried on the partially deactivated catalyst. H_2 was passed through the reactor while maintaining inlet and outlet fluid temperatures at ca 1000°F for 20 minutes. No significant increase in activity could be demonstrated during the initial run conditions established for Series 10018-55. If any enhancement of catalyst activity occurred, it was very temporary and had dissipated during the time required to bring the unit to an operating condition corresponding to the final run of the preceding series. The test was continued, increasing power input in steps, until a heat flux of 376,000 Btu/(hr·ft^2) was attained. At this point the tube wall temperature at a point 1/2 in. from the exit end started increasing rapidly and the run was discontinued. This will be further discussed in a subsequent section. The increasing rate of catalyst deactivation at higher temperatures was clearly demonstrated during this series. Figure 30 shows the MCH conversion-time data taken at three temperature levels.

A fresh charge of UOP-R8 was then installed in the tube and activated in N_2 for 2 hours at 1100°F.

Series 10018-60 was a brief test at moderate power input made to confirm that catalyst activity was the same as for the first charge.

In order to provide further data for modification of the mathematical model the next tests (Series 10018-62) were made at a lower flow rate, G = 60,000 lb/(hr·ft^2). This corresponds to the mass flow rate used for a number of tests previously made in the 10-ft reactor sections. During this series a maximum heat flux of 168,000 Btu/(hr·ft^2) to the catalyst section was reached, resulting in an initial MCH conversion of 36%.

The final test series (Series 10018-64) was designed to reach the maximum heat flux permitted by the 1000 ampere power supply limitation, ca 590,000 Btu/(hr·ft^2). Feed at ambient temperature was used for these runs and power was increased in steps as usual, until at a heat flux of 570,000 Btu/(hr·ft^2) a rapid rise in tube wall temperature forced shut-down. Conversion was 47% at this condition.

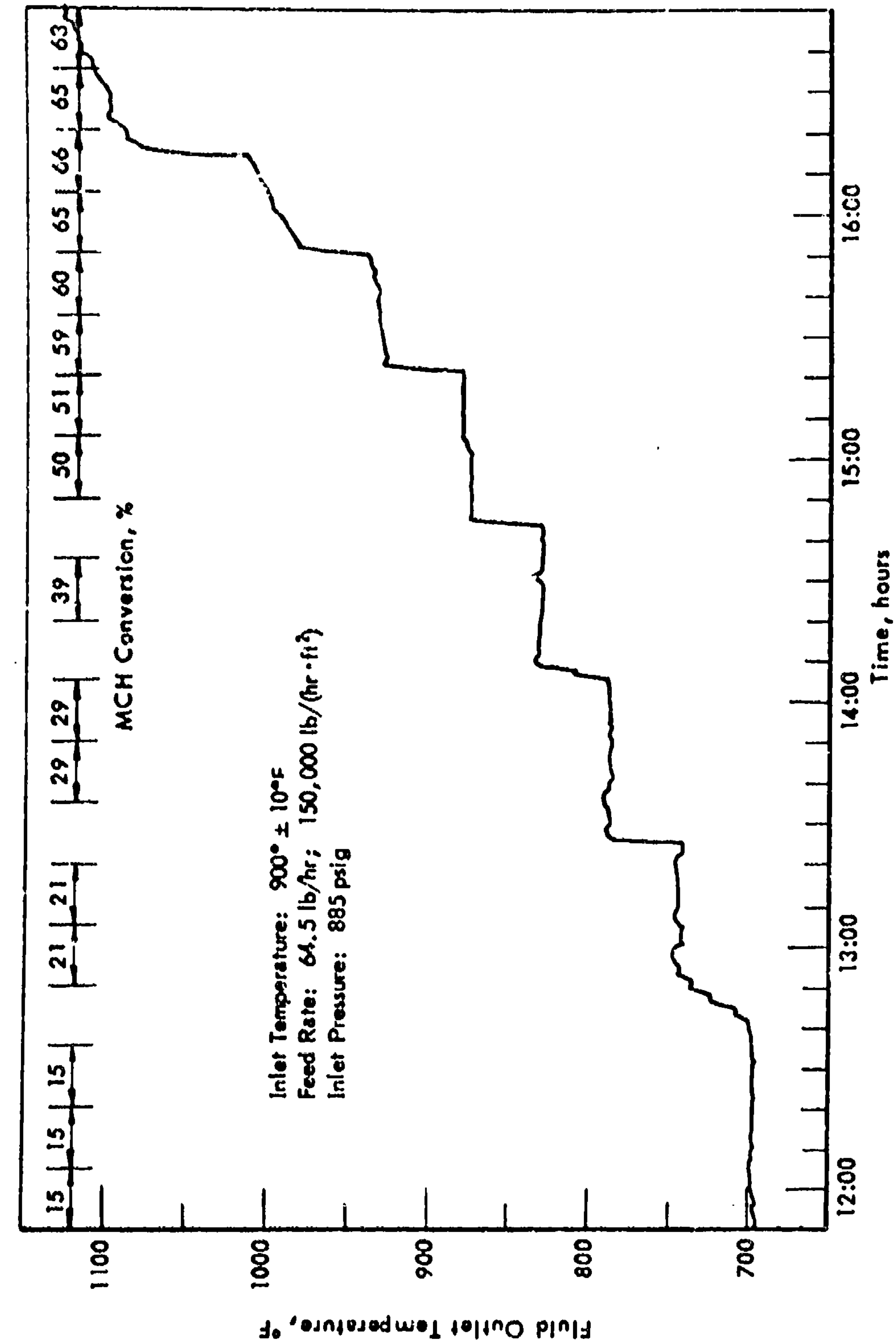

Figure 29. FSSTR - MCH OVER UOP-R-8 IN 2-FT REACTOR: CATALYST BED EXIT FLUID TEMPERATURE

63294

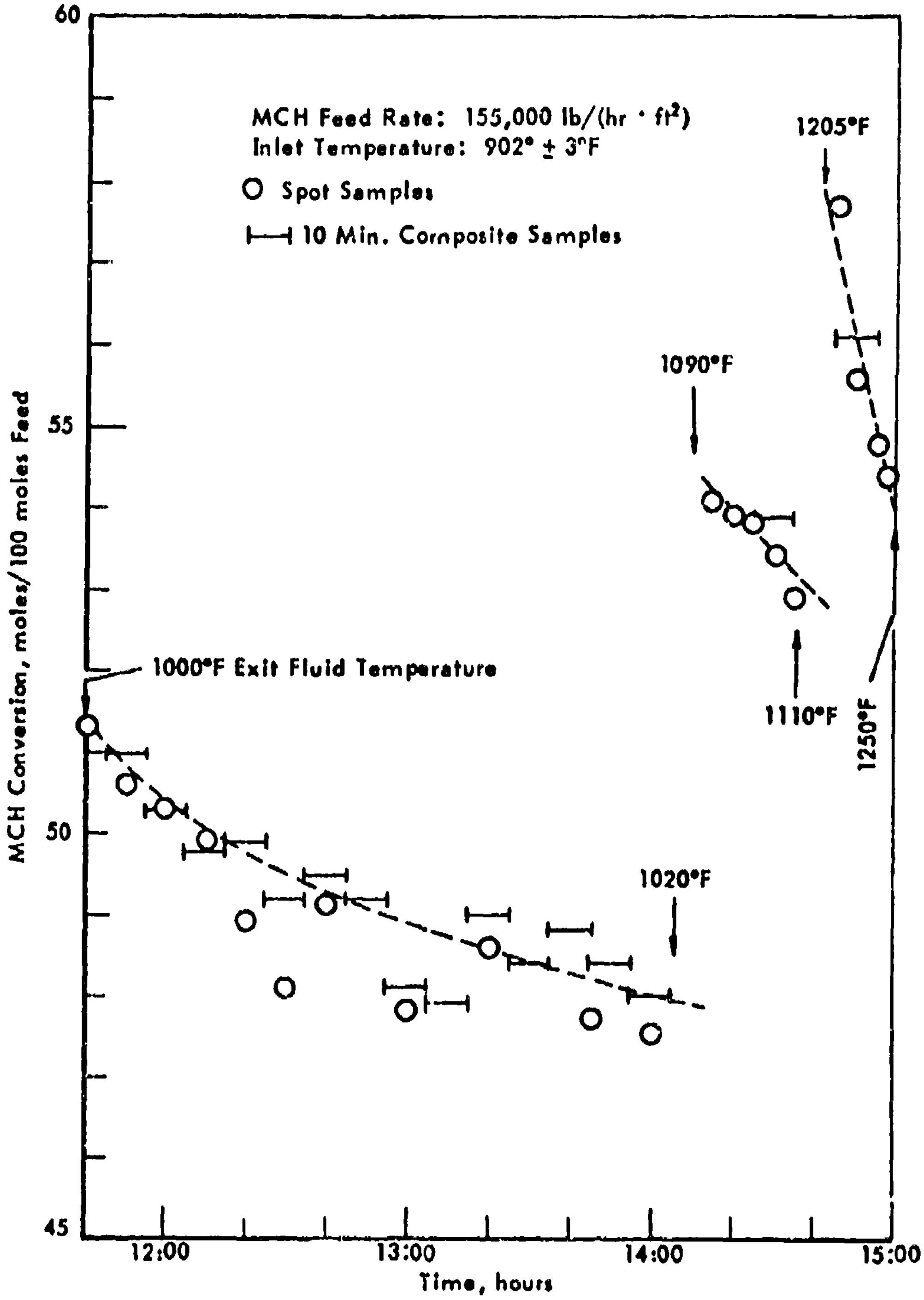

Figure 30. FSSTR - MCH OVER UOP-R8 IN 2-Ft REACTOR: DECLINE IN CATALYST ACTIVITY DURING SERIES 10018-55

Coke Deposit: Temperature Limit

Series 55 and 64 were each terminated when a runaway temperature developed after a step increase in power. The sudden increase in temperature was measured by the tube wall thermocouple located 1/2 in. before the exit end of the reactor. Figures 31 and 32 show the time-temperature data recorded during the final portions of the two series. Tube wall temperatures at 21 in. and 23-1/2 in. points and exit fluid temperatures are shown. A rapid temperature rise of this nature occurred during previous experiments on the 10-ft reactor (Figures 58 and 59),[2] at which time catalyst deactivation was caused by increasing the temperature of MCH feed to the catalyst section to 1100-1150°F. However, sudden catalyst deactivation was obviously not the mechanism involved in the present problem, since the exit fluid temperature did not follow the tube wall temperature, which would have been the case if the heat sink capacity were lost due to a sudden decline in conversion. It appeared more likely that the increase in temperature difference between tube and fluid was the result of an insulating coke layer being deposited on the tube wall and a consequent decline in overall heat transfer coefficient. This was substantiated when the catalyst charge was dumped following Series 55. The bulk of the charge poured easily from the tube but it was necessary to rod out the final 1/2 in. to 1 in. portion of the bed. Examination of the catalyst particles from this final section showed a coke sheet adhering to one tangent of some of the beads. A photomicrograph (Figure 33) of a recovered particle shows the coke sheet clearly. The broken catalyst bead was probably fractured during removal from the reactor tube. The coke film in the picture is about 0.01 in. thick. No generalized conclusions can be drawn from this single case. However, for the system involved, rapid coke build-up should be anticipated in any region where tube wall temperatures of 1350°F and fluid temperatures of 1150°F might be encountered. Whether the presence of the catalyst affects these temperatures will be checked in subsequent runs.

The R8 catalyst in the runs in the 2-ft reactor has shown much more tendency to deactivate than it did in the runs in the 10-ft reactor, due probably to the higher heat flux. Work under our catalyst development program has provided catalysts of greater stability (as indicated by bench scale tests) than the R8. Enough of one of these (10280-113) has been made up to carry out tests in the 2-ft reactor. This will be done in the subsequent period.

Cooling Program, Experimental Study

A program has been initiated to provide experimental data which will yield information on the characteristic behavior of hydrocarbon fuels under conditions of very high heat flux.

Proposed targets for this investigation are:

1. Heat sink in the region of 600 Btu/lb (from latent and sensible heat only).
2. Tube wall temperatures of 1300-1400°F.
3. Heat flux in the region of 7-8 x 10^6 Btu/(hr·ft^2).

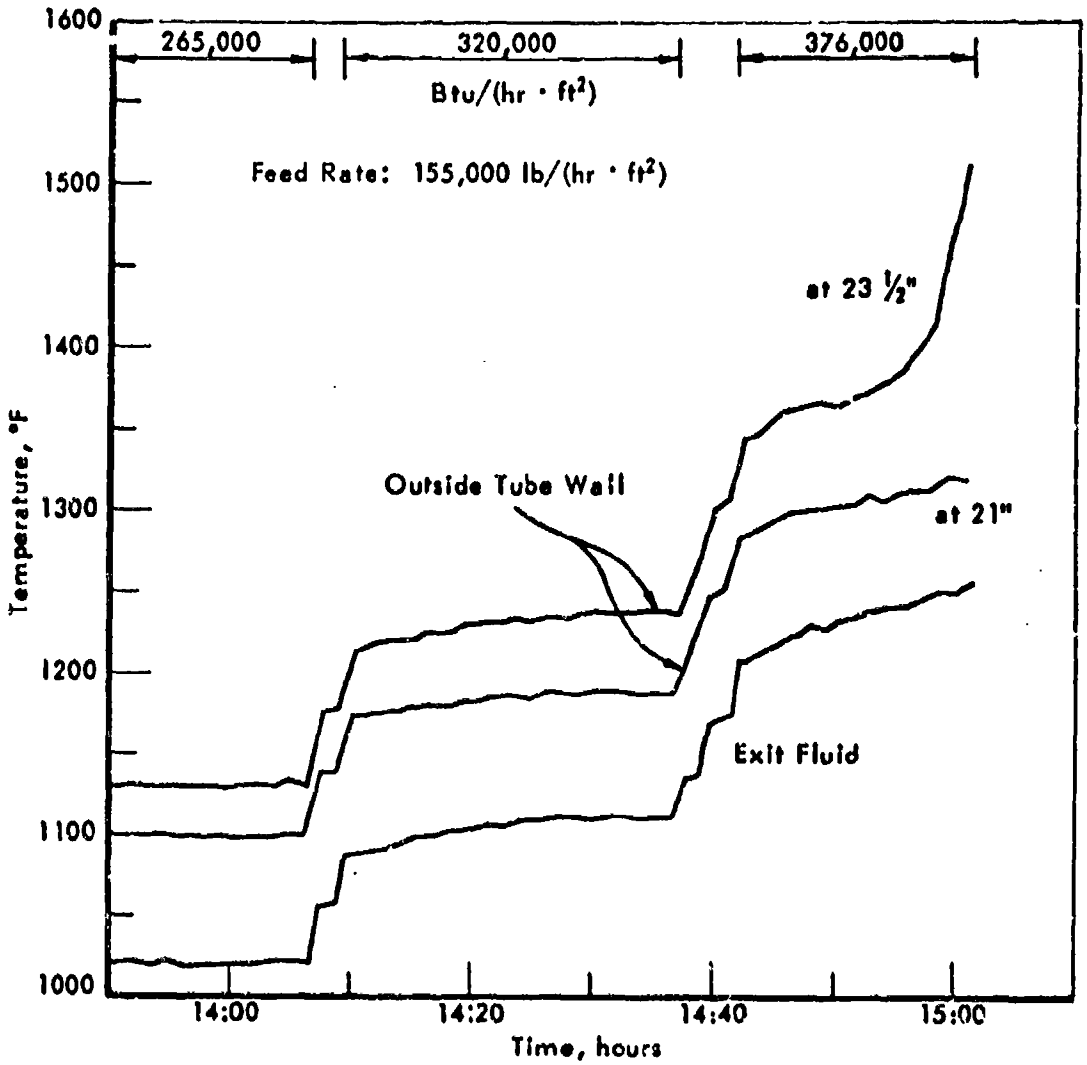

Figure 31. FSSTR - MCH OVER UOP-R8 IN 2-Ft REACTOR: EFFECT OF COKE DEPOSITION ON TUBE WALL TEMPERATURE, SERIES 10018-55

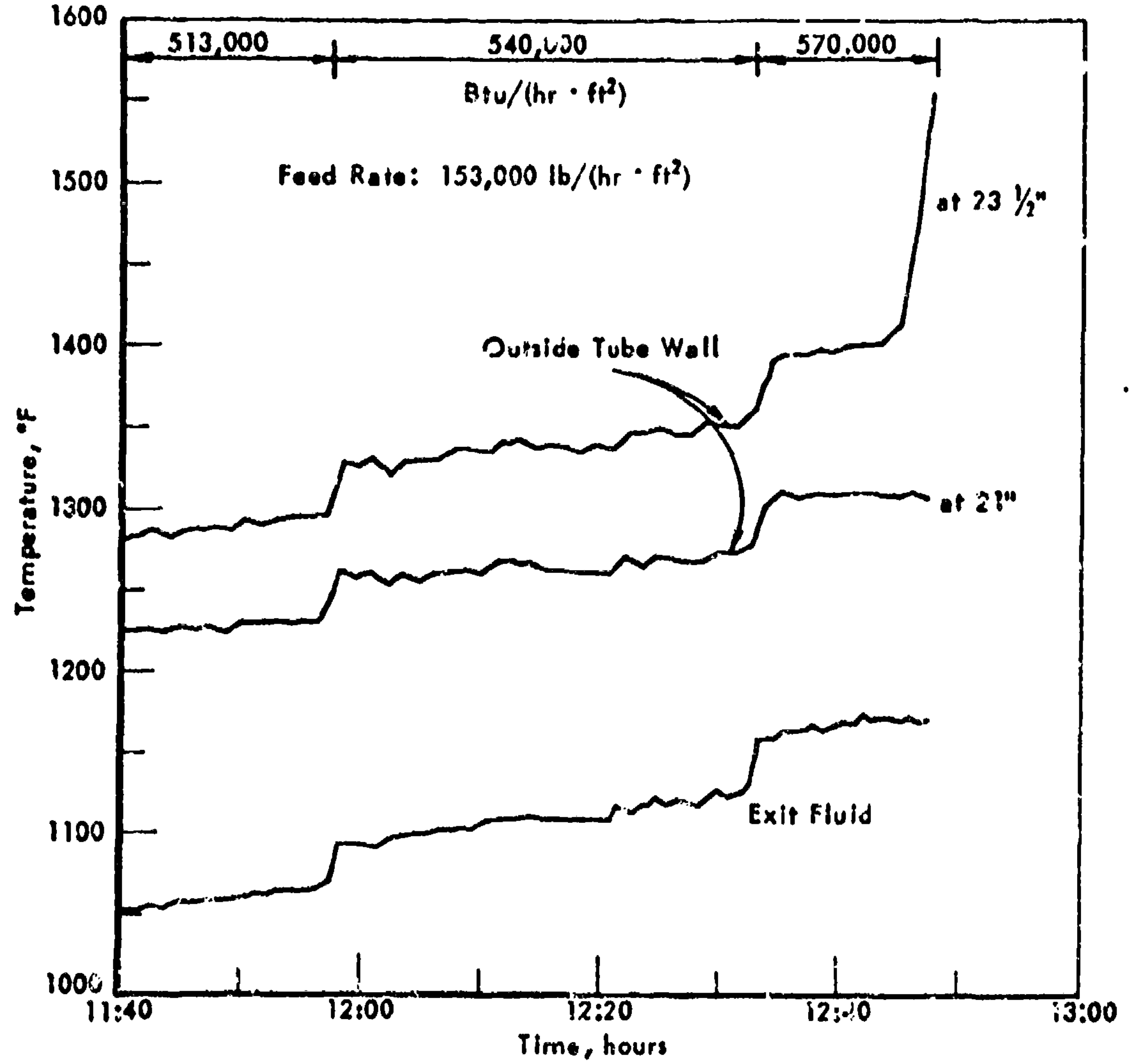

Figure 32. FSSTR - MCH OVER UOP-R8 IN 2-Ft REACTOR: EFFECT OF COKE DEPOSITION ON TUBE WALL TEMPERATURE SERIES 10018-64

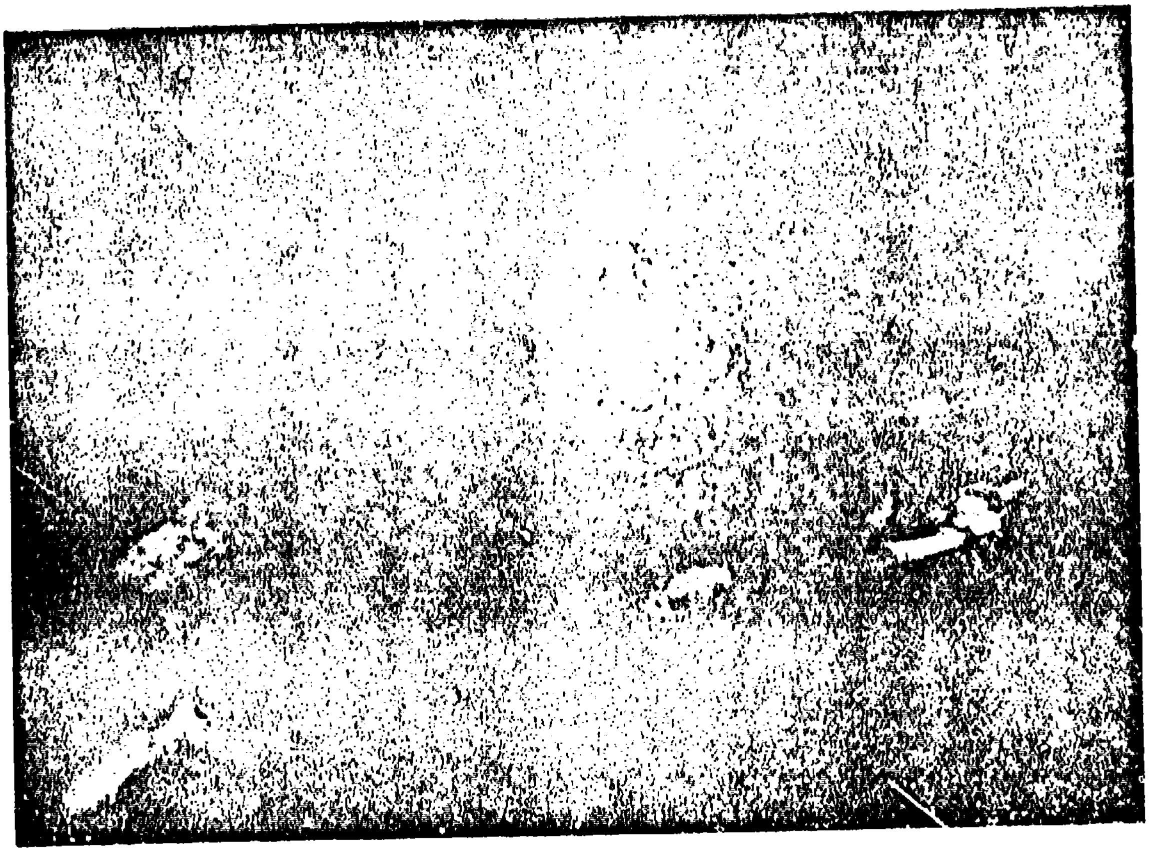

Figure 33. FSSTR - MCH OVER UOP-R8 IN 2-FT REACTOR: COKE FORMATION FROM SERIES 10018-55
Magnification: 56X

4. Tube ID between 1/4 in. and 0.02 in.

The major objective of the study is the experimental verification of, or if necessary, modification of, heat transfer correlations for use under these extreme conditions. Also, as some thermal reaction is apt to be found at the high wall temperature levels, the possibility of coke deposition on the tube walls exists and the effect of this deposit on heat transfer as well as the possibility of plugging in the small diameter tubes will have to be investigated.

0.277" ID x 2-ft Long Heat Transfer Section

The initial effort in this study, using MCH as the test fluid, was conducted using the 3/8 in. OD x 2-ft long heat transfer section which was described previously. Some changes made in thermocouple placement will be discussed later.

Test Runs

Three series of test runs have been completed at conditions which met as many of the proposed targets as possible while using this section. The range of variables covered was:

Tube Size:	0.277 in. ID x 2 ft long
Pressure:	600-900 psig
Feed Rate:	241,000 lb/(hr·ft^2) ≈ 2500 LSHV
Max Heat Flux:	163,000 Btu/(hr·ft^2)
Max Bulk Fluid Temp:	913°F
Max Tube Wall Temp:	1350°F (outside) 1320°F (inside)

In none of these tests was there any indication of change of heat transfer coefficient that might be attributed to coke deposition. Data from these tests is summarized in Table 49.

In the original design this tube section was constructed with all tube wall thermocouples spot welded to the bottom of the horizontal tube. Series 10018-71 was carried out without any change in this configuration, therefore, temperature differences between top and bottom surfaces of the tube were not measured. Difficulty in obtaining heat balances during these tests led to relocation of the exit fluid thermocouple which in turn gave indication of temperature strata existing in the outlet fluid stream. To determine the extent of this temperature variation along the tube, six additional wall thermocouples were added to the reactor. Five of the new couples were located on top of the tube alternating in axial position with the original six located on the tube bottom and one was positioned on the side of the tube 16-1/2 in. from the inlet end. A sketch of the tube with the revised thermocouple arrangement is given in Figure 34.

Series 10018-75 and 78 were then carried out. In these tests differences of up to 300°F between top and bottom outside wall temperatures were measured. Temperature profiles for three of the runs which were made under similar conditions except for feed temperatures are shown in Figure 35. Data from the 1/2 in. and 23-1/2 in. locations have been deleted from this

Table 49. ESSTR - HEAT TRANSFER TO MCH IN 0.277" ID x 2-FT LONG HEAT TRANSFER SECTION: DATA SUMMARY

Run No. 10018-	MCH Feed Rate				Heat To Fuel			Bulk Fluid[d] Temp., °F		Press., psig[e]	Outside Tube Wall Temperature, °F[f]											
	lb/hr	gph	LHSV[a]	lb[b] / (hr)(ft²)	Btu / hr	Btu / lb	Btu[c] / (hr)(ft²)	In	Out		B-1/2"	B-5"	B-9"	B-15"	B-21"	B-23-1/2"	S-16-1/2"	T-1-1/2"	T-4"	T-12"	T-18"	T-22-1/2"
72-10:20	104	16.2	2590	249,000	5,460	53	37,000	70	182	602	314	441	446	446	482	471						
10:48					8,360	80	57,700	70	234	601	428	573	611	621	621	618						
11:00					12,300	118	88,600	70	313	600	581	715	810	800	815	766						
12:06					18,400	176	126,500	70	399	753	743	970	967	971	976	927						
12:30					20,700	199	142,700	74	434	755	832	1040	1028	1031	1035	979						
12:45					22,700	218	156,500	72	463	750	917	1090	1075	1074	1070	1015						
13:15					5,050	50	36,000	335	408	670	490	527	542	550	561	561						
75-10:20	102	15.9	2540	244,000	4,990	49	48,200	74	221	888	396	531	579	571	588	580	622	555	686	727	636	647
10:50					12,400	122	85,600	74	320	888	593	727	739	762	737	788	859	803	967	932	1026	1252
11:30					17,100	167	131,600	74	420	888	800	1013	1002	1017	1020	974	1125	1150	1250	1309	1335	1347
12:25					9,400	92	64,900	209	376	888	548	662	696	677	699	689	744	636	812	857	861	852
13:15					19,700	193	135,700	209	520	908	819	1038	1037	1044	1042	990	1159	1147	1236	1307	1353	1343
14:10					10,000	98	69,100	339	535	908	666	750	785	800	805	786	856	762	900	946	963	977
15:15					21,600	212	148,800	394	669	905	964	1090	1079	1048	1042	1009	1246	1192	1241	1325	1335	1335
16:30					21,900	215	151,000	498	739	880	993	1025	970	973	1053	1061	1080	1093	1117	1231	1220	1258
16:55					21,800	214	150,200	595	824	875	1034	1077	1046	1081	1118	1124	1164	1145	1177	1252	1275	1300
78-10:15	101	15.7	2510	241,000	9,860	98	68,000	70	272	885	500	642	689	697	698	694	748	698	845	877	878	877
11:10					19,100	189	131,600	70	423	882	798	1009	1001	1003	1016	971	1118	1148	1244	1208	1337	1353
12:25					21,000	208	144,500	415	671	891	957	1085	1077	1054	1044	1005	1149	1187	1244	1320	1337	1324
13:55					22,300	220	153,400	660	902	885	1069	1164	1158	1147	1186	1201	1217	1158	1273	1273	1319	1341
15:55					23,700	234	163,100	628	913	894	1053	1159	1195	1186	1222	1247	1245	1130	1267	1316	1339	1358

a) LHSV based on 2-ft length of 0.277" ID tube.
b) Mass velocity.
c) Corrected for loss along tube. Heat flux based on inside tube surface.
d) Measured fluid temperatures have been corrected for heat loss between tube end and thermocouple location.
e) Pressure drop was < 2 psi.
f) Temperature at indicated inches from tube inlet. B = thermocouple junction on bottom of tube, S = TC on side of tube, T = TC on top of tube.

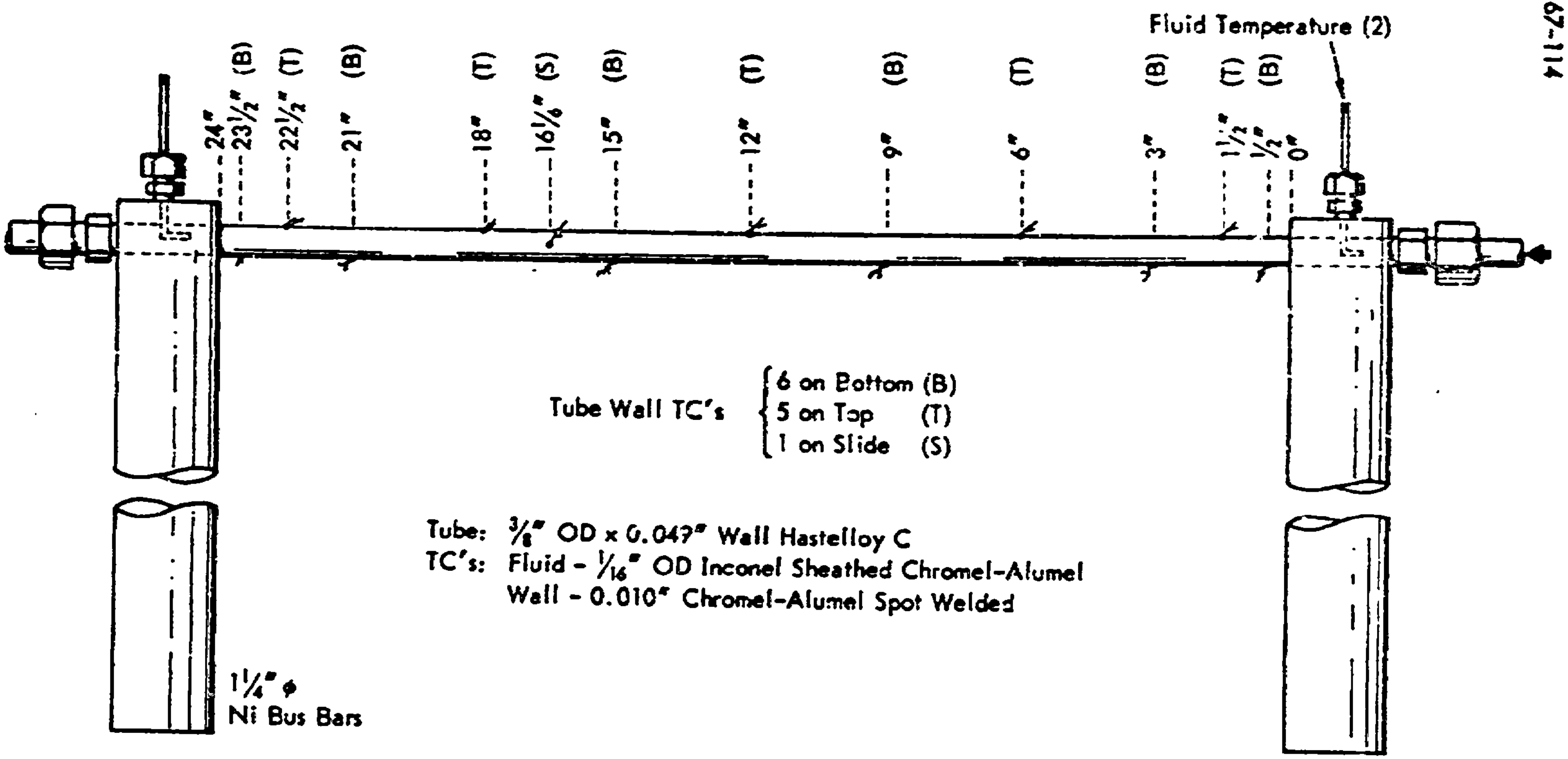
Fluid Temperature (2)
24"
23½" (B)
22½" (T)
21" (B)
18" (T)
16 1/6" (S)
15" (B)
12" (T)
9" (B)
6" (T)
3" (B)
1½" (T)
½" (B)
0"
1¼" ϕ
Ni Bus Bars

Tube Wall TC's
- 6 on Bottom (B)
- 5 on Top (T)
- 1 on Slide (S)

Tube: ⅜" OD x 0.049" Wall Hastelloy C
TC's: Fluid - $1/16$" OD Inconel Sheathed Chromel-Alumel
Wall - 0.010" Chromel-Alumel Spot Welded

Figure 34. FSSTR - 0.277" ID x 2 FT-LONG HEAT TRANSFER SECTION

Run No. 10018-	Location of TC on Tube Wall			Bulk Fluid Temperature, °F		Heat Flux, Btu/(hr · ft²)
	Top	Side	Bottom	In	Out	
75-15:15	○	⊙	●	395	668	152,000
75-16:30	◇	◈	◆	499	738	154,000
75-16:55	□	▣	■	596	823	153,000

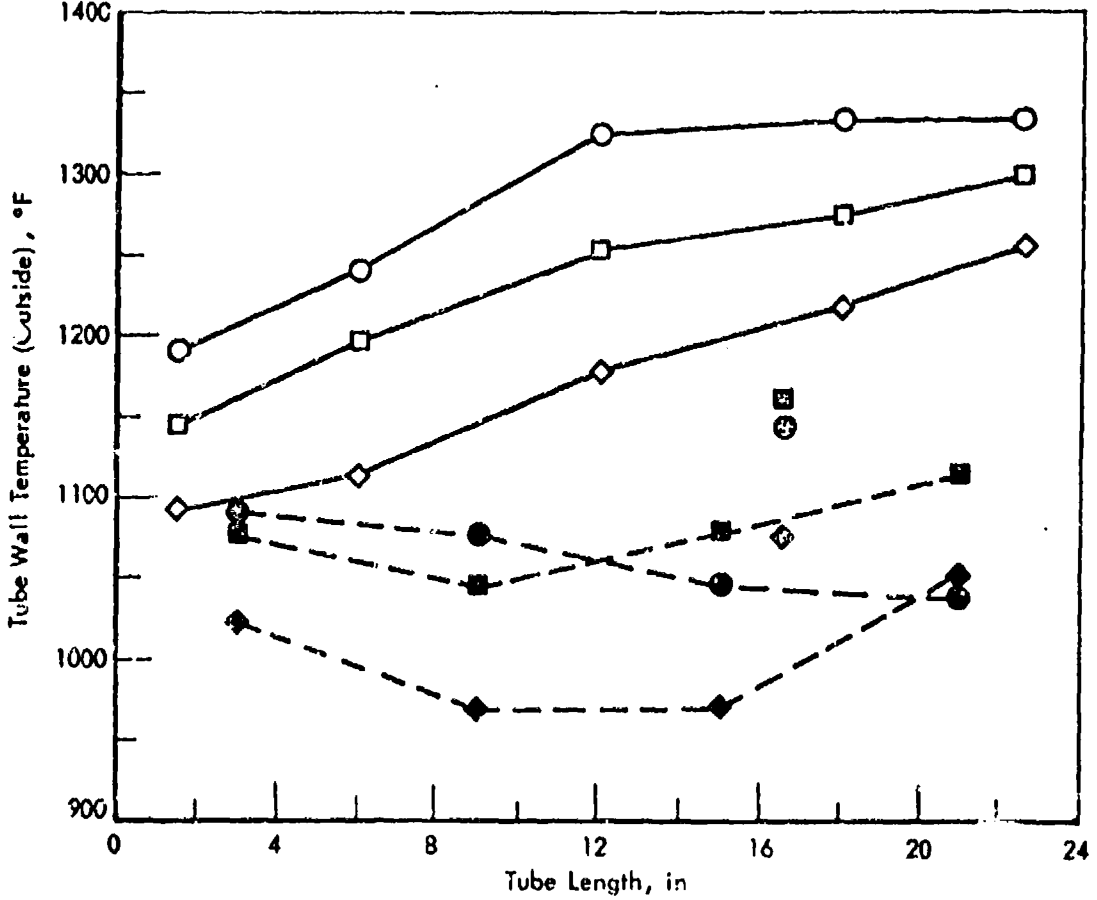

Figure 35. FSSTR - HEAT TRANSFER TO MCH IN EMPTY 0.277" ID x 2-FT LONG HEAT TRANSFER SECTION: VARIATION OF TUBE WALL TEMPERATURE WITH THERMOCOUPLE LOCATION

figure as these temperatures are influenced by the proximity of the bus bars. A comparison of the experimental data with several heat transfer correlations is given in another section of this report.

It is assumed that this temperature difference is due to stratification of the flowing fluid rather than being the result of non-uniformity of the wall thickness. A section of the tube from which the reactor was made was measured and a variation of only ± 0.001" was found in the nominal 0.049" wall thickness. When time is available this reactor will be operated in an inverted position to see if the hot wall will remain on the top or will move to the bottom with the tube inversion.

Heat losses from the uncompensated 2-ft long reactor section were determined by measuring the temperature drop of a heated N_2 stream passing through the tube in the same manner as was described when it was used as a catalytic reactor. Figure 36 illustrates the measurement for one temperature level. The heat losses determined over the entire temperature range are shown in Figure 28 along with the data obtained using the reactor packed with catalyst. Note that heat loss to the bus bars ("end" loss) is much less important when the catalyst is no longer present to promote turbulence and increased heat transfer.

Temperature data from Sections I and II of the FSSTR (3/8 in. OD x 10-ft long tubes) taken during lined-out periods of operation when they were being used as preheaters for the 2-ft section are listed in Table 74 in the Appendix.

0.0265" ID x 6" and 4" Heat Transfer Sections

A test set-up designed to operate at higher heat flux conditions than was possible using the larger reactor sections has been assembled and a photograph of the test stand with a 1/16" OD x 6" long heat exchange section in place is shown in Figure 37. The reactor is connected into the FSSTR system and makes use of the feed supply and pressure control system of that unit. Power for resistance heating of the tube is supplied by an 18 KVA variable reactance transformer. The discharge end of the reactor is grounded and is fixed in position to the mounting framework. The upstream end is supported on rails by a movable bracket, and a pulley and weight system is used to keep a constant tension on the tube, moving the bracket as necessary along the rails as the tube expands.

The heat exchange sections used in this rig have all been constructed of 1/16" OD x 0.018" wall type 316 S.S. tube (0.0265" ID) silver soldered to 3/4" diameter copper bus bars. Sketches giving dimensions and thermocouple locations for the five sections used to the present time are given in Figures 38 through 41.

Fluid temperatures are measured in the expanded end fittings before and after the heat exchange section as shown and outside tube wall temperatures are measured by thermocouples which are spot welded to the tube. The wall thermocouple leads are wrapped at least one full turn around the tube before running through ceramic insulation tubes to a junction board. The leads are insulated from direct contact with the tube and each other by a layer of ceramic cement. The rest of the tube has been covered with a

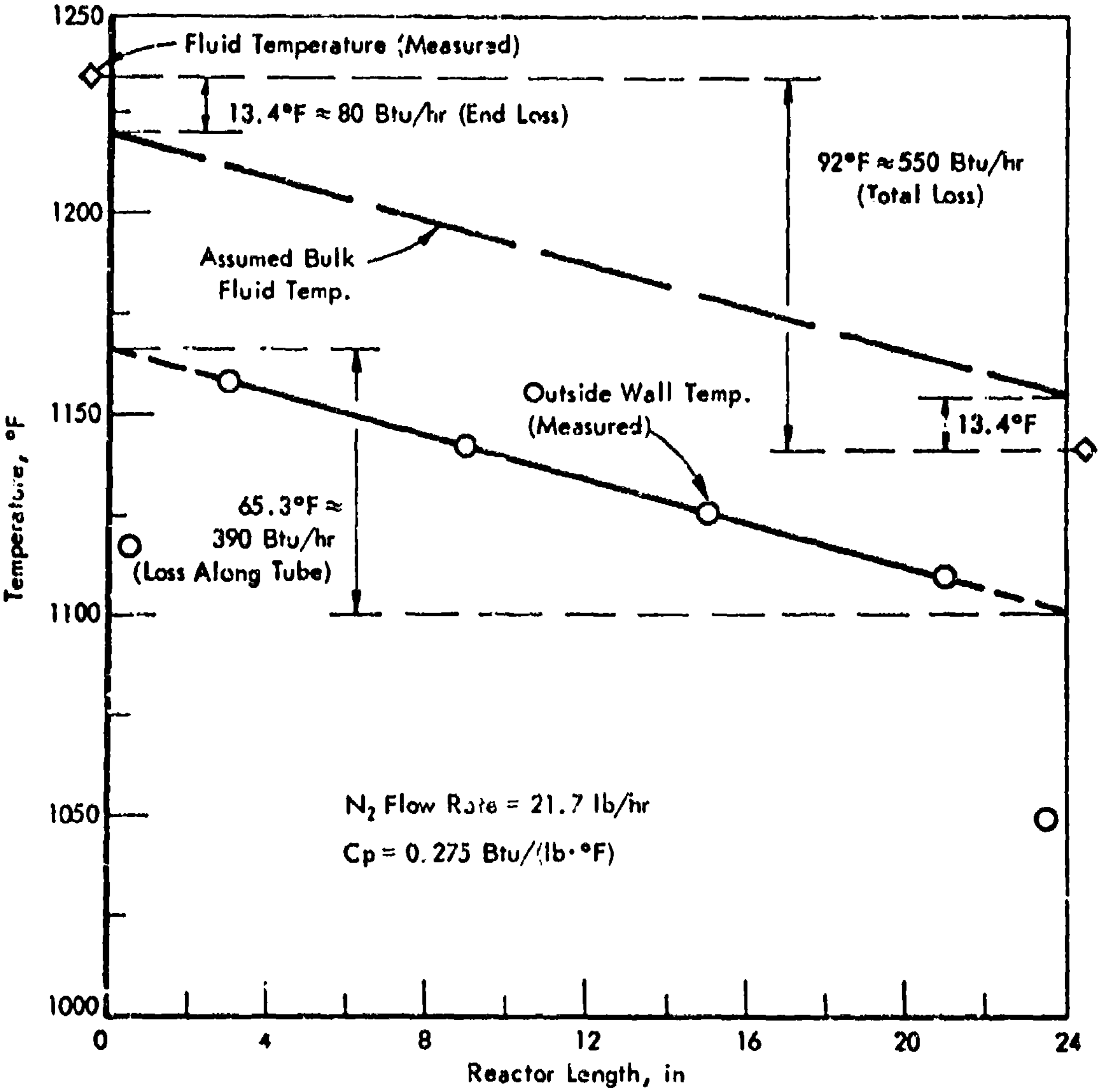

Figure 36. FSSTF: EXAMPLE OF HEAT LOSS MEASUREMENT FROM 2-FT LONG HEAT TRANSFER SECTION

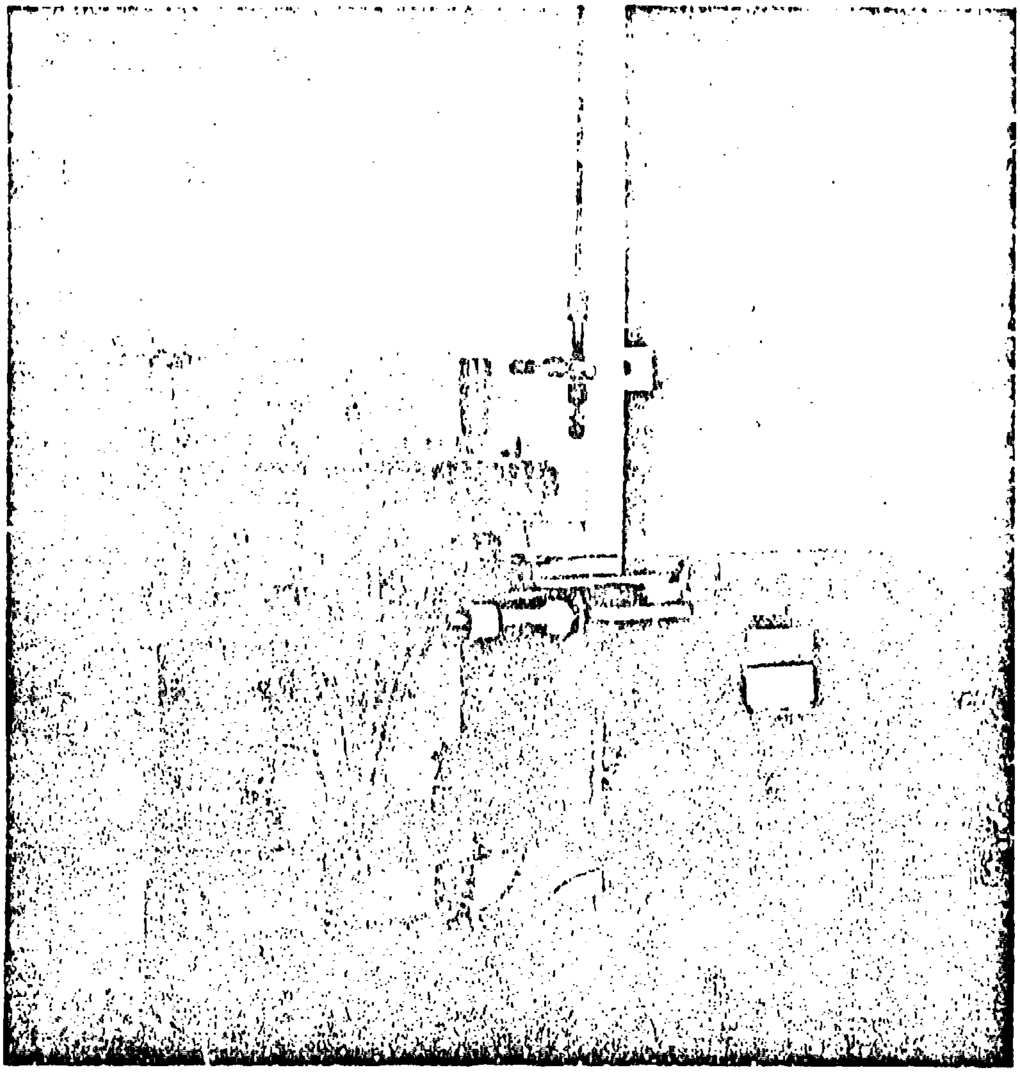

Figure 37. FSSTR - MINIATURE HEAT TRANSFER SECTION TEST STAND

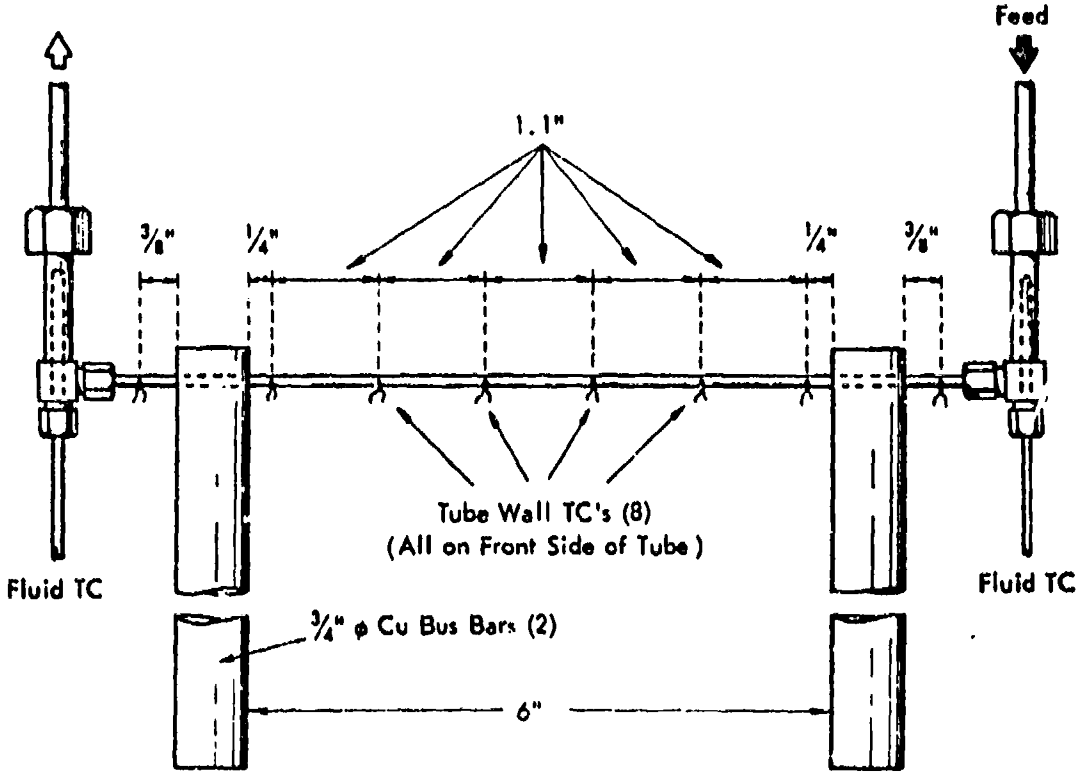
Feed
1.1"
3/8"
1/4"
1/4"
3/8"
Tube Wall TC's (8)
(All on Front Side of Tube)
Fluid TC
Fluid TC
3/4" φ Cu Bus Bars (2)
6"

Tube: 1/16" OD x 0.018" Wall Type 316 SS (1/16" Tube 10 1/4" Long Overall)
Thermocouples: Fluid - 1/16" OD inconel Sheathed Chromel-Alumel
Wall - 0.005" Chromel-Alumel Spot Welded
Scale: None

Figure 38. FSSTR - MINIATURE HEAT TRANSFER SECTION: REACTOR NO 10018-82

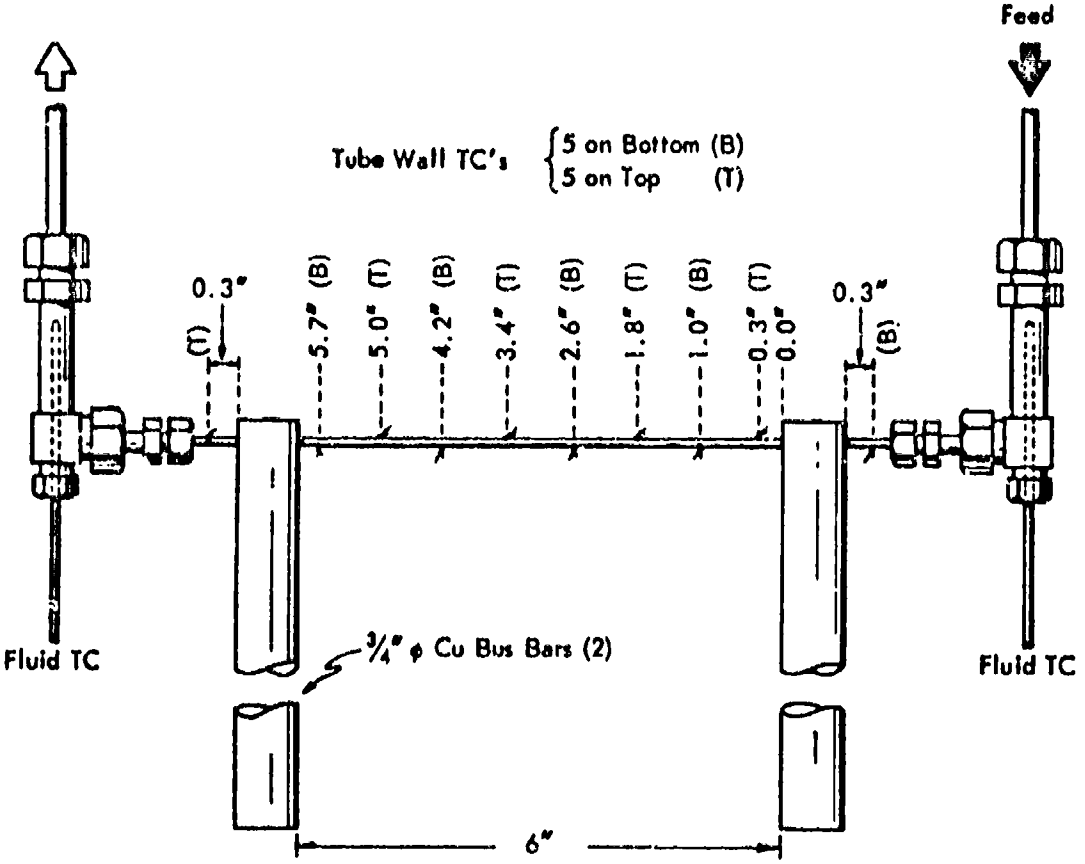
Feed
Tube Wall TC's {5 on Bottom (B) 5 on Top (T)
0.3"
(T)
5.7" (B)
5.0" (T)
4.2" (B)
3.4" (T)
2.6" (B)
1.8" (T)
1.0" (B)
0.3" (T)
0.0"
0.3"
(B)
Fluid TC
3/4" φ Cu Bus Bars (2)
Fluid TC
6"

Tube: 1/16" OD x 0.018" Wall Type 316 SS (1/16" Tube 9½" Long Overall)
Thermocouples: Fluid - 1/16" OD Inconel Sheathed Chromel-Alumel
Wall - 0.005" Chromel-Alumel Spot Welded
Scale: None

Figure 39. FSSTR - MINIATURE HEAT TRANSFER SECTION: REACTOR NO. 10018-97

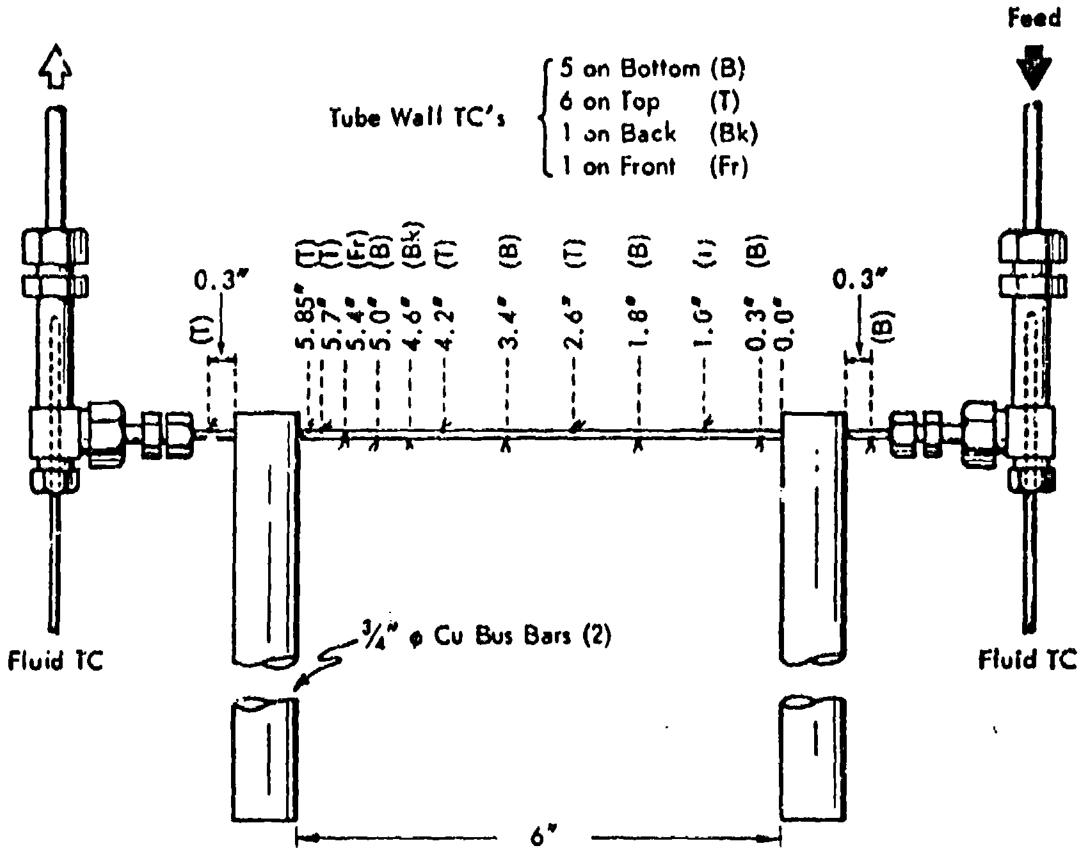
Feed
Tube Wall TC's
5 on Bottom (B)
6 on Top (T)
1 on Back (Bk)
1 on Front (Fr)
0.3"
(T)
5.85" (T)
5.7" (T)
5.4" (Fr)
5.0" (B)
4.6" (Bk)
4.2" (T)
3.4" (B)
2.6" (T)
1.8" (B)
1.6" (T)
0.3" (B)
0.0"
0.3"
(B)
Fluid TC
¾" φ Cu Bus Bars (2)
Fluid TC
6"

Tube: 1/16" OD x 0.018" Wall Type 316 SS (1/16" Tube 9½" Long Overall)
Thermocouples: Fluid - 1/16" OD Inconel Sheathed Chromel-Alumel
Wall - 0.005" Chromel-Alumel Spot Welded
Scale: None

Figure 40. FSSTR - MINIATURE HEAT TRANSFER SECTION: REACTOR NO's. 10018-103 and 110

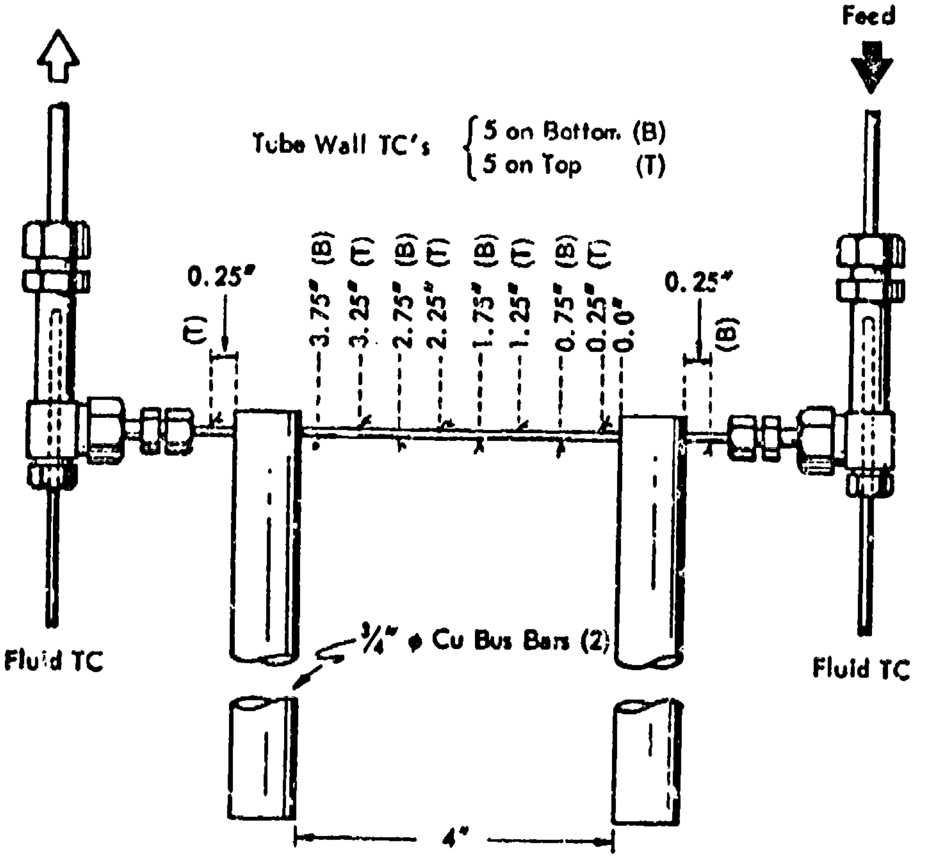
Feed
Tube Wall TC's { 5 on Bottom (B)
5 on Top (T)
0.25"
(T)
3.75" (B)
3.25" (T)
2.75" (B)
2.25" (T)
1.75" (B)
1.25" (T)
0.75" (B)
0.25" (T)
0.0"
0.25"
(B)
Fluid TC
3/4" ϕ Cu Bus Bars (2)
Fluid TC
4"

Tube: 1/16" OD x 0.018" Wall Type 316 SS (1/16" Tube 7 3/4" Long Overall)
Thermocouples: Fluid - 1/16" OD Inconel Sheathed Chromel-Alumel
Wall - 0.005" Chromel-Alumel Spot Welded
Scale: None

Figure 41. FSSTR - MINIATURE HEAT TRANSFER SECTION; REACTOR NO. 10018-122

similar layer of cement to make heat losses more uniform. Except for runs using the first tube (Reactor 10018-82) the tests have been conducted with ceramic fiber and magnesia block insulation covering the tube and end fittings.

As illustrated in Figure 38 all of the thermocouple junctions were spot welded to the side of the tube when the first miniature section was constructed. The second (Reactor 10018-97) and subsequent tubes were fabricated with alternate couples located on top and bottom of the horizontal tubes (Figures 39 through 41). This was done as tests in the 3/8 in. OD x 2 ft reactor reported above had shown large temperature differences existing between top and bottom of that tube and it was desired to determine if a similar effect could be found in the present small diameter tubes. Data obtained using the second miniature reactor (10018-97) clearly showed that there was indeed a systematic difference between top and bottom wall temperatures. Figure 42 illustrates this difference for a typical run using water feed, where the bottom of the tube was some 20-30°F hotter than the top. Unfortunately, this tube failed before further tests could be made.

The first tests made using the third miniature reactor (Reactor 10018-103) sketched in Figure 40 were made only to clarify these temperature differences. Runs were made under similar conditions, first with the tube in its normal position and then inverted. Figure 43 shows the results of one pair of tests. Contrary to the results from Reactor 10018-97, in this case the top side of the tube was hot when in its normal position. On inverting the tube the hot side moved to the bottom. This indication of nonuniformity in the tube led to further examination of the recovered portion of Reactor 10018-97. The tube was sectioned at three locations (1/2, 3, and 5 in. from the inlet end) and wall thicknesses were measured using a microscope equipped with a micrometer eyepiece. At these three locations the bottom wall was thicker than the top by 0.0021, 0.0015, and 0.006 in., respectively. Nominal wall thickness for this tube was 0.018 inch. Since more heat will be generated in the heavier wall side this explains the observed temperature difference.

For calculation purposes the top and bottom wall temperatures were smoothed as shown in Figure 42, wherever possible, and a uniform wall thickness was assumed. For Series 10018-90 and 94 this could not be done as the thermocouples were all mounted in a single row on the side of the tube. The results for these tests, therefore, are subject to the uncertainty of not knowing if the thermocouples were located where a high, low, or average wall temperature existed.

Heat losses from the miniature heat transfer sections were determined as follows. Loss from the tube wall was found by applying a small amount of power to the section with no fluid flowing. Temperatures were allowed to equilibrate and temperature and power data were recorded. While the tube wall temperature fell off at either end of the section due to heat loss to the bus bars, the profile was flat enough over the central portion of the tube that end losses could be neglected and power input was, therefore, a direct measure of tube wall heat loss at the temperature of that point. This procedure was followed with the tube insulated as was the normal practice when making test runs and also uninsulated to duplicate the conditions for the initial tests using Reactor 10018-82. Loss to the bus bars and end fittings was found by

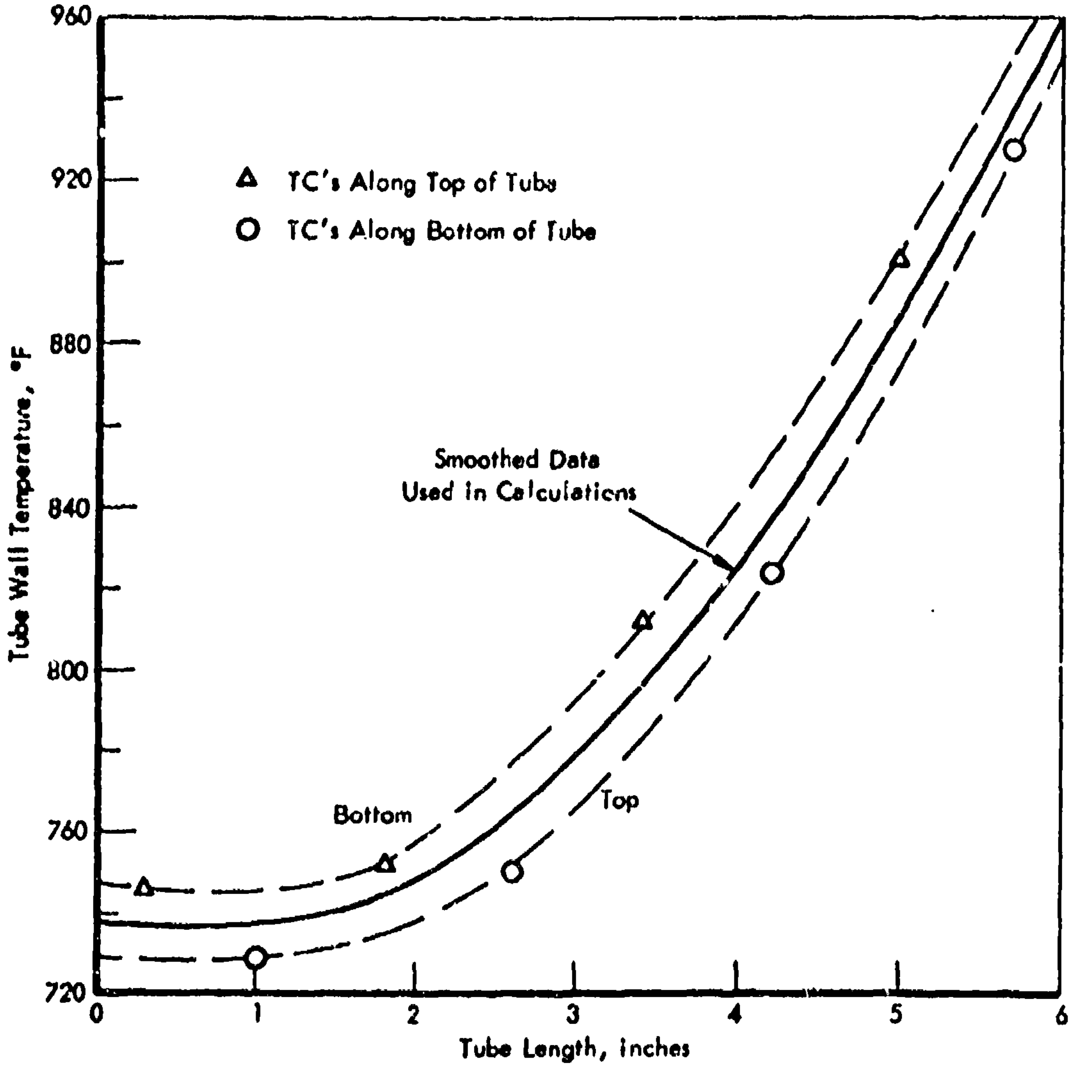

Figure 42. FSSTR: EXAMPLE OF TUBE WALL TEMPERATURE DATA FROM MINIATURE HEAT TRANSFER SECTION
Run 10018-101-13:01

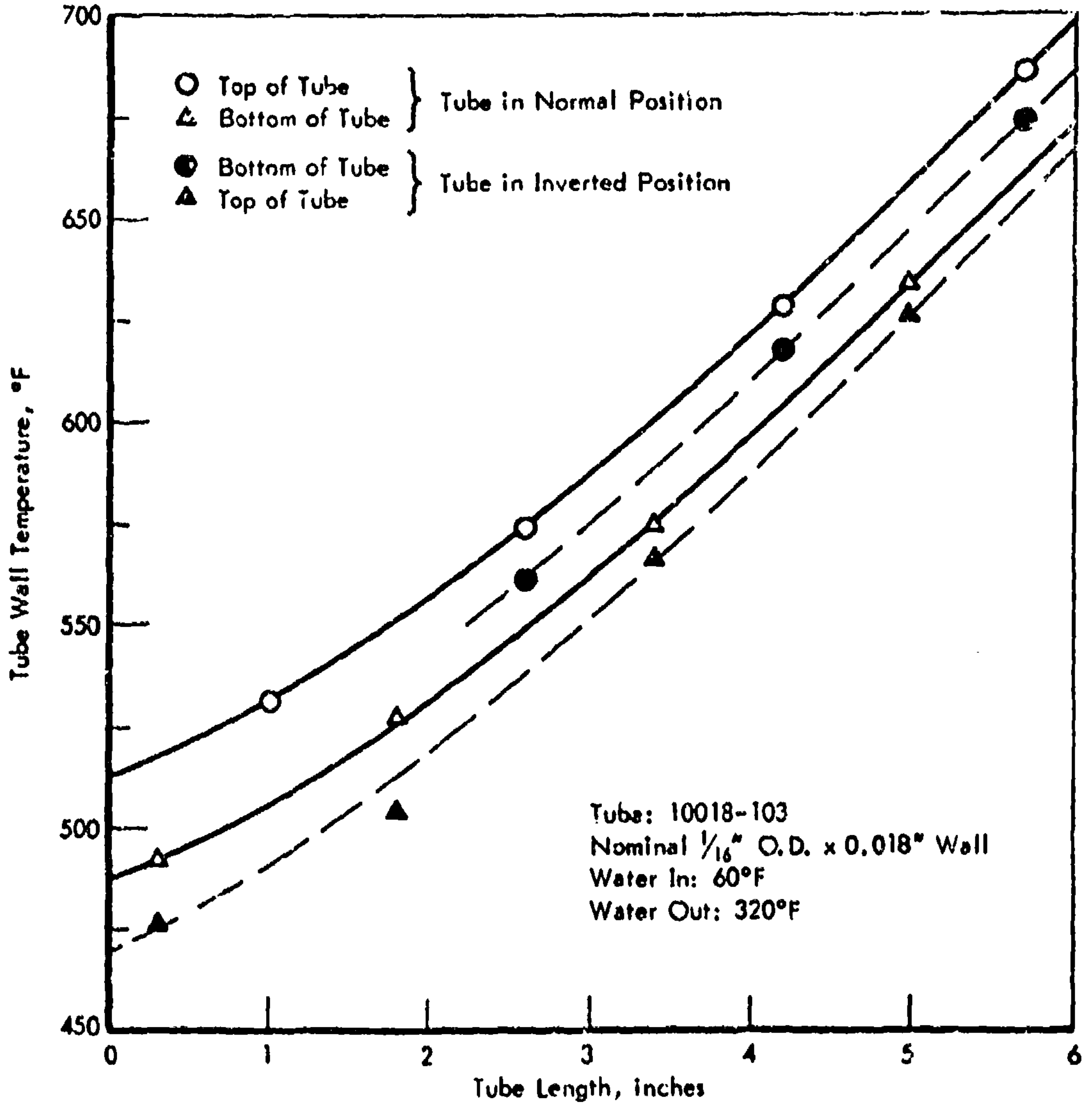

Figure 43. FSSTR: EFFECT OF INVERTING MINIATURE HEAT TRANSFER SECTION ON TUBE WALL TEMPERATURES

passing a heated feed stream through the tube, measuring the temperature drop and calculating the overall heat loss. The portion of the loss which was directly from the tube wall was determined from the wall temperature and was subtracted from the total to give the loss to the two bus bars and end fittings. This end loss depends on heat transfer between the flowing fluid and the passage through the bus bar and will therefore change with flow rate as well as with temperature of the fluid. Heat loss measurements were therefore made with all fluids used in the test runs and at several different flow rates.

Figure 44 gives the heat loss for the tube wall vs. outside wall temperature and Figure 45 gives the loss to the bus bars as functions of fluid flow rate and temperature.

Test Runs

Table 50 presents a brief survey of the operating conditions for which heat transfer data have been obtained using the miniature reactor sections. Tabulated for each test run are the fluid flow rate, inlet and outlet fluid temperature and pressure, heat flux and maximum inside tube wall temperature. Time at temperature is included for the tests using MCH feed where possible deposit formation is of interest.

Two series of tests were conducted using MCH as feed in Reactor 10018-82. The first series (10018-90) was terminated when, at a heat flux of ca 3,500,000 Btu/(hr•ft^2), flow and pressure surging became so severe that operation could not continue. Following this test the system was modified so that the product would be cooled and condensed before reaching the pressure control valve. The second test series (10018-94) was made at a higher MCH feed rate and reached a maximum heat flux of ca 4,000,000 Btu/(hr•ft^2) without any difficulty. At this point, however, with outlet pressure of 530 psig, bulk fluid temperature of 539°F and maximum inside wall temperature ca 870°F, the tube plugged as a further increase in power was made. The plug was removed by forcing a wire through the tube; however, several of the tube wall thermocouples were damaged and a new tube was constructed before testing was resumed. At this point it was decided to interrupt the MCH tests and continue operations using N_2 and water so heat transfer data could be taken at high heat flux without the added complications of reactor plugging.

Two series of tests (10018-98 and 101) were made using Reactor 10018-97. The first series, using N_2 at a feed rate of 6.4 lb/hr, was limited to a maximum heat flux of ca 500,000 Btu/(hr•ft^2) when wall temperature reached > 1500°F. In the second series (10018-101) water was used as the feed. This test terminated when the tube burned out as the heat flux was raised above 6,000,000 Btu/(hr•ft^2).

The third tube (Reactor 10018-103) burned out during its first test series when the power level was increased beyond a heat flux of 1,500,000 Btu/(hr•ft^2). Note that the outlet pressure was essentially atmospheric during this test. This reduced the boiling point and caused a lower burn-out heat flux.

Less severe conditions were then selected and the next tube (Reactor 10018-110) was used to obtain data while transfering heat to boiling water (Series 10018-116) and to superheated steam (Series 10018-119).

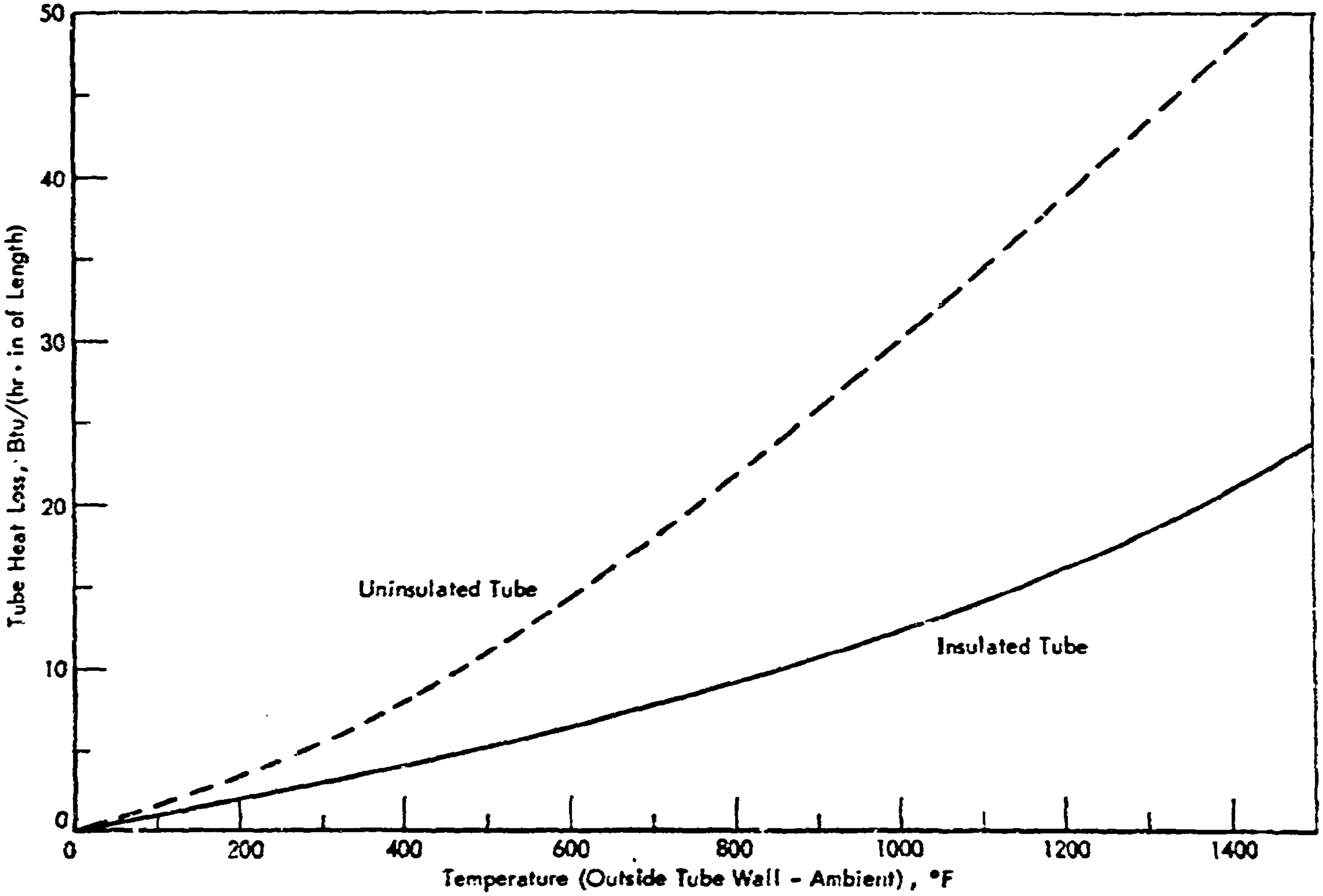

Figure 44. FSSTR - TUBE HEAT LOSS FROM MINIATURE HEAT TRANSFER SECTIONS

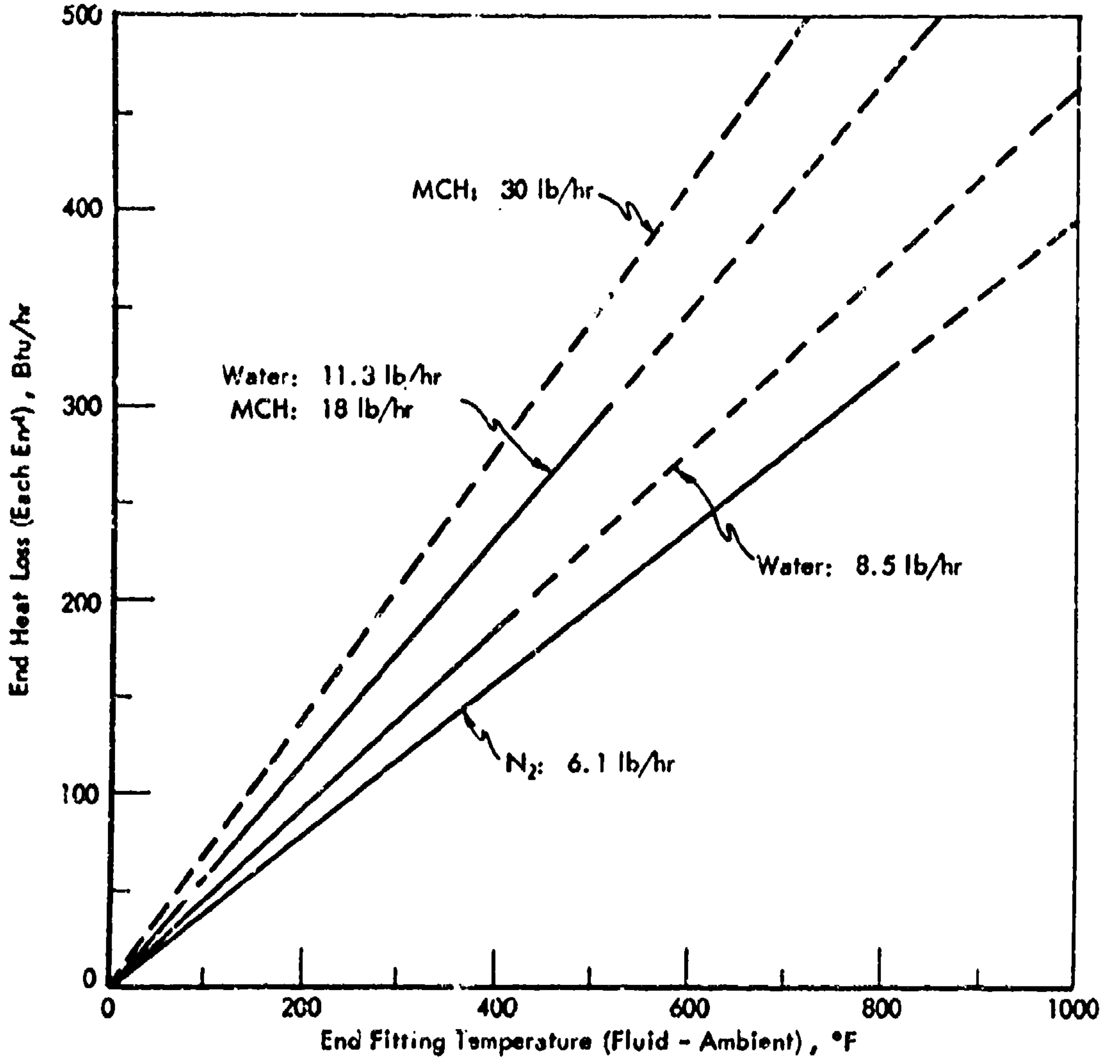

Figure 45. FSSTR - END FITTING HEAT LOSS FROM MINIATURE HEAT TRANSFER SECTIONS

Table 50. FSSTR - SUMMARY OF OPERATING CONDITIONS FOR MINIATURE HEAT TRANSFER SECTIONS

[illegible]	[illegible]	[illegible]	[illegible]	[illegible]	[illegible]	[illegible]	[illegible]	[illegible]	[illegible]	[illegible]	[illegible]	[illegible]	[illegible]
			[illegible]	[illegible]	[illegible]	In	Out	In	Out				
[illegible]	[illegible]	[illegible]	[illegible]	[illegible]	[illegible]	[illegible]	[illegible]	[illegible]	[illegible]	[illegible]	[illegible]	[illegible]	[illegible]
[illegible]													
[illegible]	[illegible]	[illegible]	[illegible]	11.03	[illegible]	[illegible]	[illegible]	[illegible]	[illegible]	[illegible]	[illegible]	[illegible]	[illegible]
[illegible]													
[illegible]	[illegible]	[illegible]	[illegible]	[illegible]	[illegible]	[illegible]	[illegible]	[illegible]	[illegible]	[illegible]	[illegible]	[illegible]	
[illegible]													
[illegible]	[illegible]	water	[illegible]	[illegible]	[illegible]	[illegible]	[illegible]	[illegible]	[illegible]	[illegible]	[illegible]	[illegible]	
[illegible]													
[illegible]	[illegible]	water	[illegible]	[illegible]	[illegible]	[illegible]	[illegible]	[illegible]	[illegible]	[illegible]	[illegible]	[illegible]	
[illegible]													
[illegible]	110	water	[illegible]	[illegible]	[illegible]	[illegible]	[illegible]	[illegible]	[illegible]	[illegible]	[illegible]	[illegible]	
[illegible]													
[illegible]	110	water	[illegible]	[illegible]	[illegible]	[illegible]	[illegible]	[illegible]	[illegible]	[illegible]	[illegible]	[illegible]	
[illegible]													
[illegible]	[illegible]	water	[illegible]	[illegible]	[illegible]	[illegible]	[illegible]	[illegible]	[illegible]	[illegible]	[illegible]	[illegible]	
[illegible]													
[illegible]	[illegible]	[illegible]	[illegible]	[illegible]	[illegible]	[illegible]	[illegible]	[illegible]	[illegible]	[illegible]	[illegible]	[illegible]	[illegible]
[illegible]													
[illegible]	[illegible]	[illegible]	[illegible]	[illegible]	[illegible]	[illegible]	[illegible]	[illegible]	[illegible]	[illegible]	[illegible]	[illegible]	[illegible]
[illegible]													
[illegible]	110	[illegible]	[illegible]	[illegible]	[illegible]	[illegible]	[illegible]	[illegible]	[illegible]	[illegible]	[illegible]	[illegible]	[illegible]
[illegible]													
[illegible]	110	[illegible]	[illegible]	[illegible]	[illegible]	[illegible]	[illegible]	[illegible]	[illegible]	[illegible]	[illegible]	[illegible]	[illegible]
[illegible]													
[illegible]	110	[illegible]	[illegible]	[illegible]	[illegible]	[illegible]	[illegible]	[illegible]	[illegible]	[illegible]	[illegible]	[illegible]	[illegible]
[illegible]													
[illegible]	[illegible]	[illegible]	[illegible]	[illegible]	[illegible]	[illegible]	[illegible]	[illegible]	[illegible]	[illegible]	[illegible]	[illegible]	[illegible]
[illegible]													

a) [illegible]
b) [illegible]
c) [illegible]
d) [illegible]
e) [illegible]
f) [illegible]

The desired maximum 8,000,000 Btu/(hr·ft²) heat flux required the construction of a 4 inch long heat exchange section (Reactor 10018-122) so that a higher feed rate could be used and a burn-out heat flux would not be reached. A maximum heat flux of 8,450,000 was attained in Series 10018-166 using this short section.

Tests with MCH were then resumed using Reactor 10018-110. Five series of runs were made at various flow rates as shown, with the power input being limited in most cases when a very sharp pressure drop increase accompanied the final power increase. For the final test using MCH the 4 inch long reactor was reinstalled and used in Series 10018-133 to reach a heat flux of 8,160,000 Btu/(hr·ft²).

More complete tabulations of the data from all of the tests made to date using the miniature heat transfer sections are given in Tables 75 through 88 in the Appendix. Flow, fluid and tube wall temperatures, and pressure readings obtained during the tests are recorded as well as smoothed outside and calculated inside wall temperatures. Heat input values in these tables have been corrected for losses along the tube but no correction has been made for heat loss to the bus bars. This will have to be considered if it is necessary to make an overall heat balance as the outlet temperatures are low as a result of these losses.

Analysis of these results and comparison with several heat transfer correlations is in progress and will be discussed in another section of this report.

While Series 94 was terminated when the reactor plugged there has been no evidence of coke formation during any of the other tests using MCH. It seems possible, therefore, that the plug was not the result of normal operation at the conditions of the run but was formed when a pressure and/or flow upset, perhaps caused by a too abrupt power increase, decreased the fluid flow rate momentarily.

The high fluid and tube wall temperature conditions which would produce coking have been avoided in these tests so that heat transfer data could be accumulated in the region of operation not subject to coking. When this heat transfer data is complete temperature levels will be raised until coke formation is an important factor. It is expected that, with these small tubes and high heat fluxes, even a thin coke deposit will have a considerable effect on heat transfer coefficient and the tube wall temperature will increase rapidly when a coke build-up commences. The possibility of tube failure, during these tests, is to be expected. A further complication will be the necessity for removal of any coke deposit between test runs.

Decalin, SHELLDYNE H, jet fuel F-71, and possibly methane are expected to be tested as this cooling program continues.

Inside Tube Wall Temperature Calculations[a)]

Inside tube wall temperatures (T_{WI}) were calculated from the measured outside wall temperatures (T_{WO}) by the following procedure:

The equation for temperature drop across a cylindrical wall with heat being generated uniformly throughout the wall and being transferred both to a fluid stream on the inside and lost to the surroundings on the outer surface is;

$$T_{WO} - T_{WI} = -\frac{(q/A_i)}{2k_W} R_i \left[\frac{1 - (R_i/R_o)^2 + 2\ln(R_i/R_o)}{1 - (R_i/R_o)^2}\right] + \frac{(q_L/A_i)}{k_W} R_i[\ln(R_i/R_o)] \qquad (6)$$

For the 0.0625 in. OD x 0.0265 in. ID tubes used the above equation reduces to:

$$\Delta T_W = \frac{(q/A_i)}{k_W(1659)} - \frac{(q_L/A_i)}{k_W(1056)} \qquad (7a)$$

or

$$\Delta T_W = \frac{I^2 r}{k_W}(3.561) - \frac{q_L}{k_W}(1.638) \qquad (7b)$$

where

$q = I^2 r\ (3.415)$ Btu/hr
$A_i = 0.0005780$ ft²/inch tube length.

Resistance and thermal conductivity of type 316 S.S. vary with temperature as shown in Figure 46. Resistance values for the tubes used were determined by measuring resistance at ambient temperature and correcting for temperature variation by applying ratios of resistance between ambient and elevated average wall temperatures obtained from Figure 46. The following equations show the resulting resistance and thermal conductivity for a typical tube with resistance equal to 0.0120 ohm/inch of length at 68°F.

---

a) Symbols used in this section are as follows:

A	tube surface area, ft²/unit length; A_i inside, A_o outside
h	heat transfer coefficient, Btu/(hr·ft²·°F)
I	current, amperes
k_W	thermal conductivity of tube material, Btu/(hr·ft·°F)
q	heat generated in wall, Btu/hr
q_L	heat lost to air, Btu/hr
R	tube radius, ft; R_i inside, R_o outside
r	tube resistance, ohm/unit length
T	temperature, °F; T_{WI} = inside wall, T_{WO} = outside wall, T_{WA} = average wall, T_F = bulk fluid, $\Delta T_W = T_{WO} - T_{WI}$.

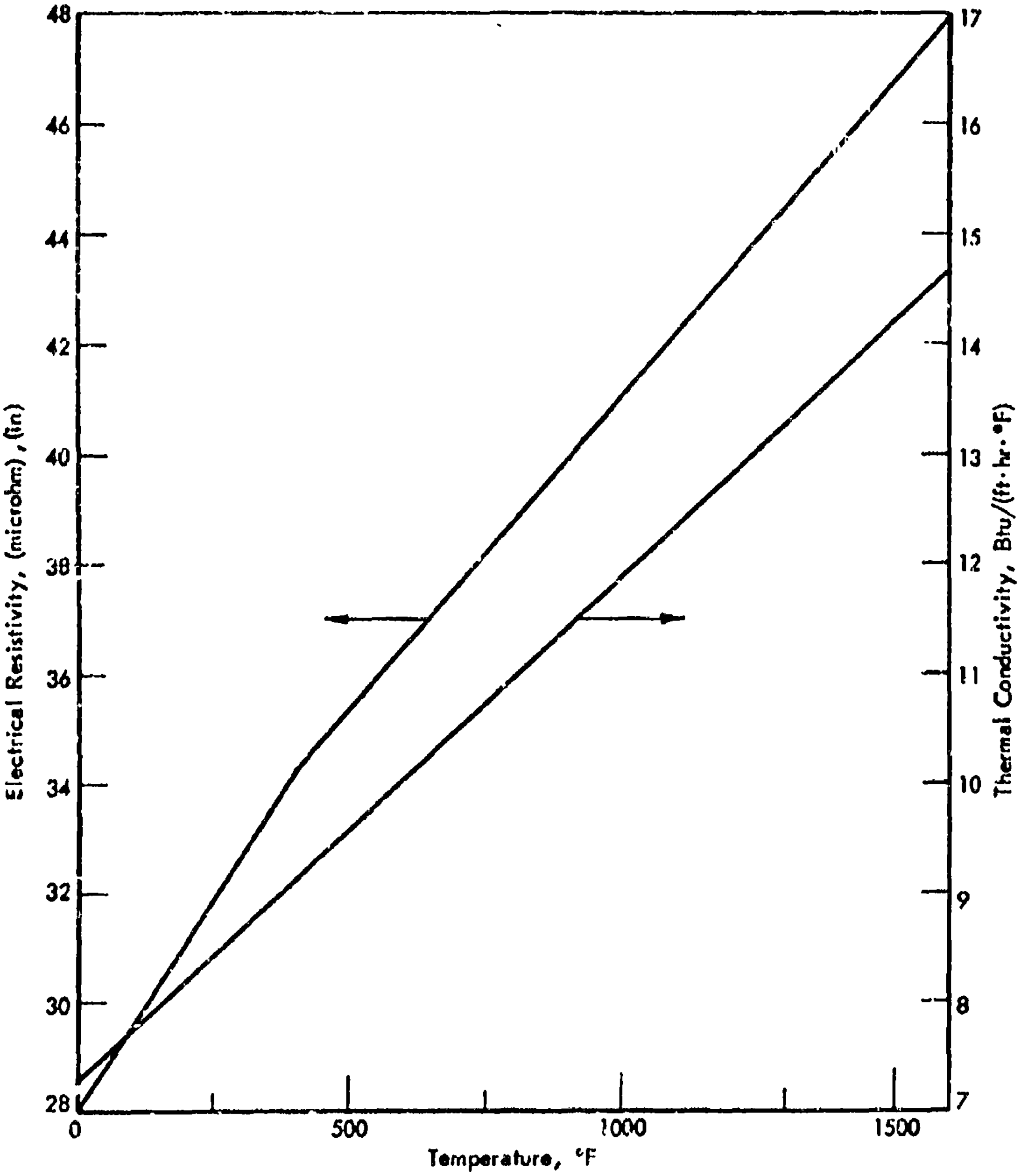

Figure 46. FS5TR - THERMAL CONDUCTIVITY AND ELECTRICAL RESISTIVITY USED FOR TYPE 316 SS MINIATURE HEAT TRANSFER SECTIONS

From 0-400°F, $r = 0.01156(1 + 0.0005597\ T_{WA})$ (8a)

From 400-1500°F, $r = 0.01234(1 + 0.0003729\ T_{WA})$ (8b)

From 0-1500°F, $k_w = 7.33(1 + 0.0006248\ T_{WA})$ (9)

On substituting these expressions in Equation (7a)

From 0-400°F,

$$\Delta T_W = I^2(0.005616)\frac{(1 + 0.0005597\ T_{WA})}{(1 + 0.0006248\ T_{WA})} - q_L\frac{(0.2235)}{(1 + 0.0006248\ T_{WA})} \qquad (10a)$$

From 400-1500°F,

$$\Delta T_W = I^2(0.005995)\frac{(1 + 0.0003729\ T_{WA})}{(1 + 0.0006248\ T_{WA})} - q_L\frac{(0.2235)}{(1 + 0.0006248\ T_{WA})} \qquad (10b)$$

These equations were solved for ΔT_W as follows:

A parabolic temperature gradient through the wall was assumed such that

$$T_{WA} = T_{WO} - 0.333\ \Delta T_W$$

Making this substitution into the first term of Equation (10a) or (10b) and using the measured values of I and T_{WO}, an approximate value for ΔT_W was obtained which in turn gave a close approximation of T_{WA}. The heat loss correction to ΔT_W was then determined by using this approximate value of T_{WA} along with the value of q_L from Figure 44 in the second (heat loss) term of Equations (10a) or (10b). Since this correction to ΔT_W was very small (2°F or less) which resulted in < 1°F change in the original approximation of T_{WA} it was not necessary to repeat the calculation with modified T_{WA} values.

Heat flux and total heat to the fluid at intermediate points along the tube were determined as follows:

Actual heat flux to the fluid is $(q/A_i) - (q_L/A_i)$. Heat generated in the tube per unit length (q) can be determined using the measured current (I) and the approximate resistance (r) from Equation (8a) or (8b) evaluated at the average tube wall temperature at that point (T_{WA}). For these tubes the inside surface area per unit length (A_i) is 0.0005780 ft^2/inch of tube length. Total heat transferred to the fluid up to any point along the tube was determined simply by averaging the heat flux up to that point and multiplying this average by the inside surface area up to that point.

Model of a Packed Bed Reactor

Influence of Physical Properties

In the packed bed reactor program, physical properties for MCH dehydrogenation (compressibility factor, thermal conductivity and viscosity) were changed to improved values. These were then varied separately to determine the sensitivity of calculated results to a change in each property. Values of the properties and the results are shown in Table 13 along with corresponding experimental measurements. The properties for Case A were determined at an average pressure and temperature for the experimental runs. The compressibility factor in Case B is in the range of low MCH conversion. However, it increases rapidly with increasing conversion and is approximately 1.0 at moderate and high conversions. Hence, 1.0 is a reasonable value in most calculations. The thermal conductivity in Case C and the viscosity in Case D were determined at the highest pressure and temperature encountered in the experiments.

Variations in the thermal conductivity and the viscosity had negligible effect on the calculated results. A change in the compressibility factor had some effect on the outlet temperature and conversion; however, the changes are comparable to differences between the calculated and experimental results. The only significant change in the results is the increase in outlet pressure due to a decrease in the compressibility factor. For the four runs shown, the ratio of the pressure drop for Case B to that for Case A is approximately 0.8, slightly less than the ratio of the compressibility factors for the two cases. In general, the agreement between calculated and experimental results is good for a compressibility factor close to 1.0, which is to be expected since it rises rapidly to 1.0 as MCH reacts.

The above results show that the use of constant properties in the packed bed reactor program is justified, since the sensitivity of these results to property changes in a single phase is small.

Reaction Kinetics for MCH Dehydrogenation

Kinetic Parameters From FSSTR Data

Further calculations with the packed bed reactor program have improved the values of kinetic parameters for MCH dehydrogenation. The kinetic model for MCH dehydrogenation is similar to the desorption-controlling model proposed by Sinfelt et al,[53] and is the same as rate expressions used in a previous report:[18]

$$r_{MCH} = \frac{(1-\epsilon)k_1 k_2 c_{MCH}}{1 + k_2 c_{MCH}} \left[1 - \frac{P_{TOL} P_{H_2}{}^3}{P_{MCH} K_{eq}} \right] \qquad (11)$$

where r_{MCH} = rate of MCH dehydrogenation
ϵ = void fraction
k_1 = $A_1 \exp(B_1/RT)$

Table 51. EFFECT OF CHANGES IN PHYSICAL PROPERTIES ON MCH DEHYDROGENATION

Run Number	140-1540	198-1420	5-1620	50-1310
G, lb/ft^2-hr	60400	36800	33200	154100
T_0, °F	1090	894	900	900
P_0, psig	890	407	903	885
q, Btu/ft^2-hr	27500	13300	24100	35900
Outlet Temperature, °F				
Experiment	1009	682	838	745
Calculation, Case				
A	1005	697	833	756
B	995	707	836	755
C	1005	697	833	755
D	1005	697	833	756
Outlet Pressure, psig				
Experiment	448	219	790	671
Calculation, Case				
A	478	230	792	668
B	572	291	813	710
C	478	230	792	668
D	478	229	792	658
MCH Conversion, %				
Experiment	94	44	62	21.3
Calculation, Case				
A	94.4	44.1	64.4	20.1
B	95.5	43.5	64.3	20.2
C	94.4	44.1	64.4	20.1
D	94.4	44.1	64.4	20.1

Case	Properties		
	Z	k, Btu/ft-hr-°F	μ, lb/ft-hr
A	0.97	0.0543	0.0417
B	0.88	0.0543	0.0417
C	0.97	0.0670	0.0417
D	0.97	0.0543	0.0430

k_2 = $A_2 \exp(B_2/RT)$

A_1, A_2 = pre-exponential factors

B_1 = activation energy for toluene desorption

B_2 = energy of reaction for MCH to adsorbed toluene

R = universal gas constant

T = absolute temperature

c_{MCH} = concentration of MCH

P_{TOL} = partial pressure of toluene

P_{H_2} = partial pressure of hydrogen

P_{MCH} = partial pressure of MCH

K_{eq} = $A_3 \exp(B_3/RT)$

A_3 = 4.0×10^{20} atm^2

B_3 = -92,500 Btu/lb mole

The latest calculations utilized experimental results which were obtained on a 2-ft section in the FSSTR and were not previously available, along with earlier data obtained on 10 ft sections in the FSSTR. Data and results for selected runs are shown in Table 52. Reasonable agreement between calculation and experiment was obtained by varying one of the kinetic parameters, A_1, from the value used in previous calculations.

The improved kinetic parameters are

A_1 = 1.2×10^{13} lb mole/ft^3-hr

A_2 = 4.5×10^{-8} ft^3/lb mole

B_1 = -59,000 Btu/lb mole

B_2 = 54,000 Btu/lb mole

The values of B_1 and B_2 are approximately the same as those determined by Sinfelt, but A_1 has a much larger value, which is indicative of a more active catalyst.

Better agreement between calculation and experiment also resulted when the more accurate reactor lengths shown in Table 52 were used instead of the approximate values of 2 and 10 feet.

Figures 47 and 48 show calculated and experimental results for two MCH dehydrogenation runs in the 2-ft section of the FSSTR. The agreement is good for the outlet pressure and conversions. There is some disagreement between the calculated and experimental temperature profiles. This may be due to different values of the heat transfer coefficient in the calculations and the experiment. In the calculations, the heat transfer coefficient is constant and yields an almost constant temperature difference between the fluid and the wall. In the real case, the number of moles of gas increases. Hence, the linear velocity and the heat transfer coefficient increase, causing the temperature difference between the fluid and the wall to decrease,

Table 52. CALCULATED AND EXPERIMENTAL RESULTS FOR MCH DEHYDROGENATION IN THE PACKED BED REACTOR

Data									
Run Number	146-1340	148-1540	198-1420	5-1620	9-1400	50-1430	50-1610	62-1300	62-1419
Reactor diameter, in.	0.277	0.277	0.652	0.652	0.652	0.277	0.277	0.277	0.277
Reactor length, ft	9.31	9.31	9.55	9.55	9.55	2.04	2.04	2.04	2.04
Fluid mass flux, lb/ft^2 hr	36700	60400	36800	33200	36700	154100	154100	60000	60000
Wall heat flux, Btu/ft^2 hr	11100	28000	13900	25200	52350	142400	311300	29050	156000
Fluid enthalpy change, Btu/lb	514	780	266	534	1003	327	715	171	920
Inlet pressure, psig	430	890	487	903	886	885	885	891	889
Inlet temperature, °F	797	1090	894	900	905	893	910	901	895
Calculated Results									
Outlet pressure, psig	243	489	246	797	697	596	452	857	830
Outlet temperature, °F	731	985	695	832	1025	827	1069	766	1053
MCH conversion, %	61.9	96.1	44.1	64.3	98.0	40.1	62.8	29.1	84.8
Experimental Results									
Outlet pressure, psig	192	448	219	790	676	604	466	855	825
Outlet temperature, °F	775	1009	682	838	1034	831	1011	770	1011
MCH conversion, %	59	94	44	62	97	39.1	65.9	28.7	86

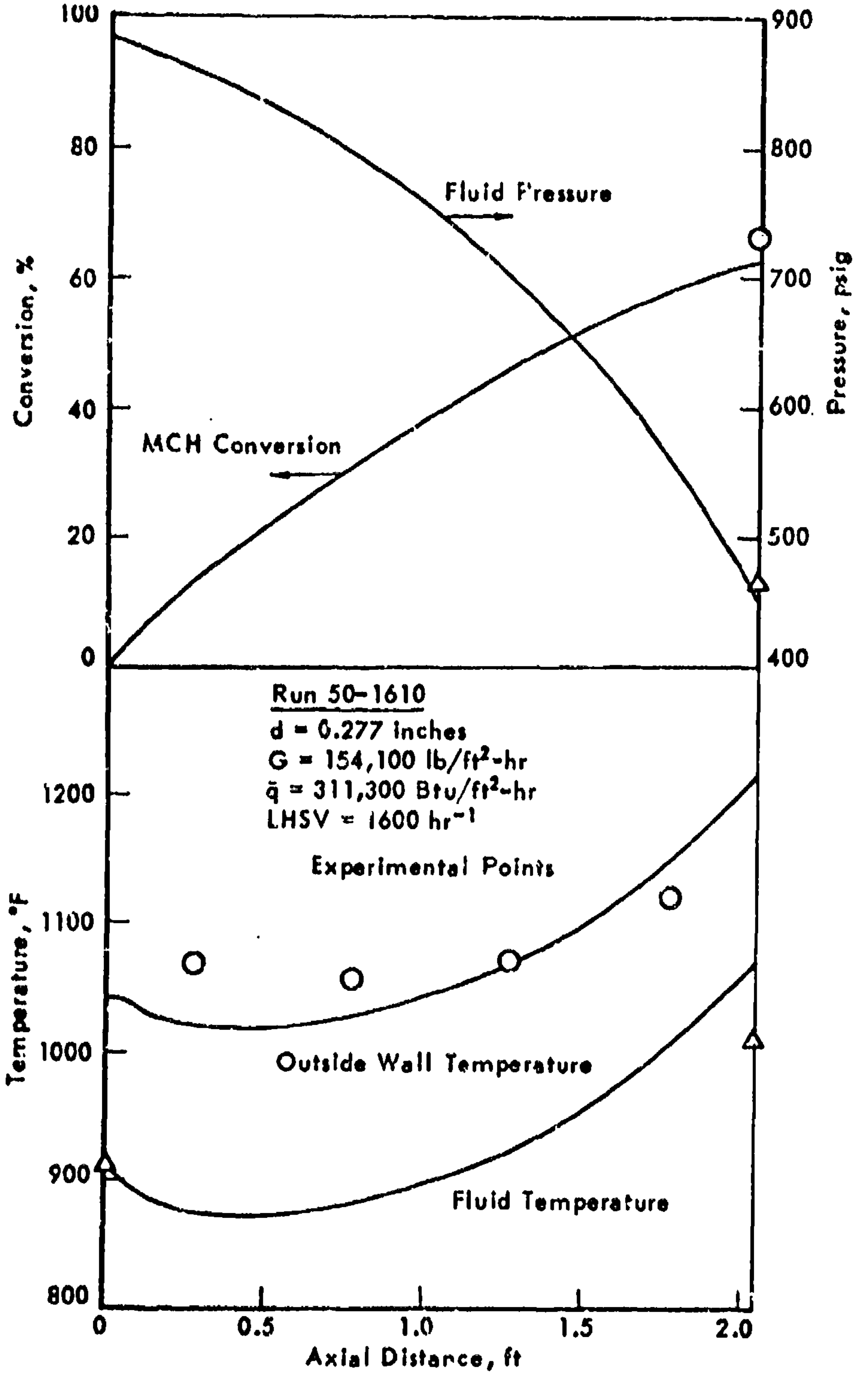

Figure 47. CALCULATED PROFILES FOR MCH DEHYDROGENATION IN THE FSSTR FROM FSSTR KINETIC DATA

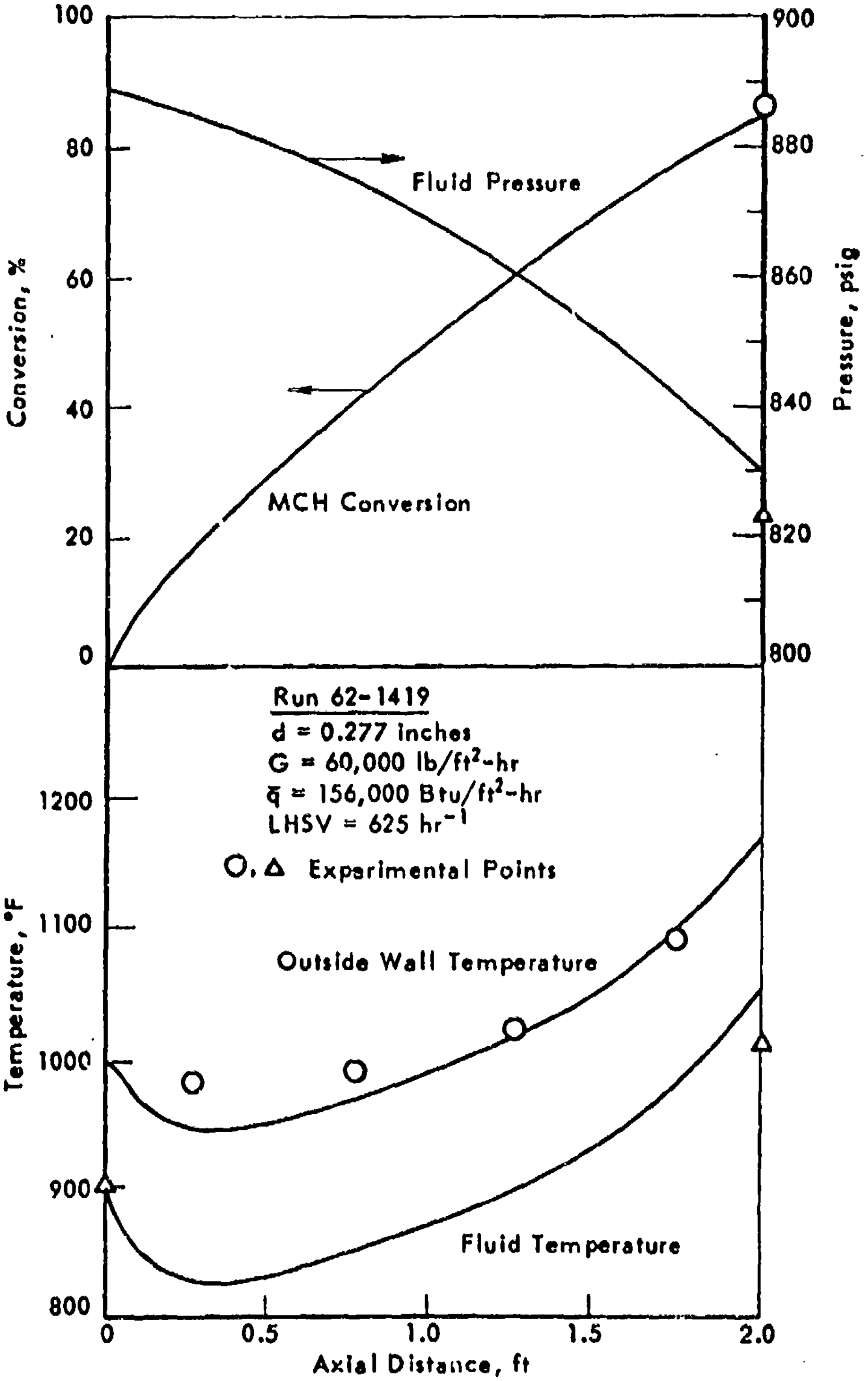

Figure 48. CALCULATED PROFILES FOR MCH DEHYDROGENATION IN THE FSSTR FROM FSSTR KINETIC DATA

as indicated by the decreasing difference between the curve for the fluid temperature and the experimental points for the wall temperature.

Kinetic Parameters From Bench-Scale Data

In order to determine the feasibility of using bench-scale data to calculate kinetic parameters for Decalin dehydrogenation, data obtained on the bench-scale reactor have been used to determine the kinetic parameters for MCH dehydrogenation for comparison with the results calculated from the FSSTR data. The bench-scale data were evaluated for a desorption-controlling kinetic model by a nonlinear estimation technique.

The kinetic model is a simplified version of Equation (11). Since equilibrium was not important in any bench-scale runs, the binomial factor was dropped and Equation (11) reduced to

$$r_{MCH} = \frac{(1-\epsilon)k_1k_2c_{MCH}}{1 + k_2c_{MCH}} \tag{12}$$

The model was developed for an integral reactor, since high conversions occurred on several runs. Isothermal conditions were assumed to simplify the integration. Steady-state conditions were assumed for the continuity equation:

$$\nabla \cdot \underline{N}_{MCH} = r_{MCH} \tag{13}$$

where $\underline{N}_{MCH}$ = molar flux of MCH.

The MCH flux is assumed to be due entirely to convection in the axial direction. Hence

$$\frac{d(c_{MCH}v_z)}{dz} = r_{MCH} \tag{14}$$

where v_z = average velocity in axial direction
z = axial distance.

The MCH concentration is related to the molar concentration of the gas by the reaction stoichiometry:

$$c_{MCH} = c\left(\frac{1-g}{1+3g}\right) \tag{15}$$

where c = molar concentration of the gas
g = fractional conversion for dehydrogenation of pure MCH.

The stoichiometry of the reaction also relates the average velocity at any time to the initial velocity. The compressibility factor is assumed to be unity, which is valid for moderate and high conversions and reasonable for low conversions. Hence

$$v_z = v_{zo}(1 + 3g) \tag{16}$$

where v_{zo} = initial average velocity.

Also

$$c = \frac{P}{RT} \tag{17}$$

where P = absolute pressure.

By substitution of Equations (12), (15), and (16) the continuity equation is transformed to

$$cv_{zo}\frac{dg}{dz} = \frac{(1-\epsilon)k_1k_2c(1 - g)}{1 + 3g + k_2c(1 - g)} \tag{18}$$

Integration along the axial direction from z = 0 yields

$$\frac{(1-\epsilon)k_1k_2z}{v_{zo}} = \int_0^g \left(k_2c - 3 + \frac{4}{1 - g}\right) dg$$

$$\frac{(1-\epsilon)k_1k_2z}{v_{zo}} = (k_2c - 3)g - 4\ \ln(1 - g) \tag{19}$$

Introduction of the mass flux for the initial velocity, reactor volume for axial distance, and Equation (17) for concentration yields

$$\frac{k_1k_2PVM_0(1-\epsilon)}{RT\ GA} = \left(\frac{k_2P}{RT} - 3\right)g - 4\ \ln(1 - g) \tag{20}$$

where V = volume of tubular reactor
M_0 = molecular weight of feed
G = mass flux
A = cross-sectional area of tubular reactor.

Equation (20) relates the reactor volume to the MCH conversion for given values of the mass flux, pressure, and temperature.

The kinetic parameters in the rate equation were determined by nonlinear estimation after rearrangement of Equation (16) to

$$V = \frac{GA}{M_0(1 - \epsilon)}\left\{\frac{g}{k_1} - \frac{RT}{k_1k_2P}\left[3g + 4\ \ln(1 - g)\right]\right\} \tag{21}$$

The reactor volume was taken as the response function with mass flux, pressure, temperature, and conversion as independent variables. The error sum of squares for the reactor volume was minimized to yield the following kinetic parameters:

$A_1 = 1.8 \times 10^{11}$ lb-mole/ft^3-hr
$A_2 = 3.6 \times 10^{-4}$ ft^3/lb-mole
$B_1 = -48800$ Btu/lb-mole
$B_2 = 31700$ Btu/lb-mole

Attempts to evaluate a confidence region for the parameters were unsuccessful. These parameters are significantly different from those in the previous section. B_1 and B_2 are less, and since these are exponents A_1 and A_2 are quite different.

Comparison of Results

MCH dehydrogenation rates were determined for kinetic data from two different sources and are shown in Table 53. Rates based on data from the bench-scale reactor and FSSTR are generally similar although the former data predict slightly higher rates. However, these rates are 10 to 100 times faster than the corresponding rates based on Sinfelt's work. Rates predicted from Sinfelt's data are questionable at 800°K, since these were determined by extrapolation from data at 588-645°K.

Table 53. DEHYDROGENATION RATES FOR PURE MCH

Source Kinetic Data	Reaction Rate, g-mole/hr-g Catalyst					
	600°K (620°F)		700°K (800°F)		800°K (980°F)	
	20 atm	50 atm	20 atm	50 atm	20 atm	50 atm
Bench-Scale Reactor	0.29	0.30	5.5	6.7	27.	47.
FSSTR	0.16	0.16	5.6	6.8	18.	39.
Sinfelt et al[7]	0.017	0.019	0.11	0.23	(0.16)	(0.39)

The kinetic parameters determined from bench-scale data were used in the packed-bed reactor program. The conditions shown in Table 54 for various experimental runs were used as data for the calculations. The predicted results are compared with experimental measurements in Tables 55 to 57. The calculated conversions in Table 55 are slightly higher than the experimental conversions. In Tables 56 and 57 most of predicted and experimental conversions agree with each other. Outlet temperatures for each run show the same degree of agreement as the conversions, since energy balances on the reacting fluid were used to determine the heat fluxes.

Figures 49 and 50 show calculated and experimental results for MCH dehydrogenation in the 2-ft section of the FSSTR. These are the same runs as shown in Figures 47 and 48. The agreement is good for fluid temperature, pressure, and conversion. There is some disagreement between the calculated and experimental wall temperature with the greatest difference being approximately 30°F near the reactor inlet. Other runs in the 2-ft reactor had good agreement except for Runs 50-1630 and 60-1336. The difference between the calculated and observed results in the former run is due to significant catalyst deactivation. However no apparent cause accounts for the disagreement in Run 60-1336.

Table 54. DATA FOR THE PACKED BED PROGRAM PREDICTIONS OF MCH DEHYDROGENATION RUNS

Run No.	Mass Flux of Fluid, lb/ft^2-hr	Heat Flux to Fluid, Btu/ft^2-hr	Inlet Pressure, psig	Inlet Temp, °F
Catalyst Bed Dimensions: 0.277-in. D x 9.81-ft L				
120-1400	59,500	33,800	890	925
123-1505	71,700	38,200	887	955
144-1330	37,600	0	626	782
144-1430	37,500	9,600	630	790
144-1530	37,500	21,500	638	788
144-1640	37,500	19,100	434	786
146-1340	36,700	11,200	430	797
146-1500	35,800	7,300	890	801
146-1620	35,800	19,700	891	793
148-1320	60,400	28,600	886	935
148-1540	60,400	27,900	890	1090
Catalyst Bed Dimensions: 0.652-in. D x 9.55-ft L				
198-1300	35,500	15,100	911	895
198-1420	36,800	13,400	487	894
5-1200	17,200	12,400	901	898
5-1320	17,200	23,900	903	900
5-1620	33,200	24,400	903	900
9-1300	36,700	35,700	886	904
9-1400	36,700	52,200	886	905
Catalyst Bed Dimensions: 0.277-in. D x 2.04-ft L				
50-1210	154,100	-5,000	885	899
50-1310	154,100	37,000	885	900
50-1400	154,100	83,000	885	891
50-1430	154,100	139,500	885	893
50-1510	154,100	202,400	885	902
50-1540	154,100	253,700	885	908
50-1610	154,100	306,200	885	910
50-1630	154,100	338,100	885	899
60-1300	154,100	-5,000	894	900
60-1336	154,100	267,300	892	903
62-1130	60,000	-3,400	892	902
62-1300	60,000	28,800	891	901
62-1400	60,000	115,100	894	901
62-1419	60,000	152,600	889	895
62-1650	60,000	30,200	891	898

Table 55. EXPERIMENTAL AND PREDICTED RESULTS FOR MCH DEHYDROGENATION IN THE FSSTR (0.277-IN. D x 9.81-FT L)

Run No.	Conv., %	Outlet Pressure, psig	Outlet Temp, °F	Centerline Fluid Temperature, °F, at		
				2.5 ft	5.0 ft	7.5 ft
120-1400	96.	502	1030	795	830	880
Prediction	98.2	508	1019	785	830	880
123-1505	91.	125	1040	800	829	873
Prediction	95.3	194	988	783	821	860
144-1330	9.	570	637	659	650	646
Prediction	10.5	555	621	635	630	625
144-1430	49.	524	784	712	738	751
Prediction	50.5	518	765	693	724	748
144-1530	93.	469	963	751	790	835
Prediction	95.8	467	928	737	786	834
144-1640	85.	44	915	728	754	734
Prediction	89.5	128	861	707	743	775
146-1340	59.	192	775	707	719	734
Prediction	62.4	231	732	681	707	722
146-1500	40.	820	800	729	751	771
Prediction	41.3	826	783	707	739	763
146-1520	90.	773	958	772	812	862
Prediction	92.4	790	929	757	812	858
148-1320	88.	516	947	791	821	858
Prediction	91.5	530	904	776	814	848
148-1540	94.	443	1009	811	838	882
Prediction	97.1	467	971	802	835	875

Table 56. EXPERIMENTAL AND PREDICTED RESULTS FOR MCH DEHYDROGENATION IN THE FSSTR (0.652-IN. D x 9.55-FT L)

Run No.	Conv., %	Outlet Pressure, psig	Outlet Temp, °F	Centerline Fluid Temperature, °F, at		
				2.5 ft	5.0 ft	7.5 ft
198-1300	43.	809	782	732	750	764
Prediction	42.9	803	783	725	749	766
198-1420	44.	219	682	687	687	684
Prediction	43.7	215	686	678	688	690
5-1200	64.	871	825	746	777	800
Prediction	63.4	872	835	742	778	805
5-1320	98.	860	1013	773	824	872
Prediction	98.4	863	1007	773	828	879
5-1620	62.	790	838	749	777	798
Prediction	62.8	789	828	743	777	802
9-1300	77.	720	872	758	792	817
Prediction	78.0	720	853	753	793	821
9-1400	97.	676	1034	777	822	866
Prediction	98.6	678	1014	772	823	870

Table 57. EXPERIMENTAL AND PREDICTED RESULTS FOR MCH DEHYDROGENATION IN THE FSSTR (0.277-IN. D x 2.04-FT L)

Run No.	Conv., %	Outlet Pressure, psig	Outlet Temp, °F	Outside Wall Temperature, °F, at			
				0.27 ft	0.77 ft	1.27 ft	1.77 ft
50-1210	15.2	700	688	801	738	715	703
Prediction	15.6	670	683	800	732	702	687
50-1310	21.3	671	745	839	787	772	771
Prediction	21.8	647	738	831	778	761	757
50-1400	28.5	645	788	885	846	841	846
Prediction	28.9	623	783	862	825	818	820
50-1430	39.1	604	831	937	906	907	919
Prediction	39.1	585	831	903	880	882	890
50-1510	51.2	548	880	987	965	970	989
Prediction	50.7	532	887	952	940	950	968
50-1540	59.6	505	935	1025	1007	1016	1046
Prediction	59.0	485	944	990	986	1004	1036
50-1610	65.9	466	1011	1061	1048	1063	1108
Prediction	66.2	432	1014	1027	1033	1061	1112
50-1630	65.3	432	1101	1098	1097	1119	1200
Prediction	69.3	405	1058	1046	1060	1095	1160
60-1300	14.7	709	696	802	739	713	700
Prediction	15.6	681	684	800	732	702	687
60-1336	63.	505	926	1023	1011	1027	1050
Prediction	60.8	488	953	998	998	1018	1053
62-1130	13.9	865	699	756	711	702	701
Prediction	14.8	862	686	747	695	688	685
62-1300	28.7	855	770	806	782	790	801
Prediction	29.0	856	766	791	762	771	782
62-1400	72.3	836	901	931	932	957	990
Prediction	72.0	842	905	903	909	939	971
62-1419	86.	823	1011	981	990	1022	1089
Prediction	87.0	828	1002	949	966	1007	1066
62-1650	28.0	854	788	815	787	793	809
Prediction	29.5	856	768	792	764	774	785

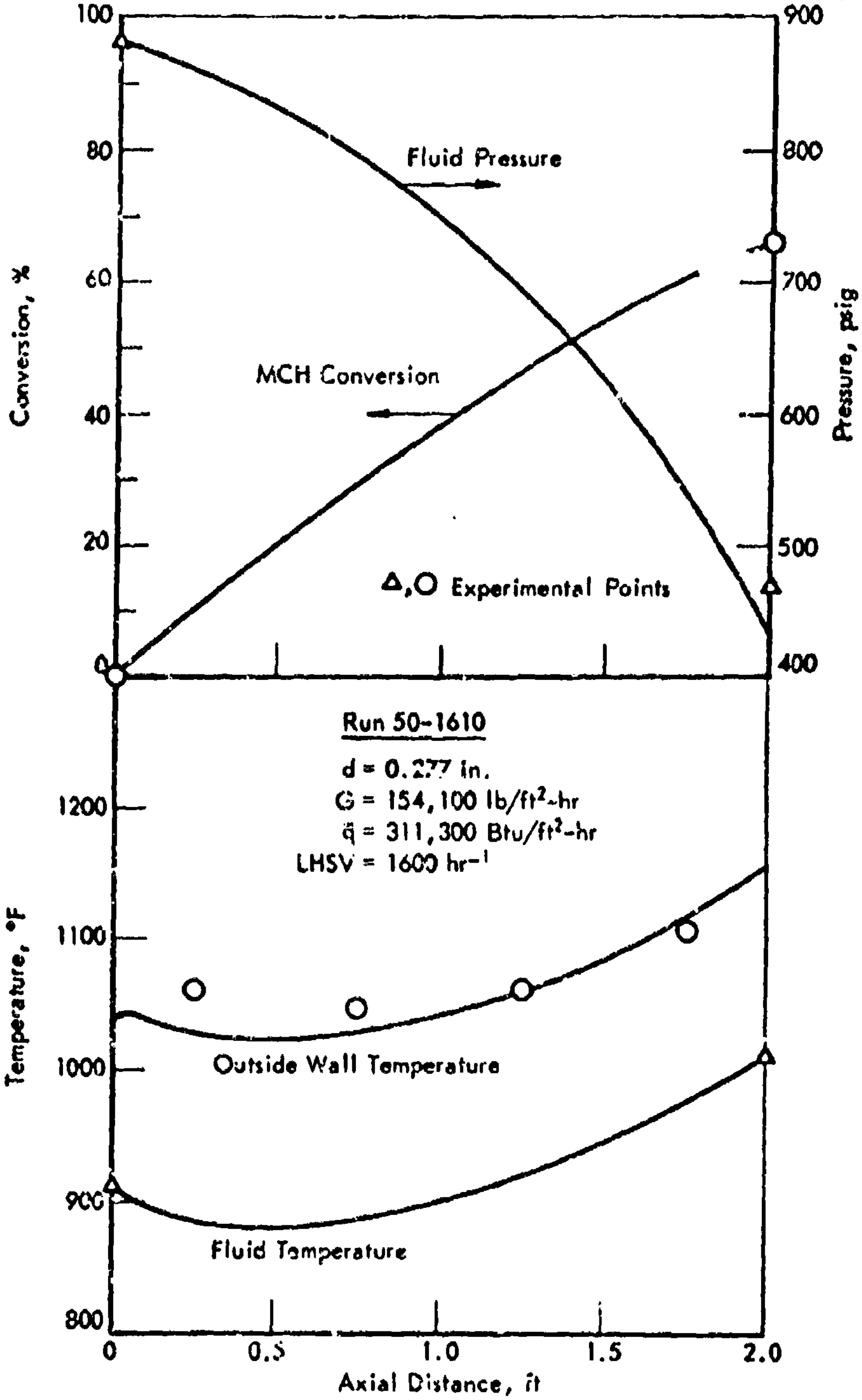

Figure 49. CALCULATED PROFILES FOR MCH DEHYDROGENATION IN THE FSSTR FROM BENCH-SCALE KINETIC DATA

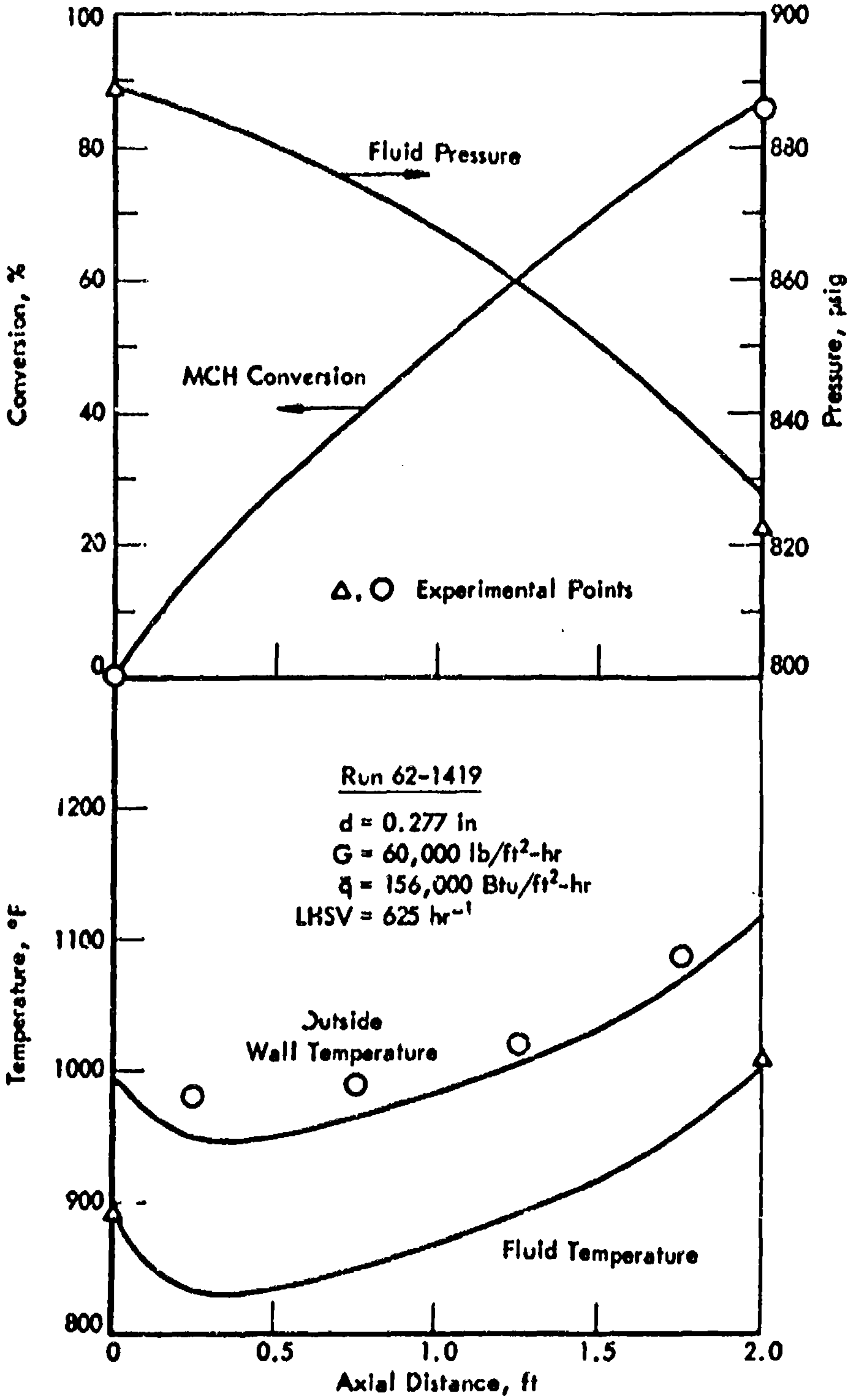

Figure 50. CALCULATED PROFILES FOR MCH DEHYDROGENATION IN THE FSSTR FROM BENCH-SCALE KINETIC DATA

Figures 57 to 60 generally show slight differences in the predictions based on the two sets of data. The kinetic parameters based on the bench-scale data do predict slightly higher conversion and pressure drop and slightly lower temperature, which becomes appreciably lower at the reactor exit, than the parameters based on FSSTR data. They also predict a temperature profile that is a slightly better fit of the experimental data and has a curvature more like the experimental profile. Because of this the bench-scale reactor should be suitable for collecting kinetic data, the kinetic parameters calculated from bench-scale data for MCH dehydrogenation should be reasonable, and available bench-scale data can be used to determine a kinetic scheme for Decalin dehydrogenation.

Reaction Kinetics for Decalin Dehydrogenation

Decalin-Tetralin-Naphthalene Equilibria

A computer program was developed and used to calculate equilibrium compositions of the Decalin-tetralin-naphthalene system at various conditions. Since the program will ultimately be used in kinetic calculations for Decalin dehydrogenation, it is presently restricted to mixtures that result from the dehydrogenation of pure Decalin.

The independent chemical reactions used for the system are

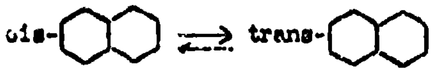

(22)

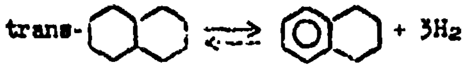

(23)

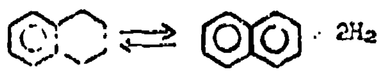

(24)

Equilibrium constants for the above reactions are:

$$k_1 = \frac{\gamma_{tD} X_{tD}}{\gamma_{cD} X_{cD}} = k_{\gamma_1} \frac{g_1 - g_2}{1 - g_1} \tag{25}$$

$$k_2 = \frac{\gamma_T \gamma_{H_2}^{3} X_T P_{H_2}^{3}}{\gamma_{tD} X_{tD}} = k_{\gamma_2} P_{H_2}^{3} \left(\frac{g_2 - g_3}{g_1 - g_2} \right) \tag{26}$$

$$k_3 = \frac{\gamma_N \gamma_{H_2}^{2} X_N P_{H_2}^{2}}{\gamma_T X_T} = k_{\gamma_3} P_{H_2}^{2} \left(\frac{g_3}{g_2 - g_3} \right) \tag{27}$$

where

k_i = equilibrium constant of reaction i

k_{γ_i} = equilibrium constant for the activity coefficients of reaction i

g_i = equilibrium conversion of reaction i

γ_j = activity coefficient of chemical species j

X_j = mole fraction of chemical species j

P_j = partial pressure of chemical species j

and chemical species are represented by the subscripts

cD = cis-Decalin

tD = trans-Decalin

T = tetralin

N = naphthalene

H_2 = hydrogen

The partial pressure of hydrogen is related to conversion by

$$P_{H_2} = \left(\frac{3g_2 + 2g_3}{1 + 3g_2 + 2g_3}\right) P \tag{28}$$

where

P = total pressure

Value of the equilibrium constants are determined from a least squares fit of data[21][22] by

$$\log K_i = a_i + \frac{b_i}{T} \tag{29}$$

where

a_i, b_i = constants

T = absolute temperature

Equations (25) to (28) are solved by iteration to determine the reaction conversions at any given temperature. The iteration logic follows:

1. Assumed values are assigned to the reaction conversions.

2. Mole fractions are calculated for each chemical species.

3. The fugacity of the mixture is calculated by Pitzer and Curl's equation of state for the second virial coefficient.[54][55]

4. Activity coefficients are determined for each species by the method of Gamson and Watson.[56][57]

5. Equilibrium constants for the activity coefficients are calculated.

6. The hydrogen partial pressure is calculated by Equation (28).

7. Equations (25) to (27) are solved simultaneously to yield the reaction conversions.

The conversions calculated in step (7) are assumed as the starting point for the following iteration. The iterations are terminated when the calculated conversions match the assumed conversions. Rapid convergence was achieved when the starting point was the complete conversion of initially pure Decalin to naphthalene and hydrogen. If feeds other than pure Decalin are used, the same starting point and logic should likewise result in rapid convergence to a solution.

Equilibrium compositions and reaction conversions are shown in Figures 16 and 51 as functions of temperature at various pressures. The curves are based on equilibrium mixtures that result when pure Decalin dehydrogenates to tetralin, naphthalene, and hydrogen. At 10 atm, Decalin has reacted completely at 740°F with 10% converted to tetralin and 90% to naphthalene. At 50 atm the 90% conversion to naphthalene occurs at 870°F. Hence, over most of the conditions to be expected in the FSSTR (700-1100°F, 10-60 atm), the equilibrium conversion of Decalin is almost complete, and the conversion to naphthalene is equilibrium limited only at the lower temperatures and higher pressures.

Kinetic Parameters From Bench-Scale Data

Present work on Decalin dehydrogenation consists of evaluating experimental data from bench-scale studies to determine a kinetic model for use in the packed bed reactor program. The data are being used to select the best form of the rate expression and to estimate kinetic parameters. Later FSSTR data will be used to confirm the model and improve the values of the parameters.

In the reaction model, cis- and trans-Decalin are considered as separate chemical species. Both isomerize to each other and dehydrogenate to tetralin, which dehydrogenates to naphthalene. The reverse hydrogenation steps will be included if the kinetic model is significantly improved. Basically the model has one isomerization and two dehydrogenation steps. In the kinetic scheme three conversions are associated with these steps. In the analysis of the bench-scale data, reaction rates for the three steps will be integrated numerically for each run to obtain conversions. Least squares analysis will be used on the conversions to optimize kinetic parameters and then select the best kinetic model.

Model of a Regenerative Heat Exchanger for Missile Application

Model Development

One of the near term applications of Air Force programs on vaporizing and endothermic fuels involves utilization of supersonic combustion ramjet engines for powering missiles. Present plans contemplate using only

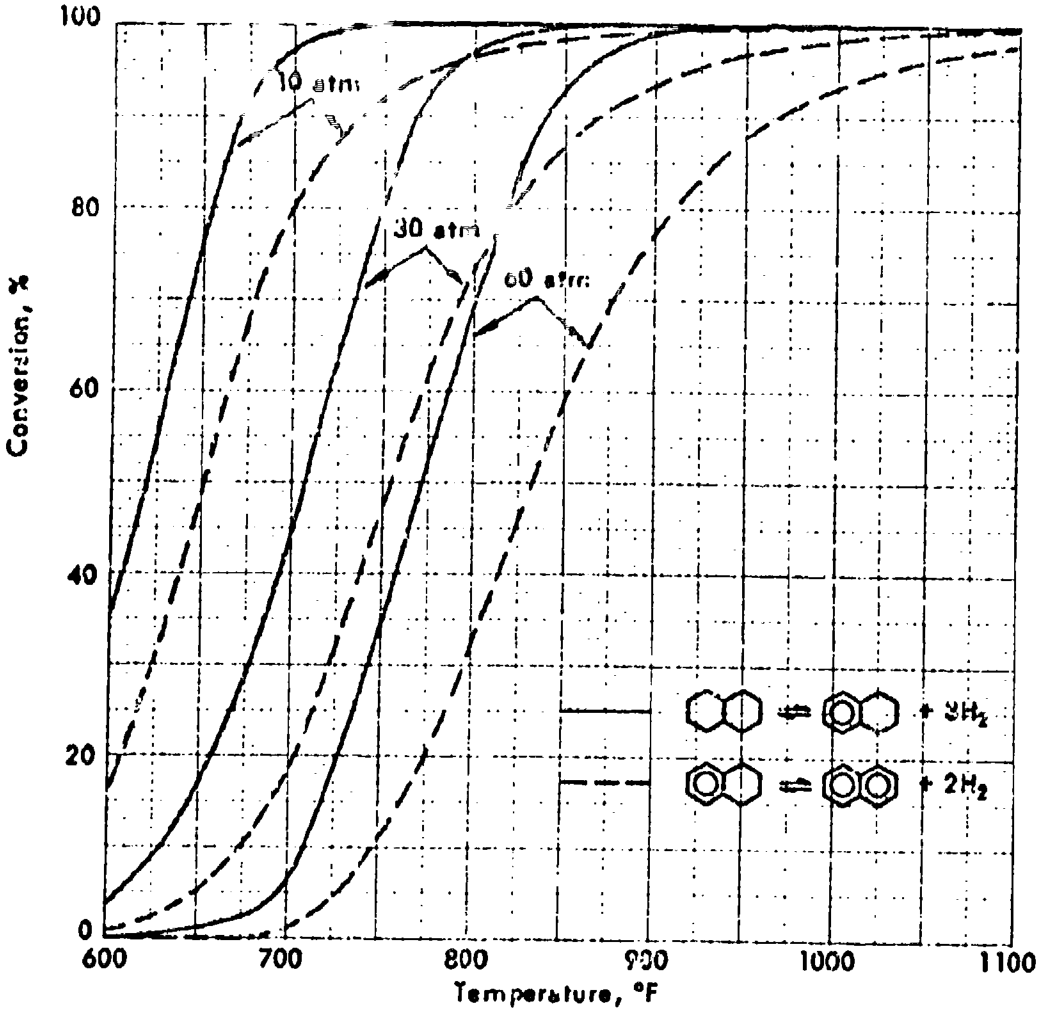

Figure 51. EQUILIBRIUM CONVERSIONS OF THE DECALIN-TETRALIN-NAPHTHALENE SYSTEM

the latent and sensible heat capacity of the fuel for cooling the engine. Under the current contract the behavior of candidate fuels will be investigated both analytically and experimentally.

In order to arrive at the optimum design of experimental equipment a computer model has been developed to be used in predicting the effect of geometric and experimental variables on heat transfer and profiles of pressure and temperature. Fuel is considered to flow through a cylindrical heat exchanger of constant cross-sectional area and increase in temperature prior to injection into the combustion chamber. The computer program predicts the pressure and temperature profiles of the fuel. Required input consist of pressure and temperature of the fuel at either end of the heat exchanger, mass flux of the fuel, heat flux profile at the wall tube dimensions, and fuel properties. The program is organized so that properties for any fuel can be inserted. The calculation is limited to single-phase flow; however, work is being done to extend the model to two-phase flow.

The model, one-dimensional along the tube axis, is based on a momentum balance, an energy balance and a mass balance:

$$v_z \frac{dv_z}{dz} + \frac{1}{\rho}\frac{dP}{dz} + \frac{2fv_z^2}{d} = 0 \qquad (30)$$

$$v_z \frac{dv_z}{dz} + c_p \frac{dT}{dz} + \left(\frac{1}{\rho} + \frac{T}{\rho^2}\frac{\partial \rho}{\partial T}\right)\frac{dP}{dz} + \frac{4q}{Gd} = 0 \qquad (31)$$

$$\rho v_z = G \qquad (32)$$

where z = axial distance from tube entrance
P = fluid pressure
T = fluid temperature
d = tube diameter
v_z = average velocity of fluid
ρ = fluid density
c_p = fluid specific heat at constant pressure
G = average mass flux of fluid
f = friction factor
q = heat flux at the wall (positive value in the direction of increasing radius).

The friction factor for turbulent flow in a smooth pipe is given implicitly by[8)]

$$f^{-1/2} = 4.0 \log(\mathrm{Re}\cdot f^{1/2}) - 4.0 \qquad (33)$$

where Re = Reynolds number.

In the program, Equation (33) is solved by iteration to determine the friction factor for a known Reynolds number. The friction factor for laminar flow is

$$f = \frac{16}{\mathrm{Re}} \qquad (34)$$

Equations (30) to (32) were solved to yield explicit expressions for the pressure and temperature derivatives in terms of the mass flux, the heat flux and properties of the fuel. Numerical integration of the derivatives then yields the pressure and temperature profiles. To obtain the derivatives the energy equation is simplified by subtracting Equation (30):

$$c_p \frac{dT}{dz} + \frac{T}{\rho^2}\frac{\partial\rho}{\partial T}\frac{dP}{dz} + \frac{4q}{Gd} - \frac{2fv_z^2}{d} = 0 \qquad (35)$$

Equations (30), (32), and (35) are now solved simultaneously. The fluid velocity in Equations (30) and (35) is replaced by the mass flux using Equation (32) and the resulting equations rearranged and made dimensionless:

$$\frac{1}{\rho}\frac{\partial\rho}{\partial P}\frac{dP}{dz} + \frac{d}{\rho}\frac{\partial\rho}{\partial T}\frac{dT}{dz} - \frac{\rho d}{G^2}\frac{dP}{dz} - 2f = 0 \qquad (36)$$

$$\frac{\rho^2 c_p d}{G^2}\frac{dT}{dz} + \frac{Td}{G^2}\frac{\partial\rho}{\partial T}\frac{dP}{dz} + \frac{4\rho^2 q}{G^3} - 2f = 0 \qquad (37)$$

These equations are written in matrix form:

$$\begin{bmatrix} a_{11} & a_{12} \\ a_{21} & a_{22} \end{bmatrix} \begin{bmatrix} x_1 \\ x_2 \end{bmatrix} = \begin{bmatrix} b_1 \\ b_2 \end{bmatrix} \qquad (38)$$

where

$$x_1 = \frac{\rho d}{G^2}\frac{dP}{dz} \qquad (39)$$

$$x_2 = \frac{\rho^2 d}{G^2}\frac{dT}{dz} \qquad (40)$$

$$a_{11} = -1 + \frac{G^2}{\rho^2}\frac{\partial\rho}{\partial P} \qquad (41)$$

$$a_{12} = \frac{G^2}{\rho^3}\frac{\partial\rho}{\partial T} \qquad (42)$$

$$a_{21} = \frac{T}{\rho}\frac{\partial\rho}{\partial T} \qquad (43)$$

$$a_{22} = c_p \qquad (44)$$

$$b_1 = 2f \qquad (45)$$

$$b_2 = 2f - \frac{4\rho^2 q}{G^3} \qquad (46)$$

The solution to Equation (38) is

$$x_1 = \frac{a_{22}b_1 - a_{12}b_2}{a_{11}a_{22} - a_{12}a_{21}} \qquad (47)$$

$$x_2 = \frac{-a_{21}b_1 + a_{22}b_2}{a_{11}a_{22} - a_{12}a_{21}}. \qquad (48)$$

In the computer program Equations (47) and (48) are integrated numerically by the Runge-Kutta-Gill method.[58] Fluid pressures and temperatures are then obtained as functions of the axial distance.

The critical velocity for choking is calculated at each integration step for comparison with the linear velocity. The critical velocity occurs as the pressure drop approaches infinty. Hence the critical velocity can be found by letting x_1 approach infinity in Equation (47). The denominator on the right side is then zero and the critical velocity is given by rearrangement:

$$v_c = \frac{G_c}{\rho} = \left[\frac{\partial\rho}{\delta P} - \frac{T}{\rho^2 c_p}\left(\frac{\partial\rho}{\delta T}\right)^2\right]^{-1/2} \tag{49}$$

where v_c = critical velocity of fluid
G_c = critical mass flux of fluid.

At periodic intervals during the integration a film heat transfer coefficient and a wall temperature are determined. The film coefficient is determined by any suitable heat transfer correlation, which can be inserted easily into the computer model.

In order to analyze data obtained in a resistance-heated heat exchanger, a pair of wall transfer coefficients, one for the heat generated and the other for the heat lost, are used to calculate the temperature drop across the wall. This temperature drop is given by

$$T_i - T_o = \frac{q_G}{h_G} + \frac{q_L}{h_L} \tag{50}$$

where

$$h_G = -\frac{2k_w}{R_i}\left[\frac{1 - \left(\frac{R_i}{R_o}\right)^2}{1 - \left(\frac{R_i}{R_o}\right)^2 + 2\ln\left(\frac{R_i}{R_o}\right)}\right] \tag{51}$$

= heat transfer coefficient for heat generated by resistance heating in tube wall

$$h_L = \frac{k_w}{R_i \ln\left(\frac{R_i}{R_o}\right)} \tag{52}$$

= heat transfer coefficient for heat transferred to surroundings

q_G = heat generated by resistance heating expressed as an inside wall heat flux to the fluid

q_L = heat lost to surroundings expressed as an inside wall heat flux from the fluid

T_i = inside wall temperature

T_o = outside wall temperature

R_i = inside tube radius

R_o = outside tube radius

k_w = wall thermal conductivity

The inside wall temperature is determined by

$$T_i - T_f = \frac{q_G - q_L}{h_f} \tag{53}$$

where T_f = fluid temperature

h_f = film heat transfer coefficient.

Comparison With Experiments

Experiments have been run at low and high heat fluxes. The calculations at low heat flux (1.36-1.63×10^5 Btu/ft^2-hr) compare favorably with experimental results. At high heat flux (4.50-8.22×10^6 Btu/ft^2-hr) the calculations are different from experimental observations. The predicted wall temperatures are higher than the observed values. Experimental results at low heat flux were obtained on a 0.277-in. diameter tube and at high flux on a tube of 0.0265-in. diameter.

Predicted temperature profiles at low heat flux are compared with experimental results in Figures 52 to 54. The mean bulk temperatures on the three figures lie in the subcritical, critical, and supercritical temperature regions. The calculated outlet bulk temperature in each figure agrees closely with the experimental value.

The profiles of the wall temperature were calculated from the heat flux, fluid temperature, and heat transfer coefficients based on different correlations. Two of the curves are based on the Dittus-Boelter correlation:59)

$$Nu = 0.023\ Re^{0.8} Pr^{0.4} \tag{54}$$

where $Nu = \frac{h_f d}{k}$ = Nusselt number

$Re = \frac{dG}{\mu}$ = Reynolds number

$Pr = \frac{C_p \mu}{k}$ = Prandtl number

k = fluid thermal conductivity

μ = fluid viscosity.

Fluid properties for one curve are based on the mean bulk temperature and for the second curve on the average film temperature (the average of the mean bulk temperature and the inside wall temperature). The third curve is based on the Sieder-Tate correlation:59)

$$Nu_B = 0.023\, Re_B^{0.8} Pr_B^{1/3} \left(\frac{\mu_B}{\mu_W}\right)^{0.14} \qquad (55)$$

where the subscripts refer to properties at either the mean bulk temperature (B) or the inside wall temperature (W).

On each figure the measured wall temperatures on the top and bottom of the tube are close together at the tube inlet, diverge for 1 ft, and maintain a large difference for the remaining tube length. This temperature difference is probably due to secondary circulation inside the tube driven by density gradients. Hot fluid at the side rises to the top forcing colder fluid down across the centerline to the bottom of the tube.

The predicted wall temperatures generally tend to lie in the region of the bottom wall temperature. At subcritical bulk temperatures ($T < 570.5$°F, Figures 32 and 53) the Dittus-Boelter correlation based on the average film temperature shows less agreement with experiment than do the other two correlations. At ambient bulk temperatures the wall temperatures are high due to a large fluid viscosity, which decreases rapidly with increasing temperature. At the critical temperature, discontinuities in the fluid properties cause discontinuities in the heat transfer coefficient and hence the wall temperature. At supercritical temperatures (Figures 53 and 54) all three correlations predict essentially the same heat transfer coefficient. In Figure 54 the wall temperature for the Sieder-Tate correlation (not shown) lies between the wall temperatures predicted by the other two correlations.

Predicted temperatures at high heat flux are shown in Figures 55 and 56. The mean bulk temperature is subcritical on both graphs. Outside wall temperatures based on three correlations are plotted for comparison with experimental temperatures. All three correlations predict conservative values of the heat transfer coefficient and hence high values for the wall temperature, although the temperatures based on the Dittus-Boelter correlation using fluid properties at the average film temperature are somewhat reasonable. The experimental wall temperatures are close together and show no evidence of secondary circulation. Actually the bottom wall temperatures are higher than the wall temperatures on top. This is probably due to a greater wall thickness at the bottom of the tube.

Shock Tube Studies of Ignition Delays of Hydrocarbons

The measurement of ignition delays has been extended to other high molecular weight hydrocarbons. Experimental methods and equipment have been described in previous reports.2)3)19) The latest measurements have been made on fuels that are possible candidates for regenerative cooling of ramjet engines. The fuels used include both as-is components(DMD(dimethanodecalin), SHELLDYNE, and SHELLDYNE H) and mixtures (SHELLDYNE-Decalin and SHELLDYNE-Binor-S). Correlating equations were determined by linear regression for each fuel.

Experimental Work

Mixtures were prepared at 80°C in order to have a sufficient concentration of fuel. The reaction section of the shock tube was heated to the same temperature, while the driver section was maintained at 43°C (except

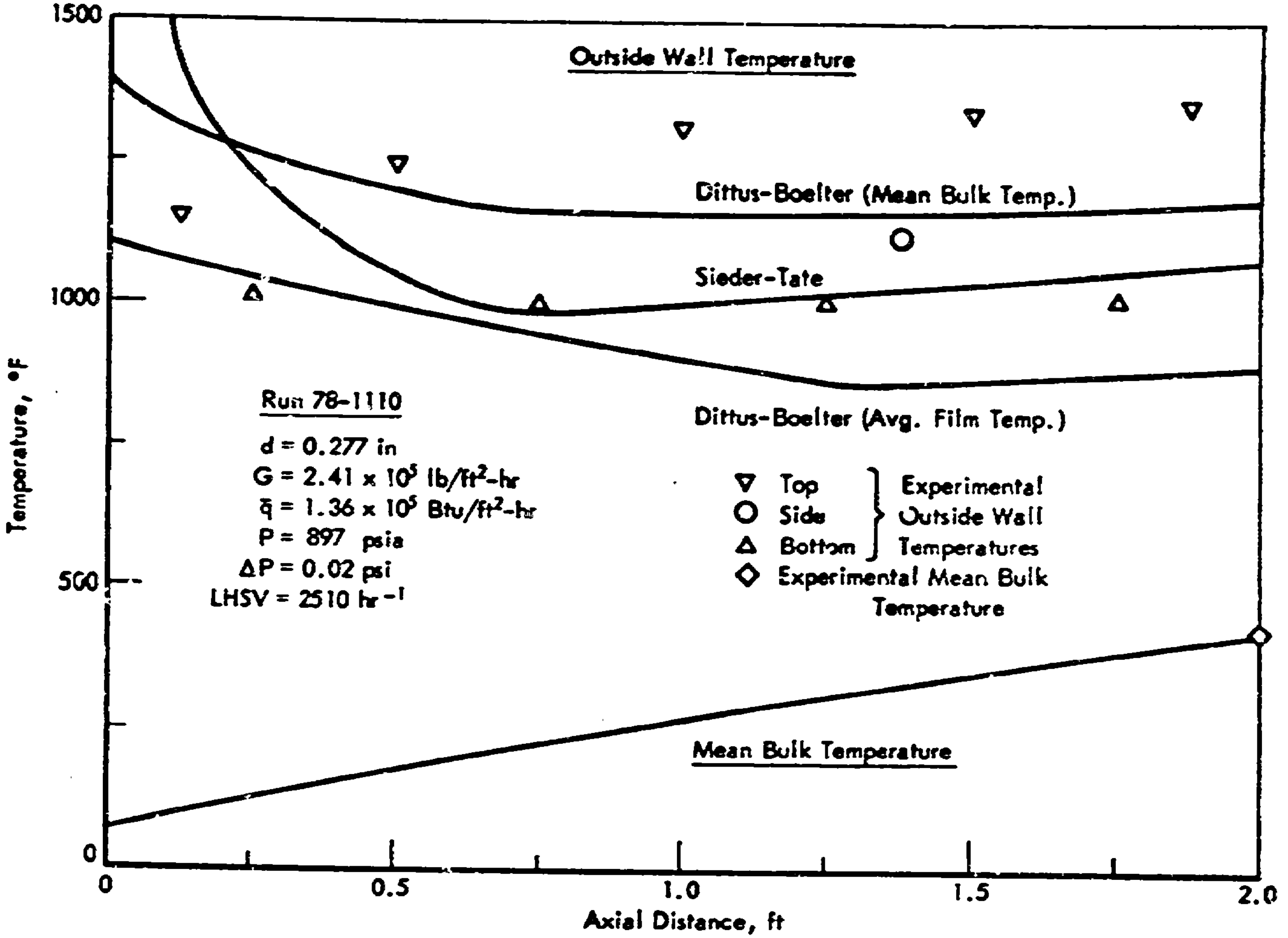

Figure 52. CALCULATED AND EXPERIMENTAL TEMPERATURE PROFILES FOR REGENERATIVE HEAT EXCHANGE STUDIES

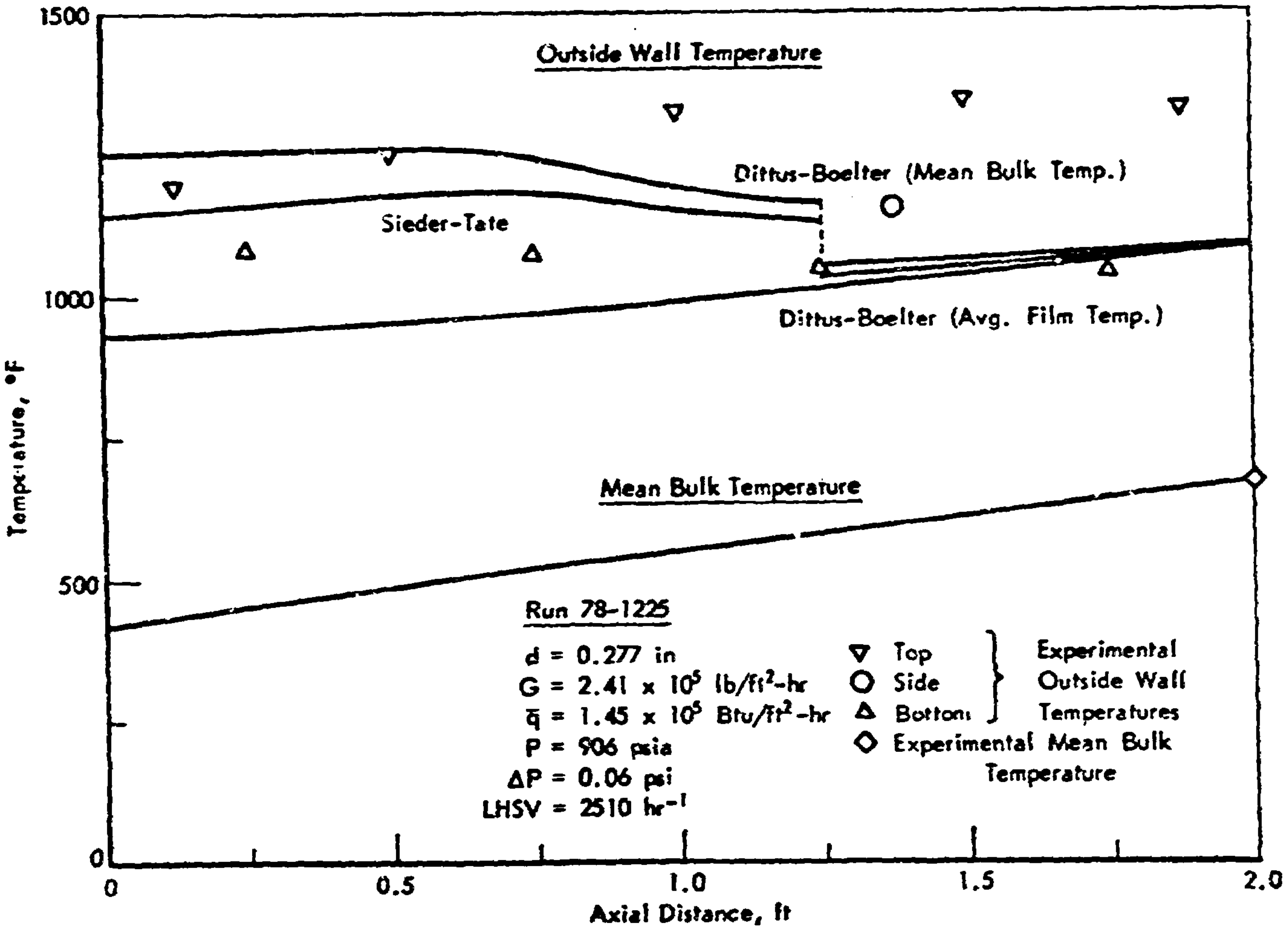

Figure 53. CALCULATED AND EXPERIMENTAL TEMPERATURE PROFILES FOR REGENERATIVE HEAT EXCHANGE STUDIES

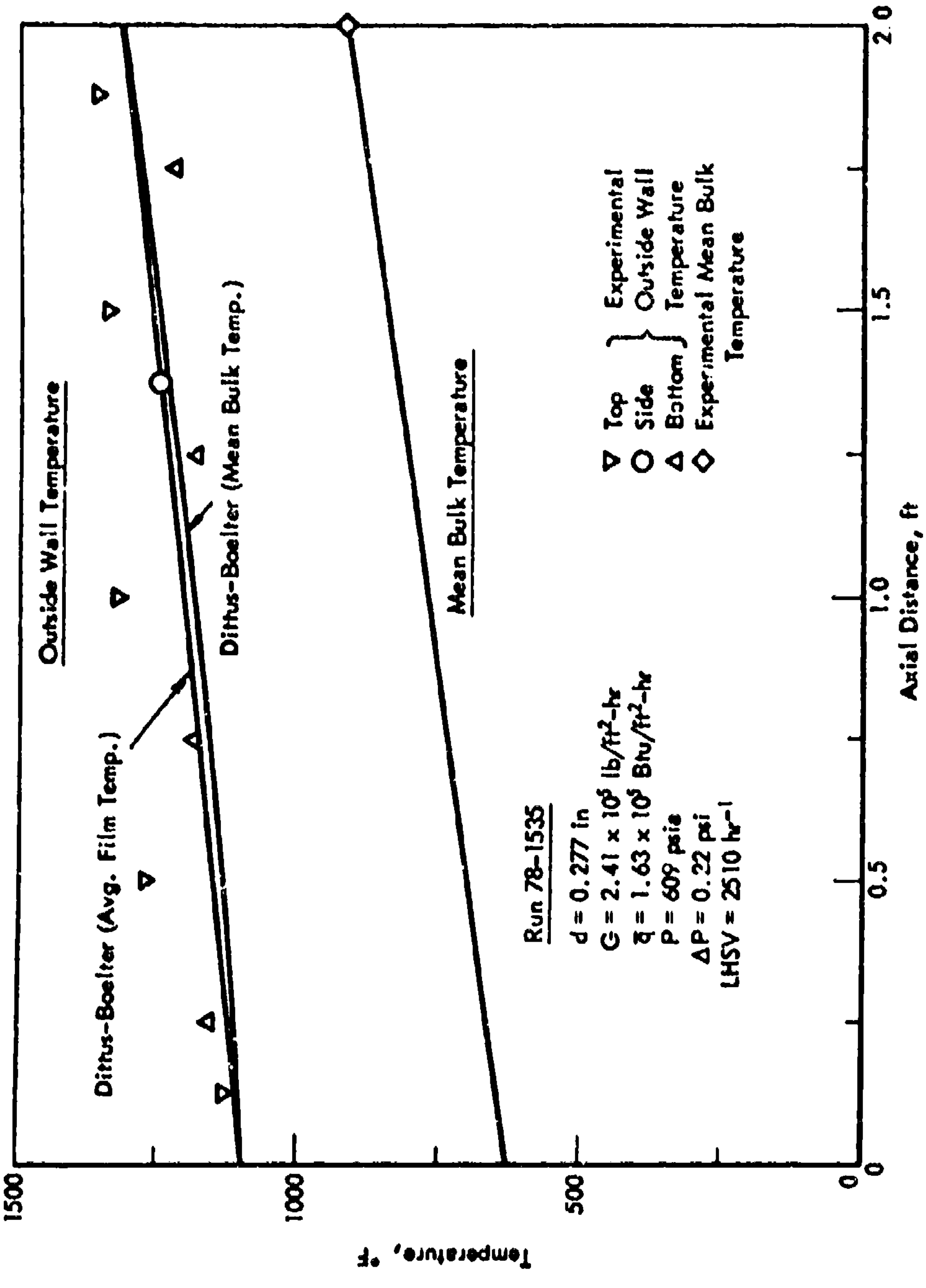

Figure 54. CALCULATED AND EXPERIMENTAL TEMPERATURE PROFILES FOR REGENERATIVE HEAT EXCHANGE STUDIES

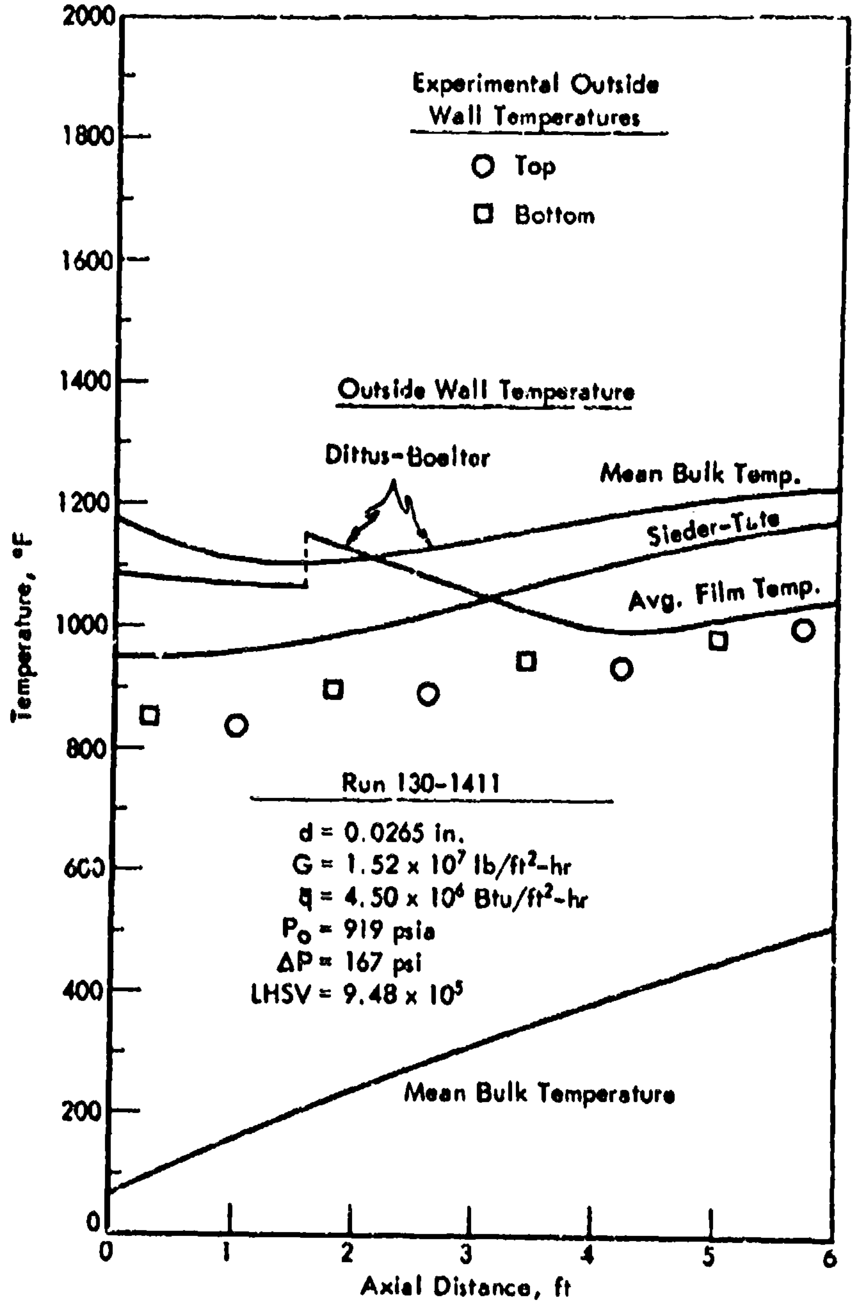

Figure 55. CALCULATED AND EXPERIMENTAL TEMPERATURE PROFILES FOR REGENERATIVE HEAT EXCHANGE STUDIES

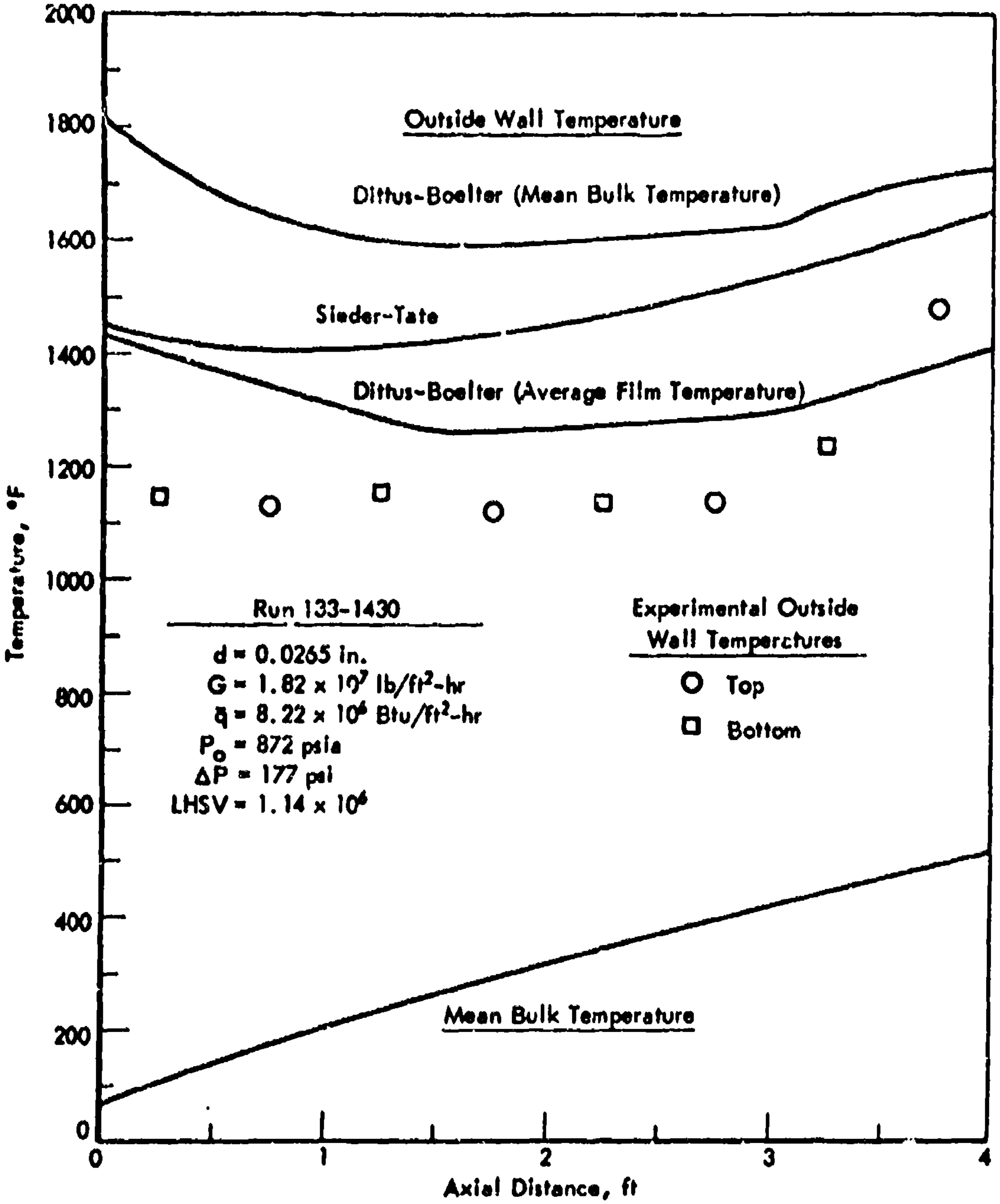

Figure 56. CALCULATED AND EXPERIMENTAL TEMPERATURE PROFILES FOR REGENERATIVE HEAT EXCHANGE STUDIES

near the diaphragm flange, where the temperature was also 80°C).

During each firing of the tube the apparent delay time of the mixture was determined by measuring the infrared emission from CO_2 at a frequency of 2350 cm^{-1}. The CO_2 emission was displayed as an oscilloscope trace, examples of which are the lower traces in the photographs of Figure 57. The upper trace in each photograph is the pressure history at the measuring station. Photographs (a) and (b) are characteristic of the results obtained on most of the shock tube runs. During the passage of the shock wave there is a sudden increase in the pressure, which is followed soon afterwards by a marked increase in CO_2 emission. A few of the runs with SHELLDYNE exhibited two breakpoints in the CO_2 traces, as shown in photographs (c) and (d). The initial increase was followed shortly by a dip and then a second increase in the CO_2 emission.

Data Analysis

The calculation procedure for analyzing data has been written as a computer program that furnishes the ignition delay and physical conditions for the combustion front. The calculation is based on the equations for conservation of mass, energy, and momentum in a one-dimensional shock wave. Perfect gas behavior and a logarithmic dependence of specific heat on temperature are assumed. The apparent delay time is corrected to the true delay time using the velocities of the shock wave and the following gas. Conditions at the combustion front are calculated from the conditions immediately behind the shock wave by assuming an exponential attenuation of the shock wave pressure. The pressure following the shock wave is assumed to decrease with distance according to

$$\frac{P_2}{P_1} - 1 = \left(\frac{P_{2,\ \text{ideal}}}{P_1} - 1\right) \exp\left(-\frac{Ax}{r_H}\right) \qquad (56)$$

where P_1 = pressure ahead of shock wave
P_2 = pressure following shock wave
x = axial distance
r_H = hydraulic radius of shock tube
A = attenuation coefficient.

An attenuation coefficient of 0.001 was used, which is in the range of 0.0005 to 0.001 estimated from attenuation coefficients for other shock tubes.(60)

Results

Ignition delay times and conditions calculated from experimental data are listed in Tables 89 through 95 of the Appendix. The calculated delay times for each hydrocarbon or hydrocarbon mixture were fitted to correlating equations by multiple regression to determine the effects of independent variables. Temperature and oxygen concentration were found to be the only variables with significant effects. Hence the correlating equation used was

$$\ln \tau = b_0 + b_1 \ln c_{O_2} + \frac{E}{RT} \qquad (57)$$

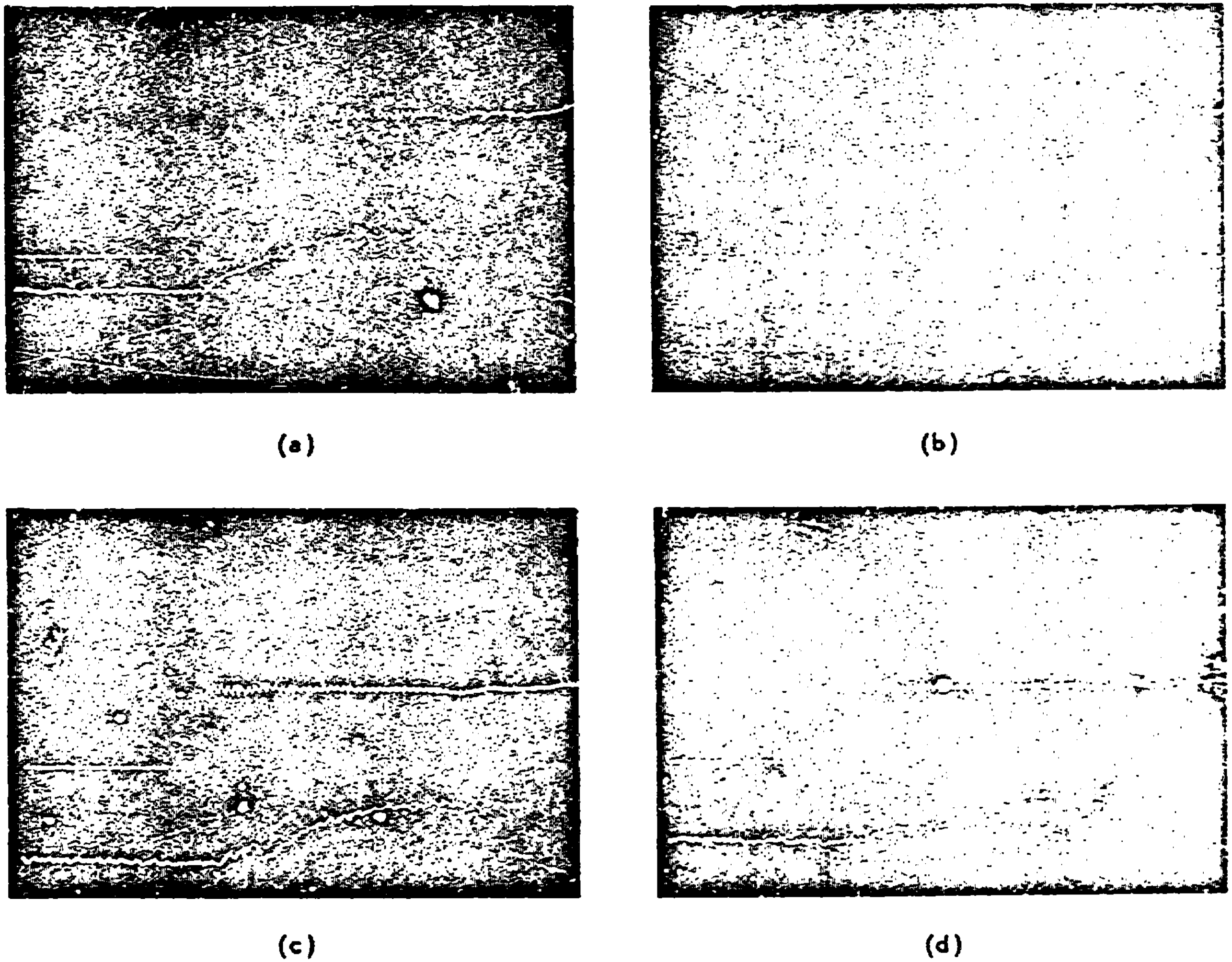

(a) (b)

(c) (d)

Figure 57. OSCILLOSCOPE TRACES OF PRESSURE AND CO_2 INFRARED EMISSION IN SHOCK TUBE RUNS

where τ = ignition delay time, μsec

c_{O_2} = oxygen concentration, g mole/liter

T = absolute temperature, °K

R = 1.987×10^{-3} kcal/g mole-°K

b_1, b_2 = correlating parameters

E = correlating parameter (activation energy), kcal/g mole.

Results of the correlation are listed in Table 58. The values of b_1 vary from -1.32 to -0.59 with most of the values close to -1. This led to the use of the following correlating equation:

$$\ln(\tau c_{O_2}) = b_0 + \frac{E}{RT} \qquad (58)$$

Regression results for Equation (58) are listed in Table 59. Activation energies are just slightly different from those in Table 58. The standard error for $\ln(\tau c_{O_2})$ is only a fraction larger in Table 59 than in Table 58. Hence the simpler and more general Equation (58) is almost as good a fit as Equation (57).

Plots of $\ln(\tau c_{O_2})$ vs 1/T are shown among Figures 58 to 65 for various fuels. These illustrate the goodness of fit for Equation (58).

Figures 58 and 59 show the correlating equations for ignition of n-octane and Decalin. The delay times have been recalculated from earlier data[3] using the computer program described above. There is some scatter of data on both plots. n-Octane seems to have no pattern for the scatter of its data. At low temperature, Decalin has delay times that correlate well. However at high temperature and low fuel-oxygen concentration there seems to be a dependence on the equivalence ratio or fuel concentration, since the delay time is almost proportional to the fuel concentration.

Results of shock tube runs for SHELLDYNE are plotted in Figure 60. In a few runs CO_2 emission increased at ignition and dipped afterwards (Figure 57, c and d). This was followed by another increase in the emission to a high level. The delay times for both of these increases fall along the two lines shown in Figure 60. Both lines are equations of the same form as Equation (58). Most of the points for SHELLDYNE fall along the upper line. However, the delay times for a few other runs and also the early delay times for those runs having two breakpoints in the CO_2 trace lie along the lower line. These runs with early ignition are indicated in Table 91 and are not restricted to a single mixture or set of conditions. The parameters for the two ignition delay lines are given in Table 59.

Figure 61 shows the ignition delays for a particular mixture of SHELLDYNE-oxygen-argon. The solid lines are the correlating equations for SHELLDYNE. Six CO_2 traces had two breakpoints each, three of whose delay times are the pairs of points connected by dotted lines in Figure 61. The other points were determined from CO_2 traces that had single breakpoints. The points on the graph appear to form two distinct lines similar to the ones shown. Hence it seems that the ignition of SHELLDYNE is complicated by two possible delay times. At the present time we have no satisfactory explanation

Table 58. IGNITION DELAY PARAMETERS IN EQUATION (57)

Fuel	Standard Error of $\ln(\tau_{CO_2})$	b_0	b_1	Standard Error of b_1	E, kcal/g mole	Standard Error of E
n-Octane	0.55	-17.19	-0.76	0.08	40.5	3.7
Decalin	0.61	-14.90	-0.59	0.07	39.2	3.9
SHELLDYNE	0.30	-22.09	-1.03	0.05	48.6	2.3
SHELLDYNE (Early Ignition)	0.26	-22.44	-1.05	0.10	46.4	3.1
SHELLDYNE H	0.35	-20.08	-0.93	0.05	43.9	1.8
DMD	0.62	-20.06	-0.95	0.19	45.6	4.2
SHELLDYNE-Decalin	0.60	-20.43	-1.10	0.13	40.7	4.0
SHELLDYNE-Binor-S	0.29	-27.77	-1.32	0.12	53.9	3.7

Table 59. IGNITION DELAY PARAMETERS IN EQUATION (58)

Fuel	Standard Error of ln(τp_{O_2})	b_o	E, kcal/g mole	Standard Error of E
n-Octane	0.56	-16.72	50.3	5
Decalin	0.67	-19.88	58.1	2.4
SHELLDYNE	0.30	-14.61	47.9	1.9
SHELLDYNE (Early Ignition)	0.25	-14.48	45.1	1.4
SHELLDYNE H	0.32	-14.44	45.4	1.2
DMD	0.62	-13.84	46.2	3.3
SHELLDYNE-Decalin	0.60	-11.45	38.1	2.1
SHELLDYNE-Binor-S	0.37	-13.66	43.8	2.2

for this behavior of SHELLDYNE. However, it occurs with sufficient frequency to make it improbable that it is adventitious.

Ignition delay results for SHELLDYNE H and DMD are shown in Figures 62 and 63. SHELLDYNE H data correlate well with Equation (58), whereas the DMD has some scatter.

Additional shock tube runs at lower DMD-oxygen concentration would extend the data to higher temperatures and probably improve the correlation.

The correlating equations for the various fuels are compared in Figure 64. DMD and most of the SHELLDYNE points have similar ignition delay times. SHELLDYNE H has delay times that correspond to the early ignition delay times of SHELLDYNE. The delay times of n-octane and Decalin are shorter at high temperature. At lower temperatures these times are similar to those of SHELLDYNE H.

Shock tube runs were made for fuel mixtures of SHELLDYNE-Decalin and SHELLDYNE-Binor-S. Figures 65 and 66 show the results of these experiments. The least-squares linear fit is shown for each mixture along with ignition delay curves for other fuels. The SHELLDYNE-Decalin data at 1% fuel-oxygen concentration do not correlate well with the rest of the data. The data for the 1% fuel-oxygen concentration falls along the SHELLDYNE curve, while the rest of the data is more consistent with the delay times of Decalin and SHELLDYNE H. The SHELLDYNE-Decalin line is the best for all the mixture data. The SHELLDYNE-Binor-S data in Figure 66 correlate well. The best fit for the mixture is close to that of SHELLDYNE H.

Estimation of Physical Properties of Hydrocarbons

The available physical properties of a JP-7 type jet fuel (F-71), trans-Decalin, and SHELLDYNE are shown in Tables 96 through 104 of the Appendix. Most of the properties for F-71 and Decalin were estimated by the Sternling-Brown Properties Program. Most of the SHELLDYNE properties were calculated by a modification of the PPP-3 Physical Properties Program.

Critical properties of the normal paraffins were used in calculating properties of F-71, since previous analysis has shown the fuel to be composed mainly of paraffins with some naphthenes, olefins, and aromatics. In view of the possible variation in composition of available JP-7 type fuels, the assumption of a paraffinic composition should be sufficiently accurate for calculating properties, and the properties in Tables 96 through 98 should be representative of this fuel.

The current physical properties program, a modification of the A. I. Ch. E. program, is being revised, and when this is completed better estimates of the properties for trans-Decalin will be determined along with properties for cis-Decalin. In the meantime the properties in Tables 99 through 101 should be reasonably satisfactory for both isomers of Decalin.

Properties of F-71 and SHELLDYNE will also be recalculated with the revised program if they can be improved significantly. Otherwise the current properties should be adequate, since these two fuels are mixtures and the actual fuels available now or later may vary slightly in composition

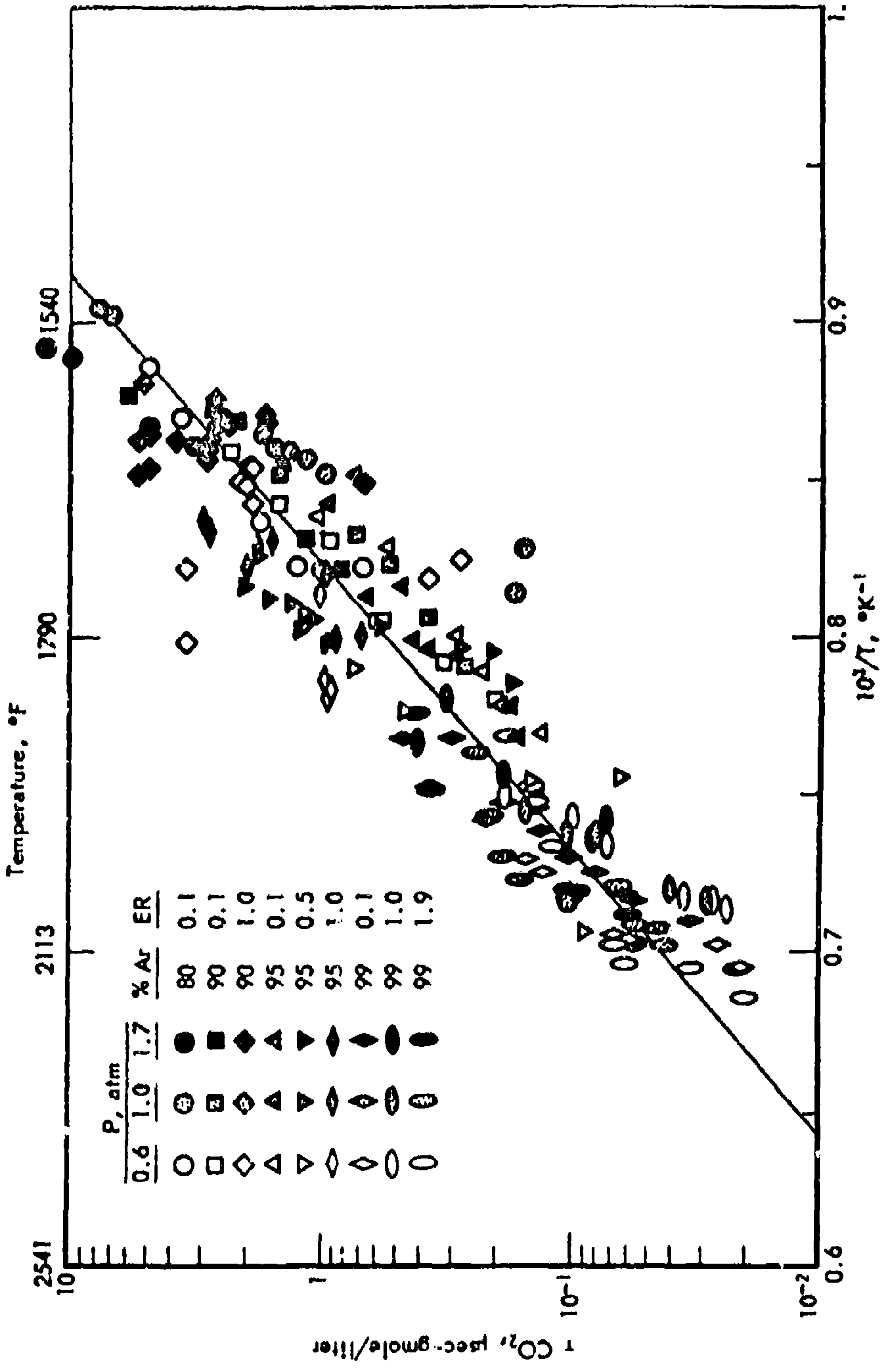

Figure 58. CORRELATION OF IGNITION DELAYS FOR n-OCTANE-OXYGEN-ARGON

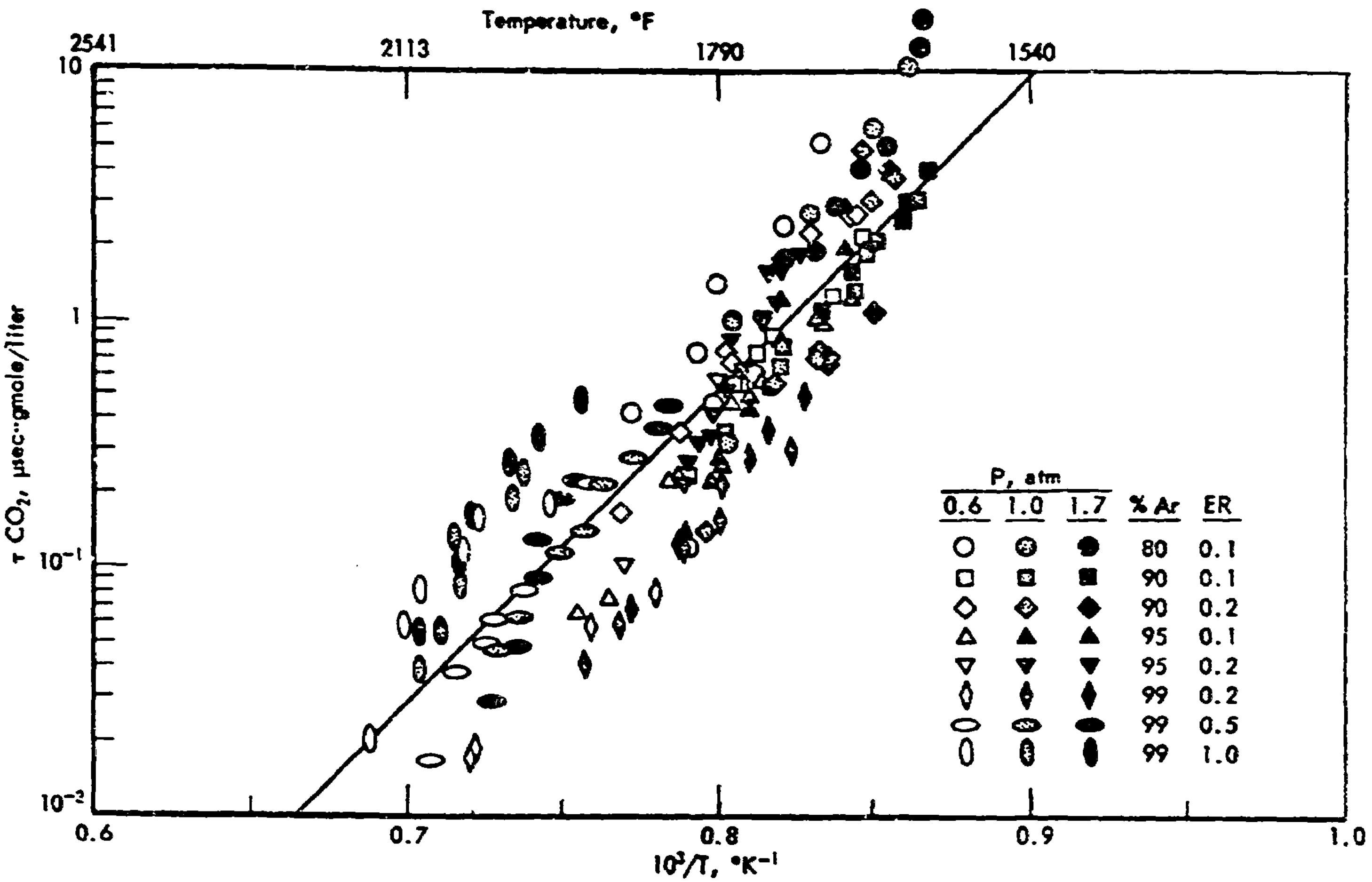

Figure 59. CORRELATION OF IGNITION DELAYS FOR DECALIN-OXYGEN-ARGON

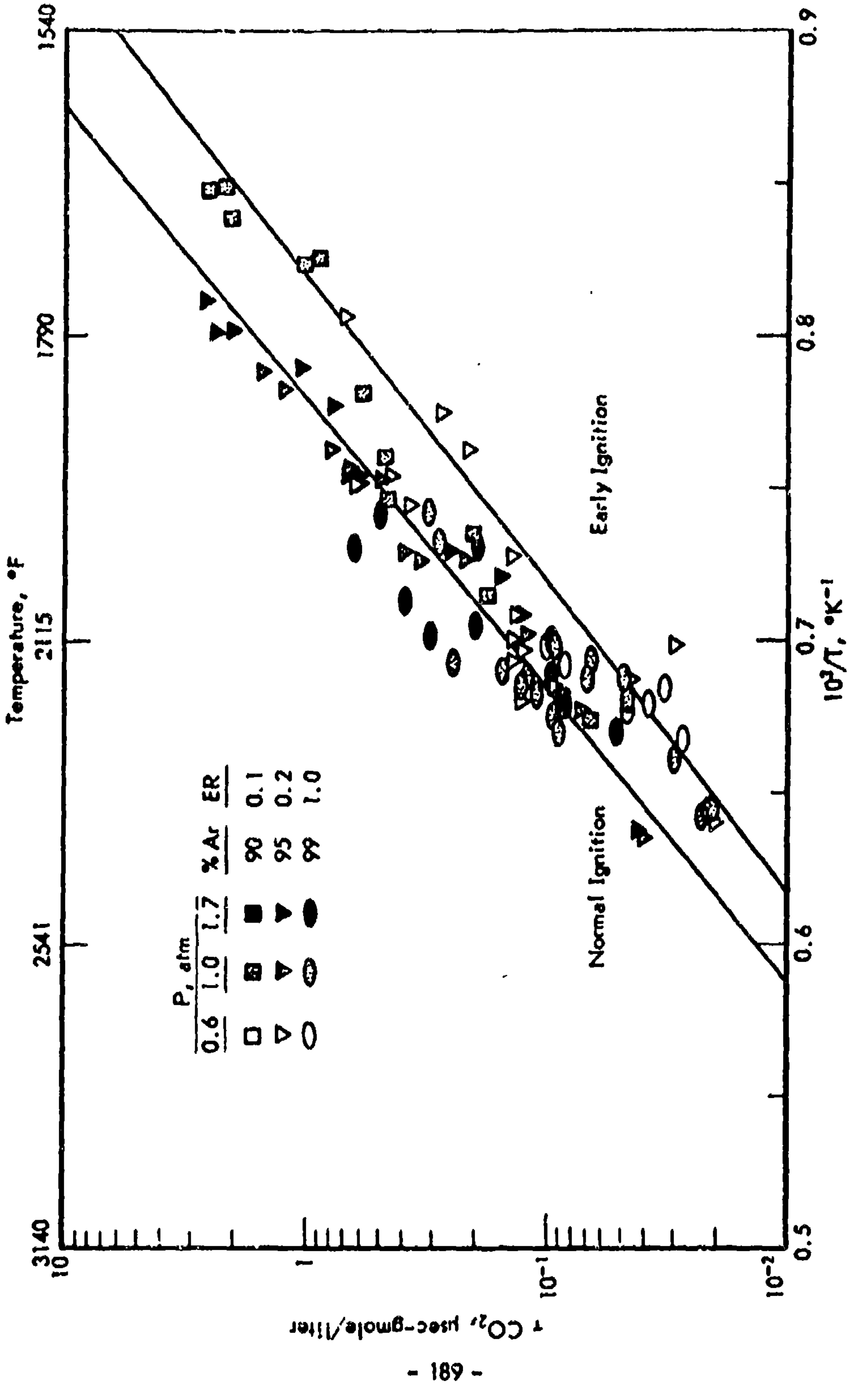

Figure 60. CORRELATION OF IGNITION DELAYS FOR SHELLDYNE-OXYGEN-ARGON

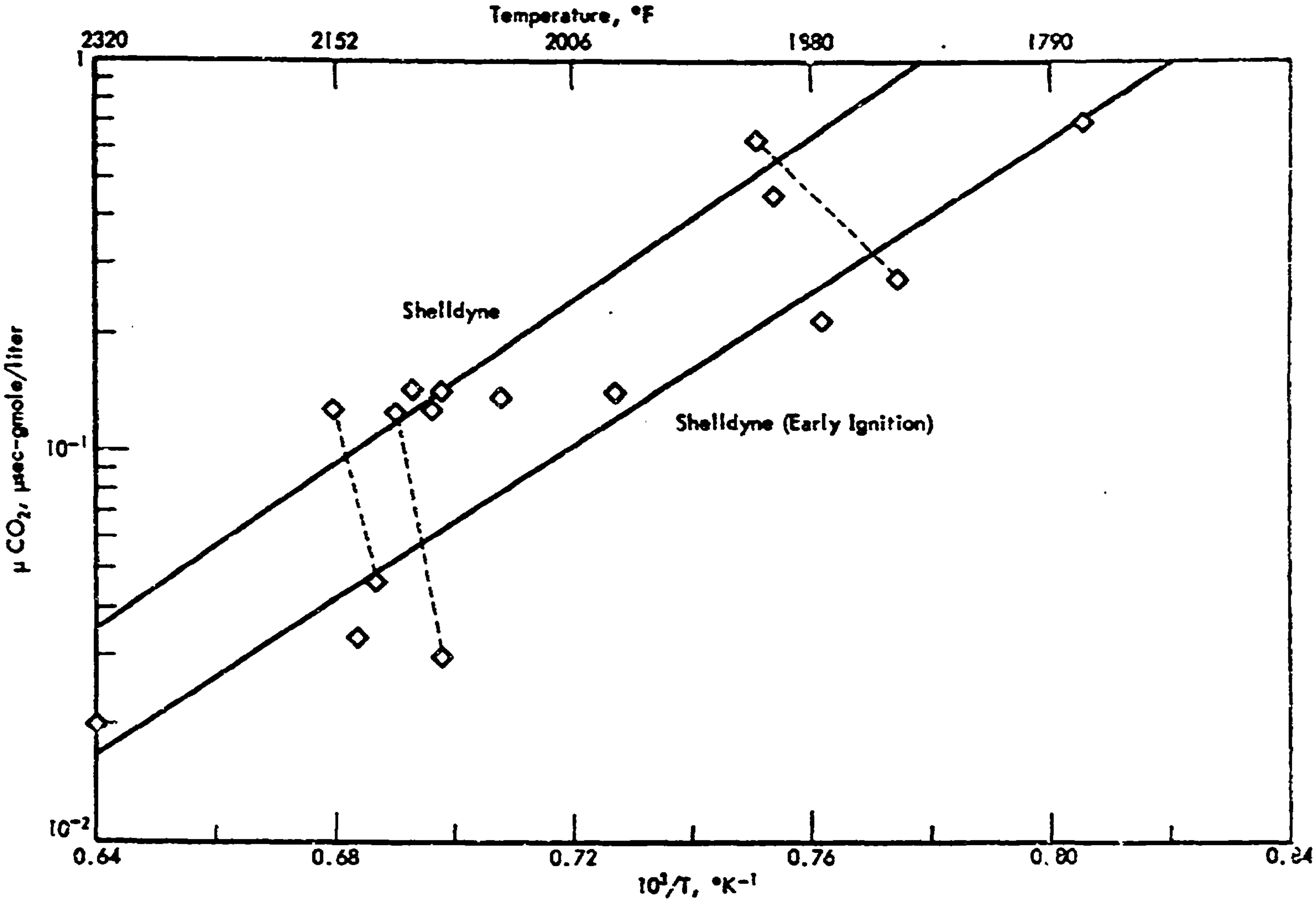

Figure 61. IGNITION DELAY TIMES FOR SHELLDYNE-OXYGEN-ARGON

64458

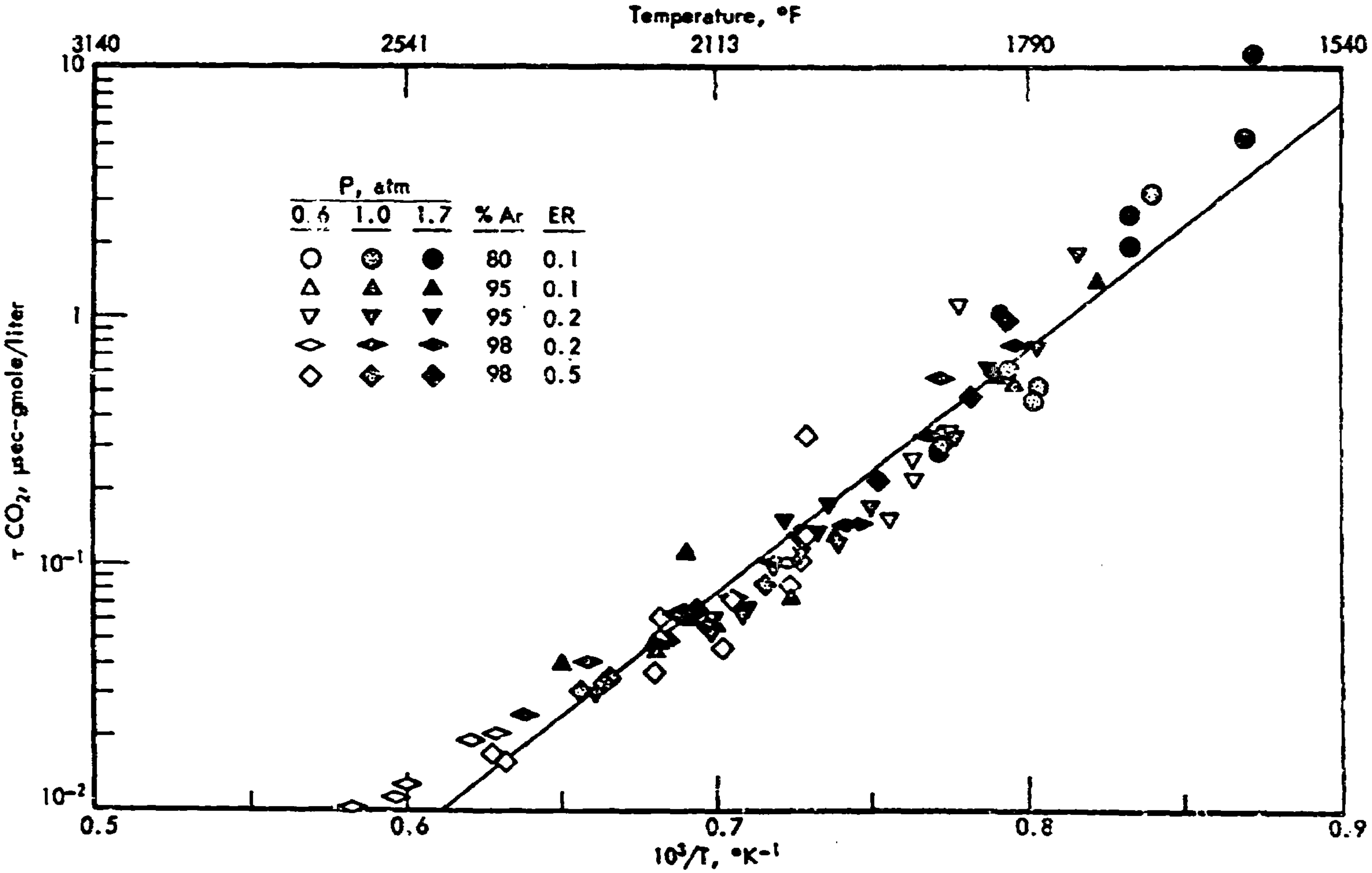

Figure 52. CORRELATION OF IGNITION DELAYS FOR SHELLDYNE H-OXYGEN-ARGON

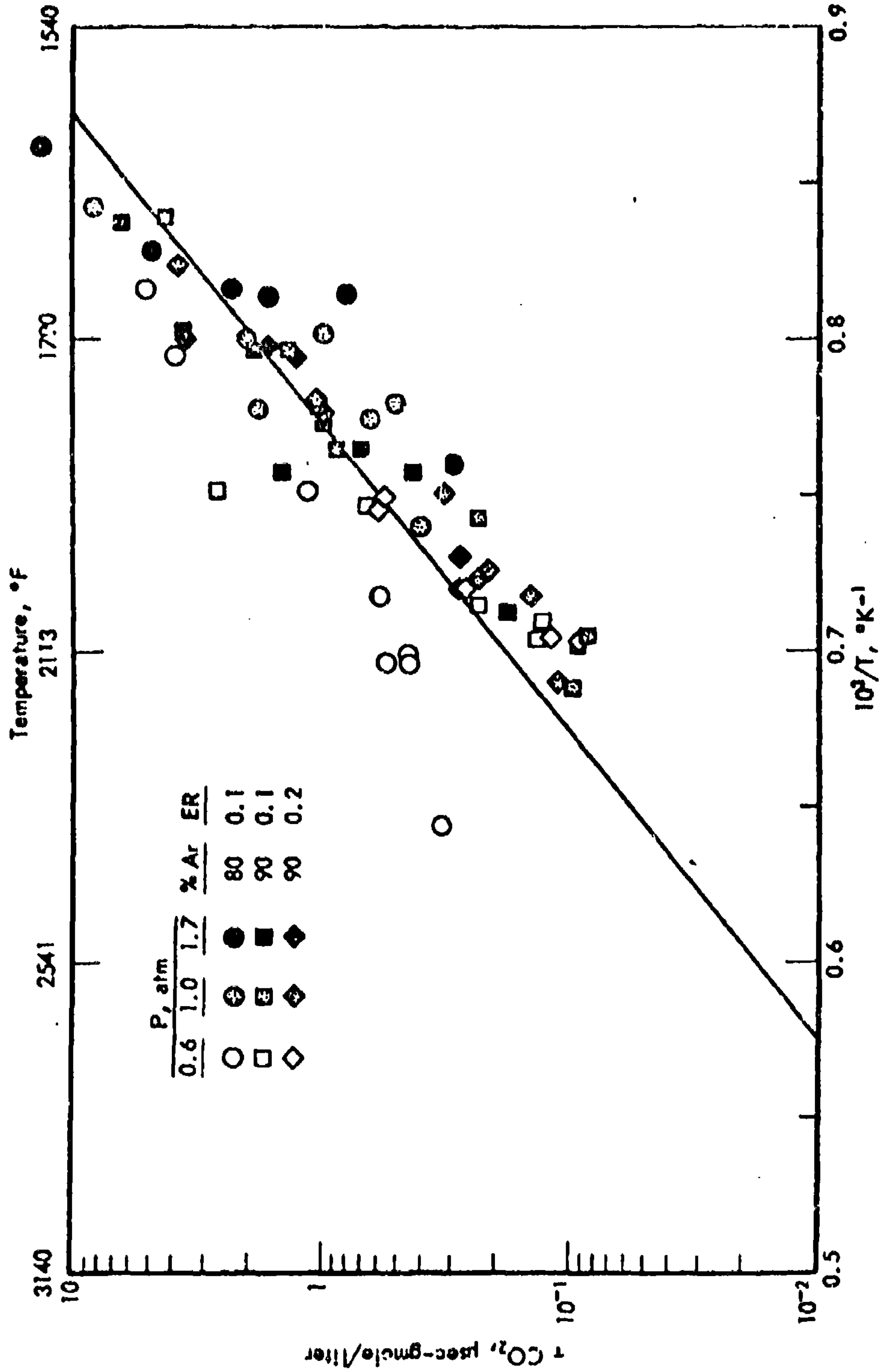

Figure 63. CORRELATION OF IGNITION DELAYS FOR DMD-OXYGEN-ARGON

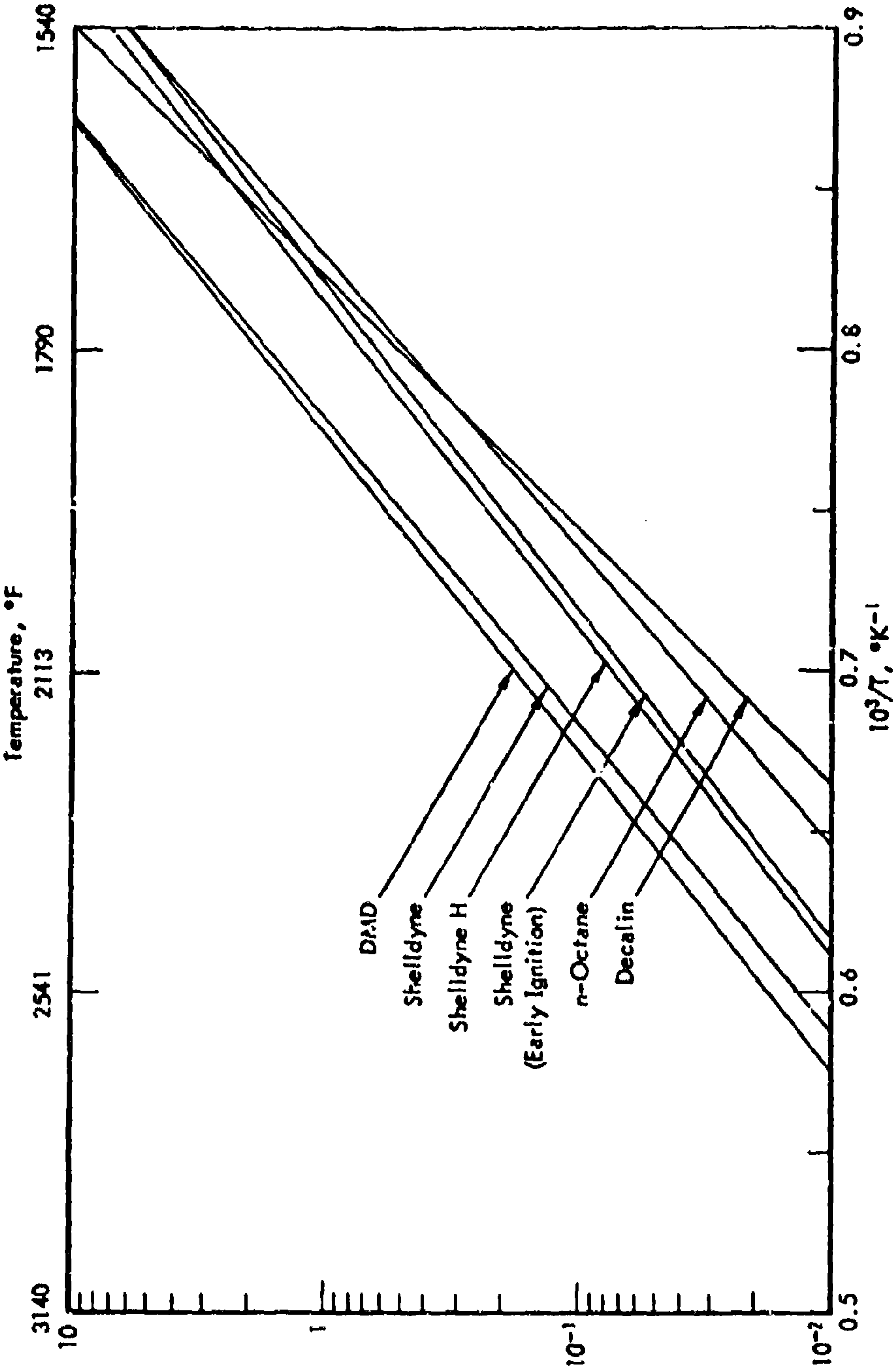

Figure 64. COMPARISON OF IGNITION DELAY CORRELATIONS FOR DMD, SHELLDYNE, SHELLDYNE H, DECALIN, AND n-OCTANE

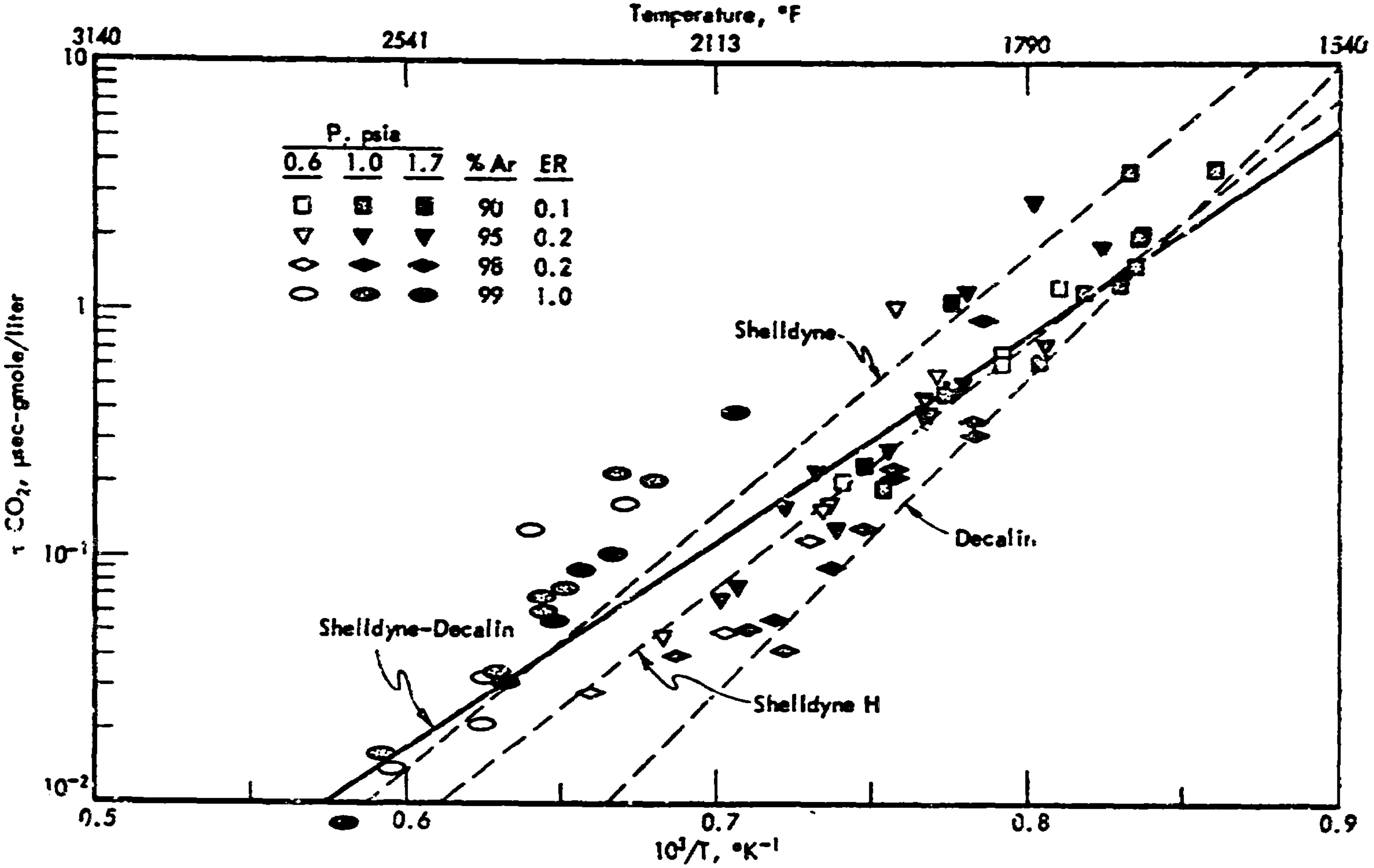

Figure 65. CORRELATION OF IGNITION DELAYS FOR SHELLDYNE-DECALIN-OXYGEN-ARGON

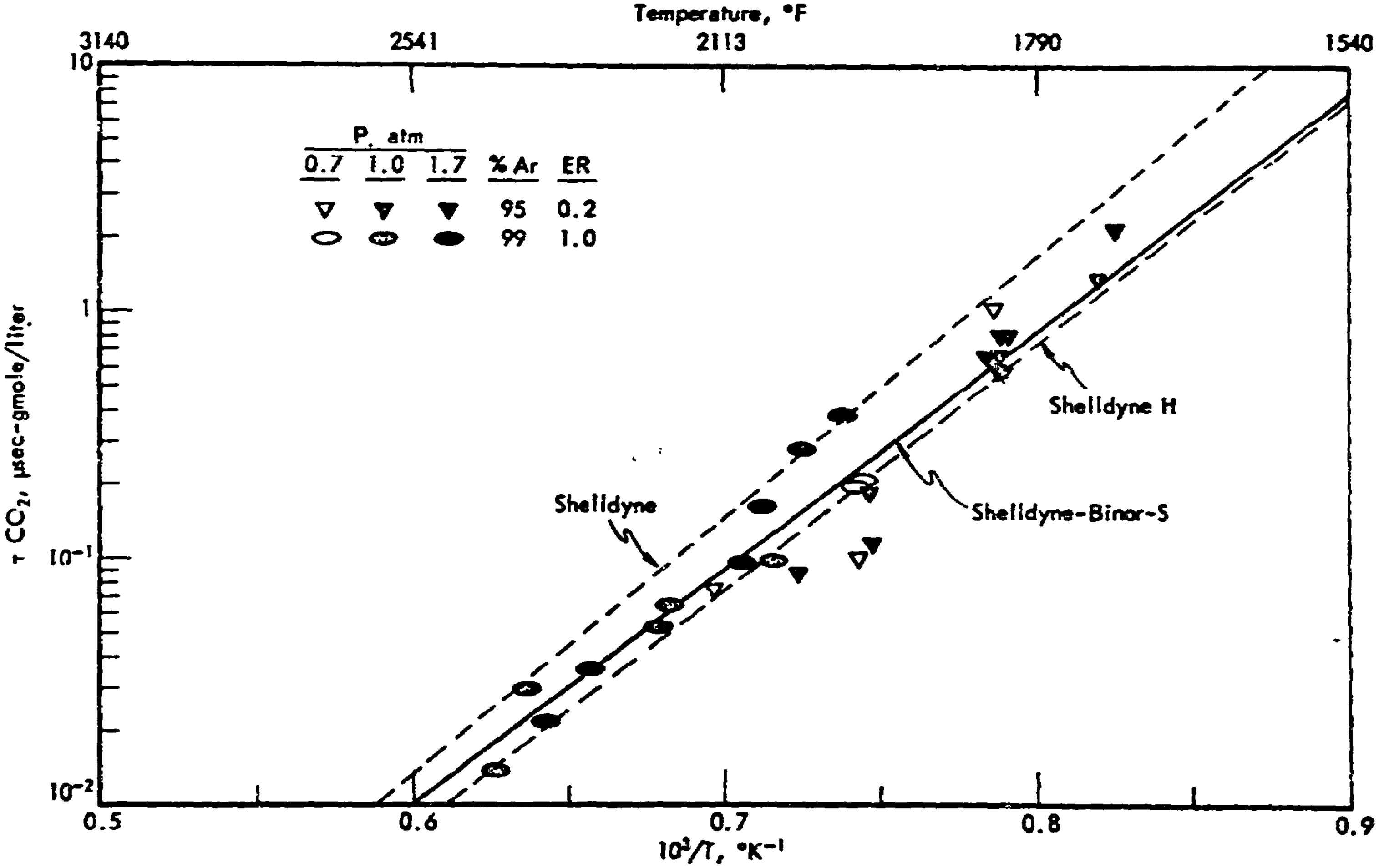

Figure 66. CORRELATION OF IGNITION DELAYS FOR SHELLDYNE-BINOR-S-OXYGEN-ARGON

and properties.

The following section contains a summary of the various methods used for estimating physical properties. The list is essentially an identification of the formulas and correlations used in the calculation. The accuracy of these techniques is difficult to assess. The gas properties should be within 3% except in the critical region where errors of 10-30% may be likely. The liquid properties are less accurate: density 2%, heat capacity 10%, enthalpy 8%, heat of vaporization 5%, vapor pressure 3%, surface tension 10%, viscosity 10%, and thermal conductivity 15%.

Description of Estimation Methods

1. Compressibility factor calculated by the Ackerman modification of the Redlich-Kwong equation of state.[61]

2. Liquid density from the Francis equation[62] for $T \leq T_c - 60°F$

$$\rho = A - BT - \frac{C}{E-T} \tag{59}$$

and from the Guggenheim equation[63] for $T > T_c - 60°F$

$$\rho_r = 1 + a(1-T_r)^{1/3} + b(1-T_r) \tag{60}$$

3. Gas heat capacity at zero pressure from data or Rihani-Doraiswamy method.[64] Pressure effect from a modified form of the Redlich-Kwong equation of state.

4. Liquid heat capacity by numerical differentiation of liquid enthalpy.

5. Gas enthalpy at zero pressure from integration of ideal gas heat capacity. Effect of pressure from a modified form of the Redlich-Kwong equation of state.

6. Liquid enthalpy at saturation pressure by difference between gas enthalpy and heat of vaporization.

7. Gas fugacity by numerical integration of

$$\ln \frac{f}{P} = \int_0^P \frac{Z-1}{P}\, dP \tag{61}$$

8. Gas free energy from the ideal gas free energy and the pressure effect on free energy

$$G - G° = RT \ln \frac{f}{f°} \tag{62}$$

9. Gas entropy from the enthalpy and free energy at the same conditions

$$S = \frac{H - G}{T} \tag{63}$$

10. Gas specific heat ratio by differentiation of the Redlich-Kwong equation of state to evaluate

$$c_p - c_v = - \frac{T\left(\frac{\partial V}{\partial T}\right)_P^2}{\left(\frac{\partial V}{\partial P}\right)_T} \tag{64}$$

11. Gas Joule-Thomson coefficient by differentiation of the modified Redlich-Kwong equation of state to evaluate

$$\mu_{JT} = - \frac{1}{C_p}\left(\frac{\partial H}{\partial P}\right)_T \tag{65}$$

12. Gas sonic velocity from

$$Vs = V\left[- \frac{\gamma}{M\left(\frac{\partial V}{\partial P}\right)_T}\right]^{1/2} \tag{66}$$

using the Redlich-Kwong equation of state.

13. Heat of vaporization from the Theisen correlation64)

$$\Delta H_V = a(T_c - T)^n \tag{67}$$

or the Watson correlation ($n = 0.38$).64)

14. Vapor pressure by the reduced Frost-Kalkwarf-Thodos correlation.64)

15. Surface tension from an empirical correlation55)

$$\sigma = a(1 - T_r)^b$$

or the MacLeod-Sugden correlation.64)

16. Gas viscosity from the Chapman-Enskog theory with Kihara potential parameters.64) Correction for pressure by the Stiel and Thodos method.65)

17. Liquid viscosity from an ASTM standard viscosity-temperature chart for $T < 200°F$, from

$$\ln \mu = a + \frac{b}{T} \tag{68}$$

for $200°F \leq T < 0.7\ T_c$, and from the Stiel and Thodos dense gas method for $T_r > 0.7$.64)

18. Gas thermal conductivity from the Chapman-Enskog theory.64) Correction for pressure by the Stiel and Thodos method.65)

19. Liquid thermal conductivity from the Robbins-Kingrea correlation for $T_r < 0.9$ and from the Stiel and Thodos dense gas correlation for $T_r > 0.9$.64)

Present Status and Future Projections

1. A considerable effort has been made during this year to gather data to allow us to advance Decalin to the same status as a candidate fuel as is now occupied by MCH. Decalin is a promising candidate fuel in its own right and would be valuable as a component of a mixed fuel in which the Decalin is incorporated to decrease the vapor pressure or modify the freeze point or viscosity. The Decalin system is considerably more involved than is MCH because of complexity of the dehydrogenation reactions. We have apparently been successful in obtaining kinetic data in bench-scale apparatus under "isothermal" conditions (vide infra) for Decalin over Pt/Al_2O_3. This will enable us to complete the mathematical model and then run Decalin in the FSSTR in order to check it.

2. Preliminary examination of the thermal reactivity of the high density fuel SHELLDYNE in our all metal bench-scale reactor equipment revealed that it displays susceptibility to cracking reactions even at as low a temperature as 800°F; the extent of reaction depending on the contact time in the reaction zone. Although the reaction is relatively clean at low conversion, at high conversions (i.e., high temperature or long reaction time) coking can occur. The reactivity of the SHELLDYNE can be greatly reduced by hydrogen treatment, which is readily accomplished. Thus, under similar conditions, the ratio of SHELLDYNE to SHELLDYNE H reaction is around 1500 while the reactivity of SHELLDYNE H is comparable with that of Decalin. Since the effect of hydrogen treating on the heat of combustion and physical properties of SHELLDYNE is relatively minor, it is evident that SHELLDYNE H should be used in any application involving cooling. While this conclusion must be tentative and will await further work in the mini-FSSTR under more representative conditions, it is unlikely that it will be modified. There is some indication that the metal used in our bench-scale equipment had a catalytic effect on the decomposition of the SHELLDYNE. The hydrotreating also improved the thermal stability of SHELLDYNE as measured in the SD/M-7 coker, being superior to Decalin in tube deposits and somewhat inferior in pressure drop effects. The next step will be to determine the behavior of SHELLDYNE H in the mini-FSSTR in order to get basic data for heat transfer calculations.

3. Other areas of interest in connection with the development of endothermic fuels involve studying the rates and extent of dehydrogenation of DMD, SHELLDYNE H, BCH (bicycloheptane), hydrogenated fulvenes, adamantane and higher naphthenes over our standard catalyst. It will also be of interest to study dehydrocyclative reactions for molecules involving spatially favored hydrogen atoms. An attempt will also be made to bring about rapid dehydrogenation of TIB in the presence of a volatile strong acid which could serve as a vapor phase catalyst.

4. Although a substantial number of the 536 catalysts that have been evaluated under our catalyst development program have shown greater activity (and in some cases greater stability) than the standard Pt/Al_2O_3 catalyst, we have not achieved the sought-for order of magnitude increase in activity desired nor the hoped-for cheap equivalent catalyst. Recent work has been concerned with the production of catalysts containing two or more catalytic elements to which one or more auxiliary elements have been added in an effort to promote substantially higher catalytic activity. Few synergistic effects have been noted as a result of these attempts. We intend in the future to systematically broaden our experimentation by increasing still further the number of elements included in a single catalyst.

A few catalysts which had been shown to be more active than the standard catalysts in MICTR tests were further examined in the bench-scale apparatus under a broader range of conditions with results substantially in agreement with the screening test results. Further testing of this type will be done as more improved catalysts become available.

5. Our efforts to develop nonconventional catalysts are basically along two routes. One, to develop a catalyst which can be coated on the inside of a heat exchanger tube. The other, to provide a catalyst precursor which can be dissolved or dispersed in the fuel and will be converted in the heated zone into a volatile or dispersed catalyst having the requisite activity to bring about the heat sink reaction. A number of thixotropic formulations have been devised which, when dried and platinized, result in a catalyst with at least as much activity as our standard catalyst and at the same time can be converted into a slip which can be applied to the inside of a catalyst tube and fixed by calcining to give an adherent coating. The coating is then platinized in situ. Experiments to check the catalytic activity of such surface catalysts have yielded some encouraging preliminary information as to the practicability of this approach. The best catalysts will be examined further in FSSTR experiments.

In the area of possible dispersed, soluble or vaporizable catalysts some success has been achieved in the past in static experiments carried out in a heated autoclave. These and additional possible catalysts which have been prepared or purchased will be further checked in two different types of apparatii which are now in hand, namely a heated injection autoclave and a pulse type reactor. Preliminary experiments in the pulse reactor have turned up three model compounds which had some activity. It is expected that a large number of materials will be examined during the next year.

6. The mathematical model devised to represent the catalytic dehydrogenation of MCH based on an axisymmetric packed reactor successfully represents the reaction under various flow and reaction conditions (although it had to be modified to accept the 2-ft reactor data). We have been for some months past attempting to develop a similar model for the Decalin system utilizing kinetic data obtained in the bench-scale reactor with diluted beds to supply the basic kinetic parameters. So far it has not been possible to successfully represent the reaction over a wide enough range of reaction variables. Accordingly, some additional data was obtained in the bench-scale reactor using a differential reaction system in order to reduce the uncertainty introduced by the indeterminate temperature variations. The model now seems to be rounding into shape. Similarly, we are attempting to develop a

satisfactory model for a regenerative heat exchanger operating under the conditions anticipated for the near term supersonic combustion missile application. Applying the model to the data obtained in the mini-FSSTR results in satisfactory representation of the data in the supercritical region but is less successful in the critical and subcritical regions. Additional work on this model will be done as more experimental data are obtained.

7. In order to provide heat flux conditions closer to those that might be encountered under application conditions, a two-foot by three-eighths inch OD tube was constructed for the FSSTR and operated at heat fluxes up to 600,000 Btu/hr/sq ft, using R-8 catalyst with MCH feed. By introducing liquid MCH at 70°F into the reactor tube, it was possible to operate at close to the maximum heat load of the section; however, it was evident that catalyst deactivation was beginning to occur at temperatures as low as 900°F. This was accompanied by a rise in the exit fluid temperature as well as the outside wall temperature and by a decline in the MCH conversion. Final fluid temperatures of 1250°F were encountered and a maximum wall temperature of 1500°F. For the system involved, it appears that rapid coke buildup should be anticipated in any region where tube wall temperatures are greater than 1350°F and fluid temperatures above 1150°F are found. These results emphasize the necessity for developing more thermally stable and more active catalysts. Fortunately, these have been provided by our catalyst development program and will be tested in future work in the high flux section.

8. Heat transfer, pressure drop, and coking data are being obtained for candidate missile fuels using a short small diameter electrically heated section substituted for the down stream section of the FSSTR (this has been dubbed the mini-FSSTR). The application being modeled here is that of a nonreactive heat sink in which the fuel will not exceed 900°F at the outlet with an inlet pressure not exceeding 1000 psi. During the recent year tubes 4 or 6 inches long by 26.5 mils ID have been used for the study section and nitrogen, MCH and water have been used as test fluids. With each test section fairly high heat fluxes and flow rates have been achieved. Each of the first three tubes used failed for one reason or another, the first by plugging with carbon and the next two by burnout, although not at the most severe condition encountered. It is suspected that fluctuations in the flow rate due to uneven exit valve operation or to surging in the feed pressure may have been the cause of the failures. It has been shown that the radial variation of wall temperatures which were of alarming proportions in the case of earlier work with a 3/8 inch OD tube section also exists in the small diameter tubes, although of a lesser magnitude. In the latter case, however, we have found that this variation is due to unequal thickness of the tube wall and, hence, unequal generation of heat by passage of the electrical current. Whether this was also the case with the 3/8 inch tube remains to be seen. Additional identical 4 or 6 inch by 26.5 mil sections have been manufactured. These were used for experimentation with water and MCH; Decalin and SHELLDYNE H will be the next test fuels, followed by F-71 and methane. Following this some experimentation with larger tube size sections will be done. A maximum heat flux of 8.5×10^6 Btu/hr/sq ft has been achieved to date.

9 We have two devices that we have been chiefly relying on for determining the thermal stability of fuels in this study: the SD coker, and the CAFSTR. The former is essentially an improved ASTM coker but we have operated it in a recycle mode in order to conserve fuel. In the past, the

feed section has been at atmospheric pressure and a Zenith pump has been used as a combination metering and pressure developing device. Because of the considerable difficulty we have had with this pump and the amount of pump wear which has occurred, we modified the SD coker to operate with the whole system under test pressure, using the pump merely as a metering device. This modification seems to be quite successful and we have used it for obtaining data on a number of fuels, including SHELLDYNE, SHELLDYNE H, and Decalin, as noted above.

No operational problems have been encountered with the CAFSTR. Runs which have been made to date on it have shown that the design concepts were quite sound. The problem here is to rate the tubes in a meaningful manner. The three possible types of evaluations favored are deposit removal by solvent action, deposit removal by combustion and deposit thickness evaluation by electron recoil. All of these are, hopefully, nondestructive to the tube. A large number of solvents were evaluated for their efficacy as deposit removers at 100°C. The only significantly promising solvent found was dimethyl formamide. This will be checked against other evaluation methods. Although the conditions necessary for utilizing combustion as an evaluation method were checked out previously utilizing the CAFSTR tube heater as the heat source for the combustion, we are also evaluating a method utilizing an external furnace as the source of the combustion, with the expectation that this will be less destructive to the tube, and, particularly, to the tube heater. Other devices, including a H_2 ring burner, a plasma torch and a laser are under consideration.

10. In the past we have been limited in our ability to determine the ignition delay of candidate fuels in our shock tube on the basis of fuel volatility, since we require a vapor phase mixture of the fuel, oxygen, and argon to charge into the tube. In order to extend our capabilities into the higher molecular weight materials such as SHELLDYNE and dimethanodecalin (DMD) we modified the tube to utilize electric heaters to increase the ambient temperature of the fuel, oxygen, diluent mixture prior to carrying out the shocking experiment. It was also necessary to eliminate all cool crannies which might provide sites for condensation. Thus, it was necessary to replace the precision pressure gauge used in making up the mixture with a pressure transducer. We have now operated the tube at an ambient temperature of 80°C to compare the ignition delay of DMD, SHELLDYNE and SHELLDYNE H. We find this to be the order of decreasing ignition delay (with the SHELLDYNE H having a delay approximating that of n-octane). A presently inexplicable peculiar behavior was noted on a number of occasions with SHELLDYNE, which gave two correlatable ignition delay times in the same experiment. The shorter delay was approximately the same as that exhibited by SHELLDYNE H while the longer delay was about the same as that shown by DMD. Future work is intended to go to higher ambient temperatures (and, hence, higher equivalence ratios) for these and other high molecular weight molecular types, and to higher pressures for a range of molecular weights. We also hope to improve the sensitivity of the IR detection system to enable us to follow more precisely the production of CO_2 and hence the combustion rate during the reaction.

11. We are keeping in constant touch with improvements being made in the various correlation schemes for computer production of properties of various molecules. We are utilizing two proprietary programs, the Sternling

Brown and the PCP program as well as the A. I. Ch. E. program (in part). We have also taken advantage of a proprietary effort to calculate the properties of molecules from the molecular structure. We utilized this in connection with the correlative programs to determine the properties of SHELLDYNE over a broad range of temperature and pressure. We have also similarly calculated the properties of a JP-7 type fuel (F-71) and trans-Decalin. Unfortunately, each time the properties are calculated, we have to make the proviso that these are subject to revision at some future date if better experimental data or improved calculation methods become available. We must do so in the present instance.

12. Decalin has a number of advantages as an endothermic fuel (compared to MCH), mainly in its lower vapor pressure, higher density, and its better thermal stability and lubricity. In order to have an adequate supply of this material on hand, we obtained thirty drums from the Air Force fuel bank (RAF-161-60). This had been in storage since 1960. In spite of the fact that it was inhibited, care taken in the selection of the material and the low temperature storage conditions, its color and thermal stability had deteriorated substantially. Laboratory work showed that it could be regenerated by silica gel treatment, so this operation was carried out on the thirty drums, resulting in a material of practically pristine quality. Some of this material has been supplied to Pratt and Whitney and to the Air Force at Wright Field. Interestingly, the impurity removed seemed to be fairly simple in character and relatively volatile containing three major components of about the same emergence time from a GLC column as naphthalene. A considerable quantity of this material was desorbed from the silica gel column used in the thirty drum purification and will be examined further to try and identify the materials responsible for the poor thermal stability behavior of the Decalin. The material also had vesicant properties, causing a severe dermatitis to susceptible individuals.

REFERENCES

1. "Vaporizing and Endothermic Fuels for Advanced Engine Application", Technical Documentary Report No. APL TDR 64-100 Part I. Contract No. AF 33(657)-11096, Shell Development Company, September 1964.

2. Ibid, Part II, September 1965.

3. Ibid, Part III, September 1966.

4. A. Terri, J. Aircraft 5, 3 (1968).

5. E. W. Ungar, Science 158, 740 (1967).

6. N. F. Amin, S. Molder, J. Spacecraft 4, 1089 (1967).

7. W. Chinitz and P. Bauer, Pyrodynamics 4, 119 (1966).

8. A. A. Lombard, Proc. Roy. Aero. Soc. 28, 31 (1967).

9. J. F. Lewis, T. Kubota and L. Lees, AIAA Journal, 6, 7 (1968).

10. B. E. Edney, Ibid. 15.

11. A. L. Laganelli, W. F. Ames and J. P. Hartnett, ibid. p. 205.

12. F. W. Spaid and E. E. Zukoski, ibid. p. 205.

13. E. J. Felderman, ibid. p. 408.

14. H. Cunningham and J. Geankoplis, Chem. Eng. Sci. 22, 11 (1967).

15. M. F. L. Johnson and J. Moli, Preprints Division of Pet. Chem., Am. Chem. Soc., 12 (3) 204 (1967).

16. S. Landa, J. Vais and J. Berkhard, Collection Czech Chem., Commun. 32 (2) 570 (1967).

17. Kunugi, Tominaga, Abiko, "Sekieyu Gakkii Shi", No. 11 (1966).

18. R. L. Smith and C. D. Prater, Kinetic Catalysis, Chem. Eng. Symp. Series 63 (73) (1967).

19. "Vaporizing and Endothermic Fuels for Advanced Engine Application", Technical Documentary Report No. AFAPL-TR-67-114, Part I. Contract No. AF 33(615)-3789, Shell Development Company, October 1967.

20. R. P. Merrill, personal communication.

21. M. I. Allam and J. C. Vlugter, J. Inst. Pet. 52 385 (1966).

22. T. Miyazawa and K. S. Pitzer, J. Amer. Chem Soc. 80, 60 (1958).

REFERENCES (CONTD-1)

23. Robert W. Coughlin, "Classifying Catalysts" - Some Broad Principles. Ind. Eng. Chem 59, 45 (1967).

24. A. M. Sokolskaya, S. M. Reshetnikov, A. B. Fasmar and Sololskii, "Dependence of the Catalytic Activity of Metals on Their Position in the Periodic System of the Elements", Ind. Chem. Eng. 7, 525 (1966).

25. Robert L. Burwell, Jr., "The Mechanism of Heterogeneous Catalysis", Chem. Eng. News, 44, 56 (1966).

26. Paul B. Weisy, "Catalysis and Chemical Engineering", Kinetics and Catalysis, 63, 1 (1967).

27. G. M. Schwab, "Methods of Catalyst Investigation", Chem. Eng. Techn. 39, 1191 (1967).

28. Miller, Ryle, "Molecular Sieve Catalysts", Chem. Week, p. 77, Nov. 14, 1964.

29. Anon., Chem. Eng. News, 45, 134 (1967).

30. F. Solymosi, "Importance of the Electric Properties of Supports in the Carrier Effect". Cat. Reviews 1 (2), 233 (1967).

31. Anon., "Precious Metals Become Dearer", Chem. Week, p. 49, May 18, 1968.

32. F. A. Smith, USP 3, 357, 916 (12/12/67), assigned to Mobil Oil Corp.

33. W. A. Alexander, USP. 2,829,116 (3/1/58), assigned to National Res. Council, Ottawa, Ontario, Canada.

34. John M. Chambers and Germann C. Schutt, Can. 626,080 (8/22/61), assigned to Stone and Webster Engineering Corp., Boston, Massachusetts.

35. J. K. Goodwine, "On the Nature of CFR Coker Tube Deposits", Chevron Research Company, Richmond, California, June 17, 1966. Communicated to A. C. Nixon by J. A. Bert, Chevron Research.

36. Autooxidation and Antioxidants, Vl. II, p. 752 et. seq., Lundberg (Editor). Interscience Publishers, 1962 (Chapter 17 by Alan C. Nixon).

37. G. H. Meguerian, W. Hillstom, E. H. Hirschberg, F. W. Rakosky and A. Zlets, "Fundamental Investigation of the Catalytic Degradation of Hydrocarbon Fuels", American Oil Company, January 31, 1965.

38. Bagneto, Lucien, "Thermal Stability of Hydrocarbon Fuels", API TDR 64-89, Part III, Phillips Petroleum Company, September, 1966.

39. W. F. Taylor and T. J. Wallace, "The Study of Hydrocarbon Fuel Vapor Phase Deposits", Quarterly Progress Report No. 4, Contract No. AF(615)-3575, Esso Research and Engineering Company.

REFERENCES (CONTD-2)

40. W. F. Taylor and T. J. Wallace, "The Study of Hydrocarbon Fuel Vapor Phase Deposits", Quarterly Progress Report No. 5, Contract No. AF(615)-3575, Esso Research and Engineering Company.

41. Henry C. Barnett and Robert R. Hibbard, "Properties of Aircraft Fuels", Technical Note 3276, August 1956, National Advisory Committee for Aeronautics, Lewis Flight Propulsion Laboratory.

42. A. E. Zengel, "A Comparison of the Capabilities of a Fuel Coker and the Minex Heat Exchanger for Determining Hydrocarbon Fuel Thermal Stability, Technical Report AF APL-TR 64-154, March 1965. Air Force Aero Propulsion Laboratory, Wright-Patterson Air Force Base, Ohio.

43. N. Sherriff, P. Gumley and J. France, "Heat Transfer Characteristics of Roughened Surfaces", Chemical and Process Engineering 45, No. 11, 1964.

44. F. Burggraf and M. Shayeson, "A New Small-Scale Method for Measuring Fuel Thermal Stability", Paper presented to International Automotive Engineering Congress, Detroit, Michigan, January 11 to 15, 1965.

45. A. C. Nixon and C. A. Cole, Shell Development Report S-13284, April 30, 1951, for WADC (Contract No. AF 33(038-7277); A. C. Nixon and C. A. Cole, WADC, Technical Report 53-63, September 1952.

46. A. C. Nixon, "Autoxidation and Antioxidants", Vol. II, Chapter 17, W. O. Lundberg (Editor), Interscience Publishers, New York, 1962.

47. Federation of Societies for Paint Technology. Federation Series on Coatings Technology, Unit 6, Solvents, Philadelphia, Pennsylvania, May, 1967.

48. H. Burrell, Official Digest, November 1957.

49. A. Z. Bikkulou and N. I. Chernozhukov, Chemistry and Technology of Fuels and Oils 2, February 1967, pp. 104-107.

50. Mellan, Ibert, "Compatibility and Solubility," Noyes Development Corporation, Park Ridge, New Jersey, 1968.

51. Personal communication of M. W. Shayeson to A. C. Nixon, January 16, 1968, at a meeting of the CRC - Aviation Fuel, Lubricant and Equipment Research Committee, Cincinnati, Ohio.

52. T. R. Lusebrink, "Thermal Stability of Experimental High Temperature Fuels", ASD TR-61-687, Contract No. AF 33(616)-7667, Shell Development Company.

53. J. H. Sinfelt, H. Hurwitz and R. A. Shulman, J. Phys. Chem. 64, 1559 (1960).

54. K. S. Pitzer and R. F. Curl, Jr., J. Am. Chem. Soc. 79, 2367 (1957).

REFERENCES (CONTD-3)

55. G. N. Lewis, M. Randall, K. S. Pitzer and L. Brewer, "Thermodynamics", 2nd ed., pp. 608-611, 630-634, McGraw-Hill, New York, 1961.

56. B. W. Gamson and K. M. Watson, Natl. Petrol. News 36, R623 (1944).

57. J. Joffe, Ind. Eng. Chem. 40, 1738 (1948).

58. L. Lapidus, "Digital Computation for Chemical Engineers", pp. 89-90, McGraw-Hill, New York, 1962.

59. J. G. Knudsen and D. L. Katz, "Fluid Dynamics and Heat Transfer", pp. 394-395, McGraw-Hill, New York, 1958.

60. R. J. Emrich and D. B. Wheeler, Jr., Physics of Fluids 1, 14 (1958).

61. A. Redlich et al, I & EC Fund. 4, 369 (1965).

62. "Technical Data Book - Petroleum Refining", American Petroleum Institute, Division of Refining, 1271 Avenue of the Americas, New York, 1966.

63. E. A. Guggenheim, J. Chem. Phys. 13, 253 (1935).

64. R. C. Reid and T. K. Sherwood, "The Properties of Gases and Liquids", McGraw-Hill, New York, 1966.

65. L. I. Stiel and G. Thodos, AIChE 10, 26 (1964) and 10, 275 (1964).

APPENDIX

Page

Description of the Pulse Reactor. 210

Tables

60. Dehydrogenation of Decalin Over Various Catalysts. 215
61. Dehydrogenation of Decalin Over Shell 46 Laboratory Catalyst. 216
62. Dehydrogenation of Decalin Over Shell 108 Laboratory Catalyst. 217
63. Dehydrogenation of Decalin Over Shell 107A Laboratory Catalyst. 218
64. Dehydrogenation of Decalin Over Shell 91A Laboratory Catalyst. 219
65. Dehydrogenation of Decalin Over Shell 105B Laboratory Catalyst. 220
GLC Analysis System 221
Micro Catalyst Test Reactor Data. 221

Tables

66. MCH Dehydrogenation With Various Catalysts in MICTR: Runs 263-450. 224
67. MCH Dehydrogenation With Various Catalysts in MICTR: Runs 484-572. 233
68. MCH Dehydrogenation With Various Catalysts in MICTR: Runs 573-676. 235
69. MCH Dehydrogenation With Various Catalysts in MICTR: Various Supports. 243
70. n-Heptane Dehydrocyclization With Various Catalysts in MICTR. 244
SD/M-7 Coker Flushing Procedure 246
Purification of RAF-161-60 Decalin. 246
Analysis 247
Table 71. GLC Analyses of RAF-161-60 Decalin 247
Purification and Evaluation. 247
Table 72. Dehydrogenation of RAF-161-60 Decalin. 249
Table 73. Comparative Effectiveness of Davison Grades 950 and 28 Silica Gel in the Purification of RAF-161-60 Decalin 250
Purification of a 30-Drum Batch of Decalin 251

APPENDIX (Contd-1)

Page

Tables

74. FSSTR-Heat Transfer to MCH in Empty 5/8" OD x 10' Long Sections: Data Summary. 254
75. FSSTR-Data Summary Series 10018-90: Heat Transfer to MCH in Miniature Heat Transfer Section 255
76. FSSTR-Data Summary Series 10018-94: Heat Transfer to MCH in Miniature Heat Transfer Section 257
77. FSSTR-Data Summary Series 10018-98: Heat Transfer to H_2 in Miniature Heat Transfer Section. 258
78. FSSTR-Data Summary Series 10018-101: Heat Transfer to Water in Miniature Heat Transfer Section 259
79. FSSTR-Data Summary Series 10018-108: Heat Transfer to Water in Miniature Heat Transfer Section 260
80. FSSTR-Data Summary Series 10018-116: Heat Transfer to Water in Miniature Heat Transfer Section 261
81. FSSTR-Data Summary Series 10018-119: Heat Transfer to Water in Miniature Heat Transfer Section 262
82. FSSTR-Data Summary Series 10018-126: Heat Transfer to Water in Miniature Heat Transfer Section 263
83. FSSTR-Data Summary Series 10018-127: Heat Transfer to MCH in Miniature Heat Transfer Section 264
84. FSSTR-Data Summary Series 10018-129: Heat Transfer to MCH in Miniature Heat Transfer Section 265
85. FSSTR-Data Summary Series 10018-130: Heat Transfer to MCH in Miniature Heat Transfer Section 266
86. FSSTR-Data Summary Series 10018-131: Heat Transfer to MCH in Miniature Heat Transfer Section 267
87. FSSTR-Data Summary Series 10018-132: Heat Transfer to MCH in Miniature Heat Transfer Section 268
88. FSSTR-Data Summary Series 10018-133: Heat Transfer to MCH in Miniature Heat Transfer Section 269
89. Ignition Delays for n-Octane-Oxygen-Argon. 270
90. Ignition Delays for Decalin-Oxygen-Argon 273
91. Ignition Delays for SHELLDYNE-Oxygen-Argon 275
92. Ignition Delays for SHELLDYNE H-Oxygen-Argon 277
93. Ignition Delays for DMD-Oxygen-Argon 279
94. Ignition Delays for SHELLDYNE-Decalin-Oxygen-Argon 280
95. Ignition Delays for SHELLDYNE-Binor S-Oxygen-Argon 281

APPENDIX (Contd-2)

Page

Tables (Contd)

96. Characteristic Properties of F-71 282
97. Liquid Properties of F-71 at Saturation Pressure 282
98. Gas Properties of F-71 283
99. Characteristic Properties of trans-Decalin 284
100. Liquid Properties of trans-Decalin at Saturation Pressure 284
101. Gas Properties of trans-Decalin 285
102. Characteristic Properties of SHELLDYNE 286
103. Liquid Properties of SHELLDYNE at Saturation Pressure 287
104. Gas Properties of SHELLDYNE 288

Description of the Pulse Reactor

The pulse reactor was a 1/4 in. OD stainless steel tube (no. 304) 9-1/4 in. long and 0.028 in. wall thickness. Swagelok Tees were fastened at each end and one arm of the Tee served as an injection port. A rubber septum (GLC type) was held in place by the fitting nut and the feed was injected through this septum from a syringe. A five inch length of the reactor tube was surrounded by a secondary furnace liner and the whole was heated by an electric furnace. The secondary liner had seven radial drilled holes for thermocouples, and the holes were located as shown in Figure 67. A schematic diagram of the pulse reactor is shown in Figure 68.

All lines were 1/4 in. OD stainless steel tubing (no. 304). About 28 in. of line just prior to the reactor was wrapped with heating tape and constituted a gas preheater. About 8 in. of the preheater section was filled with quartz chips (10-20 mesh size).

In the pulse reactor system the carrier gas was metered through a rotameter (Figure 68) and passed through the preheater section and into the reactor. The exit gas passed into a manifold and then into the GLC. The purpose of the manifold was to maintain the exit gas pressure slightly greater than the gas pressure in the GLC. This was done by adjusting the pressure control valve and the vent valve. The manifold was wrapped with heating tape and was maintained at 302° to 356°F. The injection port temperature was about 450°F. The pressure control and the vent valves were needle valves (Hoke No. 1315) and the GLC valve was a lever operated valve (Hoke No. 490).

To carry out an experiment the reactor was brought to temperature and the carrier gas flow rate, reactor pressure and manifold pressure were adjusted by means of the appropriate flow control valves. Then with inert gas flowing to the GLC a pulse was injected through the lower injection port and subsequently analysed. This gave an analysis of the starting material. A pulse was then injected in the top injection port, passed over the catalyst and analysed.

In this system the space velocity was obtained from the inert gas flow rate. Figure 69 shows the pulse reactor system with the secondary furnace liner in place; Figure 70 shows the GLC analysis system.

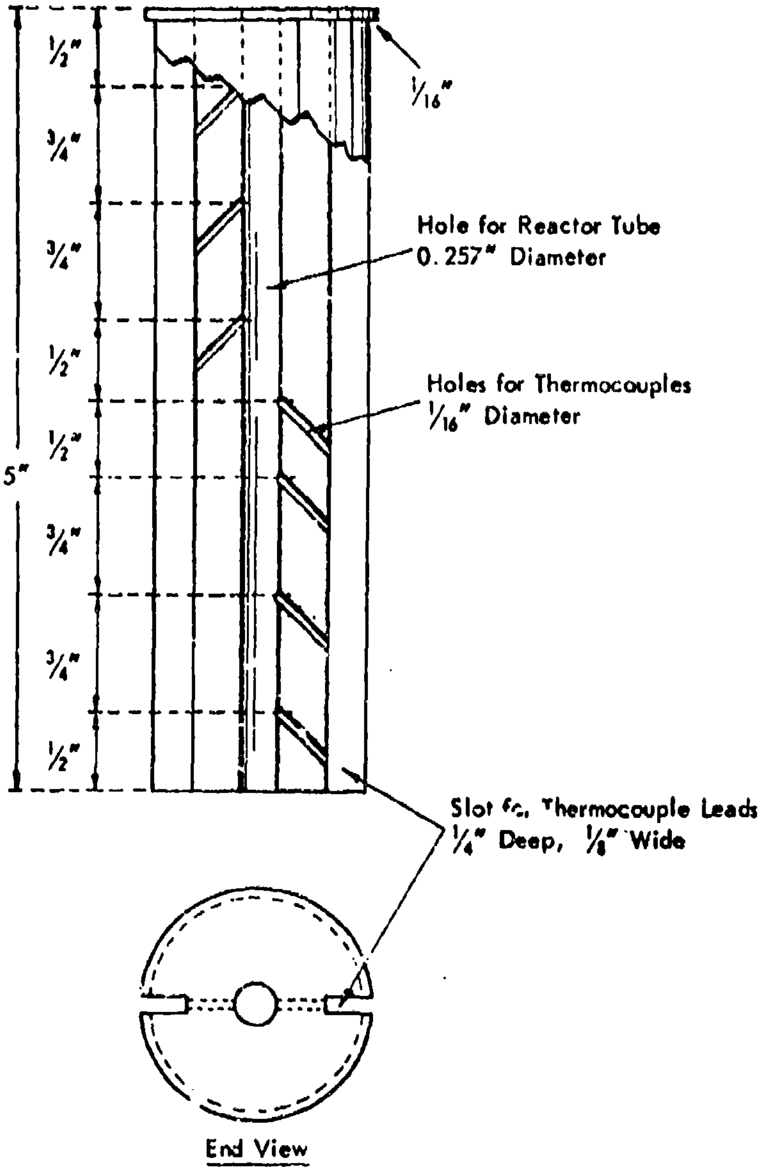
1/2"
3/4"
3/4"
1/2"
1/2"
5"
3/4"
3/4"
1/2"
1/16"
Hole for Reactor Tube
0.257" Diameter
Holes for Thermocouples
1/16" Diameter
Slot for Thermocouple Leads
1/4" Deep, 1/8" Wide
End View

Figure 67. SECONDARY FURNACE LINER FOR PULSE REACTOR

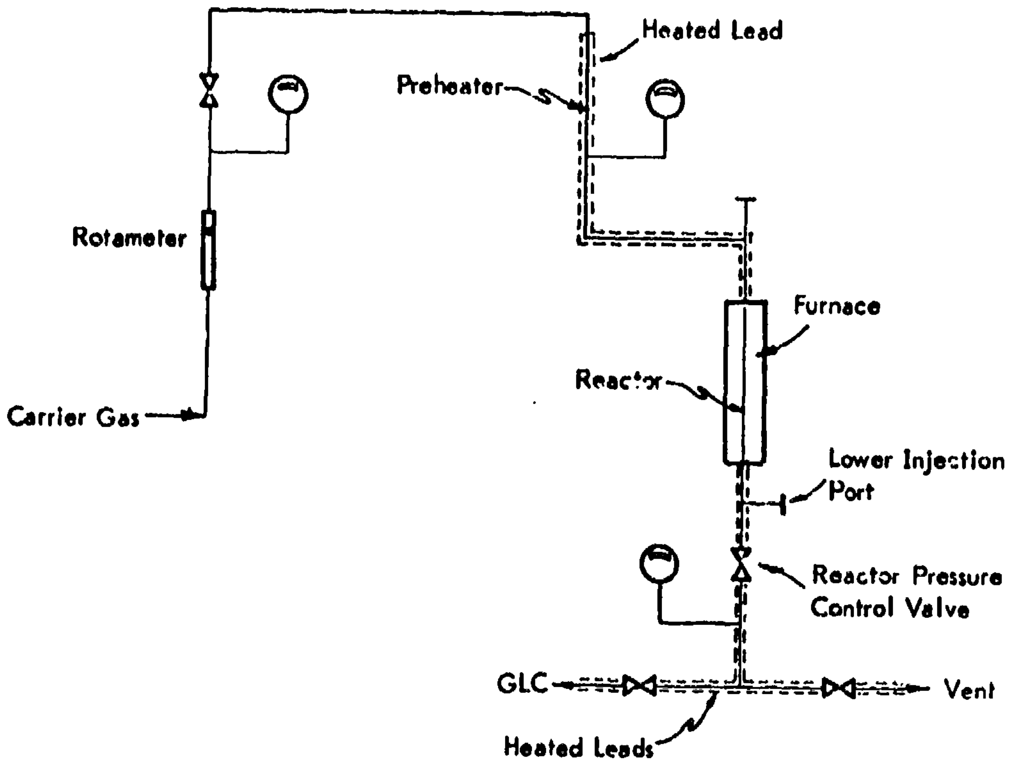
Heated Lead
Preheater
Rotameter
Carrier Gas
Furnace
Reactor
Lower Injection Port
Reactor Pressure Control Valve
GLC
Vent
Heated Leads

Figure 68. PULSE REACTOR: SCHEMATIC

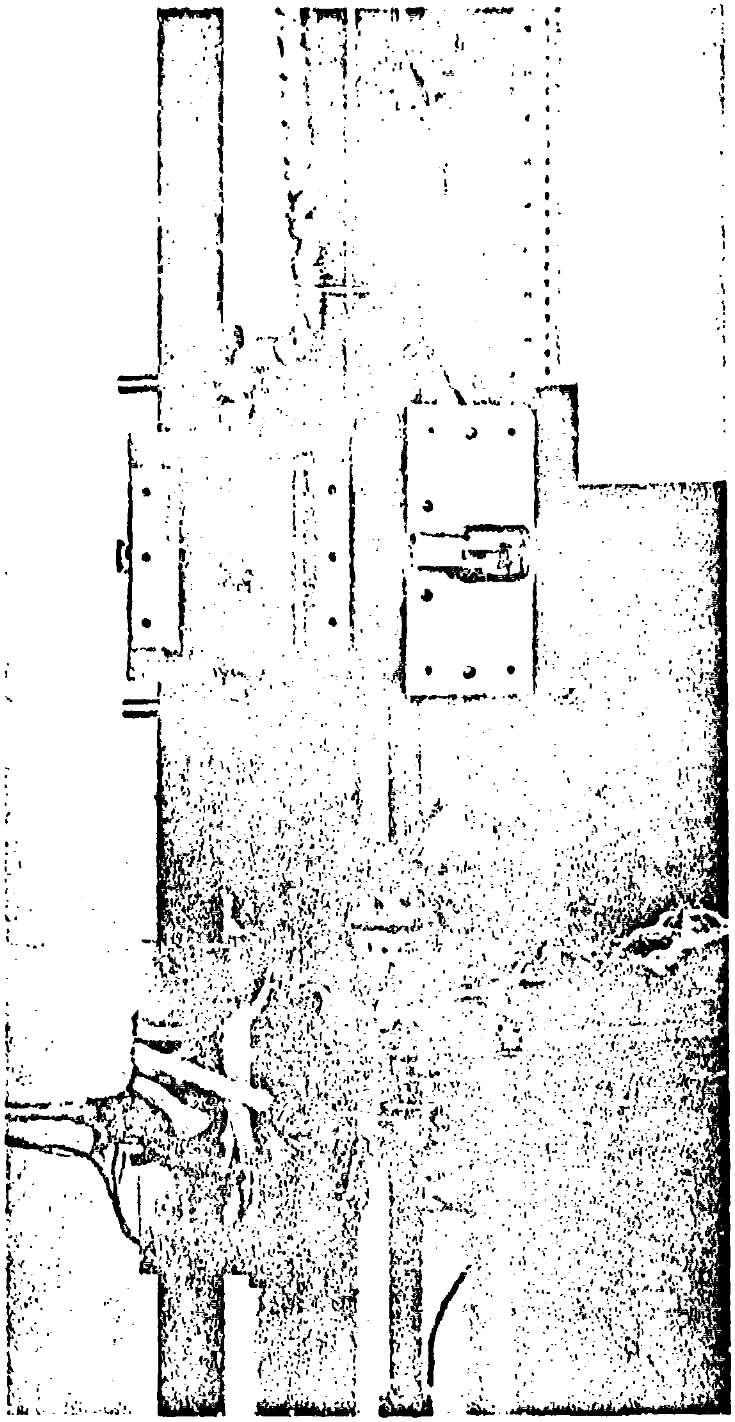

Figure 69. PULSE REACTOR SYSTEM

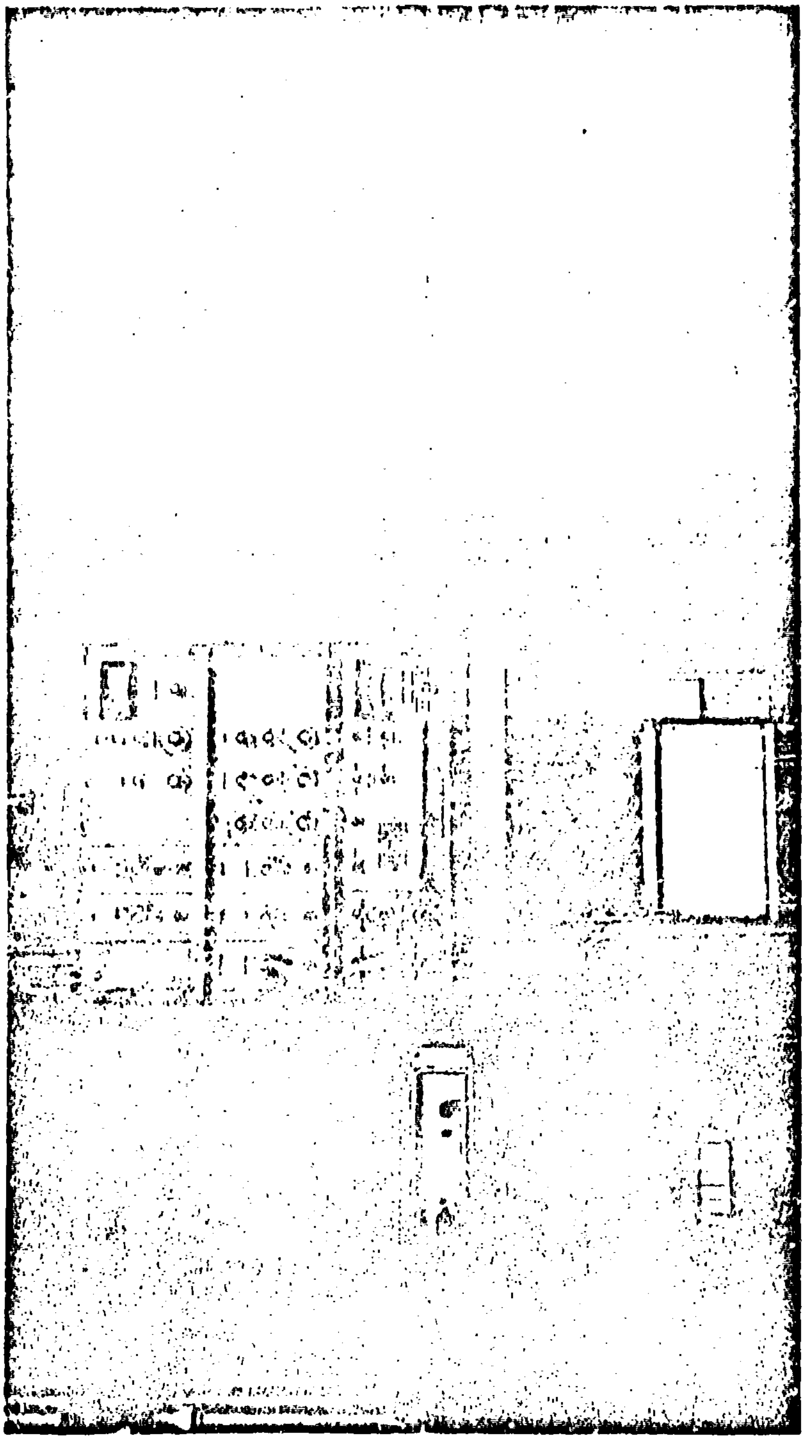

Figure 70. GLC ANALYSIS SYSTEM

Table 60. DEHYDROGENATION OF DECALIN OVER VARIOUS CATALYSTS

Feed: F-113 Decalin
Catalyst Volume: 7 ml
Pressure: 10 atm
LHSV: 100
Reaction Period: 30 min

Catalyst	1% Pt on Harshaw 0104 Alumina (Standard Catalyst)			UOP-R8			American Cyanamide Aeroform PHF-4; 0.6% Pt			Sinclair-Baker RD-150; 0.6% Pt			10280-46			10290-45		
Run No. 17342-	120	121	122	57	58	59	34	35	36	31	32	33	55	56	57	52	53	54
Temperature, °F																		
Block	842	932	1022	842	932	1022	842	932	1022	842	932	1022	842	932	1022	842	932	1022
Wall	741	799-806	660-69	765-68	804-36	896-927	720	776-79	836-69	754-59	806-13	827-92	740-41	790-92	960-66	714-19	701	819-20
Catalyst Bed Profile	657-66 653-60 658-62 678-82	694-725 689-98 693-702 720-25	752-813 730-47 738-47 770-76	644-58 617-21 617-21 628-32	695-736 651-67 651-62 649-73	783-943 698-779 694-729 720-725	624-30 617 622-24 639-41	660-69 650-55 658-62 680-82	716-842 639-712 698-705 792-27	676-82 655-62 655-62 658-64	720-33 693-701 693-702 702-07	766-97 732-45 727-32 740-43	606-15 606-12 614-17 630-33	642-53 642-43 649-53 671-73	694-727 682-88 691-93 718-20	619-24 594-93 630-10 615-19	664-71 635-57 649 662	707-18 775-78 691 709
ΔTmax, °F, catalyst bed	9	51	61	14	45	160	6	20	126	7	19	31	9	11	9	5	7	11
Product Analysis, %w																		
trans-DHN	25.4	23.3	21.0	34.9	29.7	24.7	35.7	32.3	25.3	27.4	23.4	18.8	33.2	29.0	23.1	35.5	27.8	22.6
cis-DHN	41.5	36.8	35.5	28.7	26.2	27.4	27.8	23.7	22.3	41.8	36.3	30.2	26.2	21.7	17.9	21.5	19.4	16.2
U(a)	0.0	0.0	0.0	0.1	0.3	1.7	0.1	0.4	2.1	0.4	0.2	1.3	0.0	0.0	0.4	0.0	0.0	0.2
THN	8.5	6.6	4.7	16.6	13.1	7.7	15.8	12.4	8.6	10.0	10.8	9.7	18.0	13.9	10.6	3	18.9	11.5
U(a)	0.0	0.0	0.0	0.1	0.2	0.2	0.1	0.1	0.1	0.0	0.0	0.0	0.2	0.1	0.		0.3	0.2
Naphthalene	24.5	33.2	40.7	19.4	30.2	37.7	20.6	31.6	40.9	20.2	28.6	39.6	23.2	35.0	47.		33.4	49.0
U(a)	0.1	0.1	0.1	0.2	0.3	0.4	0.1	0.3	0.4	0.2	0.2	0.4	0.2	0.3	0.3		0.2	0.3
Cracked, liquid	0.0	0.0	0.0	0.0	0.0	0.2	0.0	0.0	0.4	0.0	0.0	0.0	0.0	0.0	0.0	..	0.0	0.0
Yield THN, %w	8.1	6.2	4.3	16.2	12.7	7.3	15.4	12.2	8.2	9.6	10.4	9.3	17.6	13.5	10.2	23.4	16.5	11.1
Selectivity for N, %w	75.0	84.0	90.3	53.8	69.2	79.4	57.2	70.6	78.7	66.8	72.3	78.4	58.0	71.5	81.3	46.4	63.6	80.6
DHN Conversion, %	32.8	39.7	45.3	36.2	45.9	47.7	36.2	44.8	52.2	30.4	39.7	50.8	40.2	49.1	58.8	44.9	52.6	61.0
First Order Rate Constant, sec^{-1}	0.39	0.52	0.65	0.45	0.60	0.75	0.43	0.60	0.79	0.36	0.52	0.78	0.50	0.69	0.95	0.56	0.74	0.97
E, act, kcal/mole	9.1		-	8.7		-	9.1		-	11.4		-	10.4		-	8.5		-

a) Unidentified.

Table 61. DEHYDROGENATION OF DECALIN OVER SHELL 46 LABORATORY CATALYST

Catalyst Volume:	7 ml	Feed:	F-213 Decalin
LHSV:	100		74.6% cis-DHN
Reaction Time:	30 min		25.0% trans-DHN
			0.4% THN
		Pressure:	10 atm

Run No.	←———	———	10548-9	———	———→
Temperature, °F					
Block	842	932	1022	1112	1202
Wall	725-29	784-90	853-60	941-52	1094-98
Catalyst Bed Profile	604-17	639-53	673-89	716-40	801-66
	597-95	630-35	662-66	704-07	774-84
	606-10	640-44	676-80	725-25	799-95
	617-21	655-57	698-99	752-50	837-30
ΔT_{max}, °F$^{a)}$	13	14	16	24	65
Product Analysis, %w					
trans-DHN	34.2	29.7	24.5	18.6	11.9
cis-DHN	23.7	20.1	16.2	13.4	11.9
$U^{b)}$	0.0	0.0	0.0	0.1	0.9
THN	20.5	16.4	11.1	6.1	5.0
$U^{b)}$	0.0	0.0	0.0	0.0	0.0
N	21.4	33.6	47.9	60.5	67.6
$U^{b)}$	0.2	0.2	0.3	0.4	0.5
Cracked, liq.	0.0	0.0	0.0	0.5	2.2
Yield THN, %w	20.1	16.0	10.7	5.7	4.6
DHN Conversion, %w	41.9	50.0	59.2	67.9	81.2
Selectivity for THN + N, %w	99.5	99.2	99.0	98.1	89.0
Rate Constants					
Zero Order, atm, sec^{-1}	4.02	5.05	6.30	7.73	10.22
First Order, sec^{-1}	0.52	0.70	0.95	1.29	2.10
E_{act}, kcal/mole	←— 7.8 —→				

a) Maximum increase in catalyst bed temperature during the 30 minute run.
b) Unidentified.

Table 62. DEHYDROGENATION OF DECALIN OVER SHELL 108 LABORATORY CATALYST

Catalyst Volume: 7 ml
LHSV: 100
Reaction Time: 30 min
Run No.: 10548-5

Feed: F-113 Decalin
74.6% cis-DHN
25.0% trans-DHN
0.4% THN
Pressure: 10 atm

Temperature, °F					
Block	842	932	1022	1112	1202
Wall	709-11	768-72	838-42	916-14	1008-22
Catalyst Bed Profile	617-28	653-66	689-705	732-54	822-946
	615-21	651-55	687-91	730-34	806-37
	624-26	662-66	705-07	756-54	830-33
	635-37	676-80	725	784-80	862-56
ΔT_{max}, °F$^{a)}$	11	13	16	22	124
Product Analysis, %w					
trans-DHN	30.5	27.4	23.3	18.1	11.6
cis-DHN	32.1	27.8	22.4	19.1	16.9
U$^{b)}$	0.0	0.0	0.0	0.0	0.5
THN	14.6	10.5	7.0	4.9	5.2
U$^{b)}$	0.1	0.1	0.1	0.1	0.3
N	22.6	34.0	46.8	56.8	62.0
U$^{b)}$	0.1	0.2	0.3	0.5	0.4
Cracked, liq.	0.0	0.0	0.1	0.5	3.1
Yield THN, %w	14.2	10.1	6.6	4.3	4.8
DHN Conversion, %w	37.0	44.6	54.1	62.4	71.1
Selectivity for THN + N, %w	99.5	99.3	98.7	97.9	94.0
Rate Constants					
Zero Order, atm, sec^{-1}	3.50	4.43	5.69	6.91	8.42
First Order, sec^{-1}	0.44	0.59	0.82	1.08	1.48
E_{act}, kcal/mole	<——8.1——>				

a) Maximum increase in catalyst bed temperature during the 30 minute run.
b) Unidentified.

Table 63. DEHYDROGENATION OF DECALIN OVER SHELL 107A LABORATORY CATALYST

Catalyst Vol.: 7 ml
LHSV: 100
Reaction Time: 30 min
Run No.: 10342-196

Feed: F-113 Decalin
74.6% cis-DHN
25.0% trans-DHN
0.4% THN
Pressure: 10 atm

Run No.	196	197-1	198-1	198-2	199-1	199-2	199-3
Temperature, °F							
Block	842	932	1022	1112	1112$^{c)}$	1112$^{c)}$	1112$^{c)}$
Wall	714-25	788-801	866-96	945-1078	1085-87	1087	1087-92
Catalyst Bed Profile	646-62	687-712	740-815	801-1064	1071-58	1058-54	1054-72
	612-17	642-55	680-707	722-1036	1046-54	1054	1054-67
	610-14	642-48	676-86	722-959	986-1031	1031-40	1040-60
	626-28	662-68	705-09	761-907	923-1006	1006-35	1035-53
ΔT_{max}, °F$^{a)}$	16	25	75	314	-	-	-
Product Analysis, %w							
trans-DHN	30.8	27.5	23.2	19.2	22.3	24.4	25.2
cis-DHN	30.0	26.2	22.5	26.5	52.2	59.3	60.9
U$^{b)}$	0.0	0.0	0.3	3.9	9.5	7.0	6.2
THN	17.2	13.8	9.1	6.3	3.7	2.3	2.1
U$^{b)}$	0.0	0.0	0.1	0.4	2.2	1.9	1.5
N	21.8	32.5	44.5	42.3	7.7	2.7	1.5
U$^{b)}$	0.2	0.2	0.2	0.2	0.0	0.0	0.0
Cracked, liq.	0.0	0.0	0.1	1.2	2.4	2.4	2.6
Yield THN, %w	16.8	13.2	8.7	5.9	3.3	1.9	1.7
DHN Conversion, %w	38.9	46.1	54.1	54.1	25.2	16.0	13.5
Selectivity for THN - N, %w	99.5	99.6	98.7	89.4	43.9	28.9	23.8
Rate Constants							
Zero Order, atm, sec^{-1}	3.71	4.68	5.86	6.44	-	-	-
First Order, sec^{-1}	0.47	0.63	0.85	0.93	-	-	-
E_{act}, kcal/mole	←— 6.5 —→						

a) Maximum increase in catalyst bed temperature during the 30 minute run.
b) Unidentified.
c) Runs 199-1, 199-2, 199-3 were consecutive runs of 10-minute duration following Run 198-2.

Table 64. DEHYDROGENATION OF DECALIN OVER SHELL 91A LABORATORY CATALYST

Catalyst Vol.:	7 ml	Feed:	F-113 Decalin
LHSV:	100		74.6% cis-DHN
Reaction Time:	30 min		25.0% trans-DHN
Run No.:	10342-180		0.4% THN
		Pressure:	10 atm
		LHSV:	100

Temperature, °F					
Block	842	932	1022	1112	1202
Wall	705-09	770-77	842-48	918-25	1010-82
Catalyst Bed Profile	637-50	680-702	730-66	794-869	916-1121
	617-15	640-51	676-89	729-47	806-968
	621-17	644-53	682-89	736-43	804-51
	624-21	653-57	693-94	752-48	820-31
ΔT_{max}, °F a)	13	22	36	50	205
Product Analysis, %w					
trans-DHN	31.0	26.1	21.4	16.8	11.5
cis-DHN	29.8	27.6	23.5	21.4	18.0
U b)	0.0	0.0	0.0	0.4	1.6
THN	18.7	14.3	10.3	6.4	5.1
U b)	0.1	0.3	0.3	0.0	0.0
N	20.3	31.5	44.2	54.4	60.4
U b)	0.1	0.2	0.2	0.3	0.3
Cracked, liq.	0.0	0.0	0.1	0.3	3.1
Yield THN, %w	18.3	13.9	9.9	6.0	4.7
DHN Conversion, %w	39.0	46.1	54.9	61.6	68.8
Selectivity for THN + N, %w	99.5	98.1	98.7	98.3	95.0
Rate Constants					
Zero Order, atm, sec^{-1}	3.68	4.60	5.80	6.88	8.38
First Order, sec^{-1}	0.47	0.61	0.88	1.07	1.42
E_{act}, kcal/mole	←—6.3—→				

a) Maximum increase in catalyst bed temperature during the 30 minute run.

b) Unidentified.

Table 65. DEHYDROGENATION OF DECALIN OVER SHELL 105B LABORATORY CATALYST

Catalyst Vol.: 7 ml
LHSV: 100
Reaction Time: 30 min
Run No.: 188

Feed: F-113 Decalin
74.6% cis-DHN
25.0% trans-DHN
0.4% THN
Pressure: 10 atm
LHSV: 100

Temperature, °F					
Block	842	932	1022	1112	1202
Wall	707-09	763-65	827-33	898-910	1028-1148
Catalyst Bed Profile	626-33 621-26 624-26 632-35	658-69 655-60 657-62 665-69	700-20 693-98 693-98 707-09	756-831 738-61 740-52 759-63	974-1130 869-1106 842-1064 851-1006
ΔT_{max}, °F[a]	7	11	20	75	237
Product Analysis, %w					
trans-DHN	32.4	26.9	21.0	15.9	12.9
cis-DHN	28.1	25.2	22.2	21.7	31.9
U[b]	0.0	0.0	0.0	0.0	0.5
THN	17.0	13.6	9.5	5.4	5.4
U[b]	0.0	0.0	0.0	0.0	0.1
N	22.4	34.1	46.9	56.3	45.3
U[b]	0.1	0.2	0.3	0.3	0.2
Cracked, liq.	0.0	0.0	0.1	0.4	3.7
Yield THN, %w	16.6	13.2	9.1	5.0	5.0
DHN Conversion, %w	39.3	47.7	56.6	61.9	55.0
Selectivity for THN + N, %w	99.5	99.4	99.2	99.2	91.7
Rate Constants					
Zero Order, atm, sec^{-1}	3.71	4.73	5.91	6.83	-
First Order, sec^{-1}	0.47	0.64	0.87	1.07	-
E_{act}, kcal/mole	<——8.8——>				

a) Maximum increase in catalyst bed temperature during the 30 minute run.
b) Unidentified.

GLC Analysis System

Analyses for naphthene dehydrogenation systems have been made almost entirely with an F & M GLC (Models 710 and 5754A) using a packed column and a thermal conductivity detector. This technique is useful for rapid analyses and for determining trace amounts of material; but for analyzing mixtures of close boiling compounds, such as cis and trans isomers of poly methyl and ethyl substituted cyclohexanes, a capillary column is needed.[a] As future work on fuel evaluation will involve analyses of multicomponent systems having a multiplicity of close boiling components, it was expedient to convert our analysis system to the capillary technique.

At present our analyses are being made with an F & M GLC, Model 5754A using a hydrogen flame detector and a 165' stainless steel capillary column, 0.010" diameter, coated with 20% phenyl ethers in DC 710 silicone. The superior resolution of the capillary column over a packed column is shown by chromatograms of a mixture of diethylcyclohexane isomers and their cis and trans species that were analyzed by the capillary (Figure 71) and packed column (Figure 72) techniques.

Micro Catalyst Test Reactor Data

The micro catalyst test reactor (MICTR) and the operational techniques used for screening candidate catalysts have been described in the Appendix of the last Annual Report.[19] Catalysts are tested with MCH at LHSV 150 and 662,752 and 842°F and with n-heptane at LHSV 10 and 842 and 932°F, in all cases at 10 atm pressure without added hydrogen. Figures 87 through 89 of ref 19 show the apparatus in detail, except that the feed line pressure gauge has been eliminated to reduce feed line hold up and a check-valve installed to prevent accidental "blow-back".

The original Wheelco integrating recorder (for GLC peaks) became unserviceable and was replaced after run 291 by a Honeywell integrating recorder. This in turn was replaced by a Westronic integrating recorder starting with run 531. Starting with run 277, a small screen was placed above the bottom slotted separator in the MICTR tube. This was done to prevent an occasional small catalyst or quartz particle from plugging the slot which would cause an increase in back-pressure and a corresponding decrease in conversion over catalysts under test. At least once a week the reference catalysts 9874-24 or 139 were retested and the results used as a base point for performance evaluation of candidate catalysts tested for that particular week. The test results are shown chronologically in Tables 66, 67, 68 and 70. Table 69 gives preliminary results with coating candidates as described earlier. A few runs have been left out where mechanical or instrumental problems occurred and the validity of the data are in doubt. In such cases the catalysts were retested.

---

[a] An excellent discussion of the usefulness of various GLC techniques is given by L. S. Ettre in "Open Tubular Columns in Gas Chromatography", Plenum Press, New York, 1965.

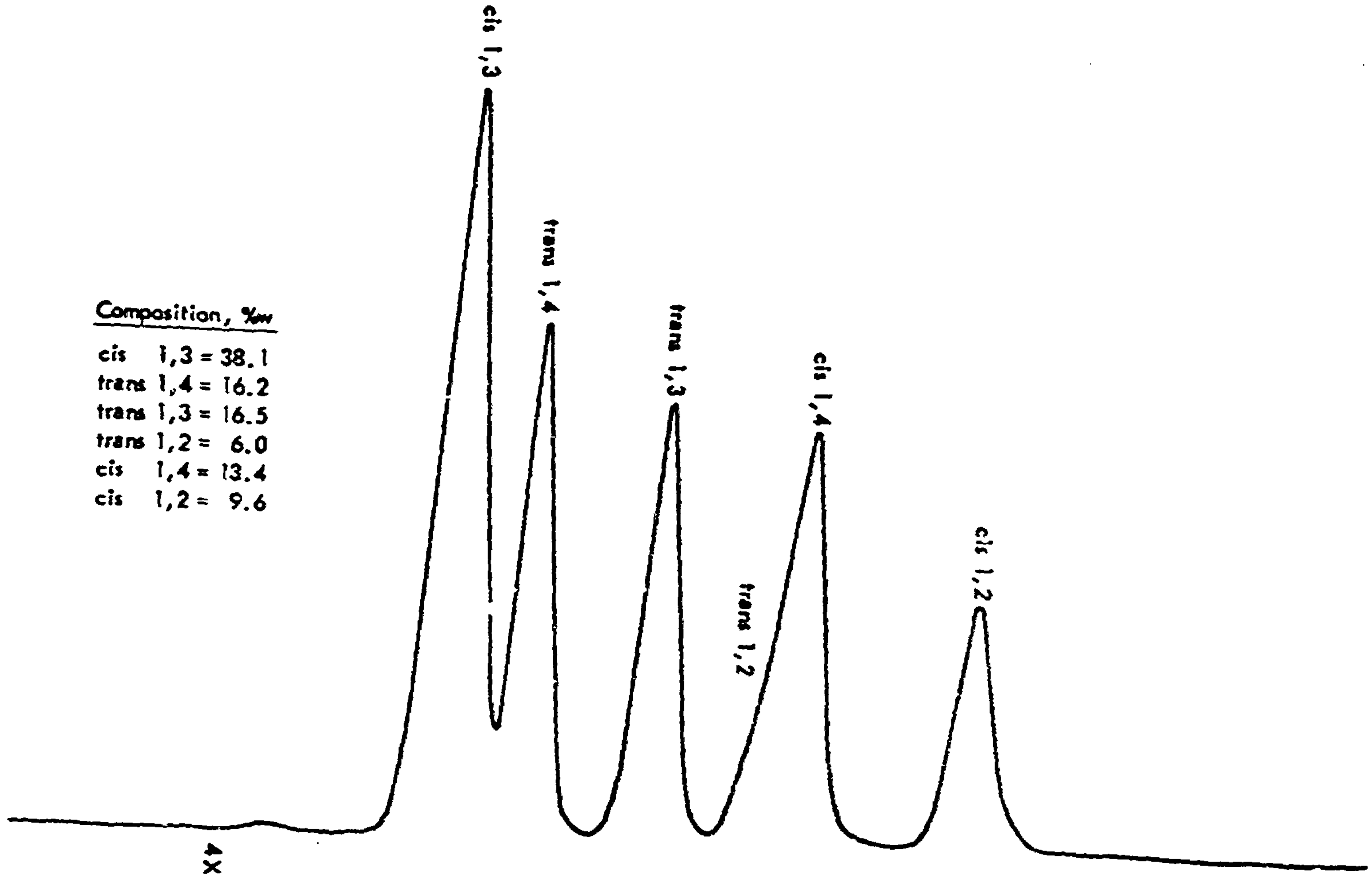

Composition, %w

cis 1,3 = 38.1
trans 1,4 = 16.2
trans 1,3 = 16.5
trans 1,2 = 6.0
cis 1,4 = 13.4
cis 1,2 = 9.6

Figure 71. GLC CHROMATOGRAM OF DIETHYLCYCLOHEXANE ISOMERS: CAPILLARY COLUMN

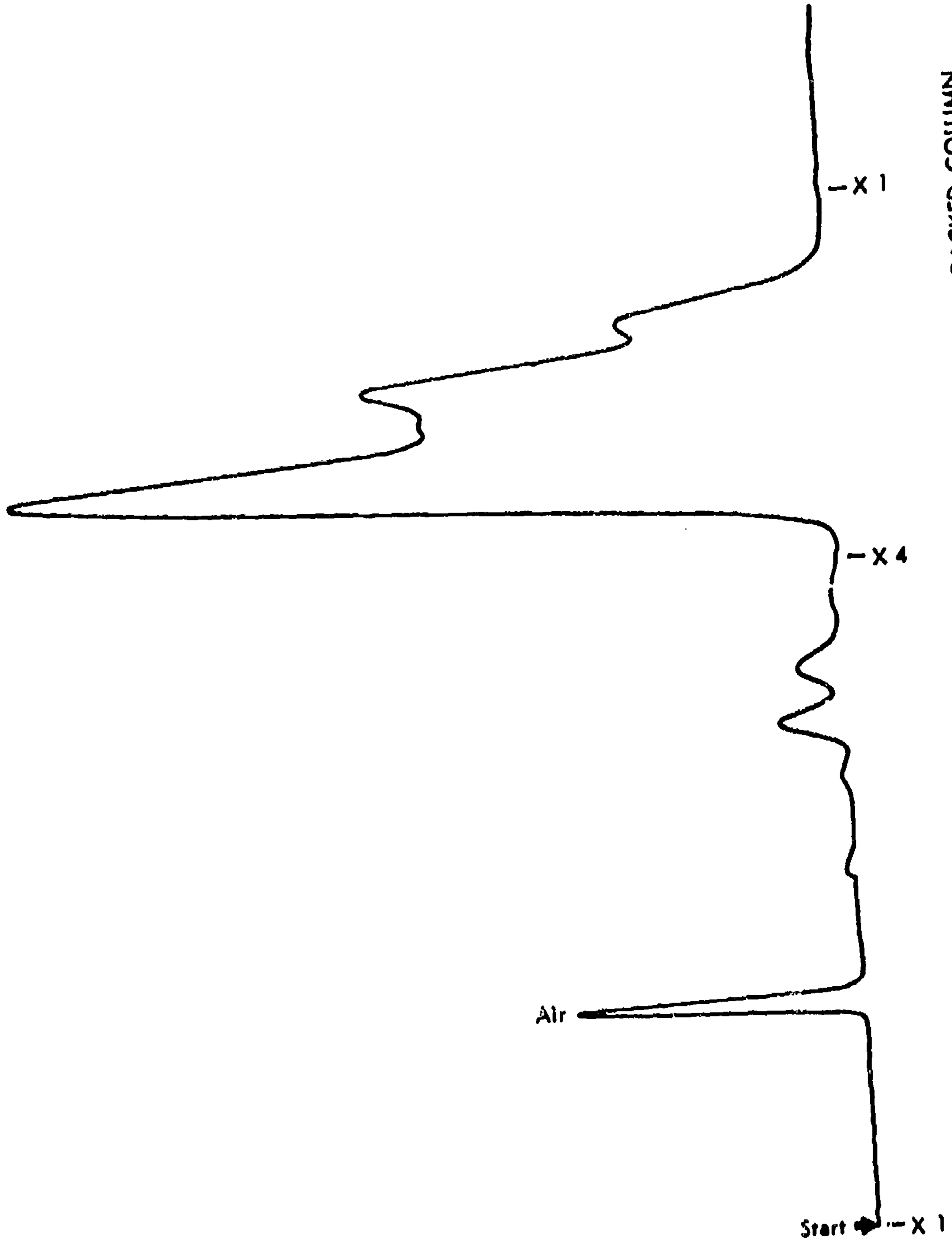

Figure 72. GLC CHROMATOGRAM OF DIETHYLCYCLOHEXANE ISOMERS: PACKED COLUMN

Table 66 MCH DEHYDROGENATION WITH VARIOUS CATALYSTS IN MICTR: RUNS 263-450

Period:	June-August 1967.
Conditions:	10 atm pressure; catalysts reduced in H_2 for 20 minutes at 796°F; GLC samples normally taken at 3-, 8- and 13-minute operation at each block temperature.
Catalyst volume:	0.9 ml catalyst diluted with 1.1 ml quartz chips; LHSV 100 (catalyst and quartz particles 10-20 mesh unless otherwise noted).

Run No.	Catalyst No.	Catalyst		% MCH Conversion, °F		
		Description	Wt, g	662	752	842
263	10280-27	5% Metal/R-8 Al_2O_3	-	0, 0, -	0, 0, -	0, 0, -
264	10280-27A	Bimetallic, 5,2% metals/R-8 Al_2O_3	-	8, 5,<1	12,11,16	33,24,32
265	9874-24	1% Pt/R-8 Al_2O_3 (ref)	0.42	22,22,23	49,53,49	70,73,69
266	9874-7	1% Pt/support type No. 1	-	25,34,30	64,61,57	86,83,79
268	9874-7	1% Pt/support type No. 1	0.77	31,32,31	63,60,56	88,84,80
269	9874-7	1% Pt/support type No. 1	0.76	36,33,30	63,63,59	87,84,82
270	10280-27B	Bimetallic, 5,2%/R-8 Al_2O_3	-	13,11, 6	19,12,10	32,30,25
271	9874-7	1% Pt/support type No. 1	0.74	30,32,37	60,62,57	83,92,86
272	10280-27C	Bimetallic, 5, 5% R-8 Al_2O_3	0.47	0, 0, -	8, 3, 3	13, 8, 6
273a)	9874-199B	4% Metal/support type No. 1b)d)	0.38	28,26,26	54,52,52	74,74,74
274a)	9874-161B	5% Metal/support type No. 6	0.28	17,18,19	26,47,38	68,60,50
277c)	9874-161Bb)	5% Metal/support type No. 6	0.42	27,30,25	48,49,45	72,71,67
278a)	10280-24C	4% Metal/support type No. 1d)	0.26	28,25,23	47,46,43	68,66,64
279a)	9874-161B	5% Metal/support type No. 6	0.28	31,25,24	44,43,40	65,56,53
280	9874-132	1% Pt/R-8 Al_2O_3 (similar to 9874-24)	0.41	24,25,26	50,48,45	77,73,68
281	10280-29	1% Pt/R-8 Al_2O_3 (exposed to CO_2 gas)	0.42	25,28,26	52,52,47	69,68,74
282	9874-94B	4% Metal/support type No. 2	0.35	26,26,24	50,49,46	74,68,65
283	10280-24A	4% Metal/support type No. 1 (14-20 m)	0.56	26,24,32	60,60,58	88,85,83
284	10280-24A	4% Metal/support type No. 1 (10-14 m)	0.56	25,23,23	53,50,48	76,71,62
286	7508-80E	2% Metal/support type No. 6	0.31	28,26,25	54,48,44	74,67,65
287	9874-24	1% Pt/R-8 Al_2O_3 (ref)	0.43	31,26,24	48,48,43	73,68,65
288	10280-45	5% Metal/support type No. 6 (repeat of 9874-161B)	0.49	20,22,26	55,56(43)	73,71,73

(Continued)

a) LHSV 200.
b) Muffled at 1082°F in air.
c) Bottom of catalyst bed screened from run 276 on to prevent plugging of slotted bottom spacer.
d) Metal tetramine hydroxide carbonated before impregnation.

Table 66 (Contd-1). MCH DEHYDROGENATION WITH VARIOUS CATALYSTS IN MICTR: RUNS 263-450

Run No.	Catalyst No.	Catalyst		% MCH Conversion, °F		
		Description	Wt, g	662	752	842
289	10280-46	4% Metal/support type No. 1 (repeat of 9874-156B	0.77	34,31,32	51,55,54	89,82,83
290	10280-36	5% Metal/support type No. 2 (acid treated)	0.39	0, 0, -	<1	5, 3, -
291	10280-36A	Bimetallic 5, 4% metal (acid treated)	0.43	-,30,24	48,49,46	68,69,(41)
292	10280-24A	4% Metal/support type No. 1	0.56	25,29,25	64,55,52	79,77,75
293	10280-39A	4% Metal/support type No. 6 (acid treated)	0.40	30,29,25	51,53,49	73,74,69
294	10280-39B	4% Metal/support type No. 6 (acid treated)	0.40	29,31,32	56,54,53	-,77,75
295	9874-24	1% Pt/R-8 Al_2O_3	0.42	28,26,27	48,48,44	76,63,66
296	10280-43D	2% Pt/pelleted R-8 Al_2O_3	0.67	33,32,30	61,59,53	78,84,78
297	10280-43B	2% Pt/pelleted support type No. 1	0.59	33,32,30	61,59,53	78,84,78
298	10280-43E	1% Metal/pelleted support type No. 1[a]	0.64	25,24,25	53,55,53	86,82,77
299	10280-42	5% Metal/R-8 Al_2O_3	0.42	<1	1	1
300	10280-42B	Bimetallic, 5,5%/R-8 Al_2O_3	0.44	<1	<1	<1
301	10280-43C	1% Pt/pelleted R-8 Al_2O_3	0.63	27,28,27	53,49,50	73,80,74
302	10280-43A	1% Metal/pelleted support type No. 1	0.56	35,32,31	57,58,54	77,77,78
303	10280-47	4% Metal/support type No. 6	0.61	33,33,30	58,59,54	83,77,72
304	9874-24	1% Pt/R-8 Al_2O_3 (ref)	0.43	30,28,28	50,53,50	77,74,70
305	9874-7	1% Metal/support type No. 1	0.76	22,22,20	45,49,45	77,73,68
306	10280-42A	Bimetallic, 5, 1%/R-8 Al_2O_3	0.45	17, 7, 9	32,26,26	49,51,50
307	9874-7[b]	1% Metal/support type No. 1	0.43	24,28,24	48,43,40	66,60,56
308	10280-58A	4% Metal/80% support type No. 1, 20% binder type No. 6	0.69	28,29,29	58,57,52	76,74,73
309	10280-57B	4% Metal/support type No. 1, formed shapes	0.57	24,31,30	58,52,51	77,74,73
310	10280-59	Bimetallic, 5,5%/R-8 Al_2O_3	0.45	23,17,17	36,26, 0	22, 9, 9
311	10280-63A	4% Metal/80% support type No. 1, 20% binder type No. 6	0.32	31,29,27	59,58,52	82,85,82
312	10280-63B	4% Metal/82% supports type No. 1, 18% binder type No. 6	0.45	33,32,27	58,55,54	89,84,79
313	9874-155B	Bimetallic, 3,2%/R-8 Al_2O_3	0.44	26,21,27	44,44,45	72,71,68
314	10280-58B	4% Metal/80% support type No. 1, 20% binder type No. 1	0.52	28,31,30	62,57,52	84,78,76
315	10280-37A	Bimetallic, 5,4%/R-8 Al_2O_3	0.47	0, 0, -	1, 1, -	1, 1, -

(Continued)

a) LHSV 200.
b) Muffled at 1082°F in air.

Table 66 (Contd-2). MCH DEHYDROGENATION WITH VARIOUS CATALYSTS IN MICTR: RUNS 263-450

Run No.	Catalyst No.	Catalyst		% MCH Conversion, °F		
		Description	Wt. g	662	752	842
316	10280-33B	4% Metal/support type No. 2 (as rec'd)	0.41	16,18,15	46,39,34	67,60,55
317	10280-33D	4% Metal/support type No. 2 (as rec'd)	0.41	25,24,32	56,61,53	85,80,76
318	9874-24	1% Pt/R-8 Al_2O_3	0.43	20,20,26	46,48,45	72,66,63
319	9874-7	1% Metal/support type No. 1[a]	0.76	33,32,30	62,58,54	87,84,78
320[b]	10280-64	4% Metal/82% support type No. 1[a] 18% support type No. 6[a]	0.26	28,31,32	29,31,31	37,33,31
321[b]	10280-65A	4% Metal/82% support type No. 1 18% support type No. 6	1.11	6, 1, -	7, -, -	47,48, -
322	9874-94B	4% Metal support type No. 2	0.36	28,28,27	51,45,48	80,76,71
323[b]	10280-65B	2% Metal/82% support type No. 1[a] 18% support type No. 6	1.23	38,43,42	13,79,80	91,94,93
324	10280-65B	2% Metal/82% support type No. 1[a] 18% support type No. 6	1.23	22,24,21	45,42,39	64,62,59
325	9874-140A	10% Metal/support type No. 2	0.37	27,26,25	50,43,40	71,59,57
326[b]	10280-68A	2% Metal/82% support type No. 1, 18% support type No. 6 on screen,	0.32	36,26,31	29, 35	43,55,53
327	10280-69A	80 Mesh, 90% Pt-10% Ir screen	0.82	17, -, -	0, -, 0	0, -, -
328	10280-49	2% Metal/support type No. 1	0.74	26,21,29	49,41,42	73,79,74
329[b]	9874-140A	10% Metal/support type No. 1	0.74	65,36,30	60,51,43	89,79, -
330[b]	10280-69A	80 Mesh, 90% Pt-10% Ir screen, Pt black coated	0.23	0, 0, -	0, 0, -	0, -, -
332	10280-50A	Bimetallic, 4, 3%/R-8 Al_2O_3	0.44	-,26,25	54,53,49	69,53,39
333	9874-24	1% Pt/R-8 Al_2O_3 (ref)	0.42	22,29,27	53,49,47	71,71,65
334	9874-24	1% Pt/R-8 Al_2O_3[c]	0.42	35,35,32	59,63,60	88,82,82
335	10280-71B	1% Pt/82% support type No. 1 18% support type No. 6[a]	0.39	29,26,26	36,37,36	75,72,75
336	10280-71D	2% Pt/82% support type No. 1[a] 2% Pt/18% support type No. 6[a]	0.34	33,27,32	56,52,53	69,69,70
337	10280-66A	4% Metal/R-8 Al_2O_3	0.47	22,20,22	29,26,26	0, 0, 0
338	10280-75E	2% Metal/41% support type No. 1, 41% support type No. 1, 18% binder type No. 6	0.51	38,32,31	62,58,55	85,83,79

(Continued)

a) Catalytic coating on exterior of 8" long, 0.11" diam hypodermic tube.
b) LHSV 50.
c) Catalyst diluted to 4 ml instead of usual 2 ml volume.

Table 66 (Contd-3). MCH DEHYDROGENATION WITH VAR[illegible]S CATALYSTS IN MICTR: RUNS 263-450

Run No.	Catalyst No.	Catalyst		% MCH Conversion, °F		
		Description	Wt, g	662	752	842
339	10280-71A	1% Metal/41% support type No. 1, 41% support, Type No. 1, 18% binder type No. 6, muffled	0.51	38,32,31	62,58,55	85,83,79
340	10280-71C	2% Metal/41% support type No. 1, 41% support, Type No. 1, 18% binder type No. 6, muffled	0.45	29,25,30	53,55,51	85,78,73
341	10280-73	Bimetallic, 1, 1%/support type No. 1	0.76	29,29,29	52,59,53	77,77,74
342	9874-24	1% Pt/R-8 Al_2O_3 (ref)	0.42	22,18,17	49,52,43	70,70,64
343	10280-70A	2% Metal/support type No. 10	0.68	25,21,21	45,46,42	70,61,50
344	10280-70B	4% Metal/support type No. 10	0.67	32,27,22	47,51,45	70,67,59
345	10280-74A	Bimetallic,5, 4%/R-8 Al_2O_3	0.48	20,24,23	42,44,41	60,54,52
346	10280-74B	Bimetallic, 5, 4%/R-8 Al_2O_3	0.46	21,18,16	38,13,32	71,43,47
347	10280-75A	1% Metal/support type No. 10	0.71	4, 7, 7	6, 9, 5	10, 6, 7
348	10280-75B	2% Metal/support type No. 10	0.71	12, 7, 7	13,11,10	7, 8, 5
350	10280-77A	2% Metal/82% of support type No. 1 18% binder type No. 6	0.49	21,21,22	49,48,48	78,74,74

Table 66 (Contd-4). MCH DEHYDROGENATION WITH VARIOUS CATALYSTS IN MICTR: [illegible] 283-450

Period: September-November, 1967
Conditions: 10 atm pressure; catalysts reduced in hydrogen at 796°F, GLC samples normally taken at 3-, 8-, and 13- minute operation at each temperature.
Catalyst: Volume 0.9 ml catalyst diluted with 1.1 ml quartz chips. LHSV = 100 (catalysts and quartz 10-20 mesh unless otherwise noted).

Run No.	Catalyst No.	Catalyst		% MCH Conversion, °F		
		Description	wt, g	662	752	842
351	10280-77B	2% metal/80% type I support - 20% type 6 binder	0.76	25, 26, 24	60, [illegible], 58	88, 85, 82
352	10280-77C	3.5% metal/type 6 support	0.43	0	0	0
353	10280-77D	4.4% metal/type 6 support	0.39	0	0	0
354[a]	9874-24	1% Pt/R-8 Al_2O_3 support (ref.)	0.21	19, 18, 16	40, 38, 34	55, 53, 51
355	9874-24	1% Pt/R-8 Al_2O_3 support (ref.)	0.43	24, 23, 24	46, 52, 48	77, 74, 69
356	9874- 7	1% Pt/0104 Al_2O_3	0.77	30, 30, 29	62, 57, 54	84, 76, 74
357	9874- 7	1% Pt/0104 Al_2O_3	0.43[b]	22, 23, 23	53, 48, 48	75, 67, 66
358	5609-181	Bimetallic, 58.6, 31.4% (no support)	0.42	0	0	0
359	6646-119	Bimetallic, 39.8, 50.2% (no support)	0.28	0	0	0
360	6646-97	Bimetallic, 78.2, 21.8% (no support)	0.75	0	0	0
361	6646-64	Bimetallic, 70.4, 29.6% (no support)	0.15	0	0	0
352	6646-46	99.4% metal (no support)	1.86	0	0	0
363	6646-114	Bimetallic, 52.4, 47.6% (no support)	0.27	0	0	0
364	6187-175B	Trimetallic, 32.9, 62, 0.1% (no support)	0.92	5, 4	8, 5, 4	16, 15, 16
365	9874-24	1% Pt/R-8 Al_2O_3 support (ref.)	0.42	26, 27, 25	50, 51, 48	75, 73, 72
366	6646-104	Bimetallic, 26.2, 73.8% (no support)	0.99	0	0	0
367	6749-161	Bimetallic, 65.1, 34.9% (no support)	1.18	0	0	0
368	6646-101	Bimetallic, 53.7, 46.3% (no support)	0.49	0	0	0
363	10280-79B	1% Pt/R-8 Al_2O_3 support (control)	0.48	27, 27, 21	56, 52, 51	74, 78, 78
370	10280-79C	Bimetallic, 1, 1%/R-8 Al_2O_3	0.41	14, 12, 12	31, 23, 22	47, 41, 38
371	10280-79D	Bimetallic, 1, 1%/R-8 Al_2O_3	0.42	18, 13, 11	33, 31, 29	54, 47, 42
372	10280-79E	Bimetallic, 1, 1%/R-8 Al_2O_3	0.43	21, 23, 22	51, 50, 48	76, 75, 70
373	10280-79F	Bimetallic, 1, 1%/R-8 Al_2O_3	0.42	25, 15, 13	45, 35, 35	68, 62, 62
374	10280-80A	Trimetallic, 1, 1, 1%/R-8 Al_2O_3	0.43	18, 18, 16	44, 39, 39	64, 58, 59

a) LHSV = 200.
b) Same charging weight as for catalyst 9874-24 (ref.)

Table 66 (Contd-5). MCH DEHYDROGENATION WITH VARIOUS CATALYSTS IN MICTR: RUNS 263-450

Run No.	Catalyst No.	Catalyst		% MCH Conversion, °F		
		Description	wt, g	662	752	842
375	10280-80C	Bimetallic, 1, 1%/R-8 Al_2O_3 support	0.42	24, 24, 23	40, 37, 39	60, 59, [illegible]
376	10280-80B	Bimetallic, 1, 1%/R-8 Al_2O_3 support	0.47	20, 18, 14	41, 39, 37	65, 65, 59
377	9874-24	1% Pt/R-8 Al_2O_3 support (ref.)	0.43	16, 24, 24	58, 50, 49	73, 69, 70
378	10280-81A	4% metal[b]/type I support (control)	0.70	31, 34, 28	51, 53, 54	81, 77, 77
379	10280-81B	4% metal[c]/type I support (control)	0.71	29, 30, 29	60, 58, 53	85, 85, 80
380	10280-81C	4% metal[d]/type I support (control)	0.74	27, 30, 31	60, 60, 57	(92), 87, 84
381	10280-81D	4% metal[e]/type I support (control)	0.73	26, 29, 27	55, 56, 56	84, 82, 77
382	10280-81E	4% metal[f]/type I support (control)	0.73	29, 33, 32	(40), 61, 57	86, 86, 83
383	10280-81F	4% metal[g]/type I support (control)	0.76	28, 35, 33	69, 65, 62	79, 91, 87
384	10280-83A	1% metal/80% type I support - 20% type 6 binder	0.73	23, 24, 23	53, 47, 47	66, 71, 66
385	10280-81A	4% metal/type I support (control)	0.74	31, 31, 30	57, 59, 55	84, 81, 77
386	10280-83B	2% metal/80% type I support - 20% type 6 binder	0.73	28, 31, 29	55, 55, 51	69, 73, 62
387	10280-83C	1% metal/80% type I support - 20% type 6 binder	0.67	26, 25, 27	52, 52, 51	72, 73, 71
388	10280-83D	2% metal/type I support	0.70	24, 28, 28	57, 59, 54	78, 75, 69
389	10280-81A	4% metal/type I support[a]	0.69	25, 36, 33	60, 58, 54	88, 85, 80
390	10280-81B	4% metal/type I support[a]	0.69	31, 33, 32	66, 61, 61	85, 89, 85
391	10280-81C	4% metal/type I support[a]	0.70	27, 25, 31	50, 51, 49	87, 80, 78
392	10280-81D	4% metal/type I support[a]	0.71	23, 35, 34	76, 62, 58	89, 84, 83
393	9874-24	1% Pt/R-8 Al_2O_3 support (ref.)	0.43	24, 24, 27	51, 50, 47	72, 65, 55
394	10280-81E	4% metal/type I support[a]	0.70	28, 33, 32	63, 60, 56	88, 85, 80
395	10280-81F	4% metal/type I support[a]	0.71	35, 34, 34	66, 64, 60	90, 88, 84
396	6646-143B	Bimetallic, 4.4, 95.6% (no support)	0.91	0	0	0
397	10280-89A	1% metal/40% type I support (1), 40% type I support (2), 20% type 6 binder	0.56	25, 23, 27	60, 56, 51	82, 80, 79

a) Calcined in air 1 hr at 965°F.

b) Unneutralized impregnate (hydroxide).

c) Acid 1 neutralized impregnate.

d) Acid 2 neutralized impregnate.

e) Acid 3 neutralized impregnate.

f) Acid 4 neutralized impregnate.

g) Acid 5 neutralized impregnate.

Table 66 (Contd-6). MCH DEHYDROGENATION WITH VARIOUS CATALYSTS IN MICTR: RUNS 263-450

Run No.	Catalyst No.	Catalyst		% MCH Conversion, °F		
		Description	wt, g	652	752	842
398	10280-89B	2% metal/40% type I support (1), 40% type I support (2), 20% type 6 binder	0.57	25, 24, 30	62, 61, 58	88, 85, 80
399	6646-79	Trimetallic, 53.5, 2, 44.5% (no support)	0.44	0	0	0
400	10280-91B^a	2% metal/type I support (spheres)	0.63	27, 24, 26	55, 53, 50	80, 75, 71
401	10280-91A	4% metal/type I support (spheres)	0.64	27, 26, 25	57, 59, 55	85, 82, 76
402	6646-88	Trimetallic, 43.9, 11.5, 44.6%	0.67	0	0	0
403	10280-89C	1% metal/85% type I support, 15% type 6 binder	0.85	31, 29, 32	56, 57, 55	82, 74, 76
404	10280-95D	2% metal/85% type I support, 15% type 6 binder	0.84	25, 26, 25	61, 58, 55	80, 81, 75
405	10280-92A	1% metal/27% type I support (1), 53% type I support (2), 20% type 6 support	0.68	28, 27, 28	60, 58, 54	85, 85, 81
406	10280-92B	2% metal/27% type I support (1), 53% type I support (2), 20% type 6 support	0.71	23, 29, 28	62, 58, 55	82, 81, 81
407	9874-24	1% Pt/R-8 Al_2O_3 support (ref.)	0.43	19, 22, 25	50, 40, 47	71, 63, 64
408	10280-92C	1% metal/13% type I support (1), 67% type I support (2), 20% type 6 binder	0.71	34, 32, 21	61, 60, 55	86, 84, 80
409	10280-92D	2% metal/13% type I support (1), 67% type I support (2), 13% type 6 binder	0.73	27, 27, 25	53, 56, 50	80, 81, 77
410	9874-24	1% Pt/R-8 Al_2O_3 support (ref.)	0.42	27, 26, 25	54, 49, 47	73, 68, 66
411	10280-95B	2% metal^b)/39% support type I (1), 39% support type I (2), 22% binder type 6	0.40	31, 29, 28	48, 52, 48	77, 67, 72
412	10280-95C	2% metal^b)c)/39% support type I (1), 39% support type I (2), 22% binder type 6	0.61	25, 32, 27	53, 52, 27	83, 83, 79

a) Prepared for beach scale evolution.

b) Carbonated metal impregnate.

c) Calcined in air at 1112°F.

Table 66 (Contd-7). MCH DEHYDROGENATION WITH VARIOUS CATALYSTS IN MICTR: RUNS 263-450

Run No.	Catalyst No.	Catalyst		% MCH Conversion, °F		
		Description	wt, g	662	752	842
413	10280-98E	2% metal$^{c)b)}$/39% support type I (1), 39% support type I (2), 22% binder type 6	0.68	27, 30, 27	57, 52, 47	78, 76, 68
414	10280-99A	[illegible]% metal/39% support type I (1), 39% support type I (2), 22% binder type 6	0.51	31, 27, 25	53, 53, 50	82, 80, 75
415	10280-98B	2% metal/39% support type I (1), 39% support type I (2), 22% binder type 6	0.51	27, 30, 34	67, 58, 57	88, 86, 82
416	10280-100A	5% metal/type 6 support$^{a)}$	0.51	25, 20, 16	37, 36, 35	47, 47, 41
417	10280-98C	3% metal/40% type I support (1), 40% type I support (2), 20% type 6 binder	0.56	37, 34, 34	65, 63, 61	91, 8[illegible], 81
418	10280-98D	4% metal/40% type I support (1), 40% type I support (2), 20% type 6 binder	0.57	28, 28, 30	53, 56, 51	80, 77, 72
419	9874-24	1% Pt/R-8 Al_2O_3 support (ref.)	0.43	22, 26, 27	49, 49, 46	73, 73, 66
420	9874-7	1% Pt/0104 Al_2O_3	0.75	30, 31, 29	54, 53, 53	75, 73, 75
421	10280-100B	4% metal$^{b)}$/type 6 support	0.59	20, 22, 20	41, 44, 41	55, 56, 51
422	10280-104B	2% metal/40% type I support (1), 40% type I support (2), 20% type 6 binder	0.61	38, 33, 30	56, 60, 57	80, 82, 80
423	10280-106C	2% metal/80% type I support$^{c)}$/20% type 6 binder	0.70	31, 29, 29	58, 58, 58	88, 87, 84
424	10280-135B	4% metal/type 6 support$^{c)}$	0.62	18, 19, 19	37, 41, 39	42, 41, 36
425	10280-102F	5% metal/type I support	0.43	0	0	0
426	10280-102A	Bimetallic, 2, 4%/type I support	0.45	19, 19, 17	37, 37, 39	53, 51, 45
427	10280-102B	Bimetallic, 5, 4%/type I support	0.46	25, 25, 25	44, 40, 39	61, 59, 56
428	10280-102C	Bimetallic, 10, 4%/type I support	0.49	18, 20, 21	40, 37, 35	56, 52, 48

a) Carbonated metal impregnate.
b) Calcined in air at 11[illegible]°F.
c) Prepared for bench scale evaluation.

Table 66 (Contd-8). MCH DEHYDROGENATION WITH VARIOUS CATALYSTS IN MICTR: RUNS 263-450

Run No.	Catalyst No.	Catalyst		% MCH Conversion, °F		
		Description	wt, g	662	752	842
429	10280-102G	Bimetallic, 5, 2%/type I support	0.46	22, 24, 21	41, 36, 36	58, 57, 52
430	10280-102E	Bimetallic, 5, 6%/type I support	0.50	25, 25, 21	40, 35, 35	50, 50, 49
431	10280-103A	Bimetallic, 6, 6%/type I support	0.80	0	0	0
432	10280-103B	Bimetallic, 6, 6%/type I support	0.78	18, 18, 18	31, 28, 23	36, 8, 6
433	9874-139	1% Pt/K-8 Al_2O_3 support (new ref. prepn.)	0.42	23, 23, 22	47, 47, 48	68, 73, 72
434c)	9874-157B	5% metal, 5% metal/type I support	0.48	43, 39, 37	84, 73, 62	76, 51, 19
435	9874-159	1% metala)/type I support	0.43	26, 23, 24	52, 48, 49	70, 67, 69
436	6749-50	Trimetallic, 4.3, 4.2, 91.5% (no support)	0.78	0	0	0
437	6749-48	Trimetallic, 4.9, 4.2, 90.9%	0.90	0	0	0
438	6749-33B	Bimetallic, 38, 62% (no support)	0.57	8, 5, 4	9, 7, 5	21, 20, 19
439c)	10280-106D	5% metal/80% type I support, 20% type 6 binder	0.69	45, 45, 43	77,b) 76, 75	89,b) 90,b) 87b)
440c)	10280-104C	5% metal/40% type I support (1), 40% type I support (2), 20% type 6 binder	0.61	46, 46, 40	83,b) 67, 66	89,b) 88,b) 86b)
441c)	10280-106E	5% metal/80% type I support, 20% type 6 binder	0.70	40, 39, 38	54, (3), 47	75,b) 30,b) 11
442	10280-103C	Bimetallic, 2, 5%/type I support d)	0.43	38, 35, 31	54, 55, 54	82, 78, 79
443	9874-90	2% metal/type I support	0.41	25, 24, 25	55, 51, 50	78, 81, 78
444	9874-193A	Bimetallic, 2, 5%/type I support	0.46	22, 25, 28	51, 52, 48	72, 71, 70
445	10280-109A	3% metal/40% type I support (1), 40% type I support (2), 20% type 6 binder	0.56	31, 25, 24	60, 61, 58	84, 87, 83
446	10280-109B	Bimetallic, 10, 4%/type I support	0.47	21, 21, 19	40, 39, 37	54, 51, 47
447	10280-139	1% Pt/P-8 Al_2O_3 support (new ref.)	0.42	30, 30, 29	53, 55, 52	77, 80, 85
448	10280-105B	4% metal/support type 6	0.62	26, 21, 22	38, 38, 37	43, 43, 39
449	10280-104C	5% metal/40% support type I (1), 40% support type I (2), 20% binder type 6	0.65	27, 22, 25	50, 51, 46	64, 60, 58
450	10280-105B	5% metal/80% support type I, 20% binder type 6	0.6[illegible]	28, 29, 26	45, 42, 43	69,b) 50, 7

a) Carbonated metal impregnate.
b) Includes substantial amounts of benzene.
c) LHSV = 50.
d) Calcined in air at 1112°F.

Table 67. MCH DEHYDROGENATION WITH VARIOUS CATALYSTS IN MICTR: RUNS 484-572

Period: December, 1967 - February, 1968.
Conditions: 10 atm pressure; catalysts reduced in hydrogen at 796°F, GLC samples normally taken at 3-, 8-, and 13-minute operation at each temperature.
Volume: 0.9 ml catalyst diluted with 1.1 ml quartz chips. LHSV = 10 (catalysts and quartz 10-20 mesh).

Run No.	Catalyst No.	Catalyst		% MCH Conversion, °F		
		Description	wt, gm	662	752	842
484	10459-118	Proprietary	0.275	10, 4, <5	7, 7, 7	8, 5, 5
485	10280-111A	20% metal/type 1 support	0.849	10, 9, 9	9, 9, 9	12, 11, 11
486	10290-111B	20% metal/type 1 support	0.770	18, 14, 14	25, 21,[a] 25	35, 31, 29[a]
487	10280-117A	2% metal/40% type 1 support (1) /40% type 2 support (2) /20% type 6 support	0.350	26, 24, 25	55, 56, 52	67, 85, 78
488	10280-117B	4% metal/40% type 1 support (1) /40% type 2 support (2) /20% type 6 support	0.334	25, 26, 24	56, 52 ( )	80, 79, 79
489	10280-117C	Trimetallic, 2,2, 2%/type 1 support	0.821	16, 15, 15	28, 27, 27	27,[a] 18, 11
490	9874-139	1% Pt/R-8 type Al_2O_3	0.424	22, 21, 29	47, 49, 47	78, 75, 67
491	10290-118	Bimetallic, 2, 6%/type 1 support	0.485	0, 0, 0	0, 0, 0	0, 0, 0
492	10280-77A	2% metal/40% type 1 support (1) /40% type 1 support (2) /20% type 6 support	0.501	22, 31, 27	57, 58, 55	82, 64, 77
493	6646-78	Trimetallic, 33.4, 2, 64.6%	0.465	0, 0	0, 0	0, 0
494	6749-26	Trimetallic, 3.8, 1.4, 94.8%	0.526	0, 0	0, 0	0, 0
495	6749-55	Trimetallic, 2.7, 4.2, 93.1%	1.45	0, 0	0, 0	0, 0
496	6646-39	Bimetallic, 48.2, 51.8%	0.295	9, 10, 0	5, 6, 5	6.5, 5
497	6749-162	Bimetallic, 68.4, 31.6%	0.824	0, 0	0, 0	0, 0
498	6749-108	Trimetallic, 33.9, 6.2, 60%	0.811	0, 0	<1	8, 8, 11
499	6646-139C	Bimetallic, 5, 95%	0.955	0, 0	0, 0	0, 0
500	5603-165	Bimetallic, 38.5, 61.5%	0.574	0, 0	0, 0	9, 7
501	9874-139	1% Pt/R-8 type Al_2O_3	0.424	b)	b)	b)
502	10280-119A	1% metal/type 1 (control) support	0.672	25, 25, 22	48, 52, 52	75, 79, 75
503	10280-119C	Bimetallic, 1, 2%/type 1 support	0.721	34, 23, 26	56, 52, 55	73, 78, 75
504	9874-139	1% Pt/R-8 type Al_2O_3 (ref)	0.426	29, 24, 24	50, 52, 49	76, 76, 72
505	10280-121	4% metal/type 1 support	0.721	80, 27, 24	55, 55, 54	79, 82, 79
506	10280-119B	Bimetallic, 1, 1%/type 1 support	0.745	20, 22, 22	48, 48, 51	71, 75, 71
507	10280-119D	Bimetallic, 1, 3%/type 1 support	0.742	27, 28, 25	51, 49, 48	69, 65, 64
508	10280-119E	1% metal/type 1 support	0.694	24, 18, 20	44, 45, 40	61, 60, 56
509	10280-121	4% metal/type 1 support	0.724	24, 28, 29	58, 55, 55	82, 85, 82
510	10280-124A	2% metal/type 1 support	0.573	22, 22, 25	55, 46, 51	78, 79, 76
511	10280-124B	4% metal/type 1 support	0.602	21, 24, 22	51, 51, 51	74, 75, 74
512	10280-119G	Bimetallic, 2, 1%/type 1 support	0.724	25, 24, 22	48, 51, 48	73, 75, 76
513	10280-119H	Bimetallic, 3, 1%/type 1 support	0.746	25, 24, 22	57, 56, 51	95, 79, 75
514	9874-139	1% metal/R-8 type Al_2O_3 (ref)	0.424	27, 24, 25	50, 55, 51	71, 74, 70
515	10280-119J	Bimetallic, 2, 3%/type 1 support	0.882	35, 25, 24	58, 55, 55	80, 84, 86
516	10280-119I	Bimetallic, 3, 3%/type 1 support	0.759	25, 26, 22	58, 57, 55	78, 82, 81
517	10280-120A	Bimetallic, 1, 1%/type 1 support	0.682	19, 19, 17	42, 40, 40	56, 57, 56
518	10280-120B	Bimetallic, 1, 2%/type 1 support	0.642	16, 20, 20	39, 38, 36	46, 47, 48
519	10280-120C	Bimetallic, 1, 3%/type 1 support	0.751	17, 24, 19	38, 35, 36	53, 58, 67[a]
520	10280-120D	1% metal/type 1 support	0.700	8, 4, 2	15, 10, 9	19, 21, 21
521	10280-120E	Bimetallic, 2, 1%/type support	0.725	25, 20, 20	42, 47, 41	61, 61, 59
522	10280-120F	Bimetallic, 3, 1%/type 1 support	0.720	20, 22, 20	46, 48, 45	72, 77, 75
523	10280-120G	Bimetallic, 3, 3%/type 1 support	0.800	16, 19, 21	45, 39, 38	55, 50, 50
524	10280-120H	Bimetallic, 3, 2%/type 1 support	0.741	25, 21, 18	45, 46, 42	69, 61, 60
525	9874-139	1 Pt/R-8 type Al_2O_3 (ref)	0.451	25, 21, 20	44, 47, 47	72, 69, 70
526	10280-129	4% metal/type 1 support[c)d)]	0.697	37, 32, 29	56, 56, [illegible]	79, 77, 76
527	10280-129E	4% metal/type 1 support[c)]	0.675	25, 26, 28	57, 57, [illegible]	72, 75, 77
528	10280-122A	Trimetallic, 1,1, 1%/type 1 support	0.748	27, 26, 26	54, 56, (48)	66, 72, 71

(Continued)

Table 67 (Contd). MCH DEHYDROGENATION WITH VARIOUS CATALYSTS IN MICTR

Run No.	Catalyst No.	Catalyst		% MCH Conversion, °F		
		Description	wt. gm	662	752	842
529	10280-122B	Trimetallic, 5,5, 5%/type 1 support	0.805	32, 24, 23	56, 52, 49	63, 67, 61
530	10280-122C	Trimetallic, 5,1, 5%/type 1 support	0.748	23, 22, 23	51, 40, 48	54, 57, 57
531	9874-139	1% Pt/R-8 type Al_2O_3 (ref)	0.430	25, 26, 26	48, 47, 49	72, 74, 72
532	10280-122A	Trimetallic, 1,1, 1%/type 1 support	0.756	22, 20, 22	49, 46, 46	62, 64, 62
533	10280-122D	Trimetallic, 1,5, 5%/type 1 support	0.780	27, 29, 28	46, 45, 47	63, 52,[a] 44
534	10280-122E	Trimetallic, 5,5, 1%/type 1 support	0.770	29, 28, 27	52, 52, 51	67, 70, 69
535	10280-122F	Trimetallic, 1,1, 5%/type 1 support	0.755	22, 25, 25	45, 44, 44	59,[a] 55, 54
536	10280-122H	Trimetallic, 5,1, 1%/type 1 support	0.771	24, 24, 25	52, 52, 56	71, 71, 72
537	10280-122I	Trimetallic, 5,5, 2%/type 1 support	0.772	22, 21, 24	48, 46, 45	66, 67, 67
538	10280-130A	10280-119A[e]	0.723	24, 24, 22	56, 55, 57	80, 76, 76
539	10280-130B	10280-119B[e]	0.740	24, 26, 23	55, 55, 52	73, 83, 77
540	10280-130C	10280-119C[e]	0.742	23, 21, 20	55, 49, 49	74, 72, 72
541	10280-130D	10280-119D[e]	0.750	22, 22, 21	49, 48, 50	78, 73, 74
542	10280-127	1% metal/type 1 support	0.593	18, 22, 23	47, 47, 46	70, 70, 69
543	10280-130E	5% metal/type 1 support[e]	0.612	28, 24, 22	47, 45, 45	71, 70, 70
544	10280-126A	2% metal/40% type 1 support (1) /40% type 1 support (2) /20% type 17 binder	0.592	13, 11, 10	30, 27, 28	60, 59, 59
545	9874-139	1% Pt/R-8 type Al_2O_3 (ref)	0.633	30, 24, 26	50, 46, 48	67, 71, 68
546	10280-126B	Similar to 10280-126A[f]	0.539	13, 12, 11	31, 25, 24	60, 54, 53
547	10280-132C	Bimetallic, 6, 6%/type 1 support	0.660	0, 0	0, 0	0, 0
548	9874-80	2% metal/type 1 support	0.619	20, 21, 23	51, 48, 48	78, 77, 74
549	10280-134A	Bimetallic, 3, 3%/type 1 support	0.744	20, 24, 26	48, 49, 50	59, 58, 58
550	10280-134B	Bimetallic, 3, 1%/type 1 support	0.716	20, 24, 26	54, 49, 49	71, 69, 74
551	10280-132A	Bimetallic, 2, 6%/type 1 support	0.729	20, 19, 26	43, 48, 45	60, 70, 64
552	10280-132B	Bimetallic, 5, 6%/type 1 support	0.717	0, 0	0, 0	0, 0
553	10280-131A	5% metal/35% type 1 support (1) /35% type 1 support (2) /10% type 6 binder /12% type 15 binder[g][j]	0.498	19, [illegible], 19	54, 51, 50	76, 77, 79
554	10280-142A	9874-139[f]	0.604	23, 19, 26	47, 44, 45	69, 64, 66
555	10280-142B	9874-90[f]	0.606	23, 20, 19	45, 41, 42	68, 67, 67
556	10280-140A	5% metal/40% support type /40% support type 1 /20% support type 6	0.590	21, 24, 21	47, 48, 48	61, 75, 71
557	10280-142C	9874-7[f]	0.719	31, 21, 22	55, 50, 51	78, 74, 70
558	9874-7	9874-7	0.752	25, 26, 22	52, 49, 51	76, 78, 73
559	9874-139	1% Pt/R-8 type Al_2O_3 (ref)	0.646	19, 28, 25	46, 46, 40	70, 72, 72
560	10280-131B	5% metal/36% type 1 support (1) /35% type 1 support (2) /22% type 6 binder[g][j]	0.562	26, 27, 25	55, 51, 50	80, 79, 77
561	10280-133D	10280-133C[f]	0.673	24, 22, 21	54, 50, 49	79, 74, 73
562	10280-133A	5% metal/40% type 1 support (1) /40% type 1 support (2) /20% type 6 binder[j]	0.681	31, 23, 25	51, 50, 50	76, 73, 76
563	10280-133B	5% metal[h]/40% type 1 support (1) /40% type 1 support (2) /20% type 5 binder[j]	0.675	19, 19, 24	43, 41, 40	73, 60, 57
564	10280-133C	5% metal/40% type 1 support (1) /40% type 1 support (2) /20% type 6 binder[j]	0.693	20, 24, 22	50, 47, 46	76, 78, 74
565	9874-199A	4% metal[d]/type 1 support	0.815	20, 30, 21	50, 51, 51	78, 80, 76
566	9874-199C	4% metal[d]/type 1 support[k][e]	0.762	22, 18, 23	49, 46, 46	74, 71, 69
567	9874-199D	4% metal/type 1 support[k][e]	0.741	21, 21, 22	56, 54, 51	73, 77, 74
568	9874-200B	4% metal[d]/type 1 support	0.960	26, 28, 27	51, 50, 50	80, 83, 79
569	9874-200C	4% metal[d]/type 1 support[e]	0.948	24, 21, 23	54, 55, 59	82, 80, 82
570	9874-199C	Repeat of Run 566	0.778	23, 20, 25	57, 56, 56	80, 79, 79
571	10280-141B	5% metal[h]/type 1 support	0.633	24, 21, 23	45, 44, 44	58, 50, 59
572	10280-141A	5% metal[h]/type 1 support	0.693	20, 21, 21	50, 47, 45	75, 67, 69

a) Includes substantial amounts of benzene.
b) GLC bleed line overheated, causing cracking of the products.
c) Muffled 1094°F
d) Carbonated impregnate.
e) Alkaline type 6 binder.
f) Support muffled at 1112°F.
g) Inclusion of 12% oxidizable metal binder.
h) Impregnate and neutralized.
i) Support muffled at 1112°F before impregnation.
j) Support 259°F dried before impregnation.
k) Support muffled at 932°F before impregnation.
l) Support muffled at 752°F before impregnation.

Table 68. MCH DEHYDROGENATION WITH VARIOUS CATALYSTS IN MICTR: RUNS 573-676

Period - March to May, 1968

Conditions: 10 atm pressure. Catalysts reduced in H_2 for 20 min at 796°F. GLC samples normally taken at 3-, 8- and 13- min operation of each block temperature. Granular catalyst volume: 0.9 ml catalyst diluted with 1.1 ml quartz chips. Lined catalyst tubes either empty or packed with quartz chips, as indicated. LHSV = 100.

Run No.	Catalyst No.	Catalyst		% MCH Conversion, °F		
		Description	Weight	562	752	842
573	9874-139	1% Pt/UOP R-8 type Al_2O_3 (ref)	0.429	19, 18, 23	47, 43, 42	66, 69, 67
574	10458-124B	Proprietary	0.663	0,0	12, 7, 7	24,a) 8, 5
575	10280-143A	4% Pt/type I support, 752°F-1-1/2 hr air	0.616	27, 25, 24	51, 50, 49	76, 72, 71
576	10280-143C	4% Pt/type I support, 1132°F-1-1/2 hr air	0.687	23, 23, 22	51, 49, 47	73, 72, 72
577	10280-143D	4% Pt/type I support, 1292°F-2 hr air	0.697	22, 21, 23	53, 47, 48	75, 72, 71
578	10280-143E	4% Pt/type I support, 1445°F-2 hr air	0.677	17, 16, 18	41, 36, 34	57, 53, 51
579	10280-144A	3% metal/type I support, stabilized	0.537	19, 21, 20	49, 46, 45	73, 72, 72
580	10280-144B	3% metal/type I support, unstabilized	0.502	21, 24, 22	54, 54, 52	83, 83, 83
581	9874-139	1% Pt/UOP R-8 type Al_2O_3 (ref)	0.435	28, 25, 22	50, 48, 48	74, 73, 71
582	10280-151	Tube No. 1, ~2% metal/40% type I support (1)[b)] 40% type I support (2) 20% type 6 binder	0.239	25, 25, 26	71, 71, 71	87, 85, 87
583	10280-151	Same as above with quartz filler	0.239	42, 37, 36	76, 75, 77	96, 97, 97
584	10280-152	Tube No. 2, ~2% metal/40% type I support (1)[c)] 40% type I support (2) 20% type 6 binder	0.406	32, 29, 29	63, 61, 61	78, 77, 76
585	10280-152	Same as above with quartz filler	0.406	41, 41, 40	77, 74, 75	97, 96, 95

a) Some benzene formed with toluene.

b) Empty tube, catalyst on wall; 0.032 in. thick wall, 1/4 in. OD.

c) Empty tube, catalyst on wall; 0.028 in. thick wall, 1/4 in. OD.

(Continued)

Table 68 (Contd-1). MCH DEHYDROGENATION WITH VARIOUS CATALYSTS IN MICTR: RUNS 573-676

Run No.	Catalyst No.	Catalyst		% MCH Conversion, °F		
		Description	Weight	662	752	842
586	10280-158	Tube No. 3, ~2% Metal/40% type 1 support (1)[a)] 40% type 1 support (2) 20% type 6 binder	1.00	38, 36, 36	67, 63, 63	79, 77, 78
587	10280-158	Same as above with quartz filler	1.00	(), 30, 29	73, 72, 70	94, 93, 91
588	10280-158	Tube No. 4, Same coating as tube No. 3[a)]	0.663	28, 28, 30	63, 58, 59	80, 77, 76
589	10280-158	Same as above with quartz filler	0.663	33, 29, 32	78, 73, 71	95, 95, 95
590	10280-158	Tube No. 5, Same coating as tube No. 3[a)]	0.291	29, 28, 26	66, 65, 67	80, 77, 76
591		Same as above with quartz filler	0.291	43, 42, 40	79, 76, 75	95, 95, 95
592	10280-165	Tube No. 6, coated with No. 18 binder, platinized	-	0, 0	0, 0	0, 0
593	9874-133	1% Pt/UOP R-8 type Al_2O_3 (ref)	0.435	19, 18, 21	50, 47, 48	74, 69, 81
594	10280-143	4% Pt/type 1 support, 248°F dried	0.778	24, 23, 23	51, 53, 49	79, 76, 76
595	10280-143A	Repeat of run 575	0.728	20, 20, 23	51, 51, 50	78, 77, 75
596	10280-143C	Repeat of run 576	0.711	23, 22, 23	52, 49, 48	78, 74, 74
597	10280-143D	Repeat of run 577	0.717	26, 22, 24	51, 47, 47	72, 69, 71
598	10280-143E	Repeat of run 578	0.707	17, 16, 19	41, 37, 35	60, 57, 56
599	10280-165	Tube No. 7, ~2% Metal/40% type 1 support[a)] 40% type 2 support 20% type 6 binder	0.128	25, 26, 27	67, 64, 65	83, 83, 82
600	10280-165	Same as above with quartz filler	0.128	31, 29, 29	77, 73, 74	95, 95, 95
601	10280-143F	4% Pt/type 1 support (chemically reduced)	0.776	23, 21, 21	(58), 51, 49	78, 76, 75
602	10280-133D	Repeat of run 561	0.494	21, 23, 22	52, 48, 50	74, 73, 74
603	9874-139	1% Pt/UOP R-8 type Al_2O_3 (ref)	0.422	23, 22, 20	51, 47, 47	70, 70, 70
604	9874-139	1% Pt/UOP diluted to 4 in. volume	0.422	29, 30, 28	62, 58, 56	87, 86, 86

a) Empty tube, catalyst on wall; 0.028 in. thick wall, 1/4 in. OD.

(Continued)

Table 68 (Contd-2). MCH DEHYDROGENATION WITH VARIOUS CATALYSTS IN MICTR: RUNS 573-676

Run No.	Catalyst No.	Catalyst		% MCH Conversion, °F		
		Description	Weight	662	752	842
605	10458-120C	Trimetallic, 4, 1, 6%/type I support	0.760	14, 12, 10	27, 21,[a] 18	30, 21, 18[a]
606	10280-167	4% Metal[d]/type I support	0.761	15, 14, 13	31, 24, 21	44, 40,[a] 35
607	10280-168A	Bimetallic, 4, 8%/type I support	0.754	14, 12, 12	29, 26, 25	40, 38, 36
608	10280-170	Tube No. 10, 3% Pt/40% type I support (1)[b] 40% type I support (2) 20% type 6 binder	0.089	23, 22, 22	47, 50, 48	69, 67, 66
609	10280-170	Same as above with quartz filler	0.089	25, 23, 24	59, 54, 52	84, 80, 80
610	10280-170	Tube No. 11, 3% Pt/40% type I support (1)[b] 40% type 2 support (2) 20% type 6 binder with quartz filler	0.201	39, 30, 30	85, 82, 80	97, 98, 98
611	10280-133E	10280-133B Muffled at 1112°F in air	0.501	25, 21, 22	50, 48, 46	75, 73, 72
612	10280-147C	3% Pt/40% type 16 support 40% type I support 20% type 6 binder	0.514	24, 24, 23	49, 50, 45	73, 74, 73
613	10280-147D	Same as above with quartz filler	0.524	22, 21, 22	48, 49, 48	74, 71, 70
614	9874 -139	1% Pt/UOP R-8 type Al_2O_3 (ref)	0.422	19, 20, 20	50, 47, 46	69, 69, 70
615	9874 -170	Tube No. 11,[b] ref to Run 610	0.201	30, 32, 29	69, 67, 67	84, 85, 85
616	9874 -153A	Bimetallic, 9, 9%/type I support	0.971	20, 22, 18	40, 34, 34[a]	(17), (13), (13) 35, 34, 35[c]

(Continued)

a) Some benzene formed with toluene.
b) Empty tube, catalyst on wall; 0.028 in. thick wall, 1/4 in. OD.
c) Bracketed numbers benzene, unbracketed numbers total conversion of MCH to benzene and toluene.
d) Impregnated in chelate form.

Table 68 (Contd-3). MCH DEHYDROGENATION WITH VARIOUS CATALYSTS IN MICTR: RUNS 573-676

Run No.	Catalyst No.	Catalyst		% MCH Conversion, °F		
		Description	Weight	662	752	842
617	9874-173	Tube No. 9, 3% Metal/40% type I support (1) 40% type I support (2) 20% type 6 binder Filled with quartz	0.335	29, 25, 28	59, 49, 50	70, 65, 62
618	9874-173	Tube No. 8, 3% Metal/40% type I support (1) 40% type I support (2) 20% type 6 binder Filled with quartz	0.1451	40, 37, 36	84, 78, 78	(28),(12),(10)a) 95, 97, 65
619	9874-174A	Tube No. 12, 3% Metal/40% type I support 40% type 19 support 20% type 6 binder Filled with quartz	0.125	42, 32, 30	70, 70, 70	95, 91, 91
620	10280-173	Tube No. 8, cf Run 618, filled with quartz	0.145	28, 25, 24	60, 57, 56	(14),(66),(69)a) 77, 57, 60
621	10280-174C	2% Pt/40% type I support 40% type 19 support 20% type 6 binder	0.525	23, 24, 22	53, 50, 49	72, 76, 77
622	10280-174D	3% Pt/40% type I support 40% type 19 support 20% type 6 binder	0.5185	23, 22, 22	55, 52, 52	82, 79, 77
623	10280-174A	Tube No. 12b), cf Run 619	0.126	27, 23, 25	51, 49, 48	63, 62, 62
624	10280-176A	4% Pt/type I support (impreg. 18 hours)	0.705	25, 25, 23	54, 51, 51	81, 78, 78
625	10280-176C	4% Pt/type I support muffled at 1112°F, in air	0.672	23, 22, 21	53, 50, 50	79, 77, 76

a) Bracketed numbers benzene, unbracketed numbers total conversion of MCH to benzene and toluene. (Continued)

b) Empty tube, catalyst on wall; 0.028 in. thick wall, 1/4 in. OD.

Table 68 (Contd-4). MCH DEHYDROGENATION WITH VARIOUS CATALYSTS IN MICTR: RUNS 573-676

Run No.	Catalyst No.	Catalyst		% MCH Conversion, °F		
		Description	Weight	662	752	842
626	10280-170	Tube No. 10, ~3% Pt/40% type I support (1) 40% type I support (2) 20% type 6 binder Filled with quartz	0.089	28, 28, 27	65, 62, 62	88, 87, 87
627	10280-170	Tube No. 10, ~3% Pt/40% type I support (1)[a] 40% type I support (2) 20% type 6 binder Filled with quartz	0.089	14, 21, 22	50, 46, 46	61, 60, 60
628	9874-139	1% Pt/ UOP R-8 type Al_2O_3 (ref)	0.424	22, 22, 23	47, 48, 48	68, 68, 70
629	10280-153B	Bimetallic, 10, 5%/type I support	0.823	20,(14),17	41, 37, 36	55, 56, 53
630	10280-154A	Bimetallic, 9, 9%/type I support	0.905	<1	13, 7, 6	17, 14, 17
631	10290-154B	Bimetallic, 10, 5%/type I support	0.828	23, 18, 18	40, 36, 35	58, 54, 50
632	10280-155C	5% metal[b]/type I support	0.798	19, 19, 17	(6),(4),(4 40, 36, 31	(14), (11), (9)[c] 55, 48, 39
633	10280-155D	5% metal[b]/type I support	0.938	24, 16, 15	41, 35, 34	(16), (14), (13) 54, 50, 46
634	10280-170	Tube No. 10, top 7-1/2" quartz filled	0.089	26, 23, 23	48, 47, 46	53, 62, 62

a) Empty tube, catalyst on wall; 0.028 in. thick wall, 1/4 in. OD.

b) Impregnated in chelated form.

c) Bracketed numbers benzene, unbracketed numbers total conversion of MCH to benzene + toluene

(Continued)

Table 68(Contd-5). MCH DEHYDROGENATION WITH VARIOUS CATALYSTS IN MICTR: RUNS 573-676

Run No.	Catalyst No.	Catalyst		% MCH Conversion, °F		
		Description	Weight	662	752	842
635	10280-157A	Bimetallic, 1, 3%/type I support	0.772	20, 22, 22	47, 43, 43	71, 68, 68
636	10280-157B	Bimetallic, 3, 1%/type I support	0.713	24, 23, 23	27, 44, 43	71, 68, 68
637	10280-159B	Bimetallic, 5, 8%/type I support	0.789	<1	<1	<1
638	10280-159A	Bimetallic, 5, 8%/type I support	0.747	13, 11, 10	28, 25, 24	46, 39, 38
639	10280-159C	Trimetallic, 1, 1,3%/type I support	0.804	22, 25, 23	47, 46, 45	71, 67, 68
640	10280-161A	Trimetallic, 1, 1, 3%/type I support	0.741	17, 17, 17	42, 39, 38	62, 62, 62
641	10280-161B	Trimetallic, 1, 1, 3%/type I support	0.748	18, 17, 19	45, 40, 40	67, 66, 65
642	9874-139	1% Pt/UOP R-8 type Al_2O_3 (ref)				
643	10280-159D	Trimetallic 1,5,8%/type I support	0.785	22, 19, 21	44, 42, 40	63, 61, 60
644	10280-161C	Trimetallic, 1,1,3%/type I support	0.750	27, 27, 22	49, 44, 44	69, 67, 67
645	10280-161D	Trimetallic, 1,1,3%/type I support	0.726	19, 18, 18	42, 40,(49)	64, 64, 64
646	10280-161E	Trimetallic, 1,1,3%/type I support	0.745	22, 19, 21	43, 41, 40	66, 61, 60
647	10280-161F	Trimetallic, 1,1,3%/type I support	0.753	20, 16, 18	38, 36, 35	59, 56, 56
648	10280-178E	3% Pt/43% type I support 43% type 19 support 14% type 6 binder	0.478	25, 21, 22	53, 51, 51	83, 79, 74
649	10280-178B	Tube No. 13, -3% Pt, lined with above (7.75")	0.327	31, 31, 32	79, 76, 76	95, 95, 96
650	10280-178C	Tube No. 14, -3% Pt, lined with above (4.25")	0.167	31, 30, 31	79, 77, 77	96, 95, 96
651	10280-170	Tube No. 10, fitted with 0.177" dia annular tube of run 626	0.069	18, 17, 16	39, 40, 37	56, 55, 56
652	9874-139	1% Pt/UOP R-8 type Al_2O_3 (ref)	0.425	25, 25, 26	52, 48, 47	75, 72, 71

(Continued)

Table 68(Contd-6). MCH DEHYDROGENATION WITH VARIOUS CATALYSTS IN MICTR: RUNS 573-676

Run No.	Catalyst No.	Catalyst		% MCH Conversion, °F		
		Description	Weight	652	752	842
653	10280-181B	Bimetallic, 10, 8%/type I support	0.810	16, 16, 17	42, 38, 42	65, 60, 59
654	10280-181C	Trimetallic, 5,5,8%/type I support	0.750	18, 17, 18	43, 40, 39	65, 60, 59
655	10280-181A	Trimetallic, 5,5,8%/type I support	0.764	15, 14, 12	25, 20, 16	30, 16, 7
656	10280-181D	Trimetallic, 5,5,8%/type I support	0.773	14, 14, 13	27, 22, 29	28, 14, 9
657	10280-163A	Trimetallic, 1,3,1%/type I support	0.777	23, 19, 21	46, 43, 44	71, 69, 69
658	10280-163B	Trimetallic, 1,3,1%/type I support	0.761	20, 20, 23	48, 45, 41	71, 69, 70
659	10280-163C	Trimetallic, 1,3,1%/type I support	0.774	24, 22, 24	50, 47, 46	75, 74, 76
660	10280-163D	Trimetallic 1,3,1%/type I support	0.774	23, 27, 26	47, 49, 49	83, 76, 76
661	10280-172	4% metal/type I support	0.740	19, 20, 19	43, 41, 42	52, 57, 57
662	10280-172A	Bimetallic 4.4%/type I support	0.803	7, 7, 7	25, 22, 22	42, 38, 37
663	10280-172B	Bimetallic 4,4%/type I support	0.820	23, 22, 24	46, 44, 43	61, 49, 50
664	10280-163A	Trimetallic 1,1,3%/type I support	0.773	27, 24, 21	48, 44, 45	72, 69, 69
665	10280-163F	Trimetallic 1,1,3%/type I support	0.757	22, 21, 19	42, 38, 36	57, 53, 52
666	9874-139	1% Pt/UOP R-8 type Al_2O_3 (ref)	0.426	23, 23, 23	51, 49, 47	74, 72, 72
667	10280-185A	4% Pt/type 2 support	0.375	39, 22, 21	55, 49, 47	78, 76, 76
668	10280-185B	Bimetallic, 3,1%/type 2 support	0.385	25, 22, 22	50, 47, 46	74, 74, 74
669	10280-185C	Bimetallic, 2,2%/type 2 support	0.398	26, 22, 22	52, 48, 46	72, 71, 71
670	10280-185D	Bimetallic, 1,3%/type 2 support	0.333	25, 22, 21	47, 43, 42	67, 66, 67
671	10280-185E	4% metal/type 2 support	0.400	23, 19, 18	47, 42, 41	68, 64, 65

(Continued)

Table 68 (Contd-7). MCH DEHYDROGENATION WITH VARIOUS CATALYSTS IN MICTR: RUNS 672-676

Run No.	Catalyst No.	Catalyst		% MCH Conversion, °F		
		Description	Weight	662	752	842
672	10280-178B	Tube No. 13 rerun, cf Run 649	0.327	32, 29, 29	80, 76, 73	96, 96, 96
673	10280-178C	Tube No. 14, rerun, cf Run 650	0.167	29, 27, 23	72, 69, 69	94, 93, 93
674	10280-185F	4% metal[a]/type I support	0.811	16, 9, 7	21, 12, 10	29, 7, 9[b]
675	10280-170	Tube No. 10, cf Run (with quartz)	0.083	33, 26, 24	52, 48, 48	74, 72, 72
676	10280-170	Tube No. 10, with 0.165" annular tube	0.089	10, 11, 12	23, 24, 26	31, 30, 32

a) Impregnated in chelated form.
b) Some benzene formed with toluene.

Table 69. MCH DEHYDROGENATION WITH VARIOUS CATALYSTS IN MICTR: VARIOUS SUPPORTS

Period: June-August 1967
Conditions: 10 atm pressure; catalyst reduced in H_2 for 20 minutes at 790°F. MCH rate and catalyst charge variable.

Run No.	MCH Rate, ml/hr	Catalyst				Wt% of MCH Converted to Toluene (752°F)
		No. 10200-	Description	Mounted on	Charging Weight, g	
Granular Catalysts						
311	90[a]	63A	4% Pt/80% support type no. 1 - 20% binder type no. 6	granular	0.32	59, 58, 52
312	90	63B	4% Pt/82% two supports type no. 1 - 20% binder type no. 6	granular	0.44	58, 55, 54
338	90	75E	2% Pt/82% two supports type no. 1 - 20% binder type no. 6	granular	0.51	62, 58, 55
Catalyst Coatings						
320	45	64	4% Pt/82% two supports type no. 1 - 18% binder type no. 6	tube	0.26	29, 31, 31
321	45	65A	4% Pt/82% two supports type no. 1 - 18% binder type no. 6	tube	1.11	7
323	45	65B	2% Pt/82% two supports type no. 1 - 18% binder type no. 6	tube	1.23	73, 79, 80
324	90	65B	2% Pt/82% two supports type no. 1 - 18% binder type no. 6	tube	1.23	45, 42, 39
326	45	66A	2% Pt/82% two supports type no. 1 - 18% binder type no. 6	screen	0.32	29, [illegible], 35
335	45	71B	1% Pt/82% two supports type no. 1 - 18% binder type no. 6	tube	0.39	36, 37, 36
336	45	71D	2% Pt/82% two supports type no. 1 - 18% binder type no. 6	tube	0.34	56, 52, 53

Table 70. n-HEPTANE DEHYDROCYCLIZATION WITH VARIOUS CATALYSTS IN MICTR

Period: September-November, 1967
Conditions: 10 atm pressure, no added hydrogen. Catalysts reduced in hydrogen at 796°F.
Catalyst: Volume 0.9 ml catalyst diluted with 1.1 ml quartz chips. LHSV = 10 (catalysts and quartz 10-20 mesh.)

Run No.	Catalyst		LHSV	Percent n-Heptane Converted To Various Products					
				842°F			932°F		
	No.	Description		Cracked Products	Benzene	Toluene	Cracked Products	Benzene	Toluene
452	9874-139	1% Pt/R-8 type alumina (ref.)	50	3	0	3	-	-	-
453	9874-139	1% Pt/R-8 type alumina (ref.)	25	5	0	7	-	-	-
454	9874-139	1% Pt/R-8 type alumina (ref.)	10	6	0	8	27-31	-	40-46
455	9874-103B	Bimetallic, 2, 2%/type 1 support	10	-a)	0	0	-a)	0	3
456	10280-81B	4% metal/type 1 support	10	51	4	36	43	18	29
457	10280-63B	4% metal/type 1 - type 6 support	10	47	0	23	43	13	39
458	9874-177B	Bimetallic, 5, 3.3%/type 1 support	10	0	0	0	-	-	-
459	9874-172A	6% metal/type 1 support	10	5	0	0	13	0	0
460	9874-121A	10% metal/type 1 support	10	0	0	0	0	0	0
461	9874- 93B	4% metal/type 2 support	10	22	0	16	41	8	40
462	10280-36	5% metal/type 2 support	10	0	0	0	50	0	0
463	9874-139	1% Pt/R-8 type alumina (ref.)	10	14	0	16	21	0	37
464	10280-7B	Bimetallic (1:9 atomic ratio)/type 1 support	10	2	0	0	6	0	0
465	10280-140B	1% metal/type 1 support	10	7	0	0	4	0	0
466	10280-74A	Bimetallic, 5, 4%/ type 1 support	10	0	0	0	0	0	0
467	10280-86B	Bimetallic, 1, 1%/ type 1 support	10	27	0	[illegible]	41	0	23
468	9874-172A	6% metal/type 1 support	10	10	0	0	21-26	0	0
469	10280-103A	Bimetallic, 6, 6%/type 1 support	10	5	0	4	8	0	0
470	10280-79E	Bimetallic, 1, 1%/type 1 support	10	14	0	4	15	0	12
471	9874-193A	Bimetallic, 2, 5%/type 1 support	10	7	0	13	10	0	12

a) Initial complete cracking, then became completely inactive.

(Continued)

Table 70 (Contd). n-HEPTANE DEHYDROCYCLIZATION WITH VARIOUS CATALYSTS IN MICTR

Run No.	Catalyst		LHSV	Percent n-Heptane Converted To Various Products					
				842°F			932°F		
	No.	Description		Cracked Products	Benzene	Toluene	Cracked Products	Benzene	Toluene
472	10280-79D	Bimetallic, 1, 1%/type I support	10	16	0	0	8	0	2
473	10280-80A	Bimetallic, 1, 1%/type I support	10	7	0	0	13	0	0
474	6749-33B	Bimetallic, 38, 62% metal	10	-	-	-	67-74	0	0
475	6546-119	Bimetallic, 40, 60% metal	10	10	0	0	10	0	0
476	6646-64	Bimetallic, 70, 30% metal	10	0	0	0	5	0	0
477	6546-97	Bimetallic, 72, 28% metal	10	2	0	0	2	0	0
478	6646-63D	Proprietary	10	0	0	0	0	0	0
479	10280-111A	20% metal/type I support	10	-	-	-	~100	0	0
480	10280-111B	20% metal/type I support	10	~100	0	0	-	-	-
481	10280-81D	4% metal/type I support	10	33	0	20	35	0	13
482	10280-117C	Bimetallic, 2, 2%/type I support	10	~100	0	0	-	-	-
483	10280-118	Bimetallic, 2, 5.5%/type I support	10	9	0	0	4	0	0

SD/M-I Coker Flushing Procedure

To assure adequate coker cleaning and avoid contamination from cold zone deposits of prior runs, a standardized solvent washing procedure has been adopted.

After the test fluid has been drained and the preheater-filter assembly removed, a 1/4" s.s. line is installed so that fluid circulation can be carried out. The water to the cooler is disconnected and replaced with a steam supply. This allows the system to be flushed with hot solvents. Further, the pump speed is increased to give several fold the normal 6 lb/hr flow. The following sequence of solvent flushes has been found satisfactory.

1st Flush:
Solvent by volume: 1/3 Dimethyl Formamide
1/3 Toluene
1/3 Acetone

Experience has shown that one 15-minute flush with this potent solvent mixture is sufficient to remove all deposits which might otherwise be dissolved by the warm hydrocarbon test fuel.

2nd Flush Series:
Solvent by volume: 1/3 Toluene
1/3 Acetone
1/3 Ethyl Acetate

A minimum of 2-15 minute flushes are made, or as many as required to produce a water-white effluent.

3rd Flush Series, Three Final 15 Minute Washes:
Solvent by volume: Normal Heptane

Following the final wash, the system is opened to atmospheric pressure at various points and each segment dried with compressed nitrogen.

Finally, the test units are replaced, the system closed, and about 25 in. Hg vacuum imposed for at least 20 minutes. The test fuel is drawn in at the end of this period, with the vacuum still on. Besides drawing residual solvent out of the system, the vacuum reduces trapped pockets of air and so helps to equilibrate the fuel with the sparge gas which has the proper oxygen content.

Purification of RAF-161-60 Decalin

Decalin has a number of advantages as an endothermic fuel, mainly its lower vapor pressure and its better thermal stability (compared to MCH). In order to have an adequate supply of this material on hand, we obtained thirty drums from the Air Force fuel bank (RAF-161-60). This had been in storage since 1960. In spite of the fact that it was inhibited, and care taken in the selection of the material and the low temperature storage conditions, its color and thermal stability had deteriorated substantially.

Samples of this material were analyzed, purified and than evaluated in the bench-scale reactor by comparing the reactivity and stability for dehydrogenations with that of our F-113 Decalin. This work was undertaken to devise a means of purifying the 1500 gal of Decalin.

Analysis

The compositions of the various drums were determined in our laboratory by standard GLC techniques. Analyses were made of drums 1, 2, 16 17 and of mixtures from drums 3 to 15 and from 18 to 30 with the following results (Table 71).

Table 71. GLC ANALYSES OF RAF-161-60 DECALIN

Drum No.	trans-DHN, %	cis-DHN, %	THN, %
1	33.2	66.0	0.8
2	33.2	66.0	0.8
3-15 mixture	33.7	65.5	0.8
16	33.1	66.1	0.8
17	34.0	65.1	0.9
18-30 mixture	33.8	65.3	0.9

On the basis of the above analyses it was concluded that the Decalin probably came from the same lot and that a purification procedure worked out for one of the drums would be suitable for the complete lot.

Sulfur content of the material as received was low and analysis of one drum showed 2.3 ppm S.

Purification and Evaluation

In previous work with Decalin the standard pretreatment was to pass the decalin through a 1-in. diameter by 12-in. long silica gel column. A high purity Davison Grade 950, 60-200 mesh silica gel was used for this purpose. As this material was suitable for removing color, olefins and sulfur, it was of interest to see if a silica gel treatment would purify the 30 drums of decalin satisfactorily. For this purpose both Davison Grade 950 (high purity; 60-200 mesh) and Grade 28 (less pure; 20-40 mesh) were tested. The cost of the former was about $7.00/lb and that of Grade 28 was 54¢/lb. Both gels appeared to be equally effective in removing the color impurities (visual inspection), neither gel lowered the sulfur content below 2 ppm, and both gels improved the reactivity of the decalin and the stability of the catalyst markedly over the decalin as received (Table 72), when tested at 10 atm pressure, 1022°F, and LHSV of 100. For example, with the untreated decalin 39.5% conversion and a catalyst temperature increase of 234°F during the run was observed, while for decalin passed through a 12-in. silica gel column, 48% conversion and catalyst bed temperature increases of 38° to 47°F were observed. The increase in catalyst bed temperature during the run was taken as a measure of catalyst deactivation. In these tests the Grade 28 silica gel appeared just as effective as the more costly Grade 950. Thus, it appears that for catalytic dehydrogenation a silica gel treatment of the RAF-161-60 will be satisfactory.

Tests were also done to see if the silica gel treatment would improve the thermal stability to an acceptable value, and also to determine how much silica gel would be needed to purify the 30 drums of Decalin. The treatment consisted in passing DHN through a silica gel column (2-in. diameter x 11-in. long, ca 500-600 ml volume) and collecting the effluent in 500-600 ml samples. Steam-jet gum, microgum and Erdco Coker tests were then done on the samples. Because the DHN as received was colored, a light transmission measurement (Beckman DU Spectrophotometer) was carried out concurrently on the effluent to see if the DHN purification could be monitored by a light transmission technique.

Steam-jet gum, microgum, and spectrophotometric light transmission observations of successive samples showed that Grade 950 and Grade 28 silica gels were not depleted until just after 40 to 1 and 60 to 1 volumes of decalin per volume of silica gel had been treated, respectively. The depletion of silica gel activity was very sharp in each case and corresponded to the exact time when the visual color band reached the bottom of the silica gel column. No gradual change in purity of the effluent was observed in either case.

Table 73 shows a comparison of the effectiveness of the two grades of silica gel for material taken as near the silica gel depletion point as possible, considering the volume of sample required for a test. However, for the coker tests this amounted to about 3 gal, or about the last 20 volumes prior to the break point. A slightly better result was indicated by light transmission for the Grade 950 compared to the Grade 28 near the saturation point, but this is probably not significant. Grade 950 also looked a little better in the coker results, but, once more, the difference is so small as to be of doubtful significance. The most interesting result was that Grade 28 purified about 50% more Decalin than Grade 950, despite the coarse grain size of the former (20-40 mesh vs 60-200 mesh). Treating rates were kept about equal by use of a stopcock flow control on the Grade 28 column. A second important observation was the approximately 300°F improvement in thermal stability effected by silica gel treatment.

No significant differences were observed in gum contents. Interestingly, the Decalin had a rather marked yellow color prior to treatment. The colored material was found to be rather volatile so that most of it was vaporized in both gum tests. Hence, the effectiveness of the silica gel was not properly disclosed by the gum analyses. Attempts will be made to characterize the adsorbate since it appears to have such a deleterious effect on thermal stability.

Table 72. DEHYDROGENATION OF RAF-161-60 DECALIN

Catalyst:	1% Pt on Al_2O_3	Feed:	33.2% trans-DHN
Catalyst Volume:	7 ml		66.0% cis-DHN
Pressure:	10 atm		0.8% THN
LHSV:	100		

Run No.	110	116-1	117	134	135	136
Feed Pretreatment Silica Gel Column	none	← Grade 950 →		← Grade 28 →		
Temperature, °F						
Block	1022	← 1022 →		842	932	1022
Wall	876-995	851-860	856-67	698-702	752-54	815-22
Catalyst Bed Profile	806-995	741-79	761-800	622-37	658-76	698-736
	727-951	797-22	711-25	635-40	671-78	711-20
	743-905	730-38	730-38	640-44	680-84	722-27
	770-842	761-66	751-66	653-60	698-704	745-52
ΔT_{max}, Catalyst bed	254	38	47	15	18	33
DHN Conversion, %w	39.5	46.3	47.9	31.5	40.2	46.6
Rate Constants						
Zero Order, atm, sec^{-1}	4.46	5.00	5.14	2.96	3.94	4.83
First Order, sec^{-1}	0.565	0.672	0.699	0.355	0.503	0.648

Table 73. COMPARATIVE EFFECTIVENESS OF DAVISON GRADES 950 AND 28 SILICA GEL IN THE PURIFICATION OF RAF-161-60 DECALIN

Analytical Test	RAF-161-60 "As Received"	RAF-161-60 Treated at 40:1 With Grade 950 SiO_2	RAF-161-60 Treated at 60:1 With Grade 28 SiO_2
Steam-jet Gum,[b] mg/100 ml	0.6 ± 0.3	0.5 ± 0.3	$0.0 \pm {}^{0.1}_{0.0}$
Microgum,[c] mg carbon/100 ml	0.16 ± 0.02	0.07 ± 0.03	0.09 ± 0.02
Erdco Coker,[d] 250 psig, °F			
300	2/5	-	-
400	4/23.5	-	-
475	6/32.5	-	-
625	--	3/20	4/24
Light Transmission,[e] % (relative)	80.0	100.0	97.5

a) Grade 950 was high purity, 60-200 mesh; Grade 28 was lower purity, 20-40 mesh.
b) ASTM Method Designation: D381-61T (450°F, steam, atmospheric pressure).
c) Method described in Technical Documentary Report No. APL TDR 64-100, Part II, pp. 180-187 (500°F, nitrogen, <2 mm Hg pressure).
d) Coker operating conditions: fuel flow, 3 lb/hr; preheater and filter at same temperature; air saturated fuel, but helium gas drive.
e) Beckman Model DU Spectrophotometer, 350 mμ wavelength; 1 cm thick cells.

Purification of a 30-Drum Batch of Decalin

Following laboratory investigation of purification techniques we have purified the entire 30 drum batch. The quality of the product obtained was equal to that of the laboratory product.

The equipment for this process consisted of a stainless steel tank about 5 feet high and 18 inches in diameter, filled to a level of 3.3 feet with the Davison Grade 28 (20-40 mesh) silica gel. The column was prepared initially by pulling a vacuum of about 29" Hg on the silica gel with the vessel tightly closed. After several hours at this pressure, about 20 gals of laboratory purified Decalin was drawn into the column to wet the gel. The column was then filled with unpurified Decalin to within a couple of inches of the top.

During operation, Decalin was pressured into the top of the column from an original drum at the rate of about 55 gal per 7 hours, and was allowed to percolate down through the silica gel bed and flow into a fresh epoxy-lined drum (the first product was recycled). Flow was monitored with a needle valve and rotameter, and samples were taken at the beginning and end of each drum. In operation, a drum was put on stream in the morning and taken off at night, requiring little attention during the day since the pressuring gas (N_2) was automatically controlled. Liquid level in the column was maintained above the level of the gel bed at all times. After the samples had been checked spectrophotometrically by comparison with a "pure" reference sample, the drum was then pumped into a clean epoxy-lined 1500 gal tank. The total 30 drums were finally stirred thoroughly in the large tank by vigorous bubbling with nitrogen to assure constant composition during usage.

A Beckman Model DU Spectrophotometer, at 350 mu wavelength with 1 cm quartz cells, was used for the light transmission measurements. Light transmission was improved ca. 25 percent by the silica gel treatment, with no significant variations in the quality of samples during the 30 drum treating process. Thus, up to a volume ratio of about 39:1, Grade 28 silica gel performed its purification function without loss in effectiveness (150 lbs or 5.4 cu. ft of silica gel for 30 55-gal drums). Previous laboratory results showed the Grade 28 silica gel would purify RAF-161-60 without loss in effectiveness until a ratio of 60:1 was reached, after which purity declined rapidly. As can be seen, better than a 50 percent safety margin was allowed in the large scale treating setup.

The 1500 gal tank is kept under nitrogen blanket at all times, and the Decalin has been nitrogen blanketed at all times since purification. Subsequently, 3 drums of this purified Decalin, now designated F-137, has been shipped to Pratt and Whitney Aircraft (Florida), 2 drums to Wright-Patterson AFB, and 1 gal to Edwards AFB. The balance is being used in our own heat transfer and thermal stability testing.

Some of the adsorbate was removed from the column by flushing with heptane and acetone and has been recovered. Interestingly, it appears to be an effective vesicant on susceptible skin. A GLC trace of some of the material recovered in a laboratory run is shown in Figure 73. There is evidence for the presence of 3 major components. Because of the potentcy of the total adsorbate as a thermal instability promoter it will be interesting to check the activity of the separate components after separation by GLC.

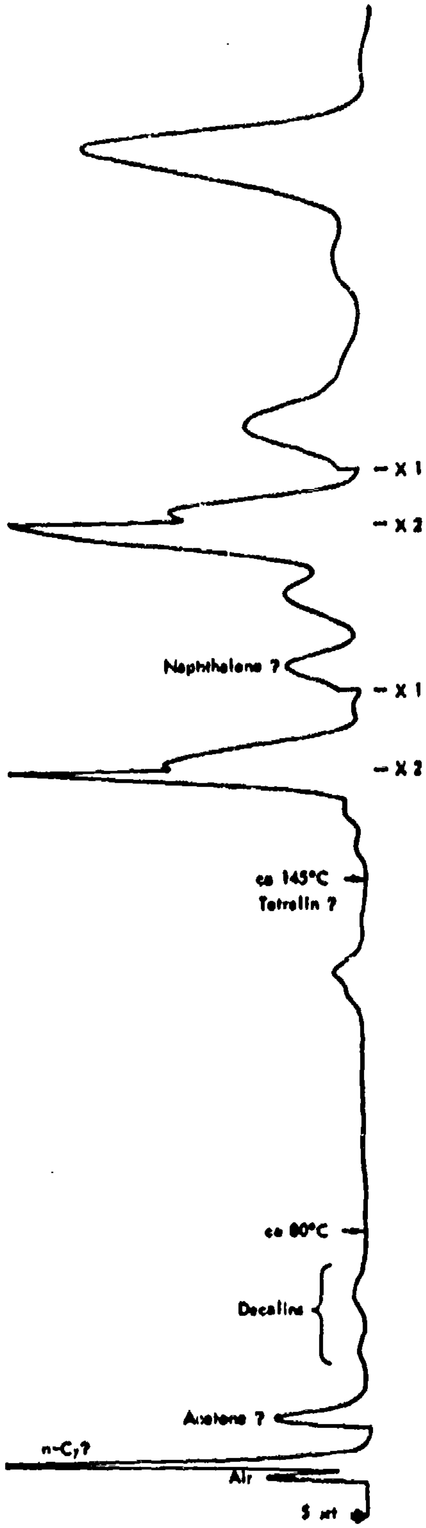

Figure 73. GLC ANALYSIS OF ADSORBATE FROM DECALIN PURIFICATION

Table 74. FSSTR-HEAT TRANSFER TO MCH IN EMPTY 3/8" OD x 10 FT LONG SECTIONS: DATA SUMMARY

Run No. 10018-	MCH Feed Rate		Press., psig	Reactor Section	Fluid Temp. at Couplings, °F		Heat Flux,b) $\frac{Btu}{(hr)(ft^2)}$	Temp., °F		Total Heat To Fluid Btu/lb
	lb/hr	$\frac{lb^{a)}}{(hr)(ft^2)}$			In	Out		Fluid	Outside Wallc)	
71-15:25	104	249,000	801	I	73	181	7,250	98 125 153	177 197 217	50
				II	181	336	12,600	218 263 298	310 347 379	136
75-15:00	102	244,000	905	I	80	210	8,580	108 142 178	204 227 250	60
				II	210	397	15,800	255 308 349	362 404 444	171
75-16:30	102	244,000	880	I	82	300	15,500	133 190 247	290 324 360	108
				II	300	501	19,000	350 406 452	450 504 545	251
75-16:55	102	244,000	875	I	82	379	21,900	154 235 313	361 401 447	153

a) Mass velocity.
b) Heat flux based on inside tube surface.
c) Wall thermocouples welded to side of tube.

(Continued)

Table 74 (Contd). FSSTR-HEAT TRANSFER TO MCH IN EMPTY 3/8" OD x 10 FT LONG SECTIONS: DATA SUMMARY

Run No. 10018-	MCH Feed Rate		Press., psig	Reactor Section	Fluid Temp. at Couplings, °F		Heat Flux,b) Btu/(hr) (ft²)	Temp., °F		Total Heat To Fluid Btu/lb
	lb/hr	lb^a)/(hr) (ft²)			In	Out		Fluid	Outside Wall^c)	
				II	379	601	23,400	438 497 548	549 599 641	317
78-12:30	101	241,000	891	I	77	310	16,800	133 195 253	300 331 370	118
				II	310	413	9,490	333 363 388	390 418 442	185
78-14:00	101	241,000	885	I	78	450	28,600	178 273 373	427 475 525	202
				II	450	660	25,500	507 561 613	610 655 695	381
78-15:40	101	241,000	584	I	82	453	28,600	178 276 380	430 478 530	202
				II	453	629	25,500	510 558 597	603 653 671	381

a) Mass velocity

b) Heat flux based on inside tube surface.

c) Wall thermocouples welded to side of tube.

Table 75. FSSTR; DATA SUMMARY SERIES 10018-90

Heat Transfer to MCH in Miniature Heat Transfer Section

Reactor No. 10018-82; 0.0265 in. ID x 0.018 in. wall x 6.0 in. long, Type 316 S.S.
Feed: MCH, 34.2 lb/hr = 8.93 x 10^6 lb/(hr·ft^2)

Run No. 10018-	Measured Power, Btu/hr	Fluid Temp, °F		Press., psig		Tube[a)] Length, in.	Wall Temperature, °F		Heat[d)] Flux, Btu/(hr·ft^2) x 10^{-3}	Cumulative[e)] Heat, Btu/hr
		In	Out	In	Out		Outside[b)]	Inside[c)]		
90-13:51	450	68	99	895	718	0.25	123	113	128	18
						1.35	125	115	128	100
						2.45	131	121	128	131
						3.55	134	124	129	263
						4.65	139	129	129	345
						5.75	146	136	129	427
						(0-6)			(128)	445
90-14:10	1,220	66	142	895	730	0.25	208	182	350	51
						1.35	209	183	350	273
						2.45	217	191	351	496
						3.35	224	198	352	720
						4.65	238	212	355	944
						5.75	252	227	357	1,171
						(0-6)			(353)	1,223
90-14:28	2,950	65	240	895	735	0.25	386	328	870	126
						1.35	369	311	865	677
						2.45	382	324	869	1,229
						3.55	392	334	874	1,783
						4.65	414	356	881	2,340
						5.75	440	382	890	2,900
						(0-6)			(875)	3,035
90-14:45	5,480	65	359	895	733	0.25	597	499	1,623	235
						1.35	555	457	1,604	1,261
						2.45	555	457	1,604	2,285
						3.55	574	476	1,612	3,305
						4.65	603	505	1,626	4,330
						5.75	637	539	1,641	5,370
						(0-6)			(1,618)	5,610
90-15:07	8,840	65	499	895	723	0.25	793	647	2,612	377
						1.35	741	594	2,576	2,030
						2.45	739	592	2,574	3,670
						3.55	765	619	2,593	5,310
						4.65	790	644	2,611	6,960
						5.75	832	687	2,640	8,603
						(0-6)			(2,601)	9,020
90-15:28	11,870	65	600	895	685	0.25	929	745	3,463	500
						1.35	877	691	3,415	2,690
						2.45	877	691	3,415	4,960
						3.55	904	719	3,440	7,040
						4.65	964	782	3,494	9,250
						5.75	1,111	932	3,630	11,510
						(0-6)			(3,476)	12,060

a) T.C.'s spot welded to outside wall at indicated inches from inlet end.
b) Measured. All T.C. junctions on one side of horizontal tube.
c) Calculated.
d) Corrected for losses. ( ) values are average for entire tube.
e) Net heat to fluid up to indicated tube length.

Table 76. FSSTR; DATA SUMMARY SERIES 10018-94

Heat Transfer to MCH in Miniature Heat Transfer Section

Reactor No. 10018-82; 0.0265 in. ID x 0.018 in. wall x 6.0 in. long, Type 316 S.S.
Feed: MCH, 45.3 lb/hr = 11.83 x 10^6 lb/(hr·ft^2)

Run No. 10018-	Measured Power, Btu/hr	Fluid Temp, °F		Press., psig		Tube[a] Length, in.	Well Temperature, °F		Heat Flux,[d] Btu/(hr·ft²) x 10^{-3}	Cumulative[e] Heat, Btu/hr
		In	Out	In	Out		Outside[b]	Inside[c]		
94-9:36	[illegible]	50	62	896	585	0.25	118	104	180	26
						1.35	119	105	181	141
						2.45	125	111	181	255
						3.55	130	116	181	371
						4.65	138	124	182	486
						5.75	145	131	182	601
						(0-6)			(181)	625
94-9:42	1,490	49	125	886	595	0.25	200	169	425	61
						1.35	205	174	426	332
						2.45	213	182	427	602
						3.55	222	191	429	874
						4.65	238	207	432	1,149
						5.75	251	220	434	1,424
						(0-6)			(429)	1,487
94-9:53	3,240	49	156	886	600	0.25	347	282	959	159
						1.35	346	281	958	748
						2.45	358	293	963	1,358
						3.55	371	306	969	1,972
						4.65	400	335	981	2,591
						5.75	420	355	989	3,217
						(0-6)			(970)	3,364
94-10:10	5,390	48	280	886	598	0.25	504	404	1,581	228
						1.35	492	392	1,575	1,232
						2.45	506	406	1,582	2,236
						3.55	526	427	1,591	3,244
						4.65	566	468	1,608	4,260
						5.75	595	497	1,622	5,288
						(0-6)			(1,593)	5,525
94-10:19	7,660	48	356	885	590	0.25	641	507	2,245	324
						1.35	621	487	2,233	1,749
						2.45	635	501	2,241	3,170
						3.55	658	524	2,257	4,600
						4.65	707	575	2,287	6,050
						5.75	742	611	2,308	7,500
						(0-6)			(2,262)	7,850
94-10:27	10,210	48	437	886	573	0.25	764	597	2,943	465
						1.35	743	575	2,925	2,292
						2.45	760	593	2,940	4,160
						3.55	783	617	2,957	6,030
						4.65	826	661	2,992	7,920
						5.75	878	714	3,035	9,830
						(0-6)			(2,965)	10,280
94-10:36	13,720	48	539	886	530	0.25	917	705	3,975	574
						1.35	892	679	3,948	3,095
						2.45	904	691	3,960	5,610
						3.55	936	724	3,996	8,140
						4.65	967	755	4,028	10,690
						5.75	1,078	871	4,147	13,280
						(0-6)			(4,004)	13,900

a) T.C.'s spot welded to outside wall at indicated inches from inlet end.
b) Measured. All T.C. junctions on one side of horizontal tube.
c) Calculated.
d) Corrected for losses. ( ) values are average for entire tube.
e) Net heat to fluid up to indicated tube length.

Table 77. FSSTR; DATA SUMMARY SERIES 10018-98

Heat Transfer to Nitrogen in Miniature Heat Transfer Section

Reactor No. 10018-97; 0.0265 in. ID x 0.018 in. wall x 6.0 in. long, Type 316 S.S.
Feed: Nitrogen, 6.31 lb/hr = 1.65 x 10^6 lb/(hr·ft^2)

Run No. 10013-98-	Measured Power, Btu/hr	Experimental Data							Smoothed and Calculated Data				
		Fluid Temp, °C		Press., psig		Tube Wall Thermocouples			Length, Inches	Wall Temp, °F[c]		Heat Flux[d] Btu/(hr·ft²) x 10⁻³	Cumulative[e] Heat, Btu/hr
						Location		Temp, °F					
		In	Out	In	Out	Inches[a]	Position[b]			Outside	Inside		
14:19	193	68	160	524	405	0.3	B	117	0	(111)	(108)	52.7	0
						1.0	T	132	1	135	130	53.1	31
						1.8	B	150	2	155	150	53.3	61
						2.6	T	166	3	174	171	53.7	92
						3.4	B	182	4	195	192	54.0	123
						4.2	T	200	5	216	213	54.2	155
						5.0	B	216	6	(237)	(234)	54.5	186
						5.7	T	230	(0-6)			(53.7)	
14:44	665	68	389	524	366	0.3	B	227	0	(210)	(197)	180	0
						1.0	T	281	1	281	268	186	106
						1.8	B	339	2	352	339	191	214
						2.6	T	394	3	422	410	196	326
						3.4	B	452	4	493	481	200	440
						4.2	T	504	5	565	551	203	557
						5.0	B	567	6	(634)	(622)	206	675
						5.7	T	614	(0-6)			(195)	
15:05	1,059	68	586	524	325	0.3	B	326	0	(300)	(281)	270	0
						1.0	T	420	1	481	400	284	160
						1.8	B	508	2	533	515	293	327
						2.6	T	595	3	650	633	302	499
						3.4	B	690	4	765	748	310	676
						4.2	T	778	5	881	864	318	857
						5.0	B	880	6	(995)	(979)	325	1042
						5.7	T	962	(0-6)			(301)	
15:25	1,646	68	878	524	227	0.3	B	482	0	(455)	(429)	416	0
						1.0	T	654	1	634	609	437	246
						1.8	B	777	2	813	788	457	504
						2.6	T	911	3	991	968	476	774
						3.4	B	1,060	4	1,170	1,147	495	1,054
						4.2	T	1,198	5	1,349	1,327	513	1,346
						5.0	B	1,353	6	(1,528)	(1,506)	531	1,648
						5.7	T	1,478	(0-6)			(475)	

a) T.C.'s spot welded to outside wall at indicated inches from inlet end bus bar.
b) Location of T.C. junction on horizontal tube. B = Bottom, T = Top.
c) Outside wall temperatures by smoothing experimental data. Inside temperatures by calculation.
d) Corrected for losses. Values in ( ) are average over entire heated length.
e) Net heat to fluid up to indicated tube length.

Table 78. FSSTR: DATA SUMMARY SERIES 10018-101

Heat Transfer to Water in Miniature Heat Transfer Section

Reactor No. 10018-97; 0.0265 in. ID x 0.018 in. wall x 6.0 in. long, Type 316 S.S.
Feed: Water, 54.1 lb/hr = 14.13 x 10^6 lb/(hr·ft²)

Run No. 10018-101-	Experimental Data									Smoothed and Calculated Data				
	Measured Power, Btu/hr	Fluid Temp, °F		Press., psig		Tube Wall Thermocouples			Length, Inches	Wall Temp, °F c)		Heat Flux d), Btu/(hr·ft²) x 10^{-3}	Cumulative e) Heat, Btu/hr
						Location		Temp, °F					
		In	Out	In	Out	Inches a)	Position b)			Outside	Inside		
11:01	1,870	58	95	889	567	0.3	B	149	0	(148)	(107)	542	0
						1.0	T	145	1	146	105	542	313
						1.8	B	147	2	146	105	542	626
						2.6	T	146	3	149	106	543	940
						3.4	B	152	4	155	114	544	1,255
						4.2	T	154	5	169	128	548	1,569
						5.0	B	173	6	(193)	(152)	555	1,887
						5.7	T	178	(0-6)			(544)	
11:31	6,550	58	181	889	586	0.3	B	344	0	(347)	(215)	1,906	0
						1.0	T	350	1	352	200	1,892	1,098
						1.8	B	322	2	321	189	1,882	2,188
						2.6	T	325	3	330	198	1,890	3,279
						3.4	B	344	4	355	225	1,914	4,379
						4.2	T	349	5	397	265	1,953	5,500
						5.0	B	404	6	(441)	(309)	1,993	6,650
						5.7	T	421	(0-6)			(1,913)	
12:05	10,180	58	254	889	579	0.3	B	497	0	(505)	(314)	2,959	0
						1.0	T	470	1	471	279	2,926	1,701
						1.8	B	459	2	455	262	2,911	3,388
						2.6	T	450	3	465	273	2,920	5,070
						3.4	B	485	4	502	311	2,956	6,770
						4.2	T	495	5	563	375	3,016	8,500
						5.0	B	576	6	(647)	(461)	3,097	10,270
						5.7	T	602	(0-6)			(2,960)	
12:31	14,810	58	336	889	575	0.3	B	647	0	651	387	4,340	0
						1.0	T	606	1	613	347	4,290	2,496
						1.8	B	597	2	591	325	4,260	4,970
						2.6	T	588	3	611	345	4,290	7,440
						3.4	B	633	4	645	380	4,340	9,950
						4.2	T	648	5	687	423	4,390	12,450
						5.0	B	689	6	(733)	(472)	4,260	15,010
						5.7	T	716	(0-6)			(4,330)	
13:01	21,040	58	445	889	571	0.3	B	746	0	(737)	(389)	5.950	0
						1.0	T	729	1	737	389	5,850	3,379
						1.8	B	752	2	747	400	5,860	6,760
						2.6	T	759	3	779	434	5,920	10,170
						3.4	B	812	4	827	484	6,010	13,620
						4.2	T	824	5	888	548	6,070	17,110
						5.0	B	900	6	(958)	(621)	6,250	20,670
						5.7	T	927	(0-6)			(5,960)	

a) T.C.'s spot welded to outside wall at indicated inches from inlet end bus bar.
b) Location of T.C. junction on horizontal tube. B = Bottom, T = Top.
c) Outside wall temperatures by smoothing experimental data. Inside temperatures by calculation.
d) Corrected for losses. Values in ( ) are average over entire heated length.
e) Net heat to fluid up to indicated tube length.

Table 72. HSSTR; DATA SUMMARY SERIES 10018-108

Heat Transfer To Water In Miniature Heat Transfer Section

Reactor No. 10018-103; 0.0265" ID x 0.018" wall x 6" long, Type 316 S.S.
Feed: Water, 30.1 lb/hr = 7.86 x 10^6 lb/(hr·ft²)

Run No. 10018-108	Experimental Data								Smoothed and Calculated Data				
	Measured Power, Btu/hr	Fluid Temp, °F		Press., psig		Tube Wall Thermocouples			Length, In.	Wall Temp,[c] °F		Heat[d] Flux, Btu/(hr·ft²) x 10⁻³	Cumulative[e] Heat, Btu/hr
						Location		Temp, °F					
		In	Out	In	Out	In.[a]	Position[b]			Outside	Inside		
14:30	772	62	87	111	1	0.3	B	100	0	(100)	(83)	218	0
						1.0	T	107	1	105	88	219	126
						1.8	B	106	2	109	92	219	252
						2.6	T	112	3	113	96	219	379
						3.4	B	113	4	117	100	220	506
						4.2	T	120	5	121	104	220	633
						5.0	B	120	6	(126)	(109)	221	761
						5.7	T	125	(0-6)			(219)	
14:40	1,209	62	103	107	1	0.3	B	122	0	(124)	(98)	337	0
						1.0	T	132	1	129	103	338	195
						1.8	B	131	2	133	109	339	390
						2.6	T	140	3	140	114	340	586
						3.4	B	140	4	146	120	341	783
						4.2	T	149	5	151	125	342	980
						5.0	B	150	6	(157)	(131)	343	1,178
						5.7	T	157	(0-6)			(340)	
14:47	1,967	62	129	104	1	0.3	B	155	0	(157)	(116)	547	0
						1.0	T	172	1	166	125	550	317
						1.8	B	171	2	175	134	552	636
						2.6	T	182	3	184	143	555	956
						3.4	B	183	4	193	152	558	1,277
						4.2	T	197	5	202	161	560	1,600
						5.0	B	199	6	(210)	(169)	563	1,925
						5.7	T	210	(0-6)			(555)	
14:55	3,500	62	179	99	1	0.3	B	219	0	(225)	(151)	1,008	0
						1.0	T	243	1	235	161	1,013	584
						1.8	B	241	2	247	173	1,019	1,171
						2.6	T	260	3	260	186	1,026	1,762
						3.4	B	260	4	274	200	1,033	2,356
						4.2	T	280	5	289	215	1,041	2,956
						5.0	B	285	6	(305)	(231)	1,050	3,560
						5.7	T	305	(0-6)			(1,027)	
15:02	4,150	62	200	100	1	0.3	B	243	0	(251)	(165)	1,186	0
						1.0	T	271	1	260	174	1,191	687
						1.8	B	264	2	274	188	1,200	1,378
						2.6	T	288	3	290	204	1,209	2,074
						3.4	B	291	4	307	221	1,220	2,777
						4.2	T	316	5	326	240	1,231	3,490
						5.0	B	321	6	(346)	(260)	1,243	4,200
						5.7	T	344	(0-6)			(1,211)	
15:15	5,370	62	236	106	6	0.3	B	288	0	(295)	(190)	1,497	0
						1.0	T	313	1	306	201	1,505	868
						1.8	B	313	2	321	216	1,516	1,741
						2.6	T	339	3	341	236	1,531	2,622
						3.4	B	344	4	364	259	1,548	3,510
						4.2	T	374	5	390	285	1,568	4,410
						5.0	B	385	6	(417)	(312)	1,588	5,320
						5.7	T	415	(0-6)			(1,555)	

a) T.C.'s spot welded to outside wall at indicated inches from inlet end bus bar.
b) Location of T.C. junction on horizontal tube. B = Bottom, T = Top.
c) Outside wall temps by smoothing experimental data. Inside temps by calculation.
d) Corrected for losses. Values in ( ) are average over entire heated length.
e) Net heat up to indicated tube length.

Table 80. FSSTR: DATA SUMMARY SERIES 10018-116

Heat Transfer To Water In Miniature Heat Transfer Section

Reactor No. 10018-110; 0.0265" ID x 0.018" wall x 6" long, Type 316 S.S.
Feed: Water, 5.33 lb/hr = 1.39×10^6 lb/(hr·ft^2)

Run No. 10018-116-	Measured Power, Btu/hr	Experimental Data							Smoothed and Calculated Data				
		Fluid Temp, °F		Press., psig		Tube Wall Thermocouples			Length, In.	Wall Temp, °F [c]		Heat [d] Flux, Btu/(hr·ft²) x 10⁻³	Cumulative [e] Heat, Btu/hr
						Location		Temp, °F					
		In	Out	In	Out	In. [a]	Position [b]			Outside	Inside		
10:58	280	250	225	20	4	0.3	B	245	0	(240)	(255)	76.8	0
						1.0	T	256	1	255	250	"	44
						1.8	B	265	2	265	260	"	89
						2.6	T	265	3	265	260	"	133
						3.4	B	265	4	264	259	"	178
						4.2	T	265	5	262	257	"	222
						5.0	B	261	6	(259)	(254)	"	266
						5.7	T	260	(0-6)			(76.8)	
11:32	557	285	250	71	6	0.3	B	312	0	(309)	(298)	156	0
						1.0	T	327	1	326	315	"	90
						1.8	B	314	2	336	325	"	180
						2.6	T	339	3	339	328	"	271
						3.4	B	338	4	335	324	"	361
						4.2	T	334	5	328	317	"	451
						5.0	B	327	6	(318)	(307)	"	541
						5.7	T	321	(0-6)			(156)	
11:59	956	360	242	144	10	0.3	B	395	0	(395)	(377)	265	0
						1.0	T	395	1	395	375	"	153
						1.8	B	390	2	391	373	"	306
						2.6	T	389	3	386	368	"	459
						3.4	B	384	4	381	362	"	612
						4.2	T	380	5	375	355	"	765
						5.0	B	375	6	(365)	(347)	"	918
						5.7	T	367	(0-6)			(265)	
12:24	1,395	365	248	172	12	0.3	B	417	0	(417)	(392)	389	0
						1.0	T	414	1	415	390	"	225
						1.8	B	414	2	412	387	"	450
						2.6	T	410	3	409	384	"	575
						3.4	B	408	4	406	381	"	900
						4.2	T	405	5	402	377	"	1,165
						5.0	B	405	6	(399)	(374)	"	1,350
						5.7	T	400	(0-6)			(389)	
12:45	1,892	334	251	194	13	0.3	B	435	0	(435)	(397)	552	0
						1.0	T	436	1	437	401	"	319
						1.8	B	440	2	440	404	"	638
						2.6	T	441	3	442	406	"	957
						3.4	B	442	4	443	407	"	1,276
						4.2	T	442	5	441	405	"	1,594
						5.0	B	442	6	(436)	(400)	"	1,913
						5.7	T	436	(0-6)			(552)	
13:15	2,394	367	260	247	16	0.3	B	464	0	(459)	(416)	670	0
						1.0	T	474	1	474	431	"	387
						1.8	B	478	2	479	436	"	775
						2.6	T	473	3	480	437	"	1,162
						3.4	B	481	4	480	437	"	1,549
						4.2	T	480	5	479	436	"	1,936
						5.0	B	480	6	(475)	(432)	"	2,324
						5.7	T	475	(0-6)			(670)	

a) T.C.'s spot welded to outside wall at indicated inches from inlet end bus bar.
b) Location of T.C. junction on horizontal tube. B = Bottom, T = Top.
c) Outside wall temps by smoothing experimental data. Inside temps by calculation.
d) Corrected for losses. Values in ( ) are average over entire heated length.
e) Net heat to fluid up to indicated tube length.

Table 81. FSSTR; DATA SUMMARY SERIES 10018-119

Heat Transfer To Water In Miniature Heat Transfer Section

Reactor No. 10018-110; 0.0265" ID x 0.018" wall x 6" long, Type 316 S.S.
Feed: Water, 4.97 lb/hr = 1.30 x 10^6 lb/(hr·ft^2)

Run No. 10018-119-	Experimental Data								Smooth and Calculated Data				
	Measured Power, Btu/hr	Fluid Temp, °F		Press., psig		Tube Wall Thermocouples			Length, In.	Wall Temp,[c] °F		Heat[d] Flux, Btu/(hr·ft²) x 10^{-3}	Cumulative[e] Heat, Btu/hr
						Location		Temp, °F					
		In	Out	In	Out	In.[a]	Position[b]			Outside	Inside		
15:20	229	475	281	457	31	0.3	B	446	0	(449)	(445)	59.0	0
						1.0	T	445	1	444	400	59.0	34
						1.8	B	437	2	439	435	58.8	68
						2.6	T	438	3	434	430	56.8	102
						3.4	B	430	4	429	425	58.9	136
						4.2	T	430	5	444	440	59.0	170
						5.0	B	449	6	(453)	(449)	58.9	204
						5.7	T	451	(0-6)			(58.9)	
15:44	495	478	368	477	34	0.3	B	458	0	(460)	(452)	134	0
						1.0	T	453	1	454	446	134	78
						1.8	B	449	2	448	440	134	155
						2.6	T	495	3	502	494	136	233
						3.4	B	510	4	523	515	136	312
						4.2	T	530	5	545	537	137	390
						5.0	B	544	6	(567)	(559)	137	470
						5.7	T	562	(0-6)			(135)	
15:56	642	476	419	490	35	0.3	B	462	0	(462)	(451)	171	0
						1.0	T	460	1	461	450	171	99
						1.8	B	460	2	460	449	171	198
						2.6	T	538	3	547	537	175	298
						3.4	B	557	4	577	567	176	399
						4.2	T	585	5	607	597	177	501
						5.0	B	605	6	(637)	(627)	178	604
						5.7	T	630	(0-6)			(174)	
16:16	1,062	482	550	516	39	0.3	B	478	0	(480)	(463)	275	0
						1.0	T	474	1	474	457	274	159
						1.8	B	598	2	607	590	283	320
						2.6	T	642	3	662	646	289	484
						3.4	B	684	4	719	703	291	652
						4.2	T	732	5	774	758	295	821
						5.0	B	771	6	(830)	(814)	298	992
						5.7	T	817	(0-6)			(286)	
16:28	1,462	486	666	540	43	0.3	B	491	0	(555)	(532)	380	0
						1.0	T	555	1	555	532	380	220
						1.8	B	684	2	698	676	395	444
						2.6	T	749	3	778	756	403	674
						3.4	B	811	4	858	836	410	909
						4.2	T	877	5	938	917	418	1,150
						5.0	B	940	6	(1,018)	(997)	425	1,390
						5.7	T	996	(0-6)			(401)	
16:50	1,909	485	800	557	46	0.3	B	504	0	(687)	(658)	504	0
						1.0	T	687	1	687	658	504	291
						1.8	B	792	2	808	780	520	587
						2.6	T	877	3	914	886	523	888
						3.4	B	958	4	1,020	993	546	1,197
						4.2	T	1,043	5	1,128	1,102	560	1,517
						5.0	B	1,128	6	(1,234)	(1,208)	573	1,844
						5.7	T	1,207	(0-6)			(532)	

a) T.C.'s spot welded to outside wall at indicated inches from inlet end bus bar.
b) Location of T.C. junction on horizontal tube. B = Bottom, T = Top.
c) Outside wall temps by smoothing experimental data. Inside temps by calculation.
d) Corrected for losses. Values in ( ) are average over entire heated length.
e) Net heat to fluid up to indicated tube length.

Table 82. FSSTR: DATA SUMMARY SERIES 10018-126

Heat Transfer To Water In Miniature Heat Transfer Section

Reactor No. 10018-122; 0.0265" ID x 0.018" wall x 4" long, Type 316 S.S.
Feed: Water, 99.4 lb/hr = 26.0 x 10^6 lb/(hr·ft^2)

Run No. 10018-126-	Experimental Data								Smoothed and Calculated Data				
	Measured Power, Btu/hr	Fluid Temp, °F		Press., psig		Tube Wall Thermocouples			Length, In.	Wall Temp,[c] °F		Heat[d] Flux, Btu/(hr·ft²) x 10^{-3}	Cumulative[e] Heat, Btu/hr
						Location		Temp, °F					
		In	Out	In	Out	In.[a]	Position[b]			Outside	Inside		
13:40	2,360	67	92	981	204	0.25	B	174	0	(169)	(92)		0
						0.75	T	178	1	179	102	1,050	594
						1.25	B	181	2	183	106	1,052	1,192
						1.75	T	131	3	188	111	1,054	1,788
						2.25	B	185	4	(193)	(116)		2,386
						2.75	T	187	(0-4)			(1,052)	
						3.25	B	190					
						3.50	T	190					
13:48	6,030	67	129	981	229	0.25	B	320	0	(303)	(120)		0
						0.75	T	325	1	330	1 7	2,600	1,496
						1.25	B	335	2	336	153	2,610	3,000
						1.75	T	330	3	348	165	2,620	4,510
						2.25	B	342	4	(364)	(181)		6,050
						2.75	T	345	(0-4)			(2,610)	
						3.25	B	353					
						3.50	T	355					
13:56	9,900	67	168	981	242	0.25	B	462	0	(432)	(149)		0
						0.75	T	465	1	476	194	4,260	2,450
						1.25	B	485	2	484	202	4,280	4,920
						1.75	T	475	3	504	222	4,320	7,400
						2.25	B	493	4	(532)	(250)		9,900
						2.75	T	489	(0-4)			(4,280)	
						3.25	B	511					
						3.50	T	511					
14:04	15,960	67	226	981	248	0.25	B	645	0	(608)	(196)		0
						0.75	T	655	1	664	254	6,650	3,820
						1.25	B	675	2	679	270	6,670	7,660
						1.75	T	666	3	704	297	6,720	11,530
						2.25	B	690	4	(758)	(352)		15,420
						2.75	T	689	(0-4)			(6,670)	
						3.25	B	720					
						3.50	T	721					
14:10	17,390	67	244	981	249	0.25	B	697	0	(666)	(211)		0
						0.75	T	706	1	715	262	7,460	4,290
						1.25	B	727	2	732	280	7,500	8,620
						1.75	T	719	3	765	315	7,580	12,970
						2.25	B	747	4	(816)	(367)		17,360
						2.75	T	746	(0-4)			(7,510)	
						3.25	B	782					
						3.50	T	783					
14:25	19,440	67	265	981	256	0.25	B	764	0	(737)	(237)		0
						0.75	T	770	1	783	286	8,380	4,820
						1.25	B	797	2	807	311	8,440	9,690
						1.75	T	792	3	841	348	8,530	14,590
						2.25	B	820	4	(900)	(408)		19,540
						2.75	T	822	(0-4)			(8,450)	
						3.25	B	860					
						3.50	T	860					

a) T.C.'s spot welded to outside wall at indicated inches from inlet end bus bar.
b) Location of T.C. junction on horizontal tube. B = Bottom, T = Top.
c) Outside wall temps by smoothing experimental data. Inside temps by calculation.
d) Corrected for losses. Values in ( ) are average over entire heated length.
e) Net heat to fluid up to indicated tube length.

Table 83. FSSTR: DATA SUMMARY SERIES 10018-127

Heat Transfer To MCH In Miniature Heat Transfer Section

Reactor No. 10018-110; 0.0265" ID x 0.018" wall x 6" long, Type 316 S.S.
Feed: MCH, 31.4 lb/hr = 8.20 x 10^6 lb/(hr·ft²)

Run No. 10018-127-	Experimental Data								Smoothed and Calculated Data				
	Measured Power, Btu/hr	Fluid Temp, °F		Press., psig		Tube Wall Thermocouples			Length, In.	Wall Temp,[c] °F		Heat[d] Flux, Btu/(hr·ft²) x 10^{-3}	Cumulative[e] Heat, Btu/hr
		In	Out	In	Out	Location In.[a]	Location Position[b]	Temp, °F		Outside	Inside		
10:45	1,834	61	180	985	844	0.3	B	265	0	(246)	(230)	513	0
						1.0	T	276	1	277	241	516	298
						1.8	B	291	2	289	253	518	596
						2.6	T	294	3	300	264	520	896
						3.4	B	304	4	311	275	523	1,198
						4.2	T	305	5	322	286	526	1,500
						5.0	B	322	6	(336)	(300)	529	1,807
						5.7	T	330	(0-6)			(521)	
11:05	3,380	60	278	984	848	0.3	B	431	0	(421)	(355)	1,007	0
						1.0	T	433	1	436	370	1,012	584
						1.8	B	432	2	451	386	1,017	1,170
						2.6	T	436	3	466	401	1,022	1,760
						3.4	B	473	4	481	416	1,027	2,350
						4.2	T	469	5	496	431	1,032	2,950
						5.0	B	496	6	(511)	(446)	1,037	3,540
						5.7	T	506	(0-6)			(1,022)	
11:20	7,020	60	445	985	841	0.3	B	700	0	(642)	(527)	1,997	0
						1.0	T	658	1	665	548	1,976	1,148
						1.8	B	691	2	687	571	1,990	2,300
						2.6	T	697	3	709	593	2,003	3,450
						3.4	B	721	4	731	616	2,016	4,610
						4.2	T	725	5	753	638	2,029	5,780
						5.0	B	756	6	(775)	(660)	2,043	6,960
						5.7	T	767	(0-6)			(2,006)	
11:48	10,370	60	584	986	821	0.3	B	884	0	(835)	(772)	3,020	0
						1.0	T	836	1	846	682	2,990	1,737
						1.8	B	873	2	871	707	3,010	3,470
						2.6	T	878	3	898	733	3,030	5,220
						3.4	B	916	4	951	768	3,060	6,980
						4.2	T	929	5	975	813	3,100	8,720
						5.0	B	981	6	(1,045)	883	3,170	10,370
						5.7	T	1,014	(0-6)			(3,048)	
12:05	1,713	60	178	985	844	0.3	B	254	0	(253)	(229)	472	0
						1.0	T	265	1	266	236	475	274
						1.8	B	280	2	278	244	478	549
						2.6	T	285	3	291	257	481	827
						3.4	B	293	4	303	269	484	1,103
						4.2	T	299	5	316	282	487	1,387
						5.0	B	317	6	(329)	(294)	490	1,668
						5.7	T	325	(0-6)			(481)	

a) T.C.'s spot welded to outside wall at indicated inches from inlet end bus bar.
b) Location of T.C. junction on horizontal tube. B = Bottom, T - Top.
c) Outside wall temps by smoothing experimental data. Inside temps by calculation.
d) Corrected for losses. Values in ( ) are average over entire heated length.
e) Net heat to fluid up to indicated tube length.

Table 84. ESSTR: DATA SUMMARY SERIES 10018-129

Heat Transfer to MCH In Miniature Heat Transfer Section

Reactor No. 10018-110; 0.0265" ID x 0.018" wall x 6" long, Type 316 S.S.
Feed: MCH, 76.5 lb/hr = 19.98 x 10^6 lb/(hr·ft²)

Run No. 10018-129-	Experimental Data								Smoothed and Calculated Data				
	Measured Power, Btu/hr	Fluid Temp, °F		Press., psig		Tube Wall Thermocouples			Length, in.	Wall Temp,[c] °F		Heat[d] Flux, Btu/(hr·ft²) x 10^{-3}	Cumulative[e] Heat, Btu/hr
						Location		Temp, °F					
		In	Out	In	Out	In.[a]	Position[b]			Outside	Inside		
11:05	5,160	60	306	999	258	0.3	B	341	0	(330)	(231)	1,444	0
						1.0	T	350	1	354	255	1,460	839
						1.8	B	379	2	376	277	1,476	1,688
						2.6	T	385	3	397	298	1,490	2,550
						3.4	B	410	4	413	314	1,503	3,410
						4.2	T	405	5	424	325	1,509	4,280
						5.0	B	425	6	(432)	(333)	1,516	5,150
						5.7	T	429	(0-6)			(1,486)	
11:30	9,650	60	403	988	190	0.3	B	536	0	(515)	(342)	2,710	0
						1.0	T	533	1	545	373	2,730	1,572
						1.8	B	580	2	574	403	2,760	3,160
						2.6	T	582	3	600	430	2,780	4,760
						3.4	B	620	4	620	450	2,800	6,370
						4.2	T	615	5	635	464	2,810	7,990
						5.0	B	634	6	(641)	(472)	2,820	9,620
						5.7	T	637	(0-6)			(2,770)	
11:40	10,400	59	515	999	193	0.3	B	563	0	(541)	(357)	2,910	0
						1.0	T	565	1	575	392	2,940	1,692
						1.8	B	613	2	606	424	2,970	3,400
						2.6	T	615	3	634	453	3,000	5,130
						3.4	B	656	4	658	477	3,020	6,870
						4.2	T	649	5	676	496	3,040	8,620
						5.0	B	682	6	(685)	(505)	3,050	10,360
						5.7	T	680	(0-6)			(2,990)	
11:50	11,090	59	535	986	64	0.3	B	596	0	(572)	(379)	3,100	0
						1.0	T	594	1	605	413	3,130	1,800
						1.8	B	640	2	637	446	3,160	3,630
						2.6	T	643	3	666	476	3,190	5,450
						3.4	B	691	4	691	501	3,220	7,310
						4.2	T	685	5	710	521	3,230	9,170
						5.0	B	717	6	(721)	(532)	3,250	11,040
						5.7	T	711	(0-6)			(3,180)	
12:05	5,380	59	306	994	225	0.3	B	348	0	(335)	(233)	1,489	0
						1.0	T	354	1	359	257	1,507	866
						1.8	B	385	2	381	279	1,522	1,741
						2.6	T	389	3	402	300	1,537	2,630
						3.4	B	413	4	418	316	1,549	3,520
						4.2	T	410	5	432	330	1,559	4,420
						5.0	B	435	6	(442)	(340)	1,566	5,330
						5.7	T	437	(0-6)			(1,534)	

a) T.C.'s spot welded to outside wall at indicated inches from inlet end bus bar.
b) Location of T.C. junction on horizontal tube. B = Bottom, T = Top.
c) Outside wall temps by smoothing experimental data. Inside temps by calculation.
d) Corrected for losses. Values in ( ) are average over entire heated length.
e) Net heat to fluid up to indicated tube length.

Table 85. FSSTR: DATA SUMMARY SERIES 10018-130

Heat Transfer to MCH In Miniature Heat Transfer Section

Reactor No. 10018-110, 0.0265" ID x 0.018" wall x 6" long, Type 316 S.S.
Feed: MCH, 58.3 lb/hr = 5.23 x 10^6 lb/(hr·ft^2)

Run No. 10018-130-	Experimental Data								Smoothed and Calculated Data				
	Measured Power, Btu/hr	Fluid Temp, °F		Press., psig		Tube Wall Thermocouples			Length, In.	Wall Temp,[c] °F		Heat[d] Flux, Btu/(hr·ft^2) x 10^{-3}	Cumulative[e] Heat, Btu/hr
						Location		Temp, °F					
		In	Out	In	Out	In.[a]	Position[b]			Outside	Inside		
13:06	1,806	61	130	991	517	0.3	B	190	0	(18[illegible])	(150)	506	0
						1.0	T	200	1	199	162	509	294
						1.8	B	210	2	21[illegible]	174	512	588
						2.6	T	216	3	22[illegible]	184	515	886
						3.4	B	228	4	230	193	517	1,184
						4.2	T	227	5	239	202	519	1,483
						5.0	B	239	6	(245)	(208)	521	1,783
						5.7	T	241	(0.6)			(514)	
13:21	3,580	62	190	991	526	0.3	B	300	0	(288)	(218)	998	0
						1.0	T	308	1	312	242	1,009	580
						1.8	B	332	2	331	261	1,019	1,166
						2.6	T	337	3	346	276	1,026	1,757
						3.4	B	355	4	359	289	1,032	2,351
						4.2	T	354	5	371	301	1,038	2,950
						5.0	B	372	6	(381)	(311)	1,043	3,550
						5.7	T	379	(0.6)			(1,024)	
13:32	7,190	62	300	991	519	0.3	B	498	0	(478)	(348)	2,017	0
						1.0	T	500	1	508	379	2,037	1,172
						1.8	B	540	2	536	407	2,056	2,355
						2.6	T	546	3	562	434	2,073	3,550
						3.4	B	578	4	584	456	2,087	4,750
						4.2	T	574	5	603	476	2,099	4,960
						5.0	B	604	6	(618)	(491)	2,109	7,180
						5.7	T	611	(0.6)			(2,069)	
13:44	10,490	63	388	991	502	0.3	B	649	0	(626)	(499)	2,930	0
						1.0	T	637	1	654	477	2,950	1,699
						1.8	B	690	2	687	511	2,980	3,410
						2.6	T	696	3	717	542	3,010	5,150
						3.4	B	739	4	743	569	3,030	6,890
						4.2	T	730	5	760	586	3,050	8,650
						5.0	B	765	6	(773)	(599)	3,060	10,410
						5.7	T	764	(0.6)			(3,000)	
14:03	14,130	64	474	991	472	0.3	B	790	0	(768)	(541)	3,960	0
						1.0	T	777	1	795	569	3,990	2,298
						1.8	B	834	2	828	603	4,030	4,620
						2.6	T	835	3	858	634	4,070	6,960
						3.4	B	863	4	885	661	4,100	9,320
						4.2	T	874	5	909	686	4,130	11,700
						5.0	B	912	6	(926)	(703)	4,150	14,090
						5.7	T	916	(0.6)			(4,060)	
14:11	15,630	65	509	991	457	0.3	B	850	0	(827)	(581)	4,370	0
						1.0	T	835	1	851	606	4,410	2,537
						1.8	B	895	2	884	640	4,450	5,100
						2.6	T	890	3	916	673	4,490	7,680
						3.4	B	945	4	947	705	4,530	10,280
						4.2	T	954	5	976	735	4,570	12,970
						5.0	B	980	6	(1,003)	(763)	4,600	15,560
						5.7	T	993	(0.6)			(4,490)	

a) T.C.'s spot welded to outside wall at indicated inches from inlet end bus bar.
b) Location of T.C. junction on horizontal tube. B = Bottom, T = Top.
c) Outside wall temps by smoothing experimental data. Inside temps by calculation.
d) Corrected for losses. Values in ( ) are average over entire heated length.
e) Net heat to fluid up to indicated tube length.

Table 86. FSSTR-DATA SUMMARY SERIES 10018-131: HEAT TRANSFER TO MCH IN MINIATURE HEAT TRANSFER SECTION

Reactor No. 10018-110; 0.0265" ID X 0.018" Wall X 6" Long Type 316 S.S.
Feed: MCH, 5.95 lb/hr = 1.56 x 10^6 lb/(hr·ft^2)

Run No. 10018-131-	Experimental Data								Smoothed and Calculated Data				
	Measured Power, Btu/hr	Fluid Temp, °F		Press., psig		Tube Wall Thermocouples			Length, In.	Wall Temp,[c] °F		Heat[d] Flux, Btu/(hr·ft^2) x10^{-3}	Cumulative[e] Heat, Btu/hr
						Location		Temp, °F					
		In	Out	In	Out	In.[a]	Position[b]			Outside	Inside		
14:03	392	67	173	897	828	0.3	B	233	0	(165)	(158)	92	0
						1.3	T	343	1	345	338	102	60
						1.8	B	432	2	450	443	105	117
						2.6	T	505	3	535	529	106	178
						3.4	B	570	4	610	604	107	239
						4.2	T	622	5	637	631	107	301
						5.0	B	637	6	(585)	(579)	107	363
						5.7	T	608	(0-6)			(105)	
14:16	582	68	228	897	893	0.3	B	310	0	(250)	(240)	144	0
						1.0	T	465	1	465	455	155	86
						1.8	B	587	2	610	601	159	177
						2.6	T	682	3	725	716	162	270
						3.4	B	771	4	825	816	165	365
						4.2	T	830	5	560	551	158	458
						5.0	B	560	6	(385)	(375)	152	547
						5.7	T	416	(0-6)			(158)	
14:27	859	88	300	896	833	0.3	B	431	0	(340)	(325)	213	0
						1.0	T	647	1	645	631	235	131
						1.8	B	821	2	860	847	246	270
						2.6	T	847	3	770	757	242	411
						3.4	B	694	4	575	561	232	547
						4.6	T	635	5	527	513	229	651
						5.0	B	523	6	(527)	(514)	229	813
						5.7	T	531	(0-6)			(235)	

a) T.C.'s spot welded to outside wall at indicated in. from inlet end bus
b) Location of T. C. junction on horizontal tube. B = Bottom, T = Top.
c) Outside wall temp's by smoothing experimental data. Inside temp's by calculation.
d) Corrected for losses. Values in ( ) are average over entire heated length.
e) Net heat to fluid up to indicated tube length.

Table 87. FSSTR: DATA SUMMARY SERIES 10018-132

Heat Transfer To MCH In Miniature Heat Transfer Section

Reactor No. 10018-110; 0.0265" ID x 0.018" wall x 6" long, Type 316 S.S.
Feed: MCH, 30.3 lb/hr = 7.91 x 10⁶ lb/(hr·ft²)

Run No. 10018-132-	Experimental Data								Smoothed and Calculated Data				
	Measured Power, Btu/hr	Fluid Temp, °F		Press., psig		Tube Wall Thermocouples			Length, In.	Wall Temp,[d] °F		Heat[e] Flux, Btu/(hr·ft²) x 10⁻³	Cumulative[f] Heat, Btu/hr
						Location		Temp, °F					
		In[a]	Out	In	Out	In.[b]	Position[c]			Outside	Inside		
14:37	778	528	538	972	798	0.3	B	549	0	(547)	(534)	218	0
						1.0	T	554	1	554	541	218	126
						1.8	B	558	2	560	547	218	252
						2.6	T	565	3	566	553	219	378
						3.4	B	567	4	571	558	219	505
						4.2	T	572	5	577	564	219	632
						5.0	B	576	6	(582)	(569)	220	758
						5.7	T	581	(0-6)			(219)	
14:52	1,836	530	578	971	788	0.3	B	600	0	(594)	(563)	516	0
						1.0	T	607	1	609	578	518	299
						1.8	B	620	2	622	591	520	599
						2.6	T	631	3	633	602	522	900
						3.4	B	638	4	644	613	523	1,202
						4.2	T	645	5	653	623	525	1,505
						5.0	B	653	6	(662)	(632)	527	1,809
						5.7	T	660	(0-6)			(522)	
15:02	3,490	530	626	972	746	0.3	B	671	0	(657)	(599)	986	0
						1.0	T	682	1	685	628	994	572
						1.8	B	707	2	710	653	1,000	1,149
						2.6	T	720	3	730	673	1,006	1,729
						3.4	B	742	4	747	690	1,012	2,312
						4.2	T	745	5	762	705	1,015	2,899
						5.0	B	762	6	(776)	(720)	1,019	3,485
						5.7	T	772	(0-6)			(1,005)	
15:20	3,900	533	634	974	697	0.3	B	691	0	(680)	(616)	1,108	0
						1.0	T	704	1	707	645	1,116	645
						1.8	B	730	2	732	668	1,125	1,290
						2.6	T	749	3	756	693	1,132	1,942
						3.4	B	763	4	778	715	1,139	2,600
						4.2	T	771	5	797	734	1,145	3,260
						5.0	B	797	6	(812)	(749)	1,150	3,920
						5.7	T	806	(0-6)			(1,131)	

a) Temp at inlet fitting. Fluid loses ca 10.6 Btu/lb before entering heated section.
b) T.C.'s spot welded to outside wall at indicated inches from inlet end bus bar.
c) Location of T.C. junction on horizontal tube. B = Bottom, T = Top.
d) Outside wall temps by smoothing experimental data. Inside temps by calculation.
e) Corrected for losses. Values in ( ) are average over entire heated length.
f) Net heat to fluid up to indicated tube length.

Table 88. FSSTR; DATA SUMMARY SERIES 10018-133

Heat Transfer To MCH In Miniature Heat Transfer Section

Reactor No. 10018-122; 0.0265" ID x 0.018" wall x 4" long, Type 316 S.S.
Feed: MCH, 69.8 lb/hr = 18.23 x 10^6 lb/(hr·ft^2)

Run No. 10018-133-	Experimental Data								Smoothed and Calculated Data				
	Measured Power, Btu/hr	Fluid Temp, °F		Press., psig		Tube Wall Thermocouples			Length, In.	Wall Temp, °F[c]		Heat[d] Flux, Btu/(hr·ft²) x 10⁻³	Cumulative[e] Heat, Btu/hr
						Location		Temp, °F					
		In	Out	In	Out	In.[a]	Position[b]			Outside	Inside		
13:31	4,710	66	204	976	493	0.25	B	453	0	(448)	(317)		0
						0.75	T	460	1	463	332	2,020	1,165
						1.25	B	467	2	475	344	2,030	2,334
						1.75	T	471	3	488	358	2,030	3,510
						2.25	B	477	4	(507)	(377)		4,690
						2.75	T	489	(0-4)			(2,030)	
						3.25	B	493					
						3.75	T	498					
13:44	9,320	66	320	975	494	0.25	B	743	0	(738)	(506)		0
						0.75	T	742	1	747	515	4,000	2,310
						1.25	B	754	2	757	525	4,020	4,610
						1.75	T	750	3	771	540	4,030	6,960
						2.25	B	759	4	(791)	(561)		9,290
						2.75	T	766	(0-4)			(4,020)	
						3.25	B	780					
						3.75	T	783					
13:57	13,920	66	423	976	457	0.25	B	959	0	(954)	(633)		0
						0.75	T	950	1	954	633	5,980	3,460
						1.25	B	963	2	955	634	5,980	6,910
						1.75	T	943	3	975	655	6,010	10,370
						2.25	B	960	4	(1,035)	(718)		13,870
						2.75	T	963	(0-4)			(6,000)	
						3.25	B	996					
						3.75	T	997					
14:07	16,500	66	473	976	443	0.25	B	1,056	0	(1,050)	(680)		0
						0.75	T	1,044	1	1,050	680	7,150	4,120
						1.25	B	1,063	2	1,051	681	7,150	8,240
						1.75	T	1,041	3	1,082	713	7,150	12,360
						2.25	B	1,068	4	(1,148)	(782)		16,530
						2.75	T	1,053	(0-4)			(7,150)	
						3.25	B	1,098					
						3.75	T	1,127					
14:30	18,730	67	518	977	430	0.25	B	1,146	0	(1,135)	(729)		0
						0.75	T	1,129	1	1,135	729	8,050	4,650
						1.25	B	1,153	2	1,135	729	8,050	9,300
						1.75	T	1,122	3	1,170	765	8,120	13,970
						2.25	B	1,136	4	(1,600)	(1,213)		18,860
						2.75	T	1,237	(0-4)			(8,160)	
						3.25	B	1,234					
						3.75	T	1,474					
14:44	4,770	67	210	976	496	0.25	B	463	0	(539)	(324)		0
						0.75	T	468	1	470	336	2,080	1,198
						1.25	B	477	2	480	346	2,080	2,400
						1.75	T	476	3	495	361	2,090	3,610
						2.25	B	484	4	(521)	(388)		4,820
						2.75	T	489	(0-4)			(2,080)	
						3.25	B	502					
						3.75	T	511					

a) T.C.'s spot welded to outside wall at indicated inches from inlet end bus bar.
b) Location of T.C. junction on horizontal tube. B = Bottom, T = Top.
c) Outside wall temps by smoothing experimental data. Inside temps by calculation.
d) Corrected for losses. Values in ( ) are average over entire heated length.
e) Net heat to fluid up to indicated tube length.

Table 89. IGNITION DELAYS FOR n-OCTANE-OXYGEN-ARGON

Press, psia	Temp, °K	Delay, µsec	Press, psia	Temp, °K	Delay, µsec	Press, psia	Temp, °K	Delay, µsec
80% Argon, ER = 0.1								
9.7	1218	755	16.1	1208	72	25.2	1121	3489
9.6	1220	720	15.7	1158	777	26.0	1169	355
9.4	1217	539	16.5	1175	426	27.0	1163	849
10.0	1214	934	15.2	1106	3471	27.1	1154	1270
9.6	1130	3500	16.0	1164	602	26.9	1125	2516
9.7	1165	2124	15.5	1109	3058			
9.9	1196	1286	16.3	1164	672			
9.7	1151	2678	17.6	1228	72			
			16.6	1167	496			
			16.6	1151	1057			
90% Argon, ER = 0.1								
9.3	1281	339	15.1	1215	533	25.2	1183	1056
9.2	1242	939	15.7	1265	270	25.1	1203	664
9.3	1263	539	15.3	1201	697	24.7	1218	500
9.5	1242	939	15.3	1174	1385	25.6	1169	1611
9.4	1206	1462	15.4	1152	1963	26.0	1160	2033
9.6	1188	2248	15.8	1147	2417	25.5	1141	3260
9.6	1166	3284	15.4	1240	369			
90% Argon, ER = 1.0								
10.1	1221	595	17.4	1164	2484	28.7	1192	873
10.6	1216	5202	16.8	1136	4559	28.8	1157	2551
10.0	1180	3085	17.3	1159	4742	29.4	1173	2565
9.9	1171	2930	16.9	1154	2039	28.2	1150	909
10.8	1252	5259	16.8	1155	2404	29.0	1179	367
10.0	1213	445	16.4	1142	2466	28.4	1175	2861
9.8	1188	2946	16.5	1160	2554			
9.6	1177	3303						

(Continued)

Table 89 (Contd-1). IGNITION DELAYS FOR n-OCTANE-OXYGEN-ARGON

Press, psia	Temp, °K	Delay, μsec	Press, psia	Temp, °K	Delay, μsec	Press, psia	Temp, °K	Delay, μsec
95% Argon, ER = 0.1								
9.3	1285	651	15.8	1243	773	24.8	1177	1900
9.1	1249	968	15.1	1226	962	25.3	1169	2276
9.0	1268	778	15.6	1285	358	25.5	1256	453
9.1	1300	457	15.9	1187	1715	24.0	1175	886
9.4	1259	938	16.1	1169	2465	24.8	1231	803
9.4	1207	1724	16.1	1302	327	25.1	1252	517
9.5	1193	3181						
95% Argon, ER = 0.5								
9.8	1252	2921	16.5	1273	334	26.9	1226	2307
10.2	1326	473	16.5	1255	531	27.1	1246	663
11.3	1416	275	17.1	1231	2905	27.1	1246	1392
10.1	1288	1473	16.5	1211	3120			
10.5	1324	203	16.6	1233	2444			
10.0	1242	3641	16.5	1242	1986			
9.9	1245	3644	16.5	1258	399			
9.8	1238	3638						
9.8	1267	2398						
9.7	1255	2989						
95% Argon, ER = 1.0								
9.6	1230	3404	15.4	1220	1969	27.2	1195	3371
9.7	1278	3171	16.9	1217	3731	27.2	1201	3242
10.1	1283	3106	16.1	1206	3517	27.1	1205	1826
9.9	1273	3236	16.7	1252	1712			
			16.4	1250	1369			

(Continued)

Table 89 (Contd-2). IGNITION DELAYS FOR n-OCTANE-OXYGEN-ARGON

Press, psia	Temp, °K	Delay, μsec	Press, psia	Temp, °K	Delay, μsec	Press, psia	Temp, °K	Delay, μsec
99% Argon, ER = 0.1								
9.8	1379	2243	16.0	1348	2294	26.5	1330	2222
10.0	1370	2560	16.0	1303	2967	26.5	1302	2841
9.9	1421	1001	15.9	1370	1088	25.8	1336	1144
9.7	1424	452	15.9	1354	1403	25.2	1341	954
9.6	1422	1034	15.6	1387	706	24.9	1392	418
9.5	1417	1226	15.1	1379	897	25.0	1395	386
9.4	1438	389	15.0	1408	387			
10.2	1422	937						
99% Argon, ER = 1.0								
9.8	1335	3283	15.2	1282	3501	26.7	1323	1188
9.9	1362	1295	15.9	1357	1164	26.1	1334	965
9.8	1394	651	16.2	1362	874	24.9	1348	516
9.5	1397	521	16.0	1398	326	25.6	1391	65
9.5	1403	457	15.9	1390	456	27.8	1305	2559
9.9	1348	1743	16.4	1359	906			
			16.6	1343	1612			
99% Argon, ER = 1.9								
10.0	1338	2573	16.3	1346	2479	27.1	1330	2471
9.9	1363	2291	16.5	1310	2655	27.6	1290	2707
10.1	1459	400	16.4	1413	661	26.8	1383	1150
10.3	1436	1195	15.9	1413	562	26.2	1391	724
10.1	1440	664	15.9	1425	530	25.8	1440	166
10.3	1425	1291	16.7	1397	1186	25.4	1389	790
10.2	1331	2602	16.5	1370	2164	25.1	1393	790
10.2	1301	3037				25.0	1405	462

Table 90. IGNITION DELAYS FOR DECALIN-OXYGEN-ARGON

Press, psia	Temp, °K	Delay, µsec	Press, psia	Temp, °K	Delay, µsec	Press, psia	Temp, °K	Delay, µsec
80% Argon, ER = 0.1								
10.4	1218	1743	17.4	1243	439	28.9	1233	159
10.4	1251	1040	17.5	1217	753	29.4	1193	708
10.3	1261	561	18.3	1206	1106	29.4	1204	474
10.3	1295	324	18.5	1178	2349	29.9	1157	2956
10.8	1201	3627	18.8	1162	3895	29.9	1183	980
						30.0	1172	1211
						29.9	1156	3887
90% Argon, ER = 0.1								
9.3	1224	1402	14.6	1185	1321	24.6	1187	958
9.1	1231	1204	14.7	1220	667	24.2	1200	663
9.2	1266	405	14.7	1247	369	24.1	1226	334
9.1	1241	905	15.1	1180	1781	25.0	1163	1706
9.0	1239	938	15.6	1177	1977	25.6	1164	1444
9.3	1196	1987	15.7	1158	2686	25.8	1154	2225
9.6	1182	3299						
90% Argon, ER = 0.2								
10.0	1247	1157	16.0	1257	137	26.4	1198	369
9.7	1244	1088	15.9	1197	672	26.5	1176	601
9.6	1269	582	15.8	1223	541	27.1	1172	2199
9.8	1301	276	16.4	1168	3329			
9.8	1185	4015	16.5	1201	672			
9.7	1189	4019	16.4	1183	4346			
9.7	1025	3499	16.5	1203	639			
			16.1	1178	2738			
95% Argon, ER = 0.1								
8.8	1200	3186	15.1	1253	452	25.6	1235	514
8.9	1243	1611	15.2	1250	548	26.0	1220	1409
8.9	1230	1926	15.2	1218	1569	25.6	1219	961
8.9	1275	779	15.4	1248	516	25.9	1190	2224
9.1	1325	230	15.6	1246	645	31.6	1190	2542
8.7	1270	843	15.7	1235	932	36.0	1170	3161
9.0	1308	262	15.9	1203	1913			
			16.1	1187	2222			

(Continued)

Table 90 (Contd-1). IGNITION DELAYS FOR DECALIN-OXYGEN-ARGON

Press, psia	Temp, °K	Delay, µsec	Press, psia	Temp, °K	Delay, µsec	Press, psia	Temp, °K	Delay, µsec
95% Argon, FR = 0.2								
9.4	1260	1075	15.4	1267	457	26.1	1244	1006
9.0	1254	1203	15.4	1253	845	25.9	1266	326
9.2	1300	362	15.8	1238	1231	25.6	1246	649
9.9	1250	1820	16.2	1228	1971	26.3	1226	1809
9.7	1222	3678	15.8	1177	3826	26.5	1220	1935
9.1	1252	1560	16.5	1228	1874	26.9	1219	1806
						26.9	1211	2057
99% Argon, ER = 0.2								
8.8	1265	2195	15.2	1321	444	25.6	1266	847
8.7	1282	1448	15.3	1302	632	25.0	1271	785
8.7	1317	1078	15.2	1265	1254	24.8	1295	442
9.0	1385	354	15.4	1249	1593	25.6	1254	1681
9.1	1388	322	16.2	1247	2092	26.0	1224	2112
			15.9	1214	2850	26.2	1207	2845
99% Argon, ER = 0.5								
9.8	1374	1063	15.7	1322	1466	26.6	1327	1404
9.4	1356	1444	15.5	1337	1247	26.0	1336	1215
9.3	1380	903	15.5	1372	515	25.2	1348	609
9.1	1393	711	15.1	1360	707	25.4	1376	193
9.0	1415	325	16.2	1311	2227	25.5	1361	321
9.9	1320	3633	16.5	1296	2726	26.5	1281	2212
9.9	1349	2179				26.8	1276	2683
99% Argon, ER = 1.0								
9.9	1341	3223	16.5	1398	1467	27.4	1323	2954
10.0	1384	2860	15.9	1395	977	27.3	1347	2130
9.8	1393	2149	15.8	1420	458	26.9	1364	1749
9.6	1420	1571	15.7	1407	653	26.3	1388	1106
9.5	1431	1115	16.6	1356	2586	25.8	1397	717
9.6	1453	395	16.4	1363	2137	26.0	1422	393

Table 91. IGNITION DELAYS FOR "SHELLDYNE"-OXYGEN-ARGON

* Delay times for early ignition.
[ ] Delay times for two ignition points
on the same shock tube run.

Press, psia	Temp, °K	Delay, μsec	Press, psia	Temp, °K	Delay, μsec	Press, psia	Temp, °K	Delay, μsec
90%m Argon, ER = 0.1								
			13.9	1426	155			
			14.3	1400	214			
			14.4	1341	528			
			14.3	1280	643			
			13.7	1212	965*			
			14.1	1178	2255*			
			14.2	1215	1064*			
			14.8	1193	2032*			
			15.8	1180	2313*			
			13.8	1361	249			
			15.0	1484	82			
			13.9	1316	554			
95%m Argon, ER = 0.2								
8.5	1436	531	14.0	1378	833	23.5	1344	533
[8.4	1456	193*]	14.7	1466	216	24.3	1414	191
8.5	1471	542]	14.5	1480	224	24.1	1387	226
[8.0	1432	130*]	14.0	1478	187	24.1	1372	360
8.1	1449	546]	14.7	1574	104	23.7	1325	832
8.7	1563	87*	14.9	1569	110	24.6	1331	818
8.1	1463	144*	14.8	1377	502	24.8	1327	980
8.3	1443	610	15.2	1372	884	24.8	1287	928
8.3	1412	571	15.5	1328	1040	25.0	1267	1314
8.8	1433	567	15.3	1279	2546	25.3	1233	3134
8.8	1375	543*	15.7	1322	1387	25.1	1249	2896
8.8	1312	785*	16.1	1312	1609	24.5	1249	2559
[8.7	1242	2430*]	16.0	1269	3006			
8.9	1291	983*]						
9.3	1332	2189						
8.6	1326	1703						

(Continued)

Table 91 (Contd-1). IGNITION DELAYS FOR "SHELLDYNE"-OXYGEN-ARGON

Press, psia	Temp, °K	Delay, μsec	Press, psia	Temp, °K	Delay, μsec	Press, psia	Temp, °K	Delay, μsec
99%m Argon, ER = 0.1								
9.0	1433	2096	⎡14.9	1444	830*⎤	24.7	1473	649
8.7	1498	611*	⎣15.2	1466	1378⎦	24.4	1493	406
8.7	1472	843*	⎡14.6	1456	600*⎤	25.1	1454	726
8.8	1447	1808	⎣14.9	1481	1200⎦	25.0	1420	1461
8.9	1478	981*	14.9	1514	389*	24.6	1371	1433
9.0	1461	1946	15.2	1558	298*	26.9	1403	2629
			14.9	1552	278*	24.5	1427	2280
			15.3	1446	2983	25.6	1350	3336
			15.2	1454	1509	26.8	1370	4217
			⎡15.4	1472	574*⎤			
			⎣15.7	1495	1091⎦			
			15.5	1461	1558			
			15.6	1451	1847			
			14.6	1434	1187			
			14.5	1456	882			
			15.3	1554	281*			
			15.3	1431	1222			
			15.3	1349	3537			
			15.1	1368	3284			
			15.4	1430	1176			

Table 92. IGNITION DELAYS FOR "SHELLDYNE" H-OXYGEN-ARGON-MIXTURES

Press, psia	Temp, °K	Delay, μsec	Press, psia	Temp, °K	Delay, μsec	Press, psia	Temp, °K	Delay, μsec
80%m Argon, ER = 0.1								
			14.2	1261	331	24.0	1264	321
			14.6	1247	339	24.1	1298	92
			15.3	1245	256	23.7	[illegible]	601
			15.1	1191	1507	24.3	1201	785
						24.2	1151	1539
						24.7	1147	3195
95%m Argon, ER = 0.1								
			14.7	1470	108	24.6	1537	59
			14.6	1428	136	24.0	1472	65
			14.0	1355	308	24.6	1450	156
						24.5	1447	84
						24.2	1382	99
						24.0	1312	365
						24.1	1265	730
						24.1	1217	1715
						23.9	1257	676
95% Argon, ER = 0.2								
9.3	1423	228	14.3	1432	130	24.5	1386	206
8.5	1311	329	14.9	1514	73	24.7	1366	183
9.1	1392	368	14.9	1412	143	25.3	1360	231
8.6	1323	572	15.2	1376	241	24.4	1271	777
9.0	1311	953	14.8	1408	155			
9.2	1291	1196	14.7	1354	269			
9.7	1286	3622	15.1	1334	362			
			15.2	1288	676			
			15.6	1246	1483			
			15.8	1225	3403			

(Continued)

Table 92 (Contd-1). IGNITION DELAYS FOR "SHELLDYNE" H-OXYGEN-ARGON-MIXTURES

Press, psia	Temp, °K	Delay, μsec	Press, psia	Temp, °K	Delay, μsec	Press, psia	Temp, °K	Delay, μsec
98% Argon, ER = 0.2								
6.6	1285	1945	14.9	1519	247	23.7	1466	175
8.7	1717	123	15.1	1567	155	24.2	1450	222
8.8	1677	132	15.0	1456	368	22.9	1349	512
9.0	1667	145	15.0	1393	551	24.1	1418	261
9.0	1611	209	14.8	1295	3033	24.1	1341	489
9.1	1590	215	15.4	1385	557	24.1	1303	1092
						24.6	1256	2445
98% Argon, ER = 0.5								
8.6	1470	382	14.4	1503	220	24.1	1461	183
9.0	1583	167	14.9	1525	191	24.4	1442	236
9.5	1593	180	15.4	1507	200	24.4	1377	463
9.0	1466	612	15.0	1433	328	24.0	1331	747
9.0	1418	639	15.2	1397	471	24.1	1280	1580
9.4	1465	478	15.0	1295	1602	24.9	1261	3046
8.7	1382	804	15.7	1295	1716			
9.3	1425	432						
9.3	1376	947						
9.4	1372	1154						
9.7	1372	2867						

Table 93. IGNITION DELAYS FOR DMD-OXYGEN-ARGON

Press, psia	Temp, °K	Delay, μsec	Press, psia	Temp, °K	Delay, μsec	Press, psia	Temp, °K	Delay, μsec
80% Argon, ER = 0.1								
11.0	1553	282	15.3	1351	219	25.6	1316	92
10.1	1436	388	15.5	1393	80	23.9	1228	249
10.1	1432	395	14.7	1283	278	24.7	1230	495
10.0	1436	484	15.2	1292	332	26.0	1225	660
10.4	1394	486	15.9	1287	884	26.0	1161	3699
10.2	1331	910	16.0	1248	466	26.3	1208	1329
9.6	1225	3969	15.9	1187	3768			
9.6	1258	3122	16.6	1250	912			
90% Argon, ER = 0.1								
8.8	1408	252	14.5	1346	268	25.8	1403	117
8.9	1422	179	15.6	1453	112	24.5	1320	283
9.2	1421	253	15.2	1418	98	25.2	1321	917
9.5	1398	419	14.8	1307	937	25.6	1307	432
9.7	1338	1096	15.4	1285	1022	26.2	1256	1079
10.3	1331	4051	16.2	1293	959	25.7	1195	3634
			16.4	1256	1268	26.6	1247	2061
			16.0	1191	3855			
90% Argon, ER = 0.2								
9.4	1419	226	15.2	1384	261	25.3	1369	186
9.2	1425	175	15.8	1449	127	26.6	1388	180
9.6	1388	468	15.8	1378	230	26.3	1349	266
9.9	1342	1003	15.9	1333	331	25.3	1260	777
10.4	1334	891	15.8	1282	1036	26.5	1255	937
			16.8	1269	939	27.3	1251	1962
			16.7	1215	3348			

Table 94. IGNITION DELAYS FOR "SHELLDYNE"-DECALIN-OXYGEN-ARGON

Press, psia	Temp, °K	Delay, μsec	Press, psia	Temp, °K	Delay, μsec	Press, psia	Temp, °K	Delay, μsec
90% Argon, ER = 0.1								
9.4	1350	357	14.5	[illegible]	210	31.5	1338	122
9.3	1263	1037	14.8	[illegible]	486	24.8	1290	316
9.7	1234	1916	14.7	[illegible]	649	25.0	1288	674
9.7	1263	1057	14.3	[illegible]	1257	24.8	1195	1244
			15.8	1196	1817			
			15.8	1162	3303			
			16.1	1201	3269			
			15.2	1198	1429			
			15.5	1223	1124			
95% Argon, ER = 0.2								
9.6	1464	180	15.0	1425	146	25.1	1415	107
8.9	1361	583	14.6	1366	500	24.4	1354	176
9.2	1358	599	15.3	1384	354	24.0	1305	486
9.1	1301	1298	14.7	1304	951	24.7	1283	635
9.5	1297	1800	15.4	1320	571	25.9	1281	1429
10.1	1319	3219	15.6	1302	770	25.6	1247	3247
			15.4	1241	1419			
			15.9	1214	3351			
98% Argon, ER = 0.2								
9.1	1516	289						
8.7	1370	1116	14.4	1407	305	23.9	1391	200
9.1	1422	479	14.6	1455	244	24.0	1357	314
			14.7	1385	241	24.3	1322	706
			14.8	1338	727	24.4	1272	2870
			15.5	1320	1192	23.9	1278	1186
			15.3	1277	1594			
99% Argon, ER = 1.0								
9.5	1493	3264	15.2	1471	2550	24.4	1416	2887
9.5	1563	2686	15.3	1550	776	24.7	1500	804
9.2	1598	730	15.2	1497	2732	25.0	1585	250
8.8	1601	486	15.2	1535	964	24.6	1545	446
9.0	1679	327	14.9	1553	925	24.5	1523	708
			14.9	1590	459			
			15.6	1690	218			
			18.8	1724	96			

Table 95. IGNITION DELAYS FOR "SHELLDYNE"-BINOR S-OXYGEN-ARGON

Press, psia	Temp, °K	Delay, μsec	Press, psia	Temp, °K	Delay, μsec	Press, psia	Temp, °K	Delay, μsec
95% Argon, ER = 0.2								
8.6	1346	386	13.9	1339	274	23.5	1346	275
8.3	1436	323	14.1	1382	213	24.1	1343	287
8.3	1273	3774	14.5	1340	421	23.2	1267	770
			14.6	1267	1231	22.9	1212	2735
			14.8	1220	2667	23.9	1276	847
			15.1	1268	1356	23.8	1265	1023
						24.3	1268	1017
99% Argon, ER = 1.0								
9.1	1777	170	14.3	1466	834	24.5	1557	178
			15.0	1597	186	24.5	1523	283
			15.2	1572	393	24.3	1479	415
			15.3	1476	651	24.1	1418	716
			15.1	1399	1165	25.1	1404	1182
			15.9	1378	2541	25.9	1356	2569
						25.8	1384	1934

Table 96. CHARACTERISTIC PROPERTIES OF F-71

Hydrogen-Carbon Ratio	2.16
Molecular Weight	177.3
Critical Temperature	737 °F
Critical Pressure	252 psia
Critical Volume	0.0683 ft^3/lb
Melting Point	-51 °F
Heat of Combustion	18930 Btu/lb
Normal Boiling Range	420-543 °F

Table 97. LIQUID PROPERTIES OF F-71 AT SATURATION PRESSURE

Temperature, °F	Heat of Vaporization, Btu/lb	Vapor Pressure, psia	Specific Heat, Btu/lb-°F	Density, lb/ft^3	Viscosity, lb/ft-hr	Thermal Conductivity, Btu/ft-hr°F	Enthalpy, Btu/lb
0	157.7	0.0	0.344	50.7	6.85	0.0417	-181.7
100	148.7	0.005	0.412	48.4	2.50	0.0455	-140.7
200	138.8	0.147	0.471	45.9	1.23	0.0483	- 93.0
300	127.7	1.59	0.522	43.2	0.734	0.0493	- 38.6
400	114.6	8.76	0.569	40.1	0.494	0.0487	21.3
500	98.8	31.3	0.615	36.7	0.354	0.0468	85.8
600	78.1	84.4	0.674	32.3	0.259	0.0434	155.8
700	44.4	192.0	0.876	25.5	0.175	0.04	233.6

Table 98. GAS PROPERTIES OF F-71

Temp., °F	Pressure, psia																
	0	100	200	300	400	500	600	700	800	900	1000	1100	1200	1300	1400	1500	1600
Viscosity, lb/ft-hr																	
500	[illegible]																
600	[illegible]																
700	[illegible]																
800	[illegible]	[illegible]	[illegible]	[illegible]	[illegible]												
900	[illegible]	[illegible]	[illegible]	[illegible]	[illegible]	[illegible]	0.0798	0.1189									
1000	[illegible]	[illegible]	[illegible]	[illegible]	[illegible]	[illegible]	0.0932	[illegible]	[illegible]	0.0962	0.1163	0.1273					
1100	[illegible]	[illegible]	[illegible]	[illegible]	[illegible]	[illegible]	[illegible]	[illegible]	[illegible]	[illegible]	[illegible]	[illegible]	0.1016	0.1134	0.1211	0.1303	0.1372
1200	[illegible]	[illegible]	[illegible]	[illegible]	[illegible]	[illegible]	[illegible]	[illegible]	[illegible]	[illegible]	[illegible]	[illegible]	[illegible]	[illegible]	0.0984	0.1148	0.1146
1300	[illegible]	[illegible]	[illegible]	0.0846	0.0860	[illegible]	[illegible]	[illegible]	[illegible]	[illegible]	[illegible]	[illegible]	[illegible]	[illegible]	[illegible]	0.0888	0.0912
Thermal Conductivity, Btu/(ft-hr-°F)																	
500	[illegible]																
600	0.0190																
700	[illegible]																
800	[illegible]	0.0457	0.0522	0.0616	[illegible]												
900	[illegible]	[illegible]	[illegible]	[illegible]	[illegible]	[illegible]	0.0968	[illegible]									
1000	[illegible]	[illegible]	[illegible]	[illegible]	[illegible]	[illegible]	[illegible]	[illegible]	[illegible]	[illegible]	0.1008	0.1074					
1100	[illegible]	[illegible]	0.0810	[illegible]	[illegible]	[illegible]	[illegible]	[illegible]	[illegible]	[illegible]	[illegible]	[illegible]	0.1100	0.1146	[illegible]	0.1138	0.1168
1200	[illegible]	[illegible]	[illegible]	[illegible]	[illegible]	[illegible]	[illegible]	[illegible]	[illegible]	[illegible]	[illegible]	[illegible]	[illegible]	[illegible]	0.1090	0.1076	0.1117
1300	[illegible]	[illegible]	[illegible]	0.0516	[illegible]	[illegible]	[illegible]	[illegible]	[illegible]	[illegible]	[illegible]	[illegible]	0.0901	0.0987	0.0982	0.1056	0.1070
Specific Heat at Constant Pressure, Btu/lb-°F																	
100	[illegible]																
200	[illegible]																
300	[illegible]																
400	[illegible]																
500	[illegible]																
600	0.571																
700	[illegible]																
800	[illegible]	0.649	0.648	0.667	0.768												
900	0.665	0.679	0.690	0.716	0.777	0.882	0.871	0.811									
1000	[illegible]	0.701	0.712	0.727	0.746	0.785	0.780	0.816	0.869	0.959	0.818	0.909					
1100	[illegible]	0.729	0.735	0.746	0.751	0.765	0.776	0.787	0.777	[illegible]	0.820	0.827	0.804	0.816	0.806	0.797	0.791
1200	[illegible]	0.755	0.760	0.766	0.772	0.771	0.778	0.742	0.784	[illegible]	0.810	0.816	0.821	0.825	0.816	0.820	0.821
1300	0.771	0.781	0.785	0.790	0.796	0.799	0.805	0.807	0.812	0.815	0.814	0.825	0.826	0.830	0.830	0.836	0.835
Enthalpy, Btu/lb																	
100	7.9																
200	43.8																
300	84.5																
400	137.5																
500	[illegible]																
600	244.8																
700	319.3																
800	[illegible]	344.3	369.8	336.9	308.5												
900	[illegible]	[illegible]	415.8	410.3	[illegible]	390.9	382.5	375.1									
1000	[illegible]	[illegible]	488.5	483.2	477.6	471.9	466.5	460.9	455.6	450.2	446.6	455.6					
1100	[illegible]	[illegible]	560.8	556.7	552.5	548.5	546.2	540.6	536.7	533.8	529.8	526.5	523.8	521.7	520.1	518.9	518.0
1200	642.2	[illegible]	635.6	636.1	628.8	625.6	[illegible]	[illegible]	616.3	613.6	611.0	608.3	606.1	603.9	601.9	600.3	598.8
1300	718.7	715.8	712.6	710.9	707.1	704.3	701.7	[illegible]	696.0	[illegible]	692.6	690.6	688.6	686.6	684.8	683.2	681.7
Entropy, Btu/lb-°F																	
800	0.903	0.930	0.921	0.907	0.889												
900	0.996	0.987	0.977	0.968	0.957	0.971	0.962	0.936									
1000	1.050	1.030	1.030	1.022	1.016	1.010	1.009	1.000	0.996	0.990	0.988	0.987					
1100	1.098	1.079	1.081	1.076	1.069	1.064	1.060	1.056	1.053	1.050	1.047	1.044	1.042	1.040	1.038	1.037	1.036
1200	1.146	1.137	1.130	1.126	1.117	1.119	1.110	1.108	1.106	1.103	1.100	1.098	1.096	1.095	1.092	1.090	1.089
1300	1.194	1.188	1.179	1.173	1.168	1.165	1.161	1.158	1.156	1.153	1.151	1.149	1.147	1.145	1.144	1.142	1.141
Density, lb/ft³																	
800	0.	1.499	3.66	7.64	21.81												
900	0.	1.337	3.36	5.20	8.10	11.41	17.15	22.50									
1000	0.	1.218	2.65	4.50	6.22	8.61	10.80	13.57	16.38	19.19	21.36	22.79					
1100	0.	1.118	2.37	3.75	5.21	6.97	8.62	10.57	12.17	14.24	15.91	17.75	19.35	20.69	21.67	22.69	23.16
1200	0.	1.039	2.16	3.37	4.65	6.00	7.38	8.78	10.18	11.57	12.99	14.38	15.7	17.06	18.30	19.38	20.20
1300	0.	0.970	2.00	3.08	4.31	5.56	6.54	7.72	8.87	10.06	11.22	12.56	13.46	14.57	15.63	16.63	17.57
Compressibility Factor																	
800	1.	0.875	0.717	0.516	0.261												
900	1.	0.909	0.806	0.701	0.540	0.510	0.425	0.381									
1000	1.	0.929	0.859	0.780	0.727	0.671	0.625	0.548	0.557	0.531	0.530	0.569					
1100	1.	0.947	0.890	0.844	0.803	0.767	0.737	[illegible]	0.656	0.675	0.646	[illegible]	0.637	0.667	0.686	0.706	0.732
1200	1.	0.952	0.917	0.876	0.843	0.813	0.810	0.778	0.752	0.773	0.744	[illegible]	0.759	0.760	0.766	0.776	0.788
1300	1.	0.964	0.930	0.906	0.875	0.855	0.842	0.832	0.806	0.800	0.797	[illegible]	0.816	0.827	0.841	0.857	[illegible]
Ratio of Specific Heats																	
800	1.018	1.063	1.136	1.861													
900	1.017	1.058	1.062	1.129	[illegible]	1.444	1.773										
1000	1.016	1.036	1.048	1.087	1.109	1.156	1.298	1.309	1.459	1.567	1.691						
1100	[illegible]	1.023	1.033	1.066	1.069	1.096	1.105	1.127	1.152	1.181	1.216						
1200	1.015	1.020	1.027	1.036	1.044	1.057	1.067	1.078	1.098	1.100	1.112						
1300	1.019	1.019	1.024	1.030	1.036	1.049	1.049	1.049	1.064	1.069	1.073						
Sonic Velocity, ft/sec																	
800	600	537	437	396													
900	619	568	509	454	418	417	488										
1000	645	600	561	529	468	479	519	491	500	532	517						
1100	667	636	603	571	530	547	539	537	540	566	559						
1200	687	661	638	620	577	600	581	590	579	604	610						
1300	708	681	670	656	648	643	642	643	639	635	660						
Joule-Thomson Coefficient, °F/psia																	
800	0.1363	0.1356	0.1618	0.2372													
900	0.0734	0.0877	0.1174	0.1116	0.1171	0.1176	0.1004										
1000	0.0613	0.0703	0.0723	0.0777	0.0751	0.0736	0.0719	0.0676	0.0621	0.0590	0.0561						
1100	0.0517	0.0559	0.0541	0.0559	[illegible]	0.0548	0.0504	0.0476	0.0449	0.0425	0.0497						
1200	0.0427	0.0459	0.0446	0.0448	0.0440	0.0428	0.0396	0.0370	0.0364	0.0330	0.0356						
1300	0.0373	0.0373	0.0376	0.0367	0.0354	0.0338	0.0319	0.0300	0.0292	0.0266	0.0253						

Table 99. CHARACTERISTIC PROPERTIES OF TRANS-DECALIN

Molecular Weight	138.3
Critical Temperature	767 °F
Critical Pressure	422 psia
Critical Volume	0.0565 ft^3/lb
Heat of Combustion	18,289 Btu/lb

Table 100. LIQUID PROPERTIES OF TRANS-DECALIN AT SATURATION PRESSURE

Temperature, °F	Heat of Vaporization, Btu/lb	Vapor Pressure, psia	Specific Heat, Btu/lb-°F	Density, lb/ft^3	Viscosity, lb/ft-hr	Thermal Conductivity, Btu/ft-hr°F	Enthalpy, Btu/lb
0	150.3	0.001	0.366	56.3	3.74	0.054	-173.3
100	143.2	0.065	0.423	53.8	1.679	0.058	-135.5
200	135.2	0.905	0.475	51.1	0.967	0.061	- 90.6
300	126.0	5.75	0.520	48.2	0.642	0.062	- 40.4
400	115.1	22.3	0.563	45.1	0.464	0.061	14.3
500	101.8	62.5	0.608	41.6	0.352	0.059	72.6
600	84.6	141.5	0.660	37.4	0.271	0.058	135.8
700	58.9	278.0	0.784	31.6	0.201	0.053	206.7

Table 101. GAS PROPERTIES OF TRANS-DECALIN

Temp, °F	Pressure, psia: 0	100	200	300	400	500	600	700	800	900	1000
Viscosity, lb/ft-hr											
400	[illegible]										
500	0.0443										
600	0.0473	0.0517									
700	0.0522	0.0537	0.0553								
800	0.0544	0.0561	0.0575	0.0646	0.0696	0.0856	0.1616				
900	0.0577	0.0597	0.0570	0.0616	0.0635	0.0646	0.0717	0.0817	0.0877	0.1064	0.1447
1000	0.0613	0.0613	0.0625	0.0636	0.0651	0.0671	0.0686	0.0731	0.0780	0.0846	0.0798
1100	0.0629	0.0630	0.0644	0.0658	0.0671	0.0686	0.0706	0.0736	0.0755	0.0796	0.0849
Thermal Conductivity, Btu/ft-hr-°F											
400	0.0146										
500	0.0177										
600	0.0208	0.0271									
700	0.0240	0.0254	0.0287								
800	0.0273	0.0282	0.0316	0.0351	0.0409	0.0541	0.1071				
900	0.0307	0.0317	0.0349	0.0377	0.0414	0.0465	0.0552	0.0651	0.0777	0.0919	0.1068
1000	0.0343	0.0352	0.0396	0.0410	0.0440	0.0475	0.0516	0.0567	0.0626	0.0695	0.0771
1100	0.0378	0.0389	0.0423	0.0445	0.0472	0.0502	0.0536	0.0574	0.0615	0.0659	0.0707
Specific Heat, Btu/lb-°F											
0	0.278										
100	0.334										
200	0.385										
300	0.442										
400	0.478										
500	0.511										
600	0.541	0.575									
700	0.569	0.589	0.649								
800	0.596	0.609	0.628	0.664	0.768	1.902	0.667				
900	0.623	0.631	0.642	0.654	0.683	0.724	0.799	0.876	1.024	0.877	0.796
1000	0.649	0.655	0.662	0.671	0.685	0.697	0.718	0.740	0.765	0.790	0.818
1100	0.676	0.678	0.686	0.690	0.697	0.706	0.715	0.726	0.737	0.748	0.763
Enthalpy, Btu/lb											
0	-23.0										
100	7.8										
200	44.5										
300	86.5										
400	132.5										
500	181.8										
600	234.5	225.0									
700	290.0	283.1	276.1								
800	348.5	342.9	336.7	328.9	317.9	302.1	279.5				
900	409.2	404.9	400.1	394.8	388.6	381.4	372.9	363.2	352.6	341.5	330.6
1000	472.8	469.2	465.5	461.2	456.8	452.0	446.9	441.6	435.2	430.8	425.6
1100	538.9	535.8	532.6	529.2	525.7	522.1	518.4	514.6	510.0	507.1	503.6
Entropy, Btu/lb-°F											
600	0.780	0.765									
700	0.830	0.817	0.781								
800	0.878	0.867	0.833	0.822	0.811	0.799	0.776				
900	0.924	0.896	0.881	0.872	0.865	0.857	0.849	0.841	0.830	0.824	0.801
1000	0.968	0.939	0.928	0.920	0.915	0.907	0.902	0.897	0.890	0.887	0.883
1100	1.015	0.984	0.972	0.965	0.959	0.954	0.949	0.945	0.941	0.936	0.935
Density, lb/ft³											
600	0.	1.438									
700	0	1.253	2.88								
800	0.	1.126	2.48	4.27	7.68	15.79	27.74				
900	0.	1.009	2.17	3.53	[illegible]	7.31	12.08	15.75	18.73	25.16	27.55
1000	0.	0.906	1.950	3.09	4.38	5.94	7.49	9.95	11.82	13.67	16.16
1100	0.	0.851	1.781	2.78	3.86	5.03	6.24	7.64	9.07	10.56	12.13
Compressibility Factor											
600	1.	0.834									
700	1.	0.887	0.765								
800	1.	0.918	0.836	0.718	0.578	0.326	0.222				
900	1.	0.939	0.876	0.806	0.729	0.648	0.564	0.482	0.405	0.390	0.387
1000	1.	0.953	0.905	0.846	0.806	0.756	0.707	0.661	0.618	0.581	0.547
1100	1.	0.964	0.927	0.871	0.855	0.821	0.786	0.757	0.729	0.704	0.681
Ratio of Specific Heats											
600	1.027	1.082									
700	1.026	1.052	1.137								
800	1.025	1.041	1.075	[illegible]	1.446						
900	1.024	1.036	1.051	[illegible]	1.139	1.253	1.521	2.365			
1000	1.023	1.030	1.041	[illegible]	1.080	1.114	1.160	1.221	1.306	1.416	1.548
1100	1.022	1.028	1.035	[illegible]	1.057	1.072	1.091	1.113	1.139	1.164	1.201
Sonic Velocity, ft/sec											
600	626	527									
700	654	586	[illegible]								
800	681	629	570	[illegible]	418						
900	708	667	624	[illegible]	533	491	472	505			
1000	733	701	664	[illegible]	605	577	553	556	528	528	526
1100	757	732	706	[illegible]	660	640	625	610	601	595	588
Joule-Thomson Coefficient, °F/psi											
600	0.1477	0.2070									
700	0.1107	0.1316	0.1743								
800	0.876	0.0944	0.1049	0.1570	0.1764						
900	0.0682	0.0713	0.0779	0.0873	0.0981	0.1081	0.1155	0.1182			
1000	0.0539	0.0569	0.0601	0.0636	0.0676	0.0712	0.0727	0.0726	0.0707	0.0689	0.0648
1100	0.0451	0.0466	0.0481	0.0499	0.0512	0.0520	0.0523	0.0519	0.0510	0.0500	0.0487

Table 102. CHARACTERISTIC PROPERTIES OF "SHELLDYNE" II

Critical Temperature	945.4 °F
Critical Pressure	448 psia
Critical Volume	0.0478 ft^3/lb
Heat of Combustion	17845 Btu/lb
Normal Boiling Point	501.8 °F

Table 103. LIQUID PROPERTIES OF "SHELLDYNE" AT SATURATION PRESSURE

Temp, °F	Density, lb/cu ft	Viscosity, lb/ft/hr	Thermal Conductivity, Btu/hr/ft/°F	Surface Tension pndl[a]/ft	Heat Capacity, Btu/lb/°F	Heat Content, Btu/lb	Heat of Vaporization, Btu/lb	Vapor Pressure, psia
-60	72.07	12000.	.098	.0994	.207	-13.6	144.7	-
-40	71.53	4850.	.097	.0970	.220	-9.3	143.6	-
-20	70.99	1403.	.097	.0946	.232	-4.8	142.5	-
0	70.45	532.	.096	.0922	.245	0.0	141.4	-
20	69.91	167.	.095	.0898	.257	5.0	140.3	.0000
40	69.37	108.	.095	.0874	.270	10.3	139.1	.0001
60	68.82	72.9	.094	.0851	.282	15.8	137.9	.0002
80	68.27	50.4	.094	.0827	.295	21.6	136.7	.0006
100	67.72	35.7	.093	.0804	.307	27.6	135.5	.0014
120	67.16	25.9	.092	.0781	.319	33.9	134.3	.0033
140	66.60	19.2	.092	.0758	.332	40.4	133.1	.0071
160	66.04	14.5	.091	.0735	.344	47.1	131.8	.0144
180	65.47	11.2	.090	.0712	.356	54.1	130.5	.0277
200	64.89	8.78	.090	.0689	.369	61.4	129.2	.0510
220	64.31	6.96	.089	.0667	.381	68.9	127.9	.0900
240	63.72	5.60	.088	.0644	.393	76.6	126.5	.1528
260	63.13	4.56	.087	.0622	.406	84.6	125.1	.2505
280	62.53	3.75	.086	.0600	.418	92.8	123.7	.3976
300	61.92	3.12	.085	.0578	.430	101.3	122.3	.6129
320	61.31	2.61	.084	.0556	.441	110.0	120.9	.9199
340	60.69	2.21	.083	.0535	.452	119.0	119.4	1.347
360	60.07	1.89	.082	.0513	.463	128.1	117.9	1.928
380	59.43	1.62	.080	.0492	.473	137.5	116.3	2.703
400	58.79	1.41	.079	.0471	.483	147.0	114.7	3.718
420	58.13	1.23	.078	.0450	.493	156.8	113.1	5.023
440	57.47	1.07	.076	.0429	.503	166.8	111.5	6.677
460	56.80	.952	.075	.0408	.513	176.9	109.8	8.743
480	56.11	.844	.073	.0388	.522	187.3	108.0	11.28
500	55.42	.752	.072	.0367	.532	197.8	106.2	14.38
520	54.71	.674	.070	.0347	.541	208.6	104.4	18.11
540	53.99	.619	.069	.0327	.550	219.5	102.5	22.56
560	53.25	.573	.067	.0308	.559	230.5	100.6	27.81
580	52.50	.531	.066	.0288	.568	241.8	98.5	33.96
600	51.73	.492	.064	.0269	.577	253.3	96.5	41.09
620	50.94	.457	.063	.0250	.586	264.9	94.3	49.32
640	50.13	.424	.061	.0232	.594	276.7	92.0	58.75
660	49.29	.394	.060	.0213	.603	288.7	89.7	69.48
680	48.43	.367	.058	.0195	.611	300.8	87.3	81.63
700	47.54	.341	.057	.0177	.620	313.1	84.7	95.31
720	46.61	.318	.055	.0160	.629	325.6	82.0	110.6
740	45.65	.296	.053	.0143	.638	338.2	79.2	127.7
760	44.63	.275	.052	.0126	.648	351.1	76.1	146.8
780	43.57	.256	.050	.0109	.658	364.2	72.9	167.9
800	42.43	.238	.048	.0094	.669	377.4	69.4	191.3
820	41.22	.221	.046	.0078	.682	390.9	65.6	217.1
840	39.89	.205	.045	.0063	.697	404.7	61.4	245.5
860	38.43	.189	.043	.0049	.715	418.8	56.7	276.7
880	36.76	.172	.041	.0035	.740	433.4	51.3	310.9
900	34.77	.155	.040	.0023	.779	448.5	44.6	348.5
920	32.17	.135	.039	.0011	.863	464.8	35.8	389.8
940	27.50	.104	.036	.0002	1.537	484.7	19.9	435.2

a) 32.2 poundals = 1 lb.

Table 104. GAS PROPERTIES OF "SHELLDYNE"

Temp, °F	Pressure, psia										
	0	100	200	400	600	800	1000	1200	1400	1600	1800
	Enthalpy,$^{a)}$ Btu/lb										
-100	124.6										
0	141.1										
100	163.1										
200	190.6										
300	223.8										
400	262.4										
500	305.9										
600	353.9										
700	405.6										
800	460.9	454.6									
900	519.3	514.2	508.0								
1000	580.6	576.4	571.5	558.1	546.0	526.7	513.3	511.4	510.2	509.4	508.9
1100	644.4	640.8	636.9	627.4	615.7	598.1	590.8	587.2	585.1	583.7	582.8
1200	710.4	707.4	704.1	697.6	687.8	677.6	669.2	664.1	661.0	659.0	657.6
1300	778.5	775.9	773.1	767.1	760.5	[illegible]	746.4	741.2	737.5	735.0	733.2
1400	847.7	845.5	843.1	838.1	832.7	827.2	821.8	817.2	813.5	810.8	808.8
1500	918.5	916.5	914.5	910.1	905.7	901.2	896.8	892.9	889.5	886.8	884.8
1600	990.4	988.6	986.7	983.0	979.1	976.2	971.6	968.2	965.2	962.7	960.7
1700	1062.9	1061.3	1059.6	1056.2	1052.9	1049.8	1046.4	1043.4	1040.7	1038.4	1036.5
1800	1135.9	1134.6	1132.9	1129.9	1126.9	1123.9	1121.1	1118.[illegible]	1116.1	1114.0	1112.2
	Fugacity, psia										
900			166.4								
1000			173.9	294.9	359.1	396.5	425.0	455.1	485.3	514.1	549.7
1100			179.2	317.5	416.0	470.1	520.9	573.3	616.2	659.0	702.4
1200			183.8	335.6	456.6	550.0	624.0	688.6	749.1	807.7	865.7
1300			187.6	350.3	489.1	606.0	709.3	792.9	874.2	952.2	1028.6
1400			190.5	362.0	515.1	651.3	773.0	883.6	986.8	1085.9	1182.7
1500			192.7	371.1	535.6	687.3	827.9	959.5	1084.5	1204.6	1322.5
1600			194.5	378.3	551.8	715.9	871.9	1021.5	1165.6	1306.7	1444.6
1700			196.0	384.0	564.7	738.8	907.2	1071.2	1232.0	1390.7	1548.0
1800			197.1	388.7	575.1	757.8	935.7	1111.6	1286.0	1459.8	1633.6
	Free Energy, Btu/lb										
900	-185.31		-149.95								
1000	-229.17		-190.34	-181.99	-178.89	-177.90	-176.38	-175.24	-174.22	-173.25	-172.31
1100	-277.12		-235.08	-225.47	-220.93	-218.52	-216.89	-215.34	-214.32	-213.19	-212.12
1200	-329.23		-284.04	-273.87	-267.76	-264.13	-262.18	-260.41	-258.91	-257.56	-256.32
1300	-385.38		-337.08	-325.23	-318.90	-314.84	-311.96	-309.74	-307.69	-306.27	-304.81
1400	-446.15		-394.80	-381.93	-374.86	-370.16	-366.73	-364.05	-361.83	-359.92	-358.21
1500	-510.69		-456.53	-442.70	-434.95	-429.68	-425.75	-422.64	-420.05	-417.83	-415.86
1600	-579.87		-522.53	-507.77	-499.39	-493.61	-489.23	-485.72	-482.79	-480.26	-478.03
1700	-653.14		-592.85	-577.19	-568.27	-561.97	-557.19	-553.32	-550.06	-547.24	-544.75
1800	-730.80		-667.57	-651.06	-641.49	-634.80	-629.64	-625.45	-621.90	-618.81	-616.07
	Entropy, Btu/lb/°F										
900	.41437		.37978								
1000	.45729		.42498	.41001	.38590	.37050	.37544	.37340	.37189	.37069	.36970
1100	.50006		.46829	.45603	.44437	.43279	.42706	.42391	.42178	.42019	.41890
1200	.54110		.51009	.49917	.49048	.48252	.47589	.47175	.46897	.46695	.46537
1300	.58094		.55046	.54034	.53293	.52652	.52103	.51677	.51365	.51128	.50944
1400	.61968		.58953	.57998	.57323	.56771	.56298	.55904	.55589	.55340	.55140
1500	.65718		.62737	.61812	.61188	.60688	.60264	.59905	.59602	.59352	.59145
1600	.69363		.66403	.65504	.64911	.64444	.64091	.63716	.63429	.63184	.62976
1700	.72905		.69960	.69080	.68508	.68064	.67695	.67378	.67104	.66867	.66661
1800	.76348		.73418	.72548	.71993	.71566	.71214	.70912	.70649	.70420	.70218

(Continued)

Table 104 (Contd-1). GAS PROPERTIES OF "SHELLDYNE"

Temp, °F	Pressure, psia										
	0	100	200	400	600	800	1000	1200	1400	1600	1800
	Viscosity, lb/ft/hr										
-100	.0157										
0	.0186										
100	.0214										
200	.0240										
300	.0264										
400	.0287										
500	.0309										
600	.0333										
700	.0351										
800	.0371	.0391									
900	.0391	.0410	.0424								
1000	.0410	.0428	.0440		.0938		.1474		.1786		.2011
1100	.0429	.0445	.0455		.0599		.1092		.1423		.1651
1200	.0447	.0464	.0472		.0571		.0843		.1147		.1390
1300	.0466	.0482	.0490		.0555		.0725		.0960		.1178
1400	.0484	.0500	.0507		.0559		.0674		.0848		.1008
1500	.0502	.0518	.0524		.0568		.0652		.0781		.0929
1600	.0520	.0535	.0541		.0579		.0646		.0744		.0863
1700	.0538	.0552	.0558		.0592		.0647		.0725		.0821
1800	.0555	.0570	.0575		.0605		.0653		.0718		.0796
	Thermal Conductivity, Btu/hr/ft/°F										
-100	.0026										
0	.0044										
100	.0065										
200	.0091										
300	.0119										
400	.0147										
500	.0176										
600	.0204										
700	.0233										
800	.0262	.0265									
900	.0290	.0292	.0295								
1000	.0317	.0319	.0322		.0377		.0430		.0454		.0470
1100	.0344	.0346	.0348		.0367		.0428		.0452		.0469
1200	.0371	.0373	.0373		.0387		.0439		.0458		.0475
1300	.0398	.0399	.0401		.0410		.0457		.0471		.0485
1400	.0420	.0422	.0424		.0430		.0476		.0486		.0497
1500	.0443	.0445	.0446		.0458		.0496		.0504		.0518
1600	.0465	.0466	.0467		.0478		.0516		.0522		.0529
1700	.0484	.0485	.0487		.0491		.0534		.0539		.0545
1800	.0501	.0503	.0504		.0507		.0551		.0555		.0560
	Compressibility Factor										
800		.881									
900		.908	.800								
1000		.929	.849		.316		.357		.441		.531
1100		.945	.885		.571		.434		.485		.561
1200		.958	.912		.699		.549		.554		.604
1300		.968	.934		.781		.655		.645		.665
1400		.975	.950		.841		.747		.714		.732
1500		.981	.962		.884		.820		.789		.796
1600		.986	.972		.917		.874		.854		.857
1700		.990	.980		.941		.915		.907		.912
1800		.993	.986		.960		.946		.947		.953
	Heat Capacity, Btu/lb/°F										
-100	.128										
0	.188										
100	.246										
200	.303										
300	.361										
400	.412										
500	.458										
600	.500										
700	.536										
800	.570	.584									
900	.599	.609	.626								
1000	.625	.634	.645	.702	.949	.794	.765	.751	.744	.738	.734
1100	.650	.656	.664	.691	.718	.822	.784	.765	.755	.748	.744
1200	.671	.676	.682	.699	.729	.770	.781	.772	.765	.757	.755
1300	.691	.694	.699	.710	.727	.748	.765	.769	.767	.763	.760
1400	.705	.705	.709	.717	.728	.740	.752	.760	.762	.761	.760
1500	.714	.717	.719	.725	.733	.741	.749	.756	.759	.760	.760
1600	.723	.725	.727	.731	.737	.743	.748	.753	.757	.758	.759
1700	.728	.730	.732	.735	.740	.744	.748	.752	.755	.757	.758
1800	.731	.732	.734	.737	.741	.744	.748	.751	.754	.756	.757

(Continued)

Table 104 (Contd-2). GAS PROPERTIES OF "SHELLDYNE"

Temp, °F	Pressure, psia										
	0	100	200	400	600	800	1000	1200	1400	1600	1800
	Heat Capacity Ratio, C_p/C_v										
900			1.039								
1000			1.032	1.085	1.305	1.158	1.108	1.085	1.075	1.068	1.062
1100			1.027	1.052	1.129	1.173	1.121	1.095	1.081	1.072	1.065
1200			1.024	1.039	1.068	1.109	1.114	1.097	1.083	1.073	1.066
1300			1.022	1.032	1.048	1.069	1.094	1.085	1.078	1.071	1.065
1400			1.021	1.028	1.039	1.051	1.063	1.069	1.068	1.065	1.062
1500			1.020	1.026	1.033	1.041	1.050	1.055	1.058	1.058	1.056
1600			1.019	1.024	1.029	1.035	1.041	1.046	1.049	1.051	1.050
1700			1.018	1.022	1.027	1.031	1.036	1.040	1.043	1.044	1.045
1800			1.018	1.021	1.025	1.028	1.032	1.035	1.038	1.040	1.041
	Joule-Thomson Coefficient, °F/psia										
900			.1129								
1000			.0820	.1290	.1070	.0300	.0158	.0098	.0064	.0042	.0026
1100			.0496	.0810	.1090	.0674	.0304	.0173	.0110	.0074	.0050
1200			.0435	.0577	.0672	.0649	.0425	.0252	.0160	.0108	.0075
1300			.0403	.0446	.0485	.0484	.0402	.0286	.0196	.0137	.0098
1400			.0339	.0368	.0379	.0376	.0338	.0273	.0206	.0153	.0113
1500			.0291	.0303	.0309	.0304	.0281	.0242	.0197	.0155	.0120
1600			.0255	.0261	.0262	.0256	.0239	.0213	.0181	.0150	.0121
1700			.0227	.0229	.0228	.0221	.0207	.0188	.0165	.0140	.0117
1800			.0204	.0204	.0201	.0194	.0183	.0167	.0149	.0130	.0111
	Sound Velocity, ft/sec										
900			490.								
1000			537.	506.	389.	346.	676.	777.	868.	938.	1006.
1100			577.	482.	374.	408.	542.	653.	769.	825.	897.
1200			610.	540.	469.	456.	488.	577.	664.	763.	819.
1300			641.	585.	533.	501.	510.	568.	609.	693.	760.
1400			668.	624.	584.	557.	553.	577.	621.	676.	731.
1500			694.	657.	625.	604.	597.	609.	638.	677.	723.
1600			718.	687.	662.	644.	638.	644.	664.	695.	729.
1700			740.	715.	694.	680.	674.	678.	692.	715.	744.
1800			762.	740.	723.	712.	707.	710.	721.	739.	763.

a) The reference state is the liquid at saturation pressure and 0°F.

BIBLIOGRAPHY[a]

1. Abramov, V. G., Gontkovskaya, V. T., Merzhanov, A. G., THEORY OF THERMAL IGNITION. I. SOME CONDITIONS GOVERNING THE TRANSITION FROM SELF-IGNITION TO INDUCED IGNITION. Izv. Akad. Nauk. SSSR, Ser. Khim. 1966 (3), 429-37 (Russ); C.A. 64, 19308 (1966).

2. Abramov, V. G., Gontkovskaya, V. T., Merzhanov, A. G., THEORY OF THERMAL IGNITION. II. EFFECT OF EXTERNAL HEAT TRANSFER ON IGNITION CHARACTERISTICS. Izv. Akad. Nauk. SSSR, Ser. Khim. 1966 (5), 823-7 (Russ); C.A. 65, 6987 (1966).

3. Abramov, V. N., Leont'eva, T. P., Fisak, V. I., COMBUSTION OF LEAN METHANE-AIR MIXTURES. Probl. Teploenerg. i Prikl. Teplofiz., Sb. (Alma-Ata: Nauka) 1965 (2), 50-7 (Russ); C.A. 65, 18416 (1966).

4. Accorsi, R., OXYGEN AND COMBUSTION. THEORETICAL AND EXPERIMENTAL FUNDAMENTAL INFORMATION. II COMBUSTION MECHANISMS IN FLAMES. Rev. Gen. Thermique 4 (41), 533-42 (1965) (Fr); C.A. 63, 9722 (1965).

5. Ackerman, G. H. and Nixon, A. C., A FUEL SYSTEM SIMULATOR FOR HYPERSONIC AIRCRAFT ENDOTHERMIC FUELS, 155th ACS National Meeting (San Francisco March 31-April 5, 1968) ACS Div. Petrol., Chem. Inc. Preprints V13 N.1 31-41 (March 1968).

6. Adams, E., AERODYNAMIC HEAT PROTECTION IN HIGH VELOCITY FLIGHT. Jahrbuch 1965 der WGLR nd 130; Deutsche Versuchsanstalt Fuer Luft-Und Raumfahrt E. V. Freiburg-Im-Breisgau (West Germany), Report No. DVL-603, 1965, 13 pp. (AD 657218) (text in German).

7. Adiutori, E. F., NEW AND SIMPLE CONCEPT FOR THE ANALYSIS OF NONLINEAR HEAT-TRANSFER PHENOMENA SUCH AS BOILING. Brit. Chem. Eng. 10 (12), 840-5 (1965); C.A. 64, 4621 (1966).

8. Adomeit, G., THERMAL IGNITION OF FLOWING GAS MIXTURE ON A HOT SURFACE UNDER STATIONARY CONDITIONS. Forsch. Ingenieurw. 32 (2), 33-44 (1966) (Ger); C.A. 65, 16781 (1966).

9. Adushkin, V. V. and Nemchinov, I. V., APPROXIMATE DEFINITION OF GAS PARAMETERS AFTER THE SHOCK WAVE FRONT BY THE LAW OF FRONT MOTION. Zh. Prik. Mekhan. i Techn. Fiz. (Moscow) 1964 (4), 75-88; U.S. Air Force Translation FTD-HT-66-261, TT-67-63189 (AD 660 248)

10. Affens, W. A., FLAMMABILITY PROPERTIES OF HYDROCARBON FUELS. PART 2. THE IMPORTANCE OF VOLATILE COMPONENTS AT LOW CONCENTRATION ON THE FLAMMABILITY OF LIQUID FUELS. U.S. Naval Research Laboratory Report No. NRL-6578, July 1967, 22 pp. (AD 657 455).

11. Affens, W. A., FLAMMABILITY PROPERTIES OF HYDROCARBON FUELS. PART 3. FLAMMABILITY PROPERTIES OF HYDROCARBON SOLUTIONS IN AIR. U.S. Naval Research Laboratory Interim Report No. NRL-6617, November 1967, 27 pp. (AD 663 881).

---

a) This extends the survey of the literature presented in reference 19.

12. Aliev, A. S. Kasimova, N. P., Gasanzade, A. A., Khalafova, T. V., CATALYTIC DEHYDROGENATION OF METHYLCYCLOPENTENE ISOMERS TO THE CORRESPONDING HYDROCARBON DIENES. Azerb. Khim. Zh. 1966 (3), 11-16 (Russ); C.A. 65, 19972 (1966).

13. All-Union Scientific-Research Institute of Petrochemical Processes (by N. R. Bursian, S. B. Kogan, and Z. A. Davydova), PREPARATION OF AN ALUMINA-PLATINUM CATALYST. U.S.S.R. 182,119 (Cl. B 01J), May 25, 1966, Appl. July 29, 1964; C.A. 65, 16117 (1966).

14. Alvermann, W. and Ulken, R., FLOW INVESTIGATIONS COMBUSTORS WITH AERODYNAMIC FLAME STABILIZATION, PART 2. PREHEATED FLOW. Deutsche Forschungsanstalt fur Luft-und Raumfahrt Report DLR-FB-67-77, Pt. 2, September 1967, 29 pp. (N68-17486).

15. Amann, J. A. R., POST - 1970 INTERCEPTORS - AN EXPLORATORY STUDY. SHAPE, Technical Center, The Hague Technical Memo Report No. TM-149, April 1967, 212 pp. (AD 382 225) (REPORT CLASSIFIED SECRET).

16. Allam, M. I., Gerritsen, A. W., Vlugter, J. C., AROMATIZATION OF KEROSINE FRACTIONS CONTAINING BICYCLONAPHTHENES. Part 3. Conversion of Methylindan and Related Compounds Over a Platinum Reforming Catalyst. J. Inst. Petrol. 53, no. 518, 94-9 (1967). Part 4. Reactions of Alkyl Derivatives of Decalin on Platinum Reforming Catalyst CK-303, ibid 53, no. 525, 285-93 (1967). Part 5. Hydrodealkylation of 1,6-Dimethylnaphthalene and the Aromatization and Dealkylation of Industrial Oil Fractions, ibid 53, no. 526, 328-37 (1967).

17. Andreev, A. A. and Selwood, P. W. (University of California, Santa Barbara), FERROMAGNETIC RESONANCE OF SUPPORTED NICKEL WITH ADSORBED HYDROGEN, OXYGEN, AND ETHYLENE. Journal of Catalysis 8, no. 4, 375-82 (1967); U.S. Army AROD-6799:2, Grant DA-ARO(D)-31-124-G863, May 1967, App. (AD 663 452).

18. Andreev, A. A. and Kiperman, S. L., KINETICS OF CYCLOHEXANE DEHYDROGENATION IN A GRADIENTLESS SYSTEM. Kinetika i Kataliz 6 (5), 869-77 (1965) (Russ); C.A. 64, 4901 (1966).

19. Andreev, A. A., Shopov, D. M., Kiperman, S. L., KINETICS OF CYCLOHEXANE DEHYDROGENATION IN A HETEROGENEOUS SYSTEM. II. Kinetika i Kataliz 7 (1), 120-7 (1966) (Russ); C.A. 64, 17375 (1966).

20. Appeldoorn, J. K. and Dukek, W. G., LUBRICITY OF JET FUELS, SAE Meeting Paper N.660712 (1966); SAE (Soc Automot. Eng.) Trans V75 N.3 428-40 (1967).

21. Appeldoorn, J. K., Feng, I., Tao, F. F., LUBRICITY PROPERTIES OF HIGH-TEMPERATURE JET FUELS. Esso Research and Engineering Co., Products Research Div., Quarterly Report No. 5, 15 May - 15 August 1966, U.S. Air Force Contract AF 33(615)-2828, August 1966, 4 pp. (AD 801 260).

22. Appeldoorn, J. K. and Tao, F. F., LUBRICITY PROPERTIES OF HIGH-TEMPERATURE JET FUELS. Esso Research and Engineering Co., Products Research Div., Quarterly Report No. 6, 15 August - 15 November 1966, U.S. Air Force Contract AF 33(615)-2828, November 1966, 33 pp. (AD 808 673).

23. Appeldoorn, J. K. and Tao, F. F., LUBRICITY PROPERTIES OF HIGH-TEMPERATURE JET FUELS. Esso Research and Engineering Co., Products Research Div., Quarterly Progress Report No. 7, 15 November 1966 - 15 February 1967, U.S. Air Force Contract AF 33(615)-2828, February 1967, 43 pp. (AD 815 710).

24. Aslonov, S. K., REMARKS TO THE WORK OF R. M. ZAYDEL "ON THE POSSIBILITY OF STABLE BURNING". Zh. Prik. Mekhan. i Techn. Fiz. (Moscow) 1964 (4), 133-5; U.S. Air Force Translation FTD-HT-66-261; TT-67-63189. (AD 660 248) (N68-11562).

25. Atkins, T. G., HYPERSONIC RAMJET HEAT TRANSFER AND COOLING PROGRAM. VOLUME I. RESULTS OF REGENERATIVE COOLING EXPERIMENTS. Marquardt Corp., Final Report, 1 June 1965 - 31 January 1966 on Task 3, Report No. 6/07, AFAPL TR-66-84-Vol. 1, U.S. Air Force Contract AF 33(615)-1467, August 1966, 209 [illegible]. (AD 377 525L) (REPORT CLASSIFIED CONFIDENTIAL).

26. Avery, D. H., TECHNIQUES FOR THE DETECTION AND ESTIMATION OF INTERMEDIATES FORMED IN COMBUSTION REACTIONS. Johns Hopkins University, Applied Physics Lab., Report No. CM-366, prepared in cooperation with Arthur D. Little, Inc., October 1946, 33 pp. (AD 659 104).

27. Axe, W. N. and Linnard, R. E. (Phillips Petroleum Co.), ADDITIVES FOR GASOLINE, DIESEL FUEL, AND JET FUEL, 7th World Petrol. Congr. (Mexico City April 2-8, 1967) Paper N.PD-28(2).

28. Bachman, K. C., (Esso Research + Engineering Co.), HEAT TRANSFER UNIT EVALUATES PERFORMANCE OF JET FUELS FOR SUPERSONIC AIRCRAFT, SAE Meeting Paper N.650803 (1965); SAE (Soc. Automotive Engrs.) Trans V74 (Pt. 3). 626-40 (1966).

29. Bagnetto, L., THERMAL STABILITY OF HYDROCARBON FUELS. Phillips Petroleum Co., Final Summary Report, 1 June 1965 - 31 May 1966, Report No. 4559-66R, APL TDR-64-89-Part 3, U.S. Air Force Contract AF 33(657)-10639, September 1966, 270 pp. (AD 641 419).

30. Bahn, G. S., SIMPLE ANALYTICAL APPROACH TO CONSIDERATION OF KINETIC FACTORS IN DIFFUSION FLAMES, WITH EXAMPLES. Western States Sect. Combust. Inst. Paper, WSS-CI-66-10, 35 pp. (1966); C.A. 65, 6990 (1966).

31. Bajars, L. (Petro-Tex Chemical Corp.), DEHYDROGENATION OF HYDROCARBONS. U.S. 3, 207, 808 (Cl. 260-680), September 21, 1965, Appl. November 29, 1960, October 18, 1961, and December 4, 1962; 7 pp.; C.A. 64, 7950 (1966).

32. Bajars, L. (Petro-Tex Chemical Corp.), DEHYDROGENATION OF HYDROCARBONS. U.S. 3, 207, 809 (Cl. 260-680), September 21, 1965, Appl. November 29, 1960, October 18, 1961 and December 4, 1962; 7 pp.; C.A. 64, 7951 (1966).

33. Bajars, L. (Petro-Tex Chemical Corp.), DEHYDROGENATION OF HYDROCARBONS. U.S. 3,268,611 (Cl. 260-680), August 23, 1966, Appl. June 11, 1965, 4 pp.; Continuation-in-part of U.S. 3,207,811; C.A. 65, 16857 (1966).

34. Bajars, L. (Petro-Tex Chemical Corp.), DEHYDROGENATION OF HYDROCARBONS. U.S. 3,268,612 (Cl. 260-680), August 23, 1966, Appl. June 11, 1965, 4 pp.; C.A. 65, 16858 (1966).

35. Bajars, L. (Petro-Tex Chemical Corp.), ALIPHATIC HYDROCARBON DEHYDROGENATION. U.S. 3,274,285 (Cl. 260-680), September 20, 1966, Appl. October 18, 1961, and June 11, 1965, 4 pp.; Continuation-in-part of U.S. 3,207,111; C.A. 65, 20003 (1966).

36. Bakhman, N. N. and Kondrashkov, Yu. A., AN EXPRESSION FOR THE BURNING VELOCITY IN SIMULTANEOUS HOMOGENEOUS AND HETEROGENEOUS REACTIONS. Doklady Akadamiya Nauk (SSSR) 168, No. 4, 844-5 (1966); U.S. Library of Congress Aerospace Technology Division, Translation Report No. ATD-66-98; TT 66-62590, August 1966, 7 pp. (AD 641 866).

37. Balent, R. L. and Stava, D. J., TEST RESULTS OF A SUPERSONIC/HYPERSONIC COMBUSTION FORCE-BALANCE INLET MODEL. U.S. Air Force Flight Dynamics Laboratory, Wright-Patterson A.F.B., Report No. AFF DL-TR-66-95, U.S. Air Force Project AF-1366, October 1966, 39 pp. (AD 378 952L) (REPORT CLASSIFIED CONFIDENTIAL).

38. Balec, E. L., ON HEAT TRANSFER WITHIN AND ACROSS NEARLY CIRCULAR CAVITIES INCLUDING THE EFFECTS OF VARIABLE WALL TEMPERATURE AND MASS BLEED. University of Illinois, Urbana Ph.D. Thesis, U.S. National Aeronautics and Space Administration Report NASA-CR-90233, Grant NsG-13-59, 1967 100 pp. (N68-10985).

39. Baltakis, F. P., HEAT TRANSFER RATES IN THE VICINITY OF SURFACE PROTUBERANCES AT MACH 6.3. General Dynamics/Convair Report No. GDC-RT-60-106, March 1961, 34 pp. (AD 664 597).

40. Bar-Gadda, I., Bogdan, S., Roberts, S. (Rep. Aviation Corp.), SUPERSONIC COMBUSTION - NEW EXPERIMENTAL TECHNIQUES. IAA Accession No. A65-26596, 16 pp. (1965); C.A. 63, 17787 (1965).

41. Barningham, R. C., COMPONENT PROPULSION PROGRAM FOR FUTURE HIGH-PERFORMANCE STRATEGIC AIRCRAFT. VOLUME I. SUMMARY. (AD 379 041L); VOLUME III. CYCLE PERFORMANCE STUDIES. (AD 379043L); VOLUME IV. ENGINE DESIGN STUDIES. (AD 379 043L); VOLUME V. INLET SCALE MODEL. (AD 379 044L); VOLUME VI. FAN AND LOW PRESSURE COMPRESSOR. (AD 379 045); VOLUME VII. HIGH PRESSURE COMPRESSOR (AD 379 046L); VOLUME IX. BURNERS. (AD 379 047L); VOLUME X. TURBINE AERODYNAMICS. (AD 379 048L); VOLUME XI. TURBINE COOLING. (AD 379 049L); VOLUME XII. AUGMENTERS. (AD 379 050L); VOLUME XIII. NOZZLES. (AD 379 051L); VOLUME XV. BEARINGS. (AD 379 052L); VOLUME XVI. SEALS. (AD 379 053L); VOLUME XVII. CONTROLS. (AD 379 054L); VOLUME XVIII. DEMONSTRATOR ENGINE (Ad 379 055L). Pratt and Whitney Semiannual Report No. 3, 1 August 1966-

31 January 1967, Reports No. PWA-2991- Vols. 1, 3, 4, 5, 6, 7, 9, 10, 11, 12, 13, 15, 16, 17, 18, U.S. Air Force Contract AF 33(657)-14903, February 1967. (REPORTS CLASSIFIED CONFIDENTIAL).

42. Bataafse Petroleum Maatschappij N.V. (by J. H. Raley and R. D. Mullineaux), DEHYDROGENATION OF HYDROCARBONS. Ger. 1,194,400 (Cl. C 07c), June 10, 1965, U.S. Appl. July 30, 1956, 5 pp.; CA 63, 14697-8 (1965).

43. Beatty, H. A., JET FUEL DECONTAMINATION STUDIES. Ethyl Corp. Interim Technical Report, 15 December 1965 - 15 June 1966, Report No. GR-66-30, U.S. Army Contract DA-44-009-AMC-1165(T), July 1966, 79 pp. (AD 815 527L).

44. Beatty, H. A., JET FUEL DECONTAMINATION STUDIES. Ethyl Corp. Interim Technical Report, 15 June 1966 - 9 January 1967, Report No. GR-67-2, U.S. Army Contract DA-44-009-AMC-1165(T), January 1967, 29 pp. (AD 815 528L).

45. Belo, G. and Churchill, A. V. (Gulf Research and Development Co.), THERMAL STABILIZATION OF JET FUELS. U.S. 3,218,137 (Cl. 44-66), November 16, 1965, Appl. December 28, 1960, 3 pp.; C.A. 64, 1879 (1966).

46. Belo, C. and Churchill, A.V. (Gulf Research and Development Co.), STABILIZATION OF JET TURBINE FUELS AT HIGH TEMPERATURES. U.S. 3,222,145 (Cl. 44-66), December 7, 1965, Appl. December 28, 1960, 7 pp.; C.A. 64, 4841 (1966).

47. Bennet, W. J., HEAT TRANSFER THRU UNBOUNDED CERAMIC LINERS AND WALLS OF THE COMBUSTION CHAMBER. General Dynamics/Fort Worth, Report No. ZJ-4033-001, prepared in cooperation with Johns Hopkins University, Applied Physics Laboratory CM-421, U.S. Navy Contract NOrd-9028, October 1947, 26 pp. (AD 659 109).

48. Bert, J. L., COMBUSTION OF HEPTANE DROPLETS IN A HOT GAS FLOW. M.S. Thesis, University of California, Lawrence Radiation Laboratory Report No. UCRL-17438, Contract W-7405-Eng-48, October 1967, 74 pp. (N68-16886).

49. Bhaduri, D., EVALUATION OF FLAME SPEED IN TURBULENT FLOW. Indian J. Technol. 3 (10), 308-13 (1965); C.A. 64, 6122 (1966).

50. Bialy, J. J., Norris, T. A., Frascati, F. P., RESEARCH ON THERMAL EFFECTS ON FUELS. Texaco Research Center Annual Report, May 1965-June 1966, AF APL TR-66-101, U.S. Air Force Contract AF 33(657)-10746, October 1966, 41 pp. (AD 801 913).

51. Billig, F. S., EXTERNAL BURNING IN SUPERSONIC STREAMS. Johns Hopkins University, Applied Physics Laboratory, Technical Memo Report No. TG-912, U.S. Navy Contract NOw-62-0604, May 1967, 132 pp. (AD 655 460).

52. Billig, F. S., SUPERSONIC COMBUSTION (ANALYSIS). Johns Hopkins University, Applied Physics Laboratory Research and Development Programs, March 1967, 2 pp. (N67-33384).

53. Billig, F. S. and Grenleski, S. E., EXPERIMENTAL STUDIES OF HYDROGEN-AIR IGNITION IN A SUPERSONIC COMBUSTOR. Johns Hopkins University Technical Memo, Report No. TG-848, U.S. Navy Contract NOw-62-00604, August 1966, 33 pp. (AD 376 857) (REPORT CLASSIFIED CONFIDENTIAL). Presented at the AIAA Joint Propulsion Specialists Conference, June 13-17, 1966, Colorado Springs, Colorado.

54. Biot, M. A. (Biot (MA)), COMPLEMENTARY FORMS OF THE VARIATIONAL PRINCIPLE FOR HEAT CONDUCTION AND CONVECTION. Journal of the Franklin Institute 283, No. 5, 372-8 (1967); U.S. Air Force AFOSR-68-0098, Contract AF 49(638)-1329, 1967, 9 pp. (AD 563 780).

55. Biot, M. A. (Biot (MA)), SIMPLIFIED VARIATIONAL AND PHYSICAL ANALYSIS OF HEAT TRANSFER IN LAMINAR AND TURBULENT FLOW. The Physics of Fluids 10, No. 7, 1424-37 (1967); U.S. Air Force AFOSR-68-0103, Contract AF 49(638)-1329, March 1967, 16 pp. (AD 66[illegible] 865).

56. Bittrich, H. J. and Werner, U., THE INFLUENCE OF REAL GAS CORRECTIONS ON THE CALCULATION OF THERMODYNAMIC FUNCTIONS FROM LIQUID-VAPOR EQUILIBRIUM MEASUREMENTS. Wiss. Z. Tech. Hochsch. Chem. Leuna-Merseburg 7 (3), 247-56 (1965) (German).

57. Blade, O. C., (U.S. Bureau of Mines, American Petroleum Institute), AVIATION TURBINE FUELS, 1967, U.S. Bur. Mines Mineral Ind. Survs. (Petrol. Prod. Surv. N.54) (February 1968) 14 pp.

58. Bland, R. B. and Ewing, F. J. (Catacycle Co., Inc.), THE THERMAL CYCLE FOR CYCLOHEXANE ⟶ BENZENE + HYDROGEN. U.S. 3,225,538 (Cl. 60-37), December 28, 1965, Appl. March 25, 1960, 13 pp.; C.A. 64, 17085 (1966).

59. Blume, H., Strich, E. R., Nicolai, M., Kurpjun, C., Pfeiffer, F., Naundorf, W., HIGHLY ACTIVE FLUORINE-CONTAINING ALUMINA CARRIERS FOR PLATINUM OR PALLADIUM CATALYSTS. Ger. (East) 30, 930 (Cl. C 07b), January 5, 1966, Appl. February 25, 1963, 3 pp.; C.A. 64, 17328 (1966).

60. Boeing Co., COMMERCIAL SUPERSONIC TRANSPORT PROPOSAL - JANUARY 15, 1964. A-II. MODEL SPECIFICATIONS. (AD 803 505L); A-III. AIRCRAFT DESCRIPTION (AD 803 506L); A-VIII. GROUND SUPPORT EQUIPMENT. (AD 803 637L); A-XI. FLIGHT OPERATIONS AND SAFETY. (AD 803 640L). Report Nos. D6-2400-8, D6-2400-9, D6-2400-14, and D6-2400-17, January 1964, 183, 237, 53, 158 pp.

61. Boeing Co., Airplane Division, COMMERCIAL SUPERSONIC TRANSPORT PROGRAM. PHASE II-A. COMPREHENSIVE REPORT. VOLUME VIII-A. AIRCRAFT PROPULSION SYSTEM. Report No. D6-6680-8, U.S. Federal Aviation Agency Contract FA-SS-64-4, November 1964, 242 pp. (AD 378 352L) (REPORT CLASSIFIED CONFIDENTIAL).

62. Boeing Co., COMMERCIAL SUPERSONIC TRANSPORT PROGRAM. PHASE II-B REPORT. FUEL SYSTEM PERFORMANCE SPECIFICATION. Report No. D6-17856, U.S. Federal Aviation Agency Contract FA-SS-65-20, June 1965, 9 pp. (AD 804 426L).

63. Boeing Co., COMMERCIAL SUPERSONIC TRANSPORT PROGRAM. PHASE II-C. PROPULSION SYSTEM PERFORMANCE SPECIFICATION. GENERAL ELECTRIC GE 4/J5G ENGINE INSTALLATION. (AD 378 634L); PRATT AND WHITNEY AIRCRAFT JTF 17A-20B ENGINE INSTALLATION. (AD 378 635L); ibid. (AD 378 636L). Interim aircraft performance assessment report, Report Nos. D6-19906-1, D6-19906-2, and D6-19903, U.S. Federal Aviation Agency Contract FA-SS-66-5, November 1965, 26, 39, and 85 pp. (REPORT CLASSIFIED CONFIDENTIAL).

64. Boeing Co., Supersonic Transport Division (P.E. Johnson), SUPERSONIC TRANSPORT PROGRAM. PHASE II-C REPORT. PROPULSION SUBSYSTEM SPECIFICATION. GENERAL ELECTRIC SST BOEING MODEL 2707. (AD 805 652L); PRATT AND WHITNEY AIRCRAFT, SST BOEING MODEL 2707. (AD 805 653L); SST BOEING MODEL 2707. (AD 805 654L); SST BOEING MODEL 2707. (AD 805 655L); SST BOEING MODEL 2707. (AD 805 657L); ENGINE INLET ANTI-ICING SUBSYSTEM SPECIFICATION, SST BOEING MODEL 2707. (AD 805 658L). Report Nos. D6A 10111-1, D6A 10112-1, D6A 10113-1, D6A 10114-1, D6A 10116-1, and D6A 10117-1, U. S. Federal Aviation Agency Contract FA-SS-66-5, June 1966, 54, 52, 41, 21, 37, and 25 pp.

65. Boeing Co., Supersonic Transport Division, SUPERSONIC TRANSPORT DEVELOPMENT PROGRAM. PHASE III PROPOSAL. BOEING MODEL 2707. COORDINATED INLET/ENGINE TEST PLAN. (GENERAL ELECTRIC). (AD 378 490L); (PRATT AND WHITNEY). (AD 378 491L). Report Nos. D6A-10007-1, and D6A-10007-2, U.S. Federal Aviation Agency Contract FA-SS-66-5, September 1966, 30 and 31 pp. (REPORT CLASSIFIED CONFIDENTIAL).

66. Boeing Co., Supersonic Transport Division (W. J. Bakken), SUPERSONIC TRANSPORT DEVELOPMENT PROGRAM. PHASE III PROPOSAL. BOEING MODEL 2707. AIRFRAME/ENGINE TECHNICAL AGREEMENT. (GENERAL ELECTRIC). (AD 378 492L); (PRATT AND WHITNEY). (AD 378 493L). Report Nos. D6A 10198-1 and D6A 10199-1, U.S. Federal Aviation Agency Contract FA-SS-66-5, September 1966, 81 and 87 pp. (CONFIDENTIAL).

67. Boeing Co., Supersonic Transport Division (P. E. Johnson), SUPERSONIC TRANSPORT DEVELOPMENT PROGRAM. PHASE III PROPOSAL. BOEING MODEL 2707. PROPULSION PERFORMANCE SPECIFICATION. (GENERAL ELECTRIC). (AD 378 494L); (PRATT AND WHITNEY). (AD 378 495L). Report Nos. D6A 10111-1 and D6A 10112-1, U.S. Federal Aviation Agency Contract FA-SS-66-5, September 1966, 64 and 52 pp. (CONFIDENTIAL).

68. Boeing Co., Supersonic Transport Division, SUPERSONIC TRANSPORT DEVELOPMENT PROGRAM. PHASE III PROPOSAL. BOEING MODEL 2707. VOLUME II-12. PROPULSION REPORT-PART A. ENGINE INLET AND CONTROLS. (AD 378 496L); VOLUME II-13. PROPULSION REPORT-PART B. ENGINE INSTALLATION FUEL SYSTEM EXHAUST SYSTEM. (AD 378 497L); VOLUME II-14. PROPULSION REPORT-PART C. ENGINE EVALUATION. Report Nos. V2-B2707-12, V2-B2707-13, V2-B2707-14, U.S. Federal Aviation Agency Contract FA-SS-66-5, September 1966, 308, 112, 121 pp. (REPORT CLASSIFIED CONFIDENTIAL).

69. Bogdanoff, D. W., A STUDY OF THE MECHANISMS OF HEAT TRANSFER IN OSCILLATING FLOW. Princeton University, Department of Aerospace and Mechanical Sciences, Technical Report, July 15, 1963-September 1967, Report No. 483-f, U.S. Navy Contract Nonr-1858(29), September 1967, 339 pp. (AD 664 248).

70. Bolshakov, G. F., A STUDY OF THE THERMAL OXIDATION RESISTANCE OF T-1 (JET) FUEL. Izv. Vysshikh. Uchebn. Zavedenii Neft i Gaz V9 N.11 57-60 (1966).

71. Bol'shakov, G. F., Bruk, Yu. A., Rachinskii, F. Yu., ADDITIVE INCREASING THE THERMOOXIDATION STABILITY OF HYDROCARBON FUELS. Khim. i Tekhnol. Topliv. i Masel 11 (3), 52-4 (1966) (Russian); C.A. 65, 3633 (1966).

72. Bolshakov, G. F. and Davydov, P. I., EFFECT OF SULFUROUS COMPOUNDS ON THERMAL STABILITY AND CORROSIVE PROPERTIES OF FUELS FOR TURBOCOMPRESSOR AIR-REACTIVE ENGINES. U.S. Dept. Commerce Clear Fed. Sci. Tech. Inform. April 1966, 15 pp. (AD 641 109); (Abstr.) Corrosion Abstr. V6 N.3 229 (May 1967).

73. Bonner, B. H. and Tipper, C. F. H. (University Liverpool), COOL FLAME COMBUSTION OF HYDROCARBONS. I. CYCLOHEXANE. Combust. Flame 9 (3), 317-27 (1965); C.A. 64, 3309 (1966).

74. Bonner, B. H. and Tipper, C. F. H. (University Liverpool), THE COOL-FLAME COMBUSTION OF HYDROCARBONS. II. PROPANE AND n-HEPTANE. Combust. Flame 9 (4), 387-92 (1965); C.A. 64, 10998 (1966).

75. Borishanskii, V. M. and Gotovskii, M. A., THEORY OF THE BREAKDOWN OF HYDRAULIC STABILITY OF THE NEAR-WALL TWO-PHASE LAYER UNDER CONDITIONS OF FREE AND FORCED CONVECTION. Teplo- i Massoperenos 3, 125-30 (1965) (Russian); C.A. 65, 11805 (1966).

76. Borishanskii, V. M., Maslichenko, P. A., Fokin, B. S., MECHANISM OF PHASE MOTION IN FILM BOILING IN A LARGE VOLUME OF LIQUID. Usp. Nauchn. Fotogr., Akad. Nauk SSSR, Otd. Khim. Nauk 9, 222-7 (1964) (Russian); C.A. 64, 9260 (1966).

77. Bowden, F. P., Boddington, T., Field, J. E., GROWTH OF BURNING TO DETONATION IN LIQUIDS AND SOLIDS. Cavendish Laboratory, University of Cambridge (England), Annual Scientific Report No. 9, November 1965-1966, AFOSR 67-0520, U.S. Air Force European Office of Aeronautical Research Contract AF-EOAR-03-66, December 1966, 14 pp. (AD 647 392).

78. Bradley, R. P. and Goodman, H., ADVANCED AIRCRAFT FUEL SYSTEM SIMULATOR MODIFICATION AND PERFORMANCE REPORT. North American Aviation, Inc. Report for February 1-December 1, 1966 on Phase 1, Report No. NA-66-1380, U.S. Air Force Contract AF 33(615)-3228, December 1966, 115 pp. (AD 807 655).

79. Braun, G. W., UNCERTAINTIES IN THE PREDICTION OF SCRAMJET SPACE BOOSTER PERFORMANCE. University of Tennessee, Tullahoma Space Institute Technical Report, AEDC TR-66-268, U.S. Air Force Contract AF 40(600)-1168, December 1966, 41 pp. (AD 806 689L).

80. British Petroleum Co., Ltd. (P. J. Maile and R. A. Dean), OXIDATION INHIBITION OF AVIATION TURBINE FUELS BY NATURALLY OCCURRING SULFUR COMPOUNDS. Belg. 648,544, November 30, 1964, Brit. Appl. May 28, 1963; 2 pp.; C.A. 63, 11223 (1965).

81. Brockman, W. E. and Durall, D. S., PHYSICAL AND CHEMICAL PROPERTIES OF JP-4 JET FUEL FOR 1966. University of Dayton Research Institute Annual Report 1 May 1966 - 1 June 1967, Report No. UDRI-TR-67-139, U.S. Air Force AFAPL-TR-67-108, Contract AF 33(615)-2692, September 1967, 132 pp. (AD 660 957) (N68-11940).

82. Brokaw, R. S., ALIGNMENT CHARTS FOR TRANSPORT PROPERTIES VISCOSITY, THERMAL CONDUCTIVITY, AND DIFFUSION COEFFICIENTS FOR NONPOLAR GASES AND GAS MIXTURES AT LOW DENSITY. U.S. National Aeronautics and Space Administration, Lewis Research Center Report NASA-TR-R-81, May 1960, 26 pp. (PB 175886).

83. Brossard, J. and Manson, N., THEORY OF DISSOCIATED SHOCK AND COMBUSTION WAVES. Colloq. Intern. Centre Natl. Rech. Sci. (Paris) No. 109, 223-34 (1961) (France); C.A. 65, 15139 (1966).

84. Buchmann, O. A., EXPLORATORY DEVELOPMENT OF HIGH TEMPERATURE HEAT EXCHANGERS. Garrett Corp., AiResearch Mfg. Division, Interim Engineering Progress Report 1 July - 30 September 1966, Report No. 66-1261, RTD IR-3084 Vol 5, U.S. Air Force Contract AF 33(615)-2753, September 1966, 52 pp. (AD 801 551).

85. Buell, J., Kagiwada, H., Kalaba, R., McNabb, A., Schumitzky, A., COMPUTATION OF THE RESOLVENT FOR THE AUXILIARY EQUATION OF RADIATIVE TRANSFER. Rand Corp. Report No. RM-55-20-PR, Contract F44620-67-C-0045, January 1968, 28 pp. (AD 664 322).

86. Bukata, S. W., Castor, C. R., Milton, R. M. (Union Carbide Corp.), DEHYDROGENATION BY A CHROMIUM CONTAINING ZEOLITE. U.S. 3,236,910 (Cl. 260-683.3), February 22, 1966, Appl. December 18, 1961; 4 pp. Continuation-in-part of U.S. 3,013,998, C.A. 64, 18485 (1966).

87. Burggraf, F. and Shayeson, M., DEVICE SPOTS THERMAL BREAKDOWN OF FUELS AT HIGH MACH NUMBERS. NEW SMALL-SCALE METHOD FOR MEASURING FUEL THERMAL STABILITY. Soc Automotive Engrs. Mtg. Paper N.987A (Cond) SAE (Soc. Automotive Engrs.) J V74 N.2.82-85 (February 1966).

88. Burnette, T. D., Dunsworth, L. C., Reed, G. J., Woodgrift, K. E., EXPLORATORY DEVELOPMENT OF THE DUAL MODE SCRAMJET. PHASE I. INLET AND INLET/COMBUSTOR ANALYSIS AND EXPERIMENTAL EVALUATIONS. Marquardt Corp. Final Report April 1965-May 1966, Report No. 6114, AF APL TR-66-106, U.S. Air Force Contract AF 33(615)-2834, October 1966, 229 pp. (AD 379 (AD 379 426L) (REPORT CLASSIFIED CONFIDENTIAL).

89. Burgoyne, J. A., THE FLAMMABILITY OF MISTS AND SPRAYS. Proc. Symp. Chem. Process Hazards Spec. Reference Plant Design, 2nd, Manchester 1963, 1-5 (Pub. 1964); C.A. 63, 12962 (1965).

90. Burk, F., HOW TO COMBAT JET-FUEL CONTAMINANTS. Defense Supply Assoc. Meeting (Washington D.C.) (Cond) Oil Gas J. V62 N.1 .73-74,76 (January 6, 1964).

91. Burggraf, F. and Shayeson, M., A NEW SMALL-SCALE METHOD FOR MEASURING (SUPERSONIC JET ENGINE) FUEL THERMAL STABILITY. Soc. Automotive Engrs. Meeting (1965) Paper N.650114. SAE (Soc. Automotive Engrs.) Trans. V74.504-12 (1966).

92. Bursian, N. R., Kogan, S. B., Davydova, Z. A., AROMATIZATION OF HEXANE UNDER ATMOSPHERIC PRESSURE IN THE PRESENCE OF A SODIUM-PROMOTED PLATINUM-SILICA GEL CATALYST. Neftekhimiya 6 (1), 35-9 (1966) (Russian); C.A. 64, 19451 (1966).

93. Bursian, N. R., Kogan, S. B., Davydova, Z. A., CATALYST FOR AROMATIZATION OF PARAFFINIC HYDROCARBONS. U.S.S.R. 176,256 (Cl. B 01j), November 2, 1965, Appl. February 4, 1963; C.A. 64, 11002 (1966).

94. Bursian, N. R., Kogan, S. B., Davydova, Z. A., VARIATIONS IN THE AROMATIZING CAPACITY OF A PLATINUM-ON-ALUMINA CATALYST AS A FUNCTION OF ITS PLATINUM AND SODIUM CONTENT. Kinetika i Kataliz 6 (6), 1046-51 (1965) (Russian); C.A. 64, 12529 (1966).

95. Bursian, N. R., Kogan, S. B., Osmolovskii, G. M., Lyudkovskaya, B. G., Davydova, Z. A., EFFECT OF ALKALI METALS ON THE ACTIVITY OF CATALYSTS IN DEHYDROCYCLIZATION OF n-HEXANE. Kinetika i Kataliz 7 (3), 556-9 (1966) (Russian); C.A 65, 12075 (1966).

96. Burt, R., Skuse, F., Thomas, A. (Shell Res. Ltd.), KINETIC SPECTROSCOPY OF INTERMEDIATES IN REACTIONS LEADING TO IGNITION OF HYDROCARBONS. Combust. Flame 9 (2), 159-72 (1965); C.A. 63, 13024 (1965).

97. Bushueva, E. M. and Bespolov, I. E., EFFECT OF FRACTIONAL AND HYDROCARBON COMPOSITION OF FUELS ON THEIR THERMAL STABILITY. Khim. i Tekhnol. Topliv i Masel 8 (8), 49-54 (1963) (Russian); C.A. 64, 9479.

98. Bushueva, E. M. and Bespolov, I. E., EFFECTS OF THE STRUCTURE OF AROMATIC HYDROCARBONS ON THERMAL STABILITY OF FUELS. Khim. i Tekhnol. Topliv i Masel 11 (1), 45-8 (1966) (Russian); C.A. 64, 9481 (1966).

99. Bushueva, E. M. and Bespolov, I. E., EFFECT OF PARAFFINIC AND CYCLOPARAFFINIC HYDROCARBONS ON THE OXIDATION STABILITY OF JET FUELS AT ELEVATED TEMPERATURE. Khim i Tekhnol Topliv i Masel V11 N.12 44-46 (December 1966).

100. Calcote, H. F. and Gibbs, C. J., BURNING VELOCITY, EFFECT OF MOLECULAR STRUCTURE. Texaco Experiment, Inc. Report No. TM-641 prepared in cooperation with Johns Hopkins University, Applied Physics Lab., CF-2263, U.S. Navy Contract NOrd-9756, July 1953, 56 pp. (AD 658 335).

101. Carey, C. A. Carnevale, E. H., Marshall, T., EXPERIMENTAL DETERMINATION OF THE TRANSPORT PROPERTIES OF GASES. PART II. HEAT TRANSFER AND ULTRASONIC MEASUREMENTS. Parametrics Inc. Final Scientific Report February 1965-February 1966, AFML TR-65-141-Pt. 2, U.S. Air Force Contract AF 33(615)-1325, September 1966, 96 pp. (AD 804 604).

102. Casaccio, A. and Rupp, R. L., A SUPERSONIC COMBUSTION TEST PROGRAM UTILIZING GAS SAMPLING, OPTICAL AND PHOTOGRAPHIC MEASURING TECHNIQUES. Republic Aviation Corp. Final Report, U.S. National Aeronautics and Space Administration Report NASA-CR-66393, Contract NAS1-6314, 1967, 115 pp. (N67-34996).

103. Proc. Intern. Congr. Catalysis, 3rd, Amsterdam 1964 (Pub. 1965).

104. Chalykh, N. D. and Stekhun, A. I., MORE ATTENTION TO THE PURITY OF JET FUELS. Khim i Tekhnol Topliv i Masel V12 N.1 49-51 (January 1967).

105. Chambellan, R. E., Lubomski, J. F., Bevevino, W. A., STRUCTURAL FEASIBILITY STUDY OF PRESSURIZED TANKS FOR LIQUID-METHANE FUELED SUPERSONIC AIRCRAFT. U.S. National Aeronautics and Space Administration, Lewis Research Center Report No. NASA-TN-D-4295, December 1967, 48 pp. (N68-12370).

106. Chambers, R. P. (University of California, Berkeley), SELECTIVITY OF GOLD FOR THE HYDROGENATION AND DEHYDROGENATION OF CYCLOHEXENE. Univ. Microfilms (Ann Arbor, Michigan), Order No. 66-3560, 124 pp.; C.A. 65, 12076 (1966).

107. Chambers, R. P. and Boudart, M. (University of California, Berkeley), SELECTIVITY OF GOLD FOR HYDROGENATION AND DEHYDROGENATION OF CYCLOHEXENE. J. Catalysis 5 (3), 517-28 (1966); C.A. 65, 5321 (1966).

108. Charpenet, L., STUDY OF THE EFFECT OF ULTRASOUND ON THE COMBUSTION OF A JET OF LIQUID HYDROCARBONS. France. Ministere de l'Air Publ. Sci. et Tech. No. 424, Serv. de Doc. Sci. et Tech. de l'Armament, 1966, 89 pp. (N68-18165); C.A. 65, 19917 (1966).

109. Charwat, A. F. (ed.), PROCEEDINGS OF THE 1965 HEAT TRANSFER AND FLUID MECHANICS INSTITUTE HELD AT THE UNIVERSITY OF CALIFORNIA, LOS ANGELES, June, 1965. Stanford: Stanford Univ. Press. 1965, 372 pp.; C.A. 64, 17081 (1966).

110. Cheek, R. M., DUAL MODE SCRAMJET. Marquardt Corp. Monthly Letter Progress Report for December 1966, Report No. LR-5012-21M, U.S. Air Force Contract AF 33(615)-2834, January 1967, 5 pp. (AD 379 645) (REPORT CLASSIFIED CONFIDENTIAL).

111. Chertkov, Ya. B., Zrelov, V. N., Shchagin, V. M., PURIFICATION OF FUELS FROM MICRO IMPURITIES. U.S.S.R. 173,363 (Cl. C 10g), July 21, 1965, Appl. February 7, 1963; C.A. 64 507 (1966).

112. Chervinsky, A. and Mar, Y. M. T., ON THE DISTRIBUTION OF MOMENTUM, HEAT AND MATTER IN AXISYMMETRICAL JET DIFFUSION FLAMES. PART I: THEORETICAL STUDY. Israel Inst. of Tech., Dept. of Aeronautical Engineering Report TAE-62, March 1967, 31 pp. (N67-34355).

113. Chinitz, W., Baurer, T., Hopf, H., ANALYTICAL AND EXPERIMENTAL INVESTIGATION OF THE LOW SPEED FIXED GEOMETRY SUPERSONIC COMBUSTION RAMJET. VOLUME I. BASIC TECHNOLOGY REPORT. General Applied Science Laboratories, Inc. Final Report January 1965-March 1966, Report No. GASL-TR-621-Vol. 1, AFAPL TR-66-102-Vol. 1, U.S. Air Force Contract AF 33(615)-2436, January 1967, 92 pp. (AD 806 888).

114. Chintz, W., Marino, A., Woods, A. R., Baront, P., Spadaccini, L., STUDIES RELATED TO THE DEVELOPMENT OF A STORABLE-FUELED SUPERSONIC COMBUSTION RAMJET ENGINE. General Applied Science Laboratories, Inc. Final Report on Phase 1, Report No. GASL-TR-585, U.S. Army Contract DA-01-021-AMC-12822(Z), January 1966, 140 pp. (AD 376 452) (REPORT CLASSIFIED CONFIDENTIAL).

115. Chinitz, W. and Spadaccini, L. J., VAPORIZING AND ENDOTHERMIC FUELS FOR ADVANCED ENGINE APPLICATION: PART IV. PRELIMINARY STUDY OF THE SUPERSONIC COMBUSTION OF ENDOTHERMIC HYDROCARBON FUELS. Shell Development Co. Final Report March-September 1966, prepared in cooperation with General Applied Science Labs., Inc., Report No. GASL-TR-635, U.S. Air Force APL TDR-64-100-Pt. 4, U.S. Air Force Contract AF 33(657)-11096, February 1967, 101 pp. (AD 811 928).

116. Churchill, A. V., Ek, A., Fareri, E. L. (Gulf Research and Development Co.), THERMALLY STABLE FUELS AND STABILIZING AGENTS. U.S. 3,269,808 (Cl. 44-62), August 30, 1966, Appl. August 7, 1961; 6 pp.; C.A. 65, 16766 (1966).

117. Cizek, A. (Armour and Co.), FUEL OIL COMPOSITIONS CONTAINING AN n-ALKYL AMINOPROPIONITRILE SALT OF AN ALKYL PHOSPHORIC ACID ESTER. U.S. 3,207,586 (Cl. 44-72), September 21, 1965, Appl. August 22, 1962, 2 pp.; C.A. 63, 14624 (1965).

118. Cochran, P. (Oklahoma State Univ., Stillwater), SIMULTANEOUS INVESTIGATION OF THE ISOBARIC INTEGRAL HEAT OF VAPORIZATION AND VAPOR-LIQUID EQUILIBRIUM DATA OF METHANE-ETHYLENE MIXTURES AT HIGH PRESSURES. Univ. Microfilms (Ann Arbor, Mich.), Order No. 66-4086, 240 pp.; C.A. 65, 19366 (1966).

119. Coleman, J. E., Wallace, T. J., Weiss, H. A., FUNDAMENTAL INVESTIGATION OF THE DEGRADATION OF HYDROCARBON FUELS. Esso Research and Engineering Co., Process Research Div. Quarterly Progress Report No. 5, July-September 1966, Report No. PcRD-6M66GR, U.S. Army Contract DA-18-035-AMC-330(A), September 1966, 191 pp. (AD 801 235).

120. Coleman, J. E., Wallace, T. J., Weiss, H. A., Taylor, W. F., FUNDAMENTAL INVESTIGATION OF THE DEGRADATION OF HYDROCARBON FUELS. Esso Research and Engineering Co., Government Research Laboratory Quarterly Progress Report No. 6, October-December 1966, U.S. Army Contract DA-18-035-AMC-330(A), January 1967, 71 pp. (AD 807 334).

121. Coleman, J. E., Taylor W. F., Wallace, T. J., Weiss, H. A., FUNDAMENTAL INVESTIGATION OF THE DEGRADATION OF HYDROCARBON FUELS. Esso Research and Engineering Co., Government Research Laboratory Quarterly Progress Report No. 7, January-March 1967, Report No. GR-1-DHF-67, U.S. Army Contract DA-18-035-AMC-330(A), April 1967, 119 pp. (AD 380 944) (REPORT CLASSIFIED CONFIDENTIAL).

122. Combustion Inst., SYMPOSIUM (INTERNATIONAL) ON COMBUSTION (10th) AT THE UNIVERSITY OF CAMBRIDGE, CAMBRIDGE, ENGLAND AUGUST 17-21, 1964. ABSTRACTS OF PAPERS. U.S. Army Contract DA-31-124-ARO(D)-197, NsG-506, 1964, 176 pp. (AD 809 450).

123. Compagnie Francaise de Raffinage, CATALYTIC DEHYDROGENATION OF ALIPHATIC HYDROCARBONS. Fr. 1,413,913 (Cl. B 01j, C 07f, C 10g), October 15, 1965, Appl. July 8, 1964; 18 pp.; C.A. 64, 7950 (1966).

124. Coordinating Research Council, Inc., Alcor Inc., and Eppi Precision Products, Inc., INVESTIGATION OF HIGH-TEMPERATURE THERMAL STABILITY OF AVIATION TURBINE FUELS, Coordinating Res. Coun. Rept. N.388 (October 1965), 95 pp.

125. Coordinating Research Council, Inc. and Eppi Precision Products, Inc., EVALUATION OF MODIFIED FUEL COKER FOR MEASURING HIGH-TEMPERATURE STABILITY OF FUELS FOR HIGH-PERFORMANCE AIRCRAFT. Coordinating Res. Council Report N.392 (March 1966), 81 pp.

126. Coordinating Research Council, Inc., U.S. Federal Aviation Agency, AN INVESTIGATION OF THE PERFORMANCE OF JET ENGINE FUELS FOR SUPERSONIC TRANSPORT (SST) AIRCRAFT. SUMMARY REPORT. Coordinating Res. Council Report N.393 (June 1966), 62 pp.

127. Coordinating Research Council, Inc., U.S. Federal Aviation Agency, TECHNIQUES FOR MEASUREMENT OF PHYSICAL PROPERTIES OF POTENTIAL SUPERSONIC TRANSPORT (SST) FUELS. Coordinating Research Council Report N.394 (June 1966), 104 pp.

128. Cottington, G. I. (Texaco, Inc.), HYDROCARBON CONVERSION TO AROMATICS. U.S. 3,240,831 (Cl. 260-672), March 15, 1966, Appl. September 10, 1962; 4 pp.; C.A. 64 17327 (1966).

129. Craig, R. R. (Wright-Patterson A.F.B.), APPLYING THE METHOD OF CHARACTERISTICS TO ANALYZE THE FLOW FIELD OF A CHEMICALLY REACTING GAS IN A TWO-DIMENSIONAL OR AN AXISYMMETRIC NOZZLE. 1965, 40 pp. (AD 618 068); C.A. 64, 1682 (1966).

130. Cumby, C., Jr., INVESTIGATION OF FUEL TANK DEPOSITS - MODEL L-2000. Lockheed-California Co. Report for January-August 1965, Report No. LR-19157, June 1966, 51 pp. (AD 814 085L).

131. Dadashev, B. A., Davydova, Z. A., Kasimova, S. A., Khudiev, A. T., INFLUENCE OF SOME RARE EARTH ELEMENT OXIDES ON THE ACTIVITY OF AN Al-Mo CATALYST IN THE DEHYDROGENATION OF CYCLOHEXANE AND THE DEHYDROCYCLIZATION OF n-HEXANE. Azerb. Khim. Zh. 1965 (5), 33-7 (Russian); C.A. 64, 15773 (1966).

132. Dadashev, B. A., Kasimova, S. A., Davydova, Z. A., EFFECT OF SOME RARE EARTH OXIDES ON THE ACTIVITY OF ALUMINO-MOLYBDENUM CATALYSTS IN AROMATIZATION OF CYCLOHEXANE AND n-HEXANE. Azerb. Khim. Zh. 1964 (6), 29-31 (Russian); C.A. 63, 14727 (1965).

133. Dadashev, B. A., Mustafaev, L. S., Poladov, P. M., EFFECT OF NEODYMIUM OXIDE ON THE CATALYST ACTIVITY OF ALUMINUM-CHROMIUM CATALYSTS IN THE DEHYDROGENATION OF n-OCTANE. Uch. Zap. Azerb. Gos. Univ., Ser. Khim. Nauk 1964 (4), 67-9 (Russian); C.A. 65, 8739 (1966).

134. Dalton, B. J. and Barieau, R. E., EQUATIONS FOR CALCULATING VARIOUS THERMODYNAMIC FUNCTIONS OF A TWO-COMPONENT SYSTEM FROM AN EMPIRICAL EQUATION OF STATE, INCLUDING LIQUID VAPOR EQUILIBRIUM DATA. U.S. Bureau of Mines Report BM-RI-7076, February 1968, 77 pp. (N68-14621).

135. Da Riva, I., THE INTERNAL STRUCTURE OF HYDROGEN-AIR DIFFUSION FLAMES. Astronautica Acta 12, no. 4, 284-93 (1966); Instiuto Nacional de Tecnica Aeroespacial (Spain), U.S. Air Force AFOSR 67-0649, U.S. Air Force Contract AF-EOAR-69-65, May 1966, 13 pp. (AD 648 681).

136. Da Riva, I., Fraga, E., Linan, A., Urrutia, J. L., DIFFUSION FLAMES AND SUPERSONIC COMBUSTION. Instituto Nacional de Tecnica Aeroespacial Madrid (Spain), Final Report, AFOSR 67-0098, U.S. Air Force European Office of Aeronautical Research Contract AF-EOAR-69-65, October 1966, 44 pp. (AD 645 163).

137. Da Riva, I., Fraga, E., Linan, A., Urrutia, J. L., DIFFUSION FLAMES AND SUPERSONIC COMBUSTION. Instituto Nacional de Tecnica Aeroespacial (Spain) Final Report, U.S. Air Force AFOSR-68-0066, Grant AF-EOAR-66-41, October 1967, 50 pp. (AD 663 741) (N68-17929).

138. Da Riva, I. and Urrutia, J. L., RECENT RESEARCH IN SUPERSONIC COMBUSTION AT INTA. Instituto Nacional de Tecnica Aeroespacial, (Spain), presented at the International Astronautical Congress (15th), Madrid (Spain), 9-15 October 1966; AFOSR 66-2479, U.S. Air Force European Office of Aeronautical Research Contract AF-EOAR-41-66, 1966, 15 pp. (AD 641 758).

139. Dauba, J. L. (Massachusetts Inst. of Technol.), MAXIMUM TEMPERATURES ATTAINABLE IN COMBUSTION OF CARBON AND METHANE IN AIR. Genie Chim 92 (4), 102-10 (1964) (French); C.A. 64, 10998 (1966).

140. Davis, J. D. and Eden, R. Q. E., (Shell International Petroleum Co., Ltd., Shell Research Ltd.), SUPERSONIC AIR TRANSPORT ENGINE DEVELOPMENTS AND FUEL REQUIREMENTS - Europe. 7th World Petrol. Congr. (Mexico City April 2-8, 1967) Paper N.PD-29(5).

141. Davis, J. D. and Eden, R. Q. E., FUEL FOR CONCORDE-1 Shell Aviation News N-347 16-21 (1967) (Abstract).

142. Davydov, P. E. and Bolshakov, G. F., EFFECT OF SULFUROUS COMPOUNDS ON THERMAL STABILITY AND CORROSIVE PROPERTIES OF FUELS FOR TURBO-COMPRESSOR AIR-REACTIVE ENGINES. Borba s Korroziyey Dvigatelei Vnutrennego Sgoraniya i Gazoturbinnykh Ustanovok, n.p. 1962, p. 272-80; U.S. Air Force Translation Report No. FTD-TT-65-1276, TT 66-62520 (AD 641 109).

143. de Galan, L. and Winefordner, J. D. (University of Florida), THERMAL EQUILIBRIUM IN TURBULENT DIFFUSION FLAMES. Journal of Quantum Spectroscopy Radiation Transfer 7, 703-13 (1967); U.S. Air Force AFOSR-67-2514, Grant AF-AFOSR-1033-67, June 1967, 13 pp. (AD 660 666).

144. de Soete, G., COMBUSTION IN TURBULENT STREAMS. Oel-Gasfeurung 10 (9), 950, 952, 954, 956, 958 (1965); C.A. 64, 3085 (1966).

145. Dimitrov, Khr. and Pelova, R., KINETICS OF DEALKYLATION OF n-AMYLBENZENE IN THE PRESENCE OF AN ALUMINUM SILICATE CATALYST. THE ROLE OF DEHYDROCYCLIZATION OF THE SIDE CHAIN DURING CRACKING OF n-AMYLBENZENE. Godishnik Sofiskiya Univ. "Kl. Okhridski," Khim. Fak. 57, 149-68 (1962-3 (Pub. 1964) (Bulg); C.A. 63, 9776 (1965).

146. Dixon, G. M., Nicholls, D., Steiner, H. (Univ. Manchester, England), ACTIVITY PATTERN IN THE DISPROPORTIONATION AND DEHYDROGENATION OF CYCLOHEXENE TO CYCLOHEXANE AND C_6H_6 OVER THE OXIDES OF THE FIRST SERIES OF TRANSITION ELEMENTS. Proc. Intern. Congr. Catalysis, 3rd, Amsterdam 1964 (2), 815-28 (Pub. 1965); C.A. 64, 608 (1966).

147. Dobrinescu, D. and Apolzan, S., VARIATION OF SPECIFIC HEATS AND ADIABATIC COEFFICIENTS OF GASES WITH PRESSURE AND TEMPERATURE. Bul. Inst. Petrol. Gaze Geol. (Bucharest) 12, 81-93 (1964) (Rom); C.A. 64, 15083 (1966).

148. Dolgich, A., DEVELOPMENT OF SOVIET SUPERSONIC TRANSPORT EQUIPMENT AND SUBSYSTEMS. PART I. ANALYTICAL SURVEY OF MATERIALS. PART II. ABSTRACTS. U.S. Library of Congress, Aerospace Technology Div. work assignment No. 98, Report No. ATD-67-27, TT-67-62268, May 1967, 139 pp.; (AD 654 671).

149. Douglas, G. W. and O'Loughlin, J. R. (Tulane Univ.), THE RELATION BETWEEN FLAME SHAPE AND CHAMBER COMBUSTION EFFICIENCY FOR A FLAME STABILIZED BY AN OPPOSED - JET FLAMEHOLDER. AIAA Propulsion Joint Specialists Conference (3rd) Washington, D.C., paper no. 67-472, 11 pp. July 17-21 1967; U.S. Army AROD-4981:4, Contract DA-31-124-ARO(D)-240, 1967, 11 pp. (AD 659 864).

150. Dugan, J. F., Jr., Keith, A. L., Jr., Boxer, E., (U.S. National Aeronautics and Space Administration), PROPULSION ASPECTS OF THE SUPERSONIC TRANSPORT. Langley Research Center, Proc. NASA Conf. on Supersonic-Transport Feasibility Studies and Supporting Research, December 1963, 291-302 (N67-31622).

151. Dugan, J. F., Jr., Luidens, R. W., and Weber, R. J., METHANE-FUELED PROPULSION SYSTEMS. Am. Inst. Aeron. + Astronautics 2nd Joint Propulsion Specialist Conf. (Colorado Springs June 13-17, 1966) NASA Tech. Mem. N.X-52199, 33 pp, (1966).

152. Dugger, G. L. and Monchick, L., EXTERNAL BURNING RAMJETS PRELIMINARY FEASIBILITY STUDY. Johns Hopkins University, Applied Physics Laboratory Technical Memo Report No. TG-892, U.S. Navy Contract NOw-6[illegible]-0604, March 1967, 93 pp. (AD 655 459).

153. Dukek, W. G. and Appeldoorn, J. K., LUBRICITY OF JET FUELS. Soc. Automotive Engr. Aeron. + Space Eng. + Mfg. Meeting (Los Angeles October 3-7, 1966) Paper N.660712, 11 pp.

154. Dulaney, C. L. and Owens, M. L., Jr. (Monsanto Co.), THERMAL CRACKING OF PARAFFINS TO AROMATICS. U.S. 3,271,298 (Cl. 208-106), September 6, 1966, Appl. February 28, 1963, 3 pp.; CA 65, 16761 (1966).

155. Dunn, R. G. (U.S. Air Force Aerospace Research Laboratories), SUPERSONIC COMBUSTION SIMULATION. U.S. Air Force Office of Aerospace Res. Proc. of the OAR Res. Appl. Conf., 14 March 1967, March 1967, 157-182 (N68-16384).

156. du Pont (by W. P. Dunworth), DISTILLATE FUEL OXIDATION INHIBITOR. Brit. 1,036,384 (Cl. C 10p), July 20, 1966, Appl. March 24, 1964, 15 pp.; C.A. 65, 12050 (1966).

157. Eckert, E. R. G., Sparrow, E. M., Ibele, W. E., Goldstein, R. J. (University of Minnesota), HEAT TRANSFER - A REVIEW OF CURRENT LITERATURE. Intern. J. Heat Mass Transfer 9 (7), 599-636 (1966); C.A. 65, 8375 (1966).

158. Economos, C., EXPERIMENTAL DETERMINATION OF HEAT TRANSFER DUE TO HYDROGEN COMBUSTION IN A BASE FLOW REGION. General Applied Science Laboratories, Inc. Technical Report TR-625, U.S. National Aeronautics and Space Administration Report NASA-CR-85819, Contract NAS8-2686, October 1966, 62 pp. (N67-31186).

159. Edwards, A. C., HYPERSONIC RAMJET HEAT TRANSFER AND COOLING PROGRAM. VOLUME II. RESULTS OF SUPERSONIC COMBUSTION HEAT TRANSFER EXPERIMENT Marquardt Corporation Final Report 1 June 1965-28 February 1966 on Task 1, Report No. 6108, AFAPL TR-66-84-Vol. 2, U.S. Air Force Contract AF 33(615)-1467, August 1966, 165 pp. (AD 377 526L) (REPORT CLASSIFIED CONFIDENTIAL).

160. Eisenberg, J. D., Shovlin, M. D., Whitlow, J. B., Jr., THE POTENTIAL (USE) OF LIQUID-METHANE FUEL FOR MACH 3 COMMERCIAL (FIXED ARROW-WING) SUPERSONIC TRANSPORTS. NASA (Natl. Aeron. Space Admin.) Tech. Note N.D-3471 (July 1966) 40 pp.

161. Eisenberg, J. D. and Chambellan, R. E., TANKAGE SYSTEMS FOR A METHANE FUELED SUPERSONIC TRANSPORT. To be presented at AIAA Meeting on Aircraft Design, Washington, D.C., 12-14 February, 1968; U.S. National Aeronautics and Space Administration Report NASA-TM-X-52378, 1967, 16 pp. (N68-12827).

162. El Paso Natural Gas Products Co. (by Walter E. Steinmetz and C. F. Gerald), HYDROCARBON DEHYDROGENATION. Belg. 658,368, April 30, 1965, U.S. Appl. January 15, 1964; 21 pp.; C.A. 64, 3346 (1966).

163. Erickson, H. and Sanford, R. A. (Sinclair Research, Inc.), NICKEL CATALYSTS FOR HYDROCARBON REFINING. U.S. 3,223,652 (Cl. 252-439), December 14, 1965, Appl. September 5, 1962, 3 pp.; C.A. 64, 7947 (1966).

164. Erofeev B. V., Nikiforava, N. V., Dmitrieva, L. P., Zaretskii, M. V., DEHYDROGENATION OF CYCLOHEXANE ON MIXED CATALYSTS Cu-ZnO-MgO. Vestsi Akad. Navuk Belarusk. SSR, Ser. Khim. Navuk 1965 (3), 5-10 (Beloruss). C.A.; 64, 11914 (1966).

165. Ershin, Sh. A. and Yarin, L. P., TRANSPORT PROCESSES IN TURBULENT STREAMS IN THE PRESENCE OF AN INTENSIVE CHEMICAL REACTION. Teplo- i Masso-perenos 2, 392-8 (1965) (Russian); C.A. 65, 11805 (1966).

166. Essenhigh, R. H., APPLICATION OF THE PERFECTLY STIRRED REACTOR (P.S.R.) THEORY TO ANALYSIS OF ONE-DIMENSIONAL FLAMES. Pennsylvania State University, Department of Fuel Science Technical Report No. FS66-3(u), U.S. Navy Contract NOnr-656(29), October 1966, 51 pp. (AD 805 113).

167. Essenhigh, R. H., A NEW APPLICATION OF THE PERFECTLY STIRRED REACTOR (P.S.R.) THEORY TO DESIGN OF COMBUSTION CHAMBERS. Pennsylvania State Univ., Dept. of Fuel Science Report No. FS 67-1(u), U.S. Navy Contract NOnr-656(29), March 1967, 86 pp. (AD 812 114).

168. Faeth, G. M., Dominicis, D. P., Olson, D. R., AN INVESTIGATION OF NEAR CRITICAL AND SUPER-CRITICAL BURNING OF FUEL DROPLETS. Pennsylvania State University, Dept. of Mechanical Engineering Annual Report AR-1, U.S. National Aeronautics and Space Administration Report NASA-CR-72314, Grant NGR-39-009-077, September 1967, 35 pp. (N68-10170).

169. Faith, L. E. and Vermeulen, T., KINETICS OF COMPLEX ISOTHERMAL REVERSIBLE FIRST-ORDER REACTION SYSTEMS INVOLVING THREE COMPONENTS. A.I.Ch.E. Journal 13:5, 934 (1967).

170. Fajeau, M. and Saunier, J., CODE FLID (DEP 051): NUMERICAL PROGRAM FOR TWO-DIMENSIONAL ANALYSIS OF THE THERMODYNAMIC BEHAVIOR OF A BOILING LIQUID. French Commissariat a l'Energie Atomique, Centre d'Etudes Nucleaires Report No. CEA-R-3141, January 1967, 60 pp. (N68-12167).

171. Faucher, J. F., Jr., Goldstein, S., Seery, D. J., Tabuck, S. and E., SUPERSONIC COMBUSTION OF FUELS OTHER THAN HYDROGEN FOR SCRAMJET APPLICATIONS. United Aircraft Corp. Final Report 1 July 1965-31 December 1966, Report No. E 910358-23, AFAPL TR-67-12, U.S. Air Force Contract AF 33(615)-3179, February 1967, 109 pp. (AD 379 427L) (REPORT CLASSIFIED CONFIDENTIAL).

172. Favre, J. A. (Phillips Petroleum Co.), STABLE JET FUELS. U.S. 3,216,929 (Cl. 208-312), November 9, 1965, Appl. October 27, 1961, 6 pp.; C.A. 64, 507 (1966).

173. Fedoceyev, V. A., TRACE METHOD AND ITS APPLICATION TO THE INVESTIGATION OF DISPERSED-FUEL COMBUSTION KINETICS. Teplofiz. i Teplotekhn. (Kiev), 1964, 136-9; U.S. Air Force Translation FTD-HT-66-706 (AD 661 898) (N68-13238).

174. Fendell, F. E. (TRW Systems), COMBUSTION IN INITIALLY UNMIXED REACTANTS FOR ONE-STEP REVERSIBLE CHEMICAL KINETICS. Astronautica Acta 13, 183-91 (1967); U.S. Army AROD-6453: 4, Contract DAHC04-67-C-0015, March 1966, 12 pp. (AD 554 979).

175. Ferrell, J. K. and Stahel, E. P., HEAT TRANSFER. Ind. Eng. Chem. 57 (12), 63-71 (1965); C.A. 64, 4620 (1966).

176. Ferri, A. and Mandel, M., ANALYTICAL AND EXPERIMENTAL INVESTIGATION OF THE LOW SPEED FIXED GEOMETRY SUPERSONIC COMBUSTION RAMJET. VOLUME II-FINAL CONTRACT WORK. General Applied Science Laboratories, Inc. Final Report January 65-March 66, Report No. GASL-TR-621-Vol 2, AFAPL TR-66-102-Vol. 2, U.S. Air Force Contract AF 33(615)-2436, January 1967, 211 pp. (AD 378 928L) (REPORT CLASSIFIED CONFIDENTIAL).

177. Ferri, A., Moretti, G., Slutsky, S. (General Applied Science Laboratories, Inc.), MIXING PROCESSES IN SUPERSONIC COMBUSTION. U.S. National Aeronautics and Space Administration Report No. NASA-CR-62194, 1964, 61 pp. (N65-21457); C.A. 65, 12053 (1966).

178. Ferron, J. R., Dunham, P. G., Gajda, J. F., SHOCKTUBE STUDIES OF GAS-LIQUID REACTIONS AND OF GAS PHASE DIFFUSION. PART II. IMPROVED ANALYSIS OF GAS PHASE DIFFUSION COEFFICIENTS. Delaware University Final Report, 31 July 1965-31 March 1967, U.S. Air Force AFML TR-65-416-Pt. 2, U.S. Air Force Contract AF 33(615)-1770, April 1967, 30 pp.; (AD 651 817).

179. Foster, R. P. and Sutphin, E. M., ECONOMICAL MACH 3+ SST SUPERSONIC TRANSPORT FUEL AVAILABLE NOW. Soc Automotive Engrs. Natl. Aeron + Space Eng. + Mfg. Mtg. (Los Angeles 10 4-8 65) Paper N.650805, 9 pp.

180. Freeman, E. S. and Rudloff, W., THE CATALYTIC ACTIVITY OF METAL OXIDES ON THERMAL DECOMPOSITION REACTIONS. IIT Research Inst. Final Technical Report 22 March 1965-30 September 1966, Report No. IITRI-U6017-6, U.S. Army Contract DA-18-035-AMC-341(A), March 1967, 142 pp. (AD 814 879L).

181. Fridshtein, I. L., Shmuk, Yu. A., Mikhailin, Yu. A., Zimina, N. A., METHOD FOR REGENERATING HYDROCARBON DEHYDROGENATION CATALYSTS BASED ON ALUMINUM OXIDE. U.S.S.R. 181,050 (Cl. B 01j), April 15, 1966, Appl. December 8, 1962; C.A. 65, 8636 (1966).

182. Frilette, V. J., Hagg, W. O., Munns, G. W., Jr., (Socony Mobil Oil Co., Inc.), CATALYTIC DEHYDROCYCLIZATION. U.S. 3,207,801 (Cl. 260-673.5), September 21, 1965, Appl. August 7, 1961, 4 pp.; C.A. 63, 14757 (1965).

183. Fristrom, R. M. (Johns Hopkins Univ.), FLAME STRUCTURE AND FLAME PROCESSES. Birmingham Univ., Chem. Engr. 16 (2), 42-56 (1965); C.A. 63, 12962 (1965).

184. Fuhs, A. E. (University of Colorado), A CONTROL DEVICE FOR SUPERSONIC COMBUSTION UTILIZING SPECTRAL INTENSITY RATIO. J. Spacecraft Rockets 3 (2), 269-70 (1966); C.A. 64, 17345 (1966).

185. Gadzhi-Kasumov, V. S., Isagulyants, G. V., Balandin, A. A., ISOMERIZATION AND DEHYDROGENATION OF CYCLOHEXANE ON CHROMIUM OXIDE. Izv. Akad. Nauk SSSR, Ser. Khim. 1966 (5), 921-2 (Russ); C.A. 65, 10459 (1966).

186. Gadzhi-Kasumov, V. S., Kiperman, S. L., Isagulyants, G. V., Balandin, A. A., KINETICS OF CYCLOHEXANE DEHYDROGENATION OVER CHROMIUM OXIDE IN A GRADIENTLESS SYSTEM. Kinetika i Kataliz 7 (2), 273-8 (1966) (Russ); C.A. 65, 5323 (1966).

187. Galich, P. N., Golubchenko, I. T., Gutyrya, V. S., Il'in, V. G., Neimark, I. E., CATALYSIS ON SYNTHETIC ZEOLITES CONTAINING GROUP I METAL CATIONS. Ukr. Khim. Zh. 31 (11), 1117-22 (1965) (Russ); C.A. 64, 12571 (1966).

188. Garwood, W. E., Hamilton, L. A., Kerr, G. T., Myers, C. G. (Socony Mobil Oil Co., Inc.), SULFUR AND HYDROCARBON DEHYDROGENATION WITH ZEOLITE CATALYSTS. U.S. 3,247,278 (Cl. 260-683.3), April 19, 1966, Appl. March 21, 1963, 11 pp.; C.A. 65, 2124 (1966).

189. Garwood, W. E. and Kerr, G. T. (Socony Mobil Oil Co., Inc.), ALUMINOSILICATE CATALYSTS FOR HYDROCARBON CONVERSIONS. U.S. 3,228,889 (Cl. 252-428), January 11, 1966, Appl. April 23, 1963, 6 pp.; C.A. 64, 7947 (1966).

190. General Applied Science Laboratories, Inc., INVESTIGATIONS OF THE LOW SPEED FIXED GEOMETRY SUPERSONIC COMBUSTION RAMJET. Final Report April-September 1966, Report No. GASL-TR-635, U.S. Air Force AF APL TR-66-139, U.S. Air Force Contract AF 33(615)-5051, March 1967, 98 pp. (AD 379 779L) (REPORT CLASSIFIED CONFIDENTIAL).

191. General Applied Science Laboratories, Inc., SUPERSONIC COMBUSTION RAMJET DEVELOPMENT PROGRAM. Final Report 17 March 1966-31 January 1967, Report No. GASL-TR-649, U.S. Army Contract DA-01-021-AMC-14072(z), March 1967, 204 pp. (AD 380 591) (REPORT CLASSIFIED CONFIDENTIAL).

192. General Electric Co., Flight Propulsion Division, COMMERCIAL SUPERSONIC TRANSPORT ENGINE PROPOSAL. VOLUME I(F). SUMMARY. (AD 377 953L); VOLUME I(J). SUMMARY. (AD 377 954L); VOLUME E-II(F). COMMERCIAL ENGINE MODEL SPECIFICATION. (AD 377 955L); VOLUME E-II(J). COMMERCIAL ENGINE MODEL SPECIFICATION. (AD 377 956L); VOLUME E-III(F). ENGINE INSTALLATION DATA FOR LOCKHEED, APPENDIX. (AD 377 959L); VOLUME E-III(J). ENGINE INSTALLATION DATA FOR BOEING. APPENDIX. (AD 377 957L); VOLUME E-III(J). ENGINE INSTALLATION DATA FOR NORTH AMERICAN AVIATION. APPENDIX. (AD 377 958L); VOLUME E-IV(F). ENGINE PERFORMANCE REPORT. (AD 377 960L); VOLUME E-IV(J). ENGINE PERFORMANCE REPORT. (AD 377 961L); VOLUME E-V(F). ENGINE DESIGN REPORT. (AD 377 962L); VOLUME E-V(J). ENGINE DESIGN REPORT. (AD 377 963L); VOLUME E-VI(F). COMPONENT DESCRIPTIONS AND PERFORMANCE - PART I. (AD 377 964L); VOLUME E-VI(F). COMPONENT DESCRIPTIONS AND PERFORMANCE - PART II. (AD 377 965L); VOLUME E-VI(J). COMPONENT DESCRIPTIONS AND PERFORMANCE - PART I. (AD 377 966L); VOLUME E-VI(J). COMPONENT DESCRIPTIONS AND PERFORMANCE PART II. (AD 377 967L); VOLUME F-VII(F). ENGINE INSTALLATION. (AD 377 968L); VOLUME E-VII(J). ENGINE INSTALLATION. (AD 377 969L). Report Nos. P64-1-Vol. 1(F), P64-1-Vol. 1(J), P64-1-Vol. E-2(F), P64-1-Vol. E-2(J), P64-1-Vol. E-3(F)-L-App., P64-1-Vol. E-3(J)-B-App., P64-1-Vol. E-3(J)-NA-App., P64-1-Vol. E-4(F), P64-1-Vol. E(J), P64-1-Vol. E-5(F), P64-1-Vol. E-5(J), P64-1-Vol. E-6(F)-Pt. 1, P64-1-Vol. E-6(F)-Pt. 2, P64-1-Vol. E-6(J)-Pt. 1, P64-1-E-6(J)-Pt-2, P64-1-Vol. E-7(F), and P64-1-Vol. E-7(J), U.S. Federal Aviation Agency Contract FA-SS-64-1, January 1964, 25, 25, 10, 10, 19, 23, 21, 304, 345, 165, 164, 425, 380, 352, 360, 180, and 181 pp. REPORT CLASSIFIED CONFIDENTIAL).

193. General Electric Co., Flight Propulsion Division, SUPERSONIC TRANSPORT ENGINE REPORT. PHASE II-A. VOLUME IX-E. ENGINE SUBSTANTIATING DATA. PART II. TECHNICAL SECTION B1. ENGINE DESIGN SUMMARY AND SYSTEMS. (AD 378 353L); TECHNICAL SECTION B2. ENGINE DESIGN BASIC ENGINE COMPONENTS. (AD 378 354L); TECHNICAL SECTION B3. ENGINE DESIGN POWER CONTROL AND ACCESSORIES. (AD 378 355L). Report Nos. P64-96 Vol. 9E-Pt.-2B1, P64-96-Vol. 9E-Pt.-B2, and P64-96-Vol. 9E-Pt.-2B3, U.S. Federal Aviation Agency Contract FA-SS-64-1, November 1964, 146, 339, and 463 pp, (REPORT CLASSIFIED CONFIDENTIAL).

194. General Electric Co., Flight Propulsion Div., SUPERSONIC TRANSPORT ENGINE PROGRAM. PHASE IIC. VOLUME I. ENGINE PERFORMANCE GE 4/J5K LOCKHEED CONFIGURATION. (AD 378 982L); VOLUME II. ENGINE PERFORMANCE GE 4/J5K LOCKHEED CONFIGURATION. (AD 378 983L); ENGINE PERFORMANCE GE 4/J5G BOEING CONFIGURATION. (AD 378 984L). Report Nos. R65FPD260-Vol. 1, R65FPD260-Vol. 2, and R65FPD259, U.S. Federal Aviation Agency Contract FA-SS-66-6, November 1965, 390, 168, and 302 pp. (REPORT CLASSIFIED CONFIDENTIAL).

195. General Electric Co., Advanced Technology and Demonstrator Programs Dept., HIGH BYPASS RATIO PROPULSION SYSTEMS INVESTIGATION. Final Report August 1965-August 1966, U.S. Air Force AFAPL TR-66-112, Contract AF 33(615)-2894, November 1966, 228 pp. (AD 381 116L) (REPORT CLASSIFIED CONFIDENTIAL).

196. General Electric Co., Advanced Technology and Demonstrator Programs Dept., SCRAMJET COMBUSTOR SCIENTIFIC TECHNOLOGY. Quarterly Presentation No. 2, U.S. Air Force Contract AF 33(615)-3733, March 1967, 45 pp. (AD 380 679L) (REPORT CLASSIFIED CONFIDENTIAL).

197. General Electric Co., Flight Propulsion Division, SUPERSONIC TRANSPORT PHASE III PROGRAM. VOLUME I. SUMMARY. (AD 378 482L); VOLUME III - TECHNICAL/ENGINE, A. ENGINE PERFORMANCE REPORT. (AD 378 483L); VOLUME III - TECHNICAL/ENGINE B. ENGINE DESIGN REPORT. PART I - MAJOR COMPONENTS. (AD 378 484L). U.S. Federal Aviation Agency Contract FA-SS-66-6, September 1966, 124, 406, and 469 pp. (REPORT CLASSIFIED CONFIDENTIAL).

198. General Electric Co., Flight Propulsion Div., SUPERSONIC TRANSPORT PROPULSION. PHASE IIC. Final Report, U.S. Federal Aviation Agency Contract FA-SS-66-6, January 1967, 160 pp. (AD 376 924L) (REPORT CLASSIFIED CONFIDENTIAL).

199. General Electric Co., Flight Propulsion Div., COMMERCIAL SUPERSONIC TRANSPORT ENGINE. GE 4/J5M MODEL SPECIFICATION E-2053 LOCKHEED CONFIGURATION. Report No. Spec-E-2053, U.S. Federal Aviation Agency Contract FA-SS-66-6, May 1966, 40 pp. (AD 806 977L).

200. General Electric Co., Flight Propulsion Division, COMMERCIAL SUPERSONIC TRANSPORT ENGINE. PHASE II C DETAILED WORK PLAN. GE4/J5 ENGINE DEVELOPMENT. Revision of Report dated 20 August 1965, U.S. Federal Aviation Agency Contract FA-SS-66-6, September 1965, 132 pp. (AD 807 357L) (REPORT CLASSIFIED CONFIDENTIAL).

201. Ginevskii, A.S., HEAT - AND MASS TRANSFER IN A NONISOTHERMAL TURBULENT GAS STREAM OF A CHANGING COMPOSITION. Teplo- i Massoperenos 2, 377-90 (1965) (Russ). C.A. 65, 11805 (1966).

202. Glassman, I. (ed), RECENT ADVANCES IN AEROTHERMOCHEMISTRY, VOLUME I. Papers presented at the 7th AGARD Colloq., Oslo, 16-20 May 1967, Advisory Group for Aerospace Research and Development Report No. AGARD-CP-12, Vol. 1, 1967, 462 pp. (N67-38681).

203. Glinkov, M.A. and Liberman, L.F., THE ELECTRICAL CONDUCTIVITY OF A LUMINOUS HYDROCARBON FLAME. Izv. Vysshikh Uchebn. Zavedenii, Chern. Met. 8 (11), 176-9 (1965) (Russ) C.A. 64, 5865 (1965).

204. Gogitidze, L.D., Makarenkov, V.V., Panchenkov , G.m., Pustyrev, O.G., Yakovlevskii, V.V., METHOD OF ESTIMATION OF THE COMBUSTION CHARACTERISTICS OF THE HYDROCARBON FUELS BY MEANS OF A CHAMBER TYPE BURNER. Metody Otsenki Ekspluatatsion, Svoistv Reaktivnykh Topliv i Smaz. Materilaov, Sb. Statei 1966, 18-26 (Russ). C.A. 65, 16752 (1966).

205. Golosov, S.A., Katsobashvili, Ya.R., Sheftelevich, Yu.L., EFFECT OF FRACTIONAL COMPOSITION AND RESIDUAL AMOUNT OF AROMATIC HYDROCARBONS ON THE STABILITY OF FUELS. Khim. i Tekhnol. Topliv i Masel, Vol. 12, No. 4, 11-13 (Apr. 1967).

206. Gonikberg, M.G., Gavrilova, A.E., Komanenkova, R.A., THE MECHANISM OF HOMOGENEOUS DEALKYLATION OF ALKYLNAPHTAHALENES. Neftekhimiya 5 (4), 489-92 (1965) (Russ) C.A. 63, 17815 (1965).

207. Goodyear Tire and Rubber Co. (by K.J. Frech), SELECTIVE THERMAL CRACKING OF PARAFFINS TO OLEFINS WITH FREE RADICAL INITIATORS. Fr. 1, 401, 586 (Cl. C 07c), June 4, 1965; U.S. Appl. June 10, 1963; 20 pp. C.A. 63, 9727 (1965).

208. Gootzait, E., Rofte, G., Gaganidze, T.P., WIND TUNNEL TESTS OF A LOW IGNITION DELAY FUEL INJECTOR. General Applied Science Laboratories, Inc. Technical Memo, Report No. GASL-TM-148, U.S. Army Contract DA-01-021-AMC-14072(Z), July 1966, 35 pp. (AD 376450) (REPORT CLASSIFIED CONFIDENTIAL).

209. W.R. Grace and Co., SYNTHETIC ZEOLITES. Neth. Appl. 6, 506, 221 (Cl. C 01b), November 16, 1965, U.S. Appl. May 14, 1964; 11 pp. C.A. 64, 15434 (1966).

210. Gring, J.L. and Mooi, J. (Sinclair Refining Co.), CATALYTIC HYDROCARBON-CONVERSION PROCESS. U.S. 3, 267, 025 (Cl. 208-136), August 16, 1966; Appl. April 28, 1965; 20 pp. C.A. 65, 16760 (1966).

211. Gruzdev, V.N. and Talantov, A.V., FLIGHT REGIMES OF A VEHICLE WITH A RAMJET ENGINE WHICH PROVIDE FOR CONSTANT CONDITIONS OF FLAME STABILIZATION. Izvestiya Vysshikh Uchebnykh Zavedenii, Aviatsionnaya Tekhnika (USSR) 1966, no. 4, 121-8; U.S. Air Force Translation Report no. FTD-HT-67-24, TT67-62110, February 1967, 17 pp. (AD 653541).

212. Gryaznov, A.P. and Rozhkov, I.V., INVESTIGATION OF THE ANTIWEAR PROPERTIES OF REACTIVE FUELS. Khimiya i Tekhnologiya Topliv i Masel (USSR) 9, no. 4, 57-60 (1964); U.S. Air Force Translation Report no. FTD-TT-65-1730, TT 66-62518 (AD 641 107).

213. Gryaznov, A.P., Kukushkin, A.A., Smirnov, G.G., Englin, B.A., Golenev, N.P., STUDY OF THE EFFECT OF ETHYLCELLOSOLVE ON THE THERMAL STABILITY OF FUELS T-1 AND TS-1. Khim. i Tekhnol. Topliv i Masel, Vol. 12, No. 3, 56-58 (Mar 1967).

214. Guenther, R., COMBUSTION MECHANISM IN TURBULENT GAS FLAMES. Intern. Z. Gaswaerme 14 (1), 6-13 (1965) (Ger). C.A. 63, 17757-8.

215. Gurevich, M.A. and Sotnichneko, B.I., CRISES AND STABILITY OF THERMAL COMBUSTION REGIMES - FIRST ORDER BOUNDARY CONDITIONS. Teplo - i Massoperenos 4, 197-212 (1966) (Russ) C.A. 65, 16523 (1966).

216. Gurvich, A.V., Khachkuruzov, G.A., Medvedev, V.A., Veyts, I.V., Bergman, G.A., et al., THERMODYNAMIC PROPERTIES OF INDIVIDUAL SUBSTANCES. VOLUME I: CALCULATION OF THE THERMODYNAMIC PROPERTIES. (Chapters 1 thru 15). Izd. Akad. Nauk SSSR (Moscow), 1962, 1033 pp.; U.S. Air Force Translation FTD-HT-66-251, Vol. Pt. I; TT-67-63067 (AD 659659) (N68-10297).

217. Gurvich, A.V., Khachkuruzov, G.A., Medvedev, V.A., Veyts, I.V., Bergman, G.A., THERMODYNAMICS PROPERTIES OF INDIVIDUAL SUBSTANCES. VOLUME I: CALCULATION OF THE THERMODYNAMIC PROPERTIES. (Chapters 16 thru 27). Termod'namicheskie Svoistva Individualnykh Veschestv, TOm I; Vychislenie Termodinamicheskikh Svoistv, 2 d ed., Moscow, 1962, 437-858; U.S. Air Force Translation Report FTD-HT-66-251-Pt. 2, TT-67-63067, March 1967, 940 pp. (AD 656659).

218. Haensel, V. (Universal Oil Products Co.) CATALYSIS IN THE PETROLEUM INDUSTRY. Am. Petrol. Inst. Preprint No. 28, 6 pp. (1966) C.A. 65, 8620 (1966).

219. Hager, J.A., HIGH-TEMPERATURE HYDROCARBON FUELS AND SUBSONIC FLIGHT ENVIRONMENTS, Soc Automotive Engrs. Mtg (1965), Paper N.650115, SAE (Soc Automotive Engrs.) Trans V74.513-22 (1966).

220. Hager, J.A., HIGH-TEMPERATURE (HYDROCARBON) FUELS POSE PROBLEMS IN SUBSONIC ENVIRONMENT, Soc Automotive Engrs. Mtg Paper N.9878, (COND) SAE (Soc Automotive Engrs.) J V74, N.5.38-42, (May 1966).

221. Hangen, W.J., PROPERTIES OF JP-5 FUEL. Chrysler Corp. Technical Memo Report no. TM-MT-M44 J, Report on Field Artillery Guided Missile System Redstone, December 1957, 27 pp. (AD 291128).

222. Hansen, C.F., APPROXIMATIONS FOR THE THERMODYNAMIC AND TRANSPORT PROPERTIES OF HIGH-TEMPERATURE AIR. U.S. National Aeronautics and Space Administration Technical Report No. NASA-TR-R-50, 1959, 38 pp. (PB 175855).

223. Harrje, D.T., HEAT TRANSFER IN OSCILLATING FLOW. Princeton University, Department of Aerospace and Mechanical Sciences Final Report for 1958 - October 1967, Report no. 483-g, U.S. Navy Contract Nonr-1858(29), October 1967, 10 pp. (AD 664303).

224. Hasel, L.E., Foss, W.E., Jr., Bowditch, D.N., NASA COMPILATION OF PAPERS SUMMARIZING SOME RECENT NASA RESEARCH ON MANNED MILITARY AIRCRAFT, IV. AIR-BREATHING PROPULSION SYSTEMS FOR SUPERSONIC AIRCRAFT, October 1960, 57-71 (N67-33074).

225. Hashemi, H.T. (Univ. of Okalhoma, Norman), HEAT CONDUCTION WITH CHANGE OF PHASE. Univ. Microfilms (Ann Arbor, Mich.), Order No. 65-8355, 385 pp.; C. A. 64, 310 (1966).

226. Hashiguchi, Y., Ogahara, T., Iwasaki, M., Ozawa, K., EFFECT OF HIGH PRESSURES ON THE FLAMMABILITY LIMITS OF ETHYLENE. Kogyo Kagaku Zasshi, 69 (4), 593-7 (1966) (Japan); C. A. 65, 16781 (1966).

227. Hastings, R.C., Brown, C.S., Atkinson, S., HEAT TRANSFER IN THE VICINITY OF A 15° COMPRESSION CORNER AT MACH NUMBERS FROM 2.5 TO 4.4. Great Britian Aeronautical Research Council ARC-CP-965, London, H.M. S.O., 1967, 36 pp.; (N68-12968).

228. Haxby, L.P., Lawler, G.F., Ludwig, A.L., (Shell Oil Co.,), THERMAL STABILITY OF JET FUEL CAN BE MAINTAINED FROM REFINERY TO AIRCRAFT. (TURBINE FUEL THERMAL STABILITY...FROM REFINERY TO SUPERSONIC TRANSPORT) SAE Mtg Paper N.660719 (1966), (ADAPT) SAE (Soc Automotive Engrs.) J V75 N.7 48-49 (July 1967).

229. Heaston, R.J., FRONTIERS OF CATALYSIS. U.S. Army Research and Development Group (Europe), February 1967, 22 pp.; (AD 808824L).

230. Heath, C.A. and Costello, C.P., SOME EFFECTS OF GEMOETRY, ORIENTATION, AND ACCELERATION ON POOL FILM BOILING OF ORGANIC FLUIDS. J. Eng. Ind., 88 (1), 17-23 (1966); C. A. 66, 13779 (1966).

231. Hollander, Tj., PHOTOMETRIC MEASUREMENTS ON THE DEVIATIONS FROM THE EQUILIBRIUM STATE IN BURNT FLAME GASES. Univ. of California, Santa Barbara, Dept. of Physics Report No. TR-22, U.S. Navy Contract Nonr-4222 (01), July 1967, 16 pp. (AD 655 143).

232. Homer, J. B. and Kistiakovsky, G. B., THE OXIDATION AND PYROLYSIS OF ETHYLENE IN SHOCK WAVES. Harvard University, Department of Chemistry, U.S. Navy Contract Nonr-1866(36), July 1967, 28 pp. (AD 656 040).

233. Horn, K. P., Kolpin, M. A., Reichenbach, R. E., A STUDY OF PENETRATION OF A LIQUID INJECTION INTO A SUPERSONIC FLOW. Aerospace Corp., Report No. TR-1058(3220-10)-1, SAMSO-TR-67-65, Contract F04695-67-C-0158, October 1967, 39 pp. (AD 663 417).

234. Hsu, Y., Cowgill, G. R., Hendricks, R. C., MIST-FLOW HEAT TRANSFER USING SINGLE-PHASE VARIABLE-PROPERTY APPROACH. U.S. National Aeronautics and Space Administration Report NASA-TN-D-4149, December 1967, 81 pp. (N68-?).

235. Hufschmidt, W., Burck, E., Reibold, W., DETERMINATION OF LOCAL OR MEAN HEAT-TRANSFER COEFFICIENTS IN TUBES WITH HIGH HEAT FLUX. Intern. J. Heat Mass Transfer 9 (6), 539-65 (1966); C.A. 65, 6760 (1966).

236. Hughes, L. J. (Monsanto Co.), CATALYTIC DEHYDROGENATION OF LONG-CHAIN HYDROCARBONS. U.S. 3,248,451 (Cl. 260-683.3), April 26, 1966, Appl. April 19, 1963; 2 pp.; C.A. 65, 2123 (1966).

237. Hughmark, G. A. (Ethyl Corp.), HEAT TRANSFER IN VERTICAL ANNULAR TWO-PHASE FLOW. A.I. Ch. E. Journal 11 (5), 937 (1965); C.A. 64, 3078 (1966).

238. Hurwicz, H. (Avco Corp., Research and Advanced Development Div.), AEROTHERMOCHEMISTRY STUDIES IN ABLATION. AGARD Combustion and Propulsion Colloquium (5th), Braunschweig, 9-13 April 1962, pp. 1-50, (AD 659 766).

239. Ignatov, V. M. and Chertkov, Ya.B., A COMPARATIVE EVALUATION OF THE ACTION OF ADDITIVES FOR JET FUELS, Khim. i Tekhnol. Topliv i Masel, Vol. 11, No. 6, 53-56 (June 1966).

240. Isagulyants, G. V., Komarova, E. N., Balandin, A. A., MECHANISM OF DEHYDROGENATION OF SIX-MEMBERED CYCLANES DEHYDROGENATION OF METHYLCYCLOHEXANE OVER ALUMINOCHROMIUM CATALYSTS. Dokl. Akad. Nauk SSSR 164 (6), 1307-10 (1965) (Russ); C.A. 64, 1919 (1966).

241. Ito, T. and Nishikawa, L., TWO-PHASE BOUNDARY LAYER TREATMENT OF FORCED-CONVECTION FILM BOILING. Intern. J. Heat Mass Transfer 9 (2), 117-30 (1966); C.A. 66, 12220 (1966).

242. Ivan'kovich, Ya.F., Zaretskii, M. V., Erofeev, B. V., SPINELS AS THE CATALYST CARRIERS IN THE REACTION OF AROMATIZATION OF n-HEXANE. Vestsi Akad. Navuk Belarusk. SSR, Ser. Khim. Navuk 1965 (2), 5-9 (Belorussian); C.A. 64, 4971 (1966).

243. Ivernel, A., OXYGEN AND COMBUSTION. THEORETICAL AND EXPERIMENTAL FUNDAMENTAL INFORMATION. III. HEAT TRANSMISSION. Rev. Gen. Thermique 4 (41), 542-51 (1965) (Fr); C.A. 63, 9722 (1965).

244. Jain, V. K. and Mukunda, H. S., A REVIEW OF THE STUDIES ON FLAME STABILIZATION PHENOMENA. India Ints. of Science, India, Dept. of Aeronautical Engineering Report AE-163A, May 1966, 35 pp. (N68-11018).

245. Johnston, R. K. and Anderson, E. L., A REVIEW OF LITERATURE ON STORAGE AND THERMAL STABILITY OF JET FUELS. U.S. Dept. Com. Office Tech. Serv. Publ. (Jan. 1964) 30 pp, (ABSTR) Mater Res. Std. Vol. 4, No. 9, 520 (Sept. 1964).

246. Johnston, R. K., (U.S. Air Force and Southwest Research Institute), IMPROVING THE STORAGE STABILITY OF JET FUELS BY THE USE OF ADDITIVES. Soc. Automotive Engrs. Mtg. Paper No. S393 (ABSTR) SAE (Soc. Automotive Engrs.) J V72 No. 9, 189 (Sept. 1964).

247. Kallergis, M., NOMOGRAPH REPRESENTATION OF PROCESSES IN RAM-JET ENGINES WITH EXTERNAL COMBUSTION [NOMOGRAPHDARSTELLUNG DER VORGAENGE BEI STAUSTRAHLTRIEBWERKEN MIT AEUSSERER VERBRENNUNG.] Deutsche Forschungsanstalt für Luft-und Raumfahrt, Brunswick (West Germany). Institut Fuer Strahlantriebe Report No. DLR-FB-66-85, December 1966, 38 pp. (N67-30759) (in German, English Summary).

248. Kapitonov, E. N. and Lebedev, K. I., HYDRAULIC RESISTANCE AND HEAT TRANSFER IN THE MOTION OF BOILING SOLUTIONS IN A HORIZONTAL TUBE. Khim. Prom. 41 (7), 511-5 (1965) (Russ); C.A. 64, 312 (1966).

249. Kazanskii, B. A., Dorogochinskii, A. Z., Gitis, K. M., Rozengart, M. I., Lyuter, A. V., EFFECT OF THE MATERIAL OF THE REACTOR ON DEVELOPMENT OF AN Al-Cr-K CATALYST FOR AROMOATIZATION OF n-HEPTANE. Zh. Prikl. Khim. 39 (6), 1352-6 (1966) (Russ); C.A. 65, 9787 (1966).

250. Kazanskii, B. A., Dorogochinskii, A. Z., Rozengart, M. I., Breshchenko, E. M., Remizov, V. G., Ogloblina, L. I., Kuznetsova, Z. F., THE EFFECT OF THE POTASSIUM CONTENT ON THE DEHYDROCYCLIZATION PROPERTIES OF ALUMINUM-CHROMIUM-POTASSIUM CATALYSTS. Nauchn. Osnovy Podbora i Proizv. Katalizatorov, Akad. Nauk SSSR, Sibirsk. Otd. 1964, 312-6 (Russ); C.A. 63, 6367 (1965).

251. Kazanskii, B. A., Sterligov, O. D., Belen'kaya, A. P., THE USE OF AN ALUMINUM-CHROMIUM-POTASSIUM CATALYST FOR THE DEHYDROGENATION AND DEHYDROCYCLIZATION OF HYDROCARBONS. Nauchn. Osnovy Podbora i Proizv. Katalizatorov, Akad. Nauk SSSR, Sibirsk. Otd. 1964, 336-44 (Russ); C.A. 63, 6833 (1965).

252. Kent, E.A. (Nalco Chemical Co.), STABILIZATION OF JET FUELS WITH AMINE-CITRIC ACID REACTION PRODUCTS. U.S. 3, 258, 320 (Cl. 44-71), June 28, 1966, Appl. November 6, 1957 and May 31, 1960; 5 pp.; C. A. 65, 8659 (1966).

253. Keough, A.H. (Norton Co.), DEHYDROGENATION OF HYDROCARBONS. U.S. 3, 202, 724, (Cl. 260-668), August 24, 1965, Appl. July 17, 1961; 1 p.; C. A. 64, 1878 (1966).

254. Kessel'man, P.M. and Chernyshev, S.K., THERMODYNAMIC CHARACTERISTICS OF SOME HYDROCARBONS AT HIGHER TEMPERATURES. Teplofiz. Vysokikh Temperatur, Akad. Nauk SSSR, 3 (5), 700-7 (1965) (Russ); C. A. 64, 4339 (1966).

255. Kichkin, G.I., Rozhkov, I.V., Kornilova, E.M., EFFECT OF ADDITIVES ON ANTIWEAR PROPERTIES OF JET FUELS. USDC Clearinghouse Federal Sci. Tech. Inform. Ad No. 611, 531 (Feb 1965) 15 p. (ABSTR) Corrosion ABSTR Vol. 4, No. 6, 456 (Nov 1965).

256. Kikvidze, A.V., CATALYTIC PROPERTIES OF NICKEL ON ALUMINOSILICATE CARRIER IN HYDROGENATION AND DEHYDROGENATION REACTIONS. Poverkhn. Yavleniya na Alyumosilikatakh, Akad. Nauk Gruz. SSR, Inst. Fiz. i Or Organ. Khim., Sb. Statei 1965, 119-23 (Russ); C. A. 64, 8969 (1966).

257. Kirkby, L.L. and Schmitz, R.A., (University of Illinois), AN ANALYTICAL STUDY OF THE STABILITY OF A LAMINAR DIFFUSION FLAME. Combustion and Flame 10, No. 3, 205-20 (Sept 1966); AROD 5648:1, Contract NSF-GP-700, January 1966, 16 pp. (AD 645 198).

258. Kirkham, F.S., Cubbage, J.M., Jr., Vahl, W.A., Small, W.J., STUDIES OF AIRFRAME - PROPULSION-SYSTEM INTEGRATION FOR MACH 6 CRUISE VEHICLES. U.S. National Aeronautics and Space Administration, Langley Research Center Report NASA-TN-D-4128, October 1967, 22 pp. (N67-38848).

259. Kittredge, G.D., EFFECTS OF FLAME RADIANT HEATING ON TEMPERATURE AND DURABILITY OF LABORATORY SCALE JET COMBUSTOR FLAME TUBES. Phillips Petroleum Co., Research Div. Special Report No. 2033-58R, U.S. Navy Contract NOas-58-310, March 1958, 32 pp.; (AD 813 498).

260. Kline, R.E. and Starnes, W.C. (Gulf Research and Development Co), CATALYST FOR DEHYDROCYCLIZATION OF HYDROCARBONS. U.S. 3, 240, 719 (Cl. 252-465), March 15, 1966, Appl. May 1, 1963; 6 pp.; C. A. 64, 15653 (1966).

261. Kozlov, L.V., EXPERIMENTAL DETERMINATION OF THE LAW OF HEAT EXCHANGE FOR THE TURBULENT BOUNDARY LAYER IN A SUPERSONIC FLOW. Issledovanie Teploobmena v Potokakh Zhidkosti i Gaza, Moscow, 1965, pp. 91-102; U.S. Air Force Translation FTD-HT-66-379, TT67-62137, January 1967, 20 pp.; (AD 653 956).

262. Krein, S.E., Rubinshtein, I.A., Popova, E.A., THE ANTIOXIDANT PROPERTIES OF ORGANIC SULFUR COMPOUNDS IN PETROLEUM AND THE POSSIBLE FORMATION OF ARYL SULFIDE COMPLEXES. Neftekhimiya 6 (2), 241-8 (1966) (Russ); C. A. 65, 2025 (1966).

263. Kroll, R.W. and Billet, F., PARAMETRIC PERFORMANCE OF SUPERSONIC COMBUSTION RAMJETS. Marquardt Corp, Astro Report No. MR-20160, U.S. Air Force Contract AF 33(616)-7046, April 1962, 117 pp.; (AD 379644) (REPORT CLASSIFIED CONFIDENTIAL)

264. Kuchta, J.M., Bartkowiak, A., Zubetakis, M.G., (U.S. Dept. of the Interior), HOT SURFACE IGNITION TEMPERATURES OF HYDROCARBON FUEL VAPOR-AIR MIXTURES. J. Chem. Eng. Data 10 (3), 282-8 (1965); C. A. 63, 11239-40 (1965).

265. Kulagin, L.V. and Okhotnikov, S.S., BASIS OF REQUIREMENTS FOR QUALITY OF ATOMIZATION OF LIQUID FUEL IN HIGH-FORCED FURNACE DEVICES. Vsesoyuznyi Nauchno-Isseldovatelskii Institut Zheleznodorozhnogo Transporta Trudy (USSR) 1964, No. 264-19 (1964); U.S. Air Force Translation FTD-MT-65-487, September 1967, 23 pp.; (AD 661 932).

266. Kuznetsov, I.L. and Malanov, M.D., MEASURING THE TURBULENT VELOCITY OF FLAME PROPAGATION BY THE INVERSE-CONE METHOD. Zh. Prik. Mekhan i Techn. Fis. (Moscow) 1964 (4), 256-62; U.S. Air Force FTD-HT-66-261, TT-67-63189 (N68-11688); (AD 660 248).

267. Lagenbeck, W. and Grimm, H., HIGHLY SELECTIVE NICKEL DEHYDROGENATION CATALYST. Ger. (East) 36, 011 (Cl. C 07 c 1, B 01 j), February 5, 1965; Appl. May 16, 1964; 2 pp.; C. A. 63, 9862 (1965).

268. Lander H.R., Jr., STORAGE BEHAVIOR OF HIGH-TEMPERATURE JET FUELS, Soc Automotive Engrs. Mtg Paper No. S391 (ABSTR) SAE (Soc Automotive Engrs.) J V72 No. 9, 189 (Sept 1964).

269. Lander, H.R. and Zengel, A.E., HYDROCARBON FUELS FOR HYPERSONIC VEHICLES (U). U.S. Air Force Aero Propulsion Laboratory, Wright-Patterson AFB Technical Paper, Report No. AFAPL-CONF-67-3, September 1966, 30 pp. (AD 642 764). Presented at Annual Air Force Science and Engineering Symposium (13th), Arnold Engineering Development Center, Tenn., September 27-29, 1966.

270. Lander, H.R., Jr. and Zengel, A.E., RELATIONSHIP BETWEEN THE MINEX AND THE HELIUM--DRIVEN MODIFIED COKER IN THE MEASUREMENT OF JET FUEL THERMAL STABILITY. U.S. Air Force Aero Propulsion Lab., Wright-Patterson AFB Report No. AFAPL-TR-67-17, February 1967, 54 pp.; (AD 653 188).

271. Lavrov, N.V., SOME PHYSICAL AND CHEMICAL REGULARITIES IN COMBUSTION OF FUELS. Dokl. Adad. Nauk SSSR, 164 (5), 1111-4 (1965) (Russ); C. A. 64, 517 (1966) C. A. 63, 9707f.

272. Lawton, J. (Imperial College, London), EFFECTS OF ELECTRIC FIELDS, UPON FLAMES. Fuel Soc. J., Univ. Sheffield 16, 8-21 (1965); C. A. 64, 2745 (1966).

273. Leas, A.M. (Ashland Oil and Refining Co.), IN-FIELD CATALYTIC FILTRATION MAKES FUEL FIT FOR FUSSY SUPERSONIC PLANES. Soc Automotive Engrs. Mtg Paper No. S392 (COND) SAE (Soc Automotive Engrs.) J V73 No. 2, 55 (Feb 1965).

274. Leas, A.M., (Ashland Oil and Refining Co.), DELIVERY OF CLEAN, DRY, THERMALLY STABLE JET FUEL TO SUPERSONIC AIRCRAFT BY IN-FIELD CATALYTIC FILTRATION. Soc Automotive Engrs. Mtg Paper No. S392 (ABSTR) SAE (Soc Automotive Engrs.) J V72 No. 9, 189 (Sept 1964).

275. Le Bouc, F., JET ENGINES WITH SUPERSONIC COMBUSTION (SCRAMJETS). Rev Inst. Franc Petrole Ann Combust Liquides Vol. 22 No. 1, 162-74 (Jan 1967).

276. Le Grives, E., EXPERIMENTAL STUDY OF COMBUSTION IN SUPERSONIC FLOW. Colloq. Intern. Centre Natl. Rech. Sci. (Paris) No. 109, 273-80 (1961) (Fr); C. A. 65, 8625 (1966).

277. Lempel, M.J., A NUMERICAL METHOD FOR DETERMINING HEAT-TRANSFER CHARACTERISTICS FOR A DILUTE GAS-SOLIDS MIXTURE IN AN EXTERNALLY HEATED TUBE. U.S. Bureau of Mines Report No. BM-IC-8343, July 1967, 20 pp. (N67-34 071).

278. Le Pera, M.E., DEVELOPMENT OF A PROCEDURE FOR ANALYSIS OF FUEL DE-ICERS BY PROGRAMMED GAS-LIQUID CHROMOTOGRAPHY. U.S. Army Coating and Chemical Laboratory, Aberdeen Proving Ground Final Report No. CCL-208, July 1966, 22 pp. (AD 893 413L).

279. Le Pera, M.E., INVESTIGATION OF THE AUTOXIDATION OF PETROLEUM FUELS. Coating and Chemical Laboratory, Aberdeen Proving Ground Interim Report, Report No. CCL-204, Ju[illegible] 1966, 26 pp. (AD 641 270).

280. Levitt, B.P., Wright, N., Sheen, D.B., LIGHT EMISSION FROM SHOCK HEATED GASES. Imperial College of Science and Technology, London (England) Final Technical Report September 1965 - August 1966, U.S. Army Contract DA-91-591-EUC-3660, September 1966, 43 pp. (AD 804 966L).

281. Leyer, J.C., PRESSURE VARIATIONS PRODUCED DURING THE IGNITION OF HYDROCARBON - AIR MIXTURES. Compt. Rend., Ser. A, B 263B (3), 230-3 (1966) (Fr); C. A. 65, 19918 (1966).

282. Li, W.-C., et al. THE DETERMINATION OF THE ACIDITY OF SILICA - ALUMINA AND PLATINUM OXIDE - SILICA - ALUMINA CATALYSTS BY THE E.S.R. METHOD. Acta Foculio - Chim. Sinica 6 (3), 202-6 (1965) (Ch).; C. A. 65, 16107 (1966).

283. Liao, S. and Ch'in, H., THE EFFECT OF INITIAL TEMPERATURE ON THE RATE OF COMBUSTION OF FUEL-AIR MIXTURES. Chung-Kuo K'o Hsueh Yuan Ying Yung Hua Hsueh Yen Chiu So Chi K'an 1964 (11), 1-8 (Ch.); C. A. 64, 517 (1966).

284. Libby, P.A., (University of Calif., La Jolla), HEAT AND MASS TRANSFER AT A GENERAL THREE-DIMENSIONAL STAGNATION POINT. U.S. National Aeronautics and Space Administration Report NASA-CR-817, Grant NGR-05-009-025, July 1967, 44 pp. (N67-30133).

285. Liebman, I., Perlee, H.E., Corry, J., INVESTIGATION OF FLAME PROPAGATION CHARACTERISTICS IN LAYERED GAS MIXTURES. U.S. Bureau of Mines Report No. BM-RI-7078, February 1968, 38 pp. (N68-15703).

286. Lienhard, J.H. and Schrock, V.E. (Washington State University), GENERALIZED DISPLACEMENT OF THE NUCLEATE-BOILING HEAT FLUX CURVE, WITH PRESSURE CHANGE. Intern. J. Heat Mass Transfer 9 (4), 355-63 (1966); C. A. 64, 17073 (1966).

287. Lindquist, R.H., Mulaskey, B.F., Harnsberger, H.F. (California Research Corp.) DEHYDROGENATION CATALYST REJUVENATION. U.S. 3, 180, 903 (Cl. 260-680), April 27, 1965, Appl. August 21, 1958; 5 pp.; C. A. 63, 1640 (1965).

288. Litchfield, E.L., Hay, M.H., Kubala, T.A., Monroe, J.S., MINIMUM IGNITION ENERGY AND QUENCHING DISTANCE IN GASEOUS MIXTURES: TECHNIQUES AND APPARATUS. U.S. Bureau of Mines Report No. BM-RI-7009, August 1967, 16 pp. (N67-34598).

289. Lockheed - California Co., PROPOSAL FOR THE DEVELOPMENT OF A COMMERCIAL SUPERSONIC TRANSPORT. Volume A-II. MODEL SPECIFICATIONS. (AD 802 2536). Report No. LAC-LR-17321, January 1964, 79 pp. Volume A-III. AIRCRAFT DESCRIPTION. (AD 802 229L). Report No. LAC-LR-17322, January 1964, 368 pp. Volume M-III. PRODUCT SUPPORT PLAN. (AD 802 342L). Report No. LAC-LR-17332, January 1964, 385 pp.

290. Lockheed - California Co., SUPERSONIC TRANSPORT DEVELOPMENT PHASE II-C. Volume IV. AIRCRAFT SYSTEM CONCEPT(CLASSIFIED PAGES). (AD 378 897L). Report No. LR-19162 - CLASSIFIED, U.S. Federal Aviation Agency Contract FA-SS-66-7, November 1965, 6 pp. Volume VII. AIRCRAFT PROPULSION SYSTEM. (AD 378 935L). Report No. LAC-606034, LR-19163, U.S. Federal Aviation Agency Contract FA-SS-66-7, November 1965, 22 pp. (REPORTS CLASSIFIED CONFIDENTIAL.)

291. Lockheed - California Co., SUPERSONIC TRANSPORT DEVELOPMENT PHASE II-C. VOLUME III-BOOK 2. SYSTEM PERFORMANCE SPECIFICATIONS. Report No. LAC-60631-BK 2, U.S. Federal Aviation Agency Contract FA-SS-66-7, July 1966, 58 pp. (AD 378 932L). (REPORT CLASSIFIED CONFIDENTIAL)

292. Lockheed - California Co., SUPERSONIC TRANSPORT DEVELOPMENT PROGRAM. PHASE III PROPOSAL. Volume II-E. PROPULSION REPORT, BOOK 1. (AD 804 541L). Report No. LR-19841-Bk-1, U.S. Federal Aviation Agency Contract FA-SS-66-7, September 1966, 269 pp. Volume II-E. PROPULSION REPORT. BOOK 3. (AD 804 652L). Report No. LR-19841-Bk-3, U.S. Federal Aviation Agency Contract FA-SS-66-7 September 1966, 106 pp. Volume II-F. ENGINE SELECTION REPORT. (AD 378 3516). Report No. LR-19842, LAC-610806, U.S. Federal Aviation Agency Contract FA-SS-66-7, September 1966, 168 pp. (REPORT CLASSIFIED CONFIDENTIAL). Appendix A. INSTALLED ENGINE PERFORMANCE DATA--GENERAL ELECTRIC. (AD 378 985L). Report No. LAC-610807, LR-19852, U.S. Federal Aviation Agency Contract FA-SS-66-7, September 1966, 350 pp. (REPORT CLASSIFIED CONFIDENTIAL).

293. Long, G.A., IGNITION OF FUEL DROPLETS IN HOT STAGNANT GASES. M.S. Thesis, University of California, Lawrence Radiation Laboratory Report UCRL-17811, September 1967, 76 pp. (N68-16885).

294. Long, R.B. (Esso Research and Engineering Co.), REACTOR COOLANT SYSTEM (EMPLOYING NAPHTHENE ENDOTHERMIC DEHYDROGENATION EXOTHERMIC REHYDROGENATION CYCLE). U.S. 3, 198, 710 (Cl. 176-39), August 3, 1965, Appl. November 12, 1958; 5 pp.; C.A. 63, 12656 (1965).

295. Longwell, J.P., Eames, J.P., Yahnke, R.L., STUDY OF COMBUSTORS FOR SUPERSONIC RAM-JET (ODS PROJECT). Esso Research and Engineering Co., Process Research Division Progress Report for 1 November 1945-31, January 1945, Report No. PDN-4136, U.S. Navy Contract NOrd-9233, February 1946, 34 pp. (AD 645 226).

296. Luebbon, M., COMBUSTION AND MIXING PROCESSES IN TURBULENT FLAMES. Ph:D Thesis, Technische Hochschule, Hannover (West Germany), 1966, 84 pp. (N68-15044).

297. Lummus Corp., DEHYDROGENATION OF C_3-C_8 PARAFFINS WITH SUSPENDED CATALYST. Brit. 1, 107, 432 Corresponds to Fr. 1, 446, 101.

298. Lydiard, W.G., FUEL PROBLEMS IN HIGH SPEED SUPERSONIC AIRCRAFT. Roy. Aeron. Soc. Conf. (1963); J Roy Aeron Soc Vol. 68, 11 (1964) (AESTR).

299. Madejski, J., ACTIVATION OF NUCLEATION CAVITIES ON A HEATING SURFACE WITH TEMPERATURE GRADIENT IN SUPERHEATED LIQUID. Intern. J. Heat Mass Transfer 9 (4), 295-300 (1966); C. A. 64, 17073 (1966).

300. Markov, S. and Ofrossimov, B., PROPELLANTS AND COMBUSTION: COMPILATION OF ABSTRACTS. U.S. Library of Congress, Aerospace Technology Div. Report No. 1 on ATD work assignment Nos. 68 and 77, Report No. ATD-66-146, TT67-62064, December 1966, 74 pp. (AD 652 845).

301. Marquardt Corp., SCRAMJET THERMAL PROTECTION PROGRAM. Progress Report 1-28 February 1967, Report No. PR-5023-9, U.S. Air Force Contract AF 33(615)-3776, March 1967, 19 pp. (AD 813 405).

302. Marquardt Corp., SUPERSONIC CHEMICAL PROPULSION FEASIBILITY FLIGHT DEMONSTRATION FOR A LOW ALTITUDE SHORT RANGE MISSILE. VOLUME VI. SLURRY FUELED RAMJET TECHNOLOGY. Technical Summary Report 15 February 1965 - 15 October 1966, Report No. MR-6127, U.S. Air Force ASD TR-67-2-Vol-6, U.S. Air Force Contract AF 33(657)-14295, May 1967, 385 pp. (AD 381 958) (REPORT CLASSIFIED CONFIDENTIAL).

303. Martin Co., COMPILATION OF ABSTRACTS, AFOSR COMBINED CONTRACTORS MEETING ON COMBUSTION DYNAMICS RESEARCH (3rd), June 27-30, 1967, RAMADA INN COCOA BEACH, FLORIDA. U.S. Air Force AFOSR-67-0391, Contract AF 49(638)-1566, June 1967, 66 pp. (AD 654 669).

304. Mason, E.A., THERMAL DIFFUSION AND OTHER TRANSPORT PHENOMENA IN GASES. University of Maryland, Inst. for Molecular Physics Final Report 1 September 1965 - 31 August 1967, U.S. Army AROD-5366:14-P, Grant DA-ARO(D)-31-124-0617, August 1967, 8 pp. (AD 661 644) (N68-13312).

305. McCabe, A., DESIGN OF A SUPERSONIC NOZZLE. Great Britian Aeronautical Research Council Report ARC--R and M-3440, Supersedes ARC-25716, 1967, 38 pp. (N67-34665).

306. McCarter, R.J. and Broido, A. (U.S.D.A. Range Expt. Sta.), A CALORIMETER FOR DETERMINING RADIATION AND CONVECTION IN SMALL-SCALE COMBUSTIONS. Western States Sec. Combust. Inst., Paper WSS-CI-66-14, 16 pp. (1966); C. A. 65, 15137 (1966).

307. McGraw - Hill Inc., F.W. Dodge Co., THE SUPERSONIC COMBUSTION RAMJET (SCRAMJET). Report No. MHR-66-54, U.S. Air Force Contract AF 33(657)-14782, June 1966, 20 pp. (AD 378 977L) (REPORT CLASSIFIED SECRET).

308. McKenna, W.W., AN INVESTIGATION OF THE BEHAVIOR OF A DETONATION WAVE IN A FLOWING COMBUSTIBLE MIXTURE. Doctoral Thesis, U.S. Air Force Aerospace Research Laboratories, Office Aerospace Research, Report No. ARL-66-0112, June 1966, 133 pp. (AD 642 240).

309. McLain, W.H., Knight, R.E., Evans, R.W., IDENTIFICATION OF EXHAUST SPECIES FROM THE COMBUSTION OF LM AND LMH FUELS. Denver Research Inst. Quarterly Report No. 1, 1 September - 1 December 1966, Report No. DRI-943-6612-Q, U.S. Air Force AFRPL-TR-67-38, Contract F04611-67-C-001, February 1967, 46 pp. (AD 808 681).

310. McManus, H.N., AN INVESTIGATION OF THE HEAT TRANSFER ASPECTS OF HORIZONTAL TWO-PHASE FLOW. Aeronca Mfg. Corp. Final Report, U.S. Army Contract DA-ARO(D)-31-124-G 188, November 1966, 8 pp. (AD 646 398).

311. Mead, C.F. and Spoecker, W.W., SUMMARY OF AUTO IGNITION TESTS. Lockheed - California Co. Report for 3 September 1964 - 8 January 1965, Report No. LR-18475, May 1965, 1 97 pp. (AD 814 080L). Revision of report dated 8 January 1965.

312. Meier Zu Koecker, H., COMBUSTION CHARACTERISTICS OF HYDROGEN-RICH COAL-TAR DERIVATIVES FOR SUPERSONIC JET FUELS OF HIGH THERMAL STABILITY. Erdoel Kohle Vol. 19 No. 9, 654-59 (Sept 1966).

313. Mertwoy, H.E. and Gisser, H. (Frankford Arsenal), SUBSTITUTED BIPHENYLS AND TERPHENYLS AS OXIDATIVELY AUTOINHIBITIVE COMPOUNDS. I + EC Product Research and Development 6, 108-12 (June 1967); Frankford Arsenal FA-A67-8, February 1967, 8 pp. (AD 657 084).

314. Mikhailov, L.E., Naboichenko, K.V. Kiryutin, A.A., [CRITICAL HEAT FLUXES DURING] BOILING UNDER FORCED CONVECTION OF ACETONE, BENZENE, AND MONOISOPROPYLBIPHENYL. Nekotorye Vopr. Fiz. i Tekhn. Yadern. Rektorov, Mosk. Inzh.-Fiz. Inst. 1965, 143-50 (Russ); C. A. 64, 12221 (1966).

315. Millan, G. and Da Riva, I. (Instituto Nacional de Tecnica Aerospacial Madrid, Spain), DISTRIBUTION OF RADICALS IN LAMINAR FLAMES. Published in Symposium (International) on Combustion (3th) 1960; AFO SR 2495, U.S. Air Force Contracts AF 61(052)-221, AF 61(514)-997, 1960, 15 pp. (AD 645 063).

316. Miller, W.J., FLAME IONIZATION AND COMBUSTION INHIBITION. Aero Chem Research Laboratories TP-151; TR-1, Contract CST-102, January 1967, 26 pp. (N68-17035).

317. Minachev, Kh. M., Kondrat'ev, D.A., Slyunyaev, P.I., STUDY OF THE INFLUENCE OF THIOPHENE ON PROPERTIES OF Pd-, Rh-, Ru-, and Pt-Al_2O_3 CATALYSTS IN CYCLOHEXANE DEHYDROGENATION. Izv. Akad, Nauk SSSR, Ser. Khim. 1965 (6), 999-1003 (Russ); C. A. 63, 9830 (1965).

318. Minachev, Kh. M. and Markov, M.A., DEHYDROGENATION OF CYCLOHEXANE ON RARE-EARTH OXIDES DEPOSITED ON HIGH-ASH CARBON. Izv. Akad, Nauk SSSR, Ser. Khim. 1965 (9), 1680-2 (Russ); C. A. 63, 17832 (1965).

319. Monarch, J., (Continental Aviation and Engineering Co.), ENVIRONMENTAL TESTING OF A GAS TURBINE ENGINE WITH EMULSIFIED JP-4 FUEL. SAE Natl. Aeron. Mtg (New York 4/24-27/67) Paper No. 670367 14 p.

320. Monchick, L., ON THE SIMULTANEOUS MIXING AND REACTION OF PARALLEL GAS STREAMS. Johns Hopkins Univ., Applied Physics Lab. Report No. CF-2830, U.S. Navy Contract NOrd-7386, September 1959, 41 pp. (AD 654 412).

321. Mondain - Monval, G., OXYGEN AND COMBUSTION. THEORETICAL AND EXPERIMENTAL FUNDAMENTAL INFORMATION, I. THEORETICAL CONSIDERATIONS ON THE THERMODYNAMICS OF COMBUSTION. Rev. Gen Thermique 4 (41), 527-33 (1965) (Fr); C. A. 63, 9722 (1965).

322. Monsanto Co., DEHYDROGENATION CATALYST. Neth. Appl. 6, 517, 032 (Cl. B 01J), June 29, 1966, U.S. Appl. December 28, 1964; 13 pp.; C. A. 65, 15223 (1966).

323. Monsanto Co., DEHYDROGENATION CATALYSTS. Neth. Appl. 6, 517, 033 (Cl. B 01J), June 29, 1966, U.S. Appl. December 28, 1964; 12 pp.; C. A. 65, 15223 (1966).

324. Monsanto Co., PROCESS FOR PREPARING A CATALYST COMPOSITION. Neth. Appl. 6, 517, 031 (Cl. B 01J), June 29, 1966, U.S. Appl. December 28, 1964) 14 pp.; C. A. 65, 15223 (1966).

325. Movikov, S.S. and Ryazantsev, Yu. S., THE EXISTENCE AND ONENESS OF SOLUTION OF THE EQUATIONS OF THE THERMAL THEORY OF BURNING. Zh. Prikl. Mekhan. i Tekhn. Fiz. 1965 (4), 86-8 (Russ); C. A. 64, 25 (1966).

326. Mueller, H. and Schnabel, K.H., RHENIUM, PLATINUM, AND PLATINUM-RHENIUM CATALYSTS SUPPORTED ON KOPPERS COKE AS A CARRIER. Z. Chem. 5 (8), 313-4 (1965) (Ger.); C. A. 64, 3382 (1966).

327. Mulaskey, B.F., Lindquist, R.H., Harnsberger, H.F. (California Research Corp.) DEHYDROGENATION CATALYST. U.S. 3, 189, 661 (Cl. 260-680), June 15, 1965, Appl. November 26, 1960; 5 pp.; C. A. 63, 14110 (1965).

328. Mullen, J.W., II, Fenn, J.B., Tanczos, F.I. (Texaco Experiment Inc.), TWO-STEP REACTION PROPULSION METHOD FOR RAM ROCKETS. U.S. 3, 230, 701 (Cl. 60-35.4), January 25, 1966, Appl. April 8, 1957, August 2, 1961, October 6, 1961; 19 pp.; C. A. 64, 9501 (1966).

329. Murgulescu, I.G. and Segal, E.I., PREEXPONENTIAL COEFFICIENTS OF THE RATE CONSTANTS CORRESPONDING TO THE ZERO ORDER FOR ENDOTHERMAL DECOMPOSITION REACTIONS IN SOLID-GAS SYSTEMS. Rev. Roumaine Chim. 10 (4), 307-22 (1965) (Fr.); Studii Cercetari Chim. Bucharest 14 (4), 303-17 (1965) (Rom); C. A. 63, 12776 (1965).

330. Myers, J.W. (Phillips Petroleum Co.), DEHYDROGENATION OF CYCLOHEXANES. U.S. 3, 228, 992 (Cl. 260-666), January 11, 1966, Appl. April 9, 1962; 2 pp.; C. A. 64, 7950 (1966).

331. Nagiev, A.M., CONDITIONS FOR COMPLETE COMBUSTION OF A GAS IN A FLAME. Tr. Vses. Neft. Nauchn.-Issled. Inst. po Tekhn. Bezopasnosti No. 16, 83-98 (1964) (Russ); C. A. 64, 7939 (1966).

332. Napolitano, L.G. (Naples Univ., Italy) TRANSONIC APPROXIMATIONS FOR REACTING MIXTURES. Israel Journal of Technology 4, No. 1, 159-71 (1966); U.S. Air Force AFOSR 67-0470, U.S. Air Force Contract AF 61(052)-853, January 1966, 15 pp. (AD 648 602).

333. National Aeronautics and Space Adminis. SUPERSONIC TRANSPORTS MAY BURN LNG. Oil Gas J Vol. 64 No. 41, 109-10 (10 10 66).

334. National Aeronautics and Space Adminis. (LNG FOR SUPERSONIC AIRCRAFT FUEL), Petro/Chem Engr. Vol. 39, No. 13 47 (Dec 1967).

335. Nicolescu, I.V., Gruia, M., Papia, A., Dumitrescu, V., PROMOTED CHROMIA-ALUMINA CATALYST I. ACIDITY, DEGREE OF SURFACE OXIDATION, MAGNETIC SUSCEPTIBILITY, AND MECHANISM OF n-OCTANE DEHYDROCYCLIZATION. Rev. Roumaine Chim. 10 (6), 523-36 (1965) (Eng.); Studii Cercetari Chim. 13 (6), 535-47 (1965) (Rom.); C. A. 63, 17817 (1965).

336. Nixon, A.C., Ackerman, G.H., Faith, L.E., Hawthorn, R.D., Henderson, H.T., Ritchie, A.W., Ryland, L.B. VAPORIZING AND ENDOTHERMIC FUELS FOR ADVANCED ENGINE APPLICATION. PART I. STUDIES OF THERMAL AND CATALYTIC REACTIONS, AND COMBUSTION PROPERTIES OF HYDROCARBON FUELS. Shell Development Co., U.S. Air Force AFAPL-TR-67-114, Part I, Contract No. AF33(615)-3789, October 1967, 381 pp.

337. Nixon, A.C. and Henderson, H.T. (Shell Development Co.), THERMAL STABILITY OF ENDOTHERMIC HEAT-SINK FUELS. Ind. Eng. Chem., Prod. Res. Develop. 5 (1), 87-92 (1966); C. A. 64, 10994 (1966).

338. Nixon, A.C., Ritchie, A.W., Hawthorn, R.D. (Shell Development Co.), CATALYTIC DEHYDROGENATION OF HYDROCARBONS OVER A CHROMIA-ON-ALUMINA CATALYST IN THE ABSENCE OF ADDED HYDROGEN. Am. Chem. Soc., Div., Petrol. Chem., Preprints 9 (3) 85-100 (1964); C. A. 64, 12431 (1966).

339. Nixon, A.C. and Henderson, H.T., EFFECT OF OXYGEN CONCENTRATION ON THE THERMAL STABILITY OF NAPTHENES, 153rd ACS Natl. Mtg (Miami Beach 4/9-14/67) ACS Div. Petrol Chem. Inc. Preprints Vol. 12 No. 1, 119-27 (Mar 1967).

340. Nixon, A.C. and Ritchie, A.W., DEHYDROGENATION OF DECALIN. EFFECT OF REACTION VARIABLES ON SELECTIVITY AND CATALYST STABILITY. 154th ACS Natl. Mtg (Chicago 9/10-15/67) ACS Div. Petrol Chem. Inc. Preprints Vol. 12 No. 3 117-47 (Aug 1967).

341. Nixon, A.C. and Ritchie, A.W., THE DEHYDROGENATION OF NAPTHENE MIXTURES. 155th ACS Natl. Mtg (San Francisco 3/31-4/5/68) ACS Div. Petrol Chem. Inc. Preprints Vol. 13 No. 1 15-28 (Mar 1968).

342. Northern, Research and Engineering Corp., COMPUTER PROGRAM FOR THE ANALYSIS OF ANNULAR COMBUSTORS. VOLUME I: CALCULATION PROCEDURES. Final Report No. 1111-1, Vol. 1, U.S. National Aeronautics and Space Administration Report NASA-CR-72374, Contract NAS 3-9402, January 1968, 246 pp. (N68-17557).

343. Northern Research and Engineering Corp., COMPUTER PROGRAM FOR THE ANALYSIS OF ANNULAR COMBUSTORS. VOLUME 2: OPERATING MANUAL. Final Report No. 1111-2, Vol. 2, U.S. National Aeronautics and Space Administration Report NASA-CR-72375, Contract NAS3-9402, January 1968, 301 pp. (N68-17556).

344. Novak, J.P., CALCULATION OF THERMODYNAMIC PROPERTIES OF REAL GAS SYSTEMS. Chem. Listy 60 (3), 385-430 (1966) (Czech); C. A. 64, 15079 (1966).

345. Novikov, S.S. and Ryazantsev, Yu. S., THE INTERACTION OF WEAK PRESSURE WAVES AND A FLAME FRONT. Akademiya Nauk SSSR, Doklady, 137 No. 6, 1409-12 (1961); U.S. Air Force Foreign Technology Div., Wright-Patterson AFB Report No. MCL-1415, October 1961, 9 pp. (AD 648 036).

346. Novak, S. and Vieweg, H.G., RELATIONS BETWEEN CHEMICAL ACTIVITY AND PHYSICAL AND CHEMICAL PROPERTIES OF Cr_2O_3-Al_2O_3 CATALYSTS, INVESTIGATED ON THE DEHYDROCYCLIZATION OF HEXANE. Erdoel Kohle 18 (8), 618-21 (1965) (Ger.); C.A. 63, 15609 (1965).

347. O'Connell, J.P. and Prausnitz, J.M. (University of California, Berkeley), APPLICATION OF THE KIHARA POTENTIAL TO THERMODYNAMIC AND TRANSPORT PROPERTIES OF GASES. Symp. Thermophys. Properties, Papers, 3rd, Lafayette, Ind. 1965, 19-31; C. A. 63, 9120 (1965).

348. O'Donnell, R.M., AN EXPERIMENTAL INVESTIGATION OF A SIMPLIFIED METHOD FOR MEASURING HEAT TRANSFER AT SUPERSONIC SPEEDS. University of Texas, Defense Research Laboratory Report No. DRL-427, prepared in cooperation with Johns Hopkins University, Applied Physics Laboratory, CF-2709, U.S. Navy Contract NOrd-16498, August 1958, 39 pp. (AD 655 463).

349. Olsen, H.L., Gayhart, E.L., Bennett, L.W., GAS FLOW TRACING IN BAFFLE-STABILIZED FLAMES. Johns Hopkins University, Applied Physics Lab. Report No. CF-2236, U.S. Navy Contract NOrd-7386, July 1954, 9 pp. (AD 658 130).

350. O'Shea, F.X. (United States Rubber Co.), DIALKYL(HYDROXYBENZYL) HYDRAZINES. U.S. 3, 243, 459 (Cl. 260-569), March 29, 1966, Appl. July 28, 1961, and April 8, 1964; 4 pp.; C. A. 65, 5399 (1966).

351. Otasek, F. and Bajer, M., ESTIMATION OF COMBUSTIBILITY LIMITS OF FLAMMABLE GASES. Sb. Ved. Praci Vysoke Skoly Banske Ostrave 11 (2), 229-39 (1965) (Czech); C. A. 65, 2038 (1966).

352. Palermo, L.G. and O'Loughlin, J.R., THE INFLUENCE OF TAILPIPE LENGTH ON FLAME STABILITY. Tulane University. U.S. Army AROD4981:1, U.S. Army Contract DA-31-124-ARO(D)-240, December 1966, 11 pp. (AD 651 612).

353. P'ang, L., et al., KINETICS OF CYCLOHEXANE DEHYDROGENATION ON PLATINUM REFORMING CATALYSTS BY THE FLOW-CIRCULATING METHOD. Acta Foculto-Chim. Sinica 6 (2), 175-86 (1965) (Ch.); C. A. 65, 18379 (1966).

354. Park, E.L., Jr., (University of Oklahoma), NUCLEATE-AND FILM-BOILING HEAT TRANSFER TO METHANE AND NITROGEN FROM ATMOSPHERIC PRESSURE TO THE CRITICAL PRESSURE. Univ. Microfilms (Ann Arbor, Mich.), Order No. 65-4892, 128 pp.; C. A. 63, 15872 (1965).

355. Park, E.L., Jr., Colver, C.P., Sliepcevich, C.M. (University of Oklahoma, Norman), NUCLEATE-AND FILM-BOILING HEAT TRANSFER TO NITROGEN AND METHANE AT ELEVATED PRESSURES AND LARGE TEMPERATURE DIFFERENCES. Advan. Cryog. Eng. 11, 516-28, discussion 528-9 (1965) (Pub. 1966); C. A. 65, 6761 (1966).

356. Paxhia, V.B., DESIGN CONSIDERATIONS OF ANNULAR BEE DUCT CONFIGURATION. Johns Hopkins University, Applied Physics Lab. Report No. CM-331, prepared in cooperation with Cornell University, July 1946, 9 pp. (AD 659 090).

357. Pearson, G.S., PERCHLORIC ACID FLAMES. PART 7: MIXED FUEL-RICH FLAMES. Great Britian Rocket Propulsion Establishment Report No. RPE-TR-67/3, March 1967, 34 pp. (N68-12535).

358. Pearson, L.W. and Fields, A.K., ANALYTICAL AND EXPERIMENTAL INVESTIGATION OF HYPERSONIC INLETS FOR DUAL MODE COMBUSTION APPLICATIONS. North American Aviation, Inc., Los Angeles Div. Quarterly Progress Report No. 3, 1 May-31 July 1966, Report No. NA-65-1070-9, prepared in cooperation with General Applied Science Labs., Inc., U.S. Air Force Contract AF 33(615)-3211, August 1966, 127 pp. (AD 381 854) (REPORT CLASSIFIED CONFIDENTIAL).

359. Peskin, R.L. and Yeh, P., A THEORETICAL STUDY OF THE EFFECT OF CONVECTION ON THE IGNITION OF SINGLE AEROSOL DROPLETS. Rutgers-the State University, New Jersey Technical Report, U.S. Army EA 67-10, Contract DA-AMC-18-035-80(A), June 1967, 99 pp. (AD 816 345).

360. Phillips, D.G., DEMAND-MODE INTEGRAL ROCKET-RAMJET, Marquardt Corp., Astro Final Technical Report 17 January 1966 - 16 January 1967, Report No. MR-25217, U.S. Navy Contract NOw-66-0488, March 1967, 244 pp. (AD 380 978) (REPORT CLASSIFIED CONFIDENTIAL).

361. Pietrangeli, G.J. and Nice, E.V., THE FEASIBILITY OF A MACH 7 TRANSPORT EMPLOYING AIRBREATHING PROPULSION SYSTEMS. Johns Hopkins Univ. Applied Physics Lab. Report No. CF-2900 Revised ed., U.S. Navy Contract Nord-7386, July 1961, 173 pp. (AD 654 428). Revision of manuscript received 15 Nov 1960.

562. Pines, H. et al. (Northwestern University), ALUMINA: CATALYST AND SUPPORT. XXIV. 13. AROMATIZATION OF HYDROCARBONS. DISCUSSION OF THE MECHANISM OF THE AROMATIZATION OF ALKANES IN THE PRESENCE OF CHROMIA-ALUMINA CATALYSTS. J. Org. Chem. 30 (10), 3530-6 (1965). Ibid, XXV. 14. AROMATIZATION OF 2-METHYLHEXANE-$6^{14}C$, 3-METHYLHEXANE-3-^{14}C, AND 3-METHYL-^{14}C-HEXANE OVER CHROMIA-ALUMINA CATALYST. CONTRIBUTION TO THE MECHANISM OF AROMATIZATION. J. Org. Chem. 30 (10), 3537-40 (1965). Ibid, XXVI. 15. AROMATIZATION AND DEHYDROISOMERIZATION OF DIMETHYLHEXANES OVER CHROMIA-ALUMINA CATALYST. CONTRIBUTION TO THE MECHANISM OF AROMATIZATION. J. Org. Chem. 30 (10), 3540-4 (1965). Ibid, XXVII. 16. AROMATIZATION OF METHYLCYCLOHEPTANE AND METHYL-^{14}C-CYCLOHEPTANE OVER CHROMIA-ALUMINA CATALYST. CONTRIBUTION TO THE MECHANISM OF AROMATIZATION. J. Org. Chem. 30 (10), 3544-8 (1965). Ibid, XXVIII. 17. AROMATIZATION AND DEHYDROISOMERIZATION OF 3- AND 4-METHYLHEPTANE AND 3- AND 4- METHYL-^{14}C-HEPTANE. CONTRIBUTION TO THE MECHANISM OF AROMATIZATION. J. Org. Chem. 30 (10), 3548-52 (1965); C. A. 63, 17816-7 (1965).

563. Pinkel, B. and Watts, F., A STUDY OF SCRAMJET APPLICATION MERIT AND DEVELOPMENT COST. Rand Corp. Report No. RM-4926-PR, U.S. Air Force Contract AF 49(638)-1700, December 1966, 108 pp. (AD 377 985) (REPORT CLASSIFIED SECRET).

564. Piskunov, V.A. and Zrelov, V.N., ABRASIVE EFFECTS OF MICROIMPURITIES AND OXIDATION PRODUCTS IN JET FUELS. Khim. i Tekhnol. Topliv i Masel, Vol. 10, No. 5, 49-52 (May 1965).

565. Pitzer, E.W. and Sailors, H.R. (Phillips Petroleum Co.), CATALYST REGENERATION. U.S. 3, 219, 587 (Cl. 252-419), November 23, 1965, Appl. September 30, 1960; 4 pp.; C. A. 64, 4839 (1966).

566. Pleier, J.R., IMPROVEMENT OF TAFDS FUEL RECIRCULATION AND PROCEDURES. U.S. Marine Corps Landing Force Development Center Final Report, March 1967, 11 pp. (AD 811 462L).

567. Pleshanov, A.S., GAS-DYNAMIC ANALYSIS OF THE NONSTEADY-STATE PROPAGATION OF FLAME. Zh. Prik. Mekhan. i Techn. Fiz. (Moscow) 1964 (4), 250-5; U.S. Air Force Translation FTD-HT-66-261, TT-67-63189 (AD 660 248) (N68-11687).

568. Polataiko, R.I., Kruglikova, N.S., Frolova, V.S., Galich, P.N., Skarchenko, V.K., DEHYDROGENATION OF n-HEXANE ON MOLYBDENUM SULFIDE CATALYSTS. Neft, i Gaz. Prom., Inform. Nauchn.-Tekhn. Sb. 1965 (2), 53-4 (Russ); C. A. 63, 11393 (1965).

569. Pollitzer, E.L. (Universal Oil Products Co.), HYDROCARBON-FUEL STABILIZERS. U.S. 3, 205, 170 (Cl. 252-32.5), September 7, 1965, Appl. August 8, 1953; 4 pp; C. A. 63, 12951 (1965).

370. Ponizko, T.A. and Rozlovskii, A.I., LIMITS OF INFLAMMATION OF COMBUSTIBLE AIR MIXTURES UPON IGNITION WITH HOT BODIES. Fiz. Goreniya i Vzryva 1965 (4), 10-19 (Russ); C. A. 65, 5294 (1966).

371. Popescu, A., Duta, D., Baiulescu, E., ACTIVITY OF Ni-Al_2O_3 CATALYSTS AND INFLUENCE OF THE Pt PROMOTER IN CYCLOHEXANE DEHYDROGENATION. Analele Univ. Bucuresti, Ser. Stiint, Nat. 13 (1), 9-18 (1964) (Rom); C. A. 64, 14055 (1966).

372. Porter, R.P., Clark, A.H., Kaskan, W.E., Browne, W.G., A STUDY OF HYDROCARBON FLAMES. General Electric Co., Missile and Space Div. Technical Report 1 January - 30 June 1966, Report No. 66 SD 952, BSD TR-66-310, U.S. Air Force Contract AF 04(694)-897, October 1966, 24 pp. (AD 800 496).

373. Powell, R.W., Ho, C.Y., Liley, P.E., THERMAL CONDUCTIVITY OF SELECTED MATERIALS. Purdue University, Thermophysical Properties Research Center, U.S. National Bureau of Standards NSRDS-NBS-8, November 1966, 175 pp. (N67-34492).

374. Pratt and Whitney Aircraft, Research and Development Center, A STUDY OF THE SUPPRESSION OF COMBUSTION OSCILLATIONS WITH MECHANICAL DAMPING DEVICES. Final Report, 1 July, 1966 - 30 September, 1967, Report No. PWA-FR-2596, U.S. National Aeronautics and Space Administration Report NASA-CR-90094, Contract NAS8-11038, November 1967, 87 pp. (N68-10627).

375. Pratt and Whitney Aircraft, SUPERSONIC TRANSPORT AIRCRAFT ENGINE. PHASE II-A DEVELOPMENT PROGRAM. VOLUME I. (AD 380 820L). Final Report 1 June - 30 November 1964, Report No. PWA-2397- Vol - 1, U.S. Federal Aviation Agency Contract FA-SS-64-2 November 1964, 1 Vol. VOLUME II. (AD 380 8216). Final Report 1 June - 30 November 1964, Report No. PWA-2397-Vol-2, U.S. Federal Aviation Agency Contract FA-SS-64-2, November 1964, 475 pp; (REPORTS CLASSIFIED CONFIDENTIAL).

376. Pratt and Whitney Aircraft, SST. VOLUME II E. BOEING SPECIFICATION 2681 ENGINE MODEL STF 219-B. (AD 378 376L) U.S. Federal Aviation Agency Contract FA-SS-64-2, October 1964, 300 pp. LOCKHEED SPECIFICATION 2682 ENGINE MODEL STF 219-L. (AD 378 377L) ibid, 289 pp. (REPORTS CLASSIFIED CONFIDENTIAL).

377. Pratt and Whitney Aircraft, SST. PHASE II-A. DATA SUBMISSION. VOLUME I E. SUMMARY. U.S. Federal Aviation Agency Contract FA-SS-64-2, November 1964, 21 pp. (AD 378 375L) (REPORT CLASSIFIED CONFIDENTIAL).

377a. Pratt and Whitney Aircraft, COMMERCIAL SUPERSONIC TRANSPORT ENGINE. VOLUME IX E. ENGINE. PART 2. TECHNICAL SECTION E. TEST AND CERTIFICATION. PHASE II-A. DATA SUBMISSION. U.S. Federal Aviation Agency Contract FA-SS-64-2, November 1964, 12 pp. (AD 378 378L) (REPORT CLASSIFIED CONFIDENTIAL).

378. Pratt and Whitney Aircraft, SUPERSONIC TRANSPORT AIRCRAFT ENGINE. PHASE II-B DEVELOPMENT PROGRAM. VOLUME I. (AD 379 231L) Final Report 1 January - 30 June 1965, Report no. PWA-2600-Vol. 1, U.S. Federal Aviation Agency Contract FA-SS-65 18, June 1965, 268 pp. VOLUME II. (AD 379 232L) Final Report 1 January - 30 June 1965, Report no. PWA-2600-Vol. 2, U.S. Federal Aviation Agency Contract FA-SS-65-18, June 1965, 453 pp. VOLUME III. (AD 379 233L) Final Report 1 January - 30 June 1965, Report no. PWA-2600-Vol. 3, U.S. Federal Aviation Agency Contract FA-SS-65-18, June 1965, 286 pp. REPORTS CLASSIFIED CONFIDENTIAL).

379. Pratt and Whitney Aircraft, SUPERSONIC TRANSPORT AIRCRAFT ENGINE. PHASE II-B DEVELOPMENT PROGRAM. FUEL CONTROL SYSTEM STUDY. APPENDIX A. Final Report 1 January - 8 June 1965, Report no. PWA-2600-App-A, U.S. Federal Aviation Agency Contract FA-SS-65-18, June 1965, 187 pp. (AD 807 389L) Prepared in cooperation with Bendix Corp., Bendix Products Aerospace Div., Report no. BPAD-863-16595R.

380. Pratt and Whitney, Florida Research and Development Center, DEVELOPMENT OF A SUPERSONIC TRANSPORT AIRCRAFT ENGINE. PHASE II C. Final Report 1 July 1965 - 31 December 1966, Report no. PWA-FR-2250, U.S. Federal Aviation Agency Contract FA-SS-66-8, January 1967, 486 pp. (AD 378 925L) (REPORT CLASSIFIED CONFIDENTIAL).

381. Pratt, D. T. and Starkman, E. S., (International Harvester Company Solar Div.). GAS TURBINE COMBUSTION OF AMMONIA. SAE Combined Fuels + Lubricants Powerplant + Transp. Mtgs. (Pittsburgh 10/30-11/3/67) Paper N.670938 9P.

382. Predvoditelev, A. S., ed., STUDIES IN PHYSICAL GAS DYNAMICS. Issledovaniya po Fizicheskoy Gazodinamike, Moscow, Nauka Press, 1966; U.S. National Aeronautics and Space Administration Translation NASA-TT-F-505, February 1968, 267 pp. (N68-16839).

383. Quigg, H. T. and Schirmer, R. M., EFFECT OF JP FUEL COMPOSITION ON HOT CORROSION. Phillips Petroleum Company. Summary Report 1 April 1965 - 31 March 1966, Report no. 4493-66R, U.S. Navy Contract NOw-65-0310, September 1966, 141 pp. (AD 800 987).

384. Rabo, J. A., Pickert, P. E., Boyle, J. E. (Union Carbide Corp.), ZEOLITE MOLECULAR-SIEVE CATALYSTS FOR HYDROCARBON CONVERSION. U.S. 3, 236, 761 (Cl. 208-11), February 22, 1966, Appl. December 30, 1959 and February 7, 1962; 28 pp. Continuation-in-part of U.S. 3, 130, 006; C.A. 65, 553 (1966).

385. Ragland, K. W., SOLUTION OF THE BLASIUS BOUNDARY LAYER EQUATION BEHIND A SHOCK WITH VAPORIZATION AND COMBUSTION AT THE WALL. University of Michigan, Gas Dynamics Laboratory, U.S. National Aeronautics and Space Administration NASA-CR-72235, July 1967, 61 pp. (N67-34546).

386. Rakowsky, F. W. and Meguerian, G. H. (Research and Development Dept., American Oil Company), PRECOMBUSTION DEPOSITS. Combust. Flame 10 (2), 182-7 (1966); C.A. 65, 10392 (1966).

387. Ratiani, G. V. and Avaliani, D. I., NUMBER OF ACTIVE CENTERS OF VAPOR FORMATION AND CRITICAL HEAT DELIVERY DURING BOILING OF ORGANIC LIQUIDS IN LARGE VOLUMES, Soobshch. Akad. Nauk Gruz. SSR 37 (3), 653-60 (1965) (Russ); C.A. 63, 15588 (1965).

388. Raushenbakh, B. V., Belyi, S. A., Bespalov, I. V., Borodachev, V. Ya., Volynskii, M. S., PHYSICAL PRINCIPLES OF THE WORKING PROCESS IN COMBUSTION CHAMBERS OF JET ENGINES. mono. Fizicheskie Osnovy Rabochego Protsessa v Kamerakh Sgoraniya Vozdushno - Reaktivnykh Dvigatelei, Moscow, 1964, p1-526; U.S. Air Force Translation FTD-MT-65-78; TT-67-62866, May 1967, 503 pp. (AD 558 372) (N67-39782).

389. Reiter, F. W. and Link, W., DETERMINATION OF THERMAL CONDUCTIVITY IN SATURATED VAPORS OF BENZENE, DIPHENYL, o-, m-, AND p-TERPHENYL. European At. Energy Comm. Report no. EUR-2282.d., U.S. Atomic Energy Commission Accession No. 24541, 1965, 28 pp. (Ger.); C.A. 64, 11896.

390. Renich, W. T., THEORETICAL COMBUSTION PERFORMANCE OF RAMJET FUELS: HYDROGEN. Johns Hopkins University, Applied Physics Laboratory Report no. CF-2601, U.S. Navy Contract NOrd-7386, December 1956, 12 pp. (AD 657 150).

391. Renich, W. T., THEORETICAL COMBUSTION PERFORMANCE OF RAMJET FUELS: PROPANE. Johns Hopkins University, Applied Physics Laboratory Report no. CF-2609, U.S. Navy Contract NOrd-7386, December 1956, 12 pp. (AD 657 152).

392. Richardson, P. D. (Brown University), EFFECTS OF SOUND AND VIBRATIONS OF (sic) HEAT TRANSFER. Applied Mechanics Reviews 20, no. 3, 201-17 (1967); ARL-67-0128, Contract F33615-67-C-1754, 1967, 21 pp. (AD 657 281).

393. Richmond, J. K. and Shreeve, R. P., WIND TUNNEL MEASUREMENTS OF IGNITION DELAY, USING SHOCK-INDUCED COMBUSTION. Boeing Scientific Research Labs., Flight Science Lab. Report no. D1-82-0609, March 1967, 50 pp. (AD 652 451).

394. Ritchie, A. W., Hawthorn, R. D., Nixon, A. C., DEHYDROGENATION OF HYDROCARBONS OVER A CHROMIA-ALUMINA CATALYST IN THE ABSENCE OF ADDED HYDROGEN. Ind. Eng. Chem., Prod. Res. Develop. 4 (2), 129-36 (1965); C.A. 63, 396 (1965).

395. Ritchie, A. W. and Nixon, A. C. (Shell Development Company), DEHYDROGENATION OF METHYLCYCLOHEXANE OVER A PLATINUM-ALUMINA CATALYST IN THE ABSENCE OF ADDED HYDROGEN. Ind. Eng. Chem., Prod. Res. Develop. 5 (1), 59-64 (1966); C.A. 64, 12490 (1966).

396. Rohsenow, W. M. (Massachusetts Inst. of Technol.), NUCLEATION WITH BOILING HEAT TRANSFER. Ind. Eng. Chem. 58 (1), 40-7 (1966); C.A. 64, 10780 (1966).

397. Rosen, P., THE INTERACTION OF SOUND WAVES WITH FLAME IN A DUCT. Johns Hopkins University, Applied Physics Lab. Report no. CF-2180, U.S. Navy Contract NOrd-7386, February 1954, 21 pp. (AD 658 133).

398. Rosner, D. E. (AeroChem. Research Labs., Inc.), ON LIQUID DROPLET COMBUSTION AT HIGH PRESSURES. AIAA Journal 5, no. 1, 163-6 (1967); U.S. Air Force AFO SR-67-2042, revised ed., Contract AF 49(638)-1654, August 1966, 6 pp. (AD 657 890).

399. Rosner, D. E. (AeroChem. Research Labs., Inc.), TRANSPIRATION COOLING WITH CHEMICAL REACTIONS. Pyrodynamics 2 (4), 221-47 (1965); C.A. 64, 4621 (1966).

400. Rouse, R. W. and Sochor, J. J., 1965 ADVANCED RAMJET CONCEPTS PROGRAM. VOLUME I. LOW VOLUME RAMJET INVESTIGATIONS. PART II. APPLICATIONS AND MISSIONS. Marquardt Corp. Final Report 1 March 1965 - 15 April 1966, Report no. 25188-Vol. 1-Pt. 2, AFAPL TR-66-49-Vol. 1-Pt. 2, U.S. Air Force Contract AF33(615)-2399, January 1967, 143 pp. (AD 378 622L) (REPORT CLASSIFIED SECRET).

401. Rozengart, M. I., Polkovnikov, B. D., Polinin, V. L., Taber, A. M., Gitis, K. M., AROMATIZING ABILITY OF BORIDE CATALYSTS OF PLATINUM GROUP METALS. Izv. Akad. Nauk SSSR, Ser. Khim. 1965 (5), 919-22 (Russ); C.A. 63, 5544 (1965).

402. Rozengart, M. I., Mortikov, E. S., Kazanskii, B. A., DEHYDROCYCLIZATION OF n-HEPTADIENE AND n-HEPTRATRIENE OVER AN ALUMINA-CHROMIA-POTASSIUM OXIDE CATALYST. Dokl. Akad. Nauk SSSR 166 (3), 619-22 (1966) (Russ); C.A. 64, 12531 (1966).

403. Ruckenstein, E., REMARKS ON NUCLEATE BOILING HEAT TRANSFER FROM A HORIZONTAL SURFACE. Intern. J. Heat Mass Transfer 9 (3), 229-37 (1966); C.A. 64, 15405 (1966).

404. Ruckenstein, E., TURBULENT HEAT OR MASS TRANSFER. Chem. Eng. Sci. 21 (2), 113-6 (1966); C.A. 64, 17069 (1966).

405. Rudikoff, N. and Roffe, G., AN EXPERIMENTAL INVESTIGATION OF SEVERAL ABLATION MATERIALS FOR SCRAMJET ENGINE APPLICATIONS. General Applied Science Laboratories, Inc. Technical Memo, Report no. GASL-TM-147, U.S. Army Contract DA-01-021-AMC-14072 (Z), July 1966, 24 pp. (AD 376 449) (REPORT CLASSIFIED CONFIDENTIAL).

406. Ruf, H., METHODS OF ESTIMATION OF STORAGE STABILITY OF MOTOR FUELS IN LABORATORY AND BEHAVIOR IN BULK STORAGE IN PRACTICE. Schweiz. Arch. Angew. Wiss. Tech. V29.428-44 (1963) (Abstr) J. Inst. Petrol. V50 N.487.136A (July 1964).

407. Ryan, P. W. (Sinclair Research, Inc.), CONVERSION OF C_8 AND HIGHER ALIPHATICS TO AROMATICS WITH A FREE ALKALI METAL CATALYST. U.S. 3, 240, 832 (Cl. 260-673.5), March 15, 1966, Appl. August 13, 1962; 3 pp.; C.A. 64, 17478 (1966).

408. Ryashentseva, M. A., Minachov, Kh. M., Kolesnikor, M., Pronenkov, G. M., KINETICS OF THE DEHYDROGENATION OF CYCLOHEXANE UNDER REFORMING CONDITIONS. Kinetics and Catalysis (Trans. in Engl.) 8 (4), 788 (1967).

409. Salooja, K. C. (Shell Res. Ltd.), COMBUSTION PROCESSES LEADING TO IGNITION OF AROMATIC HYDROCARBONS. Combust. Flame 9 (2), 121-9 (1965); C.A. 63, 12943 (1965).

410. Salooja, K. C. (Shell Res. Ltd.), THE ROLE OF ALDEHYDES IN COMBUSTION: STUDIES OF THE COMBUSTION CHARACTERISTICS OF ALDEHYDES AND OF THEIR INFLUENCE ON HYDROCARBON COMBUSTION PROCESSES. Combust. Flame 9 (4), 373-82 (1965); C.A. 64, 10998 (1966).

411. Schelkin, K. I., INSTABILITY FOR THE COMBUSTION AND DETONATION OF GASES. Usp. Fiz. Nauk 87 (2), 273-302 (1965) (Russ.); C.A. 64, 3274 (1966).

412. Shchelkin, K. I. and Troshin, Ya. K., GAS DYNAMICS OF COMBUSTION. Translated from Russian. Baltimore, Md.: Mono Book Corp. 1965. 222 pp.; C.A. 65, 10167 (1966).

413. Schep, K. C., SYMPOSIUM ON SHOCK TUBES, HELD 12-14 APRIL 1967 AT FREIBURG I BR., GERMANY. Advies bureau der Genie, The Hague (Netherlands) Report - 163; TDCK-48937, April 1967, 128 pp. (N67-40536).

414. Schetz, J. A., TURBULENT MIXING (ANALYSIS). Johns Hopkins University, Applied Physic Laboratory Research and Development Programs, March 1967, 2 pp. (N67-33385).

415. Schwartz, F. L. (Univ. of Florida, Gainesville), and Silen, L. G., CORRELATION OF SOUND GENERATION AND HEAT TRANSFER IN BOILING. J. Heat Transfer 87 (4), 436-8 (1965); C.A. 64, 310 (1966).

416. Scribner, W. G. and Lander, H. G., THERMAL STABILITY OF TEN JP-6 FUELS AFTER 1-YEAR STORAGE. Monsanto Research Corp. Report for September 1964-November 1965, AFAPL TR-66-66, U.S. Air Force Contract AF 33 (615)-1317, August 1966, 34 pp. (AD 646 440).

417. Schultz, H. D., THERMAL ANALYZER COMPUTER PROGRAM FOR THE SOLUTION OF GENERAL HEAT TRANSFER PROBLEMS. Lockheed-California Company, Report no. LR-18902, NASA-CR-65581, U.S. National Aeronautics and Space Administration Contract NAS9-3349, July 1965, 355 pp. (N67-31357).

418. Selwood, P. W., MOLECULAR INTERACTIONS AT SOLID SURFACES. University of California, Santa Barbara, Final Report 1 July 1962 - 31 December 1966, U.S. Army Grants DA-ARO(D)-31-124-G323, DA-ARO(D)-31-124-G486, December 1966, 4 pp. (AD 658 201).

419. Sergienko, S. R., Medvedeva, V. D., Petrova, A. A., Chirova, E. V., EFFECT OF THE LENGTH OF n-PARAFFIN CHAINS ON THE SELECTIVITY OF DEHYDROGENATION ON A Zn-Cr CATALYST. Izv. Akad. Nauk Turkm. SSR, Ser. Fiz.-Tekhn., Khim. i Geol. Nauk 1964 (5), 61-8 (Russ); C.A. 63, 11532 (1965).

420. Shakhnov, I. F., IGNITION OF A STOICHIOMETRIC MIXTURE IN A LAMINAR SUPERSONIC BOUNDARY LAYER OF A FLAT PLATE. Izvestiya Akademiya Nauk SSSR, Mekhanika, 1965, no. 3, 17-24; U.S. Air Force Translation no. FTD-HT-66-472, TT67-60782, September 1966, 21 pp. (AD 646 426).

421. Shell Company of the U.K., A NEW SHELL HIGH-ENERGY JET FUEL, Inst. Petrol Rev. V19 N.224.287 (August 1965).

422. Shell Internationale Research Maatschappij N.V., DEHYDROGENATION OF HYDROCARBONS. Brit. 983,907 (Cl. C 07c), February 17, 1965, Neth. Appl., December 27, 1962; 4 pp. Addn. to Brit. 895,500; C.A. 63, 490 (1965).

423. Shell Internationale Research Maatschappij N.V., DEHYDROGENATION OF HYDROCARBONS. Fr. Addn. 85,654 (Cl. C 07c), September 27, 1965; Neth. Appl., December 27, 1962; 9 pp. Addn. to Fr. 1,279,630; C.A. 64, 7951 (1966).

424. Shell Internationale Research Maatschappij N.V., DETERMINATION OF FLAME POINTS OF LIQUIDS AND VAPORS. Neth. Appl. 6,510,165 (Cl. G 01n), February 8, 1966, Brit. Appl., August 7, 1964; 14 pp.; C.A. 64, 19300 (1966).

425. Shell Research Ltd. (by P. S. Timmons), HYDROCARBON OILS, Brit. 1,031,533 (Cl. 10i), June 2, 1966, Appl. July 27, 1962; 9 pp.; C.A. 65, 10403-4 (1966).

426. Shell Research Ltd. (P. S. Timmons), STABILIZING AVIATION KEROSINE. Brit. 1,010,714 (Cl. C 10g), November 24, 1965, Appl. January 31, 1962; 6 pp.; C.A. 64, 6378 (1966).

427. Shimulis, V. I., KINETICS OF DEHYDROGENATION OF CYCLOHEXENE ON A PALLADIUM FILM. II. DELOCALIZED ADSORPTION. Kinetika i Kataliz 7 (3), 498-507 (1966) (Russ); C.A. 65, 10453 (1966).

428. Shipikin, V. V., Maslyanskii, G. N., Zharkov, B. B., Bursian, N. R., HYDROCARBON CONVERSIONS IN THE PRESENCE OF USED AND REACTIVATED PLATINUM REFORMING CATALYSTS. Neftekhimiya 6 (3), 401-6 (1966) (Russ); C.A. 65, 16741 (1966).

429. Shopov, D. and Andreev, A., APPLICATION OF DELOCALIZATION (MOLECULAR ORBITALS) METHOD IN DEHYDROGENATION OF CYCLOHEXANE HYDROCARBONS. Compt. Rend. Acad. Bulgare Sci. 18 (9), 853-6 (1965) (Eng.); C.A. 64, 4893 (1966).

430. Shopov, D. and Andreev, A., CATALYTIC DEHYDROGENATION OF CIS- AND TRANS-ISOMERS OF DECALIN AND 1,2-DI-METHYLCYCLOHEXANE ON VARIOUS METALS. Neftekhimiya 6 (4), 539-43 (1966) (Russ); C.A. 65, 18462 (1966).

431. Shopov, D. and Andreev, A., DEHYDROGENATION OF TETRALIN AND CIS- AND TRANS-DECALIN ON α-IRON. Compt. Rend. Acad. Bulgare Sci. 19 (1), 37-40 (1966) (Eng.); C.A. 65, 7113 (1966).

432. Shunick, J. R. and Schuh, J. R., HYPERSONIC RAMJET HEAT TRANSFER AND COOLING PROGRAM. VOLUME III: RESULTS ON TRANSPIRATION COOLING EXPERIMENTS IN A SUPERSONIC GAS STREAM. Marquardt Corp. Technical Report 1 June 1965 - 30 April 1966, Report no. 6109-Vol. 3, AFAPL TR-66-84-Vol. 3, U.S. Air Force Contract AF 33 (615)-1467, August 1966, 43 pp. (AD 802 044L)

433. Slutsky, S., Tamagno, J., Trentacoste, N. (General Applied Science Labs., Inc.), SUPERSONIC COMBUSTION IN PREMIXED HYDROGEN-AIR FLOWS. AIAA (Am. Inst. Aeron. Astronaut.) J. 3 (9), 1599-605 (1965); C.A. 63, 14071 (1965).

434. Smith. F. L., HIGH TEMPERATURE ONE GALLON FUEL TANK AUTO-IGNITION TESTS. North American Aviation, Inc., Engineering Dept., Report no. NA-59-1083, U.S. Air Force Contract AF 33(600)-38669, September 1959, 21 pp. (AD 814 119).

435. Smith, J. O., Satterfield, C. N., Fabuss, B. M. (Monsanto Research Corp.), ENDOTHERMIC CRACKING OF HYDROCARBON FUELS TO PROVIDE COOLING AND FUEL FOR FLIGHT VEHICLES. U.S. 3,173,247 (Cl. 60-35.4), March 16, 1965, Appl. November 30, 1962; 4 pp.; C.A. 63, 412 (1965).

436. Sochet, L. R. and Lucquin, M., HIGH-TEMPERATURE COMBUSTION OF PROPANE, MORPHOLOGICAL INVESTIGATION. J. Chim. Phys. 62 (7-8), 796-807 (1965) (Fr.); C.A. 63, 16098 (1965).

437. Socony Mobil Oil Co., Inc. (by P. Y. C. Gee and H. J. Andress), DEPOSIT INHIBITORS FOR AVIATION KEROSINE FUELS. Belg. 648,648, November 30, 1964, U.S. Appl. May 31, 1963; 19 pp.; C.A. 63, 11224 (1965).

438. Sokolik, A. S., Karpov, V. P., Semenov, E. S., TURBULENT COMBUSTION OF GASES. Teoriya i Prakt. Szhiganiya Gaza, Nauchn-Tekhn. Obshchestvo Energ. Prom. 2, 139-56 (1964) (Russ); C.A. 63, 425 (1966).

439. Sokolov, V. A., Vol'kenshtein, F. F., Brik, O.G., Kondratenko, M. B., ROLE OF RADICAL-RECOMBINATION PROCESSES DURING CANDOLUMINESCENCE. Izv. Akad. Nauk SSSR, Ser. Fiz. 30 (4), 635-6 (1966) (Russ); C.A. 65, 6535 (1966).

440. Sokol'skii, D. V. and Toibaev, I. K., DEPENDENCE OF ELECTRICAL CONDUCTIVITY OF POWDERED NICKEL ON THE DEGREE OF DEHYDROGENATION. Khim. i Khim. Tekhnol., Alma-Ata Sb. 2, 155-9 (1964) (Russ); C.A. 64, 16756 (1966).

441. Soloukhin, R. I., REFRACTION OF A SHOCK WAVE ON A FLAME FRONT. Zh. Prik. Mekhan. i Techn. Fiz. (Moscow) 1964 (4), 49-59; U.S. Air Force Translation FTD-HT-66-261; TT-67-63189 (AD 660 248) (N68-11553).

442. Solvay et Cie (U. Heusser), FINELY DIVIDED CATALYST DISPERSION OR SOLUTION BY DISSOLVING SUPPORT. Fr. 1,513, 020, Corresponds to Belg. 694,889.

443. Spengler, G., Kern, J., Gemperlein, H., COMBUSTION OF FUEL IN A JET PROPULSION UNIT BY MEANS OF EMISSION SPECTROSCOPY. Deut. Luft-Raumfahrt, Forschungsber. DLR-FB 65-45, 26 pp. (1965) (Ger.); C.A. 64, 10998 (1966).

444. Spengler, G., Wolff, H., Gemperlein, H., BURNING CHARACTERISTICS AND CHEMICAL COMPOSITION OF FUELS FOR AIR-BREATHING JET PROPULSION UNITS. Deut. Luft-Raumfahrt, Forschungsber. 64-36, 39 pp. (1964) (Ger.); C.A. 63, 14628 (1965).

445. Stainback, P. C. and Weinstein, L. M., AERODYNAMIC HEATING IN THE VICINITY OF CORNERS AT HYPERSONIC SPEEDS. National Aeronautics and Space Administration Report NASA-TN-D-4130, November 1967, 28 pp. (N67-40568).

446. Standard Oil Co., Ohio, COMPOUND PROTECTS HYDROCARBON FUELS, Oil Gas J. V65 N.50 144 (12/11/67).

447. Starkman, E. S. and Newhall, H. K., AMMONIA VERSUS HYDROCARBONS AS GAS TURBINE FUELS. (THE THEORETICAL PERFORMANCE OF AMMONIA AS A GAS TURBINE FUEL), SAE Mtg. Paper N.660768 (1966) (Adapt) SAE (Soc. Automotive Engrs.) J. V75 N.6 71-77 (June 1967).

448. Sterman, L. S. and Vilemas, Yu. V., CRITICAL HEAT FLUXES FOR BOILING ORGANIC HEAT-TRANSFER MEDIA. Teplofiz. Vysokikh Temperatur, Akad. Nauk SSSR 3 (4), 609-16 (1965) (Russ); C.A. 63, 17500 (1965).

449. Steinmetz, E. A. and Harris, J. C. (Monsanto Research Corp., U.S. Army, EMULSIFIED JET ENGINE FUEL. SAE Natl. Aeron. Mtg. (New York 4/24-27/67) Paper N.670365 6P.

460. Swithenbank, J. and Parsons, A. J. (University of Sheffield, England), EXPERIMENTAL TECHNIQUES FOR SUPERSONIC COMBUSTION RESEARCH IN A SHOCK TUNNEL. Propulsion and Energetics Panel Meeting on New Exptl. Tech. in Propulsion and Energetics Probl., Munich, September, 1967, 64 pp. (N68-11770).

461. Tarifa, C. S. and Torralbo, A. M., FLAME PROPAGATION ALONG THE INTERFACE BETWEEN A GAS AND A REACTING MEDIUM. Symposium (International) on Combustion (11th) Berkeley, p. 533-44, August 14-20 (1967); Instituto Nacional de Tecnica Aeroespacial Madrid (Spain) Scientific Interim, U.S. Air Force AFOSR-67-2681, Grant AFOSR-67-2681, November 1967, 15 pp. (AD 661 709).

462. Tarzimanov, A. A. and Mashirov, V. E., TRANSFER COEFFICIENTS OF NORMAL SATURATED HYDROCARBONS AND ALCOHOLS. Izv. Vysshikh Uchnebn. Zavedenii, Netfi Gas 9 (2), 70-2 (1966) (Russ); C.A. 65, 7038 (1966).

463. Tao, F. F., Appeldoorn, J. K., Campion, R. J., Dukek, W. G., Furey, M. J., LUBRICITY PROPERTIES OF HIGH-TEMPERATURE JET FUELS. (Quarterly Report) U.S. Dept. Commerce Tech. Inform. AF N.33(615)-2828 (1965) 45 pp. (Abstr.) Corrosion Abstr. V5 N 5 368 (Sept. 1966).

464. Taylor, W. F. and Wallace, T. J., THE STUDY OF HYDROCARBON FUEL VAPOR PHASE DEPOSITS. Esso Research and Engineering Co., Process Research Division Quarterly Progress Report no. 2, 16 August - 16 November, 1966, Report no. PcRD-8MGR-66, U.S. Air Force Contract AF 33(615)-3575, November 1966, 32 pp. (AD 804 329).

465. Taylor, W. F. and Wallace, T. J., THE STUDY OF HYDROCARBON FUEL VAPOR PHASE DEPOSITS. Esso Research and Engineering Co., Government Research Lab. Quarterly Progress Report no. 3, 16 November 1966 - 16 February 1967, Report no. GR-1-VPD-67, U.S. Air Force Contract AF 33(615)-3575, February 1967, 21 pp. (AD 808 288).

466. Taylor, W. F. and Wallace, T. J., KINETICS OF DEPOSIT FORMATION FROM HYDROCARBON (JET) FUELS AT HIGH TEMPERATURES. GENERAL FEATURES OF THE PROCESS. 154th ACS. Mtg. (Chicago Sept. 1967); Ind. Eng. Chem. Prod. Res. Develop. V6 N.4 258-62 (Dec. 1967).

467. Taylor, W. F. and Wallace, T. J., KINETICS OF DEPOSIT FORMATION FROM HYDROCARBONS (AT 200 DEGREES - 500 DEGREES F IN THE PRESENCE OF OXYGEN) --2. EFFECT OF TRACE SULFUR COMPOUNDS. Res. Results Serv Ms. (Manuscript) N.67-492 21P; Ind. Eng. Chem. V60 N.1 94-96 (Jan. 1968).

468. Thomann, H., HEAT TRANSFER MEASUREMENTS AT M = 7.17 - FIRST STEP OF A COMPARISON BETWEEN TUNNEL TEST AND FREE FLIGHT. Aeronautical Research Institute of Sweden Report no. FFA-110, February 1967, 14 pp. (N67-37662).

450. Sterligov, O. D. and Eliseev, N. A., INFLUENCE OF THE NATURE OF ALUMINUM OXIDE ON THE PROPERTIES OF AN ALUMINA-CHROMIA-POTASSIA CATALYST FOR ISOPENTANE DEHYDROGENATION. Neftekhimiya 5 (6), 809-14 (1965) (Russ); C.A. 64, 11069 (1966).

451. Strauss, K. H., FUEL FOR THE SUPERSONIC TRANSPORT. Soc. Automotive Engrs Mtg. Paper N.650297 (1965); SAE (Soc. Automotive Engrs) Trans V74 (Pt. 2).179-84 (1966).

452. Streets, W. L. and Schirmer, R. M., GAS TURBINE AND JET ENGINE FUELS. SUMMARY REPORT. April 1, 1962-March 31, 1963. U.S. Dept. Com. Office Tech. Serv. AD-414 467 (March 1963) 81 pp. (Abstr.) Corrosion Abstr. V3 N.3.204 (May 1964).

453. Strehlow, R. A. and Rubins, P. M., EXPERIMENTAL AND ANALYTICAL STUDY OF THE H_2-AIR REACTION KINETICS USING A STANDING-WAVE NORMAL SHOCK. AIAA Propulsion Joint Specialist Conference (3rd), Washington, D.C., 17-21 July 1967, AIAA-Paper-67-479; U.S. Air Force Arnold Engineering Development Center Report no. AEDC-TR-67-177 prepared in cooperation with ARO, Inc., U.S. Air Force Contract AF 40(600)-1200, September 1967, 30 pp. (AD 658 434).

454. Stull, F. D. (Wright-Patterson A.F.B.) SCRAMJET COMBUSTION PROSPECTS. Astronaut. Aeron. 3 (12), 48-52 (1965); C.A. 64, 4849 (1966).

455. Subbotin, V. I. and Papovyants, A. K., RECENT DATA ON HEAT TRANSFER IN A TURBULENT FLOW OF LIQUID DROPS IN ROUND TUBES. Presented at IAEA Symp. on Alkali Metal Coolants, Corrosion Studies, and System Operating Experience, Vienna, 29 November - 2 December, 1966; Brookhaven National Laboratory Translation BNL-TR-144, April 1967, 22 pp. (N67-37722).

456. Subrahmanyam, N. and Ghosh, S. S., VAPOR PHASE AROMATIZATION OF n-HEPTANE. Current Sci. (India) 35 (5), 118-9 (1966); C.A. 64, 15774 (1966).

457. Suzumura, H., Yoshida, H., Tomita, Y., Fujiwara, H., THE PREPARATION OF AROMATICS FROM PETROLEUM HYDROCARBONS. I. THE RELATIVE REACTIVITIES OF NORMAL PARAFFINS IN AROMATIZATION. Sekiyu Gakkai Shi 8 (4), 249-53 (1965) (Japan); C.A. 65, 15128 (1966).

458. Swihart, J. M. and Henry, J. R., COMPILATION OF PAPERS SUMMARIZING SOME RECENT NASA RESEARCH ON MANNED MILITARY AIRCRAFT. VI. HYPERSONIC CRUISE VEHICLES. U.S. National Aeronautics and Space Administration Report NASA-TM-X-420, October 1950, 87-105 (N67-33076).

459. Swithenbank, J. (Sheffield Univ., England), HYPERSONIC AIR-BREATHING PROPULSION. Progress in Aeronautical Sciences 8, 229-94 (1966); U.S. Air Force AFOSR 67-0842, U.S. Air Force Contract AF-EOAR-23-65, 1966, 70 pp. (AD 649 936).

469. Thompson, W. H. and Braun, W. G. (Pennsylvania State Univ.), EVALUATION OF SEVERAL METHODS FOR PREDICTING HEATS OF VAPORIZATION OF PURE HYDROCARBONS AS A FUNCTION OF TEMPERATURE. Proc. Am. Petrol. Inst., Sect. III, 44, 45-60 (1964); C.A. 64, 15014 (1966).

470. Timofeeva, E. A., CONVERSION OF VARIOUS HYDROCARBONS OVER VARIOUS DEHYDROGENATION CATALYSTS. Kinetika i Kataliz 7 (3), 494-7 (1966) (Russ); C.A. 65, 10477 (1966).

471. Tipper, C. F. H. (ed.), OXIDATION AND COMBUSTION AND COMBUSTION REVIEWS, Vol. 1, New York: Elsevier, 1965, 344 pp.; C.A. 63, 17180 (1965).

472. Tolstopyatova, A. A., Ch'i, C., Gorshkova, L. S., CATALYTIC PROPERTIES OF PRASEODYMIUM OXIDE IN THE DEHYDROGENATION AND DEHYDRATION OF ALCOHOLS AND THE DEHYDROGENATION OF TETRALIN. Kinetika i Kataliz 6 (3), 466-70 (1965) (Russ); C.A. 63, 8159 (1965).

473. Transcontinental Gas Pipe Line Corp., NATURAL GAS: FUTURE FUEL FOR JET PLANES, Chem. Eng. V74 N.17 200 (8/14/67).

474. Treiman, M., comp., MONTE CARLO METHODS FOR THE SOLUTION OF HEAT TRANSFER PROBLEMS, INCLUDING HYBRID COMPUTER TECHNIQUES FOR MONTE CARLO. Los Alamos Scientific Laboratory Report no. LA-3777-MS, Contract W-7405-ENG-36, October 1967, 5 pp. (N68-16141).

475. Unger, H. J. and Hill, F. K. (Johns Hopkins Univ.), SPECTROSCOPIC MEASUREMENTS OF COMBUSTION-GAS COMPOSITION IN SUPERSONIC FLOW. IAA Accession No. A65-26794, 7 pp (1965); C.A. 63, 17787 (1965).

476. United Aircraft Corp., SCRAMJET ENGINE TEST PROGRAM AND APPLICATION STUDIES. Quarterly Report no. 1, 1 October - 31 December 1966, Report no. E910505-4, Contract F33615-67-C-1045, January 1967, 35 pp. (AD 379 519) (REPORT CLASSIFIED CONFIDENTIAL).

477. U.S. Air Force Foreign Technology Division, PHYSICAL GAS DYNAMICS, HEAT TRANSFER AND THERMODYNAMICS OF HIGH TEMPERATURE GASES (SELECTED ARTICLES). Fizicheskaya Gazodinamika Teploobmen i Termodinamika Gazov Vysokikh Temperatur, 1964, 55-8, 80-99, 115-37, 150-6; Translation Report no. FTD-HT-66-365, TT-67-62287, January 1967, 96 pp. (AD 655 034).

478. U.S. Air Force Foreign Technology Division, PHYSICAL GAS DYNAMICS, HEAT TRANSFER AND THERMODYNAMICS OF HIGH TEMPERATURE GASES: SELECTED ARTICLES. Fizicheskaya Gazodynamika Teploobmen i Termodinamika Gazov Vysokikh Temperatur, n.p. 1964, 29-33, 104-14, Translation Report no. FTD-MT-65-552, TT 67-62101, March 1967, 31 pp. (AD [illegible] 513).

479. U.S. Air Force, SOVIET POLYMERIC MATERIALS AND TECHNOLOGIES APPLICABLE TO ABLATIVE AND HEAT-SHIELD FUNCTIONS IN AEROSPACE WEAPONS. Foreign Technology Division, Wright-Patterson A.F.B., Report no. FTD-PWS-114-66-2, December 1966, 31 pp. (AD 382 163L) (REPORT CLASSIFIED SECRET).

480. U.S. Army, Battelle Memorial Institute. AN ULTRASONIC BURNER FOR THE U.S. ARMY. Chem Week V97 N.9.123 (8/28/65).

481. U.S. Army, Aviation Materials Labs., INVESTIGATION OF THE FEASIBILITY OF BURNING EMULSIFIED FUEL IN GAS TURBINE ENGINES. Technical Report no. USA AVLABS-TR-67-24, March 1967, 210 pp. (AD 654 816).

482. U.S. Army, Ballistic Research Laboratories, Aberdeen Proving Ground, STABILITY AND TRANSPORT CHARACTERISTICS OF FLAMES. Technical Note, Report no. BRL-TN-191, April 1950, 10 pp. (AD 642 723).

483. U.S. Library of Congress, Aerospace Technology Div., PROPULSION TECHNOLOGY: MONTHLY SURVEY No. 2, ATD-66-137, TT 67-60621, November 1966, 62 pp. (AD 646 174).

484. U.S. National Aeronautics and Space Administration, Langley Research Center, PROCEEDINGS OF NASA CONFERENCE ON SUPERSONIC-TRANSPORT FEASIBILITY STUDIES AND SUPPORTING RESEARCH. Report NASA-TM-Y-905, Washington, NASA, December 1963, 543 pp. (N67-31605).

485. Usov, Yu. N., Skvortsova, E. V., Klyushnikova, G. G., CONVERSION OF C_8 - C_{18} n-ALKANES ON AN ALUMINOMOLYBDENUM CATALYST. Neftekhimiya 5 (6), 850-5 (1965) (Russ); C.A. 64, 8059 (1966).

486. Vahala, J. and Vyroubal, C., FERRIC CATALYST FOR THE DEHYDROGENATION OF ETHYLBENZENE. Chem. Prumysl 16 (1), 10-12 (1966) (Czech); C.A. 64, 11106 (1966).

487. Van Thiel, M. (ed.), COMPENDIUM OF SHOCK WAVE DATA. Sections B, C, D, Index, California Univ., Lawrence Radiation Laboratory Report UCRL-50108 (Vol. 2), Contract W-7405-eng-48, June 1966, 322 pp.

489. Van Tiggelen, A., EXPERIMENTAL STUDY OF THE DEFLAGRATION OF GASES AND SOLIDS. Louvain University (Belgium) Final Scientific Report, AFOSR 66-2763, U.S. Air Force European Office of Aeronautical Research Contract AF-EOAR-65-67, October 1966, 48 pp. (AD 643 439).

490. Van Tiggelen, A., Sale, B., Van Tiggelen, P., Burger, J. (Univ. Louvain, Belg.), OXIDATION AND COMBUSTION. VI. COMBUSTION THERMODYNAMICS AND AEROTHERMOCHEMISTRY THEORY. Rev. Inst. Franc. Petrole Ann. Combust. Liquides 21 (6), 955-1008 (1966) (Fr.); C.A. 66, 14520 (1966).

491. Van Tiggelen, P. J. and Duval, A. (Louvain University, Belgium), THE CONCEPT OF A MEAN TEMPERATURE IN THE FLAME REACTION ZONE. Bulletin de l'Academie Royale de Belgique (Classe des Sciences), s 5, 53, no. 4, 326-65; U.S. Air Force AFOSR-68-0131, Grant AF-EOAR-66-44, 1967, 43 pp. (AD 663 975).

492. Vasil'eva, G. V., INFLUENCE OF A DRY ZONE ON CONVECTIVE HEAT AND MASS TRANSFER DURING TRANSPIRATION COOLING. Inzh.-Fiz. Zh., Akad. Nauk Belorussk. SSR 9 (3), 405-8 (1965) (Russ); C.A. 64, 4619 (1966).

493. Vasu, G., Hart, C. E., Dunbar, W. R., PRELIMINARY REPORT ON EXPERIMENTAL INVESTIGATION OF ENGINE DYNAMICS AND CONTROLS FOR A 48-INCH RAM-JET ENGINE. U.S. National Aeronautics and Space Administration Report NACA-RM-E55J12, March 1956, 65 pp. (N67-31545).

494. Ventriglio, D. R. and McQuaid, R. W., VAPOR PRESSURE OF FLUIDS IN HIGH-PRESSURE GAS ATMOSPHERES. U.S. Navy Marine Engineering Lab. Research and Development phase Report no. MEL-456/66, March 1967, 56 pp. (AD 649 776).

495. Vieweg, H. G., Nowak, S., Koennecke, H. G., Nicolescu, J. V., Spinzi, M., INFLUENCE OF VARIOUS PROMOTERS ON THE ACTIVITY OF CHROMIC OXIDE-ALUMINUM OXIDE CATALYSTS AS SHOWN BY THE EXAMPLE OF DEHYDROCYCLIZATION OF n-HEXANE. Erdoel Kohle 19 (6), 414-7 (1966) (Ger); C.A. 65, 9786 (1966).

496. Viskanta, R., Schornhorst, J. R., Toor, J. S., ANALYSIS AND EXPERIMENT OF RADIANT HEAT EXCHANGE BETWEEN SIMPLY ARRANGED SURFACES. Purdue University Technical Report, May 1965 - June 1967, U.S. Air Force AFFDL-TR-67-94, Contract AF 33(615)-2362, June 1967, 131 pp. (AD 655 335) (N67-36717).

497. Volf, M. B., Kozik, B. L., Morozova, G. P., ON THE THERMAL STABILITY OF HYDROCARBON FUELS. Nauchno-Issledovatelskii Institut po Pererabotke Nefti. Trudy (USSR) 1960, no. [illegible]. 51-61; U.S. Air Force Translation No. FTD-MT-65-320, September 1967, 19 pp. (AD 661 441).

498. Wall, L. A., THERMAL AND OXIDATIVE DEGRADATION OF AROMATIC AND HETEROCYCLIC POLYMERS. U.S. National Bureau of Standards Report 31102-11-3110540, U.S. National Aeronautics and Space Administration NASA-CR-91659, NASA Order R-56, January 1968, 6 pp. (N68-15002).

499. Weber, R. J., LIQUID METHANE WAS PROPOSED AS A SUPERSONIC TRANSPORT FUEL. Chem Week V98 N.25.90 (6/18/66).

500. Weber, R. J. (Institute of Gas Technology), PROBLEMS BESET USE OF LNG. AS SUPERSONIC TRANSPORT FUEL. Am. Gas Assoc. Distribution Conf. (St. Louis May 1967) Oil Gas J. V65 N.27 60-62 (7/3/67).

501. Wehner, E. H., SUPERSONIC COMMERCIAL JETS NEED LOW-COST FUEL. KEROSENE FUELS FOR SUPERSONIC TRANSPORT. Soc. Automotive Engrs. Mtg. Paper N.863B (Adapt) SAE (Soc. Automotive Engrs.) J. V62 N.10.54-55 (Oct 1964).

502. Wehner, J. F. (University of Notre Dame), FLAME PROCESSES - THEORETICAL AND EXPERIMENTAL. Advan. Chem. Eng. (T. B. Drew, et al, eds., Academic) 5, 1-36 (1964); C.A. 63, 5439-40 (1965).

503. Weitkamp, A. W. (American Oil Co.), DEUTERIATION AND DEUTEROGENATION OF NAPHTHALENE AND TWO OCTALINS. Journal of Catalysis 6, 431-57 (1966).

504. Whisman, M. L. and Ward, C. C., STORAGE STABILITY OF HIGH TEMPERATURES FUELS. U.S. Bureau of Mines, Petroleum Research Center Final Report February 1966 - February 1967, AFAPL TR-65-13-Pt. 3, U.S. Air Force Project AF-3048, February 1967, 95 pp. (AD 647 787).

505. Wierzba, A., CONCERNING CERTAIN PROBLEMS RELATING TO INCOMPLETE COMBUSTION IN HEAT ENGINES. Prace Instytut Lotnictwa (Poland) 1965, no. 24, 34-48; U.S. Air Force Translation Report no. FTD-TT-65-1780 (AD 804 582).

506. Wiley, W. O., LOW-VOLUME RAMJET DEVELOPMENT. Texaco Experiment, Inc. Quarterly Progress Report 1 August - 15 November 1966, Report no. TM-1807, U.S. Navy Contract NOw-66-0259, November 1966, 42 pp. (AD 379 706) (REPORT CLASSIFIED CONFIDENTIAL).

507. Wiley, W. O., AIR-LAUNCHED LOW VOLUME RAMJET. Texaco Experiment, Inc. Quarterly Progress Report 16 November 1966 - 31 January 1967, Report no. TM-1826, U.S. Navy Contract N00019-67-C-0318, February 1967, 21 pp. (AD 381 328L) (REPORT CLASSIFIED CONFIDENTIAL) continuation of U.S. Navy Contracts NOw-64-0573 and NOw-66-0259.

508. Wiley, W. O., LVRJ AIR-LAUNCHED LOW VOLUME RAMJET. Texaco Experiment, Inc. Quarterly Progress Report 1 February - 30 April 1967, Report no. TM-1841, U.S. Navy Contract N00019-67-C-0318, May 1967, 34 pp. (AD 381 967L) (REPORT CLASSIFIED CONFIDENTIAL).

509. Williams, K. A., SUMMARY OF AIRCRAFT PROPULSION DEVICES UNITED STATES AND FOREIGN POWER PLANTS. Northrop Aircraft, Inc. Report no. NAI-58-621, August 1958, 107 pp. (AD 380 619) (REPORT CLASSIFIED SECRET).

511. Wilson, D. M., A DIGITAL COMPUTER PROGRAM FOR MAKING COMPARATIVE AERODYNAMIC HEAT TRANSFER AND SKIN FRICTION DRAG CALCULATIONS. U.S. Naval Ordnance Laboratory Report no. NOLTR-67-137, August 1967, 43 pp. (AD 660 683).

512. Winterfield, G., FLAME STABILIZATION IN SUPERSONIC FLOWS AT LOW GAS TEMPERATURES. Presented at Ann. Meeting of WGLR, Bad Godesberg, W. Germany, October, 1966; Great Britian Royal Aircraft Establishment Translation RAE-LIB-TRANS-1230, June 1967, 22 pp. (N68-12850).

513. Wood, B. J. and Rosser, W. A., Jr., IGNITION AND COMBUSTION OF SINGLE DROPLETS. Stanford Research Inst. Special Technical Report no. 8, April 1964 - December 1966, U.S. Army Contract DA-18-035-AMC-122(A), December 1966, 28 pp. (AD 808 879).

514. Wood, M. P., THE SHOCK TUNNEL AS A SUPERSONIC COMBUSTION TEST FACILITY. Fuel Soc. Journal (Sheffield Univ.) 1966, 50-60; Sheffield Univ. (England) Report no. HIC-75, U.S. Air Force AFOSR67-0847 U.S. Air Force Contract AF-EOAR-11-66, August 1966, 14 pp. (AD 650 008).

515. Yantovskii, S. A., TWO-STAGE COMBUSTION OF EXPLOSIVE MIXTURES. III. KINETIC ZONES OF SELF-IGNITION OF ISO-OCTANE - AIR AT ELEVATED PRESSURES. Kinetika i Kataliz 7 (1), 21-6 (1966) (Russ); C.A. 64, 15668 (1966).

516. Yates, C. L., Lasky, M., Schetz, J. A., TWO-DIMENSIONAL MIXING STUDIES. Johns Hopkins University, Applied Physics Laboratory Research and Development Programs, March 1967, 2 pp. (N67-33386).

517. Zakupra, V. A. and Lebedev, E. V., GAS-CHROMATOGRAPHIC INVESTIGATION OF THE PRODUCTS OF DEHYDROGENATION AND CRACKING OF NORMAL PARAFFINS. Chem. Tech. (Berlin) 17 (10), 594-8 (1965) (Ger.); C.A. 64, 494 (1966).

518. Zajic, V., INTENSIFICATION OF COOLING BY A ROUGHENED HEAT-EXCHANGE SURFACE AT A HIGH THERMAL FLUX. Jaderna Energie 11, 369-73 (1965) (Czech); C.A. 64, 3071 (1966).

519. Zeh, D. W. and Gill, W. N. (Clarkson College of Technology), HEAT TRANSFER AND BINARY DIFFUSION IN VARIABLE PROPERTY FREE CONVECTION FLOWS. International Journal Heat Mass Transfer 10, 1159-70 (1967); Prepared in cooperation with Syracuse University, Department of Chemical Engineering, U.S. Navy Contract Nonr-5053 (01). (AD 661 380).

520. N. D. Zelinskii Institute of Organic Chemistry, Academy of Sciences, U.S.S.R. (by B. A. Kazanskii, Kh. M. Minachev, O.D. Sterligov, Yu. S. Khodakov, N. A. Eliseev), CATALYST FOR DEHYDROGENATION OF PARAFFINIC HYDROCARBONS TO OLEFINS. U.S.S.R. 179,751 (Cl. B 01j), February 28, 1966, Appl. December 3, 1964; C.A. 65, 10399 (1966).

521. Zengel, A. E., Churchill, A. V., Heger, J. A., FUELS FOR ADVANCED AIR-BREATHING WEAPON SYSTEMS. SAE Mtg. Paper N.650804 (1965) SAE (Soc. Automotive Engrs.) Trans V74 (Pt. 3) .641-59 (1966).

522. Zotin, V. K. and Talantov, A. V., FLAME PROPAGATION VELOCITY IN TURBULENT FLOW OF HOMOGENEOUS MIXTURES. Izv. Vysshikh Uchebn. Zavedenii, Aviats. Tekhn. 9 (3), 98-103 (1966) (Russ); C.A. 65, 19919 (1966).

523. Zrelov, V. N., MECHANISM OF THE FORMATION OF MICRO CONTAMINANTS IN JET FUELS. Khim. i Tekhnol. Topliv i Masel V10 N.10.46-50 (Oct. 1965).

524. Zrelov, V. N. and Marinchenko, N. I., EFFECT OF THE OXIDATION PRODUCTS OF JET FUELS ON FORMATION OF MICROIMPURITIES. Khim. i Tekhnol. Topliv i Masel 11 (5), 57-61 (1966) (Russ); C.A. 65, 6972 (1966).

SUBJECT INDEX FOR BIBLIOGRAPHY

Supersonic Aircraft
60, 61, 62, 63, 64, 65, 66, 67, 68, 78, 105, 148, 150, 161, 197, 211, 289, 290, 291, 361, 377, 458, 484

Vaporizing and Endothermic Fuels
5, 105, 115, 127, 151, 160, 161, 179, 269, 298, 333, 334, 336, 337, 390, 391, 421, 435, 451, 473, 499, 500, 521

Thermal Reactions
58, 169

Catalysis and Catalytic Reactions
5, 12, 13, 16, 17, 18, 19, [illegible], 32, 33, 34, 35, 42, 59, 86, 92, 93, 94, 95, 103, 106, 107, 123, 128, 131, 132, 133, 145, 146, 154, 162, 163, 164, 180, 181, 182, 185, 186, 187, 183, 189, 206, 207, 209, 210, 218, 229, 236, 240, 242, 249, 250, 251, 253, 256, 260, 267, 282, 287, 297, 317, 318, 322, 323, 324, 326, 327, 329, 330, 332, 335, 336, 338, 340, 341, 346, 353, 362, 365, 368, 371, 384, 394, 395, 401, 402, 407, 408, 418, 419, 422, 423, 427, 428, 429, 430, 431, 440, 442, 450, 456, 457, 470, 472, 485, 486, 495, 503, 517, 520

High Temperature Stability
29, 45, 46, 50, 57, 70, 71, 72, 87, 91, 97, 98, 99, 116, 119, 120, 121, 124, 125, 126, 140, 141, 142, 172, 180, 205, 213, 219, 220, 228, 245, 268, 270, 279, 312, 337, 339, 347, 369, 406, 416, 425, 426, 497, 498, 504

Fuel Contaminants
43, 44, 72, 90, 104, 111, 130, 140, 141, 142, 273, 274, 364, 366, 452, 464, 465, 466, 467, 501, 523, 524

Fuel Additives
27, 45, 46, 71, 80, 116, 117, 140, 141, 156, 172, 239, 246, 252, 255, 262, 278, 313, 350, 369, 425, 426, 437, 446

Combustion Characteristics
1, 2, 3, 4, 8, 9, 10, 11, 14, 24, 28, 30, 36, 40, 48, 49, 51, 52, 53, 73, 74, 77, 83, 89, 96, 100, 102, 108, 112, 115, 122, 129, 135, 136, 137, 138, 139, 140, 141, 144, 166, 168, 171, 173, 174, 177, 178, 183, 184, 203, 204, 208, 214, 215, 226, 231, 232, 243, 244, 357, 264, 265, 266, 271, 272, 276, 280, 281, 283, 285, 288, 293, 296, 300, 303, 306, 308, 309, 311, 315, 316, 319, 320, 321, 325, 331, 336, 345, 349, 351, 352, 357, 359, 360, 367, 370, 372, 374, 381, 385, 386, 390, 391, 393, 397, 398, 409, 410, 411, 412, 413, 420, 424, 433, 436, 438, 439, 441, 443, 444, 447, 453, 454, 460, 461, 471, 475, 481, 482, 487, 489, 490, 499, 501, 502, 505, 512, 513, 514, 515, 522

Physical and Chemical Properties
20, 21, 22, 23, 56, 81, 82, 101, 118, 134, 147, 153, 212, 216, 217, 221, 222, 254, 304, 344, 373, 383, 389, 424, 434, 444, 449, 463, 469, 494

SUBJECT INDEX FOR BIBLIOGRAPHY (Contd)

Heat Transfer and Flow Behavior
6, 7, 25, 38, 39, 47, 54, 55, 69, 75, 76, 84, 85, 101, 109, 157, 158, 159, 165, 175, 201, 223, 225, 227, 230, 233, 234, 235, 237, 238, 241, 277, 284, 286, 294, 299, 301, 310, 314, 348, 354, 355, 356, 382, 387, 392, 396, 399, 403, 404, 415, 417, 432, 445, 448, 455, 462, 468, 474, 477, 478, 479, 480, 491, 492, 496, 511, 518, 519

Advanced Engines
14, 15, 25, 37, 40, 41, 47, 49, 51, 52, 53, 61, 63, 64, 65, 66, 67, 68, 79, 88, 102, 110, 112, 113, 114, 129, 138, 143, 149, 150, 152, 155, 159, 167, 170, 171, 176, 177, 184, 190, 191, 192, 193, 194, 195, 196, 197, 198, 199, 200, 202, 211, 224, 247, 258, 259, 261, 263, 275, 276, 290, 292, 295, 301, 302, 303, 305, 307, 328, 342, 343, 358, 361, 363, 374, 375, 376, 377a, 378, 379, 380, 388, 400, 405, 414, 433, 443, 454, 458, 459, 460, 475, 476, 483, 493, 506, 507, 508, 509, 510, 512, 514, 516